Volume 12, Issue 4, December 2022
ISSN 2158-0529

IJBM

International Journal of BIOMEDICINE

www.ijbm.org

INTERNATIONAL JOURNAL OF BIOMEDICINE

Aims and Scope: *International Journal of Biomedicine (IJBM)* publishes peer-reviewed articles on the topics of basic, applied, and translational research on biology and medicine. Original research studies, reviews, hypotheses, editorial commentary, and special reports spanning the spectrum of human and experimental and tissue research will be considered. All research studies involving animals must have been conducted following animal welfare guidelines such as the National Institutes of Health (NIH) Guide for the Care and Use of Laboratory Animals, or equivalent documents. Studies involving human subjects or tissues must adhere to the Declaration of Helsinki and Title 45, US Code of Federal Regulations, Part 46, Protection of Human Subjects, and must have received approval of the appropriate institutional committee charged with oversight of human studies. Informed consent must be obtained.

International Journal of Biomedicine endorses and behaves in accordance with the codes of conduct and international standards established by the Committee on Publication Ethics (COPE).

International Journal of Biomedicine (ISSN 2158-0510) is published four times a year by International Medical Research and Development Corp. (IMRDC), 6308, 12 Avenue, Brooklyn, NY 11219 USA

Customer Service: International Journal of Biomedicine, 6308, 12 Avenue, Brooklyn, NY 11219 USA; Tel: 1-917-740-3053; E-mail: editor@ijbm.org

Manuscript Submission: Original works will be accepted with the understanding that they are contributed solely to the Journal, are not under review by another publication, and have not previously been published except in abstract form. Accepted manuscripts become the sole property of the Journal and may not be published elsewhere without the consent of the Journal. A form stating that the authors transfer all copyright ownership to the Journal will be sent from the Publisher when the manuscript is accepted; this form must be signed by all authors of the article. All manuscripts must be submitted through the International Journal of Biomedicine`s online submission and review website. Authors who are unable to provide an electronic version or have other circumstances that prevent online submission must contact the Editorial Office prior to submission to discuss alternate options (editor@ijbm.org).

IJBM

INTERNATIONAL JOURNAL OF BIOMEDICINE

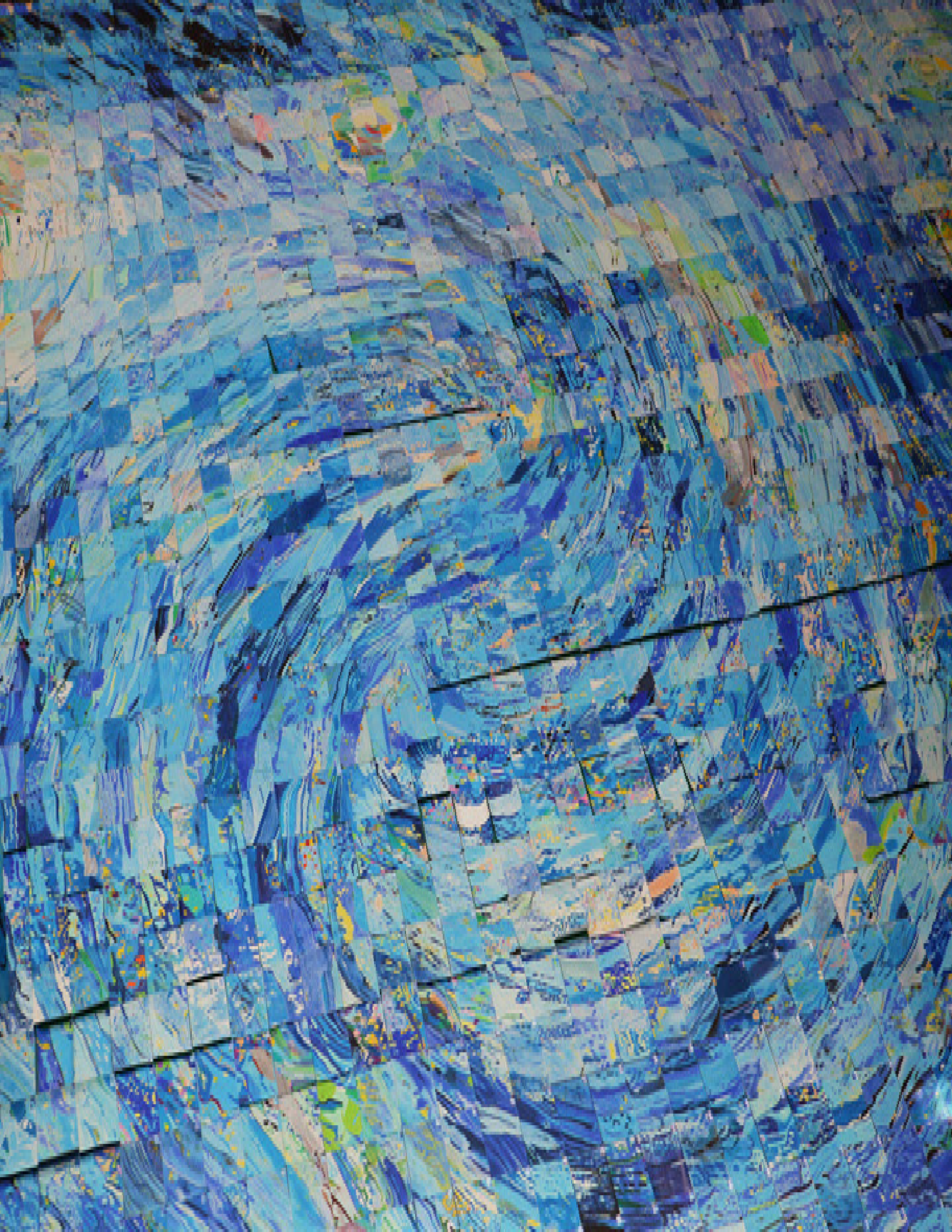

IJBM

INTERNATIONAL JOURNAL OF BIOMEDICINE

www.ijbm.org

Volume 12 Issue 4 December 2022

CONTENTS

EAPC
European Association of Preventive Cardiology

ESC Preventive Cardiology 2023

EAPC Annual Congress

13-15 April
Malaga, Spain •

#ESCPrev2023

ESC
European Society of Cardiology

EHRA
European Heart
Rhythm Association

EHRA 2023

16-18 April | Barcelona & Online

#EHRA2023

ESC
European Society
of Cardiology

International Journal of Biomedicine 12(4) (2022) 493-505
http://dx.doi.org/10.21103/Article12(4)_RA1

REVIEW ARTICLE

INTERNATIONAL JOURNAL OF BIOMEDICINE

Leading–Edge Portable Biosensors and Biomarkers Development for Raman Biospectroscopy and Imaging in Cancer Diagnosis

Alireza Heidari[1,2,3,4*], Zahra Torfeh[5], Sophia Iorgulescu[1,2,3], Olivia Robinson[1,2,3], Lin Hu[1,2,3], Charlotte Vauclin[1,2,3], Ntalie Schiltz[1,2,3], Scarlett Sondermann[1,2,3], Lucy MacLennan[1,2,3], Julia Smith[1,2,3], Lydia Williamson[1,2,3]

[1]*Faculty of Chemistry, California South University, Irvine, CA, USA*
[2]*BioSpectroscopy Core Research Laboratory (BCRL), California South University, Irvine, CA, USA*
[3]*Cancer Research Institute (CRI), California South University, Irvine, CA, USA*
[4]*American International Standards Institute (AISI), Irvine, CA, USA*
[5]*An Independent Volunteer and Unaffiliated Researcher*

Graphical Abstract

Raman spectroscopy is an important method for identifying molecules, which is widely used in determining the chemical and structural characteristics of various substances. Many materials have a special Raman spectrum, so that this phenomenon has turned the Raman device into an efficient tool for studying the structural and chemical properties of molecules. Since it is possible to obtain detailed information about the chemical and structural characteristics of biological compounds from Raman spectroscopy, the use of this method is rapidly expanding in the field of life sciences, especially in biological and medical studies. There is no need for special, time–consuming and expensive preparations in the study of materials with the help of a Raman device. In the protein Raman spectrum, distinct bands arise from the vibrational states of the peptide backbone and amino acid side chains. Therefore, based on the position and intensity of the protein's Raman spectrum, it is possible to obtain valuable information about its second, third, and fourth structures. Also, the Raman spectrum of the protein contains information about the orientation and surrounding environment of the amino acid side chains. The correct formation of the disulfide bond in the protein structure can also be studied with the help of the Raman device. In general, the Raman spectrum of proteins contains multiple discrete bands that represent the vibrational states of the molecule and is used as a selective fingerprint to accurately determine the three–dimensional structure of proteins, intramolecular dynamics, and intermolecular interactions.

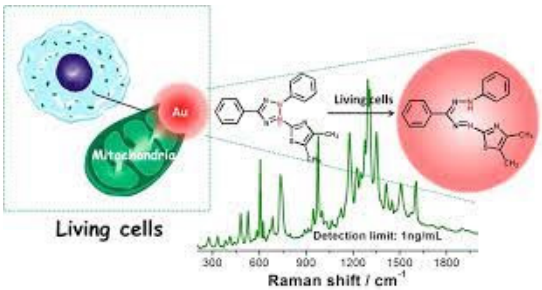

Schematic of leading–edge portable biosensors and biomarkers development for Raman biospectroscopy and imaging in cancer diagnosis.

Keywords: biosensors • biomarkers • Raman biospectroscopy • imaging • cancer • diagnosis

For citation: Heidari A, Torfeh Z, Iorgulescu S, Robinson O, Hu L, Vauclin C, Schiltz N, Sondermann S, MacLennan L, Smith J, Williamson L. Leading–Edge Portable Biosensors and Biomarkers Development for Raman Biospectroscopy and Imaging in Cancer Diagnosis. International Journal of Biomedicine. 2022;12(4):493-505. doi:10.21103/Article12(4)_RA1.

Introduction

The application of Raman spectroscopy is basically in the identification of molecules. Today, along with the many advances that have been made in the field of research equipment design, Raman spectroscopy has become more simple, accessible and affordable. Of course, despite the many advances made, the interpretation of Raman spectra is still a big challenge and requires special skills. Like all spectroscopic methods, the Raman spectrum contains information about the electromagnetic waves hitting the sample. After the electromagnetic beam hits the molecule, a part of it is scattered in all directions. Raman spectroscopy is used to observe vibrational, rotational, and other low-frequency states in a system. This type of spectroscopy typically provides a specific structural fingerprint that can be used to identify different molecules. In fact, this type of spectroscopy is based on inelastic scattering called Raman scattering (and the Raman light rays are usually laser light in the visible region, near infrared light or near ultraviolet light.[1–38]

The inelastic scattering of light upon impact with matter was not reported until 1928, while this important physical phenomenon was first predicted by Adolf Schmal in 1923. Also, Chandrasekhara Venkata Raman observed this effect for the first time after studying the passage of sunlight through organic solutions, and in 1930 he was honored to receive the Nobel Prize in Physics due to this important discovery and his other studies in this field. The development and evolution of this physical effect was carried out by George Pleczyk between 1930 and 1934. Also, in 1899, John William Reilly was able to justify the elastic scattering of light while proposing a new hypothesis. This light scattering theory was actually an answer to why the color of the sky is blue. At that time, light scattering studies were also seriously pursued in countries such as Russia, France, India, the United States of America, and Germany. In the early 20th century, people like Raman and Krishnan in India and Landsberg and Mandelstam in Russia were pioneers in this field of study. When investigating the change in the frequency of scattered light in different physical conditions, these people achieved results that they had not planned for in advance. Landsberg and Mandelstam also investigated the scattering of light in quartz and some other crystals to find the scattered rays that have undergone a frequency change compared to the incoming light. At the same time, Raman and Krishnan in India and far away from Russian scientists were studying the changes of light in the Compton effect. By publishing three articles in 1928, they recorded the change in the frequency of scattered light while encountering matter, even though the reports of Raman and Krishnan were only slightly earlier than the reports of Russian scientists. Nowadays, extensive studies are carried out on the scattering of light while interacting with matter, and the large volume of studies and the number of published scientific articles about this discovery show the special importance of this issue.[39–76]

Photons are often reflected, absorbed or scattered while hitting the molecule. In Raman spectroscopy, monochromatic light photons (light of a single wavelength) are scattered in different directions after hitting the sample. In fact, in Raman spectroscopy, photons scattered from the sample are important. Most of the photons that hit the molecule are scattered elastically. This type of scattering is called Rayleigh scattering, in which the photons scattered from the sample have the same energy or wavelength as the photons that hit the sample. In 1928, Indian physicist Chandra Sekhar Venkata Raman discovered the Raman phenomenon. In this phenomenon, the energy or wavelength of the beam scattered by the molecules is different from the wavelength of the primary beam that hits the sample. This type of scattering of light rays is called inelastic scattering. About one in ten million photons after hitting matter is scattered inelastically. Also, the amount of difference in energy or wavelength of inelastic scattered light depends on the molecular structure of the compound. In fact, Raman spectroscopy was formed based on the analysis of these differences and with the aim of determining the molecular structure of various compounds. The change in the wavelength or the initial radiation energy provides very important information about the molecular movements within the system. In Raman scattering, the photon collides with the material and after scattering its wavelength goes to the longitudinal direction. In these more or less displaced waves, the type of radiation scattering is dominated by the transmission to longer wavelengths, which is called Stokes Raman scattering. Also, the transition to lower wavelengths is called Raman anti–Stoke scattering. It has been reported that the intensity ratio of anti–Stoke to stoke scattering increases with increasing temperature. In fact, the incoming photon collides with the electron cloud of bonds of functional groups and excites the electrons to a virtual state. Then the electron returns from the virtual state to an excited vibrational or rotational state. This phenomenon causes the photon to lose some of its energy and is revealed in the form of Stokes Raman scattering. The lost energy is directly related to the chemical identity of the functional group, the molecular structure attached to it, the type of atoms in the molecule and its surrounding environment. Therefore, the Raman spectrum of each molecule is specific and can be used like a "fingerprint" to detect the chemical identity of molecular compounds in a liquid, on a surface, or in the air. [77–114]

Leading–Edge Portable Biosensors and Biomarkers Development

The degree of the Raman effect is directly related to the polarizability of the electrons of the molecule. The Raman effect is actually the interaction between the electron cloud of the sample and the external electric field of the incoming light rays. This mode creates the formation of which depends on the induced instantaneous dipole polarizability of the sample. Because the laser light does not excite the molecule, no actual transitions between energy levels occur in Raman studies. (with fluctuations, hence the Raman signal is obtained from the collision of the light beam (intermolecular photons (phonons) of the sample). Review and analysis of the information obtained in Raman spectroscopy to determine the structure, qualitative measurement, and in some cases, it takes a few molecules. Also, the study of the effect of many different physical parameters such as temperature, pressure and tension on interatomic and intermolecular oscillations. The Raman scattering spectrum and the infrared absorption spectrum of a molecule have many similarities with each other. In fact, it comes from the similarities

of these two methods. Also, despite the great similarity, these two methods are different from each other in the basic principles, so that they are usually used as complementary methods. In infrared absorption, the amount the energy absorbed from the incoming photon corresponds to the energy difference between the initial and final rotational–vibrational states, while in Raman scattering, the amount of energy of the incoming photon is not the same as the outgoing one (usually it is more or less). Also, the dependence of Raman on polarization the acceptability of its electric dipole–dipole species from infrared spectroscopy, which only observes dipole species. E is electric dependent (atomic polar tensor) differentiates. These differences indicate that transitions between rotational–vibrational states may not be active in infrared absorption, but can be studied using Raman spectroscopy. There is also the reverse of this phenomenon, so that infrared absorption spectroscopy is used in cases where Raman spectroscopy is not applicable for the study of molecules. Therefore, transitions that have a high intensity in the Raman spectrum often have weak infrared absorption and vice versa. In other words, a vibration is active in infrared spectroscopy, when a change in the momentary dipole of the molecule can be seen during its occurrence. Likewise, vibration is active in Raman spectroscopy, which changes the polarizability of the molecule as well. For example, molecules with identical nuclei, such as N2, H2, and O2 are active in the Raman study, but not active in infrared spectroscopy. In the CO2 molecule, the symmetric vibrational motion is active in Raman and not active in infrared. On the contrary, asymmetric vibrational motion is not active in Raman, but it is active in infrared. Some vibrations are also active in both infrared and Raman.

The main components of the Raman device, the system of each Raman device consists of four main parts, including the laser light source, the wavelength selector (sample illumination filter and light collecting lenses. After the light and the detector or spectrometer collide) the laser to the sample and Its scattering from its surface, the scattered light is collected by a lens and transmitted to the detector unit by a fiber. Wavelengths close to the laser wavelength (elastic or Rayleigh scattering) are absorbed by a special filter. Only the scattered rays that have changed in terms of energy or wavelength compared to the incoming light are allowed to pass and reach the detector.

The most common sources of laser generation in the Raman device are argon laser with wavelengths of 488 and 514.5 nm, krypton laser with wavelengths of 530, 568, and 647 nm, helium/neon laser with a wavelength of 632.8 nm, diode laser, with 785 and 830 nm wavelength and AG Y/d N laser with 1064 nm wavelength. The waves that change the frequency (wavelength) after hitting the sample while scattering are the Raman signals that are of special importance. The cross-section of Raman scattering is very small, and the most difficult step in this method is to separate the Rayleigh elastic beams from the frequency–shifted Raman beams known as inelastic beams. In the past, holographic gratings and multiple stages were used to obtain a high degree of Raman signal, which made the collection time relatively long. Today, notch filters or edge filters and spectrographs (or spectrometry on the axial transmitter), Zarni–Turner splitter for amplification, and detectors of the coupled device based on the Fourier transform of the Raman signal are used.

Results and Discussion

Raman, as mentioned earlier, Raman spectroscopy is widely used in various fields. In recent years, the use of Raman spectroscopy in medicine, pharmacy, food industry, defense science, and other industries has grown significantly. According to the global events of recent years, it is very important to establish methods for rapid detection of biological threats for the military and national security. In the meantime, Raman spectroscopy has received a lot of attention because it provides accurate and fast information about the molecular composition of biological materials in a non–destructive way. Currently, Raman spectroscopy is used to detect explosives, agents of chemical and bacterial warfare, and other dangerous chemical substances. With the help of this method, samples can be checked in a non–contact and non–destructive way inside transparent or semi-transparent packaging. Therefore, drugs and narcotics can be checked through the plastic bag containing them, and in this way, damage to criminal documents and evidence or their contamination can be avoided. It is also possible to equip a Raman spectroscopy probe with an optical fiber in order to measure nitrate, nitrite and hydroxide in tanks containing radioactive waste. These three chemicals are often used to display and control tank corrosion. In this way, there is no need to physically remove the sample from the tanks and the risks of transporting it to a fixed laboratory to check them. The accuracy of Raman detection depends on various factors, including the laser wavelength used and the type of material. The detection accuracy of these method variables usually ranges from a few parts per million to a few parts per billion. Raman's ability to display stress and other parameters, such as the surface temperature of the component, makes it an effective tool in the manufacture of semiconductor components. Also, the ability of this method to provide accurate images of cells allows comparison between healthy and diseased tissues, which is especially important in the study of cancerous tissues (Figures 1–5).

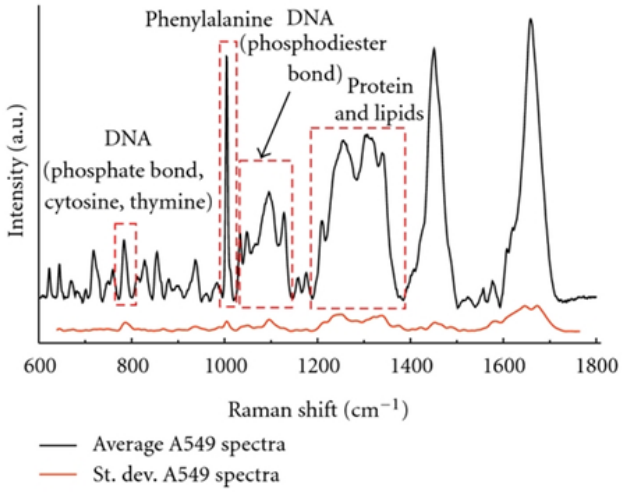

Fig. 1. *Raman spectroscopy investigation of DNA, protein and lipids in human cancer cells.*

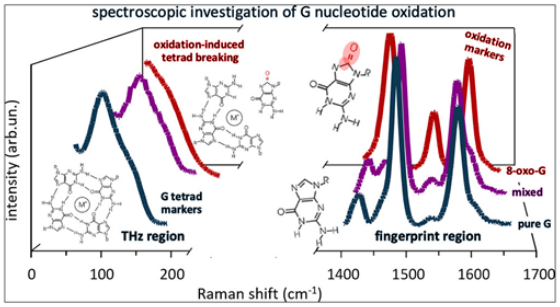

Fig. 2. Raman spectroscopy investigation of G nucleotide oxidation in human cancer cells.

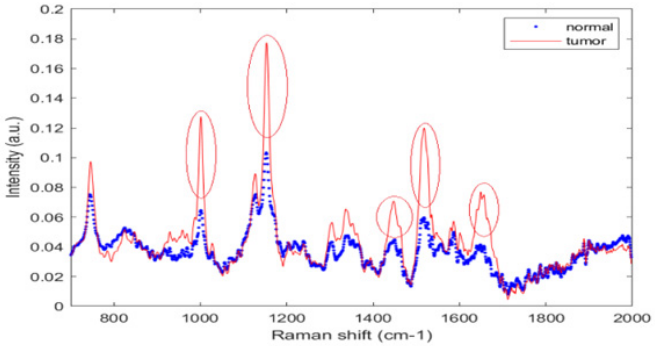

Fig. 3. Raman spectroscopy comparison between normal and cancer animal cells.

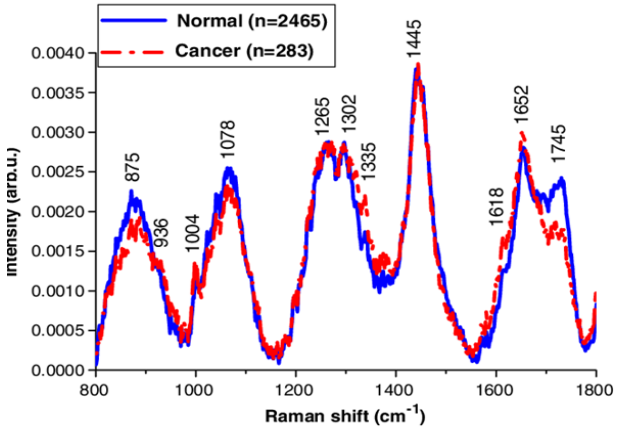

Fig. 4. Raman spectroscopy comparison between normal and cancer human cells.

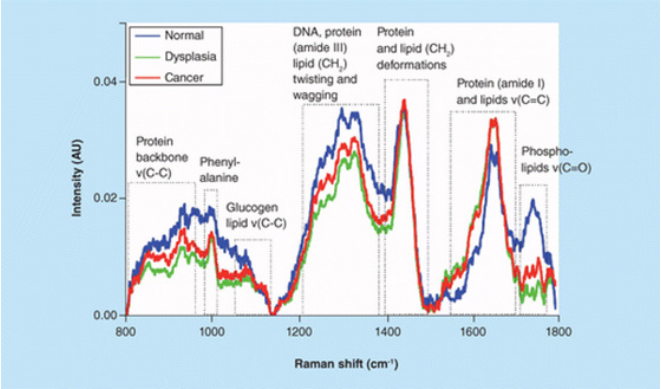

Fig. 5. Raman spectroscopy comparison among normal, dysplasia and cancer human cells.

What information can be obtained from examining the Raman scattering spectrum of materials? The vibrational frequencies of a link are very sensitive to the details and the structural features and local environment of the molecule, such as crystal phase symmetry, polymer morphology, and band position in the Raman spectrum representing the chemical species, crystal phase, or substance under study. The composition or compounds that make up the alloy, as well as the intensity of the Raman spectrum, indicates the concentration of the active group present in the composition or substance under investigation. Raman frequency shift indicates the type of functional group and temperature changes in the investigated substance. And finally, the width of the Raman spectrum indicates the presence of a disorder or structural disorder in the studied material.

Effect of solvent on the Raman spectrum of the protein. Protein in solution has a wider Raman spectrum than in powder form. The Raman spectrum of lysozyme protein in both powder and solution states. The type III amide bands of the protein in the solution state have a wider spectrum. The effect of chemical reactions on the folding and Raman spectrum of proteins in the presence of a concentration of different methanol amide bonds of type (I) alpha-synuclein protein have been modified and a detailed examination of this area after separating the sub–spectral surface, it is clear that the structure of alpha–synuclein protein under the influence of methanol gradually deviates from the normal state and in that second structures from alpha helix to structures called beta sheets and structures. The effect of reducing agents on the folding of proteins and its display in the Raman spectrum, after deconvolution of the protein Raman spectra, the amount of structural changes in the presence of reducing agents is determined. Physics such as reaction rate, free enthalpy and activation energy can be calculated from these data. Interference in protein Raman spectrum by fluorescence emission and signal–to–noise effect. Fluorescence emission can have severe destructive effects on the protein Raman spectrum. Intrinsic fluorescence usually occurs in the presence of aromatic amino acids, which can be eliminated by choosing the appropriate excitation wavelength in protein Raman studies. Also, transient fluorescence is usually due to impurity; a solvent or buffer is created to avoid interference. Transient fluorescence is necessary for Raman studies. Samples can be prepared as pure as possible. Background fluorescence was reduced by quenching or bleaching by emission light. Of course, it should be noted that increasing the temperature, in this case, may damage the sample (Tables 1–5).

Conclusion

High signal–to–noise ratio in the presence of a higher signal–to–noise ratio, the Raman spectrum of the sample is more accurate. This ratio can be increased by increasing the number of scans or the scan time.In addition, it should be noted that an excessive increase in the number of scans, as well as a change in the time interval of the scan, can cause serious damage to the sample. This method has many applications in various research fields. Also, this method provides important information about the structure of molecules, so that Raman bands can be considered as a kind of fingerprint of a compound. The similarities and differences between the Raman light scattering method and

the infrared absorption spectrometry method have made these two methods to be used for a more detailed structural study of a compound and complement each other. Raman spectroscopy provides valuable information on secondary, tertiary, and even quaternary structures of proteins. With the help of this method, it is possible to check the correct formation of disulfide bonds in the protein structure. Also, the amount of information that can be obtained from the protein Raman spectrum is far more than other conventional spectroscopic methods. Therefore, Raman spectroscopy is suggested as a useful tool to study the protein structure more precisely.

Acknowledgement

This study was supported by the Cancer Research Institute (CRI) Project of Scientific Instrument and Equipment Development, the National Natural Science Foundation of the United Sates, the International Joint BioSpectroscopy Core Research Laboratory (BCRL) Program supported by the California South University (CSU), and the Key project supported by the American International Standards Institute (AISI), Irvine, California, USA.

Table 1.

Role and applications of Raman spectroscopy and techniques in diagnosis of different types of human cancers.

Cancer Type	Technique	Raman Excitation Wavelength (nm)	Spot Size (mm)	Power (mW)	Signal Integration Time (s)	Number of Skin Lesions Studied and/or Patients	Reference
MM, BCC, SCC, actinic keratosis (AK), atypical nevi, melanocytic nevi, blue nevi, and seborrheic keratoses (SK)	Raman	785	3.5	300	1	518 (453 patients)	36
BCC, inflammatory scar tissues	Raman + OCT	785	0.044	40	30	1 patient	15
MM, BCC, SCC, pigmented nevi	Raman	785	1	150	30	50	37
MM, BCC, SCC, pigmented nevi	Raman + OCT	785	1	150	30	23, 50	38, 39
MM, BCC, SCC, pigmented nevi	Raman	785	0.1	17	10	137	40, 41
BCC, SCC, inflammatory scar tissues	Raman	825	0.005	40	30	21 (19 patients)	42
BCC	Raman	830	1.6	10	30	10 patients	43
BCC, SCC	Raman	830	–	200	20 (2 s×10 spectra)	31 (17 patients)	44
BCC, SCC, AK	Raman	830	0.17	200	20 (2 s×10 spectra)	49 (25 patients)	45
MM, BCC, SCC, actinic keratosis (AK), and non–melanoma pigmented lesions	Raman	830	0.2	100	1	137 (76 patients)	46, 47
BCC	Multi Modal	830	0.2	56	4	1 (healthy)	48
MM, eczema, psoriatic skin, malignant Kaposi sarcomas	Raman	1064	10	–	–	1 (healthy)	31
MM, BCC, pigmented nevi	Raman	1064	0.1	120	480	81 (72 patients)	49
Carotenoid concentration in BCC and actinic keratosis (AK)	Raman	488	2	10	20	14 patients	50
MM	Multi Modal	1064	0.08	–	35	Mice injected with human MM cells	51

Table 2.

Leading–edge portable biosensors and biomarkers data for Raman spectroscopy and imaging in cancer diagnosis.

	Subjects					Location			
Final lesion diagnosis	Mean age, year (range)	Male	Female	Number of lesions	Number biopsied (%)	Head and neck	Trunk	Upper limb	Lower limb
MM									
LM	69 (51–88)	12	8	20	20 (100)	19	1	0	0
LMM	67 (42–85)	7	1	8	8 (100)	8	0	0	0
SS	60 (22–77)	6	8	14	14 (100)	3	3	7	1
MM other	61 (60–62)	2	0	2	2 (100)	1	1	0	0
BCC									
Superficial	63 (34–86)	10	13	28	28 (100)	10	9	5	4
Nodular	66 (39–94)	34	29	73	73 (100)	52	10	9	2
Pigmented	67 (46–83)	2	4	6	6 (100)	2	4	0	0
Other BCC	68 (60–75)	1	1	2	2 (100)	1	1	0	0
SCC									
In situ	70 (56–88)	12	5	18	18 (100)	7	4	5	2
Invasive	66 (39–94)	16	10	28	28 (100)	16	1	5	6
Other SCC	78	0	1	1	1 (100)	1	0	0	0
Actinic keratosis (AK)	66 (43–92)	13	14	32	10 (31.3)	28	0	3	1
Atypical nevus	48 (20–75)	22	26	57	24 (42.1)	3	39	8	7
Junctional nevus	43 (18–70)	12	17	34	4 (11.8)	5	11	15	3
Compound nevus	35 (18–67)	13	15	30	6 (20)	9	8	9	4
Intradermal nevus	50 (28–83)	9	26	38	12 (31.6)	21	8	7	2
Blue nevus	37 (18–66)	4	9	13	4 (30.8)	4	1	6	2
Seborrheic keratosis (SK)	64 (25–89)	49	42	114	31 (27.2)	47	47	14	6
MM, malignant melanoma; MM subtypes: LM, lentigo maligna; LMM, lentigo maligna melanoma; SS, superficial spreading melanoma.									

Table 3.

Comparison between Mid–FTIR spectroscopy and Raman spectroscopy in cancer diagnosis.

	Mid–FTIR	Raman
Diagnostic criteria	Objective (based on biochemical spectral fingerprint)	
Wavenumber range	800–4000 cm^{-1}	400–4000 cm^{-1}
Type of spectroscopic detection	Mid–infrared light absorption using a polychromic light source	Inelastic light scattering using a monochromatic laser excitation (usually 785 or 830 nm but visible lasers also used)
Conditions for Raman/FTIR activation (selection rules)	Changes in the dipole moment	Changes in polarizability
Molecular bond sensitivities	Strong polar bonds including hydroxyl (OH), carbonyl (CO) and amide bonds	Non–polar bonds including C–C double and triple bonds including aromatic rings
SNR	Generally higher SNR in similar timescales	Weaker Raman cross–section of biological material results in lower SNR for normal Raman spectra
Spatial resolution	Lower spatial resolution due to diffraction limit (~ 10 μm). Synchrotron sources (2–5 μm)	Higher spatial resolution (~ 1 μm) due to diffraction limit
Imaging/mapping modes	Rapid scan imaging using focal plane or linear array detectors. ATR imaging can improve spatial resolutions and be applied to thicker samples	Point raster mapping, line and rapid synchronous readout mapping, Fast Raman imaging, ultrafast confocal Raman imaging, Wide–field imaging, LCTF Raman imaging
Enhanced techniques	ATR (attenuated total reflection): IR direct sample analysis by contact with an ATR crystal. Penetration is within the evanescent field which can be controlled and allows measurement from aqueous body fluids or non–dried tissue samples	SORS: the Raman scatter is collected from regions laterally offset from laser excitation, leading to significantly lower contributions from the surface layer, enabling depth probing. CARS: two laser beams are used to generate a coherent anti–Stokes frequency beam, which can be enhanced by resonance. SERS: enhancements over normal Raman scattering of typically 10^3–10^6 due to electromagnetic and chemical enhancement effects, with florescence quenching. Requires close proximity/adsorption onto a roughened metal surface, a colloidal solution or a roughened electrode (usually Ag or Au). Can tune to a specific chromophore for additional resonance enhancement (SERRS). TERS: combines high spatial resolution of an AFM and biochemical specificity of NRS
Sample preparation	Optimal thickness (transmission mode) or sample contact (ATR) may be necessary. Sample preparation is difficult	Little contact and destruction, water does not disturb measurement. Sample preparation is easier
Substrates	Mirror, CaF_2, BaF, Low e, zinc selenide (ZnSe)	CaF_2, BaF, quartz
Water	Strong water absorption and CO_2 contribution to spectrum	In vivo application possible due to weak scattering of water
Effect of paraffin–routine processing of tissue in histology	Paraffin peaks are visible in the FTIR fingerprint region. This can be overcome by deparaffinization or spectral subtraction	Strong Raman peaks in fingerprint region
Sample thickness	Spectra from thick samples (>15 μm) can cause spectral saturation	Point spectra can be obtained from thick sections (>15 μm) or bulk samples. 10–20 μm sections for mapping

Table 4.

Cancer type of interest and classification analysis groups of type of Raman system in cancer diagnosis.

Cancer type of interest	Classification analysis groups	Type of Raman system (HF/LF)	Authors (year)	Number of spectra (number of patients)	Analysis method Sensitivity: specificity	Reference
Skin cancer	Malignant + premalignant vs. benign and normal	Macro–Raman (LF)	Zeng group (2001–2012)	518 (453)	PCA–GDA and PLS 90%: 66%	20, 40–43
Skin cancer	Nonmelanoma cancers vs. normal lesions	Macro–Raman (LF)	Mahadevan–Jansen group (2008)	42 (19)	MRDF–SMLR 100%: 91%	44
Lung cancer	Malignant + premalignant vs. benign and normal	Macro–Raman (LF)	Zeng group (2008–2011)	129 (26)	PCA–LDA 90%: 91%	21, 47
Breast cancer	Tumor vs. normal (tumor tissue margin detection)	Macro–Raman (LF)	Feld group (2006)	30 (9)	Model fitting 100%: 100%	49
Colorectal cancer	Adenomatous tissue vs. hyperplastic polyps	Macro–Raman (LF)	Wilson group (2003)	19 (3)	PCA–LDA 100%: 89%	55

Table 4 (continued).
Cancer type of interest and classification analysis groups of type of Raman system in cancer diagnosis.

Cancer type of interest	Classification analysis groups	Type of Raman system (HF/LF)	Authors (year)	Number of spectra (number of patients)	Analysis method Sensitivity: specificity	Reference
Cervical cancer	Squamous dysplasia vs. normal, inflammation and metaplasia	Macro–Raman (LF)	Richards–Kortum group (2001)	27 (13)	Intensity ratios NA	63
Cervical cancer	High–grade preneoplastic lesions vs. normal	Macro–Raman (LF)	Mahadevan–Jansen group (2007)	172 (66)	Logistic regression 89%:>81%	64
Cervical cancer	1. Dysplasia vs. normal 2. High–grade dysplasia vs. normal 3. High–grade dysplasia vs normal	Macro–Raman (LF)	Huang group 1. (2009) 2. (2011) 3. (2012)	1. 92 (46) 2. 105 (29) 3. 476 (44)	PCA–LDA 1. 94%: 98% 2. 73%: 89% 3. 85%: 82%	65–67
Upper GI (esophageal cancer)	High–grade dysplasia vs. normal	Macro–Raman (LF)	Huang group (2013)	(2)	PLS–LDA 91%: 83%	71
Upper GI (stomach cancer)	1. Normal tissue 2. Benign ulcer 3. Malignant ulcer	Macro–Raman (LF)	Huang group 1. (2009) 2. (2010) 3. (2012)	65	PLS–LDA 1. 90.8%: 93.8% 2. 84.7%: 94.5% 3. 82.1%: 95.3%	68–70
Oral cavity	1. Normal vs. malignant 2. Normal vs. potentially malignant 3. Normal vs. diseased	Macro–Raman (LF)	Gupta group (2013)	802 (28 healthy + 171 nonhealthy)	MRDF–SMLR 1. 96%: 99% 2. 99%: 98% 3. 94%: 94%	72
Oral cavity	Premalignant and malignant vs. normal and benign	Macro–Raman (LF)	Sonis and Zeng group (2014)	(18)	PCA–LDA 100%: 77%	73, 74
Brain cancer	Normal brain vs. dense cancer and normal brain invaded by cancer cells	Macro–Raman (LF)	Leblond group (2015)	161 (17)	Boosted trees Machine learning 93%: 91%	77
Bladder cancer	Normal bladder vs. cancer	Macro–Raman (LF)	Bosch group (2010)	63	PCA–LDA 85%: 79%	80

Table 5.
Raman spectroscopy application, experimental set up and analysis method in cancer diagnosis.

Raman application		Experimental setup				Analysis method	Reference
		Wavelength (nm)	Power (mW)	Exposure time (sec)	Other		
Cancer detection	Breast cancer	830	100–150	10–30		Nonnegative least square (NNLS)	8
		830	82–125	1	Probe	NNLS	31
		786	N/A	4		Raman shifts	7
		830	65	10		PCA–LDA	34
		514.5	8	N/A		Hierarchical cluster	42
	Cervical cancer	785	80	5–15	Probe	Logistic regression	45
		785	80	5	Probe	Maximum representation and discrimination feature (MRDF)	47
						Sparse multinomial logistic regression (SMLR)	
		785	15	60	Probe	PCA–LDA	49
		785	10	60		Raman shifts	43
		785	100	30		PCA	50
	Colorectal cancer	785	300	5	Probe	PCA–Support vector machines (SVMs)	51
		785	70	N/A		PCA	35
						Hierarchical cluster	
						Multiple least squares (MLS)	
		782.5	11.5	60	LTRS	PCA– Logistic regression	52
		782.5	11.5	60	LTRS	PCA–Artificial neural network (ANN)	53
Allograft rejection	Cardiac rejection	785	100	10		PCA	54
	Renal rejection	785/514.5	8–12	10		PCA–Discriminant function analysis (DFA)	56

Table 5 (continued).

Raman spectroscopy application, experimental set up and analysis method in cancer diagnosis.

Raman application		Experimental setup				Analysis method	Reference
		Wavelength (nm)	Power (mW)	Exposure time (sec)	Other		
	Renal rejection	785/514.5	8–12	10		PCA–Discriminant function analysis (DFA)	56
SERS for biomarker		785	100	20		NNLS	65
		785	25	10		Raman shifts	66
		633	N/A	N/A		Raman shifts	9
SERS for in vivo		785	50	120		Partial least squares	75
		785	20	2		Raman shifts	10
SWNTs		N/A	100	2		Raman imaging using G–band	88
		785	100	3/10		Raman imaging using G–band	91
		785	80	0.5		Raman imaging using G–band	94
SERS imaging		785	60	N/A		Raman imaging using SERS peaks	100
		633	N/A	N/A		Raman imaging using SERS peaks	101
Core–shell nanoparticle		633	0.5/4	30/60		Raman shifts	105
		633	2	50		Raman shifts	109
		633	0.3	10		Raman shifts	110

References

1. Heidari A. Different High–Resolution Simulations of Medical, Medicinal, Clinical, Pharmaceutical and Therapeutics Oncology of Human Lung Cancer Translational Anti–Cancer Nano Drugs Delivery Treatment Process under Synchrotron and X–Ray Radiations. J Med Oncol. 2017;1(1):1.
2. Heidari A. A Modern Ethnomedicinal Technique for Transformation, Prevention and Treatment of Human Malignant Gliomas Tumors into Human Benign Gliomas Tumors under Synchrotron Radiation. Am J Ethnomed. 2017;4(1):10.
3. Heidari A. Active Targeted Nanoparticles for Anti–Cancer Nano Drugs Delivery across the Blood–Brain Barrier for Human Brain Cancer Treatment, Multiple Sclerosis (MS) and Alzheimer's Diseases Using Chemical Modifications of Anti–Cancer Nano Drugs or Drug–Nanoparticles through Zika Virus (ZIKV) Nanocarriers under Synchrotron Radiation. J Med Chem Toxicol. 2017;2(3):1–5.
4. Heidari A. Investigation of Medical, Medicinal, Clinical and Pharmaceutical Applications of Estradiol, Mestranol (Norlutin), Norethindrone (NET), Norethisterone Acetate (NETA), Norethisterone Enanthate (NETE) and Testosterone Nanoparticles as Biological Imaging, Cell Labeling, Anti–Microbial Agents and Anti–Cancer Nano Drugs in Nanomedicines Based Drug Delivery Systems for Anti–Cancer Targeting and Treatment. Parana Journal of Science and Education (PJSE). October 12, 2017;3(4):10-19.
5. Heidari A. A Comparative Computational and Experimental Study on Different Vibrational Biospectroscopy Methods, Techniques and Applications for Human Cancer Cells in Tumor Tissues Simulation, Modeling, Research, Diagnosis and Treatment. Open J Anal Bioanal Chem. 2017;1 (1): 014–020.
6. Heidari A. Combination of DNA/RNA Ligands and Linear/Non–Linear Visible–Synchrotron Radiation–Driven N–Doped Ordered Mesoporous Cadmium Oxide (CdO) Nanoparticles Photocatalysts Channels Resulted in an Interesting Synergistic Effect Enhancing Catalytic Anti–Cancer Activity. Enz Eng. 2017;6:1.
7. Heidari A. Modern Approaches in Designing Ferritin, Ferritin Light Chain, Transferrin, Beta–2 Transferrin and Bacterioferritin–Based Anti–Cancer Nano Drugs Encapsulating Nanosphere as DNA–Binding Proteins from Starved Cells (DPS). Mod Appro Drug Des. 2017;1(1). MADD.000504.
8. Heidari A. Potency of Human Interferon β–1a and Human Interferon β–1b in Enzymotherapy, Immunotherapy, Chemotherapy, Radiotherapy, Hormone Therapy and Targeted Therapy of Encephalomyelitis Disseminate/Multiple Sclerosis (MS) and Hepatitis A, B, C, D, E, F and G Virus Enter and Targets Liver Cells. J Proteomics Enzymol. 2017;6:1.
9. Heidari A. Transport Therapeutic Active Targeting of Human Brain Tumors Enable Anti–Cancer Nanodrugs Delivery across the Blood–Brain Barrier (BBB) to Treat Brain Diseases Using Nanoparticles and Nanocarriers under Synchrotron Radiation. J Pharm Pharmaceutics. 2017;4(2):1–5.
10. Heidari A. C. Brown, Combinatorial Therapeutic Approaches to DNA/RNA and Benzylpenicillin (Penicillin G), Fluoxetine Hydrochloride (Prozac and Sarafem), Propofol (Diprivan), Acetylsalicylic Acid (ASA) (Aspirin), Naproxen Sodium (Aleve and Naprosyn) and Dextromethamphetamine Nanocapsules with Surface Conjugated DNA/RNA to Targeted Nano Drugs for Enhanced Anti–Cancer Efficacy and Targeted Cancer Therapy Using Nano Drugs Delivery Systems. Ann Adv Chem. 2017;1(2):061–069.
11. Heidari A. High–Resolution Simulations of Human Brain Cancer Translational Nano Drugs Delivery Treatment Process under Synchrotron Radiation. J Transl Res. 2017;1(1):1–3.
12. Heidari A. Investigation of Anti–Cancer Nano Drugs' Effects' Trend on Human Pancreas Cancer Cells and Tissues Prevention, Diagnosis and Treatment Process under Synchrotron and X–Ray Radiations with the Passage of Time Using Mathematica. Current Trends Anal Bioanal Chem. 2017;1(1):36–41.
13. Heidari A. Pros and Cons Controversy on Molecular Imaging and Dynamics of Double–Standard DNA/RNA of Human Preserving Stem Cells–Binding Nano Molecules with Androgens/Anabolic Steroids (AAS) or Testosterone Derivatives through Tracking of Helium–4 Nucleus (Alpha

Particle) Using Synchrotron Radiation. Arch Biotechnol Biomed. 2017;1(1): 067–0100.
14. Heidari A. Visualizing Metabolic Changes in Probing Human Cancer Cells and Tissues Metabolism Using Vivo ^{1}H or Proton NMR, ^{13}C NMR, ^{15}N NMR and ^{31}P NMR Spectroscopy and Self–Organizing Maps under Synchrotron Radiation. SOJ Mater Sci Eng. 2017;5(2):1–6.
15. Heidari A. Cavity Ring–Down Spectroscopy (CRDS), Circular Dichroism Spectroscopy, Cold Vapour Atomic Fluorescence Spectroscopy and Correlation Spectroscopy Comparative Study on Malignant and Benign Human Cancer Cells and Tissues with the Passage of Time under Synchrotron Radiation. Enliven: Challenges Cancer Detect Ther. 2017;4(2):e001.
16. Heidari A. Laser Spectroscopy, Laser–Induced Breakdown Spectroscopy and Laser–Induced Plasma Spectroscopy Comparative Study on Malignant and Benign Human Cancer Cells and Tissues with the Passage of Time under Synchrotron Radiation. Int J Hepatol Gastroenterol. 2017;3(4):079–084.
17. Heidari A. Time–Resolved Spectroscopy and Time–Stretch Spectroscopy Comparative Study on Malignant and Benign Human Cancer Cells and Tissues with the Passage of Time under Synchrotron Radiation. Enliven: Pharmacovigilance and Drug Safety.2017;4(2):e001.
18. Heidari A. Overview of the Role of Vitamins in Reducing Negative Effect of Decapeptyl (Triptorelin Acetate or Pamoate Salts) on Prostate Cancer Cells and Tissues in Prostate Cancer Treatment Process through Transformation of Malignant Prostate Tumors into Benign Prostate Tumors under Synchrotron Radiation. Open J Anal Bioanal Chem. 2017;1(1):021–026.
19. Heidari A. Electron Phenomenological Spectroscopy, Electron Paramagnetic Resonance (EPR) Spectroscopy and Electron Spin Resonance (ESR) Spectroscopy Comparative Study on Malignant and Benign Human Cancer Cells and Tissues with the Passage of Time under Synchrotron Radiation. Austin J Anal Pharm Chem. 2017;4(3):1091.
20. Heidari A. Therapeutic Nanomedicine Different High–Resolution Experimental Images and Computational Simulations for Human Brain Cancer Cells and Tissues Using Nanocarriers Deliver DNA/RNA to Brain Tumors under Synchrotron Radiation with the Passage of Time Using Mathematica and MATLAB. Madridge J Nano Tech. Sci. 2017;2(2):77–83.
21. Heidari A. A Consensus and Prospective Study on Restoring Cadmium Oxide (CdO) Nanoparticles Sensitivity in Recurrent Ovarian Cancer by Extending the Cadmium Oxide (CdO) Nanoparticles–Free Interval Using Synchrotron Radiation Therapy as Antibody–Drug Conjugate for the Treatment of Limited–Stage Small Cell Diverse Epithelial Cancers. Cancer Clin Res Rep. 2017;1:2, e001.
22. Heidari A. A Novel and Modern Experimental Imaging and Spectroscopy Comparative Study on Malignant and Benign Human Cancer Cells and Tissues with the Passage of Time under White Synchrotron Radiation. Cancer Sci Res Open Access. 2017;4(2):1–8.
23. Heidari A. Different High–Resolution Simulations of Medical, Medicinal, Clinical, Pharmaceutical and Therapeutics Oncology of Human Breast Cancer Translational Nano Drugs Delivery Treatment Process under Synchrotron and X–Ray Radiations. J Oral Cancer Res. 2017;1(1):12–17.
24. Heidari A. Vibrational Decihertz (dHz), Centihertz (cHz), Millihertz (mHz), Microhertz (μHz), Nanohertz (nHz), Picohertz (pHz), Femtohertz (fHz), Attohertz (aHz), Zeptohertz (zHz) and Yoctohertz (yHz) Imaging and Spectroscopy Comparative Study on Malignant and Benign Human Cancer Cells and Tissues under Synchrotron Radiation. International Journal of Biomedicine. 2017;7(4):335–340.
25. Heidari A. Force Spectroscopy and Fluorescence Spectroscopy Comparative Study on Malignant and Benign Human Cancer Cells and Tissues with the Passage of Time under Synchrotron Radiation. EC Cancer. 2017;2(5):239–246.
26. Heidari A. Photoacoustic Spectroscopy, Photoemission Spectroscopy and Photothermal Spectroscopy Comparative Study on Malignant and Benign Human Cancer Cells and Tissues with the Passage of Time under Synchrotron Radiation. BAOJ Cancer Res Ther. 2017;3(3): 045–052.
27. Heidari A. J–Spectroscopy, Exchange Spectroscopy (EXSY), Nuclear Overhauser Effect Spectroscopy (NOESY) and Total Correlation Spectroscopy (TOCSY) Comparative Study on Malignant and Benign Human Cancer Cells and Tissues under Synchrotron Radiation. EMS Eng Sci J. 2017;1(2):006–013.
28. Heidari A. Neutron Spin Echo Spectroscopy and Spin Noise Spectroscopy Comparative Study on Malignant and Benign Human Cancer Cells and Tissues with the Passage of Time under Synchrotron Radiation. Int J Biopharm Sci. 2017;1:103–107.
29. Heidari A. Vibrational Decahertz (daHz), Hectohertz (hHz), Kilohertz (kHz), Megahertz (MHz), Gigahertz (GHz), Terahertz (THz), Petahertz (PHz), Exahertz (EHz), Zettahertz (ZHz) and Yottahertz (YHz) Imaging and Spectroscopy Comparative Study on Malignant and Benign Human Cancer Cells and Tissues under Synchrotron Radiation. Madridge J Anal Sci Instrum, 2017;2(1):41–46.
30. Heidari A. Two–Dimensional Infrared Correlation Spectroscopy, Linear Two–Dimensional Infrared Spectroscopy and Non–Linear Two–Dimensional Infrared Spectroscopy Comparative Study on Malignant and Benign Human Cancer Cells and Tissues under Synchrotron Radiation with the Passage of Time. J Mater Sci Nanotechnol. 2018;6(1):101.
31. Heidari A. Fourier Transform Infrared (FTIR) Spectroscopy, Near–Infrared Spectroscopy (NIRS) and Mid–Infrared Spectroscopy (MIRS) Comparative Study on Malignant and Benign Human Cancer Cells and Tissues under Synchrotron Radiation with the Passage of Time. Int J Nanotechnol Nanomed. 2018;3(1):1–6.
32. Heidari A. Infrared Photo Dissociation Spectroscopy and Infrared Correlation Table Spectroscopy Comparative Study on Malignant and Benign Human Cancer Cells and Tissues under Synchrotron Radiation with the Passage of Time. Austin Pharmacol Pharm. 2018;3(1): 1011.
33. Heidari A. Novel and Transcendental Prevention, Diagnosis and Treatment Strategies for Investigation of Interaction among Human Blood Cancer Cells, Tissues, Tumors and Metastases with Synchrotron Radiation under Anti–Cancer Nano Drugs Delivery Efficacy Using MATLAB Modeling and Simulation. Madridge J Nov Drug Res. 2017;1(1):18–24.
34. Heidari A. Comparative Study on Malignant and Benign Human Cancer Cells and Tissues with the Passage of Time under Synchrotron Radiation. Open Access J Trans Med Res. 2018;2 (1):00026–00032.
35. Gobato MRR, Gobato R, Heidari A. Planting of Jaboticaba Trees for Landscape Repair of Degraded Area. Landscape Architecture and Regional Planning. 2018;3(1)1–9.
36. Heidari A. Fluorescence Spectroscopy, Phosphorescence Spectroscopy and Luminescence Spectroscopy Comparative

Study on Malignant and Benign Human Cancer Cells and Tissues under Synchrotron Radiation with the Passage of Time. SM J Clin. Med. Imaging. 2018;4(1): 1018.
37. Heidari A. Nuclear Inelastic Scattering Spectroscopy (NISS) and Nuclear Inelastic Absorption Spectroscopy (NIAS) Comparative Study on Malignant and Benign Human Cancer Cells and Tissues under Synchrotron Radiation. Int J Pharm Sci. 2018;2(1):1–14.
38. Heidari A. X–Ray Diffraction (XRD), Powder X–Ray Diffraction (PXRD) and Energy–Dispersive X–Ray Diffraction (EDXRD) Comparative Study on Malignant and Benign Human Cancer Cells and Tissues under Synchrotron Radiation. J Oncol Res. 2018;2(1):1–14.
39. Heidari A. Correlation Two–Dimensional Nuclear Magnetic Resonance (NMR) (2D–NMR) (COSY) Imaging and Spectroscopy Comparative Study on Malignant and Benign Human Cancer Cells and Tissues under Synchrotron Radiation. EMS Can Sci, 1–1–001, 2018.
40. Heidari A. Thermal Spectroscopy, Photothermal Spectroscopy, Thermal Microspectroscopy, Photothermal Microspectroscopy, Thermal Macrospectroscopy and Photothermal Macrospectroscopy Comparative Study on Malignant and Benign Human Cancer Cells and Tissues with the Passage of Time under Synchrotron Radiation. SM J Biometrics Biostat. 2018;3(1):1024.
41. Heidari A. A Modern and Comprehensive Experimental Biospectroscopic Comparative Study on Human Common Cancers' Cells, Tissues and Tumors before and after Synchrotron Radiation Therapy. Open Acc J Oncol Med. 2018;1(1).
42. Heidari A. Heteronuclear Correlation Experiments Such as Heteronuclear Single–Quantum Correlation Spectroscopy (HSQC), Heteronuclear Multiple–Quantum Correlation Spectroscopy (HMQC) and Heteronuclear Multiple–Bond Correlation Spectroscopy (HMBC) Comparative Study on Malignant and Benign Human Endocrinology and Thyroid Cancer Cells and Tissues under Synchrotron Radiation. J Endocrinol Thyroid Res. 2018;3(1):555603.
43. Heidari A. Nuclear Resonance Vibrational Spectroscopy (NRVS), Nuclear Inelastic Scattering Spectroscopy (NISS), Nuclear Inelastic Absorption Spectroscopy (NIAS) and Nuclear Resonant Inelastic X–Ray Scattering Spectroscopy (NRIXSS) Comparative Study on Malignant and Benign Human Cancer Cells and Tissues under Synchrotron Radiation. Int J Bioorg Chem Mol Biol. 2018;6(1e):1–5.
44. Heidari A. A Novel and Modern Experimental Approach to Vibrational Circular Dichroism Spectroscopy and Video Spectroscopy Comparative Study on Malignant and Benign Human Cancer Cells and Tissues with the Passage of Time under White and Monochromatic Synchrotron Radiation. Glob J Endocrinol Metab. 2018;1(3). GJEM. 000514–000519.
45. Heidari A. Pros and Cons Controversy on Heteronuclear Correlation Experiments Such as Heteronuclear Single–Quantum Correlation Spectroscopy (HSQC), Heteronuclear Multiple–Quantum Correlation Spectroscopy (HMQC) and Heteronuclear Multiple–Bond Correlation Spectroscopy (HMBC) Comparative Study on Malignant and Benign Human Cancer Cells and Tissues under Synchrotron Radiation. EMS Pharma J. 2018;1(1):002–008.
46. Heidari A. A Modern Comparative and Comprehensive Experimental Biospectroscopic Study on Different Types of Infrared Spectroscopy of Malignant and Benign Human Cancer Cells and Tissues with the Passage of Time under Synchrotron Radiation. J Analyt Molecul Tech. 2018;3(1):8.
47. Heidari A. Investigation of Cancer Types Using Synchrotron Technology for Proton Beam Therapy: An Experimental Biospectroscopic Comparative Study. European Modern Studies Journal. 2018;2(1):13–29.
48. Heidari A. Saturated Spectroscopy and Unsaturated Spectroscopy Comparative Study on Malignant and Benign Human Cancer Cells and Tissues with the Passage of Time under Synchrotron Radiation. Imaging J Clin Medical Sci. 2018;5(1):001–007.
49. Heidari A. Small–Angle Neutron Scattering (SANS) and Wide–Angle X–Ray Diffraction (WAXD) Comparative Study on Malignant and Benign Human Cancer Cells and Tissues under Synchrotron Radiation. Int J Bioorg Chem Mol Biol. 2018;6(2e):1–6.
50. Heidari A. Investigation of Bladder Cancer, Breast Cancer, Colorectal Cancer, Endometrial Cancer, Kidney Cancer, Leukemia, Liver, Lung Cancer, Melanoma, Non–Hodgkin Lymphoma, Pancreatic Cancer, Prostate Cancer, Thyroid Cancer and Non–Melanoma Skin Cancer Using Synchrotron Technology for Proton Beam Therapy: An Experimental Biospectroscopic Comparative Study. Ther Res Skin Dis. 2018;1(1).
51. Heidari A. Attenuated Total Reflectance Fourier Transform Infrared (ATR–FTIR) Spectroscopy, Micro–Attenuated Total Reflectance Fourier Transform Infrared (Micro–ATR–FTIR) Spectroscopy and Macro–Attenuated Total Reflectance Fourier Transform Infrared (Macro–ATR–FTIR) Spectroscopy Comparative Study on Malignant and Benign Human Cancer Cells and Tissues under Synchrotron Radiation with the Passage of Time. International Journal of Chemistry Papers. 2018;2(1):1–12.
52. Heidari A. Mössbauer Spectroscopy, Mössbauer Emission Spectroscopy and ^{57}Fe Mössbauer Spectroscopy Comparative Study on Malignant and Benign Human Cancer Cells and Tissues under Synchrotron Radiation. Acta Scientific Cancer Biology 2.3: 17–20, 2018.
53. Heidari A. Comparative Study on Malignant and Benign Human Cancer Cells and Tissues under Synchrotron Radiation with the Passage of Time. Organic & Medicinal Chem IJ. 2018;6(1):555676.
54. Heidari A. Correlation Spectroscopy, Exclusive Correlation Spectroscopy and Total Correlation Spectroscopy Comparative Study on Malignant and Benign Human AIDS–Related Cancers Cells and Tissues with the Passage of Time under Synchrotron Radiation. Int J Bioanal Biomed. 2018;2(1):001–007.
55. Heidari A. Biomedical Instrumentation and Applications of Biospectroscopic Methods and Techniques in Malignant and Benign Human Cancer Cells and Tissues Studies under Synchrotron Radiation and Anti–Cancer Nano Drugs Delivery. Am J Nanotechnol Nanomed. 2018;1(1):001–009.
56. Heidari A. Vivo ^{1}H or Proton NMR, ^{13}C NMR, ^{15}N NMR and ^{31}P NMR Spectroscopy Comparative Study on Malignant and Benign Human Cancer Cells and Tissues under Synchrotron Radiation. Ann Biomet Biostat. 2018;1(1):1001.
57. Heidari A. Grazing–Incidence Small–Angle Neutron Scattering (GISANS) and Grazing–Incidence X–Ray Diffraction (GIXD) Comparative Study on Malignant and Benign Human Cancer Cells, Tissues and Tumors under Synchrotron Radiation. Ann Cardiovasc Surg. 2018;1 (2):1006.
58. Heidari A. Adsorption Isotherms and Kinetics of Multi–Walled Carbon Nanotubes (MWCNTs), Boron Nitride Nanotubes (BNNTs), Amorphous Boron Nitride Nanotubes (a–BNNTs) and Hexagonal Boron Nitride Nanotubes (h–BNNTs)

for Eliminating Carcinoma, Sarcoma, Lymphoma, Leukemia, Germ Cell Tumor and Blastoma Cancer Cells and Tissues. Clin Med Rev Case Rep. 2018;5:201.
59. Heidari A. Correlation Spectroscopy (COSY), Exclusive Correlation Spectroscopy (ECOSY), Total Correlation Spectroscopy (TOCSY), Incredible Natural–Abundance Double–Quantum Transfer Experiment (INADEQUATE), Heteronuclear Single–Quantum Correlation Spectroscopy (HSQC), Heteronuclear Multiple–Bond Correlation Spectroscopy (HMBC), Nuclear Overhauser Effect Spectroscopy (NOESY) and Rotating Frame Nuclear Overhauser Effect Spectroscopy (ROESY) Comparative Study on Malignant and Benign Human Cancer Cells and Tissues under Synchrotron Radiation. Acta Scientific Pharmaceutical Sciences. 2018;2(5):30–35.
60. Heidari A. Small–Angle X–Ray Scattering (SAXS), Ultra–Small Angle X–Ray Scattering (USAXS), Fluctuation X–Ray Scattering (FXS), Wide–Angle X–Ray Scattering (WAXS), Grazing–Incidence Small–Angle X–Ray Scattering (GISAXS), Grazing–Incidence Wide–Angle X–Ray Scattering (GIWAXS), Small–Angle Neutron Scattering (SANS), Grazing–Incidence Small–Angle Neutron Scattering (GISANS), X–Ray Diffraction (XRD), Powder X–Ray Diffraction (PXRD), Wide–Angle X–Ray Diffraction (WAXD), Grazing–Incidence X–Ray Diffraction (GIXD) and Energy–Dispersive X–Ray Diffraction (EDXRD) Comparative Study on Malignant and Benign Human Cancer Cells and Tissues under Synchrotron Radiation. Oncol Res Rev. 2018;1(1):1–10.
61. Heidari A. Pump–Probe Spectroscopy and Transient Grating Spectroscopy Comparative Study on Malignant and Benign Human Cancer Cells and Tissues with the Passage of Time under Synchrotron Radiation. Adv Material Sci Engg. 2018;2(1):1–7.
62. Heidari A. Grazing–Incidence Small–Angle X–Ray Scattering (GISAXS) and Grazing–Incidence Wide–Angle X–Ray Scattering (GIWAXS) Comparative Study on Malignant and Benign Human Cancer Cells and Tissues under Synchrotron Radiation. Insights Pharmacol Pharm Sci. 2018;1(1):1–8.
63. Heidari A. Acoustic Spectroscopy, Acoustic Resonance Spectroscopy and Auger Spectroscopy Comparative Study on Anti–Cancer Nano Drugs Delivery in Malignant and Benign Human Cancer Cells and Tissues with the Passage of Time under Synchrotron Radiation. Nanosci Technol. 2018;5(1):1–9.
64. Heidari A. Niobium, Technetium, Ruthenium, Rhodium, Hafnium, Rhenium, Osmium and Iridium Ions Incorporation into the Nano Polymeric Matrix (NPM) by Immersion of the Nano Polymeric Modified Electrode (NPME) as Molecular Enzymes and Drug Targets for Human Cancer Cells, Tissues and Tumors Treatment under Synchrotron and Synchrocyclotron Radiations. Nanomed Nanotechnol. 2018;3(2):000138.
65. Heidari A. Homonuclear Correlation Experiments Such as Homonuclear Single–Quantum Correlation Spectroscopy (HSQC), Homonuclear Multiple–Quantum Correlation Spectroscopy (HMQC) and Homonuclear Multiple–Bond Correlation Spectroscopy (HMBC) Comparative Study on Malignant and Benign Human Cancer Cells and Tissues under Synchrotron Radiation. Austin J Proteomics Bioinform & Genomics. 2018;5(1):1024.
66. Heidari A. Atomic Force Microscopy Based Infrared (AFM–IR) Spectroscopy and Nuclear Resonance Vibrational Spectroscopy Comparative Study on Malignant and Benign Human Cancer Cells and Tissues under Synchrotron Radiation with the Passage of Time. J Appl Biotechnol Bioeng. 2018;5(3):142–148.
67. Heidari A. Time–Dependent Vibrational Spectral Analysis of Malignant and Benign Human Cancer Cells and Tissues under Synchrotron Radiation. J Cancer Oncol, 2018;2(2): 000124.
68. Heidari A. Palauamine and Olympiadane Nano Molecules Incorporation into the Nano Polymeric Matrix (NPM) by Immersion of the Nano Polymeric Modified Electrode (NPME) as Molecular Enzymes and Drug Targets for Human Cancer Cells, Tissues and Tumors Treatment under Synchrotron and Synchrocyclotron Radiations. Arc Org Inorg Chem Sci. 2018;3(1).
69. Gobato R, Heidari A. Infrared Spectrum and Sites of Action of Sanguinarine by Molecular Mechanics and Ab Initio Methods. International Journal of Atmospheric and Oceanic Sciences. 2018;2(1):1–9.
70. Heidari A. Angelic Acid, Diabolic Acids, Draculin and Miraculin Nano Molecules Incorporation into the Nano Polymeric Matrix (NPM) by Immersion of the Nano Polymeric Modified Electrode (NPME) as Molecular Enzymes and Drug Targets for Human Cancer Cells, Tissues and Tumors Treatment under Synchrotron and Synchrocyclotron Radiations. Med & Analy Chem Int J. 2018;2(1):000111.
71. Heidari A. Gamma Linolenic Methyl Ester, 5–Heptadeca–5,8,11–Trienyl1,3,4–Oxadiazole–2–Thiol, Sulphoquinovosyl Diacyl Glycerol, Ruscogenin, Nocturnoside B, Protodioscine B, Parquisoside–B, Leiocarposide, Narangenin, 7–Methoxy Hespertin, Lupeol, Rosemariquinone, Rosmanol and Rosemadiol Nano Molecules Incorporation into the Nano Polymeric Matrix (NPM) by Immersion of the Nano Polymeric Modified Electrode (NPME) as Molecular Enzymes and Drug Targets for Human Cancer Cells, Tissues and Tumors Treatment under Synchrotron and Synchrocyclotron Radiations. Int J Pharma Anal Acta. 2018;2(1):007–014.
72. Heidari A. Fourier Transform Infrared (FTIR) Spectroscopy, Attenuated Total Reflectance Fourier Transform Infrared (ATR–FTIR) Spectroscopy, Micro–Attenuated Total Reflectance Fourier Transform Infrared (Micro–ATR–FTIR) Spectroscopy, Macro–Attenuated Total Reflectance Fourier Transform Infrared (Macro–ATR–FTIR) Spectroscopy, Two–Dimensional Infrared Correlation Spectroscopy, Linear Two–Dimensional Infrared Spectroscopy, Non–Linear Two–Dimensional Infrared Spectroscopy, Atomic Force Microscopy Based Infrared (AFM–IR) Spectroscopy, Infrared Photodissociation Spectroscopy, Infrared Correlation Table Spectroscopy, Near–Infrared Spectroscopy (NIRS), Mid–Infrared Spectroscopy (MIRS), Nuclear Resonance Vibrational Spectroscopy, Thermal Infrared Spectroscopy and Photothermal Infrared Spectroscopy Comparative Study on Malignant and Benign Human Cancer Cells and Tissues under Synchrotron Radiation with the Passage of Time. Glob Imaging Insights. 2018;3(2):1–14.
73. Heidari A. Heteronuclear Single–Quantum Correlation Spectroscopy (HSQC) and Heteronuclear Multiple–Bond Correlation Spectroscopy (HMBC) Comparative Study on Malignant and Benign Human Cancer Cells, Tissues and Tumors under Synchrotron and Synchrocyclotron Radiations. Chronicle of Medicine and Surgery. 2018;2(3):144–156.
74. Heidari A. Tetrakis [3, 5–bis (Trifluoromethyl) Phenyl] Borate (BARF)–Enhanced Precatalyst Preparation Stabilization and Initiation (EPPSI) Nano Molecules. Medical Research and Clinical Case Reports. 2018;2(1):113–126.
75. Heidari A. Sydnone, Münchnone, Montréalone, Mogone, Montelukast, Quebecol and Palau'amine–Enhanced Precatalyst Preparation Stabilization and Initiation (EPPSI) Nano

Molecules. Sur Cas Stud Op Acc J. 2018;1(3).
76. Heidari A. Fornacite, Orotic Acid, Rhamnetin, Sodium Ethyl Xanthate (SEX) and Spermine (Spermidine or Polyamine) Nanomolecules Incorporation into the Nanopolymeric Matrix (NPM). International Journal of Biochemistry and Biomolecules. 2018;4(1):1–19.
77. Heidari A. R. Gobato, Putrescine, Cadaverine, Spermine and Spermidine–Enhanced Precatalyst Preparation Stabilization and Initiation (EPPSI) Nano Molecules. Parana Journal of Science and Education (PJSE). July 1, 2018;4(5):1–14.
78. Heidari A. Cadaverine (1,5–Pentanediamine or Pentamethylenediamine), Diethyl Azodicarboxylate (DEAD or DEADCAT) and Putrescine (Tetramethylenediamine) Nano Molecules Incorporation into the Nano Polymeric Matrix (NPM) by Immersion of the Nano Polymeric Modified Electrode (NPME) as Molecular Enzymes and Drug Targets for Human Cancer Cells, Tissues and Tumors Treatment under Synchrotron and Synchrocyclotron Radiations. Hiv and Sexual Health Open Access Open Journal. 2018;1(1):4–11.
79. Heidari A. Improving the Performance of Nano–Endofullerenes in Polyaniline Nanostructure–Based Biosensors by Covering Californium Colloidal Nanoparticles with Multi–Walled Carbon Nanotubes. Journal of Advances in Nanomaterials. 2018;3(1):1–28.
80. Gobato R, Heidari A. Molecular Mechanics and Quantum Chemical Study on Sites of Action of Sanguinarine Using Vibrational Spectroscopy Based on Molecular Mechanics and Quantum Chemical Calculations. Malaysian Journal of Chemistry. 2018; 20 (1):1–23.
81. Heidari A. Vibrational Biospectroscopic Studies on Anti–Cancer Nanopharmaceuticals (Part I). Malaysian Journal of Chemistry. 2018;20 (1):33–73.
82. Heidari A. Vibrational Biospectroscopic Studies on Anti–Cancer Nanopharmaceuticals (Part II). Malaysian Journal of Chemistry. 2018;20 (1):74–117.
83. Heidari A. Uranocene ($U(C_8H_8)_2$) and Bis(Cyclooctatetraene) Iron ($Fe(C_8H_8)_2$ or $Fe(COT)_2$)–Enhanced Precatalyst Preparation Stabilization and Initiation (EPPSI) Nano Molecules. Chemistry Reports. 2018;1(2):1–16.
84. Heidari A. Biomedical Systematic and Emerging Technological Study on Human Malignant and Benign Cancer Cells and Tissues Biospectroscopic Analysis under Synchrotron Radiation. Glob Imaging Insights. 2018;3(3):1–7.
85. Heidari A. Deep–Level Transient Spectroscopy and X–Ray Photoelectron Spectroscopy (XPS) Comparative Study on Malignant and Benign Human Cancer Cells and Tissues with the Passage of Time under Synchrotron Radiation. Res Dev Material Sci. 2018;7(2). RDMS.000659,
86. Heidari A. C70–Carboxyfullerenes Nano Molecules Incorporation into the Nano Polymeric Matrix (NPM) by Immersion of the Nano Polymeric Modified Electrode (NPME) as Molecular Enzymes and Drug Targets for Human Cancer Cells, Tissues and Tumors Treatment under Synchrotron and Synchrocyclotron Radiations. Glob Imaging Insights. 2018;3(3):1–7.
87. Heidari A. The Effect of Temperature on Cadmium Oxide (CdO) Nanoparticles Produced by Synchrotron Radiation in the Human Cancer Cells, Tissues and Tumors. International Journal of Advanced Chemistry. 2018;6(2):140–156.
88. Heidari A. A Clinical and Molecular Pathology Investigation of Correlation Spectroscopy (COSY), Exclusive Correlation Spectroscopy (ECOSY), Total Correlation Spectroscopy (TOCSY), Heteronuclear Single–Quantum Correlation Spectroscopy (HSQC) and Heteronuclear Multiple–Bond Correlation Spectroscopy (HMBC) Comparative Study on Malignant and Benign Human Cancer Cells, Tissues and Tumors under Synchrotron and Synchrocyclotron Radiations Using Cyclotron versus Synchrotron, Synchrocyclotron and the Large Hadron Collider (LHC) for Delivery of Proton and Helium Ion (Charged Particle) Beams for Oncology Radiotherapy. European Journal of Advances in Engineering and Technology. 2018;5(7):414–426.
89. Heidari A. Nano Molecules Incorporation into the Nano Polymeric Matrix (NPM) by Immersion of the Nano Polymeric Modified Electrode (NPME) as Molecular Enzymes and Drug Targets for Human Cancer Cells, Tissues and Tumors Treatment under Synchrotron and Synchrocyclotron Radiations. J Oncol Res. 2018;1(1):1–20.
90. Heidari A. Use of Molecular Enzymes in the Treatment of Chronic Disorders. Canc Oncol Open Access J. 2018;1(1):12–15.
91. Heidari A. Vibrational Biospectroscopic Study and Chemical Structure Analysis of Unsaturated Polyamides Nanoparticles as Anti–Cancer Polymeric Nanomedicines Using Synchrotron Radiation. International Journal of Advanced Chemistry. 2018;6(2):167–189.
92. Heidari A. Adamantane, Irene, Naftazone and Pyridine–Enhanced Precatalyst Preparation Stabilization and Initiation (PEPPSI) Nano Molecules. Madridge J Nov Drug Res. 2018;2(1):61–67.
93. Heidari A. Heteronuclear Single–Quantum Correlation Spectroscopy (HSQC) and Heteronuclear Multiple–Bond Correlation Spectroscopy (HMBC) Comparative Study on Malignant and Benign Human Cancer Cells and Tissues with the Passage of Time under Synchrotron Radiation. Madridge J Nov Drug Res. 2018;2(1):68–74.
94. Heidari A. R. Gobato, A Novel Approach to Reduce Toxicities and to Improve Bioavailabilities of DNA/RNA of Human Cancer Cells–Containing Cocaine (Coke), Lysergide (Lysergic Acid Diethyl Amide or LSD), Δ^9–Tetrahydrocannabinol (THC) [(–)–trans–Δ^9–Tetrahydrocannabinol], Theobromine (Xantheose), Caffeine, Aspartame (APM) (NutraSweet) and Zidovudine (ZDV) Azidothymidine (AZT). as Anti–Cancer Nano Drugs by Coassembly of Dual Anti–Cancer Nano Drugs to Inhibit DNA/RNA of Human Cancer Cells Drug Resistance. Parana Journal of Science and Education (PJSE). 2018;4(6):1–17.
95. Heidari A, Gobato R. Ultraviolet Photoelectron Spectroscopy (UPS) and Ultraviolet–Visible (UV–Vis) Spectroscopy Comparative Study on Malignant and Benign Human Cancer Cells and Tissues with the Passage of Time under Synchrotron Radiation. Parana Journal of Science and Education (PJSE). 2018;4(6):18–33.
96. Gobato R, Heidari A, Mitra A. The Creation of $C_{13}H_{20}BeLi_2SeSi$. The Proposal of a Bio–Inorganic Molecule, Using Ab Initio Methods for the Genesis of a Nano Membrane. Arc Org Inorg Chem Sci. 2018;3(4) AOICS.MS.ID.000167.
97. Gobato R, Heidari A. Using the Quantum Chemistry for Genesis of a Nano Biomembrane with a Combination of the Elements Be, Li, Se, Si, C and H. J Nanomed Res. 2018;7(4):241–252.
98. Heidari A. Bastadins and Bastaranes–Enhanced Precatalyst Preparation Stabilization and Initiation (EPPSI) Nano Molecules. Glob Imaging Insights. 2018;3(4):1–7.
99. Heidari A. Fucitol, Pterodactyladiene, DEAD or DEADCAT (DiEthyl AzoDiCArboxylaTe), Skatole, the NanoPutians, Thebacon, Pikachurin, Tie Fighter, Spermidine and Mirasorvone Nano Molecules Incorporation into the Nano

Polymeric Matrix (NPM) by Immersion of the Nano Polymeric Modified Electrode (NPME) as Molecular Enzymes and Drug Targets for Human Cancer Cells, Tissues and Tumors Treatment under Synchrotron and Synchrocyclotron Radiations. Glob Imaging Insights. 2018;3(4):1–8.
100. Dadvar E, Heidari A. A Review on Separation Techniques of Graphene Oxide (GO)/Base on Hybrid Polymer Membranes for Eradication of Dyes and Oil Compounds: Recent Progress in Graphene Oxide (GO)/Base on Polymer Membranes–Related Nanotechnologies. Clin Med Rev Case Rep. 2018;5:228.
101. Heidari A, Gobato R. First–Time Simulation of Deoxyuridine Monophosphate (dUMP) (Deoxyuridylic Acid or Deoxyuridylate) and Vomitoxin (Deoxynivalenol (DON)) ((3α,7α)–3,7,15–Trihydroxy–12,13–Epoxytrichothec–9–En–8–One)–Enhanced Precatalyst Preparation Stabilization and Initiation (EPPSI) Nano Molecules Incorporation into the Nano Polymeric Matrix (NPM) by Immersion of the Nano Polymeric Modified Electrode (NPME) as Molecular Enzymes and Drug Targets for Human Cancer Cells, Tissues and Tumors Treatment under Synchrotron and Synchrocyclotron Radiations. Parana Journal of Science and Education (PJSE). 2018;4(6):46–67.
102. Heidari A. Buckminsterfullerene (Fullerene), Bullvalene, Dickite and Josiphos Ligands Nano Molecules Incorporation into the Nano Polymeric Matrix (NPM) by Immersion of the Nano Polymeric Modified Electrode (NPME) as Molecular Enzymes and Drug Targets for Human Hematology and Thromboembolic Diseases Prevention, Diagnosis and Treatment under Synchrotron and Synchrocyclotron Radiations. Glob Imaging Insights. 2018;3(4):1–7.
103. Heidari A. Fluctuation X–Ray Scattering (FXS) and Wide–Angle X–Ray Scattering (WAXS) Comparative Study on Malignant and Benign Human Cancer Cells and Tissues under Synchrotron Radiation. Glob Imaging Insights. 2018;3(4):1–7.
104.Heidari A. A Novel Approach to Correlation Spectroscopy (COSY), Exclusive Correlation Spectroscopy (ECOSY), Total Correlation Spectroscopy (TOCSY), Incredible Natural–Abundance Double–Quantum Transfer Experiment (INADEQUATE), Heteronuclear Single–Quantum Correlation Spectroscopy (HSQC), Heteronuclear Multiple–Bond Correlation Spectroscopy (HMBC), Nuclear Overhauser Effect Spectroscopy (NOESY) and Rotating Frame Nuclear Overhauser Effect Spectroscopy (ROESY) Comparative Study on Malignant and Benign Human Cancer Cells and Tissues under Synchrotron Radiation. Glob Imaging Insights. 2018;3(5):1–9.
105.Heidari A. Terphenyl–Based Reversible Receptor with Rhodamine, Rhodamine–Based Molecular Probe, Rhodamine–Based Using the Spirolactam Ring Opening, Rhodamine B with Ferrocene Substituent, Calix4.Arene–Based Receptor, Thioether + Aniline–Derived Ligand Framework Linked to a Fluorescein Platform, Mercuryfluor–1 (Flourescent Probe), N,N'–Dibenzyl–1,4,10,13–Tetraraoxa–7,16–Diazacyclooctadecane and Terphenyl–Based Reversible Receptor with Pyrene and Quinoline as the Fluorophores–Enhanced Precatalyst Preparation Stabilization and Initiation (EPPSI) Nano Molecules. Glob Imaging Insights. 2018;3(5):1–9.
106. Heidari A. Small–Angle X–Ray Scattering (SAXS), Ultra–Small Angle X–Ray Scattering (USAXS), Fluctuation X–Ray Scattering (FXS), Wide–Angle X–Ray Scattering (WAXS), Grazing–Incidence Small–Angle X–Ray Scattering (GISAXS), Grazing–Incidence Wide–Angle X–Ray Scattering (GIWAXS), Small–Angle Neutron Scattering (SANS), Grazing–Incidence Small–Angle Neutron Scattering (GISANS), X–Ray Diffraction (XRD), Powder X–Ray Diffraction (PXRD), Wide–Angle X–Ray Diffraction (WAXD), Grazing– Incidence X–Ray Diffraction (GIXD) and Energy–Dispersive X–Ray Diffraction (EDXRD) Comparative Study on Malignant and Benign Human Cancer Cells and Tissues under Synchrotron Radiation. Glob Imaging Insights. 2018;3(5):1–10.
107. Heidari A. Nuclear Resonant Inelastic X–Ray Scattering Spectroscopy (NRIXSS) and Nuclear Resonance Vibrational Spectroscopy (NRVS) Comparative Study on Malignant and Benign Human Cancer Cells and Tissues under Synchrotron Radiation. Glob Imaging Insights. 2018;3(5):1–7.
108. Heidari A. Small–Angle X–Ray Scattering (SAXS) and Ultra–Small Angle X–Ray Scattering (USAXS) Comparative Study on Malignant and Benign Human Cancer Cells and Tissues under Synchrotron Radiation. Glob Imaging Insights. 2018;3(5):1–7.
109. HeidariA.CuriousChloride(CmCl3)andTitanicChloride (TiCl4)–Enhanced Precatalyst Preparation Stabilization and Initiation (EPPSI) Nano Molecules for Cancer Treatment and Cellular Therapeutics. J. Cancer Research and Therapeutic Interventions. 2018;1(1):01–10.
110.Gobato R, Gobato MRR, Heidari A. A. Mitra, Spectroscopy and Dipole Moment of the Molecule C13H20BeLi2SeSi via Quantum Chemistry Using Ab Initio, Hartree–Fock Method in the Base Set CC–pVTZ and 6–311G**(3df, 3pd). Arc Org Inorg Chem Sci. 2018;3(5):402–409.
111.Heidari A. C60 and C70–Encapsulating Carbon Nanotubes Incorporation into the Nano Polymeric Matrix (NPM) by Immersion of the Nano Polymeric Modified Electrode (NPME) as Molecular Enzymes and Drug Targets for Human Cancer Cells, Tissues and Tumors Treatment under Synchrotron and Synchrocyclotron Radiations. Integr Mol Med. 2018;5(3): 1–8.
112. Heidari A. Two–Dimensional (2D) 1H or Proton NMR, 13C NMR, 15N NMR and 31P NMR Spectroscopy Comparative Study on Malignant and Benign Human Cancer Cells and Tissues under Synchrotron Radiation with the Passage of Time. Glob Imaging Insights. 2018;3(6):1–8.
113.Heidari A. FT–Raman Spectroscopy, Coherent Anti–Stokes Raman Spectroscopy (CARS) and Raman Optical Activity Spectroscopy (ROAS) Comparative Study on Malignant and Benign Human Cancer Cells and Tissues with the Passage of Time under Synchrotron Radiation. Glob Imaging Insights. 2018;3(6):1–8.
114. Heidari A. A Modern and Comprehensive Investigation of Inelastic Electron Tunneling Spectroscopy (IETS) and Scanning Tunneling Spectroscopy on Malignant and Benign Human Cancer Cells, Tissues and Tumors through Optimizing Synchrotron Microbeam Radiotherapy for Human Cancer Treatments and Diagnostics: An Experimental Biospectroscopic Comparative Study. Glob Imaging Insights. 2018;3(6):1–8.

***Corresponding author:** *Prof. Dr. Alireza Heidari, Ph.D., D.Sc.*
Full Distinguished Professor and Academic Tenure of Chemistry &
Enrico Fermi Distinguished Chair in Molecular Spectroscopy &
Head of Cancer Research Institute (CRI) &
Director of the BioSpectroscopy Core Research Laboratory (BCRL) at Faculty of Chemistry, California South University (CSU), Irvine, California, USA &
Board Member of the World Association of Theoretical and Computational Chemists (WATOC) &
President of the American International Standards Institute (AISI) Irvine, California, USA.
E–mail: scholar.researcher.scientist@gmail.com

International Journal of Biomedicine 12(4) (2022) 506-514
http://dx.doi.org/10.21103/Article12(4)_RA2

REVIEW ARTICLE

INTERNATIONAL JOURNAL OF BIOMEDICINE

Manipulation of Epigenome: Opportunities and Pitfalls in Fighting Autoimmune Diseases

Hassan Higazi[1*], Faheem Ahmed Khan[2,3], Sara Ali[1], Salma Mohamed[1], Nuruliarizki Shinta Pandupuspitasari[4], Ashraf S. Yousif[5], Praveen Kumar Kandakurti[6]

[1]Department of Medical Laboratory Science, College of Health Science, Gulf Medical University, Ajman, United Arab Emirates
[2]Laboratory of Molecular Biology and Genomics, Faculty of Science and Technology, University of Central Punjab, Lahore, Pakistan
[3]Research Center for Animal Husbandry, National Research and Innovation Agency, Indonesia
[4]Laboratory of Animal Nutrition and Feed Science, Animal Science Department, Faculty of Animal and Agricultural Sciences, Universitas Diponegoro, Semarang, Central Java, Indonesia
[5]Drugs Farm USA LLC, Massachusetts, USA
[6]Department of Physiotherapy, College of Health Sciences, Gulf Medical University, Ajman, United Arab Emirates

Abstract

Many recent studies have focused on the manipulation of the epigenome to understand the mechanistic programming in health and some disease phenotypes. These studies are designed to provide suitable drug targets to cure and/or prevent the outcome of a disease condition. Autoimmune diseases, including obesity and diabetes, are of major health concern nowadays and are the root cause of several diseases of the heart, lungs, and liver. There are several epigenetic mechanisms underlying the manifestation of autoimmune disorders. The recent advances in today's sequencing technology and genome editing have uncovered the role of epigenetic modifications in autoimmune diseases. In this review, we will cover the recent discoveries and their possible application in the control of autoimmune diseases by improving the long-term use of such technologies. The potential drawbacks will also be discussed so that future experiments may be designed to reduce or eliminate the risk factors associated with the use of recent discoveries in the field of medicine. (**International Journal of Biomedicine. 2022;12(4):506-514.**).

Keywords: autoimmune diseases • epigenome • DNA methylation

For citation: Higazi H, Khan FA, Ali S, Mohamed S, Pandupuspitasari NS, Yousif AS, Kandakurti PK. Manipulation of Epigenome: Opportunities and Pitfalls in Fighting Autoimmune Diseases. International Journal of Biomedicine. 2022;12(4):506-514. doi:10.21103/Article12(4)_RA2

Abbreviations

ADs, autoimmune diseases; **A-FABP**, adipose-fatty acid binding protein; **BMI**, body mass index; **GIT**, gastrointestinal tract; **IBD**, inflammatory bowel disease; **LSG**, labial salivary gland; **MS**, multiple sclerosis; **MeCP2**, methyl cap binding protein-2; **NAWM**, normal appearing white matter; **pSS**, primary Sjögren's syndrome; **PBMCs**, peripheral blood mononuclear cells; **RA**, rheumatoid arthritis; **SSc**, systemic sclerosis; **SLE**, systemic lupus erythematosus; **T1DM**, type 1 diabetes; **T2D,** type 2 diabetes; **WAT**, white adipose tissue.

Introduction

History has witnessed numerous famines, which cause malnutrition in the human population, thereby leading to several diseases, including anorexia; however, recently, obesity has taken the world by surprise and has become one of the leading causes of life-threatening diseases.[(1)] This long history of starved conditions has resulted in the evolution of an

organ termed adipose tissue to provide necessary nutrition in times of need.[1] This event has resulted in better regulation of energy via the central nervous system through a set of defined signaling pathways, as well as a self-system for recognizing energy demand and supply requirements.[2] Over time, the human lifestyle has changed significantly, so that now the fat tissues stored in the body cause overweight and obesity.[3] The function of adipose tissue in the era of under-nutrition and over-nutrition is distinct and requires special attention before it causes damage to other organs and tissues.

The obesity epidemic is currently posing a significant threat because it affects children and young adults, compromising their life expectancy by nearly one-half due to an increase in obesity-related disease burden.[4] Obesity can be defined in terms of BMI, where >30 kg/m^2 is considered obese, whereas >25 kg/m^2 is taken as overweight.[5] In the evolutionary context, the genotypes that support energy storage are more suited to survive in the age of famine and low food availability; however, recent developments in agriculture and the food industry have resulted in an epidemic of obesity that is strongly associated with an increase in the incidence of several diseases, including T2D, hypertension, heart ischemia, and other metabolic diseases.[4] Such genotypes termed as "thrifty genotypes"[6] became un-adaptive in recent times of low energy expenditures and are strongly associated with T2D. It was Neel who correlated obesity to sickle cell anemia, of which allele was beneficial to carry at certain times of adaptation and survival.[7] While Neel's hypothesis is partially acceptable, Hales and Barker later showed that malnutrition in the uterus actually causes a disturbance in glucose tolerance and other metabolic syndromes, which is supported by epidemiological data.[8] However, more recently, both hypotheses are being challenged with predator theory, which relates obesity to a genetic drift because of the absence of predators in the recent era.

The epigenetic changes in relation to ADs, obesity, and diabetes have been recently studied, and several target proteins have been recommended for anti-obesity and anti-diabetic targets. This review will go through the major findings and recent biological questions in the context of autoimmunity, obesity, and diabetes and pose it to the scientific community for further research and development.

Countering Obesity and Diabetes

Obesity is one of the major public health issues of the current era,[9] associated with several major diseases of vital organs, such as the heart, lungs, and kidneys, and affecting life-sustaining systems such as circulation, breathing, and excretion, causing mortality and morbidity.[10] Obesity is strongly associated with cancers; however, its molecular mechanism was vague until Hao et al.[11] discovered that circulating adipose fatty acid binding protein (A-FABP) is the cause of promoting breast cancer by direct interaction with tumor cells and activates the IL-6/STAT3/ALDH1pathway. According to the WHO, 1.9 billion adults of age 18 and above are overweight, out of which 650 million are obese. The problem continues in children, and 41 million children under age 5 are reported to be overweight or obese.[12] Much of the world's population is at risk of developing T2D because of easily available high caloric foods, which are now the routine diet of many. This includes children and adolescents, exposing them to the future threat of energy intake and expenditure imbalance.[13] Advanced research in understanding the mechanism and pathways associated with obesity and its cure is a very important need of the moment. Several labs are demonstrating obesity's linkage to epigenetic modulation, and its interaction with diets and environmental factors is becoming clearer.

Gene expression is considered at the core of the obesity problem, which is controlled by several epigenetic mechanisms, including DNA methylation, histone acetylation, and phosphorylation, affecting key pathways responsible for maintaining energy homeostasis. Today basic and advanced molecular, immunological and biotechnological procedures help diagnose several important mechanistic insights into previously unknown phenomena.[14] The following will illustrate the recent advancements in obesity research with a focus on the epigenome.

The major cause of obesity is insulin resistance, which leads to an imbalance in energy homeostasis and has been the target focus of research. It is well established that chronic inflammation of the adipose tissue, skeletal muscles, and liver is the major cause of obesity,[15] with a critical role played by miRNAs and exosomes.[16] Exosomes are the micro-vesicles that have the capability to carry miRNAs, of which the adipose tissue secreting exosomes are shown to carry miR155,[17] of which PPAR-γ is the target gene, and of which miR155 KO mice are shown to have high insulin sensitivity and glucose tolerance[16] It also demonstrates the ability of exosomes to carry the miRNAs of choice to target cells and tissues to therapeutically treat insulin sensitivity and glucose tolerance. WAT browning via activation of the AMP-activated protein kinase (AMPK) and sirtuin 1 (SIRT1) pathways or increasing the number of brown adipocytes that can dissipate energy is another approach to overcoming obesity outbreaks and is a major area of diabetes and obesity research.[15] Recently, in mouse inguinal WAT, researchers observed neural arborizations at the single-fiber level and uncovered how the sympathetic nervous system and CNS play a role in the architecture of adipose tissue.[18] The efficient induction of begging in humans remains a problem, where a recent study showed how intermittent fasting can induce beiging of WAT and help improve diabetes.[19]

The induction of beiging, however, requires activation of β-adrenergic receptors mostly by cold induction, which is why no successful therapeutic agent could be introduced until now as the β-adrenergic signaling pathway is involved in several functions of tissues and raises safety concerns. Thus what is required is a safe way to induce thermogenic fat cells that can burn fat to reduce weight without causing harm to the body. To this end, Chen et al.[20] discovered fat cells that burn only glucose and termed them glycolytic beige cells. This discovery opens a new avenue to combat obesity as it follows a previously uncharacterized pathway. If such cells are found in humans, they can help develop new therapeutic avenues.

Epigenetics of Systemic Sclerosis

A major autoimmune disease of connective tissues is SSc where skin and internal organs manifest varied clinical features of heterogeneous nature having more prevalence in females than in males.[21] The pathological outcome of SSc is

extensive fibrosis of the skin, blood vessels, lungs, and GIT.[22] The researchers are of the view that anomalous production of IL-1a in SSc patient's skin lesional fibroblasts induces IL-6 and procollagen, which has an epigenetic component that is causing fibrosis.[23] Before it is secreted, such a mechanism can operate at three different levels: gene transcriptional regulation, RNA stability control, and degradation of collagen molecules.[24]

Earlier in 2013, a study published in The Journal of Investigative Dermatology reported the upregulation of p300, an acetyl-transferase that has a predominant role in SSc and that is controlled by TGF-β.[25] The etiology of SSc is reportedly connected to dysregulation in the epigenetic landscape of certain genes. DNA methylation at the promotor region remains at the core of such research. Several important targets in this connection are reported. The hypomethylated genes in SSc are ITGA9, COL23A, ADAM12, COL4A2, and MYO1E, including transcription factors such as RUNX1, RUNX2, and RUNX3 in both diffuse cutaneous SSc and limited cutaneous SSc.[26] The hypermethylation in the promotor region of Foxp3 in SSc patients is determined as one of the other factors in the development of SSc.[27] The defective angiogenesis and micro vasculopathy in SSc patients are linked to lower expression of NRP1 that disturbs VEGF-A/VEGFR-2.[28] Recently, MeCP-2 has been shown to have a predominant role in systemic fibrosis.[29] Mechanistically, TGF-B regulates the expression of MeCP-2 in SSc fibroblasts, which regulates the expression of the extracellular matrix that epigenetically represses sFRP-1 antagonist of the Wnt signaling pathway. This in turn enhances Wnt signaling, which favors fibrosis through glycolysis. MeCP-2 can be targeted as a key regulator in SSc fibrosis.[29] Vasculopathy is one of the hallmarks of SSc and has been recently linked to trappin-2, which upregulates in absence of Fli1 to cause pathological conditions in vessels.[30] Emerging data provides a strong connection of the long noncoding RNA in driving the response of IFNs and its functional relevance in SSc.[31] Several epigenetic therapies at present are considered to cure SSc, which targets include, but are not limited to, histone modifications[32] and methylation regulation.[29] Tables 1 and 2 illustrate ADs, their epigenetic cause, and targeted genes and cells.

Epigenetics of Inflammatory Bowel Disease

IBD is a chronic condition that accompanies patients throughout their whole life. It has been widely accepted that IBD is caused by the dysregulation of cell/cell junction, causing defective barrier activity, resulting in enhanced severity of the disease.[70] It has been classified into two major classes as inflammatory ulcerative colitis and Crohn's disease.[71] Moreover, Crohn's disease affects the entire GIT, whereas ulcerative colitis only affects the large bowel.[72] Recent studies are focused on investigating the role of tight junction dynamics and factors responsible for microtubule organization. One such factor identified is ACF7,[70] the ablation of which demonstrates poor wound healing and tight junction dynamics.

Other studies have demonstrated the role of DNA methylation in the onset and prevalence of IBD influenced by the microbiome. The study by Harris et al.[73] in 2016 revealed a close relationship between the epigenome of the colon and microbiome in adolescents and children, demonstrating several differentially methylated regions having a number of possible therapeutic targets for treating IBD. Intestinal epithelial cell methylation and transcription patterns in child IBD patients define further subtypes and disease associations.[74] Another study demonstrates that a catalytic subunit PRC2, the EZH2 in epithelial cells, is responsible for keeping the epithelial cell barrier integrity.[75]

Gene regulation is a key factor in developing a certain phenotype, which is regulated by DNA methylation. Genome-wide DNA methylation studies have the potential to provide therapeutic targets, which can be used to improve disease phenotypes. A whole genome DNA methylation study performed on naïve ulcerative colitis patients determined several hypo- and hyper-methylated regions of the genome that in the future can be used as potential therapeutic targets in ulcerative colitis patients.[76] There are 577 differential DNA methylation sites with 210 target genes, which a study showed to be responsible for chronic inflammation of the colon in epithelial cells.[77] In a study by McDermott et al.,[78] the top-ranked, IBD-associated PBMC differentially methylated region (promoter region of TRIM39-RPP2) was also significantly hypomethylated in colonic mucosa from pediatric patients with ulcerative colitis; in addition, the authors confirmed TRAF6 hypermethylation using pyrosequencing and found reduced TRAF6 gene expression in PBMCs of IBD patients. Another important gene, Na_/H_exchanger-3 (NHE3), which is responsible for Na absorption and is associated with IBD, is regulated by epigenetic modulation of DNA methylation.[79]

Microbiota diversity and its response is strongly related to IBD, and recently a mechanism by which it can interact has been dissected. A study by Kelly et al. illustrated a new insight into H3K4me3 involved in key pathways of immunoglobulin, cell survival, metabolism, and cell-to-cell signaling. They identified some unexplored key targets in epithelial cells that can be influenced by commensal microbiota in infant IBD patients.[80] There are several genetic markers identified that are associated with IBD and IgG: IKZF1, LAMB1, and MGAT3. Recently, methylation in the promotor region of MGAT3 in CD3+ T cells from patients with ulcerative colitis has been detected.[81] All such targets provide an opportunity to look for further details of its involvement in disease prognosis and cure. The recent technologies of genome editing, including CRISPR-Cas9,[82] can be applied to rewrite the epigenome to its normal state, eliminating the drastic effects of environmental and other burdens on the genome. It is important to keep a full follow-up record of such experiments to eliminate the unwanted outcomes of such applications and to keep the safety concerns associated with each manipulation in mind, and do compulsory experimentation before taking any drug or therapeutic agent for clinical trials.

The Mechanistic Insights into Systemic Lupus Erythematosus

The immune system's capability to recognize self from non-self is essential to conducting defense against foreign antigens and is accomplished during the early developmental stage.[83] Females are more prone to ADs than males,[84] as is the case of SLE, a multisystem, chronic autoimmune disease[85] resulting from T cell hypomethylation, because of lower expression and activity of DNMT1 in Lupus T cells,[86] characterized by a defective ERK signaling pathway, which is reported nine times higher in females of reproductive age.[84]

Table 1.
Epigenetic alterations in autoimmune diseases at the level of DNA methylation.

Cell Type	Diseases	Genes alteration	Epigenetic alteration (DNA)		Pathological site	References
			Hyper-methylation	Hypo-methylation		
Peripheral blood CD4+ T cell	SLE, RA, SSc	CD40LG		√	CD40L (B cell costimulatory molecule encoded on the X chromosome)	(33) (34, 35)
	SLE, SSc, pSS	CD70		√	CD70, B cell costimulatory molecule associated with overproduction of IgG	(36-38)
	SSc, T1DM, RA	FOXP3	√		Forkhead box protein 3, involved in quantitative defects of regulatory T cells	(27, 39, 40)
	MS	HLA-DRB1		√	HLA class II beta chain	(41)
	SLE	IL10, IL13		√	Involved in autoantibody production and tissue damage	(42, 43)
	SLE	IRF5, IFIT2		√	Involved in type I interferon pathway	(44)
	SLE	ITGAL		√	Integrin α-L, associated with cell-cell adhesion	(45)
	SLE	PRF1		√	Perforin 1, involved in autoreactive killing	(46)
Naïve CD4+ T cell	SLE, pSS	STAT1, IFI44L, USP18		√	Involved in type I interferon pathway	(47, 48)
	pSS	LTA		√	Lymphotoxin-α	(47)
	pSS	RUNX1	√		Transcription factor associated to lymphoma	(47)
B cell	SLE	CD5		√	CD5, involved in activation and expansion of autoreactive B cells	(49)
	SLE	HRES-1		√	Human endogenous retroviruses proteins, involved in induction of cross-reactive autoantibodies	(50)
PBMC	RA	IL-6		√	IL-6, involved in B cell response	(51)
	SLE	IFNGR2, MMP14		√	IFN-γ receptor 1, Matrix metalloproteinase-14, involved in inflammation	(52)
	SLE	LCN2		√	Neutrophil gelatinase-associated lipocalin, iron transporter and marker for SLE	(52)
	MS	SHP-1	√		A negative regulator of cytokine signaling through NF-κB and STATs	(53)
CD14+ monocyte	T1DM	HLA-DQB1		√	HLA class II	(54)
	T1DM	RFXAP		√	HLA class II regulating element	(54)
	T1DM	NFKB1A		√	Regulator of apoptosis and inflammation	(54)
	T1DM	GAD2		√	GAD65, a major autoantigen involved in T1D	(54)
	T1DM	TNF	√		Key inflammatory cytokine	(54)
	T1DM	CD6	√		Involved in lymphocyte activation and differentiation	(54)
Fibroblast	SSc	FLI1	√		Involved in type I collagen expression	(55)
Fibroblast, PBMC	SSc	DKK1, SFRP1	√		Wnt signaling antagonists	(56)
Synovial fibroblast	RA	SFRP1, SFRP4	√		Wnt signaling antagonists	(57, 58)
	RA	DR3	√		Death receptor 3, associated with cell apoptosis	(59)
NAWM	MS	PAD2		√	Peptidyl argininedeiminase type II, responsible for the increased citrullinated myelin basic protein	(60)
LSG	pSS	DST	√		BP230, bullous pemphigoid antigen 1 protein	(61)

SLE, systemic lupus erythematosus; RA, rheumatoid arthritis; MS, multiple sclerosis; SSc, systemic sclerosis; T1DM, type 1 diabetes; pSS, primary Sjögren's syndrome; PBMC, peripheral blood mononuclear cell; NAWM, normal appearing white matter; LSG, labial salivary gland.

Table 2. Epigenetic alterations in autoimmune diseases at the level of histone modification.

Cell type	Disease	Epigenetic alteration	Affected gene	Dysregulation		References
				upregulation	downregulation	
T cell	SLE	H3 and H4 hypoacetylation, H3K9 hypomethylation	ND			(62)
		Increased histone H3 acetylation at lysine 18 (H3K18ac)	IL10	√		(29)
		Increased H3 acetylation, dimethylated H3 lysine4 (H3K4me2)	CD70	√		(63)
	T1DM	Increased H3K9me2	CTLA4		√	(64)
B cell	SSc	H4 hyperacetylation, decreased HDAC2 and HDAC7; H3K9 hypomethylation, decreased SUV39H2 (member of HMT), increased JHDM2A (member of HDM)	ND			(6)
Monocyte	T1DM	Increased H3K9 acetylation (H3K9Ac)	HLA-DRB1, HLA-DQB1	√		(65)
	SLE	Global H4 hyperacetylation	IRF1, RFX1, BLIMP1	√		(66)
Fibroblast	SSc	Increased H3 and H4 deacetylation	FLI1		√	(55)
		Inhibition of H3K27me3	FOSL2	√		(67)
Synovial fibroblast	RA	Increased zeste homologue 2 (EZH2, member of HMT)	SFRP1		√	(57)
		Increased sirtuin 1 (Sirt1, member of HDAC)	ND			(68)
Oligodendrocyte	MS	Increased histone H3 deacetylation	ND			(69)

SLE, systemic lupus erythematosus; T1DM, type 1 diabetes; SSc, systemic sclerosis; RA, rheumatoid arthritis; MS, multiple sclerosis; HMT, histone methyltransferases; HDAC, histone deacetylase; HDM, histone demethylase; ND, not determined.

The predominant adaptive immune cells, B lymphocytes and T lymphocytes, are both involved in the development of SLE.[83] Methylation of certain genes is one of the major reasons for ADs, and it has been found that B cell promoter hypermethylation is associated with SLE pathogenesis.[88] CD4+T cells from SLE patients with lower expression of TNFAIP3, because of hypermethylation of histone H3K4, resulting in overproduction of pro-inflammatory cytokines, appears to be a probable cause of SLE.[89] Wang et al.[6] showed that Talen(transcription activation-like effector nuclease)-mediated enhancer knockout influences TNFAIP3 gene expression and mimics a molecular phenotype associated with SLE.

Genome-wide association studies in SLE [90] identified more than 50 risk genes or loci to higher heritability of SLE. Recent genome sequencing technologies have uncovered unprecedented information regarding the development of ADs. The perturb-ATAC sequencing, for example, has shown enrichment of NF-κB binding sites near the causative variations of SLE and SSc,[91] and these sites show altered accessibility at chromatin level when NFKB1 or RELA are depleted.[92]

A shift in DNA methylation status in naïve CD4+ T cells was observed in favor of T cell activation in SLE patients with a significant increase in EZH2 binding enrichment near high methylation activity in lupus patients.[93] Furthermore, it was determined that EZH2 has a predominant role in T cell adhesion by upregulating JAM-A, hence providing a therapeutic target for lupus treatment by either blocking expression of EZH2 or JAM-A to limit T cell migration or adhesion.[94] The lupus patients demonstrated demethylated CD4+CD28+KIR+CD11a^{hi} T cells characterized by epigenetic modulation, resulting in pro-inflammatory cytokines, providing another therapeutic avenue to treat lupus by either eliminating these cells or blocking them to produce pro-inflammatory cytokines.[84]

Mechanistic Insight of Protein Acetylation and Deacetylation

Epigenetic modifications control the expression of genes that become the focus of basic and medical research to find suitable drug targets for the prevention and cure of ADs. ADs in particular are prone to histone acetylation and deacetylation, which demands a detailed investigation of the mechanistic understanding of these modifications.[95] The interaction of negatively charged DNA backbone is possible because of the positively charged histones N-terminal, which is neutralized by histone acetylation, hence weakening DNA binding and making the chromatin accessible to transcription.[96] HATs and HDACs are the two enzyme classes responsible for acetylation and deacetylation respectively. The chromatin is closed when de-acetylation takes place, consequently resulting in decreased gene expression due to no access by transcription factors. The environmental effects and diseases affect the life expectancy and living quality of an individual (Figure 1).

Currently, more than 2000 proteins are identified to be acetylated in mammalian cells, which enhance the canvas of acetylation comparable to other major post-translational mechanisms such as phosphorylation and ubiquitination.[97] A wide range of proteins involved in different cellular processes undergo acetylation, making it one of the important events to be studied in detail. Almost all enzymes involved in gluconeogenesis, glycolysis, TCA cycle, urea cycle, fatty acid oxidation, and glycogen and nitrogen metabolism are acetylated.[43] There are several mechanisms by which acetylation regulates substrate availability, one of which is by blocking the enzyme binding to a substrate; another is by blocking the binding of metabolites. Acetylation can also modulate the localization of proteins.[98]

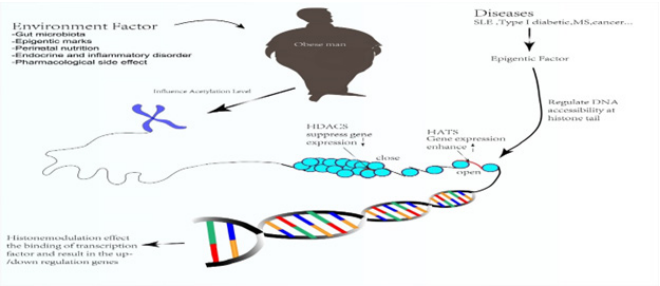

Fig. 1. *Environmental factors induce obesity and disease by affecting acetylation and de-acetylation.*

Conclusion

In summary, epigenetic modifications play a crucial role in autoimmune disease onset, which is monitored and controlled in homeostasis by certain therapies, and therapeutic agents can relieve many of the disease symptoms. DNA methylation and protein acetylation play a very important role in maintaining the epigenome of organisms; hence, more focused studies on the safety concerns of these targets are required before bringing bench research to clinical settings.

Acknowledgements

We thank Nada Jovanovic from MGH IHP for the language proof-reading and editing the manuscript.

Competing Interests

The authors declare that they have no competing interests.

References

1. Li C, Tobi EW, Heijmans BT, Lumey LH. The effect of the Chinese Famine on type 2 diabetes mellitus epidemics. Nat Rev Endocrinol. 2019 Jun;15(6):313-314. doi: 10.1038/s41574-019-0195-5.
2. Lenard NR, Berthoud HR. Central and peripheral regulation of food intake and physical activity: pathways and genes. Obesity (Silver Spring). 2008 Dec;16 Suppl 3(Suppl

***Corresponding author:** Dr. Hassan Higazi. Department of Medical Laboratory Sciences, College of Health Sciences, Gulf Medical University, Ajman, United Arab Emirates. E-mail: hhigazi8@gmail.com*

3):S11-22. doi: 10.1038/oby.2008.511.
3. Stefan N, Schick F, Häring HU. Causes, Characteristics, and Consequences of Metabolically Unhealthy Normal Weight in Humans. Cell Metab. 2017 Aug 1;26(2):292-300. doi: 10.1016/j.cmet.2017.07.008.
4. Thaiss CA, Levy M, Grosheva I, Zheng D, Soffer E, Blacher E, et al. Hyperglycemia drives intestinal barrier dysfunction and risk for enteric infection. Science. 2018 Mar 23;359(6382):1376-1383. doi: 10.1126/science.aar3318.
5. Global BMI Mortality Collaboration, Di Angelantonio E, Bhupathiraju ShN, Wormser D, Gao P, Kaptoge S, Berrington de Gonzalez A, et al. Body-mass index and all-cause mortality: individual-participant-data meta-analysis of 239 prospective studies in four continents. Lancet. 2016 Aug 20;388(10046):776-86. doi: 10.1016/S0140-6736(16)30175-1. Epub 2016 Jul 13. PMID: 27423262; PMCID: PMC4995441.
6. Wang S, Wen F, Tessneer KL, Gaffney PM. TALEN-mediated enhancer knockout influences TNFAIP3 gene expression and mimics a molecular phenotype associated with systemic lupus erythematosus. Genes Immun. 2016 Apr;17(3):165-70. doi: 10.1038/gene.2016.4.
7. NEEL JV. Diabetes mellitus: a "thrifty" genotype rendered detrimental by "progress"? Am J Hum Genet. 1962 Dec;14(4):353-62. PMID: 13937884; PMCID: PMC1932342.
8. Hales CN, Barker DJ. Type 2 (non-insulin-dependent) diabetes mellitus: the thrifty phenotype hypothesis. Diabetologia. 1992 Jul;35(7):595-601. doi: 10.1007/BF00400248. PMID: 1644236.
9. Crossman MK, Kazdin AE, Galbraith K, Eros L, Santos LR. Evaluating the Influence of the Presence of a Dog on Bias toward Individuals with Overweight and Obesity. Anthrozoös. 2018;31(1):77-88.
10. Gurzov EN, Stanley WJ, Pappas EG, Thomas HE, Gough DJ. The JAK/STAT pathway in obesity and diabetes. FEBS J. 2016 Aug;283(16):3002-15. doi: 10.1111/febs.13709.
11. Hao J, Zhang Y, Yan X, Yan F, Sun Y, Zeng J, Waigel S, Yin Y, Fraig MM, Egilmez NK, Suttles J, Kong M, Liu S, Cleary MP, Sauter E, Li B. Circulating Adipose Fatty Acid Binding Protein Is a New Link Underlying Obesity-Associated Breast/Mammary Tumor Development. Cell Metab. 2018 Nov 6;28(5):689-705.e5. doi: 10.1016/j.cmet.2018.07.006.
12. WHO. Obesity and overweight. 9 June 2021. Available at: https://www.who.int/news-room/fact-sheets/detail/obesity-and-overweight
13. Cheng J, Song J, He X, Zhang M, Hu S, Zhang S, et al. Loss of Mbd2 Protects Mice Against High-Fat Diet-Induced Obesity and Insulin Resistance by Regulating the Homeostasis of Energy Storage and Expenditure. Diabetes. 2016 Nov;65(11):3384-3395. doi: 10.2337/db16-0151. Epub 2016 Aug 23. Erratum in: Diabetes. 2017 Sep;66(9):2531.
14. Heymsfield SB, Wadden TA. Mechanisms, Pathophysiology, and Management of Obesity. N Engl J Med. 2017 Jan 19;376(3):254-266. doi: 10.1056/NEJMra1514009. PMID: 28099824.
15. Cypess AM, Lehman S, Williams G, Tal I, Rodman D, Goldfine AB, et al. Identification and importance of brown adipose tissue in adult humans. N Engl J Med. 2009 Apr 9;360(15):1509-17. doi: 10.1056/NEJMoa0810780.
16. Ying W, Riopel M, Bandyopadhyay G, Dong Y, Birmingham A, Seo JB, et al. Adipose Tissue Macrophage-Derived Exosomal miRNAs Can Modulate In Vivo and In Vitro Insulin Sensitivity. Cell. 2017 Oct 5;171(2):372-384.e12. doi: 10.1016/j.cell.2017.08.035.
17. Gaudet AD, Fonken LK, Gushchina LV, Aubrecht TG, Maurya SK, Periasamy M, et al. miR-155 Deletion in Female Mice Prevents Diet-Induced Obesity. Sci Rep. 2016 Mar 8;6:22862. doi: 10.1038/srep22862.
18. Jiang H, Ding X, Cao Y, Wang H, Zeng W. Dense Intra-adipose Sympathetic Arborizations Are Essential for Cold-Induced Beiging of Mouse White Adipose Tissue. Cell Metab. 2017 Oct 3;26(4):686-692.e3. doi: 10.1016/j.cmet.2017.08.016.
19. Li G, Xie C, Lu S, Nichols RG, Tian Y, Li L, et al. Intermittent Fasting Promotes White Adipose Browning and Decreases Obesity by Shaping the Gut Microbiota. Cell Metab. 2017 Oct 3;26(4):672-685.e4. doi: 10.1016/j.cmet.2017.08.019.
20. Chen Y, Ikeda K, Yoneshiro T, Scaramozza A, Tajima K, Wang Q, et al. Thermal stress induces glycolytic beige fat formation via a myogenic state. Nature. 2019 Jan;565(7738):180-185. doi: 10.1038/s41586-018-0801-z.
21. Wielosz E, Majdan M, Dryglewska M, Suszek D. Comparison of clinical and serological parameters in female and male patients with systemic sclerosis. Reumatologia. 2015;53(6):315-20. doi: 10.5114/reum.2015.57637.
22. Assassi S, Del Junco D, Sutter K, McNearney TA, Reveille JD, Karnavas A, et al. Clinical and genetic factors predictive of mortality in early systemic sclerosis. Arthritis Rheum. 2009 Oct 15;61(10):1403-11. doi: 10.1002/art.24734.
23. Varga J, Abraham D. Systemic sclerosis: a prototypic multisystem fibrotic disorder. J Clin Invest. 2007 Mar;117(3):557-67. doi: 10.1172/JCI31139.
24. Elkon R, Zlotorynski E, Zeller KI, Agami R. Major role for mRNA stability in shaping the kinetics of gene induction. BMC Genomics. 2010 Apr 21;11:259. doi: 10.1186/1471-2164-11-259.
25. Ghosh AK, Bhattacharyya S, Lafyatis R, Farina G, Yu J, Thimmapaya B, et al. p300 is elevated in systemic sclerosis and its expression is positively regulated by TGF-β: epigenetic feed-forward amplification of fibrosis. J Invest Dermatol. 2013 May;133(5):1302-10. doi: 10.1038/jid.2012.479.
26. Altorok N, Tsou PS, Coit P, Khanna D, Sawalha AH. Genome-wide DNA methylation analysis in dermal fibroblasts from patients with diffuse and limited systemic sclerosis reveals common and subset-specific DNA methylation aberrancies. Ann Rheum Dis. 2015 Aug;74(8):1612-20. doi: 10.1136/annrheumdis-2014-205303.
27. Wang YY, Wang Q, Sun XH, Liu RZ, Shu Y, Kanekura T, et al. DNA hypermethylation of the forkhead box protein 3 (FOXP3) promoter in CD4+ T cells of patients with systemic sclerosis. Br J Dermatol. 2014 Jul;171(1):39-47. doi: 10.1111/bjd.12913.
28. Romano E, Chora I, Manetti M, Mazzotta C, Rosa I, Bellando-Randone S, et al. Decreased expression of neuropilin-1 as a novel key factor contributing to peripheral microvasculopathy and defective angiogenesis in systemic sclerosis. Ann Rheum Dis. 2016 Aug;75(8):1541-9. doi: 10.1136/annrheumdis-2015-207483.
29. Henderson J, Brown M, Horsburgh S, Duffy L, Wilkinson S, Worrell J, Stratton R, O'Reilly S. Methyl cap binding protein 2: a key epigenetic protein in systemic sclerosis. Rheumatology (Oxford). 2019 Mar 1;58(3):527-535. doi: 10.1093/rheumatology/key327.
30. Miyagawa T, Asano Y, Saigusa R, Hirabayashi M, Yamashita T, Taniguchi T, et al. A potential contribution of trappin-2 to the development of vasculopathy in systemic

sclerosis. J Eur Acad Dermatol Venereol. 2019 Apr;33(4):753-760. doi: 10.1111/jdv.15387.
31. Mariotti B, Servaas NH, Rossato M, Tamassia N, Cassatella MA, Cossu M, et al. The Long Non-coding RNA NRIR Drives IFN-Response in Monocytes: Implication for Systemic Sclerosis. Front Immunol. 2019 Jan 31;10:100. doi: 10.3389/fimmu.2019.00100.
32. Angiolilli C, Marut W, van der Kroef M, Chouri E, Reedquist KA, Radstake TRDJ. New insights into the genetics and epigenetics of systemic sclerosis. Nat Rev Rheumatol. 2018 Nov;14(11):657-673. doi: 10.1038/s41584-018-0099-0.
33. Lu Q, Wu A, Tesmer L, Ray D, Yousif N, Richardson B. Demethylation of CD40LG on the inactive X in T cells from women with lupus. J Immunol. 2007 Nov 1;179(9):6352-8. doi: 10.4049/jimmunol.179.9.6352.
34. Lian X, Xiao R, Hu X, Kanekura T, Jiang H, Li Y, et al. DNA demethylation of CD40l in CD4+ T cells from women with systemic sclerosis: a possible explanation for female susceptibility. Arthritis Rheum. 2012 Jul;64(7):2338-45. doi: 10.1002/art.34376.
35. Liao J, Liang G, Xie S, Zhao H, Zuo X, Li F, et al. CD40L demethylation in CD4(+) T cells from women with rheumatoid arthritis. Clin Immunol. 2012 Oct;145(1):13-8. doi: 10.1016/j.clim.2012.07.006.
36. Oelke K, Lu Q, Richardson D, Wu A, Deng C, Hanash S, Richardson B. Overexpression of CD70 and overstimulation of IgG synthesis by lupus T cells and T cells treated with DNA methylation inhibitors. Arthritis Rheum. 2004 Jun;50(6):1850-60. doi: 10.1002/art.20255.
37. Jiang H, Xiao R, Lian X, Kanekura T, Luo Y, Yin Y, Zhang G, Yang Y, Wang Y, Zhao M, Lu Q. Demethylation of TNFSF7 contributes to CD70 overexpression in CD4+ T cells from patients with systemic sclerosis. Clin Immunol. 2012 Apr;143(1):39-44. doi: 10.1016/j.clim.2012.01.005.
38. Yin H, Zhao M, Wu X, Gao F, Luo Y, Ma L, et al. Hypomethylation and overexpression of CD70 (TNFSF7) in CD4+ T cells of patients with primary Sjögren's syndrome. J Dermatol Sci. 2010 Sep;59(3):198-203. doi: 10.1016/j.jdermsci.2010.06.011.
39. Li Y, Zhao M, Hou C, Liang G, Yang L, Tan Y, et al. Abnormal DNA methylation in CD4+ T cells from people with latent autoimmune diabetes in adults. Diabetes Res Clin Pract. 2011 Nov;94(2):242-8. doi: 10.1016/j.diabres.2011.07.027.
40. Janson PC, Linton LB, Bergman EA, Marits P, Eberhardson M, Piehl F, et al. Profiling of CD4+ T cells with epigenetic immune lineage analysis. J Immunol. 2011 Jan 1;186(1):92-102. doi: 10.4049/jimmunol.1000960.
41. Graves MC, Benton M, Lea RA, Boyle M, Tajouri L, Macartney-Coxson D, et al. Methylation differences at the HLA-DRB1 locus in CD4+ T-Cells are associated with multiple sclerosis. Mult Scler. 2014 Jul;20(8):1033-41. doi: 10.1177/1352458513516529.
42. Hedrich CM, Rauen T, Apostolidis SA, Grammatikos AP, Rodriguez Rodriguez N, Ioannidis C, et al. Stat3 promotes IL-10 expression in lupus T cells through trans-activation and chromatin remodeling. Proc Natl Acad Sci U S A. 2014 Sep 16;111(37):13457-62. doi: 10.1073/pnas.1408023111.
43. Zhao M, Tang J, Gao F, Wu X, Liang Y, Yin H, Lu Q. Hypomethylation of IL10 and IL13 promoters in CD4+ T cells of patients with systemic lupus erythematosus. J Biomed Biotechnol. 2010;2010:931018. doi: 10.1155/2010/931018.
44. Absher DM, Li X, Waite LL, Gibson A, Roberts K, Edberg J, et al. Genome-wide DNA methylation analysis of systemic lupus erythematosus reveals persistent hypomethylation of interferon genes and compositional changes to CD4+ T-cell populations. PLoS Genet. 2013;9(8):e1003678. doi: 10.1371/journal.pgen.1003678.
45. Lu Q, Kaplan M, Ray D, Ray D, Zacharek S, Gutsch D, Richardson B. Demethylation of ITGAL (CD11a) regulatory sequences in systemic lupus erythematosus. Arthritis Rheum. 2002 May;46(5):1282-91. doi: 10.1002/art.10234.
46. Kaplan MJ, Lu Q, Wu A, Attwood J, Richardson B. Demethylation of promoter regulatory elements contributes to perforin overexpression in CD4+ lupus T cells. J Immunol. 2004 Mar 15;172(6):3652-61. doi: 10.4049/jimmunol.172.6.3652.
47. Altorok N, Coit P, Hughes T, Koelsch KA, Stone DU, Rasmussen A, et al. Genome-wide DNA methylation patterns in naive CD4+ T cells from patients with primary Sjögren's syndrome. Arthritis Rheumatol. 2014 Mar;66(3):731-9. doi: 10.1002/art.38264.
48. Coit P, Jeffries M, Altorok N, Dozmorov MG, Koelsch KA, Wren JD, et al. Genome-wide DNA methylation study suggests epigenetic accessibility and transcriptional poising of interferon-regulated genes in naïve CD4+ T cells from lupus patients. J Autoimmun. 2013 Jun;43:78-84. doi: 10.1016/j.jaut.2013.04.003.
49. Garaud S, Le Dantec C, Jousse-Joulin S, Hanrotel-Saliou C, Saraux A, Mageed RA, et al. IL-6 modulates CD5 expression in B cells from patients with lupus by regulating DNA methylation. J Immunol. 2009 May 1;182(9):5623-32. doi: 10.4049/jimmunol.0802412.
50. Fali T, Le Dantec C, Thabet Y, Jousse S, Hanrotel C, Youinou P, et al. DNA methylation modulates HRES1/p28 expression in B cells from patients with Lupus. Autoimmunity. 2014 Jun;47(4):265-71. doi: 10.3109/08916934.2013.826207.
51. Nile CJ, Read RC, Akil M, Duff GW, Wilson AG. Methylation status of a single CpG site in the IL6 promoter is related to IL6 messenger RNA levels and rheumatoid arthritis. Arthritis Rheum. 2008 Sep;58(9):2686-93. doi: 10.1002/art.23758.
52. Allanore Y, Borderie D, Meune C, Lemaréchal H, Weber S, Ekindjian OG, Kahan A. Increased plasma soluble CD40 ligand concentrations in systemic sclerosis and association with pulmonary arterial hypertension and digital ulcers. Ann Rheum Dis. 2005 Mar;64(3):481-3. doi: 10.1136/ard.2003.020040.
53. Kumagai C, Kalman B, Middleton FA, Vyshkina T, Massa PT. Increased promoter methylation of the immune regulatory gene SHP-1 in leukocytes of multiple sclerosis subjects. J Neuroimmunol. 2012 May 15;246(1-2):51-7. doi: 10.1016/j.jneuroim.2012.03.003.
54. Rakyan VK, Beyan H, Down TA, Hawa MI, Maslau S, Aden D, et al. Identification of type 1 diabetes-associated DNA methylation variable positions that precede disease diagnosis. PLoS Genet. 2011 Sep;7(9):e1002300. doi: 10.1371/journal.pgen.1002300.
55. Wang Y, Fan PS, Kahaleh B. Association between enhanced type I collagen expression and epigenetic repression of the FLI1 gene in scleroderma fibroblasts. Arthritis Rheum. 2006 Jul;54(7):2271-9. doi: 10.1002/art.21948.
56. Dees C, Schlottmann I, Funke R, Distler A, Palumbo-Zerr K, Zerr P, et al. The Wnt antagonists DKK1 and SFRP1 are downregulated by promoter hypermethylation in systemic sclerosis. Ann Rheum Dis. 2014 Jun;73(6):1232-9. doi: 10.1136/annrheumdis-2012-203194.
57. Trenkmann M, Brock M, Gay RE, Kolling C, Speich

R, Michel BA, Gay S, Huber LC. Expression and function of EZH2 in synovial fibroblasts: epigenetic repression of the Wnt inhibitor SFRP1 in rheumatoid arthritis. Ann Rheum Dis. 2011 Aug;70(8):1482-8. doi: 10.1136/ard.2010.143040.
58. Miao CG, Yang YY, He X, Huang C, Huang Y, Qin D, Du CL, Li J. MicroRNA-152 modulates the canonical Wnt pathway activation by targeting DNA methyltransferase 1 in arthritic rat model. Biochimie. 2014 Nov;106:149-56. doi: 10.1016/j.biochi.2014.08.016.
59. Takami N, Osawa K, Miura Y, Komai K, Taniguchi M, Shiraishi M, et al. Hypermethylated promoter region of DR3, the death receptor 3 gene, in rheumatoid arthritis synovial cells. Arthritis Rheum. 2006 Mar;54(3):779-87. doi: 10.1002/art.21637.
60. Mastronardi FG, Noor A, Wood DD, Paton T, Moscarello MA. Peptidyl argininedeiminase 2 CpG island in multiple sclerosis white matter is hypomethylated. J Neurosci Res. 2007 Jul;85(9):2006-16. doi: 10.1002/jnr.21329.
61. González S, Aguilera S, Alliende C, Urzúa U, Quest AF, Herrera L, et al. Alterations in type I hemidesmosome components suggestive of epigenetic control in the salivary glands of patients with Sjögren's syndrome. Arthritis Rheum. 2011 Apr;63(4):1106-15. doi: 10.1002/art.30212.
62. Hu N, Qiu X, Luo Y, Yuan J, Li Y, Lei W, et al. Abnormal histone modification patterns in lupus CD4+ T cells. J Rheumatol. 2008 May;35(5):804-10.
63. Zhou Y, Qiu X, Luo Y, Yuan J, Li Y, Zhong Q, Zhao M, Lu Q. Histone modifications and methyl-CpG-binding domain protein levels at the TNFSF7 (CD70) promoter in SLE CD4+ T cells. Lupus. 2011 Nov;20(13):1365-71. doi: 10.1177/0961203311413412.
64. Miao F, Smith DD, Zhang L, Min A, Feng W, Natarajan R. Lymphocytes from patients with type 1 diabetes display a distinct profile of chromatin histone H3 lysine 9 dimethylation: an epigenetic study in diabetes. Diabetes. 2008 Dec;57(12):3189-98. doi: 10.2337/db08-0645.
65. Miao F, Chen Z, Zhang L, Liu Z, Wu X, Yuan YC, Natarajan R. Profiles of epigenetic histone post-translational modifications at type 1 diabetes susceptible genes. J Biol Chem. 2012 May 11;287(20):16335-45. doi: 10.1074/jbc.M111.330373.
66. Zhang Z, Song L, Maurer K, Petri MA, Sullivan KE. Global H4 acetylation analysis by ChIP-chip in systemic lupus erythematosus monocytes. Genes Immun. 2010 Mar;11(2):124-33. doi: 10.1038/gene.2009.66.
67. Krämer M, Dees C, Huang J, Schlottmann I, Palumbo-Zerr K, Zerr P, et al. Inhibition of H3K27 histone trimethylation activates fibroblasts and induces fibrosis. Ann Rheum Dis. 2013 Apr;72(4):614-20. doi: 10.1136/annrheumdis-2012-201615.
68. Niederer F, Ospelt C, Brentano F, Hottiger MO, Gay RE, Gay S, et al. SIRT1 overexpression in the rheumatoid arthritis synovium contributes to proinflammatory cytokine production and apoptosis resistance. Ann Rheum Dis. 2011 Oct;70(10):1866-73. doi: 10.1136/ard.2010.148957.
69. Pedre X, Mastronardi F, Bruck W, López-Rodas G, Kuhlmann T, Casaccia P. Changed histone acetylation patterns in normal-appearing white matter and early multiple sclerosis lesions. J Neurosci. 2011 Mar 2;31(9):3435-45. doi: 10.1523/JNEUROSCI.4507-10.2011. Erratum in: J Neurosci. 2011 Jun 1;31(22):8325.
70. Ma Y, Yue J, Zhang Y, Shi C, Odenwald M, Liang WG, et al. ACF7 regulates inflammatory colitis and intestinal wound response by orchestrating tight junction dynamics. Nat Commun. 2017 May 25;8:15375. doi: 10.1038/ncomms15375. Erratum in: Nat Commun. 2017 Jul 11;8:16121.
71. Barkas F, Liberopoulos E, Kei A, Elisaf M. Electrolyte and acid-base disorders in inflammatory bowel disease. Ann Gastroenterol. 2013;26(1):23-28. PMID: 24714322; PMCID: PMC3959504.
72. Dipiro JT, Talbert RL, Yee GC, Matzke GR, Wells BG, Posey LM. Pharmacotherapy: A Pathophysiologic Approach, ed: McGraw-Hill Medical, New York; 2014.
73. Harris RA, Shah R, Hollister EB, Tronstad RR, Hovdenak N, Szigeti R, et al. Colonic Mucosal Epigenome and Microbiome Development in Children and Adolescents. J Immunol Res. 2016;2016:9170162. doi: 10.1155/2016/9170162.
74. Howell KJ, Kraiczy J, Nayak KM, Gasparetto M, Ross A, Lee C, et al. DNA Methylation and Transcription Patterns in Intestinal Epithelial Cells From Pediatric Patients With Inflammatory Bowel Diseases Differentiate Disease Subtypes and Associate With Outcome. Gastroenterology. 2018 Feb;154(3):585-598. doi: 10.1053/j.gastro.2017.10.007.
75. Liu Y, Peng J, Sun T, Li N, Zhang L, Ren J, et al. Epithelial EZH2 serves as an epigenetic determinant in experimental colitis by inhibiting TNFα-mediated inflammation and apoptosis. Proc Natl Acad Sci U S A. 2017 May 9;114(19):E3796-E3805. doi: 10.1073/pnas.1700909114.
76. Taman H, Fenton CG, Hensel IV, Anderssen E, Florholmen J, Paulssen RH. Genome-wide DNA Methylation in Treatment-naïve Ulcerative Colitis. J Crohns Colitis. 2018 Nov 15;12(11):1338-1347. doi: 10.1093/ecco-jcc/jjy117.
77. Barnicle A, Seoighe C, Greally JM, Golden A, Egan LJ. Inflammation-associated DNA methylation patterns in epithelium of ulcerative colitis. Epigenetics. 2017 Aug;12(8):591-606. doi: 10.1080/15592294.2017.1334023.
78. McDermott E, Ryan EJ, Tosetto M, Gibson D, Burrage J, Keegan D, et al. DNA Methylation Profiling in Inflammatory Bowel Disease Provides New Insights into Disease Pathogenesis. J Crohns Colitis. 2016 Jan;10(1):77-86. doi: 10.1093/ecco-jcc/jjv176.
79. Kumar A, Malhotra P, Coffing H, Priyamvada S, Anbazhagan AN, Krishnan HR, et al. Epigenetic modulation of intestinal Na^+/H^+ exchanger-3 expression. Am J Physiol Gastrointest Liver Physiol. 2018 Mar 1;314(3):G309-G318. doi: 10.1152/ajpgi.00293.2017.
80. Kelly D, Kotliar M, Woo V, Jagannathan S, Whitt J, Moncivaiz J, et al. Microbiota-sensitive epigenetic signature predicts inflammation in Crohn's disease. JCI Insight. 2018 Sep 20;3(18):e122104. doi: 10.1172/jci.insight.122104.
81. Klasić M, Markulin D, Vojta A, Samaržija I, Biruš I, Dobrinić P, et al.; IBD consortium, Lauc G, Zoldoš V. Promoter methylation of the *MGAT3* and *BACH2* genes correlates with the composition of the immunoglobulin G glycome in inflammatory bowel disease. Clin Epigenetics. 2018 Jun 4;10:75. doi: 10.1186/s13148-018-0507-y.
82. Khan FA, Pandupuspitasari NS, Chun-Jie H, Ao Z, Jamal M, Zohaib A, et al. CRISPR/Cas9 therapeutics: a cure for cancer and other genetic diseases. Oncotarget. 2016 Aug 9;7(32):52541-52552. doi: 10.18632/oncotarget.9646.
83. Mohan C, Putterman C. Genetics and pathogenesis of systemic lupus erythematosus and lupus nephritis. Nat Rev Nephrol. 2015 Jun;11(6):329-41. doi: 10.1038/nrneph.2015.33.
84. Gensterblum E, Renauer P, Coit P, Strickland FM, Kilian NC, Miller S, et al.. CD4+CD28+KIR+CD11a^{hi} T cells correlate with disease activity and are characterized by a pro-

inflammatory epigenetic and transcriptional profile in lupus patients. J Autoimmun. 2018 Jan;86:19-28. doi: 10.1016/j.jaut.2017.09.011.
85. Chen L, Morris DL, Vyse TJ. Genetic advances in systemic lupus erythematosus: an update. Curr Opin Rheumatol. 2017 Sep;29(5):423-433. doi: 10.1097/BOR.0000000000000411.
86. Yung R, Kaplan M, Ray D, Schneider K, Mo RR, Johnson K, Richardson B. Autoreactive murine Th1 and Th2 cells kill syngeneic macrophages and induce autoantibodies. Lupus. 2001;10(8):539-46. doi: 10.1191/096120301701549660.
87. Long H, Yin H, Wang L, Gershwin ME, Lu Q. The critical role of epigenetics in systemic lupus erythematosus and autoimmunity. J Autoimmun. 2016 Nov;74:118-138. doi: 10.1016/j.jaut.2016.06.020.
88. Ulff-Møller CJ, Asmar F, Liu Y, Svendsen AJ, Busato F, Grønbaek K, Tost J, Jacobsen S. Twin DNA Methylation Profiling Reveals Flare-Dependent Interferon Signature and B Cell Promoter Hypermethylation in Systemic Lupus Erythematosus. Arthritis Rheumatol. 2018 Jun;70(6):878-890. doi: 10.1002/art.40422.
89. Zhao H, Wang L, Luo H, Li QZ, Zuo X. TNFAIP3 downregulation mediated by histone modification contributes to T-cell dysfunction in systemic lupus erythematosus. Rheumatology (Oxford). 2017 May 1;56(5):835-843. doi: 10.1093/rheumatology/kew508.
90. Bentham J, Morris DL, Graham DSC, Pinder CL, Tombleson P, Behrens TW, et al. Genetic association analyses implicate aberrant regulation of innate and adaptive immunity genes in the pathogenesis of systemic lupus erythematosus. Nat Genet. 2015 Dec;47(12):1457-1464. doi: 10.1038/ng.3434.
91. Farh KK, Marson A, Zhu J, Kleinewietfeld M, Housley WJ, Beik S, et al. Genetic and epigenetic fine mapping of causal autoimmune disease variants. Nature. 2015 Feb 19;518(7539):337-43. doi: 10.1038/nature13835.
92. Rubin AJ, Parker KR, Satpathy AT, Qi Y, Wu B, Ong AJ, et al. Coupled Single-Cell CRISPR Screening and Epigenomic Profiling Reveals Causal Gene Regulatory Networks. Cell. 2019 Jan 10;176(1-2):361-376.e17. doi: 10.1016/j.cell.2018.11.022.
93. Coit P, Dozmorov MG, Merrill JT, McCune WJ, Maksimowicz-McKinnon K, Wren JD, Sawalha AH. Epigenetic Reprogramming in Naive CD4+ T Cells Favoring T Cell Activation and Non-Th1 Effector T Cell Immune Response as an Early Event in Lupus Flares. Arthritis Rheumatol. 2016 Sep;68(9):2200-9. doi: 10.1002/art.39720.
94. Tsou PS, Coit P, Kilian NC, Sawalha AH. EZH2 Modulates the DNA Methylome and Controls T Cell Adhesion Through Junctional Adhesion Molecule A in Lupus Patients. Arthritis Rheumatol. 2018 Jan;70(1):98-108. doi: 10.1002/art.40338.
95. Zouali M. Chapter 28—epigenetics and autoimmune diseases A2—Rose, Noel R. In: Mackay IR (ed) The autoimmune diseases. Academic Press, Boston, 2014; pp 381–401.
96. Thiagalingam S, Cheng KH, Lee HJ, Mineva N, Thiagalingam A, Ponte JF. Histone deacetylases: unique players in shaping the epigenetic histone code. Ann N Y Acad Sci. 2003 Mar;983:84-100. doi: 10.1111/j.1749-6632.2003.tb05964.x.
97. Guan KL, Xiong Y. Regulation of intermediary metabolism by protein acetylation. Trends Biochem Sci. 2011 Feb;36(2):108-16. doi: 10.1016/j.tibs.2010.09.003.
98. Xiong Y, Guan KL. Mechanistic insights into the regulation of metabolic enzymes by acetylation. J Cell Biol.

International Journal of Biomedicine 12(4) (2022) 515-520
http://dx.doi.org/10.21103/Article12(4)_RA3

REVIEW ARTICLE

INTERNATIONAL JOURNAL OF BIOMEDICINE

New Concepts in Rosacea Classification and Treatment

Ramadan S. Hussein[1,2*]; Walid Kamal Abdelbasset[3,4]

[1]*Department of Internal Medicine, College of Medicine Prince Sattam Bin Abdulaziz University, Al-Kharj, Saudi Arabia*
[2]*Department of Dermatology, Andrology and STDs, Assuit Plice Hospital, Assuit, Egypt*
[3]*Department of Health and Rehabilitation Sciences, College of Applied Medical Sciences Prince Sattam bin Abdulaziz University, Al Kharj, Saudi Arabia*
[4]*Department of Physical Therapy, Kasr Al-Aini Hospital Cairo University, Giza, Egypt*

Abstract

Rosacea is a chronic, persistent, inflammatory skin disease of the central face and eyes, caused by immune dysfunction and neurovascular dysregulation, that presents with recurrent flushing, erythema, telangiectasia, papules, or pustules. Rosacea affects quality of life and social and mental health. Recent research has linked rosacea to autoimmune, gastrointestinal, neurological, and psychiatric diseases and cancer risks. This review discusses the rosacea subtype-directed approach management, new topical and systemic formulations, and therapy combinations depending on new phenotype classification.(**International Journal of Biomedicine. 2022;12(4):515-520.**).

Keywords: rosacea • skin • classification • treatment

For citation: Hussein RS, Abdelbasset WK. New Concepts in Rosacea Classification and Treatment. International Journal of Biomedicine. 2022;12(4):515-520. doi:10.21103/Article12(4)_RA3

Introduction

Rosacea is a chronic, persistent, inflammatory skin disease of the central face and eyes, caused by immune dysfunction and neurovascular dysregulation, that presents with recurrent flushing, erythema, telangiectasia, papules, or pustules. Rosacea affects between 0.09% and 22.41% of the general population and 5.46% of adults worldwide.[1] Phymatous alterations are uncommon, typically affecting the nasal area, and are more common in males. About 50% of rosacea individuals suffer eye dryness, conjunctivitis, blepharitis, and, rarely, keratitis.[2-4] Rosacea usually starts in adults but can occur at any age. Fair-skinned Celts are particularly susceptible. Because erythema and telangiectasia are more difficult to identify in deeper phototypes, rosacea is commonly misdiagnosed.[5,6] Rosacea affects quality of life and social and mental health.[7,8] Recent research has linked rosacea to autoimmune, gastrointestinal, neurological, and psychiatric diseases and cancer risks; whether these links are causative needs more study.[9] In addition to regular skin care and avoiding triggers, rosacea can be treated with active therapies. Topical brimonidine and oxymetazoline are approved for erythema, and ivermectin, azelaic acid, metronidazole, and doxycycline are for papules/pustules. Telangiectasia, erythema, and phyma can be treated with lasers and light. Phyma may need surgery.[3]

***Corresponding author:** Ramadan S. Hussein. Department of Internal Medicine, College of Medicine, Prince Sattam Bin Abdulaziz University, Alkharj, Saudi Arabia. E-mail: ramadangazeera@yahoo.com*

Pathophysiology of rosacea

Dysregulation of immunological and neurocutaneous processes contributes to rosacea development.[10] The association of rosacea with SNPs in MHC genes suggests genetic vulnerability with changed immune reactivity.[11]

Microbes like *Demodex folliculorum* and *Bacillus oleronius* can elicit innate and adaptive immune activation.[12] Innate immunity activation upregulates keratinocyte-derived TLR2 and PAR2, which promote cathelicidin. KLK-5 protease converts cathelicidin to bioactive LL-37, producing erythema.[13] TLR2 activates the NLRP3 inflammasome, causing pustule development, discomfort, and vascular responsiveness via IL-1, PGE2, and TNF-α production. TLR2 also induces

inflammation, erythema, and telangiectasia through expression of chemokines, proteases, cytokines, and angiogenic factors. PAR2 activation causes itching, inflammation, and discomfort together with T-lymphocyte, neutrophil, mast cell degranulation, and release of chemokines, cytokines, and prostaglandins.[10] Activation of the acquired immune system, shown by TH1 and TH17 cells with immunological mediators, causes inflammation and subsequent immune activation.[14]

The ankyrin (TRPA) and vanilloid (TRPV) subfamilies of the transient receptor potential (TRP) channel superfamily may mediate neurocutaneous pathways in rosacea, which indicate responsiveness to ultraviolet light, temperature variations, spicy foods, and wine. Different environmental events may cause specific subfamily receptors to react, resulting in the production of vasoactive neuropeptides. TLR2 and PAR2 are also expressed in sensory neurons, and they can continue to activate inflammatory processes.[15]

Rosacea diagnosis and classification

One or more of the following major characteristics centered on the convex parts of the face are required for rosacea diagnosis: flushing, nontransient erythema, papules/pustules, and telangiectasia. The most crucial observation is persistent facial erythema lasting at least 3 months, sparing the periocular skin. This form of erythema is the only necessary diagnostic criterion for rosacea. Flushing, papules, pustules, and telangiectasia on the convex faces are supporting, but not required, diagnostic features. Burning or stinging sensations, edema, plaques, a dry look, ocular signs, and phymatous alterations are secondary symptoms. Polycythemia vera, connective tissue disorders, carcinoid, and mastocytosis must not be present. Long-term facial steroid users are also excluded. Extrafacial erythema is usually an excluding feature, photosensitivity and allergic contact dermatitis may be considered. There are four subtypes of rosacea: erythematotelangiectatic rosacea (ETR), papulopustular rosacea (PPR), phymatous rosacea (PhR), and ocular rosacea (OR).[2,16]

ETR is characterized by prolonged flushing (lasting longer than 10 minutes). The center of the face is usually the reddest, although the periphery, ears, neck, and upper chest may also be affected. Periocular skin is sparied. Stress, hot beverages, alcohol, spicy meals, exercise, cold or hot temperatures, and hot baths can cause flushing. Episodes are sometimes unprovoked.

PPR patients have a red center face but continuous or episodic inflammation with little papules and pinpoint pustules. Symptoms may include edema. Periocular skin is seldom affected, usually in midlife women. Inflammation can cause persistent edema and phymatous changes.

PhR is characterized by pronounced skin thickening and uneven surface nodules; they can appear on the nose (rhinophyma), chin (gnathophyma), forehead (metophyma), one or both ears (otophyma), as well as the eyelids (blepharophyma). Four forms of rhinophyma (glandular, fibrous, fibroangiomatous, and actinic) are clinically distinguishable and have unique histopathologic characteristics.[16]

In OR patients with ocular symptoms, blepharitis and conjunctivitis are the most prevalent findings. Recurrent chalazion and meibomian gland irritation may occur. Hyperemia, telangiectasia, and watery or dry, itchy eyes might develop. OR frequently causes burning, stinging, itching, light sensitivity, and a feeling there is a foreign body in the eye. Keratitis, scleritis, iritis, and consequences are rare.[16]

In 2017, the worldwide ROSacea COnsensus (ROSCO) group developed a revised schema on patient attributes that incorporated clinical manifestations. This phenotypic method focused on observable traits, which can be altered by environmental or genetic causes.[17] The ROSCO panel included ophthalmologists and dermatologists from different countries all over the world to make sure that the whole world was represented. In this model, accepted by the National Rosacea Society, either one of two separate signs is diagnostic of rosacea: persistent redness in the center of the face that gets worse from time to time due to possible triggers, phymatous changes. In the absence of these signs, if two or more major signs are present (transient erythema, inflamed papules/pustules, telangiectasia, conjunctivitis/blepharitis/telangiectasia of the lids) we can make a diagnosis. Minor characteristics (edema, burning, and dry sensation of the skin) could also potentially be diagnostic or important.[5,17]

Next step, management options were aligned with the phenotypic approach to enhance patient outcomes and well-being by addressing the most problematic features.[2,18]

Therapy

General advice for patients with rosacea

The disease picture varies over time, and the aggravating factors differ from person to person. Good patient information and knowledge of the condition are prerequisites for good treatment results. Worsening of the condition can be reduced by avoiding known triggers. The literature states that sun exposure worsens the condition by up to 80%, and the use of a high sun-protection factor is generally recommended; however, because patients with rosacea have sensitive skin, a variety of skincare products, including sunscreens, moisturizers, and cosmetics, can worsen the condition. There will often be individual variations, so patients are welcome to try their hand at finding effective skin care. Creams with a green cream base will be able to camouflage redness, and mineral oils and silicone-containing preparations are generally tolerated. As a rule, people with rosacea should avoid topical steroids on the face, as these can worsen the condition. Some foods, coffee, tea, citrus fruits, red wine, blue cheese, and spices can cause rosacea to flare up because they contain vasodilators. Flare-ups are also seen with significant temperature variations and intense physical activity. There are significant differences in how patients respond to various triggers.[8]

Sunscreen and cosmetics

Choosing UVA and UVB sunscreens is very important. Titanium dioxide and zinc oxide are physical blockers best tolerated. Protective silicones should be in cosmetics and sunscreens. A light, easy-to-apply foundation can be set with powder. Foundations that have sunscreen with UVA and UVB

protection are encouraged. Green cosmetics or sunscreen can mask redness. Products should be avoided that have sodium lauryl sulfate, astringents, toners, menthol, camphor, and toners. Waterproof makeup and thick foundations that are difficult to apply and remove should also be avoided. Cleansers should be soap-free.[8]

Medical treatment

The medical treatment is primarily aimed at reducing inflammation and the symptoms it causes. Erythema persisting after anti-inflammatory treatment can be treated with lasers, intense pulsed light, or medication. Mild and moderate forms of rosacea can often be treated topically. Widespread inflammatory and PhR require oral treatment, possibly surgical treatment, and laser treatment.[2]

Topical medications

Metronidazole: A 0.75% metronidazole topical cream is recommended twice daily. Metronidazole is equally effective as low-dose tetracycline, but it works faster.[2]

Ivermectin: It is not sufficiently well documented that one type of topical treatment is significantly better than another, although a comparative study with topical ivermectin and metronidazole showed that the effect of ivermectin was somewhat better.[19]

Sodium sulfacetamide and sulfur: 10% sodium sulfacetamide and 5% sulfur have resurged in acne and rosacea therapy: cleansing twice a day with a 10% sodium sulfacetamide and a 5% sulfur solution.[3]

Azelaic acid: FDA-approved for mild-to-moderate rosacea. Azelaic acid is a saturated dicarboxylic acid. Like metronidazole, azelaic acid may suppress neutrophils' ROS generation. Pregnancy category B.[10]

Benzoyl peroxide: Some rosacea patients with barrier failure and sensitive skin can be stung by benzoyl peroxide. Non-sensitive people can quickly resolve erythematous papules and pustules. Phymatous and glandular rosacea patients take benzoyl peroxide or benzoyl peroxide–clindamycin combination treatment effectively. Pregnancy category C.[14]

Topical antibiotics: Cleaning with topical clindamycin or erythromycin twice daily for four weeks is comparable to oral tetracycline. Stinging and dryness are side effects. Clindamycin and erythromycin both are in pregnancy category B.[2]

Topical tacrolimus treats steroid-induced rosacea-like lesions. Tacrolimus is a macrolide immunosuppressant produced by the fungus *Streptomyces tsukubaensis*. Most patients clear within 1 to 2 months of using tacrolimus 0.1% and minocycline 100 mg twice daily.[14]

Brimonidine tartrate: Symptomatic improvement of erythema can be achieved by topical application of the alpha-2 agonist brimonidine tartrate. The drug can be used in parallel with anti-inflammatory rosacea treatment and has a rapid onset of action.[10] The incidence of relapse is highest in the first two weeks after starting brimonidine treatment, and the patient must be given good information about the use of the drug. Daily application over time can have a better effect than occasional use, in terms of tackling side effects.[20]

Topical tretinoin: Chronic topical tretinoin treatment enhances dermal connective tissue remodeling and reduces skin inflammation. Clinical response is delayed, typically not apparent for two or more months. The use of tretinoin in rosacea may cause telangiectasia by increasing cutaneous neovascularization; if so, avoid it. Pregnancy category C.[20]

Oral therapy

Tetracyclines: Tetracycline has long been used to treat rosacea. Symptoms normally improve after 3 to 4 weeks of oral tetracycline. Subantimicrobial-dose tetracycline has been demonstrated to be an effective treatment for rosacea, due to its inherent anti-inflammatory properties (250 mg daily or every other day for maintenance). Minocycline, doxycycline hydrate, and doxycycline monohydrate are also beneficial for rosacea, they have a longer half-life, increased bioavailability, and may be taken with meals, decreasing gastrointestinal adverse effects. Slow-release doxycycline 40mg daily has documented the same effect as doxycycline 100 mg daily, but with a lower incidence of side effects. All long-term antibiotic usage can cause resistance, even if this has not been documented for low-dose doxycycline. The treatment time for rosacea with oral tetracyclines is usually 4-12 weeks, but there are large individual variations in response.[19]

Macrolides: Oral erythromycin treatment is used for rosacea when there is tetracycline intolerance, allergy, resistance, pregnancy, breastfeeding, or age younger than 12 years. Clarithromycin and azithromycin are beneficial for rosacea. Clarithromycin: 250mg twice daily for 4 weeks, followed by 250 mg once daily for 4 weeks.[14]

Metronidazole: Metronidazole 200mg twice a day with alcohol abstinence during treatment prevents disulfiram-induced headaches. The drug is safe to use during pregnancy (category B) and is an alternative to tetracyclines.[19]

Isotretinoin: Daily low-dose isotretinoin (0.3 mg/kg) as long-term therapy should be considered where the patient needs continued oral treatment beyond three months of continuous tetracycline use. In comparison to usual treatments, isotretinoin's effect on resistant rosacea can be delayed. Isotretinoin also reduces rhinophyma nasal volume.[21]

Miscellaneous oral therapies: Oral contraceptive monotherapy for women with "historical and clinical hormonal imbalances" requires 4 months of treatment. Effects of low-dose spironolactone antiandrogenic have been studied for rosacea (50 mg daily). In refractory rosacea, flushing-blocking drugs can help. Anecdotally, beta-blockers, clonidine, and naloxone have helped reduce flushing and erythema in rosacea sufferers.[19]

Vascular laser/Intense pulsed-light (IPL) treatment

Currently, vascular lasers with short wavelengths are used to treat telangiectasia and erythema. Standard pulsed dye lasers, long-pulsed dye lasers (595 nm, 0.5 to 40 milliseconds), potassium-titanyl-phosphate lasers (532 nm, 1 to 50 milliseconds), and the diode-pumped, frequency-doubled laser (532 nm) destroy vessels without collateral tissue injury. IPL is also effective in ETR.[21] In PhR, there are good results with treatment with CO_2 laser and surgery.[13]

Combination therapy

Dermatologists frequently recommend a combination therapy, although relatively minimal data support its usefulness.[21] Topical metronidazole 1% gel in combination with doxycycline 40-mg modified-release capsules (DMR) can

help with a variety of symptoms. Over 16 weeks, doxycycline 20 mg twice daily with metronidazole 0.75% gel resulted in more improvement than did a placebo.[22] The effect of adding 0.33% brimonidine gel to 1% ivermectin cream was supported by a decrease in redness and inflammation. Topical ivermectin and DMR alleviate rosacea inflammation. The combination therapy showed a more rapid beginning of action and improved erythema, stinging, burning, flushing, and ocular symptoms. Both groups reported few adverse effects.[23]

Rosacea management: A subtype-directed approach

The fundamentals of sun avoidance and sunscreen selection have been explored in rosacea. Avoiding triggers is an essential preventative measure. Patients should be taught about recognized triggers, and if possible, should identify and avoid their own triggers. Finally, patients may be advised to use nonirritating cosmetics to mask the signs and symptoms of rosacea.[2]

Standard medical treatments for rosacea have mostly centered on reducing inflammation. Repair of vascular and connective tissue dysfunction has only lately been a treatment goal for rosacea. Topical retinoids reorganize skin collagen and blood vessels and reduce inflammation.[10]

In ETR, first-line treatment may include IPL or lasers. Symptomatic improvement of erythema can be achieved by topical application of the alpha-2 agonist brimonidine tartrate. Most ETR individuals show barrier disruption and sensitivity to topical treatments. Education on cosmetic and sunscreen options is crucial. In the morning, one or a combination of topical anti-inflammatory agents, such as metronidazole or sodium sulfacetamide–sulfur, followed by sunscreen may be administered. If irritating responses are predominant in the history of an ETR patient, or if scaling and intense erythema are present, a barrier emollient may be used in the evening. While starting oral antibiotics, using a physical sunscreen and a barrier-protective emollient twice day may be helpful.[21]

In PPR, initial therapy (generally lasting 2-3 months) frequently needs a combination of oral and topical antimicrobials. Rapid control can be obtained in 1 to 3 months using oral and topical antimicrobials. In PPR, skin sensitivity is less common; therefore, all topical therapy alternatives are well tolerated in at least half of the patients. PPR seldom requires isotretinoin. Oral tetracyclines and topical antimicrobials manage disease in these people. Long-term PPR therapy frequently involves topical medications only. Metronidazole, sodium sulfacetamide–sulfur, azelaic acid, or benzoyl peroxide, followed by sunscreen every morning, could be part of a good combination topical regimen. A protective emollient, followed by tretinoin cream, might be used in the evening. Vascular lasers and IPL are supplementary therapeutic options for erythema and telangiectasia. IPL may also reduce bouts of flushing, but more research is needed in this area.[2]

Individuals with PhR may have overlapping acne and rosacea. Topical antimicrobials have a positive effect on them. These individuals respond effectively to benzoyl peroxide and benzoyl peroxide–antibiotic combinations. In addition to the topical regimen, oral tetracyclines are necessary for the early treatment of papules and pustules. Oral medication is typically continued for one to three months. The majority of PhR patients do not develop telangiectasia; however, they may have flushing. In the initial care of mild-to-moderate PhR, topical retinoids can be used in conjunction with topical or oral antibacterial therapy. Isotretinoin can be used to treat severe inflammatory or nodulocystic illness, which should be followed by long-term treatment with topical tretinoin. Increased sebum production, big pores, and thicker skin are common complaints among females with glandular rosacea. They may have mostly perioral papules and pustules. In such instances, low-dose spironolactone (25 to 50 mg daily) or oral contraceptives, or both, may assist. Isotretinoin is also beneficial in the short-term reduction of sebum production.[2]

In mild-to-moderate PhR, there are benefits from isotretinoin monotherapy. Surgery or a combination of surgery and isotretinoin treatment should be used to treat advanced phyma. Surgical techniques that have been used to reshape rhinophyma include a heated scalpel, laser ablation, tangential excision mixed with scissor sculpturing, and radiofrequency electrosurgery. Typically, these methods are combined to provide the greatest cosmetic effect.[14]

New treatments

Minocycline Foam: FDA authorized minocycline foam 1.5% in May 2020. The US began selling the foam in October 2020. A dose-ranging, randomized, double-blind experiment investigated the safety and efficacy of minocycline foam for PPR. No treatment-related adverse events occurred. Itching was the most common skin side effect, while respiratory infection was the most common overall adverse event. More trials are needed to compare topical minocycline to other available topical therapy.[24]

Encapsulated Benzoyl Peroxide Cream: The FDA accepted for review benzoyl peroxide 5% in September 2020.[25] Concerns about skin irritation prevented research on rosacea. Encapsulating it in silica may reduce discomfort.[26]

Erenumab: Erenumab is a monoclonal antibody against the receptor of the neuropeptide CGRP, which has been implicated in migraine pathophysiology. CGRP affects nociceptive and vasodilatory signals. In June 2020, there began an open-label phase II study of erenumab 140 mg administered subcutaneously every 4 weeks for rosacea redness and flushing.[27]

Rifaximin: Rifaximin is a gut-active antibiotic for traveler's diarrhea, IBS, and hepatic encephalopathy. Rosacea and gastrointestinal illness are linked. Research on small intestine bacterial overgrowth (SIBO) in rosacea patients found that eradicating SIBO with rifaximin 400mg three times daily for 10 days resolved rosacea in 78% of patients. In a study by Weinstock & Steinhoff, 51% of 63 patients with rosacea had SIBO. Rosacea and SIBO patients took 400mg rifaximin three times daily for 10 days; 46% of patients indicated clear or notable improvement, 25% - moderate, and 11% - mild.[28]

Hydroxychloroquine: Hydroxychloroquine is used to treat systemic autoimmune disorders. It modulates costimulatory molecules and reduces pro-inflammatory cytokine. In a rosacea mouse model, hydroxychloroquine reduced pro-inflammatory factors and proteases of the mast

cells.[29] In a study of six adults with moderate to severe rosacea, hydroxychloroquine 200 mg twice a day reduced inflammatory lesions by 67% and erythema by 83%. Long-term hydroxychloroquine usage can induce permanent retinopathy.[30]

Conclusion

Individualization of the diagnostic approach to rosacea has resulted in advancements in our knowledge of the pathogenesis, therapeutic methods, and how to care for patients. Greater knowledge of the pathogenesis, innovative topical methods for active treatments, and repurposing of established dermatologic medications have led to new rosacea treatments. These innovations might enhance rosacea sufferers' results. Despite treatment adherence, not all patients obtain complete or near-complete rosacea clearance. Thus, more effective treatments, particularly combination therapies, are needed. To thoroughly meet the requirements of all rosacea patients, more pathophysiology and therapy advancements are required.

Acknowledgments

This publication was supported by the Deanship of Scientific Research at Prince Sattam Bin Abdulaziz University.

Competing Interests

The authors declare that they have no competing interests.

References

1. Parisi R, Yiu ZZN. The worldwide epidemiology of rosacea. Br J Dermatol. 2018;179:239–40. doi: 10.1111/bjd.16788).
2. Schaller M, Almeida LMC, Bewley A, Cribier B, Del Rosso J, Dlova NC, et al. Recommendations for rosacea diagnosis, classification and management: update from the global ROSacea COnsensus 2019 panel. Br J Dermatol. 2020 May;182(5):1269-1276. doi: 10.1111/bjd.18420.
3. van Zuuren EJ, Fedorowicz Z, Tan J, van der Linden MMD, Arents BWM, Carter B, Charland L. Interventions for rosacea based on the phenotype approach: an updated systematic review including GRADE assessments. Br J Dermatol. 2019 Jul;181(1):65-79. doi: 10.1111/bjd.17590.
4. van Zuuren EJ. Rosacea. N Engl J Med. 2017 Nov 2;377(18):1754-1764. doi: 10.1056/NEJMcp1506630.
5. Gallo RL, Granstein RD, Kang S, Mannis M, Steinhoff M, Tan J, Thiboutot D. Standard classification and pathophysiology of rosacea: The 2017 update by the National Rosacea Society Expert Committee. J Am Acad Dermatol. 2018 Jan;78(1):148-155. doi: 10.1016/j.jaad.2017.08.037.
6. Gether L, Overgaard LK, Egeberg A, Thyssen JP. Incidence and prevalence of rosacea: a systematic review and meta-analysis. Br J Dermatol. 2018 Aug;179(2):282-289. doi: 10.1111/bjd.16481.
7. Alexis AF, Callender VD, Baldwin HE, Desai SR, Rendon MI, Taylor SC. Global epidemiology and clinical spectrum of rosacea, highlighting skin of color: Review and clinical practice experience. J Am Acad Dermatol. 2019 Jun;80(6):1722-1729.e7. doi: 10.1016/j.jaad.2018.08.049.
8. Baldwin HE, Harper J, Baradaran S, Patel V. Erythema of Rosacea Affects Health-Related Quality of Life: Results of a Survey Conducted in Collaboration with the National Rosacea Society. Dermatol Ther (Heidelb). 2019 Dec;9(4):725-734. doi: 10.1007/s13555-019-00322-5.
9. Holmes AD, Spoendlin J, Chien AL, Baldwin H, Chang ALS. Evidence-based update on rosacea comorbidities and their common physiologic pathways. J Am Acad Dermatol. 2018 Jan;78(1):156-166. doi: 10.1016/j.jaad.2017.07.055.
10. Buddenkotte J, Steinhoff M. Recent advances in understanding and managing rosacea. F1000Res. 2018 Dec 3;7:F1000 Faculty Rev-1885. doi: 10.12688/f1000research.16537.1.
11. Chang ALS, Raber I, Xu J, Li R, Spitale R, Chen J, Kiefer AK, Tian C, Eriksson NK, Hinds DA, Tung JY. Assessment of the genetic basis of rosacea by genome-wide association study. J Invest Dermatol. 2015 Jun;135(6):1548-1555. doi: 10.1038/jid.2015.53.
12. Holmes AD. Potential role of microorganisms in the pathogenesis of rosacea. J Am Acad Dermatol. 2013 Dec;69(6):1025-32. doi: 10.1016/j.jaad.2013.08.006.
13. Yamasaki K, Kanada K, Macleod DT, Borkowski AW, Morizane S, Nakatsuji T, Cogen AL, Gallo RL. TLR2 expression is increased in rosacea and stimulates enhanced serine protease production by keratinocytes. J Invest Dermatol. 2011 Mar;131(3):688-97. doi: 10.1038/jid.2010.351.
14. Woo YR, Lim JH, Cho DH, Park HJ. Rosacea: Molecular Mechanisms and Management of a Chronic Cutaneous Inflammatory Condition. Int J Mol Sci. 2016 Sep 15;17(9):1562. doi: 10.3390/ijms17091562.
15. Schwab VD, Sulk M, Seeliger S, Nowak P, Aubert J, Mess C, Rivier M, Carlavan I, Rossio P, Metze D, Buddenkotte J, Cevikbas F, Voegel JJ, Steinhoff M. Neurovascular and neuroimmune aspects in the pathophysiology of rosacea. J Investig Dermatol Symp Proc. 2011 Dec;15(1):53-62. doi: 10.1038/jidsymp.2011.6.
16. Wilkin J, Dahl M, Detmar M, Drake L, Feinstein A, Odom R, Powell F. Standard classification of rosacea: Report of the National Rosacea Society Expert Committee on the Classification and Staging of Rosacea. J Am Acad Dermatol. 2002 Apr;46(4):584-7. doi: 10.1067/mjd.2002.120625.
17. Tan J, Almeida LM, Bewley A, Cribier B, Dlova NC, Gallo R, Kautz G, Mannis M, Oon HH, Rajagopalan M, Steinhoff M, Thiboutot D, Troielli P, Webster G, Wu Y, van Zuuren EJ, Schaller M. Updating the diagnosis, classification and assessment of rosacea: recommendations from the global ROSacea COnsensus (ROSCO) panel. Br J Dermatol. 2017 Feb;176(2):431-438. doi: 10.1111/bjd.15122.
18. Schaller M, Almeida LM, Bewley A, Cribier B, Dlova NC, Kautz G, Mannis M, Oon HH, Rajagopalan M, Steinhoff M, Thiboutot D, Troielli P, Webster G, Wu Y, van Zuuren E, Tan J. Rosacea treatment update: recommendations from the global ROSacea COnsensus (ROSCO) panel. Br J Dermatol. 2017 Feb;176(2):465-471. doi: 10.1111/bjd.15173.
19. van Zuuren EJ, Fedorowicz Z. Interventions for rosacea: abridged updated Cochrane systematic review including GRADE assessments. Br J Dermatol. 2015 Sep;173(3):651-62. doi: 10.1111/bjd.13956.
20. Steinhoff M, Schauber J, Leyden JJ. New insights into rosacea pathophysiology: a review of recent findings. J Am Acad Dermatol. 2013 Dec;69(6 Suppl 1):S15-26. doi:

10.1016/j.jaad.2013.04.045.
21. Thiboutot D, Anderson R, Cook-Bolden F, Draelos Z, Gallo RL, Granstein RD, Kang S, Macsai M, Gold LS, Tan J. Standard management options for rosacea: The 2019 update by the National Rosacea Society Expert Committee. J Am Acad Dermatol. 2020 Jun;82(6):1501-1510. doi: 10.1016/j.jaad.2020.01.077.
22. Sanchez J, Somolinos AL, Almodóvar PI, Webster G, Bradshaw M, Powala C. A randomized, double-blind, placebo-controlled trial of the combined effect of doxycycline hyclate 20-mg tablets and metronidazole 0.75% topical lotion in the treatment of rosacea. J Am Acad Dermatol. 2005 Nov;53(5):791-7. doi: 10.1016/j.jaad.2005.04.069.
23. Gold LS, Papp K, Lynde C, Lain E, Gooderham M, Johnson S, Kerrouche N. Treatment of Rosacea With Concomitant Use of Topical Ivermectin 1% Cream and Brimonidine 0.33% Gel: A Randomized, Vehicle-controlled Study. J Drugs Dermatol. 2017 Sep 1;16(9):909-916.
24. Mrowietz U, Kedem TH, Keynan R, Eini M, Tamarkin D, Rom D, Shirvan M. A Phase II, Randomized, Double-Blind Clinical Study Evaluating the Safety, Tolerability, and Efficacy of a Topical Minocycline Foam, FMX103, for the Treatment of Facial Papulopustular Rosacea. Am J Clin Dermatol. 2018 Jun;19(3):427-436. doi: 10.1007/s40257-017-0339-0.
25. Park B. FDA to Review Investigational Rosacea Treatment epsolay. MPR, September 14, 2020. https://www.empr.com/home/news/drugs-in-the-pipeline/benzoyl-peroxide-epsolay-for-rosacea-fda-review/
26. Leyden JJ. Randomized, phase 2, dose-ranging study in the treatment of rosacea with encapsulated benzoyl peroxide gel. J Drugs Dermatol. 2014 Jun;13(6):685-8.
27. Messoud Ashina, Danish Headache Center. Efficacy and tolerability of erenumab in the management of persistent redness and flushing in rosacea (STOP Ros). ClinicalTrials.gov. Identifier NCT04419259. https://c linicaltri als .gov/c t2 / show/N CT0 441925 9. Accessed 15 Nov 2020.
28. Weinstock LB, Steinhoff M. Rosacea and small intestinal bacterial overgrowth: prevalence and response to rifaximin. J Am Acad Dermatol. 2013 May;68(5):875-6. doi: 10.1016/j.jaad.2012.11.038.
29. Li J, Yuan X, Tang Y, Wang B, Deng Z, Huang Y, Liu F, Zhao Z, Zhang Y. Hydroxychloroquine is a novel therapeutic approach for rosacea. Int Immunopharmacol. 2020 Feb;79:106178. doi: 10.1016/j.intimp.2019.106178.
30. The Royal College of Ophthalmologists. Clinical guidelines. Hydroxychloroquine and Chloroquine Retinopathy: Recommendations on Monitoring. December 2020. Review date December 2023. https://www.rcophth.ac.uk/wp-content/uploads/2020/12/Hydroxychloroquine-and-Chloroquine-Retinopathy-Monitoring-Guideline.pdf

International Journal of Biomedicine 12(4) (2022) 521-525
http://dx.doi.org/10.21103/Article12(4)_RA4

SHORT REVIEW

INTERNATIONAL JOURNAL OF BIOMEDICINE

Novel Metformin Indications and Skin Disorders

Ramadan S. Hussein[1, 2*]; Walid Kamal Abdelbasset[3,4]; Osama Mahfouz[5]

[1]*Department of Internal Medicine, College of Medicine, Prince Sattam Bin Abdulaziz University, Al-Kharj, Saudi Arabia*
[2]*Department of Dermatology, Andrology and STDs, Assuit Police Hospital, Assuit, Egypt*
[3]*Department of Health and Rehabilitation Sciences, College of Applied Medical Sciences Prince Sattam bin Abdulaziz University, Al Kharj, Saudi Arabia*
[4]*Department of Physical Therapy, Kasr Al-Aini Hospital Cairo University, Giza, Egypt*
[5]*Department of Emergency, King Saud University medical city, Riyadh, Saudi Arabia*

Abstract

Metformin is the first-line medication to increase insulin sensitivity in insulin-resistant conditions such as type 2 diabetes, polycystic ovary syndrome, and obesity. However, metformin is a drug with a wide range of pharmacological properties, showing the ability to treat various skin conditions. Some inflammatory skin dermatoses, skin neoplasms, endocrinology-related dermatosis, pigmentary disorders, skin aging, and wound healing have all shown improvement when metformin is used. This review discusses the most recent research supporting the use of metformin as a treatment for common skin conditions.(**International Journal of Biomedicine. 2022;12(4):521-525.**).

Keywords: Metformin • indications • skin disorders

For citation: Hussein RS, Abdelbasset WK, Mahfouz O. Novel Metformin Indications and Skin Disorders. International Journal of Biomedicine. 2022;12(4):521-525. doi:10.21103/Article12(4)_RA4

Abbreviations

AMPK, AMP-activated protein kinase; **AN**, acanthosis nigricans; **BP-like EBA**, bullous pemphigoid-like epidermolysis bullous acquisita; **GLUT4**, glucose transporter 4; **HS**, hidradenitis suppurativa; **IR**, insulin resistance; **IGF-1**, insulin growth factor-1; **IPL**, intense pulsed light; **MITF**, microphthalmia-associated transcription factor; **OCT**, organic cation transporter; **PPARγ**, peroxisome proliferator-activated receptor γ; **PCOS**, polycystic ovary syndrome; **PKC**, protein kinase C; **T2D**, type 2 diabetes; **TRP**, tyrosinase-related protein.

Introduction

Hyperandrogenism associated with hyperinsulinemia and insulin resistance (IR) may have a significant impact on the onset of several dermatological conditions.(1) IR is defined by decreased cellular glucose absorption and average or increased insulin levels. The cytoplasmic fraction of insulin-responsive glucose transporter 4 (GLUT4) is significantly decreased in IR. Metformin counteracts this action by slowing GLUT4 endocytosis and raising GLUT4 gene expression, resulting in enhanced glucose absorption and decreased IR. Metformin may lower both fasting and induced plasma insulin levels, with this activity mediated by interactions with PPARγ.(2) It reduces blood glucose primarily by decreasing hepatic glucose production and boosting sensitivity to insulin through an AMPK-dependent mechanism.(3) Metformin is an important medicine for a variety of skin disorders. This article will look at metformin from a dermatological standpoint.

Metformin's oral bioavailability ranges between 40% and 60%. Complete gastrointestinal absorption occurs within 6 hours following medication administration. Plasma membrane

***Corresponding author**: Ramadan S. Hussein. Department of Internal Medicine, College of Medicine, Prince Sattam bin Abdulaziz University, Al-Kharj, Saudi Arabia. E-mail: ramadangazeera@yahoo.com*

monoamine transporter mediates gastrointestinal absorption.[4] Metformin is not metabolized, and its half-life is 5 hours. OCT-1 and OCT-3 aid in metformin hepatic absorption, while OCT-2 aids in metformin uptake from the bloodstream into kidney epithelial cells. Metformin is eliminated from the body by active renal excretion.[5]

Metformin and Inflammatory Dermatoses

Acne management

Acne is a relatively prevalent chronic inflammatory skin condition that affects the folliculopilosebaceous unit. Acne vulgaris affects 85% of adolescents. The pathophysiology of acne vulgaris is complex; excessive sebum, improper follicular keratinization, colonization of cutibacterium acne, and inflammation are all implicated.[6] Comedones, inflammatory papules, pustules, and cysts are characteristic lesions that may cause scarring and pigmentation changes. Typically, acne lesions are situated on the face, shoulders, back, and chest and are classified into 3 types based on the severity of the disease: mild, medium, and severe.[7] Acne development is also influenced by abnormal hormone function, hyperandrogenemia, hyperinsulinemia, and increased IGF-1. The activation of IGF-1 receptors by hyperinsulinemia is responsible for the enhanced proliferation and malfunctioning of keratinocytes. IGF-1 hypersecretion results in aberrant sebum production, sebocyte hyperproliferation, and lipogenesis.[1] Insulin and IGF-1 facilitate the production of androgens. IGF-1 also improves androgen receptor signal transduction. As a result, the increased testosterone level promotes hyperseborrhea.[8] Some investigations have indicated that hyperinsulinemia, and not elevated testosterone levels, may have been the only cause of acne.[9] According to Kartal et al.,[10] IR is a risk factor for acne that is independent of hyperandrogenemia.

Hyperinsulinemia may play a significant role in acne pathogenesis by promoting hyperandrogenemia.[11] The PPAR ligands mediate the action of androgens on sebaceous lipids. Increased PPARγ activity suppresses the GLUT4 promoter, resulting in increased IR. Metformin increases glucose absorption and improves IR via slowing GLUT4 endocytosis and raising GLUT4 expression of genes. Metformin could reduce plasma insulin and IR through PPAR interaction.[12] There are 3 PPAR isotypes: α, δ, and γ. PPARα and PPARγ predominate in human sebocytes. PPARs are found in sebocyte mitochondria, peroxisomes, and microsomes and control a variety of lipid metabolic genes.[13] IGF-1 increases acne formation by stimulating sebum hypersecretion. Metformin lowers elevated blood levels of IGF-1 and androgen in women with polycystic ovary syndrome (PCOS).[14] It may also restrict proinflammatory cytokine release and block monocyte differentiation, reducing inflammation.[15] Begin with a modest dosage of 250 mg, gradually raising it by 250 mg each week until the maximum dose of 1500-2000 mg is reached. For long-term success, a positive impact should be demonstrated within 6 months. Metformin is a safer acne treatment for women with hirsutism and acne caused by PCOS.[14]

Hidradenitis suppurativa

HS is essentially a pilosebaceous unit condition accompanied by an abnormality in hair structure, with apocrine gland participation becoming a minor feature.[16] Genetic factors linked to HS cause enlargement and deformation of the upper section of the follicle infundibulum, followed by obstruction and eventual burst, re-epithelialization, sinus tract creation, bacterial invasion, pustule, and fistula. HS has also been linked to PCOS, and with a decrease in symptoms after menopause, a link to hormonal impacts is also proposed.[16]

Metformin might be considered a viable therapy option in this situation due to the prevalence of poor glucose tolerance in a significant percentage of these individuals. Metformin works in HS via an unknown mechanism. It has been proposed, however, that metformin functions primarily via impairing androgen action, with a probable impact on gene expression implicated in this syndrome. Secondly, it enhances glucose consumption by improving the sensitivity of receptors, resulting in less IR. In pilot research, Verdolini et al.[17] established metformin's effectiveness in treating resistant HS. The treatment was maintained for 24 weeks. The dermatology life quality index improved, and the change was considerable (64%).

Psoriasis

Psoriasis is a persistent inflammatory skin disorder that develops erythematous scaly plaques.[18] Psoriasis is now considered a systemic illness. It is often linked to obesity, metabolic syndrome, and T2D.[19] Metformin works on and stimulates the enzyme AMP-activated protein kinase (AMPK). Once active, this enzyme has been found to inhibit the function of macrophages, endothelial cells, T-lymphocytes, dendritic cells, and monocytes, resulting in anti-inflammatory responses. Metformin also possesses anti-inflammatory effects that are not reliant on AMPK.[19] Metformin inhibits the generation of reactive oxygen species by complex I (NADH-ubiquinone reductase) suppression in the inner mitochondrial membrane and may significantly change T-cell responses.[20,21] Cytokines and inflammatory markers like IFN-γ, TNF-α, and C-reactive protein have been shown to decrease in response to metformin administration.[22] Metformin has been demonstrated to suppress proliferation in keratinocytes by blocking the mitogen-activated protein kinase pathway.[23] Additionally, in human keratinocyte cultures, metformin reduced growth and proinflammatory cytokines through the rapamycin signaling pathway.[24] Further, metformin has been proven in experimental investigations to reduce liver toxicity associated with methotrexate, suggesting that it might be used in conjunction with methotrexate to manage psoriasis, making methotrexate use safer. Metformin's advantages for psoriasis are established most clearly in individuals with impaired sugar tolerance and/or metabolic syndrome.[25]

BP-like EBA

BP-like EBA is a granulocyte-mediated cutaneous condition caused by autoantibodies. Pemphigoid disorders are autoimmune blistering skin illnesses characterized by an immune reaction to dermal-epidermal adhesion complex proteins.[26] Autoantibody accumulation in the PD dermis attracts immune cells, notably granulocytes. Granulocytes tear down the dermal-epidermal adhesion complex by releasing ROS and proteases, causing subepidermal clefts that appear as erosions and blisters.[27]

Because neutrophil activation by immune complexes is the key effector phase step of BP-like EBA.[28] Metabolism-modulating agents such as metformin may have systemic

effects and decrease neutrophils, especially during ongoing immunological reactions.[29] In support of these ideas, the antidiabetic medication metformin reduces OxPhos via inhibiting mitochondrial complex I.[30] It has a much better safety profile and fewer adverse effects than the immunosuppressive medications now used to treat pemphigoid disorders.[31] Metformin also reduces corticosteroid side effects, making a combined treatment of corticosteroids and metformin an attractive possibility for treating pemphigoid disorders.[32] Metformin has a variety of pharmacological actions, and in vivo efficacy is probably the average of these activities. It stimulates Tregs and M2 macrophages while suppressing M1 macrophages, resulting in greater amounts of anti-inflammatory cytokines, notably IL-10.[33,34] Metformin therapy elevated IL-10 and TGF-β in lesional skin and enhanced Tregs. IL-10 and Tregs lower inflammation in BP-like EBA skin lesions; therefore, their elevated levels may have contributed to metformin's therapeutic benefits.[35] The number of macrophages in the infiltrate was decreased. Still, there was no transition from M1 to M2 macrophages, implying that the decrement in raw numbers of M1 macrophages may have been related to metformin's therapeutic benefits.[36]

Metformin and Skin Neoplasms

Metformin's significance in skin cancer chemoprevention has recently been hypothesized.[37] There is accumulating evidence that metformin can be used to treat melanoma and squamous cell carcinoma.[38,39]

Squamous Cell Carcinoma

Metformin's impact on squamous cell carcinoma chemoprevention is due to its enhancing action on AMPK, which suppress rapamycin signaling molecular target pathway. Recent research showed that metformin has an AMPK-independent activity as an anticancer drug.[40,41] Metformin also promotes apoptosis and elevates the Bax: Bcl-2 proportion in squamous cell carcinoma cells. Bcl-2 is an antiapoptotic protein, while Bax is a proapoptotic protein. As a result, this increase promotes tumor cell apoptosis.[42] Metformin also targets the nuclear factor-kappa-beta pathway and affects the PI3K/AK+ and ERK/p38 microtubule-associated protein kinase signaling pathways, reducing these pathways that are crucial for cellular multiplication and viability. Metformin has recently been discovered to have a function in suppressing the proliferation of cancer stem cells.[43] In addition to its anticancer actions, metformin has been demonstrated to enhance the effects of traditional chemotherapeutic drugs.[38]

Melanoma

Metformin increases p53 expression, which enhances anticancer signaling in melanoma.[39] In addition, metformin inhibits transcription factors Snail and Slug and reduces epithelial-mesenchymal conversion in melanoma and matrix metalloproteinase activity, boosting anti-invasive and antimetastatic actions. In recent research, Martin et al. found that metformin might promote the proliferation of $BRAF^{V600E}$-mutated melanoma cells in vitro by upregulating VEGF. When metformin was coupled with VEGF inhibitors, the development of these cancerous cells was inhibited in vivo. Considering these findings, it may be safe to assume that combining metformin and VEGF antagonists with BRAF mutant melanoma potentially resistant to BRAF inhibitors might be an effective alternative treatment.[44]

Endocrine-Related Dermatosis

Hirsutism

Hirsutism is described as the abnormal development of male-pattern hair on a woman's body. Lips, chin, and chest are examples of specific areas. There is an underlying PCOS in around 90% of hirsute females, or an underlying cause has not yet been identified. According to some claims, lowering circulating insulin levels lowers the amount of free testosterone in free circulation, suggesting that metformin may be useful in hirsutism management.[45]

Few studies have examined the effect of metformin on hirsutism as the primary objective. After a 14-month, double-blind, placebo-controlled randomized trial, Kelly and Gordon observed a slight decrease in the Ferriman-Gallwey score. In this research, metformin 500mg was delivered initially, followed by a 3-week progressive raise to 500 mg 3 times a day until the conclusion of therapy.[45] Ibáñez et al.[46] reported that metformin medication was successful in slowing the onset of hyperandrogenism, hirsutism, and PCOS in girls aged 8 to 12 years. Finally, a randomized controlled trial of 70 PCOS patients who had metformin plus intense pulsed light (IPL) for hair removal vs. IPL alone for 5 sessions over 6 months showed the metformin-IPL regimen was better.[47] However, until additional data is collected, metformin is not a first-line hirsutism therapy.

Acanthosis Nigricans

Acanthosis nigricans (AN) is a common skin disorder that is distinguished by black, coarse, thick, and velvety skin texture. Its distribution is generally bilateral, and it may be found in the axilla, neck, groin folds, antecubital and popliteal fossas, and a few other uncommon locations. A deficiency in glucose GLUT4 diffusion to the plasma membrane of myocytes and adipocytes may enhance IGF-R activity and so play a role in the pathogenesis of acanthosis nigricans.[48] The link between benign acanthosis nigricans and IR has recently been shown, and being overweight is a common co-morbidity in these individuals. Furthermore, obese AN people had higher insulin levels than obese persons without acanthosis nigricans.[49]

The pathophysiology of acanthosis nigricans is complicated, including the interaction of many receptors and growth factors. The activation of receptors from the tyrosine kinase family is involved in the development of acanthosis nigricans.[50,51] Metformin has positive benefits in acanthosis nigricans through preventing GLUT4 receptor endocytosis, permitting its movement to the plasma membrane, and so facilitating peripheral glucose consumption, reducing hyperinsulinemia, improving insulin sensitivity, and promoting body weight and reducing fat mass. In addition, the conjunction of metformin with glimepiride or thiazolidine may enhance its effect on acanthosis nigricans when metformin alone is ineffective.[52]

Disorders of Increased Pigmentation

Metformin's involvement in treating hyperpigmentation illnesses, particularly melasma, has just lately been explored. Metformin's positive impact has been related to several molecular pathways. Metformin inhibits the production of 3 melanogenic

proteins: tyrosinase, TRP-1, and TRP-2.[53] Metformin does this by first decreasing levels of cAMP, which inhibits protein kinase A activity. As a result, the expression of the MITF is reduced. MITF is a transcription factor known as the melanocyte viability master gene. Whenever its action is inhibited, transcription of numerous melanogenic proteins like TRP-1, tyrosinase, MART-1, TRP-2, and PKC- is reduced.[54] In addition, metformin suppresses the action of PKC-β. PKCβ activated by diacylglycerol (DAG) induces melanogenesis via the activation of tyrosinase. Metformin inhibits this activation conferred by DAG to PKC-β, resulting in a decrease in pigmentation.[55] However, this effect has been proven only by topical metformin and not by systemic administration of the medication.[56]

In conclusion, although metformin is typically used to treat T2D, it also has the potential to treat a variety of cutaneous conditions, particularly those associated with IR and hyperandrogenism. There have lately been encouraging studies about the use of metformin to treat inflammatory diseases, endocrine-related dermatosis, cutaneous cancers, and hyperpigmentation illnesses. Metformin could, therefore, have systemic and topical dermatological applications.

Acknowledgments

This publication was supported by the Deanship of Scientific Research at Prince Sattam bin Abdulaziz University.

Competing Interests

The authors declare that they have no competing interests.

References

1. Napolitano M, Megna M, Monfrecola G. Insulin resistance and skin diseases. ScientificWorldJournal. 2015;2015:479354. doi: 10.1155/2015/479354.
2. Sawaya M. Antiandrogens and androgen inhibitors. In: Se W, editor. Comprehensive Dermatologic Drug Therapy. Philadelphia: W.B. Saunders Co.; 2001:385401.
3. Brauchli YB, Jick SS, Curtin F, Meier CR. Association between use of thiazolidinediones or other oral antidiabetics and psoriasis: A population based case-control study. J Am Acad Dermatol. 2008 Mar;58(3):421-9. doi: 10.1016/j.jaad.2007.11.023.
4. Gong L, Goswami S, Giacomini KM, Altman RB, Klein TE. Metformin pathways: pharmacokinetics and pharmacodynamics. Pharmacogenet Genomics. 2012 Nov;22(11):820-7. doi: 10.1097/FPC.0b013e3283559b22.
5. Graham GG, Punt J, Arora M, Day RO, Doogue MP, Duong JK, et al. Clinical pharmacokinetics of metformin. Clin Pharmacokinet. 2011 Feb;50(2):81-98. doi: 10.2165/11534750-000000000-00000.
6. Williams HC, Dellavalle RP, Garner S. Acne vulgaris. Lancet. 2012 Jan 28;379(9813):361-72. doi: 10.1016/S0140-6736(11)60321-8. Erratum in: Lancet. 2012 Jan 28;379(9813):314.
7. Gupta A, Sharma YK, Dash KN, Chaudhari ND, Jethani S. Quality of life in acne vulgaris: Relationship to clinical severity and demographic data. Indian J Dermatol Venereol Leprol. 2016 May-Jun;82(3):292-7. doi: 10.4103/0378-6323.173593.
8. Makrantonaki E, Zouboulis CC. Testosterone metabolism to 5alpha-dihydrotestosterone and synthesis of sebaceous lipids is regulated by the peroxisome proliferator-activated receptor ligand linoleic acid in human sebocytes. Br J Dermatol. 2007 Mar;156(3):428-32. doi: 10.1111/j.1365-2133.2006.07671.x.
9. Del Prete M, Mauriello MC, Faggiano A, Di Somma C, Monfrecola G, Fabbrocini G, Colao A. Insulin resistance and acne: a new risk factor for men? Endocrine. 2012 Dec;42(3):555-60. doi: 10.1007/s12020-012-9647-6.
10. Kartal D, Yildiz H, Ertas R, Borlu M, Utas S. Association between isolated female acne and insulin resistance: a prospective study. G Ital Dermatol Venereol. 2016 Aug;151(4):353-7.
11. Rena G, Hardie DG, Pearson ER. The mechanisms of action of metformin. Diabetologia. 2017 Sep;60(9):1577-1585. doi: 10.1007/s00125-017-4342-z. E
12. Sawaya M. Antiandrogens and androgen inhibitors. In: Se W, editor. Comprehensive Dermatologic Drug Therapy. Philadelphia: W.B. Saunders Co.; 2001:385401.
13. Bhambri S, Del Rosso JQ, Bhambri A. Pathogenesis of acne vulgaris: recent advances. J Drugs Dermatol. 2009 Jul;8(7):615-8.
14. Kelly CJ, Gordon D. The effect of metformin on hirsutism in polycystic ovary syndrome. Eur J Endocrinol. 2002 Aug;147(2):217-21. doi: 10.1530/eje.0.1470217.
15. Melnik BC, Schmitz G. Role of insulin, insulin-like growth factor-1, hyperglycaemic food and milk consumption in the pathogenesis of acne vulgaris. Exp Dermatol. 2009 Oct;18(10):833-41. doi: 10.1111/j.1600-0625.2009.00924.x.
16. Danby FW, Jemec GB, Marsch WCh, von Laffert M. Preliminary findings suggest hidradenitis suppurativa may be due to defective follicular support. Br J Dermatol. 2013 May;168(5):1034-9. doi: 10.1111/bjd.12233.
17. Verdolini R, Clayton N, Smith A, Alwash N, Mannello B. Metformin for the treatment of hidradenitis suppurativa: a little help along the way. J Eur Acad Dermatol Venereol. 2013 Sep;27(9):1101-8. doi: 10.1111/j.1468-3083.2012.04668.x.
18. Griffiths CE, Barker JN. Pathogenesis and clinical features of psoriasis. Lancet. 2007 Jul 21;370(9583):263-271. doi: 10.1016/S0140-6736(07)61128-3.
19. Mihaylova MM, Shaw RJ. The AMPK signalling pathway coordinates cell growth, autophagy and metabolism. Nat Cell Biol. 2011 Sep 2;13(9):1016-23. doi: 10.1038/ncb2329.
20. Glossmann H, Reider N. A marriage of two “Methusalem” drugs for the treatment of psoriasis?: Arguments for a pilot trial with metformin as add-on for methotrexate. Dermatoendocrinol. 2013 Apr 1;5(2):252-63. doi: 10.4161/derm.23874.
21. Kaminski MM, Sauer SW, Klemke CD, Süss D, Okun JG, Krammer PH, et al. Mitochondrial reactive oxygen species control T cell activation by regulating IL-2 and IL-4 expression: mechanism of ciprofloxacin-mediated immunosuppression. J Immunol. 2010 May 1;184(9):4827-41. doi: 10.4049/jimmunol.0901662.
22. Krysiak R, Okopien B. Lymphocyte-suppressing and systemic anti-inflammatory effects of high-dose metformin in simvastatin-treated patients with impaired fasting glucose. Atherosclerosis. 2012 Dec;225(2):403-7.
23. Li W, Ma W, Zhong H, Liu W, Sun Q. Metformin inhibits proliferation of human keratinocytes through a mechanism associated with activation of the MAPK signaling pathway. Exp Ther Med. 2014 Feb;7(2):389-392. doi: 10.3892/etm.2013.1416.
24. Liu Y, Yang F, Ma W, Sun Q. Metformin inhibits proliferation and proinflammatory cytokines of human keratinocytes in vitro via mTOR-signaling pathway. Pharm Biol. 2016 Jul;54(7):1173-8. doi: 10.3109/13880209.2015.1057652.
25. Hadi NR, Al-Amran FG, Swadi A. Metformin ameliorates methotrexate-induced hepatotoxicity. J Pharmacol Pharmacother. 2012 Jul;3(3):248-53. doi: 10.4103/0976-500X.99426.

26. Sadik CD, Schmidt E, Zillikens D, Hashimoto T. Recent progresses and perspectives in autoimmune bullous diseases. J Allergy Clin Immunol. 2020 Apr;145(4):1145-1147. doi: 10.1016/j.jaci.2020.02.020.
27. Egami S, Yamagami J, Amagai M. Autoimmune bullous skin diseases, pemphigus and pemphigoid. J Allergy Clin Immunol. 2020 Apr;145(4):1031-1047. doi: 10.1016/j.jaci.2020.02.013.
28. Sadik CD, Miyabe Y, Sezin T, Luster AD. The critical role of C5a as an initiator of neutrophil-mediated autoimmune inflammation of the joint and skin. Semin Immunol. 2018 Jun;37:21-29. doi: 10.1016/j.smim.2018.03.002.
29. Patel CH, Leone RD, Horton MR, Powell JD. Targeting metabolism to regulate immune responses in autoimmunity and cancer. Nat Rev Drug Discov. 2019 Sep;18(9):669-688. doi: 10.1038/s41573-019-0032-5.
30. Owen MR, Doran E, Halestrap AP. Evidence that metformin exerts its anti-diabetic effects through inhibition of complex 1 of the mitochondrial respiratory chain. Biochem J. 2000 Jun 15;348 Pt 3(Pt 3):607-14.
31. Kibsgaard L, Rasmussen M, Lamberg A, Deleuran M, Olesen AB, Vestergaard C. Increased frequency of multiple sclerosis among patients with bullous pemphigoid: a population-based cohort study on comorbidities anchored around the diagnosis of bullous pemphigoid. Br J Dermatol. 2017 Jun;176(6):1486-1491.
32. Seelig E, Meyer S, Timper K, Nigro N, Bally M, Pernicova I, et al. Metformin prevents metabolic side effects during systemic glucocorticoid treatment. Eur J Endocrinol. 2017 Mar;176(3):349-358. doi: 10.1530/EJE-16-0653.
33. Liu X, Sun Z, Wang H. Metformin alleviates experimental colitis in mice by up-regulating TGF-β signaling. Biotech Histochem. 2021 Feb;96(2):146-152. doi: 10.1080/10520295.2020.1776896.
34. Ursini F, Russo E, Pellino G, D'Angelo S, Chiaravalloti A, De Sarro G, et al. Metformin and Autoimmunity: A "New Deal" of an Old Drug. Front Immunol. 2018 Jun 4;9:1236. doi: 10.3389/fimmu.2018.01236.
35. Kulkarni U, Karsten CM, Kohler T, Hammerschmidt S, Bommert K, Tiburzy B, et al. IL-10 mediates plasmacytosis-associated immunodeficiency by inhibiting complement-mediated neutrophil migration. J Allergy Clin Immunol. 2016 May;137(5):1487-1497.e6. doi: 10.1016/j.jaci.2015.10.018.
36. Sezin T, Krajewski M, Wutkowski A, Mousavi S, Chakievska L, Bieber K, et al. The Leukotriene B_4 and its Receptor BLT1 Act as Critical Drivers of Neutrophil Recruitment in Murine Bullous Pemphigoid-Like Epidermolysis Bullosa Acquisita. J Invest Dermatol. 2017 May;137(5):1104-1113. doi: 10.1016/j.jid.2016.12.021.
37. Reddi A, Powers MA, Dellavalle RP. Therapeutic potential of the anti-diabetic agent metformin in targeting the skin cancer stem cell diaspora. Exp Dermatol. 2014 May;23(5):345-6. doi: 10.1111/exd.12349.
38. Sikka A, Kaur M, Agarwal C, Deep G, Agarwal R. Metformin suppresses growth of human head and neck squamous cell carcinoma via global inhibition of protein translation. Cell Cycle. 2012 Apr 1;11(7):1374-82. doi: 10.4161/cc.19798.
39. Cerezo M, Tichet M, Abbe P, Ohanna M, Lehraiki A, Rouaud F, et al. Metformin blocks melanoma invasion and metastasis development in AMPK/p53-dependent manner. Mol Cancer Ther. 2013;12(8):1605-15. doi: 10.1158/1535-7163.MCT-12-1226-T.
40. Chaudhary SC, Kurundkar D, Elmets CA, Kopelovich L, Athar M. Metformin, an antidiabetic agent reduces growth of cutaneous squamous cell carcinoma by targeting mTOR signaling pathway. Photochem Photobiol. 2012 Sep-Oct;88(5):1149-56. doi: 10.1111/j.1751-1097.2012.01165.x.
41. Iliopoulos D, Hirsch HA, Wang G, Struhl K. Inducible formation of breast cancer stem cells and their dynamic equilibrium with non-stem cancer cells via IL6 secretion. Proc Natl Acad Sci U S A. 2011 Jan 25;108(4):1397-402. doi: 10.1073/pnas.1018898108.
42. Hirsch HA, Iliopoulos D, Struhl K. Metformin inhibits the inflammatory response associated with cellular transformation and cancer stem cell growth. Proc Natl Acad Sci U S A. 2013 Jan 15;110(3):972-7. doi: 10.1073/pnas.1221055110.
43. Iliopoulos D, Hirsch HA, Struhl K. Metformin decreases the dose of chemotherapy for prolonging tumor remission in mouse xenografts involving multiple cancer cell types. Cancer Res. 2011 May 1;71(9):3196-201. doi: 10.1158/0008-5472.CAN-10-3471.
44. Martin MJ, Hayward R, Viros A, Marais R. Metformin accelerates the growth of BRAF V600E-driven melanoma by upregulating VEGF-A. Cancer Discov. 2012 Apr;2(4):344-55.
45. Kelly CJ, Gordon D. The effect of metformin on hirsutism in polycystic ovary syndrome. Eur J Endocrinol. 2002 Aug;147(2):217-21. doi: 10.1530/eje.0.1470217.
46. Ibáñez L, López-Bermejo A, Díaz M, Marcos MV, de Zegher F. Early metformin therapy (age 8-12 years) in girls with precocious pubarche to reduce hirsutism, androgen excess, and oligomenorrhea in adolescence. J Clin Endocrinol Metab. 2011 Aug;96(8):E1262-7. doi: 10.1210/jc.2011-0555.
47. Rezvanian H, Adibi N, Siavash M, Kachuei A, Shojaee-Moradie F, Asilian A. Increased insulin sensitivity by metformin enhances intense-pulsed-light-assisted hair removal in patients with polycystic ovary syndrome. Dermatology. 2009;218(3):231-6. doi: 10.1159/000187718.
48. Phiske MM. An approach to acanthosis nigricans. Indian Dermatol Online J. 2014 Jul;5(3):239-49. doi: 10.4103/2229-5178.137765.
49. Hermanns-Lê T, Scheen A, Piérard GE. Acanthosis nigricans associated with insulin resistance : pathophysiology and management. Am J Clin Dermatol. 2004;5(3):199-203. doi: 10.2165/00128071-200405030-00008.
50. Walling HW, Messingham M, Myers LM, Mason CL, Strauss JS. Improvement of acanthosis nigricans on isotretinoin and metformin. J Drugs Dermatol. 2003 Dec;2(6):677-81.
51. Atabek ME, Pirgon O. Use of metformin in obese adolescents with hyperinsulinemia: a 6-month, randomized, double-blind, placebo-controlled clinical trial. J Pediatr Endocrinol Metab. 2008 Apr;21(4):339-48. doi: 10.1515/jpem.2008.21.4.339.
52. Barbato MT, Criado PR, Silva AK, Averbeck E, Guerine MB, Sá NB. Association of acanthosis nigricans and skin tags with insulin resistance. An Bras Dermatol. 2012 Jan-Feb;87(1):97-104. doi: 10.1590/s0365-05962012000100012.
53. Belisle ES, Park HY. Metformin: a potential drug to treat hyperpigmentation disorders. J Invest Dermatol. 2014 Oct;134(10):2488-2491. doi: 10.1038/jid.2014.245.
54. Park HY, Lee J, González S, Middelkamp-Hup MA, Kapasi S, Peterson S, et al. Topical application of a protein kinase C inhibitor reduces skin and hair pigmentation. J Invest Dermatol. 2004 Jan;122(1):159-66.
55. Batchuluun B, Inoguchi T, Sonoda N, Sasaki S, Inoue T, Fujimura Y, et al. Metformin and liraglutide ameliorate high glucose-induced oxidative stress via inhibition of PKC-NAD(P)H oxidase pathway in human aortic endothelial cells. Atherosclerosis. 2014 Jan;232(1):156-64.
56. Lehraiki A, Abbe P, Cerezo M, Rouaud F, Regazzetti C, Chignon-Sicard B, et al. Inhibition of melanogenesis by the antidiabetic metformin. J Invest Dermatol. 2014 Oct;134(10):2589-2597. doi: 10.1038/jid.2014.202.

International Journal of Biomedicine 12(4) (2022) 526-529
http://dx.doi.org/10.21103/Article12(4)_RA5

SHORT REVIEW

INTERNATIONAL JOURNAL OF BIOMEDICINE

Hair Loss and Androgen's Role in the Era of COVID-19

Ramadan S. Hussein[1, 2*]

[1]*Department of Internal Medicine, College of Medicine, Prince Sattam Bin Abdulaziz University, Al-Kharj, Saudi Arabia*
[2]*Department of Dermatology, Andrology and STDs, Assuit Police Hospital, Assuit, Egypt*

Abstract

The new coronavirus (SARS-COV2), which causes coronavirus illness, has expanded globally, impacting millions of individuals. In comparison to female patients, males have a higher prevalence, morbidity, and death rate from this condition, according to international statistics. Androgens have been implicated in the pathophysiology of COVID-19. This review's objective is to explain the potential connection between the pathophysiology of androgen and the infectivity mechanism of the coronavirus as well as the association between SARS-COV2 and hair disorders. This might assist in clarifying androgen's involvement in COVID-19 prognosis and therapy. (**International Journal of Biomedicine. 2022;12(4):526-529.**).

Keywords: COVID-19 • androgen • androgenetic alopecia • hair loss

For citation: Hussein RS. Hair Loss and Androgen's Role in the Era of COVID-19. International Journal of Biomedicine. 2022;12(4):526-529. doi:10.21103/Article12(4)_RA5.

Abbreviations

AR, androgen receptor; **ACE2**, angiotensin-converting enzyme 2; **AGA**, androgenetic alopecia; **CAG**, cysteine-adenine-guanine; **DHT**, dihydrotestosterone; **TMPRSS2**, transmembrane serine protease 2.

Introduction

The new coronavirus (SARS-COV2), which causes coronavirus illness, has expanded globally, impacting millions of individuals.[1] SARS-CoV-2-infected males are more likely to be admitted to the ICU than females – the most common observation.[2] Several investigations have revealed that the virus's cellular entrance is aided by angiotensin-converting enzyme 2 (ACE2) and transmembrane serine protease 2 (TMPRSS2).[3] Androgens promote TMPSS2 gene expression, so COVID-19 illness has also been associated with alterations in androgen sensitivity. Androgenetic alopecia (AGA) has been connected to developing severe COVID-19, particularly in admitted patients. The role of androgen and anti-androgenic drugs could be important in the pathophysiology and management of SARS-COV2.[4] The PRISMA checklist was used to carry out this review, based on scientific articles published between 2020 and 2022 in English databases such as PubMed and Google Scholar with the keywords "SARS-COV2," "androgens," "hair loss," and "TMPSS2." We chose papers from a vast number of publications based on the role of androgens and TMPSS2 in the infectivity mechanism of the current COVID-19 virus pandemic and the therapeutic potential of anti-androgenic drugs.[5]

SARS-CoV-2 pathophysiology

SARS-CoV-2 is a member of the beta-coronavirus genus, which involves enclosed, infectious single-strand RNA viruses with similar shapes.[2] The bat is the most probable main host of coronavirus, which is why it is referred to as a zoonotic virus. By activating spike proteins with the enzyme TMPSS2 and binding to ACE2 receptors, the novel coronavirus infects host cells. The virus's cellular entrance is aided by ACE2 and TMPSS2. Androgens increase the *TMPSS2* gene expression.[4]

Possible impact of androgen on COVID-19 pathogenesis

The expression of the TMPSS2 geneis enhanced by androgens and decreased by androgen deprivation treatment. [4] The production of testosterone and TMPPRSS2 modifies the

***Corresponding author**: Ramadan S. Hussein. Department of Internal Medicine, College of Medicine, Prince Sattam bin Abdulaziz University, Al-Kharj, Saudi Arabia. E-mail: ramadangazeera@yahoo.com*

tendency of the new coronavirus infection of cells and the affinity of the spike proteins to bind to ACE2 receptors. Androgens exert their effects by binding to the androgen receptors (Ars), also known as nuclear receptors, encoded by the AR gene located in chromosome Xq11-12. Variants of this gene have varying androgen responses.[5] Because androgens increase the AR transcriptional activity, it is hypothesized that androgen-deficient individuals would have a decreased amount of active ARs; consequently, the transcription potential of TMPRSS2 will be diminished, and the possibility of new coronavirus entry into host cells will be reduced.[6] Androgen deficiency is associated with systemic inflammation and high amounts of pro-inflammatory cytokines in young and aged men.[7,8] Furthermore, there is evidence that even when testosterone levels are low, interpersonal differences in AR susceptibility caused by CAG polymorphisms may produce sensitivity.[9] The AR has 3 key domains: the DNA-binding domain, the ligand-binding domain, and the transactivation domain. The polymorphism of CAG triplet repeat (polyCAG), in the N-terminal transactivation domain of the AR protein, has been involved either in endocrine or neurological disorders in humans. Elevated AR expression may raise the risk of severe COVID-19 infection by stimulating TMPRSS2 transcription. In addition, the length of CAG repeats was identified as a potential reason for racial disparities in COVID-19 mortality rates.[10,11]

The possible link between COVID-19 and AGA, gray hairs, and trichodynia

Testosterone and DHT stimulate AR activity. Activated AR regulates the transcription of the *TMPRSS2* gene. SARS-CoV-2 engages ACE2 as the entry receptor and uses TMPRSS2 for spike protein priming.[12] In a population-based investigation, individuals with prostate cancer who had androgen restriction therapy were partly protected against COVID-19.[13] Thus, the dermatological symptoms of AR hyperactivation, such as AGA, might identify people at a greater risk for adverse consequences of COVID-19. AGA is the most common cause of moderate and severe alopecia in adults, accounting for the majority of reported cases, and this reflects the DHT level and AR sensitivity.[14] Gray hair and AGA were previously linked to an increased risk of cardiovascular disease, a recognized risk factor for COVID-19 with a poor prognosis.[15,16] In contrast, severe stress may accelerate the loss of melanocyte stem cells, leading to premature graying of the hair. Additionally, diffuse hair graying and telogen effluvium should be explored as COVID-19 side effects. Scalp allodynia has not been a common occurrence.[17]

Telogen effluvium pathophysiology in SARS-CoV-2 patients

Numerous conditions may cause pathologically excessive hair loss. Regardless of the source, the follicle tends to act similarly. While post-infectious hair disorders have been conventionally classified as telogen effluvium, they might have various pathophysiological causes and clinical characteristics. Depending on the nature and severity of the injury, the infection may cause either early-onset dystrophic anagen effluvium or late-onset telogen effluvium in the hair follicle. There have been isolated cases of dystrophic anagen and telogen effluvium associated with COVID-19; however, the former has yet to be verified by hair light microscopy. In a study performed by M. Shanshal, trichogram, of dystrophic anagen was compatible with telogen effluvium.[18] In a study by Domínguez-Santás et al., in 10 individuals with COVID-19, the onset and intensity of post-infectious hair loss were correlated with the disease's clinical severity, and fever was observed.[19] In general, hair loss is attributable to a multi-systemic, febrile inflammatory condition. To date, the etiology of hair loss in COVID-19 has not yet been understood. A pathogenic inflammatory response at the hair follicle level, or a direct invasion of the hair follicle by SARS-CoV-2, causing inflammation and cell death, has yet to be demonstrated. Interleukin-6 (IL-6), a pro-inflammatory cytokine implicated in severe COVID-19, may have a role in hair loss, according to one idea. It is believed that IL-6 contributes to hair loss by suppressing the elongation of hair shafts and the development of hair follicles.[20,21] Only a few COVID-19 patients needed hospitalization in the included trials, indicating that hair loss was most prevalent in people with moderate disease. Given the significant female predominance among individuals with hair loss, female sex hormones like estrogen and progestin could potentially play an important role in the pathophysiology behind hair loss. Estrogens and progesterone have anti-inflammatory and immunomodulating properties, suppressing pro-inflammatory cytokines.[22,23] Research is now being conducted to reuse estrogens and progestin for COVID-19 therapy.[24] Estrogen and progestin also have a protective effect on the hair follicle. Through its receptors, estradiol is known to influence hair follicle development and the hair cycle. At the same time, progestin might reduce testosterone transformation to DHT, an active metabolite of androgen that causes hair loss.[25] As a result, hair loss in female COVID-19 patients may be attributed to an acute insult caused by the viral infection, which causes a substantial decline in serum estrogens and progestin levels in female patients.

Anti-androgens impact on COVID-19 treatment

The androgen function may be significant in SARS-CoV-2 management. ARs regulate nitric oxide (NO) synthesis and activity to a certain degree, and blocking these receptors reduces NO synthesis. Moreover, NO suppresses the activities of adrenoceptor enhancers that might change the transcription of the TMPRSS2 and ACE2 genes, decreasing the virus's capacity to infiltrate host cells. NO has been shown to suppress SARS-COV-2 multiplication and also affects the virus spike proteins and their connections with ACE2, indicating that it serves many purposes in COVID-19. These data revealed that testosterone pathways are most likely the primary mechanism causing the reported NO beneficial impact. Dexamethasone, a steroid, decreased fatality by one-third in ventilated patients and one-fifth in oxygen-treatment patients without ventilators.[26] Dexamethasone has been found to suppress testosterone production in human patients and animal models. Lower testosterone levels might contribute to dexamethasone's beneficial effects, but these preliminary findings should be interpreted with care.[27] Testosterone blockers have been effective in reducing ACE2 levels, showing the utility of this strategy. Anti-androgen drugs that demonstrated therapeutic promise in current clinical studies are 5-reductase inhibitors (dutasteride, finasteride), AR blockers (apalutamide, cyproterone, spironolactone), and TMPRSS2 blockers. Anti-

androgen drugs that have shown therapeutic promise in recent clinical studies are 5-reductase inhibitors, AR blockers, and TMPRSS2 blockers (camostat, nafamostat, bromhexine).[28]

Conclusion

Androgen activity affects the *TMPRSS2* gene. As the *ACE2* and *TMPRSS2* genes are required for SARS-CoV-2 to enter host cells, they might be utilized as COVID-19 targeted therapies. The effects of androgen on TMPRSS2 may explain the reduced risk of mortality in teenagers and the gender differences in COVID-19 illness. The severity of AGA and hair loss may be considered a prognostic factor in COVID-19 infection. Even though there is still a considerable measure of the potential for the establishment of COVID-19 therapies based on androgen deprivation, ongoing studies will provide crucial information that will lead to improved management alternatives.

Acknowledgment

This publication was supported by the Deanship of Scientific Research at Prince Sattam bin Abdulaziz University.

Competing Interests

The authors declare that they have no competing interests.

References

1. World Health Organization; 2020. Coronavirus disease (COVID-19): situation report, 51. Geneva: Available from: https://apps.who.int/iris/handle/10665/331475.
2. Castagnoli R, Votto M, Licari A, Brambilla I, Bruno R, Perlini S, Rovida F, Baldanti F, Marseglia GL. Severe Acute Respiratory Syndrome Coronavirus 2 (SARS-CoV-2) Infection in Children and Adolescents: A Systematic Review. JAMA Pediatr. 2020 Sep 1;174(9):882-889. doi: 10.1001/jamapediatrics.2020.1467.
3. Jian L, Yi W, Zhang N, Wen W, Krysko O, Song WJ, Bachert C. Perspective: COVID-19, implications of nasal diseases and consequences for their management. J Allergy Clin Immunol. 2020 Jul;146(1):67-69. doi: 10.1016/j.jaci.2020.04.030.
4. Bennani NN, Bennani-Baiti IM. Androgen deprivation therapy may constitute a more effective COVID-19 prophylactic than therapeutic strategy. Ann Oncol. 2020 Nov;31(11):1585-1586. doi: 10.1016/j.annonc.2020.08.2095.
5. Lu NZ, Wardell SE, Burnstein KL, Defranco D, Fuller PJ, Giguere V, Hochberg RB, McKay L, Renoir JM, Weigel NL, Wilson EM, McDonnell DP, Cidlowski JA. International Union of Pharmacology. LXV. The pharmacology and classification of the nuclear receptor superfamily: glucocorticoid, mineralocorticoid, progesterone, and androgen receptors. Pharmacol Rev. 2006 Dec;58(4):782-97. doi: 10.1124/pr.58.4.9.
6. Rastrelli G, Di Stasi V, Inglese F, Beccaria M, Garuti M, Di Costanzo D, Spreafico F, Greco GF, Cervi G, Pecoriello A, Magini A, Todisco T, Cipriani S, Maseroli E, Corona G, Salonia A, Lenzi A, Maggi M, De Donno G, Vignozzi L. Low testosterone levels predict clinical adverse outcomes in SARS-CoV-2 pneumonia patients. Andrology. 2021 Jan;9(1):88-98. doi: 10.1111/andr.12821.
7. Bobjer J, Katrinaki M, Tsatsanis C, Lundberg Giwercman Y, Giwercman A. Negative association between testosterone concentration and inflammatory markers in young men: a nested cross-sectional study. PLoS One. 2013 Apr 18;8(4):e61466. doi: 10.1371/journal.pone.0061466.
8. Maggio M, Basaria S, Ceda GP, Ble A, Ling SM, Bandinelli S, Valenti G, Ferrucci L. The relationship between testosterone and molecular markers of inflammation in older men. J Endocrinol Invest. 2005;28(11 Suppl Proceedings):116-9.
9. Zitzmann M. The role of the CAG repeat androgen receptor polymorphism in andrology. Front Horm Res. 2009;37:52-61. doi: 10.1159/000175843.
10. Giovannucci E, Stampfer MJ, Krithivas K, Brown M, Dahl D, Brufsky A, Talcott J, Hennekens CH, Kantoff PW. The CAG repeat within the androgen receptor gene and its relationship to prostate cancer. Proc Natl Acad Sci U S A. 1997 Apr 1;94(7):3320-3. doi: 10.1073/pnas.94.7.3320. Erratum in: Proc Natl Acad Sci U S A 1997 Jul 22;94(15):8272.
11. Wambier CG, Goren A, Vaño-Galván S, Ramos PM, Ossimetha A, Nau G, Herrera S, McCoy J. Androgen sensitivity gateway to COVID-19 disease severity. Drug Dev Res. 2020 Nov;81(7):771-776. doi: 10.1002/ddr.21688.
12. McCoy J, Wambier CG, Vano-Galvan S, Shapiro J, Sinclair R, Ramos PM, Washenik K, Andrade M, Herrera S, Goren A. Racial variations in COVID-19 deaths may be due to androgen receptor genetic variants associated with prostate cancer and androgenetic alopecia. Are anti-androgens a potential treatment for COVID-19? J Cosmet Dermatol. 2020 Jul;19(7):1542-1543. doi: 10.1111/jocd.13455.
13. Montopoli M, Zumerle S, Vettor R, Rugge M, Zorzi M, Catapano CV, Carbone GM, Cavalli A, Pagano F, Ragazzi E, Prayer-Galetti T, Alimonti A. Androgen-deprivation therapies for prostate cancer and risk of infection by SARS-CoV-2: a population-based study (N = 4532). Ann Oncol. 2020 Aug;31(8):1040-1045. doi: 10.1016/j.annonc.2020.04.479.
14. Goren A, Vaño-Galván S, Wambier CG, McCoy J, Gomez-Zubiaur A, Moreno-Arrones OM, Shapiro J, Sinclair RD, Gold MH, Kovacevic M, Mesinkovska NA, Goldust M, Washenik K. A preliminary observation: Male pattern hair loss among hospitalized COVID-19 patients in Spain - A potential clue to the role of androgens in COVID-19 severity. J Cosmet Dermatol. 2020 Jul;19(7):1545-1547. doi: 10.1111/jocd.13443.
15. ElFaramawy AAA, Hanna IS, Darweesh RM, Ismail AS, Kandil HI. The degree of hair graying as an independent risk marker for coronary artery disease, a CT coronary angiography study. Egypt Heart J. 2018 Mar;70(1):15-19. doi: 10.1016/j.ehj.2017.07.001.
16. Trieu N, Eslick GD. Alopecia and its association with coronary heart disease and cardiovascular risk factors: a meta-analysis. Int J Cardiol. 2014 Oct 20;176(3):687-95. doi: 10.1016/j.ijcard.2014.07.079.
17. Zhang B, Ma S, Rachmin I, He M, Baral P, Choi S, Gonçalves WA, Shwartz Y, Fast EM, Su Y, Zon LI, Regev A, Buenrostro JD, Cunha TM, Chiu IM, Fisher DE, Hsu YC. Hyperactivation of sympathetic nerves drives depletion of melanocyte stem cells. Nature. 2020 Jan;577(7792):676-681. doi: 10.1038/s41586-020-1935-3.

18. Shanshal M. COVID-19 related anagen effluvium. J Dermatolog Treat. 2022 Mar;33(2):1114-1115. doi: 10.1080/09546634.2020.1792400.
19. Domínguez-Santás M, Haya-Martínez L, Fernández-Nieto D, Jiménez-Cauhé J, Suárez-Valle A, Díaz-Guimaraens B. Acute telogen effluvium associated with SARS-CoV-2 infection. Aust J Gen Pract. 2020 Aug 26;49. doi: 10.31128/AJGP-COVID-32.
20. Grifoni E, Valoriani A, Cei F, Lamanna R, Gelli AMG, Ciambotti B, Vannucchi V, Moroni F, Pelagatti L, Tarquini R, Landini G, Vanni S, Masotti L. Interleukin-6 as prognosticator in patients with COVID-19. J Infect. 2020 Sep;81(3):452-482. doi: 10.1016/j.jinf.2020.06.008.
21. Kwack MH, Ahn JS, Kim MK, Kim JC, Sung YK. Dihydrotestosterone-inducible IL-6 inhibits elongation of human hair shafts by suppressing matrix cell proliferation and promotes regression of hair follicles in mice. J Invest Dermatol. 2012 Jan;132(1):43-9. doi: 10.1038/jid.2011.274.
22. Mauvais-Jarvis F, Klein SL, Levin ER. Estradiol, Progesterone, Immunomodulation, and COVID-19 Outcomes. Endocrinology. 2020 Sep 1;161(9):bqaa127. doi: 10.1210/endocr/bqaa127.
23. Al-Kuraishy HM, Al-Gareeb AI, Faidah H, Al-Maiahy TJ, Cruz-Martins N, Batiha GE. The Looming Effects of Estrogen in Covid-19: A Rocky Rollout. Front Nutr. 2021 Mar 18;8:649128. doi: 10.3389/fnut.2021.649128.
24. Lovre D, Bateman K, Sherman M, Fonseca VA, Lefante J, Mauvais-Jarvis F. Acute estradiol and progesterone therapy in hospitalised adults to reduce COVID-19 severity: a randomised control trial. BMJ Open. 2021 Nov 30;11(11):e053684. doi: 10.1136/bmjopen-2021-053684.
25. Grymowicz M, Rudnicka E, Podfigurna A, Napierala P, Smolarczyk R, Smolarczyk K, Meczekalski B. Hormonal Effects on Hair Follicles. Int J Mol Sci. 2020 Jul 28;21(15):5342. doi: 10.3390/ijms21155342.
26. RECOVERY Collaborative Group, Horby P, Lim WS, Emberson JR, Mafham M, Bell JL, Linsell L, Staplin N, Brightling C, Ustianowski A, Elmahi E, Prudon B, Green C, Felton T, Chadwick D, Rege K, Fegan C, Chappell LC, Faust SN, Jaki T, Jeffery K, Montgomery A, Rowan K, Juszczak E, Baillie JK, Haynes R, Landray MJ. Dexamethasone in Hospitalized Patients with Covid-19. N Engl J Med. 2021 Feb 25;384(8):693-704. doi: 10.1056/NEJMoa2021436.
27. Mohamed MS, Moulin TC, Schiöth HB. Sex differences in COVID-19: the role of androgens in disease severity and progression. Endocrine. 2021 Jan;71(1):3-8. doi: 10.1007/s12020-020-02536-6.
28. Ghazizadeh Z, Majd H, Richter M, Samuel R, Zekavat SM, Asgharian H, Farahvashi S, Kalantari A, Ramirez J, Zhao H, Natarajan P, Goodarzi H, Fattahi F. Androgen Regulates SARS-CoV-2 Receptor Levels and Is Associated with Severe COVID-19 Symptoms in Men. bioRxiv [Preprint]. 2020 May 15:2020.05.12.091082. doi: 10.1101/2020.05.12.091082.

International Journal of Biomedicine 12(4) (2022) 530-534
http://dx.doi.org/10.21103/Article12(4)_OA1

ORIGINAL ARTICLE

Internal Medicine

INTERNATIONAL JOURNAL OF BIOMEDICINE

The Peculiarities of Six-Minute Walk Test in Patients with Chronic Obstructive Pulmonary Disease, Some with Normal Weight and Some Overweight

Evgeniy S. Ovsyannikov*, Andrey V. Budnevsky, Lilia A. Titova, Anastasia S. Ivanova, Anastasia S. Kachur

Voronezh State Medical University named after N.N. Burdenko
Voronezh, Russia

Abstract

Background: The combination of chronic obstructive pulmonary disease (COPD) and overweight/obesity is a common clinical situation in modern healthcare. The objective of this study was to conduct a comparative analysis of exercise tolerance in normal body weight (NBW) and overweight patients with COPD in the 6MWT using the original device for cardiorespiratory analysis and a method for assessing the cardiorespiratory condition.

Methods and Results: The study included 194 patients with COPD. The patients were divided into two groups. Group 1 consisted of 96 COPD patients with NBW: 77(80.21%) men and 19(19.79%) women aged 41 to 73 years (mean age of 63.33 ± 8.44 years). Group 2 consisted of 98 overweight COPD patients: 74(75.51%) men and 24(24.49%) women aged 55 to 71 (mean age of 64.84 ± 5.46 years). To assess tolerance to physical activity and to objectify the functional status of patients, the 6MWT was used and carried out according to generally accepted principles. The distance covered in 6 minutes (6MWD) was measured in meters and compared with the proper 6MWD(i). The developed device for cardiorespiratory analysis was used to obtain the most accurate 6MWT result. All patients in the study groups underwent an analysis of the composition of the body by the bioelectrical impedance method using a fat mass analyzer BC-555 (Tanita Corporation, Tokyo, Japan). The percentages of fat, water, muscle mass (MM), and bone mass were evaluated.

The average value of the 6MWD/6MWD(i) ratio in COPD patients with NBW was significantly lower than in COPD patients with overweight (P=0.0121). Before the test, the study groups did not differ in the level of SpO_2. However, according to the results of comparative analysis, this parameter was significantly lower in patients with NBW immediately after the 6MWT (P=0.0000), which, along with a lower value of the distance traveled as a percentage of the proper value in Group 1 patients, may indicate a lower tolerance to physical activity in COPD patients with NBW than in patients with overweight. In COPD patients with NBW, the percentage of fat and MM were significantly lower than in COPD patients with overweight (P=0.0000 in both cases). There was a direct correlation between 6MWD and body mass index (r=0.56, P=0.003) and between 6MWD and MM percentage (r=0.59, P=0.016).

Conclusion: Higher exercise tolerance is found in overweight COPD patients than in COPD patients with NBW. This phenomenon can be explained to some extent by the compositional components of the body, in particular, by a significantly lower percentage of lean MM in patients with NBW.(**International Journal of Biomedicine. 2022;12(4):530-534.**).

Keywords: chronic obstructive pulmonary disease • overweight • six-minute walk test

For citation: Ovsyannikov ES, Budnevsky AV, Titova LA, Ivanova AS, Kachur AS. The Peculiarities of Six-Minute Walk Test in Patients with Chronic Obstructive Pulmonary Disease, Some with Normal Weight and Some Overweight. International Journal of Biomedicine. 2022;12(4):530-534. doi:10.21103/Article12(4)_OA1.

Abbreviations

6MWT, six-minute walk test; **BMI**, body mass index; **COPD**, chronic obstructive pulmonary disease; **HR**, heart rate; **HC**, hip circumference; **MM**, muscle mass; **NBW**, normal body weight; **WC**, waist circumference.

Introduction

The combination of chronic obstructive pulmonary disease (COPD) and overweight/obesity is a common clinical situation in modern healthcare.[1] Over the past decade, a significant prevalence of obesity among COPD patients, compared with the general population of patients, has been established, which is one of the urgent problems of medicine.[2] Due to the significant increase in the prevalence of this combination of diseases, it is necessary to evaluate possible outcomes in patients with COPD and obesity.[1]

Obesity in non-COPD patients impacts lung function and is associated with dyspnea and reduced exercise capacity.[1] Also, the presence of obesity in COPD patients is accompanied by a more pronounced decrease in physical activity and an increase in the frequency of hospitalizations, in contrast to COPD patients with normal body weight (NBW).[3]

However, recent studies have shown that COPD patients with overweight/obese who have a higher lean MM have an advantage in terms of survival compared to non-obese patients.[1,3] In addition, it should be noted that COPD patients with a higher BMI may more often experience shortness of breath and activity restrictions, but it has been found that they have a relatively greater tolerance for physical activity than patients with normal BMI; however, the reason for this is not fully understood.[1,2]

Currently, spirometry is the main method of diagnosing COPD GOLD, 2021).[3] However, spirometry data do not entail an assessment of changes in patient's quality of life with COPD and weakly correlate with the severity of shortness of breath, exercise tolerance, and general health.[2,4] A simple and reproducible 6MWT can be used to determine additional functional criteria, such as exercise tolerance.[5]

The objective of this study was to conduct a comparative analysis of exercise tolerance in NBW and overweight patients with COPD in the 6MWT using the original device for cardiorespiratory analysis and a method for assessing the cardiorespiratory condition.

Materials and Methods

The study included 194 patients with COPD (GOLD 3-4, group D). The diagnosis of COPD was established in accordance with GOLD, revision 2021, based on a comprehensive assessment of the symptoms of the disease, anamnesis data, objective status data, and spirometry.[5] The patients were divided into two groups. Group 1 consisted of 96 COPD patients with NBW: 77(80.21%) men and 19(19.79%) women aged 41 to 73 years (mean age of 63.33±8.44 years). Group 2 consisted of 98 overweight COPD patients: 74(75.51%) men and 24(24.49%) women aged 55 to 71 (mean age of 64.84±5.46 years). The presence of normal or overweight was determined by BMI. 18.5-24.99 kg/m^2 – NBW, 25.0-29.99 kg/m^2 – overweight.

The criteria for exclusion from the study were: 1) participation of the patient in any intervention study, 2) COPD in the acute stage, 3) concomitant diseases of the lungs, 4) concomitant diseases of other organs and systems, such as acute cardiac pathology, chronic heart insufficiency with reduced ejection fraction, and chronic renal or hepatic insufficiency.

To assess tolerance to physical activity and to objectify the functional status of patients, the 6MWT was used and carried out according to generally accepted principles. The distance covered in 6 minutes (6MWD) was measured in meters and compared with the proper 6MWD(i). The 6MWD(i) was calculated according to the formulas, which consider age and BMI. The value of 6MWD(i) for men: 6MWD(i) = 1,140 m – (5.61 × BMI) – (6.94 × age). The value of 6MWD (i) for women: 6MWD (i) = 1,017 m – (6.24 × BMI) – (5.83 × age).[6]

In addition, we solved the problem of creating a device that gives the most accurate 6MWT result, ensuring its high safety. The device for cardiorespiratory analysis that we developed contains a housing with a control unit and an infrared pulse oximetry sensor mounted on it to measure the pulse rate and blood oxygenation. The body of the device is made in the form of a telescopic cane equipped with a handle. At the end of the cane, there is a wheel block in the form of a wheel and a sensor for counting wheel revolutions attached to it. When a submaximal HR (75% of the maximum for a given age) is reached or the oxygen saturation level decreases (<86%), a warning message appears on the device screen, and the test stops. An increase in the accuracy of measurements is achieved in the process of conducting a study and assessing the dynamics of changes in the parameters of the cardiovascular and respiratory systems when performing a test with a load.[7] All patients in the study groups underwent an analysis of the composition of the body by the bioelectrical impedance method using a fat mass analyzer BC-555 (Tanita Corporation, Tokyo, Japan). The percentages of fat, water, MM, and bone mass were evaluated.

The study was conducted in accordance with ethical principles of the WMA Declaration of Helsinki (1964, ed. 2013) and approved by the Ethics Committee of Voronezh State Medical University named after N. N. Burdenko. Written informed consent was obtained from all participants.

Statistical analysis was performed using STATGRAPHICS Plus 5.1. For descriptive analysis, results were presented as mean±standard deviation (SD). Inter-group comparisons were performed using One-Way ANOVA. Group comparisons with respect to categorical variables were performed using chi-square test. Pearson's correlation coefficient (r) was used to determine the strength of the relationship between the two continuous variables. A probability value of $P<0.05$ was considered statistically significant.

Results

Groups 1 and 2 were comparable in sex ($P=0.0817$) and age ($P=0.17$), as well as in relation to the use of long-acting anticholinergic drugs ($P=0.12$), long-acting β2-agonists ($P=0.15$), inhaled corticosteroids ($P=0.53$), and short-acting β2-agonists ($P=0.19$).

The results of the 6MWT are presented in Table 1. The distance in the 6MWT in COPD patients NBW was less than

in COPD overweight patients, but the differences were not statistically significant (*P*=0.7205). At the same time, the average value of the 6MWD/6MWD(i) ratio in COPD patients with NBW was significantly lower than in COPD patients with overweight (*P*=0.0121).

Table 1.

The results of the 6MWT of COPD patients in the study groups.

Parameter	Group 1	Group 2	*P*-value
6MWD, m	252.68±184.44	261.35±151.21	0.7205
6MWD, % of predicted	43.09±30.53	49.78±26.93	0.0121
HR before the test, bpm	87.1±16.2	86.8±18.3	0.9038
HR after the test, bpm	108.3±18.2	116.1±15.8	0.0017
SpO_2 before the test, %	94.7±3.4	93.9±2.5	0.0630
SpO_2 after the test, %	88.3±3.2	93.1±3.4	0.0000

Table 2.

The compositional components of the body of COPD patients in the study groups.

Parameter	Group 1	Group 2	*P*-value
BMI, kg/m^2	23.02±1.97	27.95±1.53	0.0000
% of fat	16.75±7.85	22.44±11.92	0.0001
% of MM	47.78±9.54	56.53±9.76	0.0000
% of water	54.38±4.94	47.19±4.55	0.0000
% of bone mass	4.19±1.05	3.25±1.61	0.0000
WC, cm	87.93±14.09	95.34±16.28	0.0009
HC, cm	96.30±5.35	92.74±23.68	0.1522
WC/HC	0.92±0.14	1.15±0.46	0.0000

Heart rate values in patients in the study groups did not significantly differ before and immediately after the test. At the same time, the average value of the heart rate in COPD patients with NBW was significantly lower than in COPD patients with overweight (*P*=0.0017). At the same time, no excess of submaximal values of this parameter was recorded in any of the subjects during the 6MWT by the device.

Before the test, the study groups did not differ in the level of SpO_2. However, according to the results of comparative analysis, this parameter was significantly lower in patients with NBW immediately after the 6MWT (*P*=0.0000), which, along with a lower value of the distance traveled as a percentage of the proper value in Group 1 patients, may indicate a lower tolerance to physical activity in COPD patients with NBW than in patients with overweight.

The results of a comparative analysis of the compositional components of the body of COPD patients in the study groups, as well as the data of an anthropometric study with the determination of BMI, hip circumference (HC), waist circumference (WC), and their ratios, are presented in Table 2. Thus, in COPD patients with NBW, the percentage of fat and MM were significantly lower than in COPD patients with overweight. The same applies to WC and WC/HC, but not HC, which was unreliably even higher in COPD patients with NBW. At the same time, there was a direct correlation between 6MWD and BMI (r=0.56, *P*=0.003) and between 6MWD and MM percentage (r=0.59, *P*=0.016).

Discussion

In recent years, the relationship between COPD and overweight/obesity has become one of the most discussed problems. It is noted that an increased risk of obesity in COPD patients may be due to a decrease in physical activity and physical performance, both as a result of long-term use of corticosteroids[8] and due to the presence of one of the main manifestations of the disease in a patient – shortness of breath.[9] Concomitant diseases,[10,11] hormonal disorders,[12] and metabolic disorders[13] can play a significant role in the formation of obesity in COPD, which, in combination with additional factors, such as smoking and a sedentary lifestyle, form a patient's reluctance to engage in any type of physical activity.[9] An interesting fact is that many studies that evaluated the effect of overweight/obesity on mortality in COPD were reduced to the same result: higher mortality risks were observed in COPD patients with NBW than in COPD patients with overweight/obesity, as a result of which this phenomenon was called "the obesity paradox."[1,8] It is important to mention that "obesity," regarded in this context in terms of BMI, cannot serve as an accurate indicator, since it only takes into account body weight, without taking into account the amount of metabolically and functionally active fat-free mass, or lean MM.[1,8] One of several theories explaining the "obesity paradox" in one way or another is based precisely on the definition of MM. Its essence lies in the fact that the presence of greater MM in obese patients allows them to better adapt during exacerbations of COPD. Patients with overweight/obesity initially have a greater resource of lean MM and therefore, better tolerate its loss, resulting in their higher chances of survival than COPD patients with NBW.[1] Our study confirmed the fact that the MM percentage in COPD patients with obesity was significantly higher than in COPD patients with NBW. Lean body mass in obese people also has several other benefits, including protection from oxidative and inflammatory stress, affecting the prognosis of COPD patients.[1]

According to GOLD 2021, objectively proven impaired exercise tolerance can be attributed to important predictive factors for assessing the risk of adverse outcomes, and various characteristics of the methods (their simplicity/complexity, availability for implementation at various levels of medical institutions) do not play a role. Thus, it is possible to carry out both simple walking tests, which are easily implemented in the conditions of any medical institution, and complex cardiopulmonary testing in a specialized laboratory. The simplest and most standardized test for assessing the functional physical performance of patients with chronic

respiratory diseases is the 6MWT. It acts as a key study, providing the functional, therapeutic response, and prognostic data. Special training of personnel is not required to perform the 6MWT, which is one of the advantages of this test. In addition, it is considered quite safe and well tolerated by most patients, regardless of the stage of the disease.[14] It is noted in the literature that complications of 6MWT are extremely rare. Various severe symptoms (severe shortness of breath, dizziness, fatigue, chest pain, pain in the legs, a decrease in oxygen saturation to 80%-86%, etc.) may cause termination of the study, but they are not complications.[15] Various parameters are assessed during the 6MWT, including the level of SpO_2, which allows an assessment of oxygen desaturation as a result of exercise. There is a direct correlation between the degree of decrease in SpO_2 and the severity of the disease. The clinical significance of desaturation is undoubted since it is associated with impaired daily physical activity, a faster decrease in FEV1, and, as a result, the progression of COPD and a worse prognosis of the disease.[16] One of the most important criteria for the reliability of SpO_2 measurements is obtaining an adequate signal. In this regard, there is a need to develop and introduce into everyday practice devices that can reliably fix the signal and continuously receive information from a specific sensor during the 6MWT. The device that we have developed meets the stated requirements.

During the 6MWT, the HR is also assessed (before and at the end of the test). An important point is the definition of such a parameter as the restoration of HR, that is, a decrease in HR at rest after the end of the 6MWT. The results of some studies conducted among patients with pulmonary arterial hypertension indicate that insufficiently rapid recovery of HR within the first minute after the end of the 6MWT was associated with negative outcomes (in particular, with high mortality).[17]

Thus, in order to ensure maximum safety of testing with the 6MWT, it is necessary to record and evaluate SpO_2 and HR. The cardiorespiratory analysis device we developed has this capability, while it also automatically monitors the distance traveled, which is the optimal solution to the task.

It should be noted that the distance in meters, covered in 6 minutes, is the main result of the 6MWT, characterized by the presence of a close relationship with clinical outcomes in patients with COPD. Recently, the development and application of proper values of 6MWD have become the most relevant that require further study.[18] In our study, we supplemented the standard 6MWD with the ratio 6MWD/6MWD (i), expressed in percentage, and reflected its significance in the form of reliable detection of differences in the results of 6MWT in COPD patients with NBW or overweight.

In conclusion, one of the main tests for assessing exercise tolerance among COPD patients (of any BMI) is the simple and safe 6MWT. The device we have created allows us to achieve more accurate test results while working in automatic mode with continuous monitoring of the following parameters: HR and oxygen saturation. This feature of the device allows, if necessary, notifying the doctor and the patient about the forced termination of the test. Taking into account the data obtained and presented in this study, it seems reasonable to compare the actual distance traveled by the patient in meters with the proper indicator depending on gender and BMI, expressed as a percentage, when conducting 6MWT. Higher exercise tolerance is found in overweight COPD patients than in COPD patients with NBW. This phenomenon can be explained to some extent by the compositional components of the body, in particular, by a significantly lower percentage of lean MM in patients with NBW. This fact must be considered when compiling complex pulmonary rehabilitation programs for this group of patients,[19] which should include individual recommendations on physical training and nutrition to eliminate the described imbalance.

Competing Interests

The authors declare that they have no competing interests.

References

1. Giri Ravindran S, Saha D, Iqbal I, Jhaveri S, Avanthika C, Naagendran MS, Bethineedi LD, Santhosh T. The Obesity Paradox in Chronic Heart Disease and Chronic Obstructive Pulmonary Disease. Cureus. 2022 Jun 5;14(6):e25674. doi: 10.7759/cureus.25674.
2. Samuleeva YuV, Zadionchenko VS, Li VV, Adasheva TV, Samorukova EI, Pikhlak AE, Logachev VA, Sokolova LB. Obesity and metabolic disorders in COPD patients: opportunities for phenotyping. PULMONOLOGIYA. 2014;(5):32-38. doi: 10.18093/0869-0189-2014-0-5-32-38. [Article in Russian].
3. WHO: Chronic obstructive pulmonary disease (COPD) [May; 2022]; Available from: https://www.who.int/news-room/fact-sheets/detail/chronic-obstructive-pulmonary-disease-(copd)
4. Lavie CJ, De Schutter A, Parto P, Jahangir E, Kokkinos P, Ortega FB, Arena R, Milani RV. Obesity and Prevalence of Cardiovascular Diseases and Prognosis-The Obesity Paradox Updated. Prog Cardiovasc Dis. 2016 Mar-Apr;58(5):537-47. doi: 10.1016/j.pcad.2016.01.008.
5. Global Initiative for Chronic Obstructive Lung Disease (GOLD). Global Strategy for the Diagnosis, Management, and Prevention of Chronic Obstructive Pulmonary Disease: 2022 Report. Available from: https://goldcopd.org/2022-gold-reports/
6. Ots ON, Maliev BM, Chushkin MI, Mandrykin YuV, Yartsev SS. [Use of walk tests in pulmonology]. Ter Arkh. 2012;84(3):62-7. [Article in Russian].
7. Tokmachev RE, Maksimov AV, Budnevsky AV, Batishcheva GA, Ovsyannikov ES, Kravchenko AYa, Kurgalin SD. Device for cardiorespiratory analysis and method for assessing cardiorespiratory condition. Patent RF N 2 637 917. 2017.[In Russian].
8. Chittal P, Babu AS, Lavie CJ. Obesity paradox: does fat alter outcomes in chronic obstructive pulmonary disease? COPD. 2015 Feb;12(1):14-8. doi: 10.3109/15412555.2014.915934.

***Corresponding author**: Prof. Evgeniy S. Ovsyannikov, PhD, ScD. Department of Faculty Therapy, Voronezh State Medical University named after N.N. Burdenko. Voronezh, Russia. E-mail: ovses@yandex.ru*

9. Yohannes AM. The Paradox of Obesity in Patients with Chronic Obstructive Pulmonary Disease. Ann Am Thorac Soc. 2022 Oct;19(10):1638-1639. doi: 10.1513/AnnalsATS.202206-525ED.
10. Budnevsky AV, Malysh EY. [Clinico-Pathogenetic Relationship of Cardiovascular Diseases and Chronic Obstructive Pulmonary Disease]. Kardiologiia. 2017 Apr;57(4):89-93. [Article in Russian].
11. Provotorov VM, Budnevskiĭ AV, Semenkova GG, Shishkina ES. [PROINFLAMMATORY CYTOKINES IN COMBINATION OF CORONARY HEART DISEASE AND CHRONIC OBSTRUCTIVE PULMONARY DISEASE]. Klin Med (Mosk). 2015;93(2):5-9. [Article in Russian].
12. Budnevskiy AV, Tsvetikova LN, Ovsyannikov ES, Goncharenko OV. A role of melatonin for occurrence of chronic obstructive pulmonary disease. Pulmonologiya, 2016, 26(3), 372–378. doi:10.18093/0869901899201662663337223 78. [Article in Russian].
13. Kozhevnikova SA, Budnevskiy AV, Ovsyannikov ES, Belov VN. Particularity of the clinical course and quality of life of patients with chronic obstructive pulmonary disease on the background of the metabolic syndrome. Medical News of North Caucasus. 2017;12(1):20–23. doi:10.14300/mnnc.2017.12006. [Article in Russian].
14. Matos Casano HA, Anjum F. Six Minute Walk Test. 2022 Jun 19. In: StatPearls [Internet]. Treasure Island (FL): StatPearls Publishing; 2022 Jan–. PMID: 35015445.
15. Chikina SYu. The role of the 6-minute walk test in the management of patients with bronchopulmonary diseases. Practical pulmonology. 2015; N4: 34-38. [Article in Russian].
16. van Gestel AJ, Clarenbach CF, Stöwhas AC, Teschler S, Russi EW, Teschler H, Kohler M. Prevalence and prediction of exercise-induced oxygen desaturation in patients with chronic obstructive pulmonary disease. Respiration. 2012;84(5):353-9. doi: 10.1159/000332833.
17. Minai OA, Gudavalli R, Mummadi S, Liu X, McCarthy K, Dweik RA. Heart rate recovery predicts clinical worsening in patients with pulmonary arterial hypertension. Am J Respir Crit Care Med. 2012 Feb 15;185(4):400-8. doi: 10.1164/rccm.201105-0848OC.
18. Singh SJ, Puhan MA, Andrianopoulos V, Hernandes NA, Mitchell KE, Hill CJ, et al. An official systematic review of the European Respiratory Society/American Thoracic Society: measurement properties of field walking tests in chronic respiratory disease. Eur Respir J. 2014 Dec;44(6):1447-78. doi: 10.1183/09031936.00150414.
19. Budnevsky AV, Isaeva YV, Malysh EY, Kozhevnikova SA. [Pulmonary rehabilitation as an effective method for optimizing therapeutic and preventive measures in patients with chronic obstructive pulmonary disease concurrent with metabolic syndrome]. Ter Arkh. 2016;88(8):25-29. doi: 10.17116/terarkh201688825-29. [Article in Russian].

International Journal of Biomedicine 12(4) (2022) 535-538
http://dx.doi.org/10.21103/Article12(4)_OA2

ORIGINAL ARTICLE

Cardiology

INTERNATIONAL JOURNAL OF BIOMEDICINE

Scenarios for Increasing, Decreasing and Stability of Tpe/QT Ratio (Simulation Study)

Natalia V. Arteyeva[1*], Jan E. Azarov[1,2]

[1]*Department of Cardiac Physiology, Institute of Physiology, Komi Science Center, Ural Branch, Russian Academy of Sciences, Syktyvkar, Russia*
[2]*Department of Physiology, Medical Institute of Pitirim Sorokin, Syktyvkar State University, Syktyvkar, Russia*

Abstract

The objective of this simulation was to study the physiological meaning of the novel index for arrhythmic risk stratification – Tpe/QT ratio (the interval from the peak to the end of the T-wave (Tpe) on electrocardiogram divided by QT interval).

Methods and Results: The role of two factors determining Tpe/QT ratio – action potential duration (APD) and dispersion of repolarization (DOR) – was studied *in silico* at two levels: ventricular wall segment and the whole heart ventricles. The simulations performed in the framework of both the segment and the entire ventricles' models showed that Tpe/QT magnitude reflects the dynamic relationship between the longest and the shortest APD rather than the magnitude of DOR, as interval Tpe does. Tpe/QT ratio remained unchanged even at large DOR, provided that the longer the ventricular APD, the greater the gap between the longest and the shortest of them. The imbalance between the longest and the shortest APD values led to the increased or decreased Tpe/QT.

Conclusion: Simulations showed that Tpe/QT is not just a corrected Tpe interval, but it reflects the balance between the longest and the shortest APD in the heart ventricles.(**International Journal of Biomedicine. 2022;12(4):535-538.**).

Keywords: action potential duration • dispersion of repolarization • arrhythmic risk stratification • electrocardiographic index

For citation: Arteyeva NV, Azarov JE. Scenarios for Increasing, Decreasing and Stability of Tpe/QT Ratio (Simulation Study). International Journal of Biomedicine. 2022;12(4):535-538. doi:10.21103/Article12(4)_OA2

Abbreviations

APD, action potential duration; **DOR**, dispersion of repolarization; **Tpe**, Tpeak-Tend interval.

Introduction

Tpeak-Tend interval (Tpe) has been demonstrated to reflect the magnitude of myocardial dispersion of repolarization (DOR),[1-3] which is considered to be one of the major prerequisites for reentrant arrhythmogenesis. However, despite the solid rationale, Tpe utility as the arrhythmic risk marker is not straightforward. In the general population, the association of Tpe with mortality has not been confirmed[4] or appeared to be U-shaped.[5] These complexities warrant further studies of the ECG predictors of arrhythmic risk.

One of the approaches to this problem may be a search for composite markers since they may reflect the interaction between different arrhythmogenic factors, including DOR manifesting as Tpe and action potential duration (APD) manifesting as QT interval. A Tpe/QT ratio has been proposed as an index of ventricular repolarization, which may be useful for arrhythmic risk stratification.[6,7]

However, the physiological meaning of this novel marker remains unclear. Since Tpe and QT reflect DOR and APD, respectively, the Tpe/QT ratio is thought to provide an estimate of DOR with respect to the total duration of repolarization excluding the confounding effects of heart rate variability and inter-individual variation of the QT interval and emphasizing disproportionate amplification of DOR.[7,8] In turn, the disproportionate amplification of DOR should arise from the abnormal proportion between the shortest and

***Corresponding author**: Natalia V. Arteyeva, PhD. Department of Cardiac Physiology, Institute of Physiology, Komi Science Center, Ural Branch, Russian Academy of Sciences, Syktyvkar, Russia. E-mail: natalia.arteyeva@gmail.com*

the longest APD. APD shortening/lengthening depends on heart rate, drug effects, myocardial pathology, etc., and this dependence may not be the same for the shortest (supposedly epicardial) and longest (supposedly endocardial) APD.

The aim of the present simulation study was to test different ways of APD shortening/lengthening and to find out which one of them is associated with the increase, decrease, or constant magnitude of Tpe/QT ratio.

Material and Methods

Morphology of action potentials

The morphology of ventricular action potentials was simulated using the model of a rabbit ventricular myocyte;[9] for each model cell, the duration of repolarization phase of action potential was scaled according to APD value set for this cell.

The effect of APD lengthening on Tpe/QT ratio was studied using two computer models: ventricular wall segment (the simple model, allowing us to exclude the effects of ventricular geometry and complicated sequences of de- and repolarization) as well as the realistic model of the rabbit heart ventricles.

Model of the heart ventricles

The rabbit ventricular model was a realistically shaped cellular automata model based on experimental data.[3] The model consisted of ≈100,000 discrete elements, with realistic 3D gradients of APD and activation times (transmural, apicobasal, anterior-posterior and left-to-right), reconstructed from experimental epicardial and intramural measurements (Fig. 1).

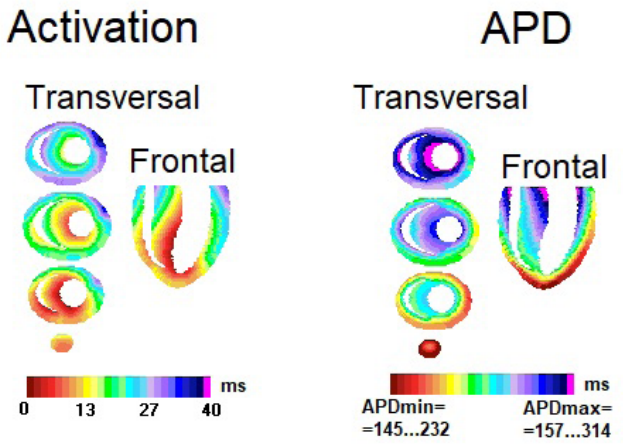

Figure 1. *Realistic activation sequence and APD distribution in the model of the rabbit heart ventricles simulated on the basis of experimental data.*[3]

Ventricular segment model

The segment of the left wall of the rabbit ventricular model consisted of ≈5,000 elements. The difference from the whole ventricular model was that only the transmural gradients of APD and activation times were present (Fig. 2).

APD lengthening

In all simulations, the same initial values of the minimal and maximal APD (APDmin and APDmax, respectively) were used (150 ms and 200 ms for the ventricular segment, 145 ms and 157 ms for the whole ventricle). APDs were prolonged in the following ways (i) proportional changes (i.e., by multiplying all APDs by the same factor), (ii) addition of the same increment to all APDs, (iii) differential changes (by multiplying APDmin and APDmax by different change factors). The change factors for intermediate APD values (neither maximum nor minimum) were calculated by the following:

Ki = Kmin + (Kmax–Kmin)*((APDi–APDmin)/(APDmax–APDmin)),

where Ki – APD change factor for i-th model element; APDi – initial APD magnitude for i-th model element;

Kmax and Kmin – change factors for APDmax and APDmin, respectively.

The moment of the T-wave peak on the simulated ECGs was determined as the instant of the maximal potential value, the T-wave end – as the point of intersection of the baseline and the tangent to the steepest part of the descending part of the T-wave (tangent method).

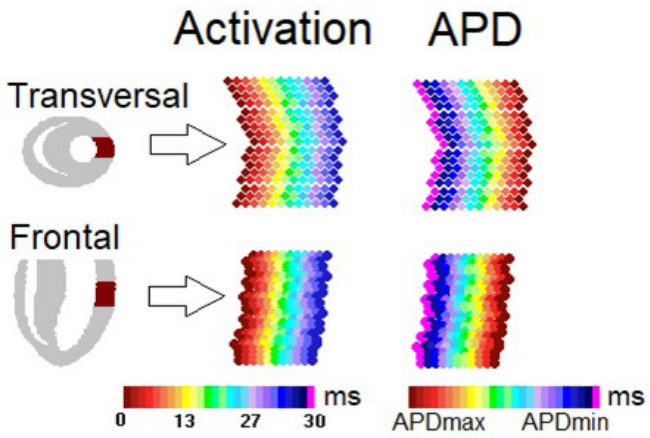

Figure 2. *The simplified activation sequence and APD distribution (only transmural gradients of APD and activation times) in the left ventricular segment of the model of the rabbit heart ventricles.*

Results and Discussion

Segment model: Stable Tpe/QT

The stable Tpe/QT ratio (even at more than twofold increase in APD) was achieved when APDmax was changed 20% less than APDmin (Fig. 3, A), which was accompanied by a moderate increase in the APDmax-APDmin difference and a slight increase in DOR and Tpe. In other words, the stable Tpe/QT ratio required that the longer the APD, the greater the difference between the longest and shortest APDs. And for this, it is necessary that the shortest and the longest APDs change with different rates. These simulation results explain the mechanisms providing a relatively unaltered Tpe/QT ratio in healthy individuals at a wide heart rate range from 60 bpm to 100 bpm.[7]

Segment model: Decreased Tpe/QT

APD prolongation when APDmax-APDmin difference remained constant or decreased was associated with a decrease

in Tpe/QT ratio. These were scenarios where APDmax and APDmin were changed by the same increment (Fig. 3, B), and the scenario where APDmax was prolonging 40% less than APDmin (Fig. 3, C). In scenario B, DOR and Tpe were stable, and the increased QT resulted in the decreased Tpe/QT ratio. In scenario C, the predominant prolongation of APDmin, compared to APDmax, decreased DOR, Tpe, and Tpe/QT ratio. In other words, the decreased Tpe/QT resulted from the less-than-expected difference between the longest and shortest APD in respect to the APD range.

Segment model: Increased Tpe/QT

APD prolongation associated with the steep increase in APDmax-APDmin difference and DOR led to the increase in Tpe/QT ratio (Fig. 3, D-F). This outcome was observed in the scenario with the proportional APDmax and APDmin changing (Fig. 3, D), and in the scenarios with differential APD increase with APDmax being changed 40% (Fig. 3, E) and 20% (Fig. 3, F) more than APDmin.

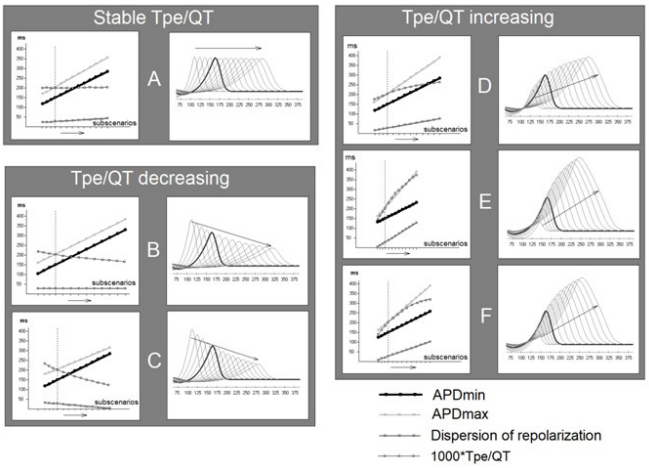

Figure 3. *The changes in morphology of the simulated T-wave and the associated changes in Tpe/QT ratio for different scenarios of APD shortening/prolongation.*

The abscissas show the subscenarios of each scenario, the ordinates – the corresponding values of APDmin, APDmax, DOR and Tpe/QT. For convenience of data presentation, Tpe/QT was scaled by a factor of 1000. The common starting point for all simulation scenarios (APDmin=150 ms, APDmax=205 ms, Tpe/QT=0.2) is indicated by a vertical dotted line, the corresponding "starting" T-wave is highlighted with a thick line.

A – APDmin were changed 20% faster than APDmax; B – APDmax and APDmin were changed by the same increment; C – APDmax was prolonging 40% less than APDmin; D – proportional changes in APDmax and APDmin; E – APDmax were changed 40% faster than APDmin; F – APDmax were changed 20% faster than APDmin.

Whole ventricles' model

The initial APDmin=145 ms and APDmax=157 ms values provided a Tpe/QT ratio of 0.2 in the model of the whole rabbit ventricles (Fig. 4). The stable Tpe/QT ratio was achieved when APDmin was prolonged 40% less than APDmax. The increase in APDmax up to 2 times (from 157 ms to 314 ms) and in APDmin up to 1.6 times (from 145 ms to 232 ms) resulted in an almost threefold increase in DOR (from 46 ms up to 124 ms), while Tpe/QT ratio of the simulated ECG remained constant (Fig.4).

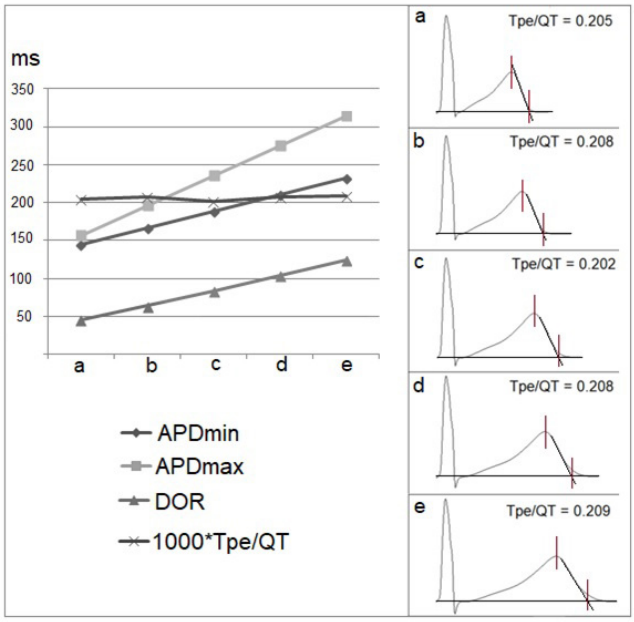

Figure 4. *Progressive APD prolongation in the model of the whole rabbit heart ventricles: APDmax changing 20% faster than APDmin provided stable magnitude of Tpe/QT ratio even at high DOR values.*

*Left panel: APDmax, APDmin, DOR and 1000*Tpe/QT values (for convenience of data presentation, Tpe/QT was scaled by a factor of 1000) in the model. Right panel: the simulated ECGs (lead V2) corresponding to cases a – e on the left panel.*

Both the simplified ventricular segment model and the realistic whole ventricles' model demonstrated that APD prolongation with the moderate increase in the APDmax-APDmin difference due to the different change factors for APDmax and APDmin was associated with the stable Tpe/QT magnitude even at high DOR values.

Experimental confirmation of the simulation results

There are experimental and clinical data that support our simulation findings. In most cases, the increased Tpe/QT is associated with increased Tpe. In this regard, Tpe/QT was considered as an index of DOR.[13] On the other hand, there is clinical evidence that Tpe/QT and Tpe can change differentially. In the febrile period, shortening of QT and Tpe intervals was accompanied by an increase in Tpe/QT ratio.[14] In the patients treated with ziprasidone, Tpe was the same as in the control group, whereas Tpe/QTc was decreased.[15]

The changes of APD and DOR are closely related to each other. However, the contributions of the two variables to arrhythmogenesis can be different. The previous studies from our group[16,17] showed that modification of APD could change the risk of the reentrant arrhythmias independently of DOR. Tpe, QT and Tpe/QT ratio reflecting DOR, APD, and APD range, respectively, may contain independent diagnostic information. Tpe/QT ratio has been demonstrated to have association with clinical outcomes, which was independent of DOR-associated and APD-associated markers. From a large number of ECG

indices (ST-segment elevation/depression, T-wave inversion, presence of Q waves, QT, QTc, QT dispersion, Tpe, Tpe dispersion, Tpe/QT, and QTpeak/QT), it was Tpe/QT ratio that was associated with major adverse cardiovascular events in the acute phase of Takotsubo syndrome.[18]

Limitations of the study

The limitations of the simulations are as follows: (1) The same action potential shape (no epicardial "spikes and domes") was assigned for all ventricular layers; (2) No electrotonic APD flattening and anisotropic fiber architecture was included in the model; (3) The model was based on the nonhuman (rabbit) experimental data, and specific calculated values could not be directly applied in clinical settings. However, the above limitations could hardly affect computation of the Tpe and QT intervals and modify the major findings of the present study.

Conclusion

The present simulation study demonstrates that Tpe/QT ratio reflects rather the relationship between the longest and the shortest APD, than DOR. In conditions of DOR and/or APD changes, the Tpe/QT ratio can be maintained at the same level, if the longest and the shortest APDs change at different rates, and vice versa; Tpe/QT ratio increases or decreases in the cases with a "disbalance" between the longest and the shortest APDs in the heart ventricles. These findings suggest that Tpe/QT ratio might serve as an independent index of arrhythmic risk to be used with other repolarization-related markers, such as Tpe and QT intervals.

Sources of Funding

The study was supported by the Program for Fundamental Research of RAS (2022-2026), Project № 1021052404529-3.

Competing Interests

The authors declare that they have no competing interests.

References

1. Yan GX, Antzelevitch C. Cellular basis for the normal T wave and the electrocardiographic manifestations of the long-QT syndrome. Circulation. 1998 Nov 3;98(18):1928-36. doi: 10.1161/01.cir.98.18.1928.
2. Meijborg VM, Conrath CE, Opthof T, Belterman CN, de Bakker JM, Coronel R. Electrocardiographic T wave and its relation with ventricular repolarization along major anatomical axes. Circ Arrhythm Electrophysiol. 2014 Jun;7(3):524-31. doi: 10.1161/CIRCEP.113.001622.
3. Arteyeva NV, Goshka SL, Sedova KA, Bernikova OG, Azarov JE. What does the T(peak)-T(end) interval reflect? An experimental and model study. J Electrocardiol. 2013 Jul-Aug;46(4):296.e1-8. doi: 10.1016/j.jelectrocard.2013.02.001.
4. Porthan K, Viitasalo M, Toivonen L, Havulinna AS, Jula A, Tikkanen JT, et al. Predictive value of electrocardiographic T-wave morphology parameters and T-wave peak to T-wave end interval for sudden cardiac death in the general population. Circ Arrhythm Electrophysiol. 2013 Aug;6(4):690-6. doi: 10.1161/CIRCEP.113.000356.
5. Bachmann TN, Skov MW, Rasmussen PV, Graff C, Pietersen A, Lind B, et al. Electrocardiographic Tpeak-Tend interval and risk of cardiovascular morbidity and mortality: Results from the Copenhagen ECG study. Heart Rhythm. 2016 Apr;13(4):915-24. doi: 10.1016/j.hrthm.2015.12.027.
6. Alvarado-Serrano C, Ramos-Castro J, Pallàs-Areny R. Novel indices of ventricular repolarization to screen post myocardial infarction patients. Comput Biol Med. 2006 May;36(5):507-15. doi: 10.1016/j.compbiomed.2005.03.003.
7. Gupta P, Patel C, Patel H, Narayanaswamy S, Malhotra B, Green JT, Yan GX. T(p-e)/QT ratio as an index of arrhythmogenesis. J Electrocardiol. 2008 Nov-Dec;41(6):567-74. doi: 10.1016/j.jelectrocard.2008.07.016.
8. Tse G, Yan BP. Traditional and novel electrocardiographic conduction and repolarization markers of sudden cardiac death. Europace. 2017 May 1;19(5):712-721. doi: 10.1093/europace/euw280.
9. Mahajan A, Shiferaw Y, Sato D, Baher A, Olcese R, Xie LH, et al. A rabbit ventricular action potential model replicating cardiac dynamics at rapid heart rates. Biophys J. 2008 Jan 15;94(2):392-410. doi: 10.1529/biophysj.106.98160.
10. Kilicaslan F, Tokatli A, Ozdag F, Uzun M, Uz O, Isilak Z, et al. Tp-e interval, Tp-e/QT ratio, and Tp-e/QTc ratio are prolonged in patients with moderate and severe obstructive sleep apnea. Pacing Clin Electrophysiol. 2012 Aug;35(8):966-72. doi: 10.1111/j.1540-8159.2012.03439.x.
11. Ciobanu A, Tse G, Liu T, Deaconu MV, Gheorghe GS, Ilieşiu AM, Nanea IT. Electrocardiographic measures of repolarization dispersion and their relationships with echocardiographic indices of ventricular remodeling and premature ventricular beats in hypertension. J Geriatr Cardiol. 2017 Dec;14(12):717-724. doi: 10.11909/j.issn.1671-5411.2017.12.001.
12. Korantzopoulos P, Letsas KP, Christogiannis Z, Kalantzi K, Massis I, Milionis HJ, et al. Exercise-induced repolarization changes in patients with stable coronary artery disease. Am J Cardiol. 2011 Jan;107(1):37-40. doi: 10.1016/j.amjcard.2010.08.038.
13. Ozawa T, Ito M, Tamaki S, Yao T, Ashihara T, Kita Y, et al. Gender and age effects on ventricular repolarization abnormality in Japanese general carriers of a G643S common single nucleotide polymorphism for the KCNQ1 gene. Circ J. 2006 Jun;70(6):645-50. doi: 10.1253/circj.70.645.
14. Gökçen E, Savrun A. The impact of fever on myocardial repolarization parameters. J Electrocardiol. 2021 Jan-Feb;64:45-49. doi: 10.1016/j.jelectrocard.2020.11.016.
15. Tümüklü MN, Tümüklü MM, Nesterenko V, Jayathilake K, Beasley CM Jr, Meltzer HY. Twenty-Four-Hour Measures of Heart Rate-Corrected QT Interval, Peak-to-End of the T-Wave, and Peak-to-End of the T-Wave/Corrected QT Interval Ratio During Antipsychotic Treatment. J Clin Psychopharmacol. 2019 Mar-Apr;39(2):100-107. doi: 10.1097/JCP.0000000000001003.
16. Bernikova OG, Durkina AV, Sedova KA, Azarov JE. Determinants of reperfusion arrhythmias: action potential duration versus dispersion of repolarization. J Physiol Pharmacol. 2021 Oct;72(5). doi: 10.26402/jpp.2021.5.04.
17. Bernikova OG, Sedova KA, Durkina AV, Azarov JE. Managing of ventricular reperfusion tachyarrhythmias - focus on a perfused myocardium. J Physiol Pharmacol. 2019 Oct;70(5). doi: 10.26402/jpp.2019.5.11.
18. Braschi A, Frasheri A, Lombardo RM, Abrignani MG, Lo Presti R, Vinci D, Traina M. Association between Tpeak-Tend/QT and major adverse cardiovascular events in patients with Takotsubo syndrome. Acta Cardiol. 2021 Sep;76(7):732-738. doi: 10.1080/00015385.2020.1776012.

International Journal of Biomedicine 12(4) (2022) 539-547
http://dx.doi.org/10.21103/Article12(4)_OA3

ORIGINAL ARTICLE

Orthopedics & Traumatology

INTERNATIONAL JOURNAL OF BIOMEDICINE

Heparin-Conjugated Fibrin Hydrogel with Chondroinductive Growth Factors and Human Synovium-Derived Mesenchymal Stem Cells for the Treatment of Articular Cartilage Defects: Evaluation of Clinical Safety

Tusipkhan Toktarov[1], Bakhtiyar Saginov[1], Yerik Raimagambetov[1], Bagdat Balbossynov[1], Gulzhanat Korganbekova[1], Marat Urazayev[1], Assel Issabekova[2], Gulsamal Zhubanova[2], Guldarigash Kaukabayeva[2], Aliya Sekenova[1], Gulshakhar Kudaibergen[2], Zhanar Akhmetkarimova[2], Saule Eskendirova[2], Yerlan Ramankulov[2,3], Olzhas Bekarissov[1], Arman Batpen[1*], Vyacheslav Ogay[1,2*]

[1]*National Scientific Center of Traumatology and Orthopedics named after Academician N. D. Batpenov*
[2]*Stem Cell Laboratory, National Center for Biotechnology*
[3]*School of Science and Humanities, Nazarbayev University*
Astana, Kazakhstan

Abstract

The purpose of this study was to evaluate the safety of an injectable heparin-conjugated fibrin (HCF) hydrogel containing human synovium-derived mesenchymal stem cells (SDMSCs), TGF-β1, and BMP-4 after implantation into articular cartilage defect in patients with osteoarthritis (OA). The study included 15 OA patients with a mean age of 44.2±18.0 years. The median articular cartilage defect size was 4.9±2.0 cm. HCF hydrogel, containing SDMSCs and growth factors (TGF-β1 and BMP-4), was implanted into the cartilage defect using DUPLOJECT two-syringe device connected with the DUPLOTIP dual lumen cannula. Clinical and radiological outcomes were evaluated with VAS, WOMAC, KOOS, and MOCART. The clinical study results showed that implantation of HCF hydrogel with autologous SDMSCs, TGF-β1, and BMP-4 appeared to be safe and did not show severe adverse events in OA patients. The assessment of clinical outcomes after 6 months showed improvement in VAS, WOMAC, and KOOS scores in all patients. The MOCART evaluation demonstrated an enhancement of cartilage tissue repair in 73.3% of OA patients at 6 months after surgery. Thus, implantation of HCF hydrogel with SDMSCs, TGF-β1, and BMP-4 was safe and demonstrated signs of improvement in articular cartilage repair. The evaluation of the long-term safety and therapeutic efficacy of HCF hydrogel is required in a further clinical study using a larger number of OA patients. (**International Journal of Biomedicine. 2022;12(4):539-547.**).

Keywords: mesenchymal stem cells • fibrin hydrogel • growth factors • cartilage defect • clinical safety

For citation: Toktarov T, Saginov B, Raimagambetov Y, Balbossynov B, Korganbekova G, Urazayev M, Issabekova A, Zhubanova G, Kaukabayeva G, Sekenova A, Kudaibergen G, Akhmetkarimova Zh, Eskendirova S, Ramankulov Y, Bekarissov O, Batpen A, Ogay V. Heparin-Conjugated Fibrin Hydrogel with Chondroinductive Growth Factors and Human Synovium-Derived Mesenchymal Stem Cells for the Treatment of Articular Cartilage Defects: Evaluation of Clinical Safety. International Journal of Biomedicine. 2022;12(4):539-547. doi:10.21103/Article12(4)_OA3.

Abbreviations

ADL, activities of daily living; **AEs**, adverse events; **BMP**, bone morphogenetic proteins; **ECM**, extracellular matrix; **HCF**, heparin-conjugated fibrin; **ICRS**, International Cartilage Repair Society; **KOOS**, Knee Injury and Osteoarthritis Outcome Score; **LMWH**, low-molecular-weight heparin; **MOCART**, Magnetic Resonance Observation of Cartilage Repair Tissue; **MSCs**, mesenchymal stem cells; **MRI**, magnetic resonance imaging; **OA**, osteoarthritis; **QoL,** Quality of Life; **SDMSCs**, synovium-derived mesenchymal stem cells; **SAEs**, severe adverse events; **TGF-β**, transforming growth factor-beta; **VAS**, Visual Analogue Scale; **WOMAC**, Western Ontario and McMaster Universities Osteoarthritis Index.

Introduction

Osteoarthritis (OA) is the most common chronic progressive joint disease, which is a serious general medical and social problem, resulting in substantial economic costs due to the high prevalence and severity of damage to the musculoskeletal system.[1,2] According to WHO, more than 300 million people in 195 countries suffer from this disease, while there is a constant increase in one of the indicators of OA – "the number of years lived by the population in a state of disability."[3] Current methods of managing articular cartilage defects include multiple microfractures, osteochondral autograft transfer, osteochondral allograft transplantation, autologous chondrocyte implantation, and matrix-assisted autologous chondrocyte implantation.[4] However, these clinical repair methods mainly lead to short-term functional regeneration with the formation of fibrocartilage and cannot provide sustainable restoration of functional hyaline cartilage.[5,6] Currently, tissue engineering technology using various hydrogel scaffolds, mesenchymal stem cells (MSCs), and growth factors is considered as the most promising therapeutic strategy for the regeneration of cartilage and osteochondral defects.[7,8] MSCs are multipotent stem cells that possess self-renewal capacity and can differentiate into various specialized cell types such as adipocytes, chondrocytes, and osteoblasts.[9,10] MSCs present in many tissues of the human body. Recent studies have revealed that MSCs can be isolated from the synovial membrane.[11,12] One of the advantages of synovium-derived MSCs (SDMSCs) is that these cells are tissue-resident stem cells, which actively participate in maintaining joint homeostasis and cartilage repair.[13,14] Moreover, it has been demonstrated that compared to MSCs isolated from other tissue sources, SDMSCs have greater proliferation activity and chondrogenic potential in vitro, rendering SDMSCs as an appropriate source for cartilage regeneration.[15,16]

It was reported that the implantation of MSCs alone often leads to the formation of fibrocartilage, indicating that the in vivo environment is not sufficient to induce chondrogenesis in the cartilage defect.[17] To induce chondrogenesis in MSCs and hyaline cartilage formation, specific growth factors such as TGF-β1, BMP-2, BMP-4, and IGF-1 are required.[6,18] Recently, several studies demonstrated that MSCs encapsulated in hydrogel scaffolds with chodroinductive growth factors significantly repaired cartilage defects in contrast to individual applications of MSCs or growth factors.[19] For example, Gugjoo et al.[20] showed that implantation of laminin gel scaffold containing MSCs with IGF-1 and TGF-β1 significantly promoted the regeneration of damaged hyaline cartilage and subchondral bone tissue in rabbit osteochondral model. Implantation of the hybrid scaffold composed of chitosan hydrogel and a decellularized bone matrix for co-delivery of rabbit SDMSCs and TGF-β1 promoted chondrogenic differentiation of loaded SDMSCs and significantly enhanced cartilage regeneration.[21] Rabbit adipose-derived MSCs encapsulated in injectable PLGA hydrogels with BMP-2 significantly improved cartilage repair in chondral defects except in untreated controls and microfracture treatment alone.[22]

Recently, we have developed an injectable heparin-conjugated fibrin (HCF) hydrogel containing SDMSCs and two chondroinductive factors (TGF-β1 and BMP-4) for the regeneration of osteochondral articular defect.[23] Our in vitro study showed that HCF hydrogel has good biocompatibility with encapsulated SDMSCs and the ability to control the release of TGF-β1 and BMP-4 for 4 weeks. A preclinical study revealed that implantation of SDMSCs in HCF hydrogel in combination with TGF-β1 and BMP-4 significantly enhanced the regeneration of osteochondral defects in rabbits through the complete formation of hyaline cartilage and subchondral bone tissue compared to HCF hydrogels with SDMSCs or growth factors alone.[24]

Thus, the purpose of this study was to evaluate the safety of HCF hydrogel containing autologous human SDMSCs, TGF-β1, and BMP-4 after implantation to articular cartilage defect in patients with osteoarthritis. At this moment, we could not find any article or clinical trial in the literature and specialized databases on the safety and efficacy of injectable hydrogel with encapsulated autologous human SDMSCs and chondroinductve factors in articular cartilage defect repair. Therefore, in this study, we present the first evidence of clinical safety of implantation of HCF hydrogel, containing SDMSCs and growth factors (TGF-β1 and BMP-4), into articular cartilage defect of OA patients.

Materials and Methods

A single-center, prospective observational study was conducted between January 2022 and August 2022 at the National Scientific Center of Traumatology and Orthopedics (Nur-Sultan, Kazakhstan).

The study was conducted in accordance with the ethical principles of the WMA Declaration of Helsinki (1964, ed. 2013). The study protocol was reviewed and approved by the Institutional Review Board of the National Center for Biotechnology (№ 00013497) and the Local Ethics Committee of the National Scientific Center of Traumatology and Orthopedics (Protocol №3, 25.12.2021). Written informed consent was obtained from all participants.

Evaluation of Patient Suitability for Study Participation

We included patients with ≥1 chondral/osteochondral lesions of the distal femur as identified by magnetic resonance imaging (MRI) analysis (Figure 1) and/or previous arthroscopies.

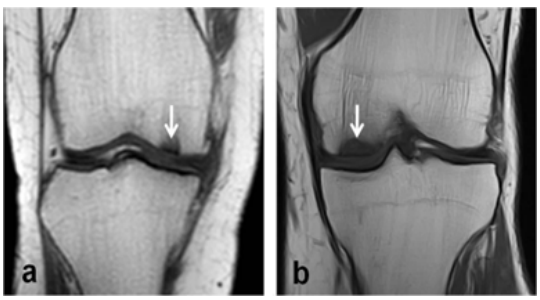

Figure 1. *MRI images of two patients with Grade 2 osteoarthritis. Preoperative MRI imaging revealed a chondral defect (arrow) on the medial femoral condyle (**a** and **b**).*

Inclusion criteria were (1) the age range of 25-65 years, (2) a symptomatic knee joint cartilage defect that was International Cartilage Repair Society (ICRS) Grade III or more under arthroscopy that was recalcitrant to more than 6 months of conservative care, and (3) size of less than 10 cm^2 for a single lesion or 15 cm^2 for multiple lesions with a relatively intact neighboring cartilage (ICRS Grades I and II).

Exclusion criteria were (1) those with more than 5° of varus or valgus deformity in the hip–knee–ankle angle, (2) the presence of instability in the affected joint, including patellofemoral instability due to any coexisting ligament problem, (3) inflammatory arthritis, synovitis, patellofemoral instability, drug and alcohol abuse, and psychological problems.

Isolation and culture of human SDMSCs

Synovial membranes were harvested aseptically from the knee joint of the patients under epidural anesthesia. Isolated synovial membranes were rinsed twice with Dulbecco's phosphate-buffered saline (DPBS) supplemented with 1% penicillin/streptomycin (Gibco, USA), minced into 1-2mm^2 pieces, and digested with 0.25% type II collagenase (Gibco, USA) at 37°C for 4 hours. The cells were washed twice by DPBS and resuspended in StemPro® MSC SFM XenoFree medium (Gibco, USA) supplemented with 1% penicillin/streptomycin. The cells were plated in CELLstart™ CTS™ (Gibco, USA) pre-coated T75 tissue culture flask (Corning, USA) and cultured in StemPro® MSC SFM Xeno Free medium at 37°C and 5% CO_2. Nonadherent cells were removed by day 2, and the adherent cells were propagated before they reached 80-90% confluence. The cells were harvested with TrypLE Express (Gibco, USA) and split in a ratio of 1:3. The culture medium was changed every 2 days. Cell viability was evaluated via trypan blue exclusion with automated cell counter BioRad TC20 (Biorad, USA). The cell culture was periodically tested for contamination with bacteria, yeast, and fungi using the Cell Culture Contamination Detection Kit (Thermo Fisher Scientific, USA).

Immunocytochemistry

Human SDMSCs were grown on a 4-well chambered cell culture slide (BD Biosciences, USA). After fixation with 4% paraformaldehyde and washing with PBS, the cells were incubated with primary antibodies against CD45 (1:100 dilution; ab40763), CD73 (1:100 dilution; ab40763), CD90 (1:100 dilution; ab226133), and CD105 (1:100 dilution; ab231774) (all from Abcam, UK) in PBS/0.1% Tween 20 and 10% normal goat serum (Abcam, UK) overnight at 4°C. The cells were washed with PBS and incubated with goat anti-rabbit IgG Alexa Fluor 488 (1:1000 dilution; A-11008) (Thermo Fisher Scientific, USA) in PBS for 45 min at room temperature. After washing in PBS, the cells were mounted in antifade reagent with DAPI (Thermo Fisher Scientific, USA) for 1 min and visualized with an inverted fluorescence microscope Axio Scope A1 (Carl Zeiss, Germany).

Detection of mycoplasma and bacterial endotoxins in cell culture

The presence of mycoplasma in human SDMSC cultures was detected with the PCR Mycoplasma Test Kit (Applichem, Germany) according to the manufacturer's instructions. The detection of gram-negative bacterial endotoxins in human SDMSC suspension was performed with Pierce™ LAL Chromogenic Endotoxin Quantitation Kit (Thermo Fisher Scientific, USA), according to the manufacturer's instructions.

Synthesis of heparin-conjugated fibrinogen

Heparin-conjugated fibrinogen was prepared according to a previously described protocol.[25] Briefly, 100 mg of low-molecular-weight heparin (LMWH) (Abcam, UK) was dissolved in 100 mL of 0.05M 2-morpholinoethanesulfonic acid monohydrate. In order to activate the -COOH groups of LMWH, 0.04 mM 1-hydroxy-2,5-pyrrolidinedione and 0.08 mM N-Ethyl-N'-(3-dimethylaminopropyl)carbodiimide hydrochloride were added and incubated at 4°C for 12 hours. The solution of activated LMWH was shaken vigorously, precipitated with an excess volume of anhydrous acetone, and lyophilized for 24 hours. Subsequently, 100 mg of human plasminogen-free fibrinogen (Sigma, USA) was dissolved in 20 mL phosphate-buffered saline (pH 7.4) at 4°C. This solution subsequently reacted with 60mg of lyophilized LMWH for 3 hours at 4°C. Following precipitation and lyophilization in similar conditions, a powder of heparin-conjugated fibrinogen was dissolved in DPBS. To remove residual LMWH, heparin-conjugated fibrinogen was dialyzed with a dialysis sack (12,000-14,000 Da) at 4°C for 24 hours and lyophilized for 48 hours to produce fibrinogen conjugated to purified heparin. Lyophilized heparin-conjugated fibrinogen was sterilized with 15 kGy dose gamma radiation using the ILU-10 irradiation unit (Park of Nuclear Technologies, Kurchatov, Kazakhstan).

Preparation of HCF hydrogel with human SDMSCs and growth factors

To prepare HCF hydrogel with human SDMSCs and growth factors, the components of fibrin sealant (TISSEEL lyo, Baxter AG, Austria) have been used. For the preparation of the component (1), 91 mg of human fibrinogen, 20mg of heparin-conjugated fibrinogen, 1μg of human recombinant TGF-β1, and 1μg of BMP-4 (Abcam, UK) were dissolved with 1ml of aprotinin solution at 37°C for 45 min using a sterile water bath. After dissolving the fibrin solution, 2×10^7 of autologous human SDMSCs were added and mixed at magnetic stir for 3 min. For the preparation of component (2), 500 IU of human thrombin was dissolved in 1ml of 40μM calcium chloride solution at 37°C for 45 min using a sterile water bath. The reconstituted components (1) and (2) were placed in two single-use syringes, inserted into the DUPLOJECT two-syringe clip, and connected this assembly to the DUPLOTIP dual lumen cannula 20G×10 cm (Baxter, USA). Both syringes were filled with equal volumes.

Surgical procedures

All surgical procedures were conducted under epidural anesthesia after patient informed consent. At the initial stage of the first procedure, arthroscopy of the patient's knee joint was performed to measure the positions, sizes, and depths of cartilage defects, as well as to identify abnormalities of the menisci and ligaments. Then, a synovial membrane biopsy was harvested and sent to the stem cell laboratory (National Center for Biotechnology) for the isolation and expansion of autologous SDMSCs. After 4-5 weeks, a suspension of cultured SDMSCs (2×10^7 cells/vial) with cell viability of more than 90% was delivered for a second surgery.

In the second stage, a mini-arthrotomy of the knee joint was performed on the medial or lateral part of the patella along the cartilage defect. Before implantation of the hydrogel, remnant articular cartilage tissue, fibrotic tissue, and sclerotic bone were debrided and removed from the edges of the cartilage defect (Figure 2).

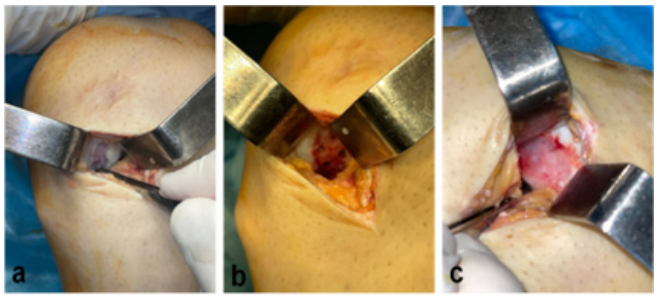

Figure 2. *Surgical procedure of HCF hydrogel implantation into the cartilage defect.* ***(a)*** *Preparation of cartilage defect;* ***(b)*** *Microperforation of subchondral bone in the defect site;* ***(c)*** *Gelated HCF hydrogel after implantation.*

After several rinsing of the defect with sterile saline, several microperforations 5 mm deep and 2.5 mm in diameter were made. After stopping bleeding from the holes using a gauze swab soaked in a solution of epinephrine, the HCF hydrogel containing synovial MSCs and growth factors (TGF-β1 and BMP-4) was implanted using DUPLOJECT two-syringe device connected with the DUPLOTIP dual lumen cannula.

Postoperative rehabilitation

Postoperative rehabilitation was performed individually for each patient, depending on the location and size of the defect, the level of physical activity, and the postoperative progress. Patients should walk with crutches for 6 weeks and not lift heavy objects. Patients should perform isometric hamstring and quadriceps contraction exercises for 6 weeks.

Clinical and radiological evaluation of the knee joint

The knee conditions of the patients before and after surgery were assessed with VAS, WOMAC, and KOOS. Before surgery, MRI was performed on all patients using a 1.5-Tesla MRI system.

Statistical analysis was performed using statistical software package SPSS version 22.0 (SPSS Inc, Chicago, IL). Baseline characteristics were summarized as frequencies and percentages for categorical variables and as mean±SD for continuous variables. The Wilcoxon criterion was used to compare the differences between the paired samples. Group comparisons with respect to categorical variables are performed using chi-square test. A probability value of $P<0.05$ was considered statistically significant.

Results

Patient characteristics

Out of the 330 screened patients with articular cartilage defects, 15 patients (66.7% women and 33.3% men) with a mean age of 44.2±18.0 years were enrolled in the study and received implantation of HCF hydrogel containing autologous SDMSCs and growth factors (TGF-β1 and BMP-4) (Figure 3). Of the study participants, 4(26.67%) patients had Kellgren-Lawrence Grade I, while 11(73.33%) had Grade II (Figure 1). OA of the right and left knee was diagnosed in 8(53.33%) and 7(46,67%) patients, respectively. The VAS median value at the damaged knee was 59 mm (range of 43–87 mm). The mean lesion size was 4.9±2.0 cm on MRI. All treated defects were on the femur, mostly on the medial femoral condyle - 11(73.33%), lateral femoral condyle - 3(20%), and trochlea - 1(6.67%) (Table 1).

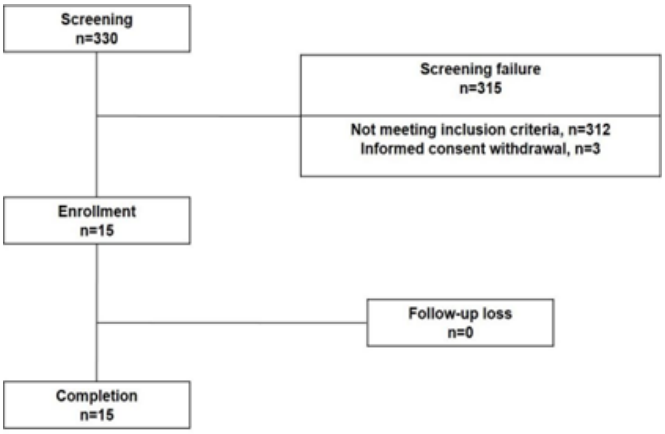

Figure 3. *The study scheme.*

Table 1.

Demographics and baseline characteristics of study participants

Experimental group (n=15)		
Age, years		44±18
Sex	Male	6 (34%)
	Female	9 (66%)
Body mass index, kg/m^2		29.38±3.9
Diagnosis	Osteoarthritis, K-L grade	
	1	4 (26.67%)
	2	11(73.33%)
Knee	Right	8 (53.33%)
	Left	7 (46.67%)
Lesion size, cm^2		4.9±2.0
Location	Medial femoral condyle	11 (73.33%)
	Lateral femoral condyle	3 (20%)
	Trochlea	1 (6.67%)
Compartment	Unicompartmental osteoarthritis	9 (60%)
	Multicompartmental osteoarthritis	6 (40%)
Concomitant procedures	Meniscectomy	13 (86.67%)
	Other procedures	6 (40%)

Evaluation of clinical safety

The safety assessment of hydrogel was based on the absence of infections, inflammation, adhesion, loose body, and tumor formation in the knee joints. Joint pain, synovitis, and edema were observed at an early date after surgery, and all symptoms had completely disappeared at Week 8 after surgery. In addition to assessing the condition of the joints, patients were monitored to determine undesirable side effects after the hydrogel implantation. The results showed no severe adverse events (SAEs) for 8 weeks after the implantation (Table 2).

Table 2.

Adverse events after hydrogel implantation

Adverse events	Before surgery	After surgery (24 h)	After surgery (8 weeks)
Joint pain	9 (60%)	5 (33.3%)	0
Joint edema	3 (20%)	2 (13.3%)	0
Synovitis	3 (20%)	2 (13.3%)	0
Joint contracture	0	0	0
Surgical wound infection	0	0	0

Furthermore, no post-operative infections were detected. There were no significant changes in body temperature and blood pressure before and after hydrogel implantation. There were no adverse events according to the criteria of the World Health Organization after surgery and for the 8-week follow-up. No significant differences were observed before and after implantation regarding overall or specific treatment-emergent adverse events in the initial 24 hours of a clinical trial or the 8-week follow-up (Table 2). No participant was withdrawn from the study because of adverse events. The pain at the incision site was the only severe adverse event considered by the investigator as "probably related" to treatment (due to mini-arthrotomy). In the 8-week follow-up, pain decreased. None of the severe adverse events were considered treatment-related by the investigators. No inflammation reactions were observed in any of the 15 participants treated with HCF hydrogel, according to the blood test.

There was no significant abnormal finding in the hematological parameters during this study (Table 3).

Clinical outcomes of the patients after 6-month follow-up were evaluated with VAS, WOMAC, and KOOS. VAS score and WOMAC-A pain score significantly decreased at all time points compared to baseline (P<0.001 in all cases) (Table 4). Knee pain, other symptoms, and QOL were measured by the corresponding KOOS subscores and showed statistically significant improvement compared to baseline at all time points (P<0.001). The subjective assessment of ADL measured by the ADL KOOS subscore also showed significant enhancement compared to the baseline at all time points.

To evaluate articular cartilage repair, we used the MOCART score. In total, 15 patients underwent MRI before and 6 months after implantation (Figure 4). A total of 11(73.3%) patients showed complete graft integration into the border zone, one had a visible demarcating border, and 3 patients still had visible defects. Intact surface tissue appeared in 11(73.3%) patients, whereas 4(26.7%) patients still had a damaged surface.

Table 3.

Hematological tests at baseline, 24 hours, and Week 8 after HCF hydrogel implantation.

Hematological parameter	Baseline	24 hours	Week 8	Changes (between baseline and 24 h)	Changes (between 24 h and Week 8)	Changes (between baseline and Week 8)	P-value
WBC, $\times 10^9$/L	6.47 ± 2.18	6.76 ± 2.02	6.78 ± 1.45	0.29 ± 1.78	0.024 ± 1.86	0.314 ± 1.96	0.5632
NEU, %	51.3 ± 5.2	58.6 ± 4.2	53.2 ± 4.4	7.3 ± 3.2	-5.4 ± 4.2	1.9 ± 4.1	0.2346
EOS, %	2.5 ± 1.2	2.2 ± 1.6	3.6 ± 1.1	-0.3 ± 1.1	1.4 ± 1.3	1.1 ± 1.3	0.7892
BAS, %	0.4 ± 0.3	0.9 ± 0.2	0.5 ± 0.4	0.5 ± 0.3	-0.4 ± 0.2	0.1 ± 0.3	0.5223
LYM, %	34.4 ± 9.2	30.6 ± 8.3	28.1 ± 7.4	-3.8 ± 6.8	-2.5 ± 7.1	-6.3 ± 7.2	0.2754
MON, %	5.5 ± 3.2	4.3 ± 2.6	4.9 ± 3.3	-1.2 ± 1.1	0.6 ± 0.8	-0.6 ± 0.9	0.3879
RBC, $\times 10^{12}$/L	4.68 ± 0.54	4.74 ± 0.61	4.65 ± 0.75	0.06 ± 0.66	-0.09 ± 0.71	-0.03 ± 0.72	0.4916
Platelet, $\times 10^9$/L	246 ± 46.79	236 ± 42.53	255 ± 50.71	-10 ± 5.54	19 ± 4.33	9.2 ± 4.12	0.3167
ESR, mm/hr	21.2 ± 12.2	23.7 ± 10.3	14.5 ± 8.4	2.5 ± 3.12	-9.2 ± 3.43	-6.7 ± 3.11	0.1257
Total protein, g/dL	6.67 ± 0.28	6.55 ± 0.4	6.34 ± 0.31	-0.12 ± 0.34	-0.21 ± 0.38	-0.33 ± 0.42	0.4021
Total bilirubin, mg/dL	0.65 ± 0.17	0.72 ± 0.13	0.63 ± 0.14	0.07 ± 0.23	-0.09 ± 0.16	-0.02 ± 0.15	0.3219
AST, IU/L	20.2 ± 9.1	21.6 ± 8.3	18.5 ± 7.9	1.4 ± 0.2	-3.1 ± 0.3	-1.7 ± 0.2	0.5223
ALT, IU/L	23.4 ± 10.2	20.2 ± 9.7	19.2 ± 8.8	-3.2 ± 9.1	-1 ± 8.2	-4.2 ± 9.3	0.4034
Total cholesterol, mg/dL	177 ± 30.4	175 ± 35.5	168 ± 20.7	-2 ± 24.8	-7 ± 22.3	-9.1 ± 25.1	0.0854

Abbreviations: *ALT, alanine transaminase; AST, aspartate transaminase; ESR, erythrocyte sedimentation rate; WBC, white blood cell; RBC, red blood cell; NEU, neutrophils; EOS, eosinophils; BAS, basophils; LYM, lymphocytes; MON, monocytes.*

Table 4.

Analysis of the changes in VAS, WOMAC, and KOOS scores before and6 months after HCF hydrogel implantation.

Parameter	Baseline (n=15)		Month 1 (n=15)		Month 6 (n=15)	
	Mean ± SD	(Range)	Mean ± SD	(Range)	Mean ± SD	(Range)
VAS-knee pain	67.54 ± 13.73	(45–84)	22.81 ± 18.21	(40–85)	14.74 ± 17.20	(0–80)
P-value			<0.001		<0.001	
WOMAC-A-knee pain	28.98 ± 14.72	(6–56)	13.63 ± 12.44	(0–37)	7.10 ± 10.12	(0–33)
P-value			<0.001		<0.001	
WOMAC-C–knee function	23.58 ± 15.95	(0–52.94)	9.29 ± 10.33	(0–35.29)	6.45 ± 12.13	(0–47.06
P-value			<0.001		<0.001	
KOOS–Knee pain	70.07 ± 13.24	(41.67–88.89)	85.66 ± 11.89	(55.56–100)	90.28 ± 10.34	(63.89–100)
P-value			<0.001		<0.001	
KOOS–Symptoms	60.65 ± 23.79	(5–95)	78.71 ± 17.89	(30–100)	83.28 ± 14.84	(40–100)
P-value			<0.001		<0.001	
KOOS–Activity of daily living	79.93 ± 14.38	(48.53–100)	92.17 ± 9.75	(64.71–100)	93.97 ± 9.19	(63.24–100)
P-value			<0.001		<0.001	
KOOS–Quality of life	45.16 ± 18.52	(6.25–93.75	61.09 ± 27.29	0–100)	68.27 ± 23.45	(0–100)
P-value			<0.001		<0.001	

Figure 4. *MRI images of the medial femoral condyle. (A-B) Images of cartilage lesion on medial femoral condyle before HCF hydrogel implantation; (C-D) Images captured after 6-month follow-up showed regeneration of articular cartilage. The white arrow indicates a cartilage lesion.*

The structure of the repaired tissue was homogenous in 12(80%) patients. An isointense signal was seen in 11(73.3%) patients, and 4(26.7%) patients had a moderately hyperintense signal; a markedly hyperintense signal was not observed. Regarding subchondral bone repair, the subchondral lamina was intact in 9(60%) patients, and all patients had intact subchondral bone. Finally, no patients exhibited adhesion, and 12(80%) patients showed no evident effusion.

Discussion

We tested HCF hydrogel as a new drug for the treatment of articulate cartilage defects in small-group OA patients to evaluate its safety and identify side effects. In the present study, an injectable HCF hydrogel for delivery of autologous human SDMSCs, TGF-β1, and BMP-4 was fabricated from FDA–approved materials: LMWH, fibrinogen, thrombin, and aprotinin. Implantation of HCF hydrogel into articular cartilage defect was performed with a mini-arthrotomy approach using DUPLOJECT two-syringe device connected with the DUPLOTIP dual lumen cannula. Our early clinical study demonstrated that implantation of HCF hydrogel with autologous human SDMSCs, TGF-β1 and BMP-4 resulted in a favorable safety profile for patients with OA. No significant severe adverse events or undesirable side effects such as joint edema, inflammation reactions, elevated body temperature, and wound infections after HCF hydrogel implantation were observed during this study. In addition, our laboratory tests showed no significant abnormal changes in the hematological parameters of the patients during post-surgical follow-up. Only the pain at the incision site was reported as a minor adverse event, but the pain gradually disappeared in 8 weeks after surgery.

To our knowledge, this is the first report of a clinical study on the safety of the implantation of HCF hydrogel with encapsulated human SDMSCs and chondroinductive factors into articular cartilage defect in OA patients.

In the literature, only two previous clinical studies used autologous MSCs loaded in fibrin glue for the treatment of cartilage defects in the human knee. A pilot study of 5 patients with full-thickness cartilage defects revealed that implantation of autologous bone marrow-derived MSCs loaded on platelet-rich fibrin glue significantly improved functional knee scores and MRI findings at 6 and 12 months postoperatively.[26] Kim and colleagues showed that fibrin glue is an effective and safe injectable scaffold in the implantation of adipose-derived stem cells for the treatment of articular cartilage defects in OA patients.[27]

In our study, we used autologous SDMSCs because they have a number of advantages in comparison to MSCs isolated from other sources: 1) SDMSCs can be easily isolated in a sufficient amount from a small piece of the synovial membrane, 2) they do not lose their phenotypic properties during cultivation, 3) the functional activity of SDMSCs remains at a high level regardless of the person's age.[11] Moreover, SDMSCs are tissue-resident stem cells that have a higher capacity to differentiate into chondrocytes than MSCs from bone marrow or adipose tissue. To obtain safe cell product, SDMSCs were propagated in serum-free and xeno-free culture medium StemPro® MSC and examined accurately for the presence of bacteria, fungi, yeast, mycoplasma, and bacterial endotoxins in cell culture. During our study, no SDMSCs containing any abovementioned contaminants were observed.

A number of studies have shown that the application of recombinant growth factors alone or in combination with MSCs can stimulate cell proliferation, extracellular matrix (ECM) formation, and tissue regeneration. However, despite the therapeutic efficacy of recombinant growth factors, the clinical application is still limited due to a short half-life and poor biological activity.[28] Large doses of TGFs and BMPs cause adverse effects, including immune response and abnormal growth of cartilage and bone tissue.[29] Therefore, to overcome the aforementioned limitations, many researchers have developed drug delivery systems based on natural and/or synthetic scaffolds for the sustained release of growth factors in a target site. Among the scaffolds for growth factors and cell delivery, injectable fibrin hydrogels demonstrated great potential in cartilage and bone tissue engineering. The fibrin hydrogel application is supported by its high-water content, biocompatibility, biodegradability, nontoxicity, porous framework, structural similarity to the ECM, and ability to match irregular defects.[30,31] Conjugating heparin to fibrinogen provides biomaterials for the controlled release of heparin-binding proteins such as TGFs and BMPs. The heparin-conjugated hydrogel can protect growth factors from proteolysis and prolong the retention of their biological activity in vivo.[29] In addition, it has been shown that heparin can modulate the biological activity of the TGF-β1, which plays a significant role in cell migration, proliferation, cartilage differentiation, and synthesis of cartilage-specific ECM, which is also involved in the suppression of immune response.[32,33]

Therefore, in our study, we used HCF hydrogel as a scaffold for the delivery of human recombinant TGF-β1 and BMP-4 in combination with SDMSCs because we supposed that HCF hydrogel could better stimulate the regeneration of articular cartilage defect in OA patients in comparison with MSC implantation in fibrin gel. Our first-in-human clinical study showed that implantation of SDMSCs with human recombinant TGF-β1 and BMP-4 in HCF hydrogel did not lead to significant adverse events and changes in hematological profiles of OA patients. Thus, we consider HCF hydrogel as a safe injectable scaffold for the delivery MSCs and chondroinductive factors for the treatment of cartilage defects.

Moreover, the analysis of clinical outcomes showed that HCF hydrogel is effective for the treatment of articular cartilage defects in OA patients between 25 and 65 years. As measured by the KOOS scores, the main clinical improvement was presented in a significant increase in knee function, which was observed 6 months post-treatment. WOMAC-C score showed a similar pattern confirmed by clinical changes during post-surgery time. The results of the present study showed that hydrogel implantation is effective in pain reduction by providing lasting therapeutic effects as also shown by changes in VAS, WOMAC-A, and KOOS scores. Function and symptom improvements led to a significant increase in ADL and QOL in 30 days. Thus, HCF hydrogel containing autologous SDMSCs and chondroinductive growth factors promotes rapid and lasting therapeutic effects in OA patients with Kellgren-Lawrence Grade I-II.

This study has some limitations. First, the number of OA patients in an experimental group was relatively small. Second, the follow-up period after implantation of HCF hydrogel with SDMSCs and growth factors was short for the examination of long-term safety. For a complete assessment of HCF hydrogel as a carrier of SDMSCs and growth factors in articular cartilage defects of OA patients, a prospective study with a larger number of patients and a long-term follow-up period is required. Currently, we have enrolled 40 subjects and carried out a 2-year clinical study to evaluate the long-term safety and therapeutic efficacy of HCF hydrogel.

Conclusion

The results of this first-in-human clinical study showed that the application of HCF hydrogel with autologous SDMSCs, TGF-β1, and BMP-4 appears to be safe and showed no serious adverse events in OA patients. The implantation of HCF hydrogel was found to be a promising method for the effective repair of cartilage defects in femoral condyles, with the effect lasting for 6 months after the HCF hydrogel implantation for the vast majority of the patients. The HCF hydrogel-based grafting technique appears to be a viable option for condylar lesions and may delay or prevent the need for arthroplasty. However, further clinical study is required to evaluate the long-term safety and therapeutic efficacy of HCF hydrogel using a larger number of subjects.

Sources of Funding

This study was funded by the Ministry of Education and Science of the Republic of Kazakhstan in frame scientific program № OR11465426: "The implementation of innovative tissue engineering technologies into medical practice for the restoration of damaged joints."

Competing Interests

The authors declare that they have no competing interests

References

1. Hiligsmann M, Reginster JY. The economic weight of osteoarthritis in Europe. J Medicographia. 2013;35:197–202.
2. Klug A, Gramlich Y, Rudert M, Drees P, Hoffmann R, Weißenberger M, Kutzner KP. The projected volume of primary and revision total knee arthroplasty will place an immense burden on future health care systems over the next 30 years. Knee Surg Sports Traumatol Arthrosc. 2021 Oct;29(10):3287-3298. doi: 10.1007/s00167-020-06154-7.
3. Safiri S, Kolahi AA, Smith E, Hill C, Bettampadi D, Mansournia MA, et al. Global, regional and national burden of osteoarthritis 1990-2017: a systematic analysis of the Global Burden of Disease Study 2017. Ann Rheum Dis. 2020 Jun;79(6):819-828. doi: 10.1136/annrheumdis-2019-216515.
4. Evenbratt H, Andreasson L, Bicknell V, Brittberg M, Mobini R, Simonsson S. Insights into the present and future of cartilage regeneration and joint repair. Cell Regen. 2022 Feb 2;11(1):3. doi: 10.1186/s13619-021-00104-5.
5. Steinert AF, Ghivizzani SC, Rethwilm A, Tuan RS, Evans CH, Nöth U. Major biological obstacles for persistent cell-based regeneration of articular cartilage. Arthritis Res Ther. 2007;9(3):213. doi: 10.1186/ar2195.
6. Huang K, Li Q, Li Y, Yao Z, Luo D, Rao P, Xiao J. Cartilage Tissue Regeneration: The Roles of Cells, Stimulating Factors and Scaffolds. Curr Stem Cell Res Ther. 2018;13(7):547-567. doi: 10.2174/1574888X12666170608080722.
7. Vinatier C, Mrugala D, Jorgensen C, Guicheux J, Noël D. Cartilage engineering: a crucial combination of cells, biomaterials and biofactors. Trends Biotechnol. 2009 May;27(5):307-14. doi: 10.1016/j.tibtech.2009.02.005..
8. Huselstein C, Li Y, He X. Mesenchymal stem cells for cartilage engineering. Biomed Mater Eng. 2012;22(1-3):69-80. doi: 10.3233/BME-2012-0691.
9. Salgado AJ, Oliveira JT, Pedro AJ, Reis RL. Adult stem cells in bone and cartilage tissue engineering. Curr Stem Cell Res Ther. 2006 Sep;1(3):345-64. doi: 10.2174/157488806778226803.
10. Ding DC, Shyu WC, Lin SZ. Mesenchymal stem cells. Cell Transplant. 2011;20(1):5-14. doi: 10.3727/096368910X.
11. Fan J, Varshney RR, Ren L, Cai D, Wang DA. Synovium-derived mesenchymal stem cells: a new cell source for musculoskeletal regeneration. Tissue Eng Part B Rev. 2009 Mar;15(1):75-86. doi: 10.1089/ten.teb.2008.0586.
12. Sasaki A, Mizuno M, Ozeki N, Katano H, Otabe K, Tsuji K, Koga H, Mochizuki M, Sekiya I. Canine mesenchymal stem cells from synovium have a higher chondrogenic potential than those from infrapatellar fat pad, adipose tissue, and bone marrow. PLoS One. 2018 Aug 23;13(8):e0202922. doi: 10.1371/journal.pone.0202922.
13. Jones BA, Pei M. Synovium-derived stem cells: a tissue-specific stem cell for cartilage engineering and regeneration. Tissue Eng Part B Rev. 2012 Aug;18(4):301-11. doi: 10.1089/ten.TEB.2012.0002.
14. Koga H, Muneta T, Ju YJ, Nagase T, Nimura A, Mochizuki T, Ichinose S, von der Mark K, Sekiya I. Synovial stem cells are regionally specified according to local microenvironments after implantation for cartilage regeneration. Stem Cells. 2007 Mar;25(3):689-96. doi: 10.1634/stemcells.2006-0281.
15. Sakaguchi Y, Sekiya I, Yagishita K, Muneta T. Comparison of human stem cells derived from various mesenchymal tissues: superiority of synovium as a cell source. Arthritis Rheum. 2005 Aug;52(8):2521-9. doi: 10.1002/art.21212.
16. Koga H, Muneta T, Nagase T, Nimura A, Ju YJ, Mochizuki T, Sekiya I. Comparison of mesenchymal tissues-derived stem cells for in vivo chondrogenesis: suitable conditions for cell therapy of cartilage defects in rabbit. Cell Tissue Res. 2008 Aug;333(2):207-15. doi: 10.1007/s00441-008-0633-5.
17. Magne D, Vinatier C, Julien M, Weiss P, Guicheux J. Mesenchymal stem cell therapy to rebuild cartilage. Trends Mol Med. 2005 Nov;11(11):519-26. doi: 10.1016/j.molmed.2005.09.002.
18. Miljkovic ND, Cooper GM, Marra KG. Chondrogenesis, bone morphogenetic protein-4 and mesenchymal stem cells. Osteoarthritis Cartilage. 2008 Oct;16(10):1121-30. doi: 10.1016/j.joca.2008.03.003.
19. Wagenbrenner M, Mayer-Wagner S, Rudert M, Holzapfel BM, Weissenberger M. Combinations of Hydrogels and Mesenchymal Stromal Cells (MSCs) for Cartilage Tissue Engineering-A Review of the Literature. Gels. 2021 Nov 16;7(4):217. doi: 10.3390/gels7040217.
20. Gugjoo MB, Amarpal, Abdelbaset-Ismail A, Aithal HP, Kinjavdekar P, Pawde AM, Kumar GS, Sharma GT. Mesenchymal stem cells with IGF-1 and TGF- β1 in laminin gel for osteochondral defects in rabbits. Biomed Pharmacother. 2017 Sep;93:1165-1174. doi: 10.1016/j.biopha.2017.07.032.
21. Huang H, Hu X, Zhang X, Duan X, Zhang J, Fu X, Dai L, Yuan L, Zhou C, Ao Y. Codelivery of Synovium-Derived Mesenchymal Stem Cells and TGF-β by a Hybrid Scaffold for Cartilage Regeneration. ACS Biomater Sci Eng. 2019 Feb 11;5(2):805-816. doi: 10.1021/acsbiomaterials.8b00483.
22. Vayas R, Reyes R, Arnau MR, Évora C, Delgado A. Injectable Scaffold for Bone Marrow Stem Cells and Bone Morphogenetic Protein-2 to Repair Cartilage. Cartilage. 2021 Jul;12(3):293-306. doi: 10.1177/1947603519841682.
23. Ogay VB, Isabekova AS, Sarsenova MA, Ramankulov EM. Patent of the Republic of Kazakhstan. A method for obtaining an injectable biocomposite hydrogel to stimulate the regeneration of bone and cartilage tissue. 2019;33784:29.

Corresponding authors:

Prof. Vyacheslav Ogay, PhD. National Center for Biotechnology. Astana, Kazakhstan. E-mail: ogay@biocenter.kz

Dr. Arman Batpen, PhD, MD. National Scientific Center of Traumatology and Orthopedics. Astana, Kazakhstan. E-mail: batpen_a@nscto.kz

24. Sarsenova M, Raymagambetov Y, Issabekova A, Karzhauov M, Kudaibergen G, Akhmetkarimova Zh, Batpen A, Ramankulov Y, Ogay V. Regeneration of Osteochondral Defects by Combined Delivery of Synovium-Derived Mesenchymal Stem Cells, TGF-β1 and BMP-4 in Heparin-Conjugated Fibrin Hydrogel. Polymers. 2022 (under review).
25. Yang HS, La WG, Bhang SH, Jeon JY, Lee JH, Kim BS. Heparin-conjugated fibrin as an injectable system for sustained delivery of bone morphogenetic protein-2. Tissue Eng Part A. 2010 Apr;16(4):1225-33. doi: 10.1089/ten.TEA.2009.0390.
26. Haleem AM, Singergy AA, Sabry D, Atta HM, Rashed LA, Chu CR, et al. The Clinical Use of Human Culture-Expanded Autologous Bone Marrow Mesenchymal Stem Cells Transplanted on Platelet-Rich Fibrin Glue in the Treatment of Articular Cartilage Defects: A Pilot Study and Preliminary Results. Cartilage. 2010 Oct;1(4):253-261. doi: 10.1177/1947603510366027.
27. Kim YS, Choi YJ, Suh DS, Heo DB, Kim YI, Ryu JS, Koh YG. Mesenchymal stem cell implantation in osteoarthritic knees: is fibrin glue effective as a scaffold? Am J Sports Med. 2015 Jan;43(1):176-85. doi: 10.1177/0363546514554190.
28. Ren X, Zhao M, Lash B, Martino MM, Julier Z. Growth Factor Engineering Strategies for Regenerative Medicine Applications. Front Bioeng Biotechnol. 2020 Jan 21;7:469. doi: 10.3389/fbioe.2019.00469.
29. Joung YK, Bae JW, Park KD. Controlled release of heparin-binding growth factors using heparin-containing particulate systems for tissue regeneration. Expert Opin Drug Deliv. 2008 Nov;5(11):1173-84. doi: 10.1517/17425240802431811.
30. Wei W, Ma Y, Yao X, Zhou W, Wang X, Li C, Lin J, He Q, Leptihn S, Ouyang H. Advanced hydrogels for the repair of cartilage defects and regeneration. Bioact Mater. 2020 Oct 10;6(4):998-1011. doi: 10.1016/j.bioactmat.2020.09.030.
31. Liu M, Zeng X, Ma C, Yi H, Ali Z, Mou X, Li S, Deng Y, He N. Injectable hydrogels for cartilage and bone tissue engineering. Bone Res. 2017 May 30;5:17014. doi: 10.1038/boneres.2017.14.
32. Palladino MA, Morris RE, Starnes HF, Levinson AD. The transforming growth factor-betas. A new family of immunoregulatory molecules. Ann N Y Acad Sci. 1990;593:181-7. doi: 10.1111/j.1749-6632.1990.tb16110.x.
33. McCaffrey TA, Falcone DJ, Du B. Transforming growth factor-beta 1 is a heparin-binding protein: identification of putative heparin-binding regions and isolation of heparins with varying affinity for TGF-beta 1. J Cell Physiol. 1992 Aug;152(2):430-40. doi: 10.1002/jcp.1041520226.

International Journal of Biomedicine 12(4) (2022) 548-553
http://dx.doi.org/10.21103/Article12(4)_OA4

ORIGINAL ARTICLE

Orthopedics & Traumatology

INTERNATIONAL JOURNAL OF BIOMEDICINE

Synovium-Derived Mesenchymal Stem Cells in Combination with Low Molecular Weight Hyaluronic Acid for Cartilage Repair

Madina Sarsenova[1,2], Ainur Mukhambetova[1], Bakhtiyar Saginov[3], Yerik Raimagambetov[3], Vyacheslav Ogay[1*]

[1]*Stem Cell Laboratory, National Center for Biotechnology, Astana, Kazakhstan*
[2]*School of Medicine, Nazarbayev University, Astana, Kazakhstan*
[3]*National Scientific Center of Traumatology and Orthopedics named after Academician N. D. Batpenov, Astana, Kazakhstan*

Abstract

Regeneration of damaged articular cartilage remains one of the most complex and unresolved problems in traumatology and orthopedics. In this study, we investigated whether intra-articular injection of synovium-derived mesenchymal stem cells (SD-MSCs) with low molecular weight hyaluronic acid (LMWHA) could promote the regeneration of damaged cartilage in rabbits. To answer this question, rabbits' SD-MSCs were harvested, expanded in culture, and characterized by CFU assay and a multilineage differentiation test. For in vivo study, we created a defect within the cartilage layer without destroying subchondral bone. Two weeks after the cartilage defect, SD-MSCs (2×10^6 cells) were suspended in 0.5% LMWHA and injected into the left knee, and hyaluronic acid (HA) solution alone was placed into the right knee. Cartilage regeneration in experimental and control groups was evaluated macroscopically and histologically at Days 30, 60, and 90. The results of the study showed an early process of cartilage regeneration in the defect area on Day 30 after intra-articular MSCs-HA injection. Histological studies revealed that cartilage defect was covered by a thin layer of spindle-shaped undifferentiated cells and proliferated chondroblasts, in contrast to a single HA injection, which did not induce cartilage regeneration. On Day 60, we observed that the size of the cartilage defect after MSCs-HA injection significantly decreased, compared to one after HA injection. On Day 90, the cartilage defect in a knee treated with MSCs-HA was fully regenerated and was similar to intact cartilage. Thus, the combined application of the MSCs, HA, and chondroinductive proteins have a high therapeutic effect on cartilage defect regeneration in rabbits.(**International Journal of Biomedicine. 2022;12(4):548-553.**).

Keywords: mesenchymal stem cells • hyaluronic acid • growth factors • cartilage defect • regeneration • cell therapy

For citation: Sarsenova M, Mukhambetova A, Saginov B, Raimagambetov Y, Ogay V. Synovium-Derived Mesenchymal Stem Cells in Combination with Low Molecular Weight Hyaluronic Acid for Cartilage Repair. International Journal of Biomedicine. 2022;12(4):548-553. doi:10.21103/Article12(4)_OA4

Abbreviations

BMP, bone morphogenic protein; **CFU**, colony-forming unit; **CCM**, complete culture medium; **CT**, cartilage tissue; **GFs**, growth factors; **HA**, hyaluronic acid; **LMWHA**, low molecular weight HA; **PBS**, phosphate-buffered saline; **SM**, synovial membrane; **SD-MSCs**, synovium-derived mesenchymal stem cells; **TGF-β**, transforming growth factor-beta.

Introduction

Regeneration of damaged articular cartilage remains one of the most complex and unresolved problems in traumatology and orthopedics.(1) The absence of its own perichondrium results in poor cellular regeneration. Only in peripheral injuries with the areas adjacent to the synovial membrane is the process of histotypical restoration of hyaline cartilage tissue (CT) observed. In deep injuries communicating with the bone marrow canal, migration of mesenchymal stem cells (MSCs) from the bone marrow to the defect area is ensured. This occurrence can serve as a

cellular source for regeneration.[2] However, even if damaged hyaline cartilage is restored in this manner, the cartilage is formed with fibrous tissue, which differs significantly in architectonics, the biochemical composition of the matrix, and mechanical properties.

The current non-surgical methods, including physiotherapy and intra-articular injections, as well as surgical procedures, such as multiple microperforations of the articular surface, abrasion, and microfractures, are aimed at stimulating the CT regeneration and are not able to provide a complete and sustainable cure without complication.[3]

Advanced options for cellular arthroplasty involve a combination of cellular technology with a complex surgical technique, among these methods - transplantation of autologous chondrocyte under a periosteal patch or a resorbable collagen membrane.[4,5] This technology is called autologous chondrocyte implantation. Even though this method is able to improve cartilage defect regeneration to some extent, it has certain limitations. The major of these are trauma, in cases when a transplant is taken from an adjacent healthy area of cartilage, difficulties in obtaining a sufficient number of chondrocytes, and the expansion of chondrocytes in culture. Additionally, another disadvantage is incomplete recovery, which is explained by the formation of fibrous cartilage but not functional hyaline tissue.[6,7] Moreover, there is a question of the optimal source of cells, their acceptable carrier to the damaged area, and immobilization for the complete and efficient recovery of damaged cartilage.

In order to develop an effective cell preparation, it was necessary to choose the optimal source of MSCs. An effective solution might be the use of synovial MSCs obtained from the same individual.[8-11] SD-MSCs are more effectively involved in the activation of chondrogenesis and have a higher proliferative and chondrogenic potential than MSCs derived from bone marrow or adipose tissue.[12-14] Other advantages of using SD-MSCs in cellular therapy for cartilage defects are the ease of isolation, less traumatic nature of material sampling using arthroscopy, and obtaining a sufficient amount of MSCs from a small fragment of synovial tissue, which can completely self-repair in a short period of time.[15]

As a biocompatible and biodegradable agent, we chose low molecular weight hyaluronic acid (LMWHA). HA plays the role of a lubricant and shock absorber, an energy-accumulating agent between opposite cartilage, and a semi-permeable barrier that regulates metabolic processes between cartilage and synovial fluid.[16] Thus, the use of this biopolymer will not only reduce pain in the joint, but also increase the therapeutic efficacy of restoring damaged CT.

Additionally, in the development of the drug, we propose the addition of chondroinductive growth factors such as TGF-β1 and BMP-4 in a certain combination and optimal concentration, which will increase the regeneration of cartilage defects and other damage to the knee joint.[17]

In this study, we obtained and characterized primary cultures of SD-MSCs from the knee joints of experimental rabbits. In addition, we studied the effect of MSCs and HA on cartilage defect regeneration in rabbits. In vivo data showed that SD-MSCs after intra-articular injection were distributed mainly in the area of the defect, suggesting that the cells have a tropism for damaged areas of CT. It was also revealed that the intra-articular injection of MSCs with HA leads to a complete repair of the cartilage defect within 90 days, compared with the individual use of HA, which did not have an effect on cartilage regeneration. In contrast, the combined administration of SD-MSCs with HA and growth factors resulted in a significant acceleration of the regeneration process in cartilage defects with a complete restoration of hyaline-like cartilage within 30 days.

Thus, the results of this study demonstrate that SD-MSCs and growth factors (TGF-β1 and BMP-4) play a crucial role in CT repair. The combined application of the MSCs, HA, and chondroinductive proteins have a high therapeutic effect on cartilage defect regeneration in rabbits. It is assumed that the results of this work might serve as a basis for the application in orthopedics, namely in cell-based therapy for cartilage defects.

Materials and Methods

Animals

Skeletally mature male grey Giant rabbits were purchased from the "KletkaMaster" company (Saint Petersburg, Russian Federation). Rabbits were held in large cages at a temperature of 23°C and relative humidity of 60%. The access to food and water for all experimental animals was ad libitum. All procedures from this study were approved by the local Ethical Committee and the Institutional Review Board of the National Center for Biotechnology (IRB 00013497). All experimental procedures were performed following the guidelines for the care and use of laboratory animals.

Isolation and cultivation of rabbit SD-MSCs

The isolation of the synovial membrane from the knee joints of rabbits was performed under general calypsol anesthesia (5 mg/kg intramuscularly). The synovium was rinsed with a mixture of antimycotic-antibiotics (100 U/mL penicillin, 100 μg/mL streptomycin, and 0.25 μg/mL amphotericin B) in phosphate-buffered saline, minced into 1-2mm^3 pieces, and processed with 0.3% collagenase type II solution for 16 hours at 37°C. The resulting cell suspension was filtered through a 70-μm cell strainer (BD Biosciences, USA) to remove the remaining tissue fragments. Following that, the cells were resuspended in α-MEM complete culture medium, counted in a hemocytometer and cultured in a T75 cell culture flask (Corning, USA) at 37°C and 5% CO_2. After 2 days, the cells unattached to the plastic were removed, and the fraction of adherent cells was cultivated until cells reached 80-90% confluence. Passaging of the MSCs was performed with TrypLE™ Express (Thermo Fisher Scientific, USA) with an interval of 5-7 days. The medium in the cell culture was changed every 2 days.

Fibroblastic colony forming unit test

Cells isolated from the rabbit synovial tissue were seeded into Petri dishes at a rate of 1cell/cm^2 and cultured in complete culture medium for 14 days at 37°C and 5% CO_2. At the end of the cultivation period, the cells were washed with phosphate-buffered saline and stained with 0.5% crystal violet solution for 5 min at room temperature. After washing twice with phosphate-buffered saline, the formed colonies were dried and counted using an SZ61 stereomicroscope (Olympus, Germany).

Multilineage differentiation test

For differentiation into chondrocytes, at passage 4 MSCs were resuspended in a differentiation medium consisting of high glucose DMEM medium, 1% ITS+Premix (BD Biosciences, USA), 100μM ascorbate-2-phosphate (Sigma, USA), 10^{-7}M dexamethasone (Sigma, USA), and 10ng/mL TGFβ1 (Sigma, USA) at a concentration of 1.25×10^6 cells/mL. To create chondrogenic cell pellets, each well of a 96-well polypropylene plate was loaded with 2.5×10^5 cells, centrifuged at 400g, and transferred to a CO_2 incubator at 37°C, and 5% CO_2. The medium was changed 3 times a week. On day 21 of differentiation, cell pellets were collected and fixed in 10% neutral buffered formalin. Samples were placed into paraffin, cut on a microtome, and processed for staining with hematoxylin-eosin (H&E).

For osteogenic differentiation of MSCs, at passage 4 we used an induction medium containing 10^{-7}M dexamethasone, 10mM β-glycerol-phosphate, and 50 μM ascorbate-2-phosphate. After 3 weeks of cultivation, the cells were stained with Alizarin Red.

MSCs were differentiated into adipocytes by culturing them in an induction medium containing 10^{-6}M dexamethasone, 0.5μM 3-isobutyl-1-methylxanthine, and 10ng/mL insulin for 3 weeks at the same passage as chondrocytes and osteoblasts and stained with Oil Red O.

Cartilage defect model and intra-articular injection of SD-MSCs

Surgical intervention was performed under ketamine anesthesia at the concentration of 5mg/kg of the rabbit body weight. After anesthesia was achieved, the experimental animals were fixed on the operating table. A 4 mm diameter cartilage defect was formed in the intercondylar area of the thigh, in the area of the femoral-patellar joint. To unify the modeled defect, we used the COR kit for mosaic chondroplasty of the femoral condyles (Johnson&Johnson, USA). To exclude the reparative function of the bone marrow, the defect was performed within the cartilage without destroying the subchondral bone. The joint cavity was washed with sterile phosphate-buffered saline, the wound was sutured in layers. Three days post-operation gentamicin was used to prevent purulent complications.

Two weeks after the cartilage defect, to evaluate the effect of HA in combination with SD-MSCs, the cells at the concentration of 2×10^6/100μL of DMEM media were suspended in 0.5% of LMWHA (*OSTENIL®*, TRB CHEMEDICA AG, Haar/Munich, Germany) and injected into the left knee. HA solution alone in the same concentration was used as a control, which was administered into the right joint of the same rabbits. The procedure was performed 3 times at an interval of 7 days. The determination of cartilage defect regeneration in the intermuscular region of the knee joint was evaluated by macroscopic and histological analyses at different time points on Days 30, 60, and 90.

To study the possibility of enhancing the regeneration of a cartilage defect, the following experimental groups were used: Group 1: 0.5% HA, TGF-β1 (100 ng/mL) and BMP-4 (500 ng/mL); Group 2: 0.5% HA, 5×10^6 of MSCs, and TGF-β1 (100 ng/mL) and BMP-4 (500 ng/mL). A 0.5% HA was used as a control.

Histological Analysis

Joints with cartilage defects were fixed in 4% paraformaldehyde solution (pH=7.2). After washing in phosphate-buffered saline, the samples were decalcified, then dehydrated consistently in 70%, 95%, 95%, 100%, and 100% ethanol and immersed in xylene. Then, the samples were infiltrated with paraffin, embedded into paraffin blocks, and cut into 5μm sections. Before staining, sections were treated with xylene and sequentially rehydrated in 100%, 100%, 95%, 95%, and 70% ethyl alcohol and distilled water in order to remove paraffin. The sections from each defect were stained with modified Mayer's H&E, sequentially dehydrated and cleared with ethyl alcohol and xylene, and mounted in histological medium Bio Mount HM (Bio-Optica, Italy). The stained samples were analyzed using a light microscope (Carl Zeiss, Germany). The cartilage defect regeneration area was measured using the AnalySIS® program (Olympus, Germany).

Statistical analysis was performed using The GraphPad Prism 8 software. Baseline characteristics were summarized as frequencies and percentages for categorical variables and as mean±SD for continuous variables. Inter-group comparisons were performed using Student's t-test. A probability value of $P<0.05$ was considered statistically significant.

Results

At the first stage of this study, MSCs were isolated from the synovium of the knee joints of 12 mature rabbits and further characterized. The isolated cells had a fibroblast-like morphology (Figure 1A), the capacity to adhere to culture plastic, and a high ability to proliferate and form cell colonies (Figure 1B-C). Moreover, it has been found that the cells also were able to differentiate into adipocytes, osteoblasts, and chondrocytes when cultured in selective differentiation media (Figure 1D-F). MSCs differentiated into adipocyte-like cells and formed lipid vacuoles in the cytoplasm, which were stained by Oil Red O. Osteoblast-like cells accumulated calcium deposits by Alizarin Red staining. Moreover, chondrogenic differentiation resulted in the formation of chondrogenic pellets with the characteristic hyaline-like morphology shown by H&E staining.

At the same stage of the synovial membrane isolation, we created a massive cartilage defect 4 mm in diameter in the intermuscular region of the knee joint. In order to avoid the release of bone marrow progenitor cells into the defect area, the defect was performed up to the border of the subchondral bone. After the synovial membrane isolation, MSCs were cultured for 14 days to produce an appropriate cell mass. The macroscopic and histological analyses after using the HA in combination with MSCs showed interesting results (Figure 2).

As shown in Figure 2G, 30 days after MSC administration, the area of cartilage defect was markedly reduced, compared to the control. On Day 60, the macroscopic analysis demonstrated that the cartilage defect was substantially repaired and looked almost like native articular cartilage (Figure 2H). On Day 90 after MSC transplantation, the area of the cartilage defect was completely recovered (Figure 2I). These results were confirmed by the histologic analysis. Histology showed that on Day 30, the formation of the fibrocartilaginous layer containing both undifferentiated cells and chondrocytes was observed (Figure 2J). On Day 60, histology showed that the formation of hyaline-like cartilage occurred. As can be seen in Figure 2K, the emerging

hyaline-like cartilage consists of three conditional layers: 1) the upper fibrous layer, consisting of undifferentiated cells surrounded by collagen fibers; 2) a layer containing chondroblasts, and 3) a layer of hyaline-like cartilage containing clusters of chondrocytes. On Day 90, the analysis showed the formation of hyaline cartilage with almost fully repaired cartilage (Figure 2L).

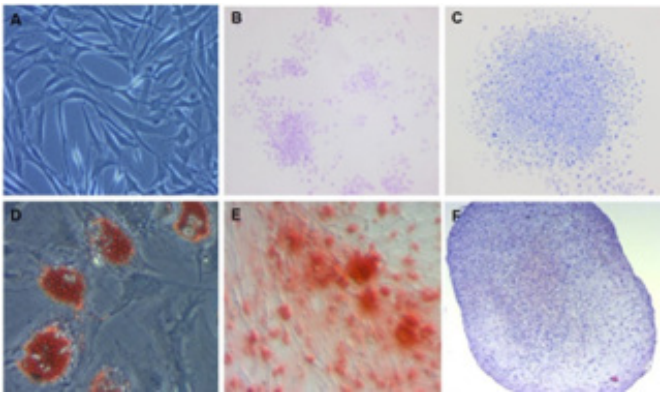

Fig. 1. *Rabbit SD-MSC characterization. A) Phase-contrast image of a live cell culture with fibroblast-like morphology. B) CFU assay. SD-MSCs are able to proliferate and form colonies rapidly. C) Enlarged image of CFU assay. D-F) Multilineage differentiation test. D) Differentiation of MSCs into adipocytes. Lipid vacuoles stained with Oil Red O are visible. E) Differentiation of MSCs into osteoblasts. Calcium deposits are visible in the cells stained with Alizarin Red. E) Differentiation of MSCs into chondrocytes. H&E staining.*

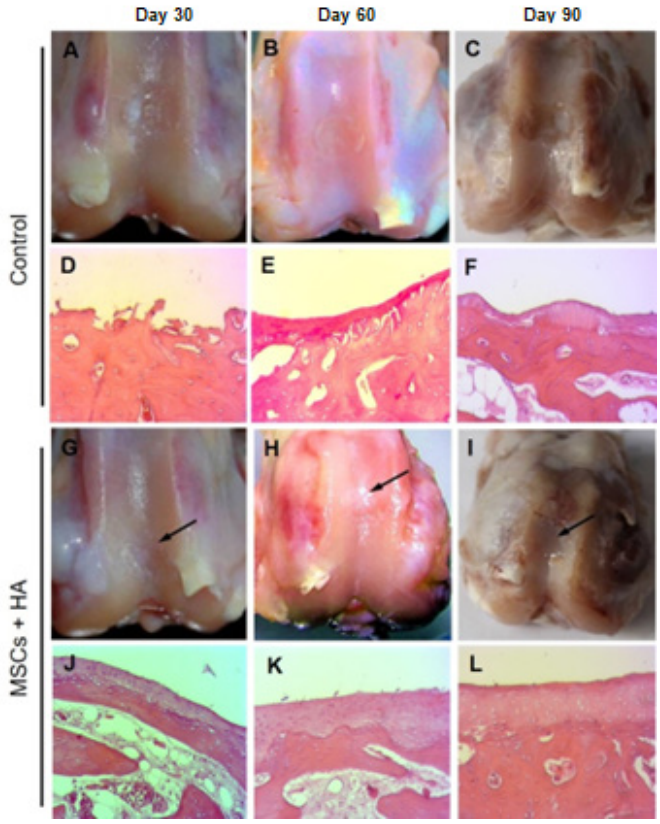

Fig. 2. *Macroscopic (A-C, G-I) and histological (D-F, J-L) analyses of cartilage defect regeneration after intra-articular injection of rabbit synovial MSCs at the indicated time points. The black arrow shows a regenerating cartilage defect. HA only was used as a control.*

Macroscopic and histological analyses of articular cartilage regeneration after the application of HA with growth factors (TGF-β1 and BMP-4) showed that on Day 30, there was a marginal repair of the defect by about 40%-50% (Figures 3B and 3E). Apparently, the addition of TGF-β1 and BMP-4 leads to the activation of the proliferation of endogenous chondroblasts, resulting in the regeneration of the cartilage defect.

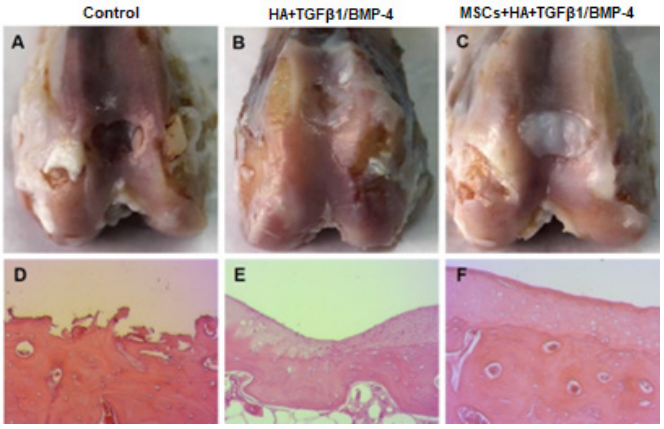

Fig. 3. *Macroscopic (A-C) and histological (D-F) analyses of cartilage defect regeneration after intra-articular injection of rabbit SD-MSCs on Day 0 and Day 30.*

The evaluation of the articular cartilage defect regeneration after the use of MSCs in combination with HA and growth factors demonstrated a significant acceleration of the regeneration in the defective area. As shown on macroscopic and histological images (Figures 3C and 3F), 30 days after the intra-articular injection, complete closure of the defect area with hyaline-like CT was observed. Spontaneous recovery was not observed in the control samples. Additionally, the macroscopic results were quantitatively evaluated. As shown in Figure 4, the regeneration area of the defect after HA in combination with growth factor administration was at the level of 2 mm and was significantly higher than the control (P<0.05). In contrast to the treatment with hyaluronic acid + growth factors, the combination of hyaluronic acid with growth factors and MSCs had a more pronounced effect with a regeneration area of 4 mm (P<0.05).

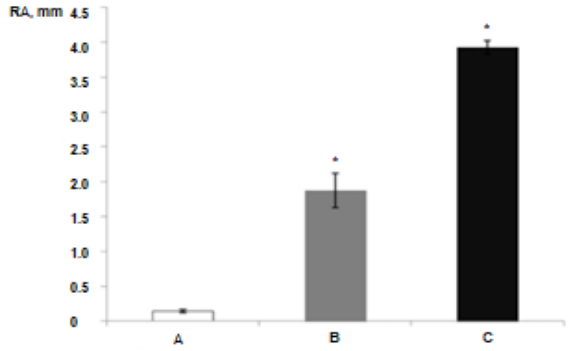

Fig. 4. *Quantitative measurements for the macroscopic analysis of cartilage defect regeneration after intra-articular administration of rabbit SD-MSCs and growth factors.* ***RA*** *- Regeneration area (mm).* ***A.*** *Control: 0.14±0.02 mm;* ***B.*** *HA+TGFβ1/BMP-4: 1.87±0.25 mm;* ***C.*** *MSCs+HA+TGFβ1/BMP-4: 3.9±0.09 mm. *- Significant difference from control, P<0.05.*

Discussion

The development and implementation of cell-based preparations for the treatment of degenerative diseases of joints remain one of the promising directions in cellular therapy and tissue engineering. In this regard, biotechnological methods for obtaining cellular preparations encounter the need to address several issues: 1) the optimal cell source; 2) a method for their delivery to the defect area; 3) an adequate biocompatible matrix.

In this study, as an optimal source of MSCs, we chose the synovial membrane, which can be easily isolated from a patient during arthroscopic procedures. It is justified by several studies, which showed that MSCs isolated from the synovial membrane have a higher proliferative potential and a higher potential than MSCs to differentiate into chondrocytes from bone marrow or adipose tissue.[15,18] At the same time, the functional activity of synovial MSCs remains at a high level, regardless of the person's age. The procedure for isolating MSCs from the synovial membrane of a human or animal is relatively simple to perform, which includes the following steps: 1) sampling of the synovial membrane from the knee joint, 2) washing in a sterile buffer with antibiotics, 3) mincing the tissue into small pieces, 4) processing with collagenase, 5) filtering through a special nylon filter, and 6) counting seeding the cells in a culture dish, followed by cultivation in a CO_2 incubator. Using this technique, we managed to obtain primary cultures of rabbit SD-MSCs. The resulting cultures of MSCs had high adhesiveness to the culture plastic and the ability to form fibroblastic CFU. Moreover, they differentiated into adipocytes, chondrocytes, and osteoblasts.

As previously described, HA is a natural biopolymer that provides the viscoelastic properties of the synovial fluid. In the synovial fluid, HA acts as a lubricant and shock absorber, an energy-accumulating agent between opposite cartilage, and regulates metabolic processes between cartilage and synovial fluid.[16,19] Moreover, HA has been shown to have an anti-inflammatory, anabolic, and analgesic effect when injected into an injured joint.[20] Thus, given its unique properties, we have chosen this biopolymer for use in the development of our cell preparation. In our study, we used a commercial Ostenil drug based on 1% LMWHA, which is commonly used for local therapy of osteoarthritis.

In addition, after observing the positive impact of HA in combination with SD-MSCs administration, we questioned how to enhance the therapeutic effect of the cellular preparation. According to the literature, there are several key GFs that increase MSC proliferation and their differentiation into chondrocytes, among which is TGF-β1, which plays a central role in chondrogenesis.[21] This factor stimulates the synthesizing activity of chondrocytes and acts against the catabolic activity of the inflammatory mediator, IL-1, and also increases the proliferation and chondrogenic differentiation of bone marrow MSCs. Moreover, the cultivation of MSCs with the addition of TGF-β1 led to the suppression of the expression of the collagen I gene, and at the same time, activated the expression of collagen II, which is synthesized during the formation of hyaline cartilage.[22]

Other important factors that participate in chondrogenesis and osteogenesis are BMPs, which are homodimeric molecules belonging to the TGF-β superfamily. There are 13 types of BMPs (from BMP-2 to BMP-14) that are involved in the regeneration of cartilage and bone tissue.[23] The most studied of them are BMP-2 and BMP-7, which are already used in clinical practice to repair nonunion fractures. In the previous study, it was found that TGF-β1 in combination with BMP-4, has a significant effect on both chondrogenic differentiation and the synthesis of extracellular matrix and glycosaminoglycans in chondrogenic micropellets.[17] Apparently, BMP-4 acts synergistically with TGF-β1, stimulating chondrogenesis in synovial MSCs and chondroprogenitor cells. Similar results were obtained by other researchers who showed that the combination of TGF-β3 and BMP-4 is necessary to stimulate chondrogenesis, while chondoprogenitor cells can differentiate into chondrocytes in the presence of BMP-4 alone.

At the next stage of the study, we evaluated the regenerative potential of SD-MSCs in rabbits with a massive defect in the cartilage of the knee joint. In order to exclude the reparative function of the bone marrow, the defect was performed within the cartilage, without destroying the subchondral bone. In our study, we used SD-MSCs in combination with HA, which served not only as a scaffold for cell delivery, but also as an anti-inflammatory and analgesic agent. The macroscopic and histological analyses for the evaluation of cartilage defect regeneration at different time points showed that intra-articular injection of synovial MSCs with HA significantly accelerates the process of regeneration of damaged CT in rabbits. In subsequent periods of observation, it was shown that a significant acceleration in the recovery of a cartilage defect led to the formation of hyaline-like cartilage on Day 90 after the introduction of MSCs with HA.

Animal studies showed that the combination of TGF-β1 and BMP-4 with SD-MSCs and HA significantly accelerated the process of cartilage defect repair in experimental rabbits. Already on Day 30 after the injection of HA and MSCs with GFs, we observed a complete closure of the defect by hyaline-like cartilage. In contrast, the intra-articular injection of HA with MSCs only resulted in the restoration of damaged CT on Day 90. Apparently, the addition of TGF-β and BMP-4 leads to stimulation of the proliferation and differentiation of MSCs and endogenous chondroblasts, resulting in the regeneration of the cartilage defect.

In conclusion, based on the obtained data, it can be said that the combined intra-articular application of SD-MSCs with HA and TGF-β+BMP-4 significantly accelerates the process of regeneration of damaged CT, compared to their separate use.

Sources of Funding

This study was funded by the Ministry of Education and Science of the Republic of Kazakhstan in frame scientific programs: № OR11465426 "The implementation of innovative tissue engineering technologies into medical practice for the restoration of damaged joints" and BR11065157 "Development and scientific rationale of innovative technologies to improve the

effectiveness of diagnosis, treatment of injures, consequences of injures, diseases of the limbs, spine and pelvis."

Competing Interests

The authors declare that they have no competing interests.

References

1. Marlovits S, Kutscha-Lissberg F, Aldrian S, Resinger C, Singer P, Zeller P, Vécsei V. [Autologous chondrocyte transplantation for the treatment of articular cartilage defects inf the knee joint. Techniques and results]. Radiologe. 2004 Aug;44(8):763-72. doi: 10.1007/s00117-004-1082-0. [Article in German].
2. Caldwell KL, Wang J. Cell-based articular cartilage repair: the link between development and regeneration. Osteoarthritis Cartilage. 2015 Mar;23(3):351-62. doi: 10.1016/j.joca.2014.11.004.
3. Kan HS, Chan PK, Chiu KY, Yan CH, Yeung SS, Ng YL, Shiu KW, Ho T. Non-surgical treatment of knee osteoarthritis. Hong Kong Med J. 2019 Apr;25(2):127-133. doi: 10.12809/hkmj187600.
4. Rahmani Del Bakhshayesh A, Babaie S, Tayefi Nasrabadi H, Asadi N, Akbarzadeh A, Abedelahi A. An overview of various treatment strategies, especially tissue engineering for damaged articular cartilage. Artif Cells Nanomed Biotechnol. 2020 Dec;48(1):1089-1104. doi: 10.1080/21691401.2020.1809439.
5. Panseri S, Russo A, Cunha C, Bondi A, Di Martino A, Patella S, Kon E. Osteochondral tissue engineering approaches for articular cartilage and subchondral bone regeneration. Knee Surg Sports Traumatol Arthrosc. 2012 Jun;20(6):1182-91. doi: 10.1007/s00167-011-1655-1.
6. Jiang S, Guo W, Tian G, Luo X, Peng L, Liu S, Sui X, Guo Q, Li X. Clinical Application Status of Articular Cartilage Regeneration Techniques: Tissue-Engineered Cartilage Brings New Hope. Stem Cells Int. 2020 Jun 30;2020:5690252. doi: 10.1155/2020/5690252.
7. Epanomeritakis IE, Lee E, Lu V, Khan W. The Use of Autologous Chondrocyte and Mesenchymal Stem Cell Implants for the Treatment of Focal Chondral Defects in Human Knee Joints-A Systematic Review and Meta-Analysis. Int J Mol Sci. 2022 Apr 6;23(7):4065. doi: 10.3390/ijms23074065.
8. Han Y, Li X, Zhang Y, Han Y, Chang F, Ding J. Mesenchymal Stem Cells for Regenerative Medicine. Cells. 2019 Aug 13;8(8):886. doi: 10.3390/cells8080886.
9. Campagnoli C, Roberts IA, Kumar S, Bennett PR, Bellantuono I, Fisk NM. Identification of mesenchymal stem/progenitor cells in human first-trimester fetal blood, liver, and bone marrow. Blood. 2001 Oct 15;98(8):2396-402. doi: 10.1182/blood.v98.8.2396.
10. Dai R, Yu Y, Yan G, Hou X, Ni Y, Shi G. Intratracheal administration of adipose derived mesenchymal stem cells alleviates chronic asthma in a mouse model. BMC Pulm Med. 2018 Aug 8;18(1):131. doi: 10.1186/s12890-018-0701-x.
11. Voga M, Adamic N, Vengust M, Majdic G. Stem Cells in Veterinary Medicine-Current State and Treatment Options. Front Vet Sci. 2020 May 29;7:278. doi: 10.3389/fvets.2020.00278.
12. Makris EA, Hadidi P, Athanasiou KA. The knee meniscus: structure-function, pathophysiology, current repair techniques, and prospects for regeneration. Biomaterials. 2011 Oct;32(30):7411-31. doi: 10.1016/j.biomaterials.2011.06.037.
13. Zha K, Sun Z, Yang Y, Chen M, Gao C, Fu L, Li H, Sui X, Guo Q, Liu S. Recent Developed Strategies for Enhancing Chondrogenic Differentiation of MSC: Impact on MSC-Based Therapy for Cartilage Regeneration. Stem Cells Int. 2021 Mar 20;2021:8830834. doi: 10.1155/2021/8830834.
14. Bae HC, Park HJ, Wang SY, Yang HR, Lee MC, Han HS. Hypoxic condition enhances chondrogenesis in synovium-derived mesenchymal stem cells. Biomater Res. 2018 Sep 26;22:28. doi: 10.1186/s40824-018-0134-x. Erratum in: Biomater Res. 2019 Mar 4;23:7.
15. Sakaguchi Y, Sekiya I, Yagishita K, Muneta T. Comparison of human stem cells derived from various mesenchymal tissues: superiority of synovium as a cell source. Arthritis Rheum. 2005 Aug;52(8):2521-9. doi: 10.1002/art.21212.
16. Li L, Duan X, Fan Z, Chen L, Xing F, Xu Z, Chen Q, Xiang Z. Mesenchymal Stem Cells in Combination with Hyaluronic Acid for Articular Cartilage Defects. Sci Rep. 2018 Jul 2;8(1):9900. doi: 10.1038/s41598-018-27737-y.
17. Hatsushika D, Muneta T, Horie M, Koga H, Tsuji K, Sekiya I. Intraarticular injection of synovial stem cells promotes meniscal regeneration in a rabbit massive meniscal defect model. J Orthop Res. 2013 Sep;31(9):1354-9. doi: 10.1002/jor.22370.
18. Gale AL, Linardi RL, McClung G, Mammone RM, Ortved KF. Comparison of the Chondrogenic Differentiation Potential of Equine Synovial Membrane-Derived and Bone Marrow-Derived Mesenchymal Stem Cells. Front Vet Sci. 2019 Jun 6;6:178. doi: 10.3389/fvets.2019.00178.
19. Ha CW, Park YB, Chung JY, Park YG. Cartilage Repair Using Composites of Human Umbilical Cord Blood-Derived Mesenchymal Stem Cells and Hyaluronic Acid Hydrogel in a Minipig Model. Stem Cells Transl Med. 2015 Sep;4(9):1044-51. doi: 10.5966/sctm.2014-0264.
20. Kang SW, Bada LP, Kang CS, Lee JS, Kim CH, Park JH, Kim BS. Articular cartilage regeneration with microfracture and hyaluronic acid. Biotechnol Lett. 2008 Mar;30(3):435-9. doi: 10.1007/s10529-007-9576-2.
21. Danišovič L, Varga I, Polák S. Growth factors and chondrogenic differentiation of mesenchymal stem cells. Tissue Cell. 2012 Apr;44(2):69-73. doi: 10.1016/j.tice.2011.11.005.
22. Blaney Davidson EN, van der Kraan PM, van den Berg WB. TGF-beta and osteoarthritis. Osteoarthritis Cartilage. 2007 Jun;15(6):597-604. doi: 10.1016/j.joca.2007.02.005.
23. Miljkovic ND, Cooper GM, Marra KG. Chondrogenesis, bone morphogenetic protein-4 and mesenchymal stem cells. Osteoarthritis Cartilage. 2008 Oct;16(10):1121-30. doi: 10.1016/j.joca.2008.03.003.

***Corresponding author:** Prof. Vyacheslav Ogay, PhD, National Center for Biotechnology. Astana, Kazakhstan. E-mail: ogay@biocenter.kz*

International Journal of Biomedicine 12(4) (2022) 554-559
http://dx.doi.org/10.21103/Article12(4)_OA5

ORIGINAL ARTICLE

Obstetrics and Gynecology

INTERNATIONAL JOURNAL OF BIOMEDICINE

Fetal Biometry and Doppler Assessment of Pregnant Women with COVID-19

Hiba Ahmed Suhail[1], Dalya Mudhafar Abdulrahman[2], Abeer Wali Ahmed[3*]

[1]*Department of Gynecology and Obstetrics, Collage of Medicine, University of Mosul, Mosul, Iraq*
[2]*Department of Obstetrics and Gynecology, Collage of Medicine, Nineveh University, Mosul, Iraq*
[3]*Department of Surgery, Collage of Medicine, Nineveh University, Mosul, Iraq*

Abstract

Background: The world has changed radically because of the worldwide COVID-19 pandemic. SARS-CoV-2, a unique strain of large, enveloped single-stranded RNA viruses, that has spread around the world. The primary objective of this research was to assess the fetal growth velocity in pregnancies complicated by SARS-CoV-2 infection and those that were not. The secondary objective was to determine if SARS-CoV-2 infection may affect maternal and fetal Doppler readings.

Methods and Results: A total of 250 pregnant women diagnosed with SARS-CoV-2 (Case group) were compared to 300 healthy pregnant women (Control group) in a prospective case-control study in Mosul from February 20 to October 20, 2021. Infections during pregnancy were detected and verified using the real-time reverse transcriptase-polymerase chain reaction (RT-PCR). All ultrasound exams were done from 24 to 40 weeks. Measuring parameters using Doppler ultrasonography included plasticity and resistive indices (PI, RI), as well as cerebroplacental ratio computed according to gestational age. Fetal development in utero was assessed by measuring biometric markers, such as parietal diameter, head size, belly circumference, leg length, and estimated fetal weight every four weeks. The US scans in the second and third trimester of pregnancy showed no evidence of congenital abnormalities (P=0.7047). There was a significant incidence of cesarean delivery (P=0.0000) and lower fetal activity at birth (P=0.0000) in the Case group, compared to the Control group. Anticoagulant treatment during pregnancy was not associated with an increased risk of postpartum hemorrhage in women of the Case group. Also, there were no significant differences in fetal biparietal diameter and femur length between groups in the second and third trimesters, and both fetal and maternal Doppler studies throughout the second and third trimesters of pregnancy yielded no significant differences in the PI and RI indices. (**International Journal of Biomedicine. 2022;12(4):554-559.**).

Keywords: pregnancy • Doppler ultrasonography • COVID-19 • fetal biometry

For citation: Suhail HA, Abdulrahman DM, Ahmed AW. Fetal Biometry and Doppler Assessment of Pregnant Women with COVID-19. International Journal of Biomedicine. 2022;12(4):554-559. doi:10.21103/Article12(4)_OA5

Abbreviations

BMI, body mass index; **BPD,** biparietal diameter; **CD**, cesarean delivery; **CPR,** cerebro-placental ratio; **DU**, Doppler ultrasonography; **FL**, femur length; **IUGR**, intrauterine growth restriction; **MCA**, middle cerebral artery; **PI**, pulsatility index; **RI**, resistance index, **UA**, umbilical artery.

Introduction

The world has changed radically because of the worldwide COVID-19 pandemic. SARS-CoV-2, a unique strain of large, enveloped single-stranded RNA viruses, that has spread around the world. As a result of the outbreak of SARS-CoV-2 infections in recent years, the virus has emerged as a significant public health threat.[1] The possible repercussions of these infections on pregnancy are a serious cause of worry for obstetric care professionals.[2-5] Since the outbreak of the pandemic, women who are expecting a child have had a higher risk of developing a life-threatening illness. When comparing nonpregnant women infected with SARS-CoV-2 to pregnant infected women, the pregnant women showed an increased

***Corresponding author**: Dr. Abeer Wali Ahmed. Department of Surgery, Collage of Medicine, Nineveh University, Mosul, Iraq. E-mail: abeerwali82@gmail.com*

chance of severe chest symptoms, need for hospitalization in critical care units, and demand for mechanical ventilators.[6-8]

Pregnant women have a higher concentration of angiotensin-converting-enzyme receptors in the uterus and placenta, making them a perfect target for the transmission of SARS-CoV-2.[9,10] Another piece of evidence supporting this conclusion comes from the higher incidence of indications of decidual arteriopathy in pregnant women infected with SARS-CoV-2, which the researchers say shows that there is a significant association between infection and impaired placental function.[11-13]

Some patients show no symptoms even if their COVID-19 test is positive. Although intrauterine vertical transmission of SARS-CoV-2 has been shown, the most prevalent finding in placental disease is fetal vascular mal perfusion. Maternal-fetal morbidity and death are clearly increased in instances of severe pneumonia, which is often associated with COVID-19. Pregnant women who have been infected should have their prenatal follow-up appointments enhanced, since this may identify a wide range of unfavorable pregnancy outcomes, including miscarriage, IUGR, preeclampsia, and fetal mortality. Consequently, in pregnant women who have recovered from COVID-19, fetal development should be evaluated by ultrasound and Doppler to identify inadequate placental supply, intrauterine growth limitation, and other obstetric problems, among other things. Ultrasound examination of uterine artery, middle cerebral artery (MCA), umbilical artery (UA), and other fetal vessels for fetal well-being, as well as other fetal vasculature, has traditionally been performed in the second and third trimesters of pregnancy to check on the health of the fetus. The assessment of pulsatility index (PI) and resistance index (RI) is a way of measuring uteroplacental perfusion. Variations in vascular resistance are referred to as downstream vascular resistance and are used to predict newborn issues such as IUGR, low birth weight, and intrauterine fetal mortality.

The risk of SARS-CoV-2 infection in pregnant women who have elevated angiotensin-converting enzyme 2 (ACE2) receptors has been linked to hypertension during pregnancy. The binding of the virus to ACE2 causes it to be down-regulated, which can make angiotensin II (Ang-II) more likely to be produced than Ang-(1-7), which can cause vasoconstriction, and which in turn can cause preeclampsia or make it worse[14] (Fig.1). The immune responses of pregnant women to SARS-CoV-2 are unclear at this time; however, data from previous pandemics suggest that pregnancy may increase the risk of disease and mortality when compared to nonpregnant women infected with the virus.[15] When an infection arises during pregnancy, it may have an impact on the mother's immune response, viral clearance, and, eventually, the fate of the child after birth. Because the first and third trimesters are pro-inflammatory in nature, it is necessary to induce implantation and labor at these times.[16] According to the researchers, pregnant women who are infected with SARS-CoV-2 throughout three trimesters may be at increased risk of developing severe viral infections (cytokine storm). Unfortunately, significant quantities of stress and inflammation are produced during delivery, and the physiological changes that occur in a mother's body after the birth of her child may result in poor maternal COVID-19 outcomes following the birth.

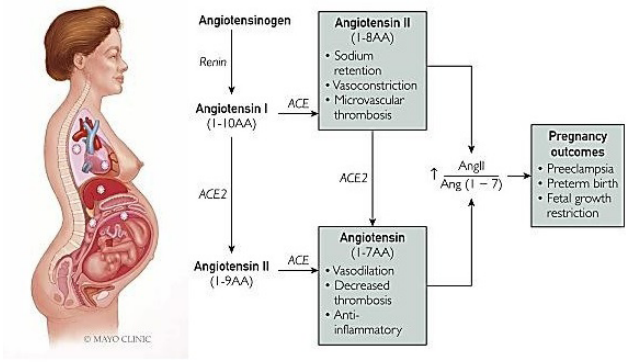

Fig.1. *Pregnancy: COVID-19 and vascular damage pathways.*

Pregnant women with moderate symptoms need postpartum hospitalization for respiratory symptoms.[14] When pregnant, the upper airways get more congested and get more congested from the secretion of mucus the chest wall increases in circumference, and the diaphragm rises higher. These changes in breathing are rather important. They reduce residual volume but increase tidal volume and air trapping. Airway resistance is also reduced significantly while diffusion capacity remains unchanged. Heart output and vascular resistance are both enhanced, and plasma volume decreases by 20% to 50% in hemodynamic alterations.[17] Women who are expecting are more susceptible to respiratory infections because of these abnormalities in their physiology and respiratory alkalosis. Pregnant women with SARS-CoV-2 infection may have symptoms that are similar to physiologic dyspnea, which may cause them to be misdiagnosed and result in more severe sickness. The symptoms of SARS-CoV-2 infection in pregnant women are likely to be more severe than those in nonpregnant women. Although there is a scarcity of data, there have been cases of rapid deterioration in women who initially showed no signs of illness but were subsequently identified with severe COVID-19. Other maternal medical illnesses (hypertension, diabetes, pregnancy cholestasis) were present in some, but not all, patients.[18,19] Cesarean deliveries (CDs) have increased because of the quickly progressing maternal difficulties, which have resulted in either deteriorating maternal status or non-reassuring fetal status as a result of the worsening maternal clinical condition. COVID-19 may increase or exacerbate pregnancy-related complications, including preeclampsia. In addition, both stages have laboratory abnormalities in common, which makes the issue even more complicated. Certain forms of preeclampsia may make it difficult to discern between abnormal test results generated by SARS-CoV-2 infection and those caused by other causes of abnormal results. Examples include thrombocytopenia and decreased liver function, both of which serve as diagnostic criteria for severe preeclampsia and are associated with a worsening COVID-19 score.[20,21] We supposed that placental alterations caused by

this infection might compromise the development of the fetus and hemodynamics in these pregnancies.

The primary objective of this research was to assess the fetal growth velocity in pregnancies complicated by SARS-CoV-2 infection and those that were not. The secondary objective was to determine if SARS-CoV-2 infection may affect maternal and fetal Doppler readings. This study also aimed to examine fetal biometric measurements for fetal growth evaluation and Doppler velocimetry in pregnant women infected with SARS-CoV-2.

Materials and Methods

A total of 250 pregnant women diagnosed with SARS-CoV-2 were compared to 300 healthy pregnant women in a prospective case-control study in Mosul from February 20 to October 20, 2021. Infections during pregnancy were detected and verified using the real-time reverse transcriptase-polymerase chain reaction (RT-PCR).

Inclusion criteria were a) singleton pregnancy, b) fetal viability, c) BMI <30kg/m^2, d) no history of diabetes mellitus, hypertension, including pregnancy hypertension, antepartum bleeding, autoimmune disorders, clinical hyperthyroidism/hypothyroidism, hematological diseases, e) negative TORCH test, f) no history of IUGR, g) informed consent from the participants.

Exclusion criteria were moderate and severe COVID-19.

A detailed history was taken, including gestational age at infection diagnosis, medical treatment for COVID-19, the time interval between Doppler measurement and COVID-19 diagnosis, and examinations including general examination, vital signs, complete obstetric examination, and BMI calculation.

All ultrasound exams were done from 24 to 40 weeks (based on the last menstrual period or early ultrasound), and by a single ultra-sonographer who was blinded to the patient's medical history. A Mindray DC-30 Full HD Ultrasound System (Shenzhen Mindray Bio-Medical Electronics Co., Ltd.) with wideband convex transducer was used.

At 24 weeks of pregnancy, the UA and MCA were checked with Doppler flowmetry. The examinations were done twice during the study, once in each trimester. Measuring parameters using Doppler ultrasonography included plasticity and resistive indices, as well as cerebroplacental ratio computed according to gestational age. Fetal development in utero was assessed by measuring biometric markers, such as parietal diameter, head size, belly circumference, leg length, and estimated fetal weight every four weeks. In addition, the amniotic fluid index was determined for each patient under consideration.

Statistical analysis was performed using statistical software package SPSS version 23.0 (SPSS Inc, Armonk, NY: IBM Corp). Baseline characteristics were summarized as frequencies and percentages for categorical variables. For descriptive analysis, results are presented as median (Me), first quartile (Q1) and third quartile (Q3). The Mann-Whitney U Test was used to compare the differences between the two independent groups Group comparisons with respect to categorical variables are performed using chi-square tests or, alternatively, Fisher's exact test when expected cell counts were less than 5. A probability value of $P<0.05$ was considered statistically significant.

Results

A total of 250 pregnant women with a positive history of COVID-19 infection (Case group) and 300 pregnant women without infection (Control group) were examined in our private clinic by a gynecologist and radiologist with over a decade of expertise. Maternal age ranged from 17 to 45 years in both control and infected cases. The pregnancy and maternal characteristics of both groups are presented in Table 1, which demonstrates no difference in maternal age, parity, gravidity, or gestational age at birth.

The US scans in the second and third trimester of pregnancy showed no evidence of congenital abnormalities (P=0.7047). There was a significant incidence of CD (P=0.0000) and lower fetal activity at birth (P=0.0000) in the Case group, compared to the Control group. Anticoagulant treatment during pregnancy was not associated with an increased risk of postpartum hemorrhage in women of the Case group. Also, there were no significant differences in fetal biparietal diameter and femur length between groups in the second and third trimesters (Table 1), and both fetal and maternal Doppler studies throughout the second and third (35-37 weeks) trimesters of pregnancy yielded no significant differences in the PI and RI indices (Table 2).

Table 1.
***The pregnancy and maternal characteristics of both** groups.*

Variable	Case group (n=250)	Control group (n=300)	*P*-value
Maternal age, years	30.04 (17-45)	30.35 (17-45)	0.43
Gravity	4.96 (3-7)	4.78 (2-6)	0.07
Parity	4.28 (3-6)	4.16 (2-6)	0.29
Second trimester US examination, weeks	20.91 (19-23)	21.01 (19.5-22)	0.39
Third trimester US examination, weeks	36.43 (35.5-37)	36.51 (35.9-37)	0.61
Gestational age at birth, weeks	37.97 (37-39)	38.13 (38-40)	0.15
Lower fetal activity at birth	64 (25.6%)	30 (10%)	0.0000
CD rate	72 (28.8%)	43 (14.3%)	0.0000
Anticoagulant treatment during pregnancy	102 (40.8%)	70 (23.3%)	0.0000
Postpartum hemorrhage	6 (2.4%)	7 (2.3%)	1.0000
Congenital abnormality	2 (0.80%)	4 (1.3%)	0.7047

Table 2.

Fetal and maternal Doppler studies in study groups

Variable	Case group (n=250)	Control group (n=300)	*P*-value
Second trimester DU			
BPD, mm	47.01 (45.4-48.5)	46. 91 (39.4-48.4)	0.08
FL, mm	36.08 (34.2-37.6)	36.00 (34.4-37.2)	0.26
UA-PI	1.06 (0.53-1.59)	1.05 (0.54-1.6)	0.59
Third trimester DU			
BDD, mm	88.34 (83.5-93.4)	88.05 (81.1-92.1)	0.25
FL, mm	71.27 (68.4-74.1)	70.27 (69.2–71.3)	0.08
UA-PI	0.72 (0.67-0.77)	0.73 (0.66-0.79)	0.63
UA-RI	0.51 (0.40-0.61)	0.52 (0.52-0.62)	0.07
MCA-PI	2.76 (2.60-2.92)	2.74 (2.51-2.70)	0.09
CPR	1.02 (0.51-1.55)	1.01 (0.53-1.52)	0.51

Discussion

The pathophysiology of SARS-CoV-2 infection during pregnancy and its association with co-morbid disorders remain unknown.[22] This case-control research is one of the few that examines the relationship between intrauterine placental flow and fetal death.[23] The US and Doppler outcomes for SARS-CoV-2 in infected and non-infected pregnant women were compared. As the results showed, there was no significant difference in terms of maternal age (17-45 years), parity, second trimester US examination (19-23 weeks), third trimester US examination (35-37 weeks), or gestational age at birth (37-40 week), while there was a significant difference between the groups in terms of fetal movement at the time of delivery and decreased fetal movement at birth (*P*=0.0000). That some pregnant women report transitory reductions in fetal movement despite the lack of substantial vascular abnormalities seen by Doppler,[24] could be explained by high doses of systemic corticosteroid given to treat the main manifestations of COVID-19, changes in maternal perception because of the fear of disease, maternal pyrexia during acute infection, or transplacental transmission of inflammatory mediators and tiny micro thrombi at the placental bed.[25] SARS-CoV-2 infection may also explain the considerable increase in the rate of CD under regional anesthesia in pregnant women having an urgent medical or obstetric cause for termination of pregnancy. Additionally, there was a statistically significant increase in the usage of prenatal and postpartum anticoagulant medication in the case group, compared to the control group, for thrombus treatment and prophylaxis without differences in postpartum bleeding, which was comparable to a study done by Anuk et al.[25] found that delivery in the maternity hospital with active management in the third stage of labor, in addition to the manipulation or discontinuation of the anticoagulant therapy at an appropriate time during labor, is the cause behind the absence of difference in the rate of postpartum hemorrhage between the groups.

No congenital anomaly was discovered post-delivery in the pregnant women diagnosed with SARS-CoV-2. According to Rizzo et al.,[26] SARS-CoV-2 infection during the second half of pregnancy without congenital anomaly indicates that the patients have passed the key time of organogenesis. However, Khalil et al.[3] compared stillbirth rates during the pandemic to the pre-pandemic era and found that the frequency of stillbirth was much greater during the pandemic. Anuk et al.[25] found that the Doppler indices were significantly changed during the pandemic. Due to the study group's features, concomitant comorbidities like diabetes, chronic hypertension, advanced age, or a higher BMI in pregnant women with COVID-19 aggravate the disease's effects. But in our study, the presence of all the listed conditions were exclusion criteria. As the long-term effects of this viral infection and its consequences during pregnancy are still being investigated, we discovered that infected women attend antenatal care more often because they are fearful of potential problems.[27]

We studied SARS-CoV-2 impact on fetal development. The primary objective of this research was to use Doppler ultrasonography to assess fetal growth and circulation throughout the second and third trimesters of pregnancy. The results of our study suggest that fetal development and growth velocity, as measured by biparietal diameter and femur length, are similar in SARS-CoV-2 infected and not infected pregnant women. The fetal and maternal Doppler studies showed no significance in the PI and RI throughout the second and third trimesters. These data suggest that infection with SARS-CoV-2 during pregnancy does not increase the risk of IUGR and hence does not need increased fetal surveillance.[26-28] It should be noted that this study included only pregnant women with mild symptoms of infection. A second point to note is a restriction on when an evaluation can be done. If an infection happened early in the pregnancy, it could have a different outcome. Even though there is a lot of evidence that the SARS-CoV-2 virus can spread during pregnancy, many unanswered concerns remain, such as how the virus may damage the fetus and placenta. SARS-CoV-2 infection can be transmitted vertically; however, this is still up for discussion. Early in the outbreak, it was claimed that transmission from mother to fetus was very low.[29] In contrast, more recent and larger studies have found that there is a higher risk of transmission from mother to child.[25] A recent review of 39 studies that looked at 936 newborns born to mothers who had COVID-19 found that 3.2% of them had SARS-CoV-2 in their nasopharyngeal swabs.[30] A subgroup analysis that looked at the effect of the location of the research revealed that the rate of vertical transmission was almost the same whether the trial was conducted in China or elsewhere (2.0% vs 2.7%).[31] Although much progress has been made, the hazards of vertical transmission and the long-term consequences it may have on a developing fetus remain poorly known. Recent research has raised questions regarding the true danger of transmission of SARS-CoV-2, which was found exclusively in the placenta but not in neonates.[28]

Among other things, placentas from pregnant women infected with SARS-CoV-2 revealed evidence of arterial necrosis, fibrinoid necrosis, and mural enlargement of the decidual arterioles.[2,27] In our research, we were unable to address this question because of the absence of an examination of placental pathology. A reduced placental function, growth limitation, or stillbirth may occur even when there is no evidence that the mother has been infected with SARS-CoV-2 or any other sickness that causes maternal vascular hypo perfusion.[3] Contrary to common opinion, the findings of this study reveal that pregnancies complicated by SARS-CoV-2 infection do not increase the likelihood of fetal growth limitation.[32] It is no longer required to do repeated scans during pregnancy to rule out certain conditions. One potential clarification for the absence of a link between women infected with COVID-19 and IUGR is that only women with moderate symptoms were included in the study, which may have represented the slighter range of COVID-19 symptoms only.[33] However, it cannot be ruled out that women with more severe COVID-19 may be at risk for IUGR. The amount of time a woman has been infected may have an impact on her likelihood of having placental lesions.[11,34] One of the most disputed issues in the treatment of pregnant women with SARS-CoV-2 infection is whether these women should be exposed to more intensive prenatal surveillance. Because there is no evidence of a relationship between illness and impaired fetal development, the results of the current study do not sustain a strategy of increased US screenings to ensure the safety of the fetus. Furthermore, it has been established that the incidence of stillbirth in women infected with SARS-CoV-2 is no different from the incidence of stillbirth in the baseline pregnant population that was not infected with the virus.[35] Gravid women infected with SARS-CoV-2 should rest assured that the risk of poor consequences for their unborn child is very minimal,[36,37] but more focused studies need to be done to confirm this finding.

Acknowledgments

The authors highly appreciate the great cooperation of included patients to complete the study.

Competing Interests

The authors declare that they have no competing interests.

References

1. Centers for Disease Control and Prevention (CDC). Data on COVID-19 during pregnancy: severity of maternal illness. Available at: https://stacks.cdc.gov/view/cdc/119588
2. Di Mascio D, Khalil A, Saccone G, Rizzo G, Buca D, Liberati M, Vecchiet J, Nappi L, Scambia G, Berghella V, D'Antonio F. Outcome of coronavirus spectrum infections (SARS, MERS, COVID-19) during pregnancy: a systematic review and meta-analysis. Am J Obstet Gynecol MFM. 2020 May;2(2):100107. doi: 10.1016/j.ajogmf.2020.100107.
3. Khalil A, Kalafat E, Benlioglu C, O'Brien P, Morris E, Draycott T, Thangaratinam S, Le Doare K, Heath P, Ladhani S, von Dadelszen P, Magee LA. SARS-CoV-2 infection in pregnancy: A systematic review and meta-analysis of clinical features and pregnancy outcomes. EClinicalMedicine. 2020 Aug;25:100446. doi: 10.1016/j.eclinm.2020.100446..
4. Poon LC, Yang H, Dumont S, Lee JCS, Copel JA, Danneels L, Wright A, Costa FDS, Leung TY, Zhang Y, Chen D, Prefumo F. ISUOG Interim Guidance on coronavirus disease 2019 (COVID-19) during pregnancy and puerperium: information for healthcare professionals - an update. Ultrasound Obstet Gynecol. 2020 Jun;55(6):848-862. doi: 10.1002/uog.22061.
5. Liang H, Acharya G. Novel corona virus disease (COVID-19) in pregnancy: What clinical recommendations to follow? Acta Obstet Gynecol Scand. 2020 Apr;99(4):439-442. doi: 10.1111/aogs.13836.
6. Zaigham M, Andersson O. Maternal and perinatal outcomes with COVID-19: A systematic review of 108 pregnancies. Acta Obstet Gynecol Scand. 2020 Jul;99(7):823-829. doi: 10.1111/aogs.13867.
7. WAPM (World Association of Perinatal Medicine) Working Group on COVID-19. Maternal and perinatal outcomes of pregnant women with SARS-CoV-2 infection. Ultrasound Obstet Gynecol. 2021 Feb;57(2):232-241. doi: 10.1002/uog.23107. Epub 2021 Jan 21. Erratum in: Ultrasound Obstet Gynecol. 2021 Sep;58(3):496.
8. Di Mascio D, Sen C, Saccone G, Galindo A, Grünebaum A, Yoshimatsu J, et al. Risk factors associated with adverse fetal outcomes in pregnancies affected by Coronavirus disease 2019 (COVID-19): a secondary analysis of the WAPM study on COVID-19. J Perinat Med. 2020 Nov 26;48(9):950-958. doi: 10.1515/jpm-2020-0355. Erratum in: J Perinat Med. 2020 Dec 02;49(1):111-115.
9. Malinowski AK, Noureldin A, Othman M. COVID-19 susceptibility in pregnancy: Immune/inflammatory considerations, the role of placental ACE-2 and research considerations. Reprod Biol. 2020 Dec;20(4):568-572. doi: 10.1016/j.repbio.2020.10.005.
10. Dhaundiyal A, Kumari P, Jawalekar SS, Chauhan G, Kalra S, Navik U. Is highly expressed ACE 2 in pregnant women "a curse" in times of COVID-19 pandemic? Life Sci. 2021 Jan 1;264:118676. doi: 10.1016/j.lfs.2020.118676.
11. Shanes ED, Mithal LB, Otero S, Azad HA, Miller ES, Goldstein JA. Placental Pathology in COVID-19. Am J Clin Pathol. 2020 Jun 8;154(1):23-32. doi: 10.1093/ajcp/aqaa089.
12. Baergen RN, Heller DS. Placental Pathology in Covid-19 Positive Mothers: Preliminary Findings. Pediatr Dev Pathol. 2020 May-Jun;23(3):177-180. doi: 10.1177/1093526620925569.
13. Schwartz DA, Baldewijns M, Benachi A, Bugatti M, Collins RRJ, De Luca D, et al. Chronic Histiocytic Intervillositis With Trophoblast Necrosis Is a Risk Factor Associated With Placental Infection From Coronavirus Disease 2019 (COVID-19) and Intrauterine Maternal-Fetal Severe Acute Respiratory Syndrome Coronavirus 2 (SARS-CoV-2) Transmission in Live-Born and Stillborn Infants. Arch Pathol Lab Med. 2021 May 1;145(5):517-528. doi: 10.5858/arpa.2020-0771-SA.
14. Narang K, Enninga EAL, Gunaratne MDSK, Ibirogba ER, Trad ATA, Elrefaei A, Theiler RN, Ruano R, Szymanski LM, Chakraborty R, Garovic VD. SARS-CoV-2 Infection and COVID-19 During Pregnancy: A Multidisciplinary Review. Mayo Clin Proc. 2020 Aug;95(8):1750-1765. doi: 10.1016/j.mayocp.2020.05.011.
15. Rasmussen SA, Jamieson DJ, Macfarlane K, Cragan JD, Williams J, Henderson Z; Pandemic Influenza and Pregnancy

Working Group. Pandemic influenza and pregnant women: summary of a meeting of experts. Am J Public Health. 2009 Oct;99 Suppl 2(Suppl 2):S248-54. doi: 10.2105/AJPH.2008.152900.
16. Mor G, Aldo P, Alvero AB. The unique immunological and microbial aspects of pregnancy. Nat Rev Immunol. 2017 Aug;17(8):469-482. doi: 10.1038/nri.2017.64.
17. Hegewald MJ, Crapo RO. Respiratory physiology in pregnancy. Clin Chest Med. 2011 Mar;32(1):1-13. doi: 10.1016/j.ccm.2010.11.001.
18. Breslin N, Baptiste C, Miller R, Fuchs K, Goffman D, Gyamfi-Bannerman C, D'Alton M. Coronavirus disease 2019 in pregnancy: early lessons. Am J Obstet Gynecol MFM. 2020 May;2(2):100111. doi: 10.1016/j.ajogmf.2020.100111.
19. Schwartz DA. An Analysis of 38 Pregnant Women With COVID-19, Their Newborn Infants, and Maternal-Fetal Transmission of SARS-CoV-2: Maternal Coronavirus Infections and Pregnancy Outcomes. Arch Pathol Lab Med. 2020 Jul 1;144(7):799-805. doi: 10.5858/arpa.2020-0901-SA.
20. Lippi G, Plebani M, Henry BM. Thrombocytopenia is associated with severe coronavirus disease 2019 (COVID-19) infections: A meta-analysis. Clin Chim Acta. 2020 Jul;506:145-148. doi: 10.1016/j.cca.2020.03.022.
21. Zhang C, Shi L, Wang FS. Liver injury in COVID-19: management and challenges. Lancet Gastroenterol Hepatol. 2020;5(5):428-430. doi: 10.1016/S2468-1253(20)30057-1.
22. Di Guardo F, Di Grazia FM, Di Gregorio LM, Zambrotta E, Carrara G, Gulino FA, Tuscano A, Palumbo M. Poor maternal-neonatal outcomes in pregnant patients with confirmed SARS-Cov-2 infection: analysis of 145 cases. Arch Gynecol Obstet. 2021 Jun;303(6):1483-1488. doi: 10.1007/s00404-020-05909-4.
23. Al-kuraishy HM, Al-Maiahy TJ, Al-Gareeb AI, Musa RA, Ali ZH. COVID-19 pneumonia in an Iraqi pregnant woman with preterm delivery. Asian Pac J Reprod 2020;9:156-8
24. Xia H, Zhao S, Wu Z, Luo H, Zhou C, Chen X. Emergency Caesarean delivery in a patient with confirmed COVID-19 under spinal anaesthesia. Br J Anaesth. 2020 May;124(5):e216-e218. doi: 10.1016/j.bja.2020.02.016.
25. Anuk AT, Tanacan A, Yetiskin FDY, Buyuk GN, Senel SA, Keskin HL, Moraloglu O, Uygur D. Doppler assessment of the fetus in pregnant women recovered from COVID-19. J Obstet Gynaecol Res. 2021 May;47(5):1757-1762. doi: 10.1111/jog.14726.
26. Rizzo G, Mappa I, Maqina P, Bitsadze V, Khizroeva J, Makatsarya A, D'Antonio F. Effect of SARS-CoV-2 infection during the second half of pregnancy on fetal growth and hemodynamics: A prospective study. Acta Obstet Gynecol Scand. 2021 Jun;100(6):1034-1039. doi: 10.1111/aogs.14130.
27. Arthurs AL, Jankovic-Karasoulos T, Roberts CT. COVID-19 in pregnancy: What we know from the first year of the pandemic. Biochim Biophys Acta Mol Basis Dis. 2021 Dec 1;1867(12):166248. doi: 10.1016/j.bbadis.2021.166248.
28. Tanacan A, Yazihan N, Erol SA, Anuk AT, Yucel Yetiskin FD, Biriken D, et al. The impact of COVID-19 infection on the cytokine profile of pregnant women: A prospective case-control study. Cytokine. 2021 Apr;140:155431. doi: 10.1016/j.cyto.2021.155431.
29. Soto-Torres E, Hernandez-Andrade E, Huntley E, Mendez-Figueroa H, Blackwell SC. Ultrasound and Doppler findings in pregnant women with SARS-CoV-2 infection. Ultrasound Obstet Gynecol. 2021 Jul;58(1):111-120. doi: 10.1002/uog.23642.
30. Ratiu D, Hide-Moser K, Morgenstern B, Gottschalk I, Eichler C, Ludwig S, Grüttner B, Mallmann P, Thangarajah F. Doppler Indices and Notching Assessment of Uterine Artery Between the 19th and 22nd Week of Pregnancy in the Prediction of Pregnancy Outcome. In Vivo. 2019 Nov-Dec;33(6):2199-2204. doi: 10.21873/invivo.11722.
31. Labò N, Ohnuki H, Tosato G. Vasculopathy and Coagulopathy Associated with SARS-CoV-2 Infection. Cells. 2020 Jun 30;9(7):1583. doi: 10.3390/cells9071583.
32. Dong L, Tian J, He S, Zhu C, Wang J, Liu C, Yang J. Possible Vertical Transmission of SARS-CoV-2 From an Infected Mother to Her Newborn. JAMA. 2020 May 12;323(18):1846-1848. doi: 10.1001/jama.2020.4621.
33. Shah PS, Diambomba Y, Acharya G, Morris SK, Bitnun A. Classification system and case definition for SARS-CoV-2 infection in pregnant women, fetuses, and neonates. Acta Obstet Gynecol Scand. 2020 May;99(5):565-568. doi: 10.1111/aogs.13870.
34. Kotlyar AM, Grechukhina O, Chen A, Popkhadze S, Grimshaw A, Tal O, Taylor HS, Tal R. Vertical transmission of coronavirus disease 2019: a systematic review and meta-analysis. Am J Obstet Gynecol. 2021 Jan;224(1):35-53.e3. doi: 10.1016/j.ajog.2020.07.049.
35. Kotlyar AM, Grechukhina O, Chen A, Popkhadze S, Grimshaw A, Tal O, Taylor HS, Tal R. Vertical transmission of coronavirus disease 2019: a systematic review and meta-analysis. Am J Obstet Gynecol. 2021 Jan;224(1):35-53.e3. doi: 10.1016/j.ajog.2020.07.049.
36. Mappa I, Distefano FA, Rizzo G. Effects of coronavirus 19 pandemic on maternal anxiety during pregnancy: a prospectic observational study. J Perinat Med. 2020 Jul 28;48(6):545-550. doi: 10.1515/jpm-2020-0182.
37. Thapa SB, Mainali A, Schwank SE, Acharya G. Maternal mental health in the time of the COVID-19 pandemic. Acta Obstet Gynecol Scand. 2020 Jul;99(7):817-818. doi: 10.1111/aogs.13894.

International Journal of Biomedicine 12(4) (2022) 560-566
http://dx.doi.org/10.21103/Article12(4)_OA6

ORIGINAL ARTICLE

Radiology

INTERNATIONAL JOURNAL OF BIOMEDICINE

Response of Human Malignant Glioma Cells to Asymmetric Bipolar Electrical Impulses

Amr A. Abd-Elghany[*1,2], A. M. M. Yousef[1,3]

[1]*Radiology and Medical Imaging Department, College of Applied Medical Sciences, Prince Sattam Bin Abdul-Aziz University, Alkharj 11942, Saudi Arabia*
[2]*Biophysics Department, Faculty of Science, Cairo University, Egypt*
[3]*Physics Department, Faculty of Science, South Valley University, Kena, Egypt*

Abstract

Electric and electromagnetic pulses have been shown to enhance the endocytosis rate, with all-or-nothing responses beyond a field strength threshold and linear responses as a function of field strength and treatment duration utilizing bipolar symmetrical and monopolar pulses, respectively. Malignant glioma (MG) is resistant to chemotherapy. The present study looked for a new electrical impulse that can aid electrochemotherapy to deliver anticancer drugs while using less electrical energy. Bipolar asymmetric electric pulses were applied to U251MG cells suspended in physiologically conductive media in the presence of molecular probes, including Bleomycin. The delivered electric pulses with a pulse duration range of 180-500 µs and a frequency range of 100-400 Hz had a low field intensity ranging from 1.5 V/cm to 7.3 V/cm. Spectrophotometric and spectrofluorometric measurements were used to investigate the impact of these variables on cancer cell survival and the molecular probe uptake induced by the electric pulses. An all-or-nothing response was observed above a specified threshold of electric field intensity of 4 V/cm. This threshold was unaffected by changes in repetition frequency or pulse duration. It was not a temperature effect that caused the molecular probe uptake to increase. When bipolar asymmetric electric pulses were applied just before electroporation, the effectiveness of the cytotoxic impact of bleomycin was increased from 80%, when employing electroporation pulses alone, to 100%.**(International Journal of Biomedicine. 2022;12(4):560-566.)**.

Keywords: electroendocytosis • asymmetric bipolar electrical impulses • spectrofluorometry • U251MG cells

For citation: Abd-Elghany AA, Yousef AMM. Response of Human Malignant Glioma Cells to Asymmetric Bipolar Electrical Impulses. International Journal of Biomedicine. 2022;12(4):560-566. doi:10.21103/Article12(4)_OA6

Abbreviations

BSA, bovine serum albumin; **BLM,** Bleomycin; **FITC**, fluorescein isothiocyanate; **MG**, malignant glioma; **PEF**, pulsed electric field; **EP,** electric pulse.

Introduction

One of the most challenging aspects of drug delivery is transporting exogenous materials into the cell's cytoplasm. Various approaches to incorporating macromolecules into cells have been explored over the last few decades.[1-3] An interesting procedure is based on an electrically driven process called electroporation, in which cells are subjected to a high-intensity pulsed electric field (PEF) for micro- to milliseconds duration. The membrane undergoes short-term permeability alterations as a result of this exposure due to transient defects in membrane structure termed "electropores," allowing small molecules to diffuse through the membrane along their electrochemical gradients or the uptake of large molecules (e.g., electrically mediated gene delivery) through mechanisms, including electrophoresis.[4-6] Electroendocytosis, i.e., electric field endocytosis, is a method for incorporating macromolecules into cells that involves exposing cells to a

***Corresponding author:** Amr A. Abd-Elghany. Radiology and Medical Imaging Department, College of Applied Medical Sciences, Prince Sattam Bin Abdul-Aziz University, Alkharj 11942, Saudi Arabia. Biophysics Department, Faculty of Science, Cairo University, Egypt. E-mail: amrabdelghany25@gmail.com*

pulsed low electric field. It is arising as a complementary method to electroporation.[7] Electroendocytosis, unlike electroporation, which causes nanometer-sized electropores to develop on the lipid bilayer of the plasma membrane, causes cell membrane internalization and fission via endocytotic vesicles.[8,9] It incorporates either macromolecules that are bound to membrane receptors by receptor-mediated endocytosis[10,11] or any soluble drugs by fluid-phase endocytosis (pinocytosis).[12,13] Exocytosis, a reciprocal mechanism, restores the cellular membrane area.[14]

Two main types of electric pulses have reported endocytosis induced by pulsed low electric fields.[7,10,11,13-15] The first pulse type used was bipolar symmetrical square pulses with field intensity ranging from 1.2 V/cm to 8 V/cm, pulse durations ranging from 75 µs to 580µs, frequencies ranging from 50 to 400 Hz, and total exposure times ranging from 5 to 90 minutes. A bipolar pulse was adopted to limit unidirectional electrophoresis and to reduce electrochemical deposits at the surface of the electrodes. On three separate cell lines, exposures lasting more than 10 minutes resulted in a ~50% improvement in fluid-phase endocytosis, compared to controls with the same exposure time but no electric pulses. This improvement was defined as an all-or-nothing incident that occurs at electric field intensity thresholds ranging from 1.6 V/cm to 2.6 V/cm, depending on the cell type. The cell response to the PEF was unaffected by changes in repetition frequency or pulse duration.[12] As the second pulse type, we used unipolar rectangular pulses with field strengths ranging from 2.5 V/cm to 20 V/cm, pulse durations ranging from 50 µs to 250 µs, at temperatures ranging from 4 to 37°C, and conductivities ranging from 6.4 mS/cm to 18.6 mS/cm. In all experiments, the total exposure time was 1 minute. The electrically induced increase in BSA-FITC uptake by two separate cell types showed a linear dependency with no sign of a field strength cut-off value. At 20 V/cm, maximum uptake could be up to 7.5 times higher than in controls. The uptake was also linearly dependent on the pulse duration and medium conductivity.[7,10,11] These two sets of data were markedly different.

MG is a form of brain tumor with a high death rate in humans and is resistant to typical cancer therapies like surgery, chemotherapy, and radiotherapy. The blood-brain barrier in the areas surrounding the tumor is reversibly damaged when electroporation is administered to the brain with specific treatment parameters, which are greatly helpful in treating the infiltrating cells with maximum delivered chemotherapeutic doses.[16-19] The response of U251MG cells to asymmetric bipolar electric pulses was investigated using various electrical parameters. Increased receptor-mediated endocytosis was detected in U251MG cells, which were characterized by an all-or-nothing response at field strength threshold just after electric pulse exposure. Such a low PEF can be used as an adjuvant with electrochemotherapy to enhance MG treatment with lower electrical parameters and lower doses of anticancer drugs.

Materials and Methods

Cell culture

Modified Eagle's medium (MEM, Sigma-Aldrich, Germany) enriched with L-glutamine, 10% fetal calf serum (FCS, Biochrom, Berlin, Germany), streptomycin (125 µg/ml) and penicillin (100 units/ml) were used to culture human MG cells U251MG driven from malignant astrocytic tumors. The cells were grown in number by adding 1 ml of MEM(1x) containing ~10^6 cells with 9 ml of MEM(1x) free of cells in culture flasks incubated at 37°C for 3 days in a CO_2 incubator (5±1% CO_2 and 95 % relative humidity). The attached cells were collected by trypsin-EDTA (0.05%, Sigma-Aldrich, Germany). After centrifugation (210 g, 5min, room temperature), the culture medium MEM(1x) was removed as a supernatant, and cells were resuspended (4-8×10^6 cells/ml) in the exposure medium S-MEM (product 21385, Invitrogen), a calcium-depleted modification of EMEM, which has a physiological conductivity (10 mS/cm). Exposure media were subjected to degassing at 23±2°C for 10min using a vacuum pump (Thermo Scientific, Germany).

Molecular probes

Receptor-mediated endocytosis was detected using either BSA (66 kDa) that has been conjugated to fluorescein isothiocyanate (5-FITC, Sigma-Aldrich, Germany) (1:4 v/v) to get a final concentration of 6.8 µM or BLM (1.5 kDa) as an anticancer drug (Laboratoire Roger Belon, France) at concentrations ranging from 30 nM to 30 µM.[10,11,13,15]

Low-intensity bipolar asymmetric electrical impulses

Suspended cells (100µl of medium containing 0.5 to 1.0×10^6 cells) were subjected to a low-intensity train of bipolar, asymmetric, rectangular voltage pulses with the area of the positive part of the pulse (above the baseline) nearly equal to the area of the negative part of the pulse (below the baseline) by employing a 50 MHz pulse generator (Model 801, Wavetek, San Diego, USA) whether or not a molecular probe was present (BSA or BLM). The exposure was performed in a vertical position by two stainless-steel electrodes with an interdistance of 0.2 cm, resulting in a medium to the electrode contact area of 0.5 cm^2 and a quasi-uniform electric field. The exposure was done in S-MEM (a physiologically conductive medium, 10 mS/cm). A digital storage oscilloscope (HITACHI, Japan) was used to monitor the electric field characteristics online. The electrical parameters comprised electric field strengths ranging from 1.5 to 7.3 V/cm, pulse individual durations from 180 to 500 µs, and pulse repetition rates from 100 to 400 Hz. All trials were carried out at 23°C, 4°C, and 37°C, with no significant changes noted between the temperatures (data not shown). A digital thermometer was used to measure the samples' temperature at the end of the exposure. For each set of exposures, a control (molecular probe only, no electric pulses) sample was placed between the same electrodes.

Application of electroporation pulses

U251MG cells previously exposed to bipolar asymmetric electric pulses (6.9 V/cm, 200 Hz repetition frequency, 400 µs pulse duration, and 2 min exposure time) in the presence of 30 µM BLM were transferred aseptically to an electroporation cuvette (Al electrodes) with a gap width of 0.2 cm and subjected to 8 square unipolar electroporation pulses of 600 ms pulse duration and 1000 V/cm field intensity using BTX Harvard electroporator (Model No. 620, BTX Harvard Apparatus, USA).

Determination of the fluorescent probe uptake using spectrofluorometry

The collected samples were centrifuged for 250 RCF for 10 min twice after washing them with PBS. After the supernatant was discarded, pellets were suspended in a one-milliliter buffer (Lysis reagent buffer), then diluted 100 times by H_2O and mixed by the vortex. Total fluorescence was spectrofluorometric (at 494 & 520 nm for BSA-FITC, Kontron SFM 25- England) evaluated to calculate released fluorescence molecules from the ruptured cell. Molecule numbers/cells were calculated according to FSC (standard curve of fluorescence). The fluorescent probe uptake by cells subjected to electric pulses was calculated and compared to the control samples treated with BSA-FITC only (no electric pulses).

Determination of the number of cells using spectrophotometry

The colorimetric detection and quantification of total protein, corresponding to the number of cells, in dilute aqueous solutions were done using Micro BCA™ Protein Assay Kit (Pierce, Rockford, USA). The water-soluble complex exhibited a strong absorbance at 562 nm, which is linear with increasing protein concentration. To avoid fluctuations in cell counts eventually resulting in cell damage caused by the electric pulses, and to determine cell content in each of the treated samples, the total protein content was measured in all the samples. Protein standards were prepared by diluting 2.0 mg/ml BSA stock standard with water to set the standard curve. The working reagent was prepared according to the manufacturer's instructions; 40 µl of cell lysate for each sample (including unknown samples treated with different electrical parameters and untreated samples of the known number of cells) were added to 110ml of water in the appropriate microwell plate wells. Blank wells only contained water (150 µl). Then 150ml of the working reagent was added to each well. The plate was covered and incubated at 37°C for 2 hours. After incubation, the plate was cooled at room temperature, and the absorbance was measured at 562 nm on a plate reader. The reading for each standard or unknown sample was deducted from the average reading for the blanks. The average blank-corrected reading for each BSA standard was plotted against its concentration in g/ml to create a standard curve. Another standard curve was created by graphing the protein concentration of the unknown untreated samples vs. cell numbers. The standard curve was used to calculate the number of cells in each electrically treated sample when the molecular probe was present.

Determination of BLM cytotoxicity and electroendocytosis

Another confirmatory method (cloning efficacy test) was used to determine the cytotoxic effect of the anticancer drug BLM in the presence or absence of the electric pulses. Half an hour after exposing them to an electric field, every 100 cells were placed in 1mL of culture medium, then 4mL of the cell suspension were sucked out, placed in a Petri dish (60 mm), and incubated for 5 days to form colonies. At the end of the incubation time, the colonies were fixed in Petri dishes with 4% formaldehyde (Sigma-Aldrich, Germany) and stained in 1% crystal violet (Biochrom, Berlin, Germany). By counting clone colonies and comparing them to the control group, the proportion of cells that survived after being exposed to electric pulses with or without BLM was calculated.

Cell observation with Inverted Light Microscope

A portion of the cell suspension that was exposed to different types of electrical pulses in the presence of BLM (30 µM) was re-cultured and incubated at 37°C in a CO_2 incubator (5±1% CO_2 and 95 % relative humidity). After 3 days the attached cells were observed under the inverted light microscope (Olympus, Tokyo, Japan) with a magnification of 100x. A negative control group represents cells with no BLM and no electric pulses.

Statistical analysis

In Figures 2-6, each value in the data indicates the mean±standard error of 3 separate experiments, each of which was repeated three times. For each Figure, the average control value and SD were determined using the individual control values from all the relevant independent experiments. Inter-group comparisons were performed using unpaired Student's t-test. A probability value of $P<0.05$ was considered statistically significant.

Results

Effect of field intensity

The influence of field intensity was studied at room temperature by exposing U251MG cells suspended in the physiologically conductive medium (10 mS/cm) with the molecular probe to pulsed bipolar asymmetric trains (200 Hz repetition frequency and 400 µs pulse duration) of different electric field strengths (1.5-7.3 V/cm) for 2 min, followed by 8 min of incubation without pulses. There was no significant response to any tested values below 3 V/cm. A significant increase in the fluorescence probe uptake was detected only for electric pulses higher than the threshold intensity of 4 V/cm (by ~38-110%) (Figure 1).

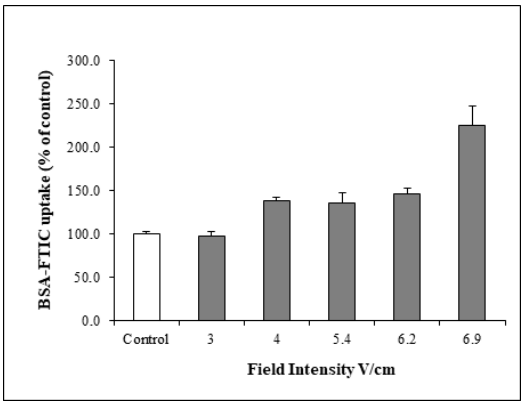

Fig. 1. *BSA-FTIC uptake by U251MG cells suspended in S-MEM (10mS/cm) as a function of field strengths of bipolar asymmetric electric pulses at 200 Hz, 400 µs, 2 min in the presence of BSA-FITC followed by exposure of 8 min to the BSA-FITC without electric pulses. (□) Control cells treated were with 6.8 µM BSA-FITC only. 100% represents the uptake of control samples in 10 min. Statistical significance: P<0.001.*

Due to the electrochemical reactions at the stainless-steel electrode surfaces, field intensities higher than 7.3 V/cm couldn't be tested. There was no cell loss at all the tested values of field intensities and no temperature increase.

Effect of frequency

To evaluate the effect of frequency on the uptake of fluorescent probes, cells were exposed in a physiologically conductive medium to bipolar asymmetric electric pulses using 4 V/cm field intensity (the threshold intensity) and 400 µs pulse duration. The exposure time was 2 min (electric pulses + BSA-FITC), followed by 8 min incubation in the presence of BSA-FTIC without pulses. The controls were incubated for 10 min with BSA-FITC only. In this group of experiments, a significant increase (P<0.001) in BSA-FITC uptake was found at frequencies higher than 100 Hz. The increase was almost identical for all the repetition frequencies tested, at ~40% higher than the unexposed controls (Figure 2). These results confirmed those obtained by changing the field intensity. No change in the number of cells was found using different repetition frequencies.

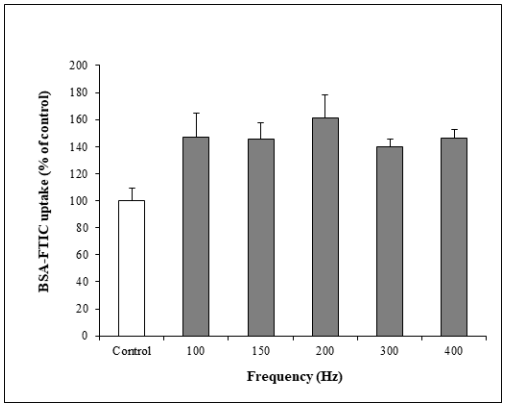

Fig. 2. *BSA-FTIC uptake by U251MGis suspended in S-MEM (10mS/cm) as a function of repetition frequency for bipolar asymmetric EP at 4 V/cm, 400 µs, 2 min, and BSA-FITC followed by exposure of 8 min to the BSA-FITC only. (□) Control cells were treated with 6.8µM BSA-FITC only. 100% represents the uptake of control samples in 10min. Statistical significance: P<0.001.*

Effect of pulse duration

To study the effect of pulse duration BSA-FITC uptake, cells were exposed to the physiologically conductive medium to electric pulses using 4 V/cm field intensity and 200 Hz repetition frequency. The exposure time was 2 min (electric pulses + BSA-FITC), followed by an 8 min incubation with BSA-FTIC only. The controls were incubated for 10 min with BSA-FITC only. A significant increase (P<0.001) in BSA-FITC uptake was found at pulse durations higher than 180 µs. The increase was almost identical for all the pulse durations tested, at a value approximately 40% higher than the unexposed controls (Figure 3). No change in cell survival was found using different pulse durations.

Electroendocytosis arises mainly during EP exposure

In this experiment, there was no BSA-FITC in the medium at the time of the electric pulses delivery medium. Thus, just after U251MG cells' exposure to electric pulses of 6.9 V/cm field strength, 200 Hz repetition frequency, and 400 µs pulse duration in physiologically conductive medium cells were incubated at room temperature (~23°C) for various durations in the presence of 6.8µM BSA-FITC. The exposed cells showed no enhanced dye uptake compared to the control cells (Figure 4). Compared to the controls, there was no cell loss in the exposed samples. One hundred percent corresponds to control cells that were only exposed to BSA-FITC for 2 minutes.

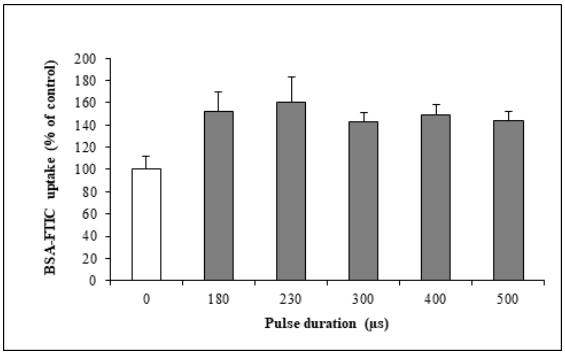

Fig. 3. *BSA-FTIC uptake by U251MG cells suspended in S-MEM (10 mS/cm) as a function of pulse duration for bipolar asymmetric electric impulses at 4 V/cm, 200 Hz, 2min in the presence of BSA-FITC followed by exposure of 8min to the BSA-FITC only. (□) Control cells were treated with 6.8µM BSA-FITC only. 100% represents the uptake of control samples in 10min. Statistical significance: P<0.001.*

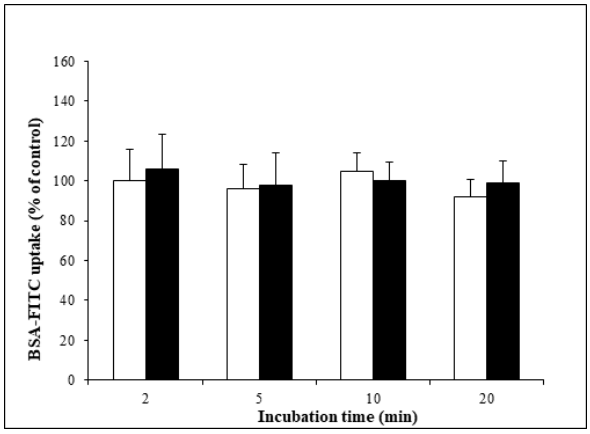

Fig. 4. *Uptake of the fluorescent probe by U251MG cells, using different incubation times, S-MEM (10 mS/cm) exposure medium, 6.9 V/cm field intensity, 200Hz repetition frequency, 400µs pulse duration, and 2min exposure time to the EP only. (□) Incubation in the presence of BSA-FITC without EP. (■) Incubation in the existence of BSA-FITC just after the exposure to EPs.*

BLM cytotoxicity triggered by low-intensity bipolar asymmetric EPs

After exposure to low-intensity bipolar asymmetric electric pulses (6.9 V/cm, 200 Hz, 400 µs, 120-sec total exposure, BLM at concentrations of 3 µM and higher), increased levels of cellular death rates were observed, which was a good predictor for the occurrence of electroendocytosis. For cells treated with bipolar asymmetric EP and BLM at various concentrations (30 nM - 30 µM), colonies were counted and standardized to the positive control (BLM alone, no electric pulses). There was no significant cell loss for cells treated with BLM at different concentrations, although survival was reduced considerably by ~18% in the absence of electric pulses at 30 µM BLM. The survival was significantly lowered (P<0.001) by ~17% and ~40% at 3 µM and 30 µM, respectively (Figure 5), in the presence of bipolar asymmetric electric pulses. Negative control represents samples without any treatment (drug-free, no EPs).

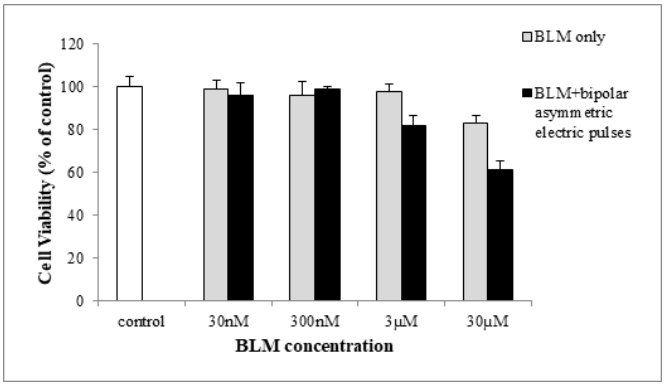

Fig. 5. *Cell survival of U251MG cells exposed to 6.9 V/cm, 200 Hz repetition frequency, 400 µs pulse duration, and 2 min exposure time in the presence of BLM. □ Control represents drug-free, and no EPs samples.*

Morphological and cell viability changes

Using an inverted light microscope, the efficacy of PEF to generate deformation and cell survival change was investigated. U251MG healthy control cells are spindle-shaped (Figure 6a). Cells in monolayer exponential growth became deformed and decreased significantly in number (Figures 6 b-d) because of the electric pulse application. Cells treated by electroporation pulses (1000 V/cm, 8 square unipolar pulses, and 600 µs pulse duration) after bipolar asymmetric bipolar PEF (6.9 V/cm, 200 Hz repetition frequency, 400 µs pulse duration, and 2 min exposure time) in the presence of BLM disappeared from the dishes, which indicates a ~100% mortality rate (Figure 6d).

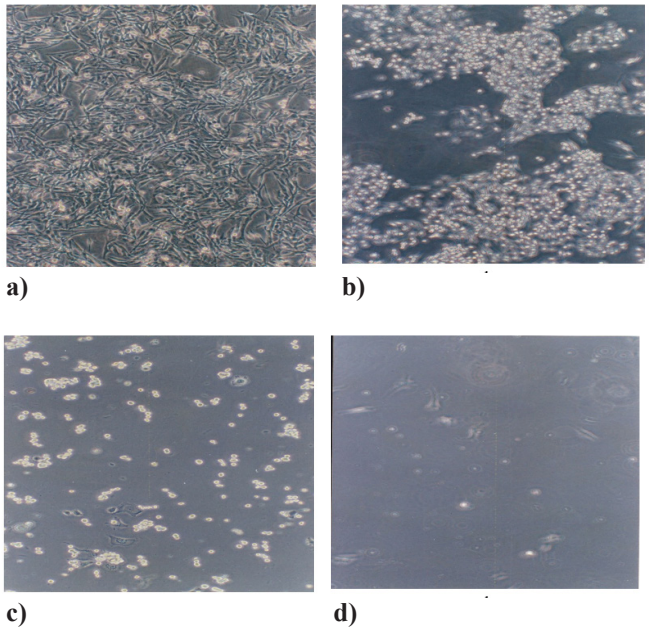

Fig. 6. *Monolayer exponential growth of U251MG cells under inverted light microscope. (a.) Negative control (healthy human malignant glioma cells without neither BLM nor electric pulses). (b.) Cells exposed to bipolar asymmetric electric pulses in the presence of 30 µM BLM. (c.) Cells exposed to electroporative pulses in the presence of 30 µM BLM. (d.) Cells exposed to bipolar asymmetric electric pulses then electroporative pulses.*

Discussion

The application of a low PEF was found to modify the cell surface, resulting in increased adsorption and subsequent uptake of macromolecules such as DNA, dextran, and BSA. [7,10,11] The electrophoretic segregation of charged moveable protein and lipid molecules in the plane of the cell membrane was attributed to this surface change. This phenomenon has previously been demonstrated both theoretically and practically. [20-24] Subsequent researchers proposed that these modifications are directly responsible for improved adsorptions and motivated uptake by a change in plasma membrane curvature that promotes endocytotic vesicle formation.[7.9.11]

A bipolar asymmetric signal with the area of the positive part of the pulse (above the baseline) nearly equal to the area of the negative part of the pulse (below the baseline) was chosen to perform the present study. The tested signal has a sort of "net" pulse in one direction (one short and relatively intense pulse "above" the threshold in one polarity and one long and much less intense pulse "below" the threshold in the other polarity). It was an attempt to approach the unipolar condition (pseudo-monopolar) of Rafi Korenstein's lab[11,13] with minimization of potential electrophoresis and electrochemical reactions at the electrodes (because the product of the pulse duration multiplied by field strength is similar between the positive and the negative part of this bipolar asymmetrical pulse).

The experimental results showed a statistically significant increase of ~38%-110% in non-permeant fluorescent probe uptake when exposed to bipolar asymmetric low-intensity square pulses for 2 minutes total exposure time using a physiologically conductive medium (10 mS/cm). This rise took place above a field intensity threshold value of 4 V/cm that was independent of the pulse duration, frequency, and temperature during the exposure. These results agreed with those obtained by Mahrour et al.[12] and disagreed with those obtained by Antov et al. in terms of cell viability and linear dependence. There was no significant uptake change using the low conductive medium (sucrose 0.25 M, 1 mS/cm) (data not shown). Conductivities of 1mS/cm were not tested in the previous studies.. The effect of conductivity may suggest that the increase in uptake is reliant on the electric current running through the cell's suspension and the resistance of the exposure medium. The resistance of the physiologically conductive medium (10mS/cm) was 40 Ω, while the resistance of the low conductive medium (1 mS/cm) was 400 Ω. The calculated current flowing through the cells suspended in S-MEM (10 mS/cm) was 20 mA at 4 V/cm compared to 2mA with that obtained by the low conductive medium (1mS/cm) using the same field intensity. The number of Coulombs liberated in the conductive medium using 4 V/cm, 200 Hz, 400 µs, and 2 min total exposure time was 0.192 Coulombs, compared to 0.0192 Coulombs liberated in the low conductive medium. The results obtained by changing either the repetition frequency or the pulse duration demonstrated an increase in BSA-FITC uptake at 0.0432 Coulomb, which corresponded to 4 V/cm, 100 Hz, 180 µs, and 2 min total exposure time in the S-MEM. Thus, the number of Coulombs (and the current intensity) in the low conductivity medium is not the limiting factor. We can therefore exclude a direct effect of

the current passing through the cell suspension. This conclusion is reinforced by the presence of a clear plateau for frequencies above 100Hz (Figure 3) or pulse durations longer than 180µs (Figure 4) at 4V/cm as the number of Coulombs is much less, but the cell response is similar.

Moreover, this "plateau" confirms that this increase is an all-or-nothing response independent of the energy liberated in the medium, as reported by Mahrour et al. The absence of cell response in the low conductivity medium can simply result from the fact that, contrary to the S-MEM, a cell culture medium at 10mS/cm, the low conductive medium at 1mS/cm is not a "physiological" medium: osmolarity is preserved by the presence of 250mM sucrose, and ion content (Na^+ and Cl^-) is very low. Thus, to increase their endocytosis rate, cells must be in "physiological" conditions.

The results also demonstrated that the increase in receptor-mediated endocytosis in PEF-exposed cells was the consequence of a rapid change: it was apparent immediately after the start of PEF exposure and was not detectable if the fluorescent probe was introduced soon after the end of PEF delivery.

The transmembrane potential was determined by the Schwan equation[25]:

$\Delta\Psi_i = 1.5\ r\ E\ \cos\theta$

where r is the cell radius (a suspended cell is a sphere), E is the field strength in the region where the cell is located, and θ is the polar angle measured from the center of the cell concerning the direction of the field.

According to this formula, the highest voltage is induced at the places where the electric field is perpendicular to the membrane, i.e., at θ = 0° and θ=180°. Thus, exposing a glioma cell with a radius of 20 µm [26] to an electric field with positive pulse strengths ranging from 4 to 6.9 V/cm resulted in an induced potential differential of 12-20.7 mV across the plasma membrane. As a result, the membrane region facing the anode was hyperpolarized by 12-20.7 mV, while the membrane region facing the cathode was depolarized by the same amount using either unipolar electric pulses, as used by Antov et al.,[11] or bipolar asymmetric electric pulses, as used in the current study. It is well understood that the calculated changes in transmembrane potential do not result in electroporation.

Fluorescence aggregates were produced with the cell exposed to field intensity higher than 7.3V/cm despite degassing the medium before exposure to electric pulses due to the electrochemical reactions at the electrode surface. The generation of the aggregates limits the study at higher field intensities.

Human MG cells were exposed to bipolar asymmetric electric pulses in the presence of the anticancer drug bleomycin to investigate the ability of the drug to provoke electroendocytosis. BLM enters cells by receptor-mediated endocytosis, but in small quantities that are not enough to kill cancer cells,[27-29] so electroporation was used to increase the permeability of the anticancer drug and thus increase its cytotoxicity.[30] The pulse under research was able to destroy a reasonable number of cells at 3µM, reinforcing the idea of employing it as an auxiliary pulse before the electroporation process to allow the use of low doses of chemotherapy.

Conclusion

The features of the tested electrical impulses, as well as the outcomes of the experimentations, suggested that electroendocytosis was triggered only during the application of electric pulses at threshold intensity, with a quick "switch off" of the molecular probe uptake rise after the exposure to electric pulses was terminated. This result allows us to exclude the mechanisms that require more than a few minutes to be stimulated, such as gene expression regulation mechanisms. The meaning of this observation is that for drug delivery by electroendocytosis into MG cells, the drug must be administered before electric pulses. The bipolar asymmetric nature of the electric pulses, as well as the brief exposure time, significantly diminish the potential mechanisms involving electrophoresis of membrane proteins over long distances within the cell membrane; the absence of any relationship with the number of Coulombs or the electric current intensity also limits the influence of electrophoretic effects. The possibility of thermal effects can be ruled out.

Acknowledgments

The present work was supported by the Deanship of Scientific Research at Prince Sattam Bin Abdulaziz University, Al-Kharj, KSA.

Competing Interests

No potential conflict of interest was reported by the authors.

References

1. Pereyra AS, Mykhaylyk O, Lockhart EF, Taylor JR, Delbono O, Goya RG, Plank C, Hereñu CB. Magnetofection Enhances Adenoviral Vector-based Gene Delivery in Skeletal Muscle Cells. J Nanomed Nanotechnol. 2016 Apr;7(2):364. doi: 10.4172/2157-7439.1000364.
2. Vigata M, Meinert C, Hutmacher DW, Bock N. Hydrogels as Drug Delivery Systems: A Review of Current Characterization and Evaluation Techniques. Pharmaceutics. 2020 Dec 7;12(12):1188. doi: 10.3390/pharmaceutics12121188.
3. Sundaram J, Mellein BR, Mitragotri S. An experimental and theoretical analysis of ultrasound-induced permeabilization of cell membranes. Biophys J. 2003 May;84(5):3087-101.
4. Ita K. Perspectives on Transdermal Electroporation. Pharmaceutics. 2016 Mar 17;8(1):9. doi: 10.3390/pharmaceutics8010009.
5. Draga M, Pröls F, Scaal M. Double electroporation in two adjacent tissues in chicken embryos. Dev Dyn. 2018 Nov;247(11):1211-1216. doi: 10.1002/dvdy.24674.
6. Kotnik T, Rems L, Tarek M, Miklavčič D. Membrane Electroporation and Electropermeabilization: Mechanisms and Models. Annu Rev Biophys. 2019 May 6;48:63-91. doi: 10.1146/annurev-biophys-052118-115451.
7. Ben-Dov N, Rozman Grinberg I, Korenstein R. Electroendocytosis is driven by the binding of electrochemically produced protons to the cell's surface. PLoS One. 2012;7(11):e50299. doi: 10.1371/journal.pone.0050299.

8. Lin R, Chang DC, Lee YK. Single-cell electroendocytosis on a micro chip using in situ fluorescence microscopy. Biomed Microdevices. 2011 Dec;13(6):1063-73. doi: 10.1007/s10544-011-9576-9.
9. Shawki MM, Farid A. Low electric field parameters required to induce death of cancer cells. Electromagn Biol Med. 2014 Jun;33(2):159-63. doi: 10.3109/15368378.2013.800105.
10. Barbul A, Antov Y, Rosenberg Y, Korenstein R. Enhanced delivery of macromolecules into cells by electroendocytosis. Methods Mol Biol. 2009;480:141-50. doi: 10.1007/978-1-59745-429-2_10.
11. Antov Y, Barbul A, Mantsur H, Korenstein R. Electroendocytosis: exposure of cells to pulsed low electric fields enhances adsorption and uptake of macromolecules. Biophys J. 2005 Mar;88(3):2206-23. doi: 10.1529/biophysj.104.051268.
12. Mahrour N, Pologea-Moraru R, Moisescu MG, Orlowski S, Levêque P, Mir LM. In vitro increase of the fluid-phase endocytosis induced by pulsed radiofrequency electromagnetic fields: importance of the electric field component. Biochim Biophys Acta. 2005 Feb 1;1668(1):126-37. doi: 10.1016/j.bbamem.2004.11.015.
13. Antov Y, Barbul A, Korenstein R. Electroendocytosis: stimulation of adsorptive and fluid-phase uptake by pulsed low electric fields. Exp Cell Res. 2004 Jul 15;297(2):348-62. doi: 10.1016/j.yexcr.2004.03.027.
14. Marshall M, Lund PE, Barg S. Molecular Mechanisms of V-SNARE Function in Secretory Granule Exocytosis. Biophysical Journal. 2017, 112 (3), 395a.
15. Abd-Elghany AA. Incorporation of electroendocytosis and nanosecond pulsed electric field in electrochemotherapy of breast cancer cells. Electromagn Biol Med. 2022 Jan 2;41(1):25-34. doi: 10.1080/15368378.2021.
16. Hjouj M, Last D, Guez D, Daniels D, Sharabi S, Lavee J, Rubinsky B, Mardor Y. MRI study on reversible and irreversible electroporation induced blood brain barrier disruption. PLoS One. 2012;7(8):e42817. doi: 10.1371/journal.pone.0042817.
17. Sharabi S, Last D, Guez D, Daniels D, Hjouj MI, Salomon S, Maor E, Mardor Y. Dynamic effects of point source electroporation on the rat brain tissue. Bioelectrochemistry. 2014 Oct;99:30-9. doi: 10.1016/j.bioelechem.2014.06.001.
18. Garcia PA, Rossmeisl JH Jr, Robertson JL, Olson JD, Johnson AJ, Ellis TL, Davalos RV. 7.0-T magnetic resonance imaging characterization of acute blood-brain-barrier disruption achieved with intracranial irreversible electroporation. PLoS One. 2012;7(11):e50482. doi: 10.1371/journal.pone.0050482.
19. Sharabi S, Guez D, Daniels D, Cooper I, Atrakchi D, Liraz-Zaltsman S, Last D, Mardor Y. The application of point source electroporation and chemotherapy for the treatment of glioma: a randomized controlled rat study. Sci Rep. 2020 Feb 7;10(1):2178. doi: 10.1038/s41598-020-59152-7.
20. Poo M. In situ electrophoresis of membrane components. Annu Rev Biophys Bioeng. 1981;10:245-76. doi: 10.1146/annurev.bb.10.060181.001333.
21. Poo M, Robinson KR. Electrophoresis of concanavalin A receptors along embryonic muscle cell membrane. Nature. 1977 Feb 17;265(5595):602-5. doi: 10.1038/265602a0.
22. Poo M, Lam JW, Orida N, Chao AW. Electrophoresis and diffusion in the plane of the cell membrane. Biophys J. 1979 Apr;26(1):1-21. doi: 10.1016/S0006-3495(79)85231-5.
23. McLaughlin S, Poo MM. The role of electro-osmosis in the electric-field-induced movement of charged macromolecules on the surfaces of cells. Biophys J. 1981 Apr;34(1):85-93. doi: 10.1016/S0006-3495(81)84838-2.
24. Sowers AE, Hackenbrock CR. Rate of lateral diffusion of intramembrane particles: measurement by electrophoretic displacement and rerandomization. Proc Natl Acad Sci U S A. 1981 Oct;78(10):6246-50. doi: 10.1073/pnas.78.10.6246.
25. SCHWAN HP. Electrical properties of tissue and cell suspensions. Adv Biol Med Phys. 1957;5:147-209. doi: 10.1016/b978-1-4832-3111-2.50008-0.
26. Jäkel S, Dimou L. Glial Cells and Their Function in the Adult Brain: A Journey through the History of Their Ablation. Front Cell Neurosci. 2017 Feb 13;11:24. doi: 10.3389/fncel.2017.00024.
27. Pron G, Belehradek J Jr, Mir LM. Identification of a plasma membrane protein that specifically binds bleomycin. Biochem Biophys Res Commun. 1993 Jul 15;194(1):333-7. doi: 10.1006/bbrc.1993.1824.
28. Pron G, Mahrour N, Orlowski S, Tounekti O, Poddevin B, Belehradek J Jr, Mir LM. Internalisation of the bleomycin molecules responsible for bleomycin toxicity: a receptor-mediated endocytosis mechanism. Biochem Pharmacol. 1999 Jan 1;57(1):45-56. doi: 10.1016/s0006-2952(98)00282-2.
29. Prausnitz MR, Lau BS, Milano CD, Conner S, Langer R, Weaver JC. A quantitative study of electroporation showing a plateau in net molecular transport. Biophys J. 1993 Jul;65(1):414-22. doi: 10.1016/S0006-3495(93)81081-6.
30. Miklavčič D, Mali B, Kos B, Heller R, Serša G. Electrochemotherapy: from the drawing board into medical practice. Biomed Eng Online. 2014 Mar 12;13(1):29. doi: 10.1186/1475-925X-13-29.

International Journal of Biomedicine 12(4) (2022) 567-569
http://dx.doi.org/10.21103/Article12(4)_OA7

ORIGINAL ARTICLE

Radiology

INTERNATIONAL JOURNAL OF BIOMEDICINE

Prevalence and Causes of Intrahepatic and Extrahepatic Bile Duct Obstruction among the Jaundiced Patients at Riyadh Hospitals Diagnosed by Ultrasound

Mahasin G. Hassan*[1], Sarah Kaabi[1], Sahar Alqahtani[1], Badryah Sharahily[1], Lamia Almodayan[1], Mona Alghanim[1], Faten Alqahtani[1], Ahmed Abdulsalam[2], Halima Hawesa[1], Zohida A. Abdelgabar[3], Ibrahim Luttfi[4]

[1]*Department of Radiological Sciences, College of Health and Rehabilitation Sciences, Princess Nourah bint Abdulrahman University, Riyadh, Saudi Arabia*
[2]*Radiology Department, American Hospital Dubai, Dubai, UAE*
[3]*Department of Radiological Sciences, Al-Ghad International Colleges for Applied Sciences, Riyadh, KSA*
[4]*Home Health Care, King Salman Hospital, Riyadh, KSA*

Abstract

The aim of this study was to assess the prevalence and causes of bile duct obstruction among patients with jaundice at the ultrasound departments in Riyadh hospitals.

Methods and Results: The study included 525 records of jaundiced patients aged ≥18 years that were referred to the ultrasound department. Data were collected from PACS (Picture Archiving and Communication System) at three different hospitals in Riyadh. Of 525 adult jaundiced patients, 69 had biliary obstruction, a 13% prevalence. In our study, 38(55.1%) cases of obstruction were caused by stones, 14(20.3%) by tumors, 9(13.0%) by inflammation, 5(7.2%) by a nonfunctioning stent, and 3(4.3%) by pnemobilia. Obstructive jaundice occurred significantly more frequently with increasing age. The study revealed no significant difference between gender and the presence of obstruction. More studies with a larger sample size of obstructive jaundice patients are suggested.(**International Journal of Biomedicine. 2022;12(4):567-569.**).

Keywords: ultrasound • jaundice • bile duct • biliary obstruction

For citation: Hassan MG, Kaabi S, Alqahtani S, Sharahily B, Almodayan L, Alghanim M, Alqahtani F, Abdulsalam A, Hawesa H, Abdelgabar ZA, Luttfi I. Prevalence and Causes of Intrahepatic and Extrahepatic Bile Duct Obstruction among the Jaundiced Patients at Riyadh Hospitals Diagnosed by Ultrasound. International Journal of Biomedicine. 2022;12(4):567-569. doi:10.21103/Article12(4)_OA7

Introduction

Ultrasound is used as a first-line investigation in the assessment of biliary pathology.[1] Ultrasonography is a sensitive imaging modality for detecting cholelithiasis (gallstones) and is often the initial procedure of choice for imaging jaundiced patients.[2] Biliary obstruction (BO) is a blockage of the bile duct. There are two types: intrahepatic, above the level of the common bile duct (CBD), and extrahepatic, which is below that level. A low bile duct obstruction occurs when the blockage is below the insertion of the cystic duct.[3]

Bile duct obstruction can be caused by stones, benign or malignant structures, obstructed stents, or parasites, though the most common causes are malignancy, choledocholithiasis, and inflammatory stricture.[4] Less common causes are sclerosing cholangitis, choledochal cyst, hemobilia, pneumobilia, duodenal diverticulum, echinococcosis, and ascariasis.[5]

There are several studies regarding the causes of obstruction in different countries. A study conducted in Japan

***Corresponding author:** Mahasin G. Hassan, Department of Radiological Sciences, College of Health and Rehabilitation Sciences, Princess Nourah bint Abdulrahman University, Riyadh, Saudi Arabia. E-mail: mghassan@pnu.edu.sa*

revealed that the most common origins of intrahepatic and extrahepatic bile duct dilatation are calculus-related.[6]

In the USA, a study found that approximately 5 cases of BO in 1000 people are caused by gall stones, which is the most common cause.[7] On the other hand, a study conducted in Sweden revealed that malignancy is the most common cause of obstruction in that country.[8]

Due to the lack of reviews in Saudi Arabia regarding this topic, the aim of this study was to assess the prevalence and causes of bile duct obstruction among patients with jaundice at the ultrasound departments in Riyadh hospitals.

Material and Methods

The study was conducted from January 2020 until April 2020. Data were collected from PACS (Picture Archiving and Communication System) at three different hospitals in Riyadh. A simple random sample of jaundiced patients` data was collected from 2018 to 2020. The study sample included 525 records of jaundiced patients that were referred to the ultrasound department. The study included adults above 18 years old. Patients who have a history of treated biliary duct obstruction were excluded. The population of the study included 5150 jaundiced patients. This number was used to calculate the sample size of this study.[9] The confidence level used was 95%, and the error estimation was 5%. The resulting sample size was 358 for this study. Because of the availability of data, larger sample size (n=525) was used.

In this cross-sectional study, data were collected from patients' records using a data collection sheet that included all the variables of the study: age, gender, presence of obstruction, type of obstruction (intrahepatic, extrahepatic, combined intra- and extrahepatic ducts), and cause.

Statistical analysis was performed using statistical software package SPSS version 23.0 (SPSS Inc, Armonk, NY: IBM Corp). Baseline characteristics were summarized as frequencies and percentages for categorical variables. Group comparisons were performed using chi-square test with Yates correction. A probability value of $P<0.05$ was considered statistically significant.

Ethical approvals were obtained from the research center at Princess Nourah Bint Abdulrahman University (PNU) before collecting data (IRB number: 20-0039) and from the hospitals to get access to the patients' data. The data was only used for study purposes without individual details identifying the patient. The IRB stated that the study is exempt from IRB review.

Results and Discussion

Of 525 adult jaundiced patients, 69 had BO, a 13% prevalence. Among those with obstruction, 33(47.8%) had combined obstruction, 22 (31.9%) extrahepatic, and 14(20.2%) intrahepatic. In our study, 38(55.1%) cases of obstruction were caused by stones, 14(20.3%) by tumors, 9(13%) by inflammation, 5(7.2%) by a nonfunctioning stent (NFS), and 3(4.3%) by pnemobilia. Obstructive jaundice occurred significantly more frequently with increasing age (P=0.000) (Table 1). The study revealed no significant difference between gender and the presence of obstruction (P=0.624) (Table 2). The chi-square test showed a significant difference between the type of BO and the cause (P=0.0125) (Table 3).

Table 1.

Association between age and prevalence of BO

Distribution of age	Presence of biliary obstruction		Total
	No	Yes	
18-38 years	169	13	182
39-58 years	200	26	226
59-79 years	87	30	117
Total	456	69	525

Table 2.

Association between gender and prevalence of BO

Distribution of gender	Presence of biliary obstruction		Total
	No	Yes	
Female	250	40	290
Male	206	29	235
Total	456	69	525

Table 3.

Association between types and causes of biliary obstruction

Types of biliary obstruction	Distribution of causes of biliary obstruction					Total
	Stone	Inflammation	Tumor	Pnemobilia	NFS	
Intrahepatic	3	0	7	1	3	14
Extrahepatic	35	9	7	2	2	55
Total	38	9	14	3	5	69

The study showed that the prevalence of BO among jaundiced patients was about 13%, which is less than the prevalence in the study conducted in Sweden (32%).[8] This result also indicates that the major source of jaundice among Riyadh patients is mostly nonobstructive, that the prevalence of BO increased significantly with age (P=0.000), and that the age group of 59-79 years had the highest percentage of obstruction (43.5%). These results may be related to the increased frequency of causes with age, like biliary stones and pancreatic tumors. In our study, the prevalence of obstruction was higher in females than in males, although the difference between genders was not significant (P=0.624).

Combined obstruction (intra- and extrahepatic obstruction) was the most prevalent (47.8%), followed by extrahepatic obstruction (31.9%). The increase in the prevalence of the combined type was due to a rise in the presence of stones at the CBD (below cystic duct insertion) and increasing biliary duct dilation to include the intrahepatic ones. Biliary stones were the major cause of BO (55.1%) followed by tumors (20.3%), which include pancreatic head carcinoma, cholangiocarcinoma, periampullary carcinoma, and duodenal papillary carcinoma. Inflammation (cholangitis)

(13%) was in third place, a nonfunctioning stent (7.2%) was in fourth place, and pnemobilia (4.3%) was the least prevalent cause. The result is compatible with a number of previous studies, showing that the major cause of intrahepatic and extrahepatic bile duct dilatation is stones.[7,8,10]

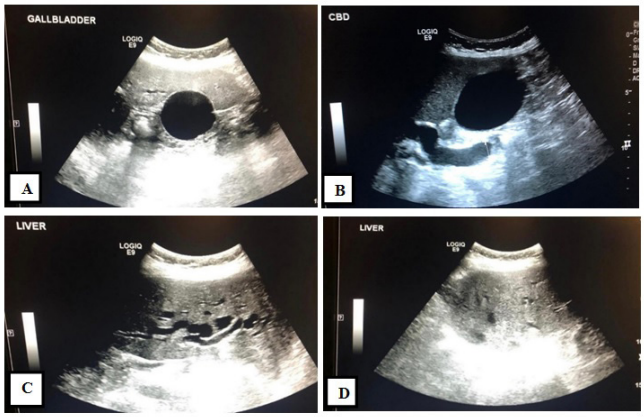

Fig. 1. *A 74-year-old female came to the department with abdominal pain and jaundice. Image (A) shows a distended gallbladder with a transverse diameter of 4.5 cm. There is mild gallbladder sludge. (B) shows dilatation of CBD measuring 1.4 cm in diameter, there is an impression of the abrupt structure at the distal end of CBD. (C) shows diffuse dilatation of intrahepatic biliary ducts. The liver demonstrates a homogenous normal echotexture and a smooth outline. It is slightly above normal limits measuring 16.9 cm. No focal liver lesions are seen (D).*
(The image was taken with permission from Prince Mohammed Bin Abdulaziz Hospital)

The study revealed that stones were the major cause of the combined and extrahepatic obstruction. For intrahepatic obstruction, the major cause was tumors. The difference was significant between the types and the causes of obstruction (P=0.0125). Our result aligns well with the Yunfu et al.[8] study showing that stones are the major cause of combined obstruction.

In conclusion, biliary obstructionis not the major cause of jaundice among patients in Riyadh (KSA). The prevalence of biliary obstruction among jaundiced patients is about 13%. In our study, 38(55.1%) cases of obstruction were caused by stones, 14(20.3%) by tumors, 9(13%) by inflammation, 5(7.2%) by a nonfunctioning stent, and 3(4.3%) by pnemobilia. Obstructive jaundice occurred significantly more frequently with increasing age. The study revealed no significant difference between gender and the presence of obstruction. More studies with a larger sample size of obstructive jaundice patients are suggested.

Competing Interests

The authors declare that they have no competing interests.

References

1. Spârchez Z, Radu P. Role of contrast enhanced ultrasound in the assessment of biliary duct disease. Med Ultrason. 2014 Mar;16(1):41-7. doi: 10.11152/mu.2014.2066.161.zs1pr2.
2. Dean D. Abdominal Ultrasound, and Instrumentation. Part 1, Module 4, 1st ed. The Burwin institute of diagnostic medical ultrasound. 2005, Luneburg; Canada.
3. Yarmohammadi H, Covey AM. Percutaneous biliary interventions and complications in malignant bile duct obstruction. Chin Clin Oncol. 2016 Oct;5(5):68. doi: 10.21037/cco.2016.10.07.
4. Jarnagin W, Blumgart L, Hann L, Belghiti J, Büchler M, Chapman W et al. Blumgart's surgery of the liver, biliary tract, and pancreas. 4th ed., 2012, Philadelphia: Elsevier Saunders.
5. Sahani D, Samir A, Abdominal imaging, 1st ed. 2011, Maryland Heights, Mo: Saunders Elsevier.
6. Tazuma S. Gallstone disease: Epidemiology, pathogenesis, and classification of biliary stones (common bile duct and intrahepatic). Best Pract Res Clin Gastroenterol. 2006;20(6):1075-83. doi: 10.1016/j.bpg.2006.05.009.
7. Naumowicz E, Białecki J, Kołomecki K. Results of treatment of patients with gallstone disease and ductal calculi by single-stage laparoscopic cholecystectomy and bile duct exploration. Wideochir Inne Tech Maloinwazyjne. 2014 Jun;9(2):179-89. doi: 10.5114/wiitm.2014.41629.
8. Yunfu Lv, Wan Yee Lau, Haiying Wu, Etiological Causes of Intrahepatic and Extrahepatic Bile Duct Dilatation. International Journal of New Technology and Research. 2015;8(1):53.
9. Calculator.net [Internet], Sample Size Calculator, Available from https://www.calculator.net/sample-size-calculator.html
10. Gameraddin M, Omer S, Salih S, Elsayed S, Alshaikh A, Sonographic Evaluation of Obstructive Jaundice. Open Journal of Medical Imaging. 2015;05(01):24-29.

International Journal of Biomedicine 12(4) (2022) 570-574
http://dx.doi.org/10.21103/Article12(4)_OA8

ORIGINAL ARTICLE

Radiology

INTERNATIONAL JOURNAL OF BIOMEDICINE

Biometric Data of Adults' Aortic Knob Diameter in Posteroanterior Chest Radiograph, Correlation to Age and Normative Heart Diameter: A Cross-Sectional Study

Maisa Elzaki[1,2]

[1]*Faculty of Applied Medical Sciences, Taibah University, Al-Madinah Al-Munawara (Madinah), Saudi Arabia*

[2]*Faculty of Radiological Sciences and Medical Imaging, Alzaiem Alazhari University, Khartoum, Sudan*

Abstract

Background: The aortic knob (AK) is an essential feature on a chest x-ray. It could be the first sign of a cardiovascular problem if there is any deformation or enlargement of the knob. This study aimed to measure the normal AK diameter (AKD) on a posteroanterior chest radiograph in healthy adult Sudanese.

Methods and Results: The study was conducted in the Department of Radiology and Imaging in Ribat Hospital (Sudan) between Jun 2019 and Jan 2020. A total of 113 participants of both sexes (45.1% males and 54.9% females) with a normal chest x-ray and no history of diabetes, blood hypertension, cardiovascular disease, or skeletal abnormality were selected. Participants' age fluctuated from 18 to 75 years. The measurements (AK, heart diameter [HD], cardiothoracic ratio [CTR]) were carried out with the measuring tools available on the software of the computed radiography system. The mean AKD was 2.8±0.8 cm (2.94±0.8 cm in males and 2.51±0.77 cm in females, P=0.005)). The mean HD was 9.22±2.8 cm (9.8±3.3 cm in males and 8.7±0.2.1 cm in females, P=0.005). The mean CTR was estimated as 46.6±7.7% with a significant difference between males and females and significantly correlated with HD and BMI (P<0.05). The AKD increased by 0.0199 cm with an increase of one year of age (AKD = 0.0199(age)+1.9469), and there was a strong positive correlation between age and AKD (P<0.001).

Conclusion: The study found a significant positive correlation between age and AKD. Increased heart sizes increase AKD. The AKD value is greater in males than in females.(**International Journal of Biomedicine. 2022;12(4):570-574.**).

Keywords: chest radiograph • aortic knob • heart diameter • cardiothoracic ratio

For citation: Elzaki M. Biometric Data of Adults' Aortic Knob Diameter in Posteroanterior Chest Radiograph, Correlation to Age and Normative Heart Diameter: A Cross-Sectional Study. International Journal of Biomedicine. 2022;12(4):570-574. doi:10.21103/Article12(4)_OA8

Abbreviations

AK, aortic knob; **AKD**, AK diameter; **BMI**, body mass index; **CTR**, cardiothoracic ratio; **HD**, heart diameter.

Introduction

Human physical variability has been a subject of great interest for scientists for a long time using a scientific technique for measuring the proportions of the human body that has evolved; this technique is known as *anthropometry*. The examination of anthropometric parameters is critical in resolving identification and pathology issues.(1) In medicine, measuring normal parts and organs is used as an index to assess pathology or for manufacturing medical devices to harmonize the bodies of patients.

Chest radiography with a posteroanterior view is one of the most significant studies; it is the primary line of investigation for many disorders. As a result, it is one of the most common inquiries in our daily work because it is the commonest imaging modality of the heart;(2) due to its

affordability and simplicity, it is most readily used. Physicians must understand how to evaluate basic chest radiographic results and summarize them. Before reading and diagnosing abnormalities,[3] the normal appearances, sizes/measurements, and variances in a chest radiograph must be familiar to physicians.

The aortic knob (AK), or aortic knuckle, is an essential feature on a chest x-ray. It could be the first sign of a cardiovascular problem[4,5] if there is any deformation or enlargement of the knob.[4] The left border of the cardiac silhouette on the posteroanterior (PA) chest radiograph is composed of a series of convex arcs. The AK, often known as the knuckle, is one of them; it is not a particular anatomical structure, although it does symbolize the aortic arch's distal end.[2] Plain radiography, computed tomography, echocardiography, magnetic resonance imaging, and radionuclide imaging can be used to determine the AK.[4] It can be expanded as a result of increased pressure flow in the aorta or changes in the elasticity of its wall, such as in systemic hypertension, medial cystic necrosis of the aorta, or aortic dissection, as well as atherosclerosis. The prominence of the AK is also seen in some instances of aortic stenosis (post stenotic dilation), coarctation of the aorta, and aortic aneurysm;[4] having a sensitivity of between 70% and 90% for cardiovascular diseases due to hypertension, it is an effective predictor of target organ damage.[6] Although many advanced investigations are required to diagnose cardiovascular disorders, these instruments are scarce in rural regions. Thus the chest x-ray remains the initial inquiry in suspected heart disease, particularly in rural areas.[4,7] As a result, the radiologic method's utility in determining and predicting direct measurement of AK size indicates the presence of any diseases in the cardiovascular system. Nonetheless, it differs depending on body type, gender, and ethnicity, according to previous studies on Africans,[6,8] Indians,[2,4] Asians,[9-11] and Caucasians. This study aimed to measure the normal AK diameter (AKD) on a posteroanterior chest radiograph presented as a baseline of dilated AK, to correlate it with different ages, genders, and body mass index (BMI), and to estimate the relationship between the AK index with various thoracic biometrics in healthy adult Sudanese.

Materials and Methods

The study was conducted in the Department of Radiology and Imaging in Ribat Hospital (Sudan) between Jun 2019 and Jan 2020. A total of 113 participants of both sexes (45.1% males and 54.9% females) with a normal chest x-ray and no history of diabetes, blood hypertension, cardiovascular disease, or skeletal abnormality were selected. Participants' age fluctuated from 18 to 75 years (mean age of 37.9±14.07 years; age range was classified with an interval of 10 years). All chest radiographs were taken with the patient erect, facing the stand bucky; the distance from the patient to the x-ray focus was 72 inches. The radiologist assessed a radiograph for the technique's normality confirmation and quality evaluation.

The measurements were carried out with the measuring tools available on the software of the computed radiography system. The AKD was measured by drawing a horizontal line from the trachea's lateral border to the aortic knob's left lateral wall.[4,6,11,12]

Transverse heart diameter (HD) was measured as the sum of the right atrium diameter from the midline plus the left ventricle diameter from the midline.[4,6] After obtaining the patient's height and weight, BMI was defined, and cardiothoracic ratio (CTR) was determined by dividing the HD by the maximum width of the chest diameter.[3] To minimize errors, all measurements were completed by a single reviewer.

Statistical analysis was performed using the statistical software package SPSS version 25.0 (Armonk, NY: IBM Corp.). Baseline characteristics were summarized as frequencies and percentages for categorical variables and as mean±SD for continuous variables. Levene's Test of Equality of Variances was used to assess meeting the statistical assumption of homogeneity of variance in between-subjects designs. A simple linear regression was performed. Pearson's Correlation Coefficient (r) was used to determine the strength of the relationship between the two continuous variables. Group comparisons with respect to categorical variables are performed using chi-square test. A probability value of $P<0.05$ was considered statistically significant.

Ethical approvals were obtained from the research center at Alzaiem Alzhari University Radiologic Sciences Faculty before collecting data. The data was only used for study purposes without individual details identifying the participant. Written informed consent was obtained from each research participant.

Results

The mean BMI was 23.6±5.03 kg/m^2 and distributed among males and females as 23.47 kg/m^2 and 25.06 kg/m^2, respectively. The mean AKD was 2.8±0.8 cm (2.94±0.8 cm in males and 2.51±0.77 cm in females, P=0.005). The mean HD was 9.22±2.8 cm (9.8±3.3 cm in males and 8.7±0.2.1 cm in females (P=0.005) (Table 1). All measurements significantly differed between both genders.

Table 1.

Mean BMI, AKD, HD, and CTR values according to gender.

	n	BMI, kg/m^2	AKD, cm	HD, cm	CTR, %
Male	51	23.47±4.28	2.94±0.8	9.8±3.3	45.3±0.7
Female	62	25.06±4.16	2.51±0.77	8.7±2.1	47.8±0.6
All	113	24.34±4.2	2.72±0.8	9.22±2.8	46.7±5.5
P-value		0.04	0.005	0.028	0.02

The study clarified a linear association between AKD and HD (Table 2). There was a strong positive correlation between the two variables (r=0.837, P=0.000). In addition, there was a significant association between AKD and age (r=0.342, P=0.000), and a significant difference was found in

AKD measurement between different age groups (P<0.001) (Table 2, Figure 1).

Table 2.
Pearson Correlations of AKD & CTR with age, BMI, and HD

Variable		r	Sig. (2-tailed)
AKD	Age	0.342	0.000
	BMI	0.104	0.275
	HD	0.837	0.000
CTR	Age	0.112	0.237
	BMI	0.302	0.001
	HD	0.358	0.000

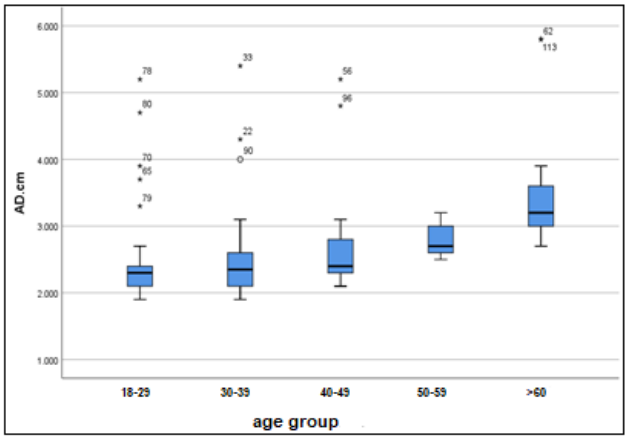

Figure 1. *Box plot. AKD in different age groups (r=0.359;P=0.000).*

A simple linear regression was developed to predict AKD based on age. A significant regression equation was found (F = 14.74, P<0.001, with R^2 = 0.1173. AKD = 0.0199(age) +1.9469 cm), the AKD increased by 0.0199 cm for each year of age (Figure 2).

The mean CTR was estimated as 46.6±7.7% with a significant difference between males and females and significantly correlated with HD and BMI (P<0.05); additionally there was an insignificant difference of CTR with AKD and age (P>0.05). CTR of females over 60 years was found to be larger than in other age groups, more than 50% (Table 1,2; Figure 3).

Discussion

As one of the highly regularly performed radiological examinations, a basic understanding and interpretation of chest radiographs is an unavoidable requirement for any physician involved in patient care.[3] Before evaluating anomalous data, it is necessary first to understand normal chest radiography characteristics and variations.

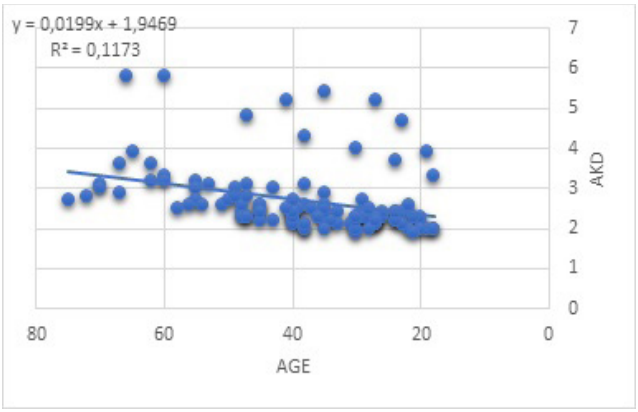

Figure 2. *Scatter plot. Linear regression of AKD predicted by age.*

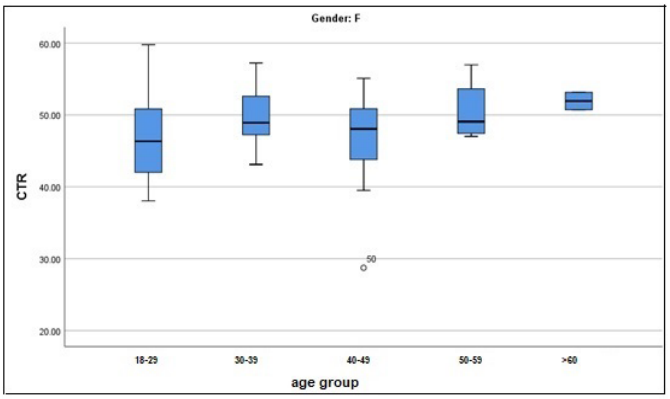

Figure 3. *Box plot. Comparison in CTR of females in different age groups.*

This study aimed to assess AKD in the Sudanese population using PA chest x-ray and to establish normative measurement to compare it with others and add a reference measurement.

In this study's sample population involving males and females, the mean AKD was 2.8±0.8cm; this is less than found in previous studies[2,4,5,7,10,11] and differs considerably from them.This value is smaller than Indian[2] AKD (3.04±0.59 cm) and Korean[10] AKD (32.29±5.30 mm) but nearly similar to the Nepal[9] population (2.786±0.19 cm). This could be due to variations in the method of measurement. In some previous studies,[2,13,14] measurements were taken from the lateral border of AKD to the midline of the body. Table 3 compares the measurements of this study with other studies in different countries.

In this study, measurements of AKD and HD were significantly different by gender; males had greater sizes than females. It could be related to differences in BMI. Many studies consistent with this study documented that males have higher values than females in the same age group.[2,5,7,15] The finding is also similar to Magera et al.[6] and Ray et al.[4] The HD in this study was smaller than in Nigerians, with a mean of 12.64±1.5cm, contrary to Magera's report.[6] Our results show a significant positive correlation between HD and AKD.

Table 3.

Comparison of the measurements made in this study with other studies in different countries.

Study	n	Age	BMI	AKD	HD	CTR
Shankar et al., 2010 (India) [2]	108			3.04±0.59 cm		
Kayastha et al., 2020 (Nepal) [9]	100	18-70 years		2.786±0.19 cm		
Lee et al., 2018 (Korea) [10]	3,970	45.45±11.56 years	23.88±3.35 kg/m^2	32.29±5.30 mm		
Anyanwu GE et al., 2007 (Nigeria) [8]	1018	32.2 years		4.7±0.46 cm	12.64±1.5 cm	46.68±4.3%
Sung et al., 2019 (Korea) [11]	696	46.85±12.89 years	24.02±3.51 kg/m^2	32.08±5.54 mm		
Current Study (Sudan)	113	37.9± 4.07 years	23.6±5.03 kg/m^2	2.8±0.8 cm	9.16±2.7 cm	46.7±5.5%

The CTR is a simple and helpful technique that can screen for cardiovascular disorders as an index of heart size.[16] In adults, the average range of CTR was determined to be 39%-50% (mean of 45%). However, it was proposed that a CTR of up to 52% be "acceptable."[17]

As exhibited in the results section, there was a notable normal mean of Sudanese CTR (46.7±5.5%). It was also observed that the mean CTR of females was higher than in males (47.8±0.6% and 45.3±0.7%, respectively). This result is similar to a study of the Indian population, which was published by Debnath et al.,[3] in their revising anatomical variations, which may be due to increasing body structure in males, or also may be due to the prevalence of increased BMI in females more than in males. This relationship was highlighted as a significant difference between the two genders.[2] Moreover, the CTR of females over 60 years was found to be more than 50%; this result was similar to the result found in the Ghanaian population by Mensah et al.[16] This was explained by the fact that older women experienced a more marked drop in trans-thoracic diameter with age.

There was a significant difference in AKD among different age groups. The AKD increased by 0.019cm with an increase of one year of age (AKD = 0.0199(age)+1.9469), and there was a strong positive correlation between age and AKD (P<0.001), which agreed with several studies.[2,4,5,7]The results of this study agree with previous studies,[2,5,8] which indicated an insignificant correlation between AKD and BMI; the result of this study is consistent with previous studies in that the AKD increases significantly with an increase in HD.[2,4,7]

Conclusion

The study found a significant positive correlation between age and aortic knob diameter; age can be used as a predictor for aortic knob diameter. The aortic knob diameter in adult Sudanese is smaller than in Nigerians, Indians, and Asians. Increased heart sizes increase aortic knob diameter. The aortic knob diameter value is greater in males than in females.

Competing Interests

The author declares that there is no conflict of interests.

Acknowledgments

The author appreciates Ehaa Abdulla, Malaz Mohammed, Marwa Alwasilla, Mathany Mohammed, Nuha Salah, and Sakina Mohammed for their cooperation.

References

1. Franciscus RG, Long JC. Variation in human nasal height and breadth. Am J Phys Anthropol. 1991 Aug;85(4):419-27. doi: 10.1002/ajpa.1330850406.
2. Shankar N, Veeramani R, Ravindranath R, Philip B. Anatomical variations of the aortic knob in chest radiographs. Eur J Anat. 2010;14(1):25-30.
3. Debnath J, Sreedhar CM, Mukherjee R, Maurya VK, Patrikar S, Reddy YRN. Revisiting anatomical variants on screening chest radiographs in Indian adolescents: A cross sectional observational pilot study. Med J Armed Forces India. 2018 Oct;74(4):337-345. doi: 10.1016/j.mjafi.2017.07.010.
4. Ray A, Mandal D, Kundu P, Manna S, Mandal S. Aortic Knob Diameter in Chest X-Ray and its Relation with Age, Heart Diameter and Transverse Diameter of Thorax in a Population of Bankura District of West Bengal, India: A Cross-Sectional Study. J Evol Med Dent Sci. 2014;3(31):8595-8600. doi:10.14260/jemds/2014/3092
5. Obikili EN, Okoye IJ. Transverse cardiac diameter in frontal chest radiographs of a normal adult Nigerian population. Niger J Med. 2005 Jul-Sep;14(3):295-8.
6. Magera S, Sereke SG, Okello E, Ameda F, Erem G. Aortic Knob Diameter in Chest Radiographs of Healthy Adults in Uganda. Reports in Medical Imaging. 2022;15:21-29. doi:10.2147/rmi.s356443
7. Anyanwu GE, Agwuna KK. Aortic arch diameter and its significance in the clinical evaluation of cardiac and aortic enlargements. Niger J Clin Pract. 2009 Dec;12(4):453-6.
8. Anyanwu GE, Anibeze CIP, Akpuaka FC. Transverse Aortic Arch Diameters and Relationship with Heart Size of Nigerians within the South East.2007;18(2):115-118.

***Correspondence:** Maisa Elzaki, Assistant Professor of Diagnostic Radiology, Faculty of Applied Medical Sciences, Taibah University, Al-Madinah Al-Munawara (Madinah), Saudi Arabia. E-mail: elzakimaisa@gmail.com*

9. Kayastha P, Paudel S, Suwal S, Adhikari B, Humagain MP, Magar BT, Adhikary KP. Variations in Measurements of the Aortic Knob in the Chest Radiograph in Normal and Hypertensive Subjects. Europasian J Med Sci. 2020;2(2):92-96. doi:10.46405/ejms.v2i2.212
10. Lee EJ, Han JH, Kwon KY, Kim JH, Han KH, Sung SY, Hong SR. The Relationship between Aortic Knob Width and Metabolic Syndrome. Korean J Fam Med. 2018 Jul;39(4):253-259. doi: 10.4082/kjfm.17.0038.
11. Sung SY, Han JH, Kim JH, Kwon KY, Park SW. The Relationship between Heart Rate Variability and Aortic Knob Width. Korean J Fam Med. 2019 Jan;40(1):39-44. doi: 10.4082/kjfm.18.0077.
12. Tomita Y, Kasai T, Ishiwata S, Daida H, Narui K. Aortic Knob Width as a Novel Indicator of Atherosclerosis and Obstructive Sleep Apnea. J Atheroscler Thromb. 2020 Jun 1;27(6):501-508. doi: 10.5551/jat.50286.
13. Debnath J, Sreedhar CM, Mukherjee R, Maurya VK, Patrikar S, Reddy YRN. Revisiting anatomical variants on screening chest radiographs in Indian adolescents: A cross sectional observational pilot study. Med J Armed Forces India. 2018 Oct;74(4):337-345. doi: 10.1016/j.mjafi.2017.07.010.
14. Bons LR, Rueda-Ochoa OL, El Ghoul K, Rohde S, Budde RP, Leening MJ, Vernooij MW, Franco OH, van der Lugt A, Roos-Hesselink JW, Kavousi M, Bos D. Sex-specific distributions and determinants of thoracic aortic diameters in the elderly. Heart. 2020 Jan;106(2):133-139. doi: 10.1136/heartjnl-2019-315320.
15. Groepenhoff F, den Ruijter HM. Sex-specific thoracic aortic dimensions and clinical implications. Heart. 2020 Jan;106(2):97-98. doi: 10.1136/heartjnl-2019-315903.
16. Mensah YB, Mensah K, Asiamah S, Gbadamosi H, Idun EA, Brakohiapa W, Oddoye A. Establishing the Cardiothoracic Ratio Using Chest Radiographs in an Indigenous Ghanaian Population: A Simple Tool for Cardiomegaly Screening. Ghana Med J. 2015 Sep;49(3):159-64. doi: 10.4314/gmj.v49i3.6.
17. Inoue K, Yoshii K, Ito H. Effect of aging on cardiothoracic ratio in women: a longitudinal study. Gerontology. 1999 Jan-Feb;45(1):53-8. doi: 10.1159/000022056.

International Journal of Biomedicine 12(4) (2022) 575-579
http://dx.doi.org/10.21103/Article12(4)_OA9

ORIGINAL ARTICLE

Radiology

INTERNATIONAL JOURNAL OF BIOMEDICINE

Evaluations of Paranasal Sinus Disease Using Multidetector Computed Tomography in Taif City, Saudi Arabia

Osama Alotaibi[1], Hamid Osman[2*], Yasser Hadi[3], Yasser Alzamil[4], Amjad Alyahyawi[4,5], Mamdouh S. Al-Enezi[4], Feras Alafer[6], Ahmad Abanomy[7], Mayeen Uddin Khandaker[8,9], Meshari Almeshari[4]

[1]King Abdulaziz Specialist Hospital-Taif, Taif, Saudi Arabia
[2]College of Applied Medical Science, Taif University, Taif, Saudi Arabia
[3]King Abdullah Medical City (KAMC), Makkah, Saudi Arabia
[4]Department of Diagnostic Radiology, College of Applied Medical Sciences, University of Ha'il, Ha'il, Saudi Arabia
[5]Centre for Nuclear and Radiation Physics, Department of Physics, University of Surrey, Guildford, UK
[6]College of Applied Medical Sciences, Jouf University, Sakaka, Saudi Arabia
[7]College of Applied Medical Sciences, King Saud University, Riyadh, Saudi Arabia
[8]Centre for Applied Physics and Radiation Technologies, School of Engineering and Technology, Sunway University, Selangor, Malaysia
[9]Daffodil International University, Dhaka, Bangladesh

Abstract

Background: This study aimed to evaluate paranasal sinusitis disease and determine if there is a relationship between the anatomical variation of sinusitis based on the age and gender of the patient and, if so, to identify the most affected demographic group.

***Methods and Results*:** This study included 130 patients (76 men and 54 women with ages ranging from 18 years to 75 years) diagnosed with PNS disease and was conducted in the Radiology Department of King Abdelaziz Specialist Hospital and King Faisal Hospital (Taif city, Saudi Arabia) from January 1 2021 to January 31 2022. The evaluation of sinusitis was conducted using multidetector computed tomography (MDCT). The clinical symptoms included 70% cases of nasal obstruction, 53% cases of headache, 28.5% cases of nasal discharge, 17.7% cases of facial pain, and 3.1% cases of general malaise. The types of sinusitis included maxillary sinusitis (88.5%), sphenoid sinusitis (28.5%), ethmoid sinusitis (43.8%), and frontal sinusitis (23.5%). The study found no significant anatomical variation of sinuses based on age and gender ($P>0.05$).

Conclusion: An evaluation of paranasal sinusitis disease using an MDCT scan shows that there are no gender or age-related differences in the prevalence of the disease. Moreover, the study demonstrates that there is no significant anatomical variation of sinuses based on age and gender.(**International Journal of Biomedicine. 2022;12(4):575-579.**).

Keywords: paranasal sinus • sinusitis • multidetector computed tomography

For citation: Alotaibi O, Osman H, Hadi Y, Alzamil Y, Alyahyawi A, Al-Enezi MS, Alafer F, Abanomy A, Khandaker MU, Almeshari M. Evaluations of Paranasal Sinus Disease Using Multidetector Computed Tomography in Taif City, Saudi Arabia.. International Journal of Biomedicine. 2022;12(4):575-579. doi:10.21103/Article12(4)_OA9.

Abbreviations

CT, computed tomography; **DNS**, deviated nasal septum; **MDCT**, multidetector CT; **PNS**, paranasal sinus.

Introduction

Sinusitis is an inflammatory condition associated with bacterial, viral, or fungal infections of the cavities around the nasal passages or allergic reactions affecting the paranasal sinuses.[1] Sinusitis affects approximately 15% of humans worldwide[2,3] and is considered a major public health problem. The prevalence of sinusitis in the United States and

Europe was 12% and 10.9%, respectively.[4] Paranasal sinus (PNS) disease is a chronic and life-threatening condition characterized by infection, growth, and inflammation of the sinuses.[5] PNS disease is a prevalent disease in humans, and it impairs their quality of life.[6,7] It is also considered the fifth most common cause of antibiotic prescription in the U.S., with medical costs of almost $2.4 billion in addition to lost and diminished productivity.[8,9]

The most widely used method for the assessment and diagnosis of PNS disease is the CT imaging modality.[1,10] CT scans are considered reliable for diagnosing PNS disease due to their high accuracy and sensitivity in defining the extent and degree of sinusitis.[2] While CT scans may not be reliable for detecting neoplasms in the paranasal sinuses, they can be used to distinguish between inflammatory diseases of the sinuses.[11] An improved form of a CT scan known as MDCT has been developed, which provides a quicker and more detailed analysis of body structures with higher spatial resolution and more coverage of the patient. MDCT can be a useful tool for assessing patients suspected of having and confirmed to have PNS disease.

Due to a lack of publication from our community regarding the efficacy of CT in diagnosing PNS, this study aims at characterizing and evaluating patients with PNS disease in Taif City, Saudi Arabia, using the MDCT technique. Preliminary research shows that sinusitis is prevalent in the Eastern Provinces, where it is associated with nasal polyposis, bronchial asthma, and analgesic intolerance.[12-14] However, the prevalence rate of PNS disease in the Kingdom of Saudi Arabia is not known due to a paucity of studies on the disease prevalence and incidence.

This study aimed to evaluate paranasal sinusitis disease and determine if there is a relationship between the anatomical variation of sinusitis based on the age and gender of the patient and, if so, to identify the most affected demographic group.

Materials and Methods

Study population, sampling criteria, and study design

This study included 130 patients (males and females with ages ranging from 18 years to 75 years) diagnosed with PNS disease and was conducted in the Radiology Department of King Abdelaziz Specialist Hospital and King Faisal Hospital (Taif city, Saudi Arabia) from January 1 2021 to January 31 2022.

This retrospective study was performed to assess and characterize paranasal sinusitis using MDCT. The dependent variable was paranasal sinusitis disease with mucosal thickening, retention cysts, opacifications, fluid level, polyp, as well as septal deviation, and enlarged nasal conchae. The independent variables were age, gender, history of the disease, and patient complaint (clinical data).

Clinical assessments and guidelines

Patient data were obtained from the Picture Archiving and Communication System (PACS) of each hospital. The data are complete and do not require any special preparation. The data were captured with CT machines installed in the hospitals, including General Electric (GE) healthcare light speed, Phillips Medical System, and Siemens, all with 128 slices each. The protocol followed during the assessment started with a patient in the supine position and supported under the knee for comfort. The lead apron was placed over the area to follow the concept of "as low as reasonably achievable" (ALARA) patient exposure to radiation.[15] The study protocol was used for the assessment with a lateral scout, axial scan, coronal and sagittal scan plane, and a scan range from the bottom of the maxillary sinus to the endpoint of the frontal sinus.

Statistical analysis was performed using statistical software package SPSS version 23.0 (SPSS Inc, Armonk, NY: IBM Corp). Baseline characteristics were summarized as frequencies and percentages. Group comparisons with respect to categorical variables are performed using One-Sample Chi-Square test. A probability value of $P<0.05$ was considered statistically significant.

Informed consent was obtained from patients before collecting the data. All identifiable information about patients was removed, and the data were coded to ensure anonymity.

Results

Analysis of the demographic characteristics of the study patients (76[59%] men and 54[41%] women) showed the age range from 18 to 65 years (21.63 ±6.36 years) with the following age groups: the age group of 18-25 years – 24.6%, 26-35 years –36.2%, 36-45 years –18.5%, 46-55 years – 9.2%, and 56-65 years – 6.9% (Table 1).

Table 1.
Distribution of the study sample according to gender and age.

Variable		Frequency (n)	Percentage (%)
Gender	Males	76	58.5%
	Females	54	41.5%
Age range (years)	18-25	32	24.6%
	26-35	47	36.2%
	36-45	24	18.5%
	46-55	12	9.2%
	56-65	9	6.9%
	<65	6	4.6%

More than half of the study sample (60.8%) was aged between 18 and 35, with a mean age of 21.63. The clinical symptoms included 70% cases of nasal obstruction, 53% cases of headache, 28.5% cases of nasal discharge, 17.7% cases of facial pain, and 3.1% cases of general malaise (Table 2). The types of sinusitis included maxillary sinusitis (88.5%), sphenoid sinusitis (28.5%), ethmoid sinusitis (43.8%), and frontal sinusitis (23.5%) (Fig.1).

Characterization of sinusitis depending on the type of sinus opacification showed that 60.8% of the cases with maxillary sinusitis had bilateral opacification, 14.7% had right

sinus opacification, and 24.5% had left sinus opacification. Of the cases diagnosed with ethmoid sinusitis, 70.2% had bilateral sinus opacification, 8.8% had right sinus opacification, and 12.1% had left sinus opacification. Of the cases diagnosed with frontal sinus, 61.3% had bilateral sinus opacification, 12.9% had right sinus opacification, and 25.8% had left sinus opacification. Sphenoid sinus opacification was present in 27.5% of the cases (Table 3).

Table 2.
Distribution of the study sample according to clinical diagnosis.

Clinical symptoms	Frequency (n)	Percentage (%)
Nasal obstruction	91	70%
Headache	69	53.1%
Nasal discharge	37	28.5%
Facial pain	23	17.7%
General malaise	4	3.1%

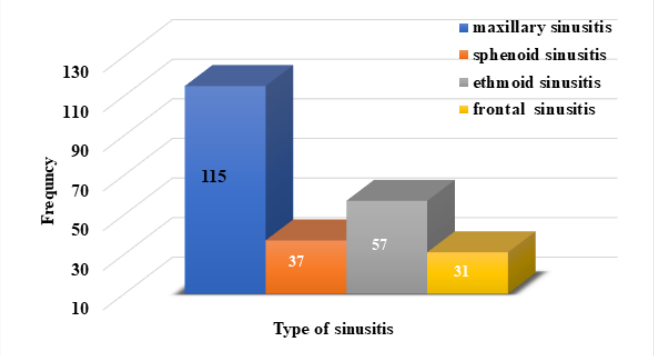

Fig. 1. *Types of paranasal sinusitis.*

Table 3.
The side of sinus opacification.

Sinus	The side of opacification		
	Right	Bilateral	Left
Maxillary sinus	17 (14.7%)	70 (60.8%)	28 (24.5%)
Ethmoid sinus	5 (8.8%)	40 (70.2%)	12 (12.1%)
Frontal sinus	4 (12.9%)	19 (61.3%)	8 (25.8%)
Sphenoid sinus	Present		Absent
	37 (28.5%)		93 (71.5%)

The most common CT findings in cross-sectional images were nasal septum deviation (72.3%), mucosal thickening (70.8%), nasal conchae enlargement (32.2%), retention cyst(16.9%), and nasal polyps (7.7%) (Figure 2 and Table 4).

Table 4.
Distribution of the study sample according to CT findings.

CT finding		Side		
		Right	Bilateral	Left
Presence of mucosal thickening		15 (16.3%)	62 (67.4%)	15 (16.3%)
Presence of retention cyst		10 (45.4%)	4 (18.2%)	8 (36.4%)
Presence of nasal polyps		2 (20%)	6 (60%)	2 (20%)
Nasal conchae enlargement	Site	Right	Bilateral	Left
	Inferior	7 (16.7%)	6 (14.3%)	16 (38.1%)
	Middle	2 (4.7%)	4 (9.5%)	7 (16.7%)
	Superior	0	0	0
Nasal septum deviation		Right	Centralize	Left
		56 (43.1%)	36 (27.7%)	38 (29.2%)
Presence of air-fluid level		2 (1.5 %)		

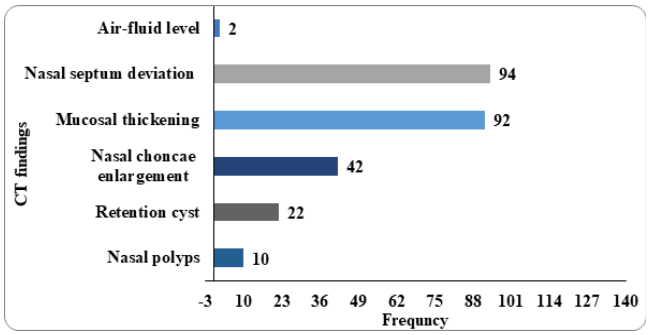

Fig. 2. *Distribution of the study sample according to CT findings.*

No gender differences in sinusitis prevalence were observed between male and female patients (P=0.178). An analysis of age differences in sinusitis showed no significant differences (P=0.762). We also did not find statistically significant anatomical variation among the age variables (P>0.05). No statistically significant differences in gender were noted in the anatomical variation of sinusitis (P>0.05).

Discussion

Sinusitis is a leading public health issue with significant cost implications. An extensive body of literature focuses on the evaluation of paranasal sinusitis using CT scans.[7,12,16,17] The findings suggest that the age of the patient influences the

pattern of infection.[7] Further research shows that the features of sinusitis vary widely among patients, including maxillary sinusitis, nasal septal deviation, enlarged nasal conchae, mucosal thickening, retention cysts, and polyps.

The samples used in this study included male and female samples of patients aged 18 years to 65 years old. The study sample indicated that more than half of the study patients (60.8%) who suffered from sinusitis were between 18 and 35 years old. Many studies have explored sinusitis prevalence among various age groups, including young children. Most of these studies have shown that sinusitis occurs among all age groups.[14,20] Consistent with the evidence from the existing literature, this study's findings indicate no statistically significant difference between the age of the subjects and the severity of sinusitis (P>0.05).

Characterization of the study sample based on the type of sinusitis showed that most patients had maxillary sinusitis (88.5%), followed by ethmoid sinusitis (43%), sphenoid sinusitis (28%), and frontal sinusitis (23%).

According to this study, 58.5% of the cases were male while 41.5% were female, with a marginal preponderance for males, which corresponds with the existing research evidence.[13,21,22] Sinusitis of the maxillary sinus was most common (88.5%), followed by ethmoid, sphenoid and frontal sinuses.[13,23,24] The most frequent clinical presentations in the present study were nasal obstruction (70%) and headache (53%), which were like those found in the study by Almutairi et al.[25] In our study, the septal deviation, mucosal thickening, and enlarged nasal conchae were the most common findings in PNS pathologies, which agrees with data in the study by Alshammari et al.[12]

According to the current study, there was no statistically significant variation in sinusitis and anatomical variables between genders and ages. Most patients with PNS pathology were in their first and second decades, with male predominance. Nasal obstruction was the most common complaint among these patients, and the most common anatomical variant observed was deviated nasal septum, more to the right and with maxillary as commonly involved.

A range of research studies has shown that various mechanisms can damage the sinuses and cause them to become inflamed.[26-32] The most common cause is an inflammation caused by a sinus infection that has not yet been identified. In this study, the differences in anatomical features between genders and between ages were not statistically significant. These findings are congruent with existing studies, which show that maxillary sinusitis is the most common type of sinusitis.[33]

In conclusion, an evaluation of paranasal sinusitis disease using an MDCT scan shows that there are no gender or age-related differences in the prevalence of the disease. Moreover, the study demonstrates that there is no significant anatomical variation of sinuses based on age and gender. Further clinical studies are required to evaluate other anatomical variations, like concha bullosa, agger nasi cell, basal lamella pneumatization, and crista Galli. The study findings will help healthcare professionals, especially ENT physicians, to make early assessments and accurate diagnoses of PNS disease for effective treatment and management.

Acknowledgments

This research has been funded by Scientific Research Deanship at the University of Hail-Saudi Arabia through project number (GR-22094).

Competing Interests

The authors declare that they have no competing interests.

References

1. Iwanaga J, Wilson C, Lachkar S, Tomaszewski KA, Walocha JA, Tubbs RS. Clinical anatomy of the maxillary sinus: application to sinus floor augmentation. Anat Cell Biol. 2019 Mar;52(1):17-24. doi: 10.5115/acb.2019.52.1.17.
2. Choby G, Thamboo A, Won TB, Kim J, Shih LC, Hwang PH. Computed tomography analysis of frontal cell prevalence according to the International Frontal Sinus Anatomy Classification. Int Forum Allergy Rhinol. 2018 Jul;8(7):825-830. doi: 10.1002/alr.22105.
3. Sobiesk JL, Munakomi S. Anatomy, Head and Neck, Nasal Cavity. National Library of Medicine. 2022, StatPearls Publishing LLC. https://www.ncbi.nlm.nih.gov/books/NBK544232/.
4. Hastan D, Fokkens WJ, Bachert C, Newson RB, Bislimovska J, Bockelbrink A, Bousquet PJ, Brozek G, Bruno A, Dahlén SE, Forsberg B, Gunnbjörnsdóttir M, Kasper L, Krämer U, Kowalski ML, Lange B, Lundbäck B, Salagean E, Todo-Bom A, Tomassen P, Toskala E, van Drunen CM, Bousquet J, Zuberbier T, Jarvis D, Burney P. Chronic rhinosinusitis in Europe--an underestimated disease. A GA²LEN study. Allergy. 2011 Sep;66(9):1216-23. doi: 10.1111/j.1398-9995.2011.02646.x.
5. Torpy JM, Lynm C, Golub RM. JAMA patient page. Chronic sinusitis. JAMA. 2011 Nov 9;306(18):2048. doi: 10.1001/jama.2011.1588.
6. Papadopoulou AM, Chrysikos D, Samolis A, Tsakotos G, Troupis T. Anatomical Variations of the Nasal Cavities and Paranasal Sinuses: A Systematic Review. Cureus. 2021 Jan 15;13(1):e12727. doi: 10.7759/cureus.12727.
7. Orman G, Kralik SF, Desai N, Meoded A, Vallejo JG, Huisman TAGM, Tran BH. Imaging of Paranasal Sinus Infections in Children: A Review. J Neuroimaging. 2020 Sep;30(5):572-586. doi: 10.1111/jon.12737.
8. Centers for Disease Control and Prevention. Sinus Infection (Sinusitis). August 27, 2019. Available from: https://www.cdc.gov/antibiotic-use/sinus-infection.html
9. Pereira JGD, Santos JBS, Sousa SP, Franco A, Silva RHA. Frontal sinuses as tools for human identification: a systematic review of imaging methods. Dentomaxillofac Radiol. 2021 Jul 1;50(5):20200599. doi: 10.1259/dmfr.20200599.
10. Naqvi SFH, Arshad N, Naeem MA, Waseem N, Batool N, Ali A. Paranasal Sinuses in the Evaluation of Sinusitis using

***Corresponding author**: Prof. Hamid Osman Hamid. Department of Radiology. College of Applied Medical Science, Taif University, Taif, Saudi Arabia. E-mail: ha.osman@tu.edu.sa*

Computed Tomography: Cross-Sectional Study. Sch J App Med Sci. 2021;9(4): 605-611.
11. Hussein AO, Ahmed BH, Omer MA, Manafal MF, Elhaj AB. Assessment of clinical, X-Ray and CT in the diagnosis of paranasal sinus diseases. International Journal of Scientific Research. 2014;3:7-11.
12. Alshammari QT, Malik BA, Salih M, Yousef M, Elnour E, Yousif E, Gameraddin M. Assessment of Paranasal Sinuses Diseases using Multi-Detector Computed Tomography Scanning in Hail city, Saudi Arabia. Bioscience Research. 2020;17:1308-1314.
13. Hamdi A, Mohtasib R, Mahmoud M. Role of Computed Tomography in Determining the Spectrum of Paranasal Sinuses Pathologies in Saudi patients. Pakistan Journal of Biological Sciences. 2020;23(3):339-344.
14. Alfarhood AA, Rayzah M, Alhassan MA, Alhassan AA, Alqahtani FA, Alanazi OH. Knowledge And Practice of Pilonidal Sinuses Among Adult Population in Zulfi City, Saudi Arabia, 2018-2019. World Journal of Pharmaceutical Research. 2018;7:270-275. doi: 10.20959/wjpr201818-13564.
15. Osman H. Evaluation of patient radiation dose in routine radiographic examinations in Saudi Arabia, Radiat Phys and Chemi. 2020;173:108883
16. Chang YS, Chen PL, Hung JH, Chen HY, Lai CC, Ou CY, Chang CM, Wang CK, Cheng HC, Tseng SH. Orbital complications of paranasal sinusitis in Taiwan, 1988 through 2015: Acute ophthalmological manifestations, diagnosis, and management. PLoS One. 2017 Oct 3;12(10):e0184477. doi: 10.1371/journal.pone.0184477.
17. Kaminsky J, Bienert-Zeit A, Hellige M, Rohn K, Ohnesorge B. Comparison of image quality and in vivo appearance of the normal equine nasal cavities and paranasal sinuses in computed tomography and high field (3.0 T) magnetic resonance imaging. BMC Vet Res. 2016 Jan 19;12:13. doi: 10.1186/s12917-016-0643-6.
18. Munhoz L, Abdala Júnior R, Abdala R, Asaumi J, Arita ES. Diffusion-Weighted Magnetic Resonance Imaging in Maxillary Sinuses Inflammatory Diseases: Report of Three Cases and Literature Review. J Oral Maxillofac Res. 2018 Jun 29;9(2):e4. doi: 10.5037/jomr.2018.9204.
19. Munhoz L, Abdala Júnior R, Arita ES. The value of the apparent diffusion coefficient calculated from diffusion-weighted magnetic resonance imaging scans in the differentiation of maxillary sinus inflammatory diseases. Oral Surg Oral Med Oral Pathol Oral Radiol. 2019 May;127(5):433-443. doi: 10.1016/j.oooo.2018.11.013.
20. Kakish KS, Mahafza T, Batieha A, Ekteish F, Daoud A. Clinical sinusitis in children attending primary care centers. Pediatr Infect Dis J. 2000 Nov;19(11):1071-4. doi: 10.1097/00006454-200011000-00008.
21. Verma J, Tyagi S, Srivastava M, Agarwal A. Computed tomography of paranasal sinuses for early and proper diagnosis of nasal and sinus pathology. International Journal of Otorhinolaryngology and Head and Neck Surgery. 2016;2(2):70-76.
22. Özer CM, Atalar K, Öz II, Toprak S, Barut Ç. Sphenoid Sinus in Relation to Age, Gender, and Cephalometric Indices. J Craniofac Surg. 2018 Nov;29(8):2319-2326. doi: 10.1097/SCS.0000000000004869.
23. Whyte A, Boeddinghaus R. The maxillary sinus: physiology, development and imaging anatomy. Dentomaxillofac Radiol. 2019 Dec;48(8):20190205. doi: 10.1259/dmfr.20190205.
24. Hui L, Hung KF, Yeung AWK, von Arx T, Leung YY, Bornstein MM. Anatomical variations of the ethmoid sinuses and their association with health or pathology of the ethmoid and maxillary sinuses in a Southern Chinese population: An analysis using cone-beam computed tomography. Imaging Sci Dent. 2022 Mar;52(1):109-115. doi: 10.5624/isd.20210277.
25. Almutairi AF, Shafi RW, Albalawi SA, Basyuni MA, Alzahrnai AA, Alghamdi AS, Alhaifi AA, Alshehri AA, Al-Gadouri MA. Acute and Chronic Sinusitis Causes and Management. The Egyptian Journal of Hospital Medicine. 2017;68(3):1513-1539. doi:10.12816/0039697.
26. Scangas GA, Gudis DA, Kennedy DW. The natural history and clinical characteristics of paranasal sinus mucoceles: a clinical review. Int Forum Allergy Rhinol. 2013 Sep;3(9):712-7. doi: 10.1002/alr.21178.
27. Sataloff RT. Sinusitis. Journal of Singing. 2007;64(1):63-66.
28. Khasnavis S. Sinusitis. In Handbook of Outpatient Medicine. Springer, Cham. 2018:215-224.
29. Liu T, Sun Y, Bai W. The Role of Epigenetics in the Chronic Sinusitis with Nasal Polyp. Curr Allergy Asthma Rep. 2020 Nov 24;21(1):1. doi: 10.1007/s11882-020-00976-8.
30. Sumathy G. Chronic Sinusitis–A Review. European Journal of Molecular & Clinical Medicine. 2020;7(10):2020.
31. Abraham J. Imaging for head and neck cancer. Surg Oncol Clin N Am. 2015 Jul;24(3):455-71. doi: 10.1016/j.soc.2015.03.012.
32. Rosenfeld RM, Andes D, Bhattacharyya N, Cheung D, Eisenberg S, Ganiats TG, Gelzer A, Hamilos D, Haydon RC 3rd, Hudgins PA, Jones S, Krouse HJ, Lee LH, Mahoney MC, Marple BF, Mitchell CJ, Nathan R, Shiffman RN, Smith TL, Witsell DL. Clinical practice guideline: adult sinusitis. Otolaryngol Head Neck Surg. 2007 Sep;137(3 Suppl):S1-31. doi: 10.1016/j.otohns.2007.06.726.
33. Lewis ME, Roberts CA, Manchester K. Comparative study of the prevalence of maxillary sinusitis in later Medieval urban and rural populations in northern England. Am J Phys Anthropol. 1995 Dec;98(4):497-506.

International Journal of Biomedicine 12(4) (2022) 580-583
http://dx.doi.org/10.21103/Article12(4)_OA10

ORIGINAL ARTICLE

Radiology

INTERNATIONAL JOURNAL OF BIOMEDICINE

Association between Renal Stones Sonographic Findings and Demographic Data among Patients at Riyadh Hospitals, Saudi Arabia

Mahasin G. Hassan[1*], Tahani Alshammrani[1], Shahad Alshammeri[1], Faten Alotaibi[1], Sara Alzeryer[1], Reem Alharbi[1], Amal Almujalli[1], Sahar Mansour[1], Ibrahim Luttfi[2], Tasneem S. A. Elmahdi[3], Lubna Bushara[4], Halima Hawesa[1]

[1]Department of Radiological Sciences, College of Health and Rehabilitation Sciences, Princess Nourah bint Abdulrahman University, Riyadh, Saudi Arabia
[2]Home Health Care, Ministry of Health, Riyadh, Saudi Arabia
[3]Department of Radiological Sciences, Al-Ghad International Colleges for Applied Sciences, Al-Medina, Saudi Arabia
[4]Department of Medical Imaging and Radiation Sciences, Collage of Applied Medical Sciences, University of Jeddah, Saudi Arabia

Abstract

Background: Ultrasound is the primary imaging modality to identify renal stones (RS) in patients with acute flank pain. This study aimed to evaluate the presence, location, and size of RS diagnosed by ultrasound in association with age, gender, and body mass index (BMI) among patients at Riyadh hospitals.

Methods and Results: In this case-control study, a total of 250 records (130/52% for males and 120/48% for females) from 2018 to 2019 were reviewed from January to March 2020 at different hospitals in Riyadh. In this study, 150(60%) records of patients with RS and 100(40%) records of patients without RS were collected to evaluate the risk factor for RS formation in the central area of Saudi Arabia. A designed data collection sheet containing all variables (demographic and sonographic) of the study was used. Demographic data included gender, age, and BMI. Sonographic data included RS presence (yes, no), RS location (right kidney, left kidney, both kidneys), and RS size (small [<0.5 cm], average [0.5–1 cm], and large [>1 cm]). Statistical analysis was performed using statistical software package SPSS version 23.0 (SPSS Inc, Armonk, NY: IBM Corp).

The study found that RS were more common among males than females ($P<0.001$). The results show that in normal body weight, the frequency of stone presence was similar for right kidney and left kidney. In overweight patients, RS were more often observed in left kidney (P=0.000). We also found a significant association between BMI and RS size (P=0.049); the presence of smaller stones increases with BMI. There was no association between sonographic data and age (P>0.05)

Conclusion: Among patients at Riyadh hospitals, females are less affected by RS than males. Gender is a significant risk factor for the development of RS. The effect of BMI is obvious on renal stone location and size. (**International Journal of Biomedicine. 2022;12(4):580-583.**).

Keywords: kidney • renal stone • gender • demographic data • ultrasound

For citation: Hassan MG, Alshammrani T, Alshammeri S, Alotaibi F, Alzeryer S, Alharbi R, Almujalli A, Mansour S, Luttfi I, Elmahdi TSA, Bushara L, Hawesa H. Association between Renal Stones Sonographic Findings and Demographic Data among Patients at Riyadh Hospitals, Saudi Arabia. International Journal of Biomedicine. 2022;12(4):580-583. doi:10.21103/Article12(4)_OA10.

Abbreviations

BMI, body mass index; **BW**, body weight; **RS**, renal stones; **RT**, right kidney; **LK**, left kidney.

Introduction

Renal stones (RS) are considered one of the most common diseases worldwide. Generally, calculi develop in one kidney, but sometimes in both kidneys.[1] Flank pain due to urolithiasis is a common problem with patients presenting to emergency departments. Radiology plays a vital role in diagnosing this problem. Many modalities can be used, including ultrasonography, X-ray and CT.[2]

Ultrasound is the primary imaging modality to identify RS in patients with acute flank pain.[3] Ultrasound detects the presence, location and size of RS. Kidney stones are seen as an echogenic focus that produces acoustic shadowing.[4]

Calculi can form in the kidneys at any age, but adults are under the threat of calculi creation in their kidneys more often than children. Climate influences people's diet plans, and it generally becomes a reason for the formation of calculi in their kidneys. Numerous other factors affect calculi formation in the kidney, including gender, the nature of the liquids consumed, and diet.[5]

In the US, a medical survey regarding calculi prevention discovered that the prevalence of calculi among women was 5% and among men, 12%.[1] In Japan, a study on the correlation of body mass index (BMI) with RS found that an increased BMI was a risk factor for Japanese men.[6]

In Saudi Arabia, result of studies in different parts of the country do not agree. A study conducted in the western region found that the middle-aged population in their third decade of life, as well as overweight and obese people, are at a high risk of developing urolithiasis.[7] However, another study in the eastern region found that the prevalence of RS is high among patients between 30 and 50 years of age, male gender and normal BMI.[8] There is a different climate in the central region of Saudi Arabia, which was the focus of our study, so the risk factors that affect the formation of RS there may differ.

This study aimed to evaluate the presence, location, and size of RS diagnosed by ultrasound in association with age, gender, and BMI among patients at Riyadh hospitals.

Materials and Methods

In this case-control study, a total of 250 records (130/52% for males and 120/48% for females) from 2018 to 2019 were reviewed using a picture archiving and communication system (PACS) from January to March 2020 at different hospitals in Riyadh. In this study, 150(60%) records of patients with RS and 100(40%) records of patients without RS were collected to evaluate the risk factor for RS formation in the central area of Saudi Arabia.

A designed data collection sheet containing all variables (demographic and sonographic) of the study was used. Demographic data included gender, age (classified into four groups: 18–37 years, 38–57 years, 58–77 years, and 78–97 years), and BMI (organized into four categories: underweight [<18.5 kg/m^2], normal weight [18.5–24.9 kg/m^2], overweight [>24.9–29.9 kg/m^2], and obese [>30 kg/m^2]). Sonographic data included RS presence (yes, no), RS location (right kidney [RK], left kidney [LK], both kidneys), and RS size (small [<0.5 cm], average [0.5–1 cm], and large [>1 cm]).[9]

Statistical analysis was performed using statistical software package SPSS version 23.0 (SPSS Inc, Armonk, NY: IBM Corp). Baseline characteristics were summarized as frequencies and percentages for categorical variables. Group comparisons were performed using chi-square test with Yates correction. A probability value of $P<0.05$ was considered statistically significant.

Ethical approvals were obtained from the research center at Princess Nourah Bint Abdulrahman University (PNU) before collecting data (IRB number: 20-0040).

Results and Discussion

Among 150(60%) records of patients with RS, about 44% of RS were located in right kidney, 50% - in left kidney, and 9% - in both kidneys simultaneously. About 20.8% of RS were small, 27.2% - average, and 12% large. Tables 1-2 show the distribution of sonographic data according to the demographic data (age, gender and BMI). There was no association between sonographic data and age ($P>0.05$) (Table 1). Gender showed an effect on the presence of RS (P0.001) (Table 2); BMI showed an effect on stone location ($P=0.010$) and stone size ($P=0.049$) (Table 3).

Table 1.

Association between age and sonographic data.

Age	RS presence		RS location			RS size		
	Yes	No	RK	LK	Both	Small	Average	Large
18-37 years	52	37	25	26	1	15	25	12
38-57 years	64	38	25	36	3	22	32	10
58-77 years	33	20	15	13	5	14	11	8
78-97 years	1	5	1	0	0	1	0	0
Total	150	100	66	75	9	52	68	30
P-value	0.156		0.596			0.474		

Table 2.

Association between gender and sonographic data.

Gender	RS presence		RS location			RS size		
	Yes	No	RK	LK	Both	Small	Average	Large
Female	57	63	27	27	3	24	22	11
Male	93	37	39	48	6	28	46	19
Total	150	100	66	75	9	52	68	30
P-value	0.000		0.799			0.300		

Table 3.

Association between BMI and sonographic data.

BMI	RS presence		RS location			RS size		
	Yes	No	RK	LK	Both	Small	Average	Large
Underweight	6	7	4	2	0	2	3	1
Normal BW	75	57	39	36	0	20	40	15
Overweight	62	36	19	35	8	29	23	10
Obesity	7	0	4	2	1	1	2	4
Total	150	100	66	75	9	52	68	30
P-value	0.082		0.010			0. 049		

Results obtained demonstrate that the age group between 38–57 years had a higher frequency of renal stones. It may be that this age group performed the most substantial activities, which led to dehydration. In the eastern region, the prevalence of renal stones was highest in patients aged 30–50 years. However, our results showed no significant association between sonographic data and age. A larger sample size may be needed to show the significance.

The left kidney was most affected by renal stones. The chi-square test indicated a nonsignificant association (P=0.596) between patients' age and the renal stone location. The presence of an average size of renal stones was observed somewhat more often, but without statistical significance (P=0.474). The study found that renal stones were more common among males than females (P<0.001). Different studies confirmed that the male gender is more affected.[8,10] There are various reasons for this result; heavy activities are performed by males, leading to dehydration, a high protein diet is spread among males, and males have a high prevalence of diabetes.[11] Gender did not affect the location or size of renal stones

The body mass index (BMI), first described by Adolphus Quetelet in the mid-19th century,[12] has been consistently used in a myriad of epidemiologic studies. However, the accuracy of body mass index in diagnosing obesity is limited, particularly for individuals in the intermediate body mass index ranges, in men, and in the elderly.[13] In a study performed by Romero-Corral et al.,[13] a BMI cutoff of ≥ 30 kg/m^2 had good specificity but misses more than half of people with excess fat.

Different studies[6,14] in different countries emphasized the effect of body mass index on the formation of renal stones. Our results regarding the effect of body mass index on the presence of renal stones is contrary to some literature data (P=0.082). However, the sample size may not be enough to show the significance. The effect of body mass index on renal stone location is obvious (P=0.010). The results show that in normal body weight, the frequency of stone presence was similar for right kidney and left kidney. In overweight patients, renal stones were more often observed in left kidney (P=0.000). However, this association needs more studies to justify these results. We also found a significant association between body mass index and renal stone size (P=0.049); the presence of smaller stones increases with body mass index. These stones can be impacted at the distal ureter and result in a hydroureter. Usually, these small stones are formed by uric acid, and the tendency toward uric stone formation increases with body mass index. On the other hand, larger stones are usually formed by calcium oxalate, which decreases with increasing body mass index.[15]

Conclusion

Among patients at Riyadh hospitals, females are less affected by renal stones than males. Gender is a significant risk factor for the development of renal stones. The effect of body mass index is obvious on renal stone location and size. The results show that in normal body weight, the frequency of stone presence was similar for right kidney and left kidney. In patients with overweight, renal stones were more often observed in the left kidney. The presence of smaller size stones increases with body mass index.

Competing Interests

The authors declare that they have no competing interests.

References

1. Coe FL, Evan A, Worcester E. Kidney stone disease. J Clin Invest. 2005 Oct;115(10):2598-608. doi: 10.1172/JCI26662.
2. Kalb B, Sharma P, Salman K, Ogan K, Pattaras JG, Martin DR. Acute abdominal pain: is there a potential role for MRI in the setting of the emergency department in a patient with renal calculi? J Magn Reson Imaging. 2010 Nov;32(5):1012-23. doi: 10.1002/jmri.22337.
3. Kanno T, Kubota M, Sakamoto H, Nishiyama R, Okada T, Higashi Y, Yamada H. The efficacy of ultrasonography for the detection of renal stone. Urology. 2014 Aug;84(2):285-8. doi: 10.1016/j.urology.2014.04.010.
4. Penny SM. Examination Review for Ultrasound: Abdomen & Obstetrics and Gynaecology, 1st edition, Lippincott Williams & Wilkins; 2011.
5. Menon M, Resnick MI. Urinary lithiasis: etiology, diagnosis and medical management. In PC Walsh PC, AB Retik AB, ED Vaughan ED, et al. (eds). Cambell's Urology, 8th edition. Saunders, Philadelphia; 2002.

***Corresponding author:** Mahasin G. Hassan, Department of Radiological Sciences, College of Health and Rehabilitation Sciences, Princess Nourah Bint Abdulrahman University, Riyadh, Saudi Arabia. E-mail: mghassan@pnu.edu.sa*

6. Yoshimura E, Sawada SS, Lee IM, Gando Y, Kamada M, Matsushita M, Kawakami R, Ando R, Okamoto T, Tsukamoto K, Miyachi M, Blair SN. Body Mass Index and Kidney Stones: A Cohort Study of Japanese Men. J Epidemiol. 2016;26(3):131-6. doi: 10.2188/jea.JE20150049.
7. Nassir AM. Prevalence and characterization of urolithiasis in the Western region of Saudi Arabia. Urol Ann. 2019 Oct-Dec;11(4):347-352. doi: 10.4103/UA.UA_56_19. Erratum in: Urol Ann. 2020 Apr-Jun;12(2):203.
8. Gamalalddin M, Yassin Z, Saleh W. Study of the renal stones composition using computed tomography among Saudi population. International Journal of Science and Research (IJSR). 2018;7(3):1873–1875.
9. Devin D, Abdominal ultrasound and instrumentation. Module 1, 1st edition, The Burwin Institute of Diagnostic Medical Ultrasound, Luneburg, Canada; 2001
10. Shirazia F, Shahpourianb F, Khachiana A, Hosseini F, Houshiarradd A, Heidari S, Sanjari M. Personal Characteristics and Urinary Stones. Hong Kong Journal of Nephrology. 2009;11(1):14–19.
11. Alqurashi KA, Aljabri KS, Bokhari SA. Prevalence of diabetes mellitus in a Saudi community. Ann Saudi Med. 2011 Jan-Feb;31(1):19-23. doi: 10.4103/0256-4947.75773.
12. Quetelet A. A Treatise on Man and the Development of His Faculties. Burt Franklin; New York: Originally published in 1842. Reprinted in 1968.
13. Romero-Corral A, Somers VK, Sierra-Johnson J, Thomas RJ, Collazo-Clavell ML, Korinek J, Allison TG, Batsis JA, Sert-Kuniyoshi FH, Lopez-Jimenez F. Accuracy of body mass index in diagnosing obesity in the adult general population. Int J Obes (Lond). 2008 Jun;32(6):959-66. doi: 10.1038/ijo.2008.11.
14. Semins MJ, Shore AD, Makary MA, Magnuson T, Johns R, Matlaga BR. The association of increasing body mass index and kidney stone disease. J Urol. 2010 Feb;183(2):571-5. doi: 10.1016/j.juro.2009.09.085.
15. Daudon M, Lacour B, Jungers P. Influence of body size on urinary stone composition in men and women. Urol Res. 2006 Jun;34(3):193-9. doi: 10.1007/s00240-006-0042-8.

International Journal of Biomedicine 12(4) (2022) 584-590
http://dx.doi.org/10.21103/Article12(4)_OA11

ORIGINAL ARTICLE

Dentistry

INTERNATIONAL JOURNAL OF BIOMEDICINE

Bacterial Leakage Evaluation of Three Root Canal Sealers with Two Obturation Techniques: An in Vitro Study

Tringa Z. Kelmendi[1], Linda J. Dula[2*], Shera Kosumi[3], Anila Kamberi[4], Nita Kelmendi[5]

[1]*Department of Dental Pathology and Endodontics, Faculty of Medicine, University of Prishtina, Prishtina, Kosovo*

[2]*Department of Prosthodontics, Dental School, Faculty of Medicine, University of Prishtina, Prishtina, Kosovo*

[3]*Dental Faculty, Alma Mater Europaea Campus College "Rezonanca", Prishtina, Kosovo*

[4]*Department of Dental Pathology and Endodontics, University Dentistry Clinical Center of Kosovo, Prishtina, Kosovo*

[5]*Department of Pharmacy, Alma Mater Europaea Campus College "Rezonanca", Prishtina, Kosovo*

Abstract

Background: The purpose of this study was to compare the quality of the coronal seal of three root canal sealers and two obturation techniques using the bacterial penetration method.

Methods and Results: A total of 132 single-rooted human teeth with fully developed apices were used. The teeth were randomly assigned to three experimental groups according to the endodontic sealer used. Group 1: Samples (n=44) were obturated using a zinc oxide eugenol-based sealer, Pulp Canal Sealer EWT. Group 2: Samples (n=44) were obturated using an epoxy resin-based sealer, AH Plus. Group 3: Samples (n=44) were obturated using a bioceramic-based root canal sealer, Well-Root ST. Each group was subdivided into 2 equal subgroups in accordance with the obturation technique being used: the cold lateral condensation technique (CLCT) and Thermafil obturation technique (ThOT). Thus, 6 subgroups were formed: Sub-1A: Pulp Canal Sealer/CLCT; Sub-2A: AH Plus/CLCT; Sub-3A: Well-ROOT ST/CLCT; Sub-1B: Pulp Canal Sealer/ThOT; Sub-2B: AH Plus/ThOT; Sub-3B: Well-ROOT ST/ThOT. A dual-chamber device was used to evaluate bacterial leakage. Fresh medium and *E. faecalis* were added to the upper chamber every 4 days. The broth was monitored for color change daily for 33 days. Significant differences were found among Sub-2A vs. Sub-1B (P=0.023), Sub-1A vs. Sub-3A (P=0.014), Sub-1A vs. Sub-2B (P=0.024), Sub-1A vs. Sub-3B (P=0.002), Sub-3A vs. Sub-1B (P=0.003), Sub-2B vs. Sub-1B (P=0.005), and Sub-1B vs. Sub-3B (P<0.0001). There was no significant difference in the average occurrence of turbidity between CLCT and ThOT (P=0.718)

Conclusion: Regardless of the obturation technique, all root canal sealers exhibited leakage; however, the bioceramic-based root canal sealer appeared to perform better than the epoxy resin-based sealer and the zinc oxide eugenol-based sealer. (**International Journal of Biomedicine. 2022;12(4):584-590.**).

Keywords: microleakage • cold lateral condensation technique • thermafil obturation technique • root canal sealer

For citation: Kelmendi TZ, Dula LJ, Kosumi S, Kamberi A, Kelmendi N. Bacterial Leakage Evaluation of Three Root Canal Sealers with Two Obturation Techniques: An in Vitro Study. International Journal of Biomedicine. 2022;12(4):584-590. doi:10.21103/Article12(4)_OA11.

Abbreviations

CLCT, cold lateral condensation technique; **CFU**, colony-forming units; **ThOT**, Thermafil obturation technique.

Introduction

Microorganisms are a major etiological factor in root canal infections, and eradicating them during root canal treatment by instrumentation, irrigation, and intracanal medication is fundamental. The root canals should be cleaned, shaped, and obturated with sterilized materials with antimicrobial properties.[(1)] It is not always possible to completely eliminate microorganisms from the root canals,[(2)] and microorganisms can also penetrate through coronal

leakage after the obturation of root canals.[3] No available filling material or technique can achieve complete sealing of the entire root canal system.[4] Therefore, there is a need to develop root canal filling materials with an improved capacity to prevent bacterial ingress in the long term.[5]

Many studies involving dyes, radioisotopes, and bacteria have been performed to evaluate coronal leakage. The use of bacteria to assess substantial coronal leakage is considered to be of greater clinical relevance than dye penetration, according to Timpawat et al.[6] *Enterococcus faecalis* is commonly isolated from primary[7] and secondary endodontic infections.[8] However, its prevalence is higher in secondary endodontic infections. This microorganism is one of the most resistant in endodontic infections and is considered to be a possible cause of endodontic treatment failure.[9]

The success of endodontic treatment depends on adequate mechanical debridement of the root canal and quality obturation with a material that must be biocompatible. Gutta-percha is the recommended material because it has been shown to be biologically inert.[10] Gutta-percha does not bond to root dentin and must be used in conjunction with a sealer cement.[11] Cold lateral condensation of gutta-percha is one of the most widely accepted canal obturation methods and is taught by numerous dental schools. Nevertheless, its capability to adapt the gutta-percha to the internal surface of the root canal has been questioned.[12] Recently, a number of plasticized gutta-percha techniques have been introduced that have claimed to seal the root canal better.[13] The Thermafil obturation technique (ThOT) involves a plastic core covered by gutta-percha that is heated in an electric oven to ensure thermoplasticization. This carrier-guided gutta-percha technique is fast and effective in obturating the canal, exhibiting less leakage in vitro compared with the cold lateral condensation technique (CLCT).[14] The flow of endodontic sealers is related to their physical-chemical properties as well as to their root canal sealing ability during the procedure of root filling.[15]

AH Plus (epoxy resin-based sealer) has gained popularity due to its radiopacity, biocompatibility, ease of use, and availability. Pulp Canal Sealer (zinc oxide eugenol sealer) has antibacterial activity, but also exhibits some toxicity when placed directly on vital tissues.[16] New endodontic sealers based on bioceramic materials have been developed in an effort to create a biocompatible sealer with ideal physical, chemical, mechanical, and biological properties. Such an endodontic sealer is Well-Root ST.[17] Bioceramic sealers have stimulated strong interest because they contain calcium phosphate, silicates, and water-free thickening vehicles to enable the sealer to be applied as a premixed paste.[18] The inorganic ingredients of the sealer are mixed with thickening agents because water is needed for the setting response. The need for water can be attributed to the inherent properties of bioceramic materials or more precisely to the hydrophilic nanoparticles that allow more water molecules to come in contact with the sealer.[19] The differences between the materials change over time, and this change has clinical implications; therefore, this study investigated the need to measure microleakage over more extended periods.[20]

The purpose of this study was to compare the quality of the coronal seal of three root canal sealers and two obturation techniques using the bacterial penetration method.

Materials and Methods

Collection of teeth

A total of 132 single-rooted human teeth with fully developed apices were used. Exclusion criteria were teeth with cracks, root caries, internal/external resorption, and untreated root canals with open apices. The teeth were stored in a sterile saline solution until use. Bone, calculus, and soft tissue on the roots were removed with scalpel blades under running tap water, taking care not to damage the root surface.

Root canal preparation and filling

Patency and working length were determined by placing a #10 K-file (Maillefer, LD Caulk Co., Milford, DE, USA) in the root canal until it just penetrated the foramen, after which 1 mm was subtracted from this, and the length was recorded. Flaring was performed with Gates Glidden Drills #1 through #3.

Canals were instrumented using K-files via the step-back technique with 2% sodium hypochlorite (Parcan, Septodont, France) and 17% EDTA (Chelaton III, Lach, Czech Republic) used as irrigants. All root canals were enlarged to the size of a #40 K-file (master apical file) (Dentsply Maillefer, Tulsa, OK, USA) at the apical foramen. The samples were stored in normal saline until obturation. Absorbent paper points were used to dry the canals (Dentsply Maillefer). After root canal preparation, the teeth were randomly assigned to three experimental groups according to the endodontic sealer used. Group 1: Samples (n=44) were obturated using a zinc oxide eugenol-based sealer, Pulp Canal Sealer EWT (PCS) (Kerr Corporation, Romulus, MI, USA). Group 2: Samples (n=44) were obturated using an epoxy resin-based sealer, AH Plus (Dentsply DeTrey GmbH, Konstanz, Germany). Group 3: Samples (n=44) were obturated using a bioceramic-based root canal sealer, Well-Root ST (Vericom, Gangwon-do, Korea).

Each group was subdivided into 2 equal subgroups in accordance with the obturation technique being used: CLCT and ThOT. Thus, 6 subgroups were formed: Sub-1A: Pulp Canal Sealer/CLCT; Sub-2A: AH Plus/CLCT; Sub-3A: Well-ROOT ST/CLCT; Sub-1B: Pulp Canal Sealer/ThOT; Sub-2B: AH Plus/ThOT; Sub-3B: Well-ROOT ST/ThOT.

Cold lateral condensation technique (CLCT)

The sealer was placed in the canal using a lentulo spiral (25 mm size 3 green, Dentsply-Maillefer), followed by inserting the gutta-percha master cone (Dentsply-Maillefer) to the predetermined working length. Nickel-titanium finger spreaders (Dentsply-Maillefer) were used to conduct the lateral compaction using accessory cones (Dentsply-Maillefer). Obturations were considered complete when the spacer could not enter the root canal area (10 mm).

Thermafil obturation technique (ThOT)

The samples of the Thermafil subgroups were obturated as specified by the manufacturer. We selected a Thermafil obturator the same size as the verifier. Sterile paper points were used to coat the walls of the canal to the working length with the allocated sealer of the subgroup. The Thermafil obturator was heated in the Therma Prep oven and inserted in the canal to the established working length. The shaft was severed level

with the orifice using a round bur in a high-speed handpiece. The total time from checking the obturator until shaft removal was measured.

Bacterial leakage device

A scintillation vial was modified to create a dual-chamber device based on a similar two-chamber method. A round bur with a diameter of 9mm was used to bore a hole through the center of the screw cap, in which the tooth was suspended and secured with wax covered by two layers of nail varnish. The lower chamber of the device was filled with sterile tryptic soy broth (TSB). Using a sterile micropipette, 0.1ml of an overnight broth culture of E. faecalis ATCC-51299 (Liofilchem, Roseto degli Abruzzi, Italy) was inoculated into the root canal of each tooth via the coronal access cavity preparation. To prevent evaporation and contamination, the opening of the pipette tip was veiled with a sterile plastic cap. All laboratory procedures were carried out under aseptic conditions. Fresh medium and *E. faecalis* were added to the upper chamber every 4 days. The broth was monitored for color change daily for 33 days. An LS-722N-2000 Spectrophotometer (Qingdao Pharmacypro Co., Ltd. Shanghai, China) was used to measure the turbidity of the samples at an absorption rate of 590 µm. The measurements were all performed in the same room.

Statistical Analysis

Statistical analysis was performed using statistical software package SPSS version 20.0 (SPSS Inc, Armonk, NY: IBM Corp). The mean, standard deviation, standard error of the mean, median, interquartile range, and confidence interval (CI) were calculated. The means and medians for the turbidity presentation time according to obturation techniques and materials used for canal obturation were analyzed using Kaplan-Meier survival curves. Data were analyzed with One-way ANOVA & Tukey's (HSD) post-hoc test. Group comparisons with respect to categorical variables are performed using chi-square tests. A probability value of $P<0.05$ was considered statistically significant.

Results

On average, tooth turbidity was observed after 25.8 days. There was no significant difference in the average occurrence of turbidity between CLCT and ThOT ($P=0.718$) (Table 1 and Figure 1).

For both canal obturation techniques, the fastest turbidity presentation time was reported in Group 1 (Sub-1A=19.3 days and Sub-1B=18.2 days), and the slowest turbidity presentation time occurred in Group 3 (Sub-3A=30.2 days and Sub-3B=31.5 days). Significant differences were found among Sub-2A vs. Sub-1B ($P=0.023$), Sub-1A vs. Sub-3A ($P=0.014$), Sub-1A vs. Sub-2B ($P=0.024$), Sub-1A vs. Sub-3B ($P=0.002$), Sub-3A vs. Sub-1B ($P=0.003$), Sub-2B vs. Sub-1B ($P=0.005$), and Sub-1B vs. Sub-3B ($P<0.0001$) (Table 2 and Figure 2). CFU levels >300 were recorded in 31.8% of teeth for both canal obturation techniques (Table 3).

Among subgroups, the highest percentage of CFU>300 was registered for Sub-1B and Sub-1A (68.2% and 50%, respectively). The lowest percentage of CFU>300 was found in Sub-3B and Sub-3A (9.1% and 18.2%, respectively). CFU>300 was also found in 18.2% of Sub-2B samples (Table 4). No significant differences were found for the mean turbidity values using spectrophotometry for samples using the obturation techniques ($P=0.58$). The highest mean turbidity value was recorded in the CLCT group (CLCT=0.57 vs. ThOT=0.54) (Table 5 and Figure 3).

There were significant differences in the mean turbidity values according to the Subgroups ($P=0.008$). The highest mean turbidity values were recorded for Sub-1A and Sub-1B (0.64 and 0.58, respectively). The lowest mean turbidity values were recorded for Sub-2B and Sub-2A (0.42 and 0.44, respectively) (Table 5).

Table 1.

Mean and median for turbidity presentation time for Cold Lateral Condensation Technique vs. Thermafil obturation technique.

Means and Medians for Survival Time

Groups	Mean[a]				Median			
	Estimate	Std. Error	95% CI		Estimate	Std. Error	95% CI	
			Lower Bound	Upper Bound			Lower Bound	Upper Bound
CLCT	25.530	1.451	22.686	28.375	.	.	.	.
ThOT	26.061	1.422	23.274	28.847	.	.	.	.
Overall	25.795	1.016	23.804	27.787	.	.	.	.

a. Estimation is limited to the largest survival time if it is censored.
Log Rank (Mantel-Cox): Chi-Square=0.131, df=1, P=0.718

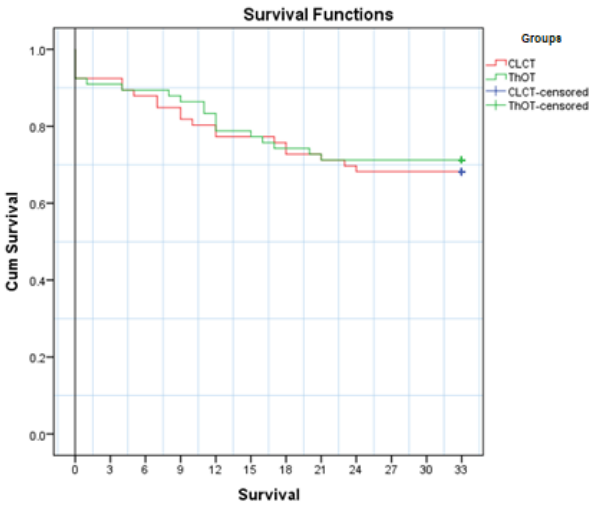

Fig. 1. *Kaplan-Meier survival curves: Turbidity presentation time for CLCT vs. ThOT.*

Table 2.

Mean and median for turbidity presentation time according to the obturation technique and paste subgroups.

Means and Medians for Survival Time								
Subgroups	Mean[a]				Median			
	Estimate	Std. Error	95% CI		Estimate	Std. Error	95% CI	
			Lower Bound	Upper Bound			Lower Bound	Upper Bound
2A	27.091	2.227	22.727	31.455	.	.	.	.
1A	19.318	3.030	13.379	25.258	18.000	.	.	.
3A	30.182	1.402	27.434	32.930	.	.	.	.
2B	28.545	2.142	24.346	32.745	.	.	.	.
1B	18.182	2.827	12.641	23.722	12.000	4.221	3.726	20.274
3B	31.455	1.090	29.317	33.592	.	.	.	.
Overall	25.795	1.016	23.804	27.787	.	.	.	.

a. Estimation is limited to the largest survival time if it is censored. Log Rank (Mantel-Cox): Chi-Square=24.754, df=5, P<0.0001

Pairwise Comparis: Log Rank Test (Mantel-Cox).

Subgroups	A / Group 2		A / Group 1		A / Group 3		B / Group 2		B / Group 1		B / Group 3	
	Chi-Square	Sig.	Chi-Square	Sig.	Chi-Square	Sig.	Chi-Square	Sig.	Chi-Square	Sig.	Chi-Square	Sig.
2A			3.001	0.083	0.643	0.423	0.453	0.501	5.153	0.023	2.425	0.119
1A	3.001	0.083			6.038	0.014	5.079	0.024	0.113	0.737	9.725	0.002
3A	0.643	0.423	6.038	0.014			0.011	0.915	9.106	0.003	0.740	0.390
2B	0.453	0.501	5.079	0.024	0.011	0.915			7.937	0.005	0.825	0.364
1B	5.153	0.023	0.113	0.737	9.106	0.003	7.937	0.005			13.01	0.000
3B	2.425	0.119	9.725	0.002	0.740	0.390	0.825	0.364	13.006	0.000		

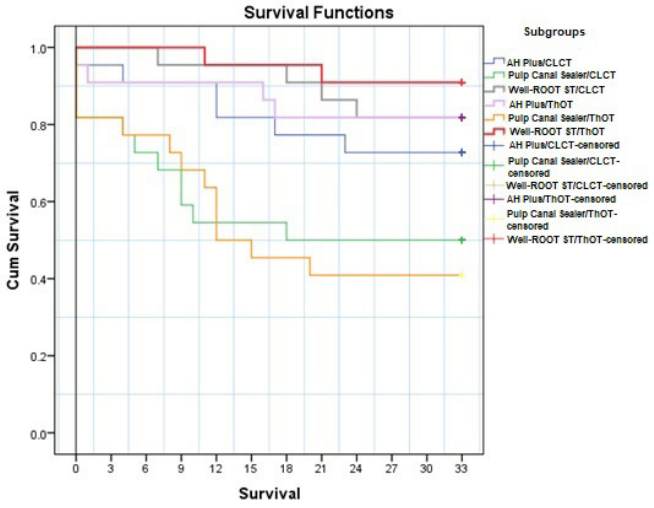

Fig. 2. *Kaplan-Meier survival curves: turbidity presentation time according to the obturation technique and paste subgroups.*

Table 3.

CFU in the teeth analyzed according to the canal obturation technique.

Groups	CFU	Frequency	Percent	Cumulative Percent
CLCT	Negative	45	68.2	68.2
	>300	21	31.8	100.0
	Total	66	100.0	
ThOT	Negative	45	68.2	68.2
	>300	21	31.8	100.0
	Total	66	100.0	

Table 4.

CFU according to the obturation technique and pastes used.

Subgroups*	CFU	Frequency	Percent	Cumulative Percent
AH Plus/CLCT	Negative	16	72.7	72.7
	>300	6	27.3	100.0
	Total	22	100.0	
Pulp Canal Sealer/ CLCT	Negative	11	50.0	50.0
	>300	11	50.0	100.0
	Total	22	100.0	
Well-Root ST/ CLCT	Negative	18	81.8	81.8
	>300	4	18.2	100.0
	Total	22	100.0	
AH Plus/ThOT	Negative	18	81.8	81.8
	>300	4	18.2	100.0
	Total	22	100.0	
Pulp Canal Sealer/ ThOT	Negative	7	31.8	31.8
	>300	15	68.2	100.0
	Total	22	100.0	
Well-Root ST/ ThOT	Negative	20	90.9	90.9
	>300	2	9.1	100.0
	Total	22	100.0	

** Pearson Chi-Square = 25.981[a], df=5, P<0.0001.*

a. 0 cells (0.0%) have expected count less than 5. The minimum expected count is 7.00.

Table 5.

The mean value of turbidity using spectrophotometry according to the obturation techniques and subgroups.

Groups/ Subgroups	N	Minimum	Maximum	Mean	Std. Dev.	ANOVA	*P*-value
CLCT	21	0.28	0.70	0.57	0.124	F=0.311	0.58
ThOT	19	0.27	0.89	0.54	0.141		

Table 5 (continued).

The mean value of turbidity using spectrophotometry according to the obturation techniques and subgroups.

Groups/ Subgroups	N	Minimum	Maximum	Mean	Std. Dev.	ANOVA	*P*-value
AH Plus/ CLCT	6	0.28	0.55	0.44	0.113	F=3.763	0.008
Pulp Canal Sealer/CLCT	11	0.44	0.70	0.64	0.088		
Well-Root ST/ CLCT	4	0.48	0.59	0.56	0.054		
AH Plus/ ThOT	4	0.27	0.58	0.42	0.131		
Pulp Canal Sealer/ ThOT	13	0.38	0.89	0.58	0.138		
Well-Root ST/ ThOT	2	0.55	0.58	0.56	0.018		

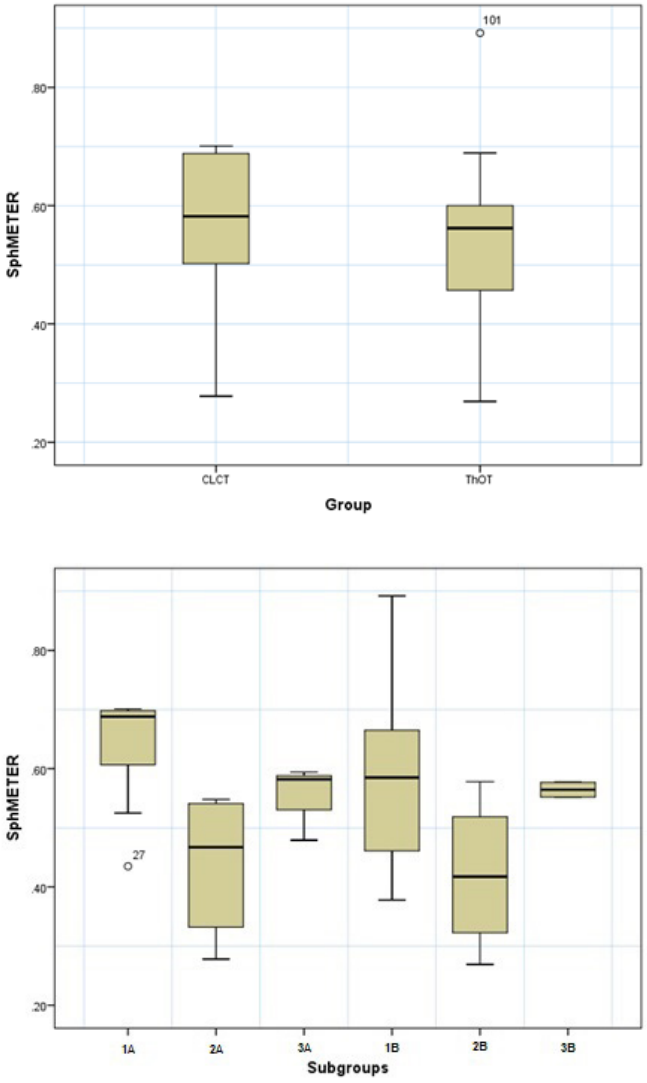

Fig. 3. *The mean value of turbidity using spectrophotometry according to the obturation techniques and subgroups.*

Multiple Comparisons						
Dependent Variable: SphMETER Tukey HSD						
(I) Subgroup	(J) Subgroup	Mean Difference (I-J)	Std. Error	Sig.	95%CI	
					Lower Bound	Upper Bound
PCS/CLCT	PCS/ThOT	0.19998*	0.05703	0.015	0.0279	0.3721
	WRST/CLCT	0.21832*	0.06560	0.024	0.0203	0.4163
* - *The mean difference is significant at the 0.05 level.*						

Discussion

Achieving an acceptable coronal seal is one of the key intentions in endodontic treatment. Many materials and obturation techniques are available. Each has its own advantages and disadvantages; therefore, the search for the ideal sealer and obturation technique continues. The present study used two obturation techniques to compare and evaluate coronal leakage in three root canal sealers.

We found no significant differences between the techniques of ThOT and CLCT. Our results, consistent with the findings of other researchers, indicated no significant differences in coronal sealing ability between ThOT and CLCT.[21,22] Gade et al.[23] found no significant differences in the quality of obturation between CLCT and ThOT. The turbidity of the samples appeared later in ThOT than in CLCT, which was in accordance with other studies in which the researchers concluded that ThOT provided better sealing than CLCT.[24,25] De Moor and Hommez[26] demonstrated that ThOT had significantly greater coronal leakage than three other condensation techniques. The important aspect of Thermafil is the margin of error permitted by the manufacturer in the production of plastic carriers. There is no evidence in the literature for the discrepancy percentage between different carriers.[27]

According to our results, Well-Root ST and AH Plus had similar leakage after 33 days, but Well-Root ST had the better sealing ability. Four of the Well-Root ST samples in the subgroup obturated with CLCT exhibited bacterial leakage, compared with only 2 samples in the subgroup obturated with ThOT. In the AH Plus/CLCT subgroup, 6 samples exhibited leakage, compared with 4 samples in the AH Plus/ThOT subgroup. In contrast, the Pulp Canal Sealer/CLCT subgroup included 11 samples with high leakage, and the Pulp Canal Sealer/ThOT subgroup included 13 samples with bacterial leakage. Our results indicated that Well-Root ST had less microleakage than other tested sealers, such as AH 26,[28] while zinc oxide eugenol had the highest microleakage, which agreed with previous findings.[29,30] One possible reason for the better sealing ability of Well-Root ST is its biocompatibility and antimicrobial effect.[31]

Turbidity in the lower chamber is an indicator of contamination by microorganisms. In the present study, the highest mean turbidity value was recorded in the CLCT group, but the differences were not significant. The highest turbidity value was recorded in the group with Pulp Canal Sealer, whereas the lowest turbidity value was in the group with AH

Plus. Because of its poor sealing and adhesion properties to dentin, Pulp Canal Sealer exhibited the highest amount of bacterial penetration compared with all groups, which is consistent with other studies.[32-34] Pommel and Camps [35] compared the lateral condensation technique and the ThOT with Pulp Canal Sealer and reported that Thermafil obturation had less leakage than lateral condensation. Our study showed no significant differences between the CLCT and ThOT subgroups in the Pulp Canal Sealer group.

This study found that regardless of the obturation technique, turbidity appeared most quickly in the groups obturated with Pulp Canal Sealer and AH Plus (18.75 and 27.82 days, respectively), compared with 30.82 days in the Well-Root ST group. This may be because the antibacterial effect of Pulp Canal Sealer and AH Plus is lower than that of Well-Root ST.[36,37] Apart from the antibacterial activity of the sealers, the physical properties, such as adhesion, adaptability, and solubility, are also important.

Obturation is the final step in root canal treatment. It can be achieved with different types of root canal sealers in combination with the core root canal filling material, such as gutta-percha cones, using different condensation techniques. In the present study, the samples were contaminated with *E. faecalis* and monitored for 33 days, which was long enough to detect early-stage leakage, although other studies monitored teeth daily from 30 to 90 days.[38,39] *E. faecalis* was used because it invades the dentin tubules and can survive in the root canal system after root canal treatment. Histological sections or high-resolution micro-CT imaging[40] should be used together with other testing methods to verify the mode of contamination for bacterial leakage.

There were some limitations in this study. The coronal restorations were missing, which increased the amount of leakage, even though the current clinical philosophy recommends that the tooth should be immediately restored to protect the root canal filling from coronal leakage. However, there are sometimes cases when the patient does not have time to finish the treatment session, or the dentist may need to postpone the placement of a coronal restoration until a subsequent appointment. In such instances, temporary filling cements are used, which may fall out of the cavity before the coronal restoration appointment, exposing the obturated root canal to saliva and oral bacteria.

Conclusion

Within the limitations of this study, our findings indicate no statistically significant difference between the CLCT and the ThOT. Regardless of the obturation technique, all root canal sealers exhibited leakage; however, the bioceramic-based root canal sealer appeared to perform better than the epoxy resin-based sealer and the zinc oxide eugenol-based sealer.

Acknowledgments

We thank Helen Jeays, BDSc AE, from Edanz (www.edanz.com/ac) for editing a draft of this manuscript.

Competing Interests

The authors declare that they have no competing interests.

References

1. Marín-Bauza GA, Silva-Sousa YT, da Cunha SA, Rached-Junior FJ, Bonetti-Filho I, Sousa-Neto MD, Miranda CE. Physicochemical properties of endodontic sealers of different bases. J Appl Oral Sci. 2012 Jul-Aug;20(4):455-61. doi: 10.1590/s1678-77572012000400011.
2. Abdulkader A, Duguid R, Saunders EM. The antimicrobial activity of endodontic sealers to anaerobic bacteria. Int Endod J. 1996 Jul;29(4):280-3. doi: 10.1111/j.1365-2591.1996.tb01382.x.
3. Tselnik M, Baumgartner JC, Marshall JG. Bacterial leakage with mineral trioxide aggregate or a resin-modified glass ionomer used as a coronal barrier. J Endod. 2004 Nov;30(11):782-4. doi: 10.1097/00004770-200411000-00008.
4. Eldeniz AU, Ørstavik D. A laboratory assessment of coronal bacterial leakage in root canals filled with new and conventional sealers. Int Endod J. 2009 Apr;42(4):303-12. doi: 10.1111/j.1365-2591.2008.01509.x.
5. Siqueira JF Jr, Rôças IN, Ricucci D, Hülsmann M. Causes and management of post-treatment apical periodontitis. Br Dent J. 2014 Mar;216(6):305-12. doi: 10.1038/sj.bdj.2014.200.
6. Timpawat S, Amornchat C, Trisuwan WR. Bacterial coronal leakage after obturation with three root canal sealers. J Endod. 2001 Jan;27(1):36-9. doi: 10.1097/00004770-200101000-00011.
7. Pathomvanich S, Edmunds DH. The sealing ability of Thermafil obturators assessed by four different microleakage techniques. Int Endod J. 1996 Sep;29(5):327-34. doi: 10.1111/j.1365-2591.1996.tb01393.x.
8. Vitti RP, Prati C, Silva EJ, Sinhoreti MA, Zanchi CH, de Souza e Silva MG, Ogliari FA, Piva E, Gandolfi MG. Physical properties of MTA Fillapex sealer. J Endod. 2013 Jul;39(7):915-8. doi: 10.1016/j.joen.2013.04.015.
9. da Silva Neto UX, de Moraes IG, Westphalen VP, Menezes R, Carneiro E, Fariniuk LF. Leakage of 4 resin-based root-canal sealers used with a single-cone technique. Oral Surg Oral Med Oral Pathol Oral Radiol Endod. 2007 Aug;104(2):e53-7. doi: 10.1016/j.tripleo.2007.02.007.
10. Williams JM, Trope M, Caplan DJ, Shugars DC. Detection and quantitation of E. faecalis by real-time PCR (qPCR), reverse transcription-PCR (RT-PCR), and cultivation during endodontic treatment. J Endod. 2006 Aug;32(8):715-21. doi: 10.1016/j.joen.2006.02.031.
11. Sedgley C, Nagel A, Dahlén G, Reit C, Molander A. Real-time quantitative polymerase chain reaction and culture analyses of Enterococcus faecalis in root canals. J Endod. 2006 Mar;32(3):173-7. doi: 10.1016/j.joen.2005.10.037.
12. Brunton PA, Burke FJ, Sharif MO, Creanor S, Hosey MT, Mannocci F, Wilson NH. Contemporary dental practice in the UK in 2008: aspects of direct restorations, endodontics and

***Corresponding author**: Linda J. Dula. Department of Prosthodontics, Dental School, Faculty of Medicine, University of Prishtina, Republic of Kosovo. E-mail: linda.dula@uni-pr.edu*

bleaching. Br Dent J. 2012 Jan 27;212(2):63-7. doi: 10.1038/sj.bdj.2012.46.
13. Pallarés A, Faus V. A comparative study of the sealing ability of two root canal obturation techniques. J Endod. 1995 Sep;21(9):449-50. doi: 10.1016/S0099-2399(06)81526-8.
14. Siqueira JF Jr, Rôças IN. Polymerase chain reaction-based analysis of microorganisms associated with failed endodontic treatment. Oral Surg Oral Med Oral Pathol Oral Radiol Endod. 2004 Jan;97(1):85-94. doi: 10.1016/s1079-2104(03)00353-6.
15. Sedgley C, Buck G, Appelbe O. Prevalence of Enterococcus faecalis at multiple oral sites in endodontic patients using culture and PCR. J Endod. 2006 Feb;32(2):104-9. doi: 10.1016/j.joen.2005.10.022.
16. Ma J, Wang Z, Shen Y, Haapasalo M. A new noninvasive model to study the effectiveness of dentin disinfection by using confocal laser scanning microscopy. J Endod. 2011 Oct;37(10):1380-5. doi: 10.1016/j.joen.2011.06.018.
17. Massi S, Tanomaru-Filho M, Silva GF, Duarte MA, Grizzo LT, Buzalaf MA, Guerreiro-Tanomaru JM. pH, calcium ion release, and setting time of an experimental mineral trioxide aggregate-based root canal sealer. J Endod. 2011 Jun;37(6):844-6. doi: 10.1016/j.joen.2011.02.033.
18. Tanomaru JM, Tanomaru-Filho M, Hotta J, Watanabe E, Ito IY. Antimicrobial activity of endodontic sealers based on calcium hydroxide and MTA. Acta Odontol Latinoam. 2008;21(2):147-51.
19. Santos AD, Moraes JC, Araújo EB, Yukimitu K, Valério Filho WV. Physico-chemical properties of MTA and a novel experimental cement. Int Endod J. 2005 Jul;38(7):443-7. doi: 10.1111/j.1365-2591.2005.00963.x.
20. Miletić I, Ribarić SP, Karlović Z, Jukić S, Bosnjak A, Anić I. Apical leakage of five root canal sealers after one year of storage. J Endod. 2002 Jun;28(6):431-2. doi: 10.1097/00004770-200206000-00003.
21. Inan U, Aydin C, Tunca YM, Basak F. In vitro evaluation of matched-taper single-cone obturation with a fluid filtration method. J Can Dent Assoc. 2009 Mar;75(2):123.
22. Yücel AC, Ciftçi A. Effects of different root canal obturation techniques on bacterial penetration. Oral Surg Oral Med Oral Pathol Oral Radiol Endod. 2006 Oct;102(4):e88-92. doi: 10.1016/j.tripleo.2006.02.007.
23. Gade VJ, Belsare LD, Patil S, Bhede R, Gade JR. Evaluation of push-out bond strength of endosequence BC sealer with lateral condensation and thermoplasticized technique: An in vitro study. J Conserv Dent. 2015 Mar-Apr;18(2):124-7. doi: 10.4103/0972-0707.153075.
24. Xu Q, Ling J, Cheung GS, Hu Y. A quantitative evaluation of sealing ability of 4 obturation techniques by using a glucose leakage test. Oral Surg Oral Med Oral Pathol Oral Radiol Endod. 2007 Oct;104(4):e109-13. doi: 10.1016/j.tripleo.2007.05.014.
25. Inan U, Aydemir H, Taşdemir T. Leakage evaluation of three different root canal obturation techniques using electrochemical evaluation and dye penetration evaluation methods. Aust Endod J. 2007 Apr;33(1):18-22. doi: 10.1111/j.1747-4477.2007.00050.x.
26. De Moor RJ, Hommez GM. The long-term sealing ability of an epoxy resin root canal sealer used with five gutta percha obturation techniques. Int Endod J. 2002 Mar;35(3):275-82. doi: 10.1046/j.1365-2591.2002.00481.x.
27. Vittoria G, Pantaleo G, Blasi A, Spagnuolo G, Iandolo A, Amato M. Thermafil: A New Clinical Approach Due to New Dimensional Evaluations. Open Dent J. 2018 Feb 22;12:173-180. doi: 10.2174/1874210601812010173.
28. Ehsani M, Dehghani A, Abesi F, Khafri S, Ghadiri Dehkordi S. Evaluation of Apical Micro-leakage of Different Endodontic Sealers in the Presence and Absence of Moisture. J Dent Res Dent Clin Dent Prospects. 2014 Summer;8(3):125-9. doi: 10.5681/joddd.2014.023.
29. Palanivelu CR, Ravi V, Sivakumar AA, Sivakumar JS, Prasad AS, Arthanari KK. An *In Vitro* Comparative Evaluation of Distribution of Three Different Sealers by Single-Cone Obturation Technique. J Pharm Bioallied Sci. 2019 May;11(Suppl 2):S438-S441. doi: 10.4103/JPBS.JPBS_64_19.
30. Ballullaya SV, Vinay V, Thumu J, Devalla S, Bollu IP, Balla S. Stereomicroscopic Dye Leakage Measurement of Six Different Root Canal Sealers. J Clin Diagn Res. 2017 Jun;11(6):ZC65-ZC68. doi: 10.7860/JCDR/2017/25780.10077.
31. Chotvorrarak K, Yanpiset K, Banomyong D, Srisatjaluk R. In vitro antibacterial activity of oligomer-based and calcium silicate-based root canal sealers. Mahidol Dent J. 2017;37(2):145-154.
32. Dultra F, Barroso JM, Carrasco LD, Capelli A, Guerisoli DM, Pécora JD. Evaluation of apical microleakage of teeth sealed with four different root canal sealers. J Appl Oral Sci. 2006 Oct;14(5):341-5.
33. Kocak MM, Er O, Saglam BC, Yaman S. Apical leakage of epiphany root canal sealer combined with different master cones. Eur J Dent. 2008 Apr;2(2):91-5.
34. Tay FR, Loushine RJ, Weller RN, Kimbrough WF, Pashley DH, Mak YF, Lai CN, Raina R, Williams MC. Ultrastructural evaluation of the apical seal in roots filled with a polycaprolactone-based root canal filling material. J Endod. 2005 Jul;31(7):514-9.
35. Pommel L, Camps J. In vitro apical leakage of system B compared with other filling techniques. J Endod. 2001 Jul;27(7):449-51.
36. Kelmendi T, Koçani F, Kurti A, Kamberi B, Kamberi A. Comparison of Sealing Abilities Among Zinc Oxide Eugenol Root-Canal Filling Cement, Antibacterial Bioceramic Paste, and Epoxy Resin, using Enterococcus faecalis as a Microbial Tracer. Med Sci Monit Basic Res. 2022 Jun 1;28:e936319.
37. Melo TV de, Prado MC, Hirata Junior R, Fidel SR, Silva EJNL da, Sassone LM. Improved sealing ability promoted by calcium silicate-based root canal sealers. Braz. J. Oral Sci. [Internet]. 2018 Jun. 5 [cited 2022 Oct. 22];17:e18148.
38. Prado M, Simão RA, Gomes BP. A microleakage study of gutta-percha/AH Plus and Resilon/Real self-etch systems after different irrigation protocols. J Appl Oral Sci. 2014 Jun;22(3):174-9.
39. Ashraf H, Faramarzi F, Paymanpour P. Sealing Ability of Resilon and MTA as Root-end Filling Materials: A Bacterial and Dye Leakage Study. Iran Endod J. 2013 Fall;8(4):177-81.
40. Consolaro A, Bramante CM, de Moraes IG, Ordinola-Zapata R, Garcia RB. Bacterial leakage in obturated root canals-part 2: a comparative histologic and microbiologic analyses. Oral Surg Oral Med Oral Pathol Oral Radiol Endod. 2010 May;109(5):788-94.

International Journal of Biomedicine 12(4) (2022) 591-595
http://dx.doi.org/10.21103/Article12(4)_OA12

ORIGINAL ARTICLE

Dentistry

INTERNATIONAL JOURNAL OF BIOMEDICINE

Shear Bond Strength of Two Self-Etching Adhesives to Air-Abraded Dentin: An in Vitro Study

Timur V. Melkumyan[1,2], Shahnoza K. Musashaykhova[1], Zurab S. Khabadze[2], Maria K. Makeeva[2,3], Marina U. Dashtieva[2], Diloro J. Kakhkharova[1], Angela D. Dadamova[1]

[1]*Tashkent State Dental Institute, Tashkent, Uzbekistan*
[2]*Peoples' Friendship University of Russia (RUDN University), Moscow, Russia*
[3]*Sechenov University, Moscow, Russia*

Abstract

Background: The aim of this research was to study the effect of air-abrasive treatment of dentin on the chemical composition of its surface and the adhesion strength of 2 self-etching adhesive systems (AS).

Methods and Results: Powders based on aluminum oxide (Al_2O_3) (27µm) (KaVo, Biberach, Germany), sodium bicarbonate (NaHCO3) (40µm) (AIR-FlOW Classic Comfort, EMS, Nyon, Switzerland), and erythritol (14µm) (AIR-FLOW Plus, EMS, Nyon, Switzerland) were used for the air-abrasive treatment of adhesive surfaces. Bonding steps were carried out with Single Bond Universal (SBU) (3M ESPE, USA) and Bond Force 2 (BF2) (Toquyama, Japan). The adhesion strength of composite to dentin was evaluated on 80 samples prepared in accordance with the Ultradent Shear Bond Strength test. All samples were divided into 4 groups depending on the method of dentin surface processing. In the samples of Group 1 (n=20), aluminum oxide was used for the air-abrasive treatment of dentin. In Group 2 (n=20) and Group 3 (n=20), samples were treated using powders based on sodium bicarbonate and erythritol, respectively. Group 4 (control, n=20) included tooth samples in which the dentin surface was not air-abraded after preparation with carbide burs. Then, each group was divided into 2 subgroups (Sub-A and Sub-B) depending on the type of adhesive system used. Adhesive resin was applied and polymerized in accordance with the manufacturer's instructions. Single Bond Universal (SBU) was used for the samples of Sub-A, and Bond Force 2 (BF2) (Toquyama, Japan) was used for the samples of Sub-B. Scanning electron microscopy and determining the surface elemental composition of samples were carried out on an SEM-EVO MA 10 (Carl Zeiss) and energy dispersive X-ray spectrometer with EDS Aztec Energy Advanced X-Act (Oxford Instruments). It was concluded that air-abrasive treatment of the dentin surface does not enhance the adhesion strength of composite material when using self-etch AS. Also, it was noted that the pH level of self-etch AS is not a crucial feature in determining the strength of the filling-tooth interface. The resulting variations in the elemental composition of dentin surface after air-abrasion with various mixtures and their effect on the efficacy of the different AS require further in vitro studies.(**International Journal of Biomedicine. 2022;12(4):591-595.**).

Keywords: air-abrasion • adhesive systems • dentin surface

For citation: Melkumyan TV, Musashaykhova ShK, Khabadze ZS, Makeeva MK, Dashtieva MU, Kakhkharova DJ, Dadamova AD. Shear Bond Strength of Two Self-Etching Adhesives to Air-Abraded Dentin: An in Vitro Study. International Journal of Biomedicine. 2022;12(4):591-595. doi:10.21103/Article12(4)_OA12.

Abbreviations

AA, air-abrasion; **AS,** adhesive systems; **SBU**, Single Bond Universal; **BF2**, Bond Force 2.

Introduction

Modern trends in minimally invasive cavity preparation, combined with the advent of self-etching adhesive systems (AS), have conceptually changed the philosophy of dental caries operative treatment.[1-5] Alternative methods of tooth preparation allow performing dental care, considering the microscopic surface features of enamel and dentin.[6-11]

Removing biofilm and the smear layer without a clinically significant impact on hard tooth tissues became possible due to the introduction into the practice of low abrasive powders based on glycine, erythritol, trehalose, etc.[12-14] At the same

time, the variety of clinical situations and increasing complexity of comprehensive tooth care unfortunately do not allow the complete abandonment of coarse-grained air-abrasive mixtures based on aluminum oxide, sodium bicarbonate, calcium carbonate, and many other substances.[15-17] Recent attempts have also been made to combine the removal of stains and tissue debris of the smear layer with a guided biofilm therapy and the formation of a bioactive layer on the surface of the tooth to promote accelerated remineralization of dentin and enamel weakened by the carious pathology.[18,19]

Therefore, the current techniques of tooth surface preparation with consideration of the features of adhesive and restorative materials can contribute to reliable and long-term restorations.

The modern concept of simultaneous etching and hybridization of hard tooth tissues is another step toward minimally invasive dentistry, and it was embodied in AS of the sixth and seventh generations.[20,21] It is important to emphasize that one of the bad features of total-etch AS is considered to be incomplete infiltration by monomers of microgaps created after etching with phosphoric acid in the surface layers of enamel and dentin.[22,23] Moreover, moisture in the demineralized extracellular matrix of dentin causes gel polymerization of Etch&Rinse adhesive monomers resulting in the formation of hydrolytically unstable polymers in a hybrid layer.[24,25

The above and many other shortcomings related to total-etch AS were considered when a new group of self-etching adhesives based on acidic monomers was introduced. The positive aspects of these adhesives are the absence of mandatory acid etching of dentin and the formation of a chemical bond between the hydroxyapatite of hard tooth tissues and adhesive resin monomers.[26,27] Also, the chemistry and mode of application of one-step bonding materials imply the incorporation of a smear layer into the structure of the adhesive layer.[28]

In this regard, it can be assumed that the composition and amount of the smear layer may affect the bond strength of the composite to tooth dentin when using self-etching adhesives.[29]

It is known that air-abrasion of prepared dentin can open a significant number of orifices of dentinal tubules and facilitate the formation of a thinner smear layer.[30] However, considering the experience of previous studies, this method may cause changes in the chemical composition of dentin surfaces and affect the strength of composite adhesion.[31,32

The aim of this research was to study the effect of air-abrasive treatment of dentin on the chemical composition of its surface and the adhesion strength of 2 self-etching adhesive systems (AS).

Materials and Methods

Powders based on aluminum oxide (Al_2O_3) (27μm) (KaVo, Biberach, Germany), sodium bicarbonate (NaHCO3) (40μm) (AIR-FlOW Classic Comfort, EMS, Nyon, Switzerland), and erythritol (14μm) (AIR-FLOW Plus, EMS, Nyon, Switzerland) were used for the air-abrasive treatment of adhesive surfaces. Bonding steps were carried out with Single Bond Universal (SBU) (3M ESPE, USA) and Bond Force 2 (BF2) (Toquyama, Japan). The adhesion strength of composite to dentin was evaluated on 80 samples prepared in accordance with the Ultradent Shear Bond Strength test.

To obtain a uniform smear layer, the exposed tooth surfaces on all samples were processed with carbide burs under constant water cooling and then washed with water spray for 30 seconds using an air-water syringe of a dental unit.

All samples were divided into 4 groups depending on the method of dentin surface processing. In the samples of Group 1 (n=20), aluminum oxide was used for the air-abrasive treatment of dentin. In Group 2 (n=20) and Group 3 (n=20), samples were treated using powders based on sodium bicarbonate and erythritol, respectively. Group 4 (control, n=20) included tooth samples in which the dentin surface was not air-abraded after preparation with carbide burs. In each case of air-abrasion, the nozzle of the handpiece was angulated at 45° to the dentin surface. The treatment was carried out with a constant flow of particles under 0.25MPa pressure for 30 seconds, slowly moving a nozzle with sweeping motions above the surface of tooth samples at a distance of 5mm, after which they were thoroughly washed with an air-water spray for 30 seconds.

Then, each group was divided into 2 subgroups (Sub-A and Sub-B) depending on the type of adhesive system used. Adhesive resin was applied and polymerized in accordance with the manufacturer's instructions. SBU was used for the samples of Sub-A, and BF2 (Toquyama, Japan) was used for the samples of Sub-B. The light-curing composite Herculite XRV (Kerr, Italy) served as a material of choice. The polymerization was carried out using a VALO lamp (Ultradent Products Inc., USA) in a standard mode. The one-day adhesive strength of bonded interfaces without aging simulation was evaluated on an UltraTester device (Ultradent Products Inc., USA). The speed of movement of the test clamp was set to 1mm/min. The top value of bonding failure was fixed in pounds.

Scanning electron microscopy and determining the surface elemental composition of samples were carried out on an SEM-EVO MA 10 (Carl Zeiss) and energy dispersive X-ray spectrometer with EDS Aztec Energy Advanced X-Act (Oxford Instruments). There were 12 additional tooth samples, which were divided into 3 groups. Each sample had 2 different areas on the dentin surface, which were subjected to air-abrasion and carbide bur (machined) processing. For air-abrasion, in the A/M group (n=4), B/M group (n=4), and E/M group (n=4), alumina particles, bicarbonate, and erythritol mixtures, respectively, were applied.

Statistical analysis was performed using StatSoft Statistica v6.0. For descriptive analysis, results are presented as mean±standard deviation (SD). Multiple comparisons were made with one-way ANOVA and post-hoc Tukey HSD test. The Mann-Whitney U Test was used to compare the differences between the two independent groups. A probability value of $P<0.05$ was considered statistically significant.

Results

It was revealed that the adhesive strength of composite material to tooth dentin depends on the type of powder used

for air-abrasion and the kind of adhesive system applied (Table 1). When compared with the control (Sub-4A), air-abrasion of the dentin surface with powders based on alumina (Sub-1A), sodium bicarbonate (Sub-2A), and erythritol (Sub-3A) did not adversely affect the strength of adhesion when SBU was used.

In the case of BF2, there was no statistical difference between the control (Sub-4B) and Sub-1B. However, we found a statistically significant decrease in the strength of adhesion in samples of Sub-2B by 1.2 times (P=0.012) and Sub-B3 by 1.7 times (P=0.000), compared to Sub-4B.

Changes in the elemental composition of dentin surfaces after air-abrasion with different mixtures were predictable to a certain extent (Table 2). Along with the minor variations in the level of basic elements of dentin, the appearance of aluminum and silicon ions was noted after exposure to powders based on aluminum oxide, sodium bicarbonate, and erythritol.

An increase in Al+ content by 8.3 times was found after air-abrasion of dentin surfaces in samples of the A/M group (P=0.000). Also, Na+ content grew by 1.28 times in the B/M group (P<0.05). The same tendency in Si+ content by 1.5 times was noted in the B/M and E/M samples; however, these changes were not statistically significant (P>0.05).

An unexpected 1.5-times elevation of Mg+ (P<0.05) was registered on dentin surfaces after air-abrasion with erythritol-based powder. However, the level of the element in the E/M group did not significantly differ from the value obtained after dentin treatment with Al_2O_3 powder in A/M samples. The high content of C+ after dentin surface processing with a carbide bur in samples of the E/M group was assumed for the contamination of scanning areas.

Discussion

A huge amount of research has been devoted to the problem of integrating dental composite with dentin, which is directly related to a large number of factors that affect the quality of adhesion and hence the longevity of restorations.[33-36] Also, the complex ultrastructure of adhesive surfaces and technical problems associated with AS of fourth and fifth generations can negatively affect the quality of dental treatment when composite materials are applied.[37,38]

That is why the use of self-etching adhesive monomers on dentin appears to be the most promising.[39] However, considering the mode of interaction of these materials with hard tooth tissues, the method of its application, and the presence

Table 1.

Adhesion strength of composite to tooth dentin in groups (lb).

Group/ Subgroup	Group 1	Group 2	Group 3	Group 4	Statistics
Subgroup A	24.57±4.72	21.42±2.03	21.82±4.7	23.53±2.27	F=1.6220 P=0.2013
Subgroup B	15.56±1.72	13.57±2.3	9.9±2.96	16.47±2.35	F=15.0697 P=0.000 P_{1B-2B}=0.2567 P_{1B-3B}=0.0000 P_{1B-4B}=0.8265 P_{2B-3B}=0.0074 P_{2B-4B}=0.0457 P_{3B-4B}=0.0000
P-value	<0.0001	<0.0001	<0.0001	<0.0001	

Table 2.

Elemental composition of dentin surfaces after processing with different methods.

Groups		C^+	O^-	Na^+	Mg^+	Ca^+	P^+	Al^+	Si^+
A/M	Al_2O_3 abraded	16.02±0.56	41.23±1.45	0.55±0.1	0.75±0.05	28.1±0.67	13.62±0.3	0.25±0.05	0.07±0.05
	P-value	>0.05	>0.05	>0.05	>0.05	<0.05	<0.05	0.000	>0.05
	Machined	15.53±0.8	39.45±0.39	0.57±0.052	0.67±0.05	29.4±0.47	14.23±0.21	0.03±0.05	0.05±0.05
B/M	Bicarbonate abraded	15.26±1.04	39.03±0.9	0.87±0.11	0.63±0.05	29.7±0.87	14.16±0.33	0.03±0.05	0.27±0.11
	P-value	>0.05	>0.05	<0.05	>0.05	>0.05	>0.05	>0.05	>0.05
	Machined	16.25±1.15	38.3±0.66	0.68±0.1	0.57±0.12	29.87±1.22	14.12±0.57	0.02±0.04	0.18±0.1
Э/М	Erythritol abraded	16.82±0.65	40±0.49	0.62±0.07	0.82±0.04	27.78±0.31	14.08±0.71	0.02±0.04	0.18±0.07
	P-value	<0.05	<0.05	>0.05	<0.05	<0.05	<0.05	>0.05	>0.05
	Machined	20.63±0.61	38.27±0.29	0.55±0.05	0.55±0.05	26.75±0.33	13.07±0.16	0.07±0.05	0.12±0.04

of a smear layer that is amorphous and weakly adhered to the underlying dentin may cause particular concern.[40]

In the available literature, there is a sufficient amount of data indicating the effective use of air-abrasive methods concerning cleaning the tooth surface from dentin debris and enamel fragments that appear after traditional preparation with diamond and carbide burs. However, the results of studies that assume to improve the adhesion strength of a composite to abraded dentin may go either way.[18,41-43] In this regard, the main purpose of this study was to evaluate the effect of various air-abrasive mixtures on the adhesion strength of composite to dentin when self-etching AS are used. It is well known that adhesive materials of the sixth and seventh generations create mechanical and chemical bonds with dentin and enamel hydroxyapatite due to the unique properties of acidic monomers.[26,27] That is why, considering the appearance of possible changes on the surface of abraded dentin, a comparative analysis of its elemental composition was also carried out. It was previously noted that self-etching AS might have a different pH, and based on the pH, they are divided into very weak (ultra-mild, pH≥2.5), weak (mild, pH≈2), medium (intermediate, pH≈1.5), and strong (strong, pH≤1). It has also been found that the depth of demineralization of hard tooth tissues directly relates to the pH level of self-etch AS.[44] Hence to reduce the level of subjectivity, we used SBU and BF2 adhesives in the study, which are slightly different from each other in terms of acidity and have pH of 2.7 and 2.8, respectively.

Results of the study demonstrated that in the case of SBU, an air-abrasion of the dentin surface with Al_2O_3 (27μm), AIR-FLOW Classic, and AIR-FLOW Plus did not cause a clinically significant variation in values of adhesion strength of composite to dentin.

However, the same processing of the dentin surface led to a significant decrease in bond strength between resin and tooth when BF2 was applied, whereas the differences were significant after abrasion with sodium bicarbonate and erythritol-based powders.

Concerning changes in the elemental composition of the dentin surface after treatment with Al_2O_3 powder (27μm), a significant increase in Al+ and a decrease in Ca+ and P+ were noted, presumably indicating the decrease in the number of hydroxyapatite crystals in the scanning sectors. However, the revealed changes were not a reason for significant variations in the bond strength values for the SBU and BF2. The accumulation of Na+ on the dentin surface after treatment with AIR-FLOW Classic powder could be one of the possible reasons for the deterioration of composite adhesion when BF2 was used. Also, the most dramatic reduction in composite bond strength with BF2 was observed after dentine treatment with AIR-FLOW Plus despite a relative increase in the surface level of Ca+ and P+. Therefore, it was concluded that air-abrasive treatment of the dentin surface does not enhance the adhesion strength of composite material when using self-etch AS. Also, it was noted that the pH level of self-etch AS is not a crucial feature in determining the strength of the filling-tooth interface. The resulting variations in the elemental composition of dentin surface after air-abrasion with various mixtures and their effect on the efficacy of the different AS require further in vitro studies.

Competing Interests

The authors declare that they have no competing interests.

References

1. Banerjee A, Watson TF. Pickard's Manual of Operative Dentistry, 9th edition. Oxford, UK: OUP Oxford; 2011
2. Hegde VS, Khatavkar RA. A new dimension to conservative dentistry: Air abrasion. J Conserv Dent. 2010 Jan;13(1):4-8. doi: 10.4103/0972-0707.62632.
3. Van Meerbeek B, Yoshihara K, Yoshida Y, Mine A, De Munck J, Van Landuyt KL. State of the art of self-etch adhesives. Dent Mater. 2011 Jan;27(1):17-28. doi: 10.1016/j.dental.2010.10.023.
4. Foxton RM. Current perspectives on dental adhesion: (2) Concepts for operatively managing carious lesions extending into dentine using bioactive and adhesive direct restorative materials. Jpn Dent Sci Rev. 2020 Nov;56(1):208-215. doi: 10.1016/j.jdsr.2020.08.003.
5. Melkumyan TV, Kakhkharova DJ, Dadamova AD; Kamilov NKh, Siddikova SSh, Rakhmatullaeva ShI, Masouleh SM. Comparative Analysis of *in vitro* Performance of Total-Etch and Self-Etch Adhesives. International Journal of Biomedicine.2016;6(4):283-286. doi: 10.21103/Article6(4)OA7.
6. Bornstein ES. Why wavelength and delivery systems are the most important factors in using a dental hard-tissue laser: a literature review. Compend Contin Educ Dent. 2003 Nov;24(11):837-8, 841, 843 passim; quiz 848.
7. Iaria G. Clinical, morphological, and ultrastructural aspects with the use of Er:YAG and Er,Cr:YSGG lasers in restorative dentistry. Gen Dent. 2008 Nov-Dec;56(7):636-9.
8. Lin T, Aoki A, Saito N, Yumoto M, Nakajima S, Nagasaka K, et al. Dental hard tissue ablation using mid-infrared tunable nanosecond pulsed Cr:CdSe laser. Lasers Surg Med. 2016 Dec;48(10):965-977. doi: 10.1002/lsm.22508.
9. de Oliveira MT, de Freitas PM, de Paula Eduardo C, Ambrosano GM, Giannini M. Influence of Diamond Sono-Abrasion, Air-Abrasion and Er:YAG Laser Irradiation on Bonding of Different Adhesive Systems to Dentin. Eur J Dent. 2007 Jul;1(3):158-66.
10. Anja B, Walter D, Nicoletta C, Marco F, Pezelj Ribarić S, Ivana M. Influence of air abrasion and sonic technique on microtensile bond strength of one-step self-etch adhesive on human dentin. ScientificWorldJournal. 2015;2015:368745. doi: 10.1155/2015/368745.
11. Lima VP, Soares K, Caldeira VS, Faria-E-Silva AL, Loomans B, Moraes RR. Airborne-particle Abrasion and Dentin Bonding: Systematic Review and Meta-analysis. Oper Dent. 2021 Jan 1;46(1):E21-E33. doi: 10.2341/19-216-L.
12. Moëne R, Décaillet F, Andersen E, Mombelli A. Subgingival plaque removal using a new air-polishing device. J Periodontol. 2010 Jan;81(1):79-88. doi: 10.1902/jop.2009.090394.
13. Kröger JC, Haribyan M, Nergiz I, Schmage P. Air polishing with erythritol powder - In vitro effects on dentin loss. J Indian Soc Periodontol. 2020 Sep-Oct;24(5):433-440. doi: 10.4103/jisp.jisp_414_19.
14. Kruse AB, Akakpo DL, Maamar R, Woelber JP, Al-Ahmad A, Vach K, Ratka-Krueger P. Trehalose powder for subgingival air-polishing during periodontal maintenance therapy: A randomized controlled trial. J Periodontol. 2019 Mar;90(3):263-270. doi: 10.1002/JPER.17-0403.

15. Kofford KR, Wakefield CW, Murchison DF. Aluminum oxide air abrasion particles: a bacteriologic and SEM study. Quintessence Int. 2001 Mar;32(3):243-8.
16. Johnson King O, Milly H, Boyes V, Austin R, Festy F, Banerjee A. The effect of air-abrasion on the susceptibility of sound enamel to acid challenge. J Dent. 2016 Mar;46:36-41. doi: 10.1016/j.jdent.2016.01.009.
17. Barnes CM, Covey D, Watanabe H, Simetich B, Schulte JR, Chen H. An in vitro comparison of the effects of various air polishing powders on enamel and selected esthetic restorative materials. J Clin Dent. 2014;25(4):76-87.
18. Sauro S, Watson TF, Thompson I, Banerjee A. One-bottle self-etching adhesives applied to dentine air-abraded using bioactive glasses containing polyacrylic acid: an in vitro microtensile bond strength and confocal microscopy study. J Dent. 2012 Nov;40(11):896-905. doi: 10.1016/j.jdent.2012.07.004.
19. Spagnuolo G, Pires PM, Calarco A, Peluso G, Banerjee A, Rengo S, Elias Boneta AR, Sauro S. An in-vitro study investigating the effect of air-abrasion bioactive glasses on dental adhesion, cytotoxicity and odontogenic gene expression. Dent Mater. 2021 Nov;37(11):1734-1750. doi: 10.1016/j.dental.2021.09.004.
20. 20 Giannini M, Makishi P, Ayres AP, Vermelho PM, Fronza BM, Nikaido T, Tagami J. Self-etch adhesive systems: a literature review. Braz Dent J. 2015 Jan-Feb;26(1):3-10. doi: 10.1590/0103-6440201302442.
21. Ozer F, Blatz MB. Self-etch and etch-and-rinse adhesive systems in clinical dentistry. Compend Contin Educ Dent. 2013 Jan;34(1):12-4, 16, 18; quiz 20, 30. PMID: 23550327.
22. Pashley DH, Tay FR, Breschi L, Tjäderhane L, Carvalho RM, Carrilho M, Tezvergil-Mutluay A. State of the art etch-and-rinse adhesives. Dent Mater. 2011 Jan;27(1):1-16. doi: 10.1016/j.dental.2010.10.016.
23. Hashimoto M, Ito S, Tay FR, Svizero NR, Sano H, Kaga M, Pashley DH. Fluid movement across the resin-dentin interface during and after bonding. J Dent Res. 2004 Nov;83(11):843-8. doi: 10.1177/154405910408301104.
24. Paul SJ, Leach M, Rueggeberg FA, Pashley DH. Effect of water content on the physical properties of model dentine primer and bonding resins. J Dent. 1999 Mar;27(3):209-14. doi: 10.1016/s0300-5712(98)00042-6.
25. Cadenaro M, Breschi L, Rueggeberg FA, Suchko M, Grodin E, Agee K, Di Lenarda R, Tay FR, Pashley DH. Effects of residual ethanol on the rate and degree of conversion of five experimental resins. Dent Mater. 2009 May;25(5):621-8. doi: 10.1016/j.dental.2008.11.005.
26. Perdigão J, Frankenberger R, Rosa BT, Breschi L. New trends in dentin/enamel adhesion. Am J Dent. 2000 Nov;13(Spec No):25D-30D.
27. Van Meerbeek B, Yoshihara K, Yoshida Y, Mine A, De Munck J, Van Landuyt KL. State of the art of self-etch adhesives. Dent Mater. 2011 Jan;27(1):17-28. doi: 10.1016/j.dental.2010.10.023.
28. Saikaew P, Sattabanasuk V, Harnirattisai C, Chowdhury AFMA, Carvalho R, Sano H. Role of the smear layer in adhesive dentistry and the clinical applications to improve bonding performance. Jpn Dent Sci Rev. 2022 Nov;58:59-66.
29. Suyama Y, Lührs AK, De Munck J, Mine A, Poitevin A, Yamada T, Van Meerbeek B, Cardoso MV. Potential smear layer interference with bonding of self-etching adhesives to dentin. J Adhes Dent. 2013 Aug;15(4):317-24. doi: 10.3290/j.jad.a29554.
30. Melkumyan TV, Musashaykhova ShK, Daurova FYu, Kamilov NKh, Sheraliyeva SSh, Dadamova AD. Effect of Air-Abrasion on Shear Bond Strength of Resin Composite to Dentin: A Study in Vitro International Journal of Biomedicine.2021;11(4):451-455. doi:10.21103/Article11(4)_OA10.
31. Melkumyan TV, Seeberger GK, Khabadze ZS, Kamilov NKh, Makeeva MK, Dashtieva MU, et al. Air Abrasion of Titanium Dental Implants with Water-Soluble Powders: An In Vitro Study International Journal of Biomedicine. 2022;12(3):428-432. doi:10.21103/Article12(3)_OA15.
32. Bester SP, de Wet FA, Nel JC, Driessen CH. The effect of airborne particle abrasion on the dentin smear layer and dentin: an in vitro investigation. Int J Prosthodont. 1995 Jan-Feb;8(1):46-50.
33. Hellyer P. The longevity of composite restorations. Br Dent J. 2022 Apr;232(7):459. doi: 10.1038/s41415-022-4163-4.
34. Opdam NJ, van de Sande FH, Bronkhorst E, Cenci MS, Bottenberg P, Pallesen U, Gaengler P, Lindberg A, Huysmans MC, van Dijken JW. Longevity of posterior composite restorations: a systematic review and meta-analysis. J Dent Res. 2014 Oct;93(10):943-9. doi: 10.1177/0022034514544217.
35. Kubo S. Longevity of resin composite restorations. Japanese Dental Science Review. 2011;47(1):43-55. doi:10.1016/j.jdsr.2010.05.002.
36. Melkumyan TV, Makhamadaminova KD, Kamilov EKh. Clinical and Experimental Evaluation of the Effectiveness of «Soft-Start» Polymerization in Dental Composite Restoration. International Journal of Biomedicine. 2012;2(3):242-245
37. Goldberg M, Kulkarni AB, Young M, Boskey A. Dentin: structure, composition and mineralization. Front Biosci (Elite Ed). 2011 Jan 1;3(2):711-35. doi: 10.2741/e281.
38. Scotti N, Bergantin E, Giovannini R, Delbosco L, Breschi L, Migliaretti G, Pasqualini D, Berutti E. Influence of multi-step etch-and-rinse versus self-etch adhesive systems on the post-operative sensitivity in medium-depth carious lesions: An in vivo study. Am J Dent. 2015 Aug;28(4):214-8.
39. Gupta A, Tavane P, Gupta PK, Tejolatha B, Lakhani AA, Tiwari R, Kashyap S, Garg G. Evaluation of Microleakage with Total Etch, Self-Etch and Universal Adhesive Systems in Class V Restorations: An In vitro Study. J Clin Diagn Res. 2017 Apr;11(4):ZC53-ZC56.
40. Pashley DH. Smear layer: overview of structure and function. Proc Finn Dent Soc. 1992;88 Suppl 1:215-24.
41. Banerjee A, Watson TF. Air abrasion: its uses and abuses. Dent Update. 2002 Sep;29(7):340-6. doi: 10.12968/denu.2002.29.7.340.
42. Mujdeci A, Gokay O. The effect of airborne-particle abrasion on the shear bond strength of four restorative materials to enamel and dentin. J Prosthet Dent. 2004 Sep;92(3):245-9. doi: 10.1016/j.prosdent.2004.05.007.
43. Freeman R, Varanasi S, Meyers IA, Symons AL. Effect of air abrasion and thermocycling on resin adaptation and shear bond strength to dentin for an etch-and-rinse and self-etch resin adhesive. Dent Mater J. 2012;31(2):180-8.
44. Poggio C, Beltrami R, Scribante A, Colombo M, Chiesa M. Shear bond strength of one-step self-etch adhesives: pH influence. Dent Res J (Isfahan). 2015 May-Jun;12(3):209-14.

***Corresponding author:** *Prof. Timur V. Melkumyan, PhD, ScD. Tashkent State Dental Institute, Tashkent, Uzbekistan. Peoples' Friendship University of Russia (RUDN University), Moscow, Russia. E-mail: t.dadamov@gmail.com*

International Journal of Biomedicine 12(4) (2022) 596-600
http://dx.doi.org/10.21103/Article12(4)_OA13

ORIGINAL ARTICLE

Dentistry

INTERNATIONAL JOURNAL OF BIOMEDICINE

Assessment of the Relationship between Expressions of CD34, p63 with Different Clinical Types of Oral Epithelial Dysplasia: A Retrospective Immunohistochemical Study

Mustafa Mohammed Abdulhussain[1*], Fawaz D. Alaswad[2]

[1]*Department of Oral Pathology, College of Dentistry, Mustansiriyah University, Baghdad, Iraq*
[2]*Department of Oral Diagnosis, College of Dentistry, Baghdad University, Baghdad, Iraq*

Abstract

Background: Potentially malignant disorders such as leukoplakia and erythroplakia are often associated with dysplastic changes that have an increased risk for malignant transformation. CD34 is considered as an important marker for tissue vascularization, which represents microvessel density. P63 has a role in epithelial proliferation and is frequently altered in dysplasia and associated with tumorigenesis. The aim of this study was to evaluate the expression of CD34 and p63 in different grades of oral epithelial dysplasia (OED).

Methods and Results: This research included 50 histopathologically confirmed OED. Grading classification of OED was determined according to the WHO criteria, in which the lesions were classified into mild, moderate, and severe grades. CD34 and P63 expressions were studied by using the immunohistochemical technique. Most OED lesions were observed in patient between 40 and 69 years of age. Buccal mucosa was the most affected site (42%). According to histopathological grades, mild OED was predominant (54%). There was a significant difference among OED grades through the P63 marker.

Conclusion: The P63 marker can be considered a good indicator for malignant transformation by grade scoring scales, and the CD34 marker can be used as a useful diagnostic indicator for OED**. (International Journal of Biomedicine. 2022;12(4):596-600.)**.

Keywords: oral epithelial dysplasia • malignancy • CD34 • P63 • immunohistochemistry

For citation: Abdulhussain MM, Alaswad FD. Assessment of the Relationship between Expressions of CD34, p63 with Different Clinical Types of Oral Epithelial Dysplasia: A Retrospective Immunohistochemical Study. International Journal of Biomedicine. 2022;12(4):596-600. doi:10.21103/Article12(4)_OA13.

Abbreviations

AUC, area under the curve; **MVD**, microvessel density; **OED,** oral epithelial dysplasia; **OSCC**, oral squamous cell carcinoma; **OPMDs**, oral potentially malignant disorders.

Introduction

Oral epithelial dysplasia (OED) is characterized by a spectrum of histologic changes in the oral mucosa with the potential to transform into oral squamous cell carcinoma (OSCC).[1,2] A meta-analysis of OED data indicates a malignant transformation rate of 12% within 2 years, increasing to 22% within 5 years.[3] Predicting the risk of malignant transformation is predominantly based on clinicopathologic correlation, histologic examination, and grading.[2,3] However, there is currently no consensus regarding the risk of malignant transformation based on histopathology.[5]

Oral potentially malignant disorders (OPMDs) are defined as a group of oral mucosal lesions (leukoplakia, erythroplakia, oral submucous fibrosis, oral lichen planus, oral dysplasia),[6,7] which are associated with an increased risk of malignant transformation. While OPMD is a clinical term, OED is a histo-morphologically spectrum of epithelial changes associated with an increased risk of transformation to carcinoma.[8] Many OPMD may be pathologically associated with OED.[9-11] The OED histological criteria reported in the WHO classification 2017 are based on “architectural” (disordered tissue organization) and “cytological” (individual cell abnormality) changes.[12-14] However, the malignant

potential of OED can be variable and unpredictable. OSCC has been shown to develop in the absence of known OED and without any evidence of neoplasia seen histologically in previously and conventionally stained oral biopsies in >20% of previously biopsied cases.[15] However, the overall evidence indicates a positive correlation between the likelihood and time of malignant transformation with increasing degrees of dysplasia. [9,11,14]

CD34 is a glycoprotein member found on the surface of a number of body cells. It is a group of differentiation compounds that act as cell adhesion proteins.[16] During the formation of a tumor, angiogenesis is the complicated creation of newly created blood vessels from pre-existing vascular complexes through vessel expansion.[17] In epithelial dysplastic lesions, angiogenesis is believed to be critical for the nourishment and proliferation of dysplastic cells as well as tumor cells, mesenchymal cells, and inflammatory cells like mast cells and macrophages secreting angiogenic materials. Amplified levels of angiogenic triggers like vascular epidermal growth factor (VEGF) result in angiogenesis.[18]

In many tumors, endothelial cells of blood vessels play an essential role in angiogenesis, and CD34 is a signal for these cells. Microvessel density (MVD) in different malignancies is evaluated using the CD34 marker. Furthermore, MVD helps in predicting tumor progression or regression.[19]

The p63 is essential for regulating epithelial cell proliferation, development, and maturation, and its level in the epithelial dysplastic lesions is usually changed.[20] The p63 is implicated in embryogenesis, cell differentiation, and defective cell death.[21] It is also involved in the formation of stratified squamous epithelium.[22] Its role in the oral epithelium might be to preserve stem cell activity rather than a direct link between tumorigenesis and metastasis transformation.[23]

The purpose of this research was to evaluate the expression of CD34 and p63 in different grades of OED.

Materials and Methods

Fifty cases of OED were retrieved from the archives of the Oral Pathology Laboratory of the Oral Diagnosis Department at the College of Dentistry (Baghdad University). Formalin-fixed paraffin-embedded (FFPE) histopathologically diagnosed tissue specimens were collected along with their relevant patient's clinical data (age, sex, and site) as provided from the oral and maxillofacial reports.

Grading classification was determined according to the WHO criteria, in which the lesions were classified into mild, moderate, and severe grades.[24] Hematoxylin and eosin (H&E) stained tissue sections were evaluated by two pathologists to confirm the diagnosis. The positive tissue controls were the human tonsil for CD34 and the human prostate for P63.

The presence of a brown granular DAB dye pattern within the particular cellular or tissue compartment for a specific antibody in positive control tissue slides, according to the product's datasheets, and the lack of staining in negative control tissue samples indicated immunohistochemical signal specificity. The markers' expression was quantitatively assessed.

CD34 and microvessel density quantification

The immunohistochemical expression of CD34 was assessed to determine microvessel density (MVD), which represents the number of microvessels in each field at 40 magnifications, and the average was calculated. Individual endothelial cells or clusters of endothelial cells with or without a lumen that established a brown color with anti-CD34 were regarded as positively stained blood vessels.[25]

P63 scoring

The positive nuclear staining for P63 was assessed using a well-established quantitative scoring system ranging from negative to strong positive staining, as follows:[26]

- Negative staining (less than 5% stained cells)
- Weak positive staining (between 5% and 25% stained cells)
- Moderate positive staining (between 25% and 50% stained cells)
- Strong positive staining (more than 50% stained cells)

Statistical analysis was performed using statistical software package SPSS version 20.0 (SPSS Inc, Chicago, IL). Baseline characteristics were summarized as frequencies and percentages. Group comparisons with respect to categorical variables are performed using One-Sample Chi-Square test. A probability value of $P<0.05$ was considered statistically significant.

Results

The distribution of socio-demographic characteristics such as age groups and gender, as well as comparison significance, were demonstrated to be sure whether these two variables regarding studied patients have randomly distributed among their different classes or not.

The age group's distribution of OED patients showed no significant difference ($P>0.05$). Thus, the probability of OED did not differ according to the age groups, as well as age pivoted in the fifth and sixth decades, with mean value and standard deviation (53.36±12.63 years). As for gender, there was no significant difference ($P>0.05$), and the probability of OED does not differ according to the gender's patients (Table 1).

Table 1.

Demographic characteristics of OED patients.

Variable		n	%	Statistics*
Age group (years)	< 40	7	14	χ^2= 5.600 P=0.231
	40 _ 49	12	24	
	50 _ 59	13	26	
	60 _ 69	13	26	
	≥ 70	5	10	
	Mean ± SD 53.36 ± 12.63			
Gender	Male	24	48	P=0.888
	Female	26	52	
(Between Age & Gender)		CC = 0.334 P = 0.178		

**Testing based on One-Sample Chi-Square test, Binomial test, and Contingency Coefficient (CC) measuring test.*

The distribution of the site and grade of OED, as well as comparison significance, are present in Table 2.

Table 2.

Site and Grade distributions of OED in study patients

Variable		n	%	Statistics*
Site	Tongue	12	24	χ^2= 8.720 *P*=0.033
	Buccal Mucosa	21	42	
	Lips	10	20	
	Others	7	14	
Grade	Mild	27	54	χ^2= 13.240 *P*=0.001
	Moderate	17	34	
	Sever	6	12	
(Site & Grade)		CC = 0.318 *P* = 0.469		

**Testing based on a One-Sample Chi-Square test and Contingency Coefficient (CC) measuring test.*

Buccal mucosa was the most affected site (42%), followed by the tongue site (24%), lips site (24%), and other sites (14%).

According to histopathological grades (Figure 1), a mild grade of OED was predominant (54%), followed by a moderate grade (34%) and a severe grade (12%) (Table 2).

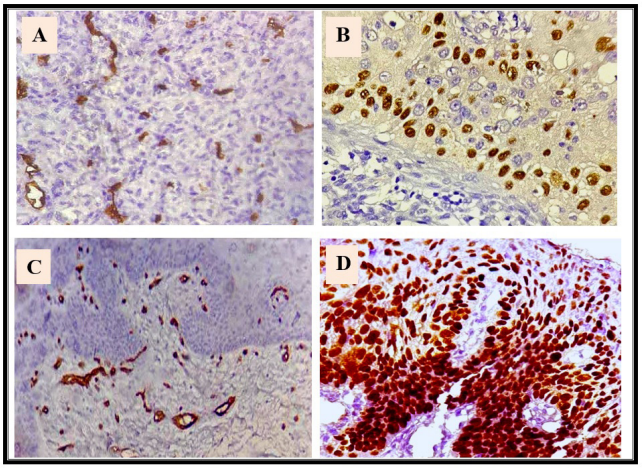

Fig. 1. *A - Photomicrograph of the positive controls of CD34 reactivity in human tonsil, B - Photomicrograph of the positive controls of P63 reactivity in human prostate, C - Positive membranous immunohistochemical expression of CD34 in OED (mild grade), D - Positive nuclear immunohistochemical expression of P63 in OED (severe grade), (magnification 20X).*

Despite there being no significant AUC by the CD34 marker (*P*>0.05) under the guideline of the lowest grade group, which was adopted as the control group, analysis for the compromised pairs (Grade III as a target group and Grade I as a baseline group and Grade III as a target group and Grade II as a baseline group) showed that CD34 marker could be more than an extended indicator for diagnosing OED and especially for the last combination since the AUC decreased by more than half, which confirms a decrease in the CD34 marker with the severe grade of OED (Figure 2).

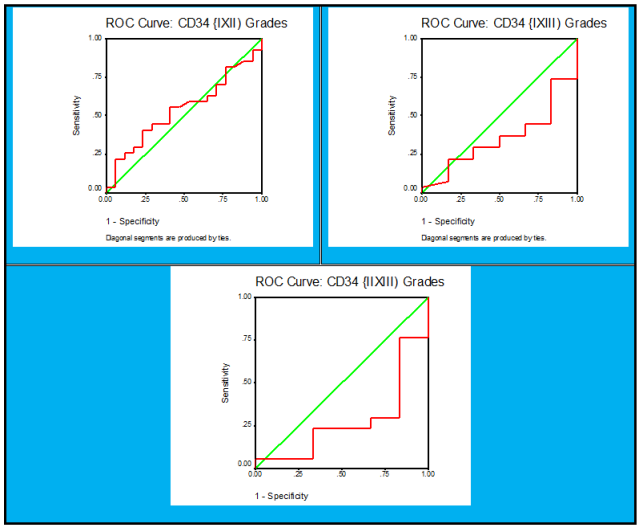

Fig. 2. *ROC-curve plots for the CD34 marker for the group grades with different probable combinations*

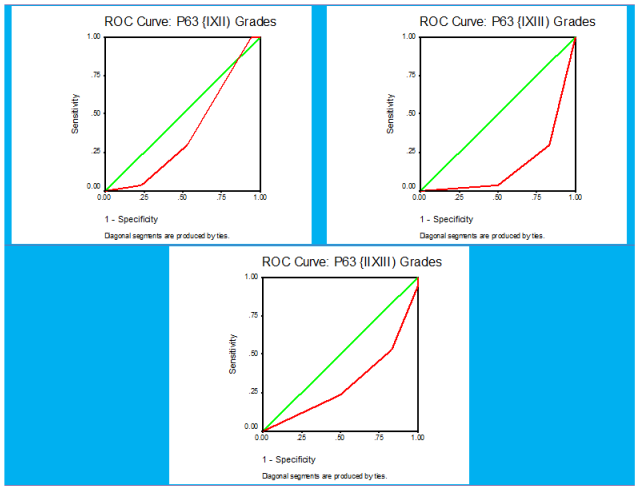

Fig. 3. *ROC-curve plots for the p63 marker for the group grades with different probable combinations*

The significant AUC by the P63 marker (*P*<0.05) under the guideline of the lowest grade group, which was adopted as the control group, and that was accounted at the compromised pair (Grade III as a target group and Grade I as a baseline group) showed that the P63 marker could be a very good indicator for predicting the malignant transformation of OED. AUC could be close to the estimated value (0.000) with a study pair, as indicated by the 95% CI (Fig. 3).

Discussion

Histopathological assessed severity of OED remains essential for the prediction of malignant transformation of precancerous lesions.[27] In this study, most of the OED cases were distributed in the fifth and sixth decades of life (mean age of 53.36±12.63 years), which was consistent with the results of another study.[28] This similarity might be due to a similar sample size and gender distribution. The association of OED development

with aging could be explained by the prolonged accumulation of genetic changes caused by genetic and/or environmental factors such as tobacco and alcohol drinking, which are considered provoking factors in epithelial dysplasia development.

Concerning gender distribution, the results of the current study showed that females were slightly more affected by OED (52%) than males (48%). Similar findings were reported in other parts of the world.[29] Batool et al.,[30] in contrast to our study, showed that 80% of oral dysplastic samples belonged to males with the M/F ratio of 4:1. There is controversy as to which gender is most affected. Specific habits, such as betel nut or tobacco chewing, could explain this in each region.

According to the site lesions, the distribution of studied cases showed that the buccal mucosa was the commonest affected site with OED (42%). This finding was in agreement with the previous study.[30] The higher prevalence of the buccal mucosa site is probably related to the widespread habit of betel/areca nut chewing in some regions and increased malignant transformation in oral leukoplakia lesions of the buccal mucosa over other sites. Napier et al.[31] found that OSCC was more likely with potentially malignant disorders on the lateral and ventral tongue, the floor of the mouth, and retromolar/soft palate complex than those elsewhere.

In our study, the distribution of OED grades (mild, moderate, and severe) was characterized by significant differences. Grading of OED continues to be a hotly debated subject due to subjectivity. Moreover, several grading systems are currently employed because of the need for a consensus. It should be recognized that OED grade is of limited utility as a risk prediction marker for OSCC. [15,30]

The high score of the CD34 marker was found in the severe grade of OED cases, followed in descending order by the mild grade and, finally, moderate grade, so no statistical significance was obtained among the grades of OED for CD34 expression. This finding is in concordance with previous studies,[31] which stated that the confirmed theory that the increased nutrient requirements of actively developing and dividing cells lead to an increase in angiogenesis, which in turn leads to tumor growth.

Pujari et al.[32] showed a strong statistical significance in MVA with the grade of dysplasia when mild and moderate epithelial dysplasia were compared to severe epithelial dysplasia. Thus, the increased MVA might be related to numerous cytokines, macrophages, mast cells, and neutrophils triggered by the dysplastic epithelium's altered keratinocytes. The number of dysplastic cells that can create chemical signals that can start the angiogenesis process grows as the dysplasia degree increases. Thus, angiogenesis promotes tumor growth by supplying nutrients and oxygen. It might be utilized as a prognostic marker to determine the aggressiveness of dysplastic lesions and their transition to carcinoma.[25] The assessment of MVD was done by one study that showed no significant correlation with the dysplastic histological grade.[33] This discrepancy in the results may be due to different sizes in the study sample or subjective assessment of epithelial dysplasia grading.

The results of this study revealed that the vast majority of the score for P63 expression was accounted within a severe grade and suggested that the expression of p63 increased significantly from the mild-to-moderate-to-severe grade of dysplasia. This finding comes in accordance with many other previous studies which showed that the P63 overexpression might be caused by a stabilization of p63 that is not caused by mutations. The rate at which cells turn over a short period of time may also contribute to stabilization by disrupting their breakdown routes or accumulating wild-type proteins.[34] Bavle et al. showed that increased expression of p63 in cases of oral submucous fibrosis can be considered as definitive quantitative markers in the prediction of malignant transformation.[35]

In conclusion, the P63 marker can be considered a good indicator for malignant transformation by grade scoring scales, and the CD34 marker can be used as a useful diagnostic indicator for OED**.**

Competing Interests

The authors declare that they have no competing interests

References

1. Thomas V, Devi SR, Jeyaseelan V, Jeyseelan L. Mucosal Disorders with Oral Epithelial Dysplasia risk–Development of a simple screening tool for general health care setting. Oral Oncol 2012;48(8):671-677.
2. Cheung VKY, Hulme K, Schifter M, Palme C, Low TH, Clark J, Gupta R. Oral Epithelial Dysplasia: A Review of Diagnostic Criteria for Anatomic Pathologists. Adv Anat Pathol. 2022 Jul 1;29(4):227-240. doi: 10.1097/PAP.0000000000000343.
3. Mehanna HM, Rattay T, Smith J, McConkey CC. Treatment and follow-up of oral dysplasia - a systematic review and meta-analysis. Head Neck. 2009 Dec;31(12):1600-9. doi: 10.1002/hed.21131.
4. McCullough MJ, Prasad G, Farah CS. Oral mucosal malignancy and potentially malignant lesions: an update on the epidemiology, risk factors, diagnosis and management. Aust Dent J. 2010;55(suppl 1):61-65. doi.org/10.1111/j.1834-7819.2010.01200.x
5. Speight PM. Update on oral epithelial dysplasia and progression to cancer. Head Neck Pathol. 2007 Sep;1(1):61-6. doi: 10.1007/s12105-007-0014-5.
6. Warnakulasuriya S, Johnson NW, van der Waal I. Nomenclature and classification of potentially malignant disorders of the oral mucosa. J Oral Pathol Med. 2007 Nov;36(10):575-80. doi: 10.1111/j.1600-0714.2007.00582.x.
7. Warnakulasuriya S. Clinical features and presentation of oral potentially malignant disorders. Oral Surg Oral Med Oral Pathol Oral Radiol. 2018 Jun;125(6):582-590. doi: 10.1016/j.oooo.2018.03.011.
8. Lorini L, Bescós Atín C, Thavaraj S, Müller-Richter U, Alberola Ferranti M, Pamias Romero J, Sáez Barba M, de Pablo García-Cuenca A, Braña García I, Bossi P, Nuciforo P, Simonetti S. Overview of Oral Potentially Malignant Disorders: From Risk Factors to Specific Therapies. Cancers (Basel). 2021 Jul 23;13(15):3696. doi: 10.3390/cancers13153696.
9. Muller S. Oral epithelial dysplasia, atypical verrucous lesions and oral potentially malignant disorders: focus on

histopathology. Oral Surg Oral Med Oral Pathol Oral Radiol 2018;125:591–602. doi.org/10.1016/j.oooo.2018.02.012
10. Speight PM, Khurram SA, Kujan O. Oral potentially malignant disorders: risk of progression to malignancy. Oral Surg Oral Med Oral Pathol Oral Radiol. 2018 Jun;125(6):612-627. doi: 10.1016/j.oooo.2017.12.011.
11. Iocca O, Sollecito TP, Alawi F, et al. Potentially malignant disorders of the oral cavity and oral dysplasia: A systematic review and meta-analysis of malignant transformation rate by subtype. Head Neck. 2020;42:539-555. doi.org/10.1002/hed.26006
12. WHO Classification of Head and Neck Tumours. El-Naggar AK, Chan JKC, Grandis JR, Takata T, Slootweg PJ, Eds. IARC Press: Lyon, France, 2017.
13. Kujan O, Oliver RJ, Khattab A, Roberts SA, Thakker N, Sloan P. Evaluation of a new binary system of grading oral epithelial dysplasia for prediction of malignant transformation. Oral Oncol. 2006 Nov;42(10):987-93. doi: 10.1016/j.oraloncology.2005.12.014.
14. Nankivell P, Williams H, Matthews P, Suortamo S, Snead D, McConkey C, Mehanna H. The binary oral dysplasia grading system: validity testing and suggested improvement. Oral Surg Oral Med Oral Pathol Oral Radiol. 2013 Jan;115(1):87-94. doi: 10.1016/j.oooo.2012.10.015.
15. Pritzker KPH, Darling MR, Hwang JT, Mock D. Oral Potentially Malignant Disorders (OPMD): What is the clinical utility of dysplasia grade? Expert Rev Mol Diagn. 2021 Mar;21(3):289-298. doi: 10.1080/14737159.2021.1898949.
16. Raffat MA, Hadi NI, Alghamdi O, Al-Aali KA, Al Deeb M, Abduljabbar T, Vohra F. Expression of Salivary S100A7 Levels in Stage I Oral Submucous Fibrosis: A Clinical and Laboratory Study. Asian Pac J Cancer Prev. 2020 Apr 1;21(4):1115-1119. doi: 10.31557/APJCP.2020.21.4.1115.
17. Roskoski R Jr. Vascular endothelial growth factor (VEGF) signaling in tumor progression. Crit Rev Oncol Hematol. 2007 Jun;62(3):179-213. doi: 10.1016/j.critrevonc.2007.01.006.
18. Menakuru SR, Brown NJ, Staton CA, Reed MW. Angiogenesis in pre-malignant conditions. Br J Cancer.2008;99(12):1961-1966. doi:10.1038/sj.bjc.6604733
19. Siar CH, V. P. A. Oo, Nagatsuka H, Nakano K, Ng. KH, Kawakami T. Angiogenic squamous dysplasia-like phenomenon in oral epithelial precursor lesions. Eur J Med Res. 2009;14(7): 315-319. doi.org/10.1186/2047-783X-14-7-315
20. Yong M, Yang L, Suyila Q, et al. Expression and clinical implications of P53, P63, and P73 protein in malignant tumor of the parotid gland. Turk J Med Sci. 2014;44(5):875-882. doi:10.3906/sag-1304-136
21. Yoon MK, Ha JH, Lee MS, Chi SW. Structure and apoptotic function of p73. BMB reports. 2015 48(2):81. doi.org/10.5483%2FBMBRep.2015.48.2.255
22. Mills AA. p63: oncogene or tumor suppressor? Curr Opin Genet Dev. 2006 Feb;16(1):38-44. doi: 10.1016/j.gde.2005.12.001.
23. Takeda T, Sugihara K, Hirayama Y, Hirano M, Tanuma JI, Semba I. Immunohistological evaluation of Ki67, p63, CK19 and p53 expression in oral epithelial dysplasias. J Oral Pathol Med 2006;35(6):369-375. doi.org/10.1111/j.1600-0714.2006.00444.x
24. Barnes L, Eveson JW, Reichart P, Sidransky D. World Health Organization Classification of Tumors. Pathology and Genetics of Head and Neck Tumours. Lyon: IARC Press; 2005.
25. Sundararajan A, Muthusamy R, Gopal Siva K, Harikrishnan P, Kumar SCK, Rathinasamy SK. Correlation of Mast Cell and Angiogenesis in Oral Lichen Planus, Dysplasia (Leukoplakia), and Oral Squamous Cell Carcinoma. Rambam Maimonides Med J 2021;12(2):e0016. doi.org/10.5041%2FRMMJ.10438
26. Kamal KAER, Mohamed MA, Abd-alwahab AS, Alazazi M. P63 & ki67 antigen expression in relation to the aggressiveness of oral squamous cell carcinoma. Egyptian Dental Journal (2-April (Oral Medicine, X-Ray, Oral Biology & Oral Pathology). 2020;(66)1091-1098. doi.org/10.21608/edj.2020.23986.1009
27. Niu LX, Feng ZE, Wang DC, Zhang JY, Sun ZP, Guo CB. Prognostic factors in mandibular gingival squamous cell carcinoma: A 10-year retrospective study. Int J Oral Maxillofac Surg. 2017;46(2):137–143. doi.org/10.1016/j.ijom.2016.09.014
28. Gopinath D, Thannikunnath BV, Neermunda SF. Prevalence of Carcinomatous Foci in Oral Leukoplakia: A Clinicopathologic Study of 546 Indian Samples. J ClinDiagn Res 2016;10:78-83. doi.org/10.7860%2FJCDR%2F2016%2F16815.8305
29. Bijina BR, Ahmed J, Shenoy N, Ongole R, Shenoy S, Baliga S. Detection of human papilloma virus in potentially malignant and malignant lesions of the oral cavity and a study of associated risk factors. South Asian Journal of Cancer. 2016;5(4):179-181. doi.10.4103/2278-330X.195337
30. Batool S, Fahim A, Qureshi A, Anas S, Qamar N, Kamran S. Significance of Expression of Cyclin D as an Early Indicator in Dysplastic Transformation of Oral Mucosa in Tobacco Users. JPDA. 2019;28(4):171-175. https://doi.org/10.25301/JPDA.284.171
31. Napier SS, Speight PM. Natural history of potentially malignant oral lesions & conditions: An overview of the literature. J Oral Pathol Med 2008;37(1):110. doi.org/10.1111/j.1600-0714.2007.00579.x
32. Pujari RV, Vanaki SS, Puranik RS, Desai RS, Motupalli N, Halawar S. Histomorphometric analysis of vascularity in normal buccal mucosa, leukoplakia, and squamous cell carcinoma of buccal mucosa. J Oral Maxillofac Pathol 2013;17:334-339.doi.org/10.4103%2F0973-029X.125178
33. Mohammad DN, Garib BT. CD34 and Wnt3 expression in potentially malignant oral disorders. J Bagh Coll Dent. 2017;29:59-67.
34. Krause DS, Fackler MJ, Civin CI, May WS. CD34: structure, biology, and clinical utility. Blood. 1996 Jan 1;87(1):1-13.
35. Bavle RM, Paremala K, Sowmya M, Sudhakara M, Reshma V, Hosthor S. Predicting the Malignant Transformation of Oral Submucous Fibrosis Using Quantitative Biomarkers p63 and CD31. J Orofac Sci. 2020;12:52-60. doi. 10.4103/jofs.jofs_6_20.

***Corresponding author:** Mustafa Mohammed Abdulhussain, MSc. Department of Oral Pathology, College of Dentistry, Mustansiriyah University. Baghdad, Iraq. E-mail: mustafa80moh@uomustansiriyah.edu.iq*

International Journal of Biomedicine 12(4) (2022) 601-605
http://dx.doi.org/10.21103/Article12(4)_OA14

ORIGINAL ARTICLE

Dentistry

INTERNATIONAL JOURNAL OF BIOMEDICINE

Determination of Mercury in Dental Hard Tissue: An in Vitro Study

Nexhmije Ajeti[1], Violeta Vula[2*], Miranda Stavileci[2], Lindihana Emini[3]

[1]*Department of Operative Dentistry and Endodontology, University for Business and Technology, Prishtina, Kosovo*

[2]*Department of Dental Pathology and Endodontics Faculty of Medicine, University of Prishtina, Prishtina, Kosovo*

[3]*Department of Dental Pathology and Endodontics, Faculty of Medical Sciences, University of Tetova, Tetova, North Macedonia*

Abstract

Background: The purpose of this study was to determine the levels of mercury in hard tissue from dental amalgam fillings under in vitro conditions.

***Methods and Results*:** The study included 30 human teeth that were extracted for various clinical reasons. The teeth were stored in a physiological solution until they were used. The teeth were divided into 3 experimental groups: Group 1 (n=10) – occlusal surface cavity preparation (class I according to Black); Group 2 (n=10) – proximal-occlusal surface cavity preparation (class II); and Group 3 (n=10) – mesio-occlusal-distal [MOD] surface cavity preparation. Each of these groups was divided into 2 subgroups: subgroup 1 (n=5) – amalgam fillings were not polished, and subgroup 2 (n=5) amalgam fillings were polished. The teeth were filled with amalgam, and those in subgroups 2 were polished after 24 hours. The amount of mercury released from the amalgam fillings was determined 9 months after the teeth were filled. Before chemical analysis, the teeth were irrigated 4 times over a period of 10 minutes in an ultrasonic bath. From each tooth, 250 mg of the powder was mineralized with royal water ($HCl+HNO_3$ in a ratio of 1:3) in a microwave oven, for 54 minutes. After mineralization, the samples were filtered and analyzed with inductively coupled plasma optical emission spectrometry. The average mercury level after polishing the amalgam filling was significantly smaller (P=0.032) only in Group 1. The average mercury levels in the 3 groups revealed significant differences between both the unpolished samples (one-way ANOVA F=69.54, P<0.001) and the polished samples (one-way ANOVA F=110.54, P<0.001). Group 3 with MOD surface cavity preparation was characterized by the highest mercury levels.

Conclusion: The more mercury is released from unpolished amalgam fillings than from polished amalgam fillings in theeth with occlusal surface cavity preparation (class I according to Black). The teeth with an MOD amalgam restoration are characterized by the highest mercury levels. (**International Journal of Biomedicine. 2022;12(4):601-605.**).

Keywords: dental fillings • amalgam • mercury • polishing

For citation:Ajeti N, Vula V, Stavileci M, Emini L. Determination of Mercury in Dental Hard Tissue: An in Vitro Study. International Journal of Biomedicine. 2022;12(4):601-605. doi:10.21103/Article12(4)_OA14.

Introduction

The use of mercury (Hg) in dentistry has been controversial since at least the middle of the 19th century. This controversy has recently intensified because of techniques that show that mercury is continually released from dental amalgam fillings.(1)

Mercury is a naturally occurring element that exists in 3 forms: organic, inorganic, and elemental. Concentrations of mercury in most foodstuffs are often below the detection limit. Fish and marine mammals are the dominant sources, mainly in the form of methylmercury compounds (70–90% of the total)(2)

The US Food and Drug Administration (FDA) recently acknowledged several important facts regarding amalgams: (1) they release Hg in the form of Hg vapor; (2) they release amounts of Hg vapor dependent on the number of existing fillings; and (3) they release Hg vapors that may be harmful to certain patients.(3)

Amalgam dental fillings with mercury can be a source of human exposure to elemental mercury vapors for many populations. Mercury vapor is released from the surface of amalgam fillings into the mouth and lungs. Depending upon the number of amalgam fillings and other factors, the estimated average daily absorption of mercury vapor from dental fillings

varies between 3μg and 17μg of mercury.[4] So ionic mercury leached out from amalgam restorations may present a risk to the dental patient.[5]

Mercury can also be released by electrochemical corrosion from amalgam fillings during chewing.[6] Additionally, materials used for tooth bleaching can cause the release of mercury from amalgam fillings. According to Bahar et al.,[7] the amount of free mercury released from amalgam fillings depends on the content of silver in the alloy. Alloys with a high percentage of silver (69%) release low levels of mercury from the amalgam, while those with a smaller percentage of silver (45%) release more mercury from the amalgam.[7]

Although bleaching gels are commonly applied to the anterior teeth, excess bleaching materials may inadvertently come into contact with amalgam restorations on premolars and molars, and may increase the susceptibility of the amalgam to corrosion and degradation. Bleaching agents such as carbamide peroxide break into free radicals that can theoretically corrode metallic alloys, such as amalgam in close proximity, to release mercury.[8]

According to Azarsina et al., polished amalgam fillings release less mercury after the application of carbamide peroxide than do unpolished amalgam fillings.[9] Another hazard of mercury is that it is a radioactive element that can be quite toxic, even in small doses.[10,11]

To determine levels of mercury in the environment and biological samples, various analytical techniques have been used, such as cold vapor atomic absorption spectrometry, cold vapor fluorescence spectrometry, inductively coupled plasma optical emission spectrometry (ICP-OES), electrothermal atomic absorption spectrometry, anodic stripping voltammetry, and cold vapor inductively coupled plasma mass spectrometry.[12] The amount of free mercury released from amalgam fillings can also be determined with nuclear tracking techniques.[13] The release of mercury from amalgam fillings can be studied with spectroscopy-induced laser femtosecond,[14] and the corrosion of amalgam can also be determined by fluorescent spectroscopy.[15]

The influence of pH on the release of mercury from amalgam fillings has also been studied. It has been reported that at variable pH values, mercury dissolves more in amalgam fillings that contain tin at all stages of amalgamation, than in amalgam fillings that do not contain tin.[16] According to Rotstein et al.,[17] one of the factors influencing the release of mercury from unpolished amalgam is the filling pH.

Researchers agree that amalgam restorations leach mercury into the mouth, but consistent findings are not available to determine whether this poses any significant health risk.[18] Mercury does not collect irreversibly in human teeth. The average half-life of mercury is 55 days for transport through the body to the point of excretion. Thus, mercury that came into the body years ago may no longer be present in the body.[14] The use of mercury in dental fillings represents approximately 10% of the total global mercury consumption; thus, dentistry is the largest consumer of mercury in the world.[19]

The purpose of this study was to determine the levels of mercury in hard tissue from dental amalgam fillings under in vitro conditions.

Materials and Methods

This in vitro research included 30 human teeth that were extracted for various clinical reasons. The teeth were stored in a physiological solution until they were used. The teeth were divided into 3 experimental groups: Group 1 (n=10) – occlusal surface cavity preparation (class I according to Black); Group 2 (n=10) – proximal-occlusal surface cavity preparation (class II); and Group 3 (n=10) – mesio-occlusal-distal [MOD] surface cavity preparation. Each of these groups was divided into 2 subgroups: subgroup 1 (n=5) – amalgam fillings were not polished, and subgroup 2 (n=5) amalgam fillings were polished.

The teeth were filled with amalgam (Dispersalloy, Johnson and Johnson Inc. Montreal, Canada), and those in subgroups 2 were polished after 24 hours.

The amount of mercury released from the amalgam fillings was determined 9 months after the teeth were filled. Before chemical analysis, the teeth were irrigated 4 times over a period of 10 minutes in an ultrasonic bath. The teeth were ground to a particle size of <75 microns with a blinder (Retsch, Grindomix GM 200, Germany). The ground tooth material was dried at a temperature of 105°C for 3 hours. The powder Ber was weighed on a scale with a precision of 4 decimal places (Kern &Sohn GmbH, Germany). From each tooth, 250 mg of the powder was mineralized with royal water ($HCl+HNO_3$ in a ratio of 1:3) in a microwave oven (Berghof products, Germany), for 54 minutes. After mineralization, the samples were filtered and analyzed with ICP-OES (Perkin Elmer, USA, Optima 2100 DW).

Statistical analysis was performed using statistical software package SPSS version 23.0 (SPSS Inc, Armonk, NY: IBM Corp). For descriptive analysis, results are presented as mean±SD. For data with normal distribution, inter-group comparisons were performed using Student's t-test. Multiple comparisons were performed with a one-way ANOVA. A probability value of $P<0.05$ was considered statistically significant.

Results

Group 1

The average level of mercury in teeth with an occlusal amalgam restoration before the amalgam was polished was (5 teeth, 10 measurements of each tooth from 2 times, n = 10) was 6.53±0.85 mg/kg (the range of 5.36-8.02). The average level of mercury in teeth with an occlusal amalgam restoration after the amalgam was polished was 5.80±0.51 mg/kg (the range of 5.12-6.53). The average mercury level after polishing the amalgam filling was smaller, and the difference was significant ($P=0.032$) (Table 1).

Group 2

The average level of mercury in teeth with a proximal-occlusal amalgam restoration before the amalgam was polished was 10.02±1.81 mg/kg (the range of 6.72-12.22). The average level of mercury in teeth with a proximal-occlusal amalgam restoration after the amalgam was polished was 8.76±1.24 mg/kg (the range of 7.74-11.4). The mercury level after polishing the amalgam filling was smaller, but the difference was not significant ($P=0.086$) (Table 1).

Group 3

The average level of mercury in teeth with an MOD amalgam restoration before the amalgam was polished was 13.18±0.88 mg/kg (the range of 11.61-14.56). The average level of mercury in teeth with an MOD amalgam restoration after the amalgam was polished was 12.54±1.14 mg/kg (the range of 10.53-14.07). The mercury level after polishing the amalgam filling was smaller, but this difference was not significant (*P*=0.177).

Table 1.

Mean value (mg/kg) of mercury in the study groups.

Group	Subgroup	N	Mean ± SD	Rank	Statistics
Group 1	Subgroup 1	10	6.53 ± 0.85	5.36 - 8.02	T=2.329 *P*=0.032
	Subgroup 2	10	5.80 ± 0.51	5.12 - 6.53	
Group 2	Subgroup 1	10	10.02 ± 1.81	6.72 - 12.22	T=1.816 *P*=0.086
	Subgroup 2	10	8.76 ± 1.24	7.74 - 11.4	
Group 3	Subgroup 1	10	13.18 ± 0.88	11.61 - 14.56	T=1.405 *P*=0.177
	Subgroup 2	10	12.54 ± 1.14	10.53 - 14.07	
	Total	60	9.47 ± 3.00	5.12 - 14.56	

The average mercury levels in the 3 groups revealed significant differences between both the unpolished samples (one-way ANOVA F=69.54, *P*<0.001) and the polished samples (one-way ANOVA F=110.54, *P*<0.001) (Figures 1 and 2). The teeth with an MOD amalgam restoration were characterized by the highest mercury levels.

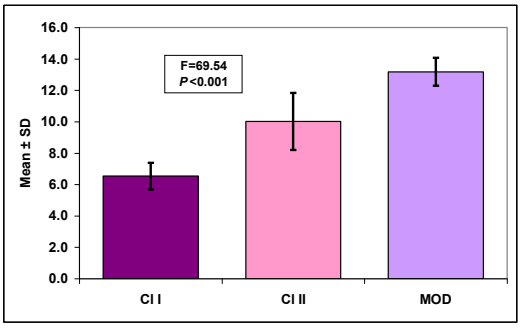

Fig. 1. *The average mercury levels in the study groups (unpolished samples)*

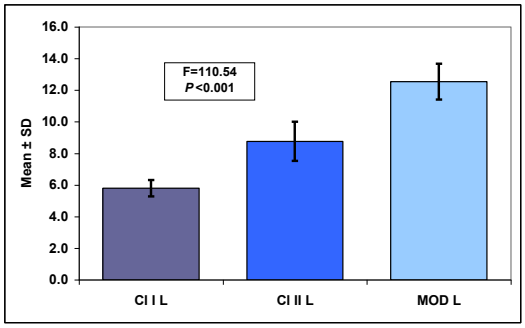

Fig. 2. *The average mercury levels in the study groups (polished samples).*

Discussion

Exposure to mercury from dental amalgams, with possible adverse health effects, has generally been considered to occur via either erosion or evaporation directly from the surface of fillings, followed by ingestion.[20]

Numerous epidemiological studies have assessed the impact of mercury exposure from oral dental amalgam. In a recent study, males with high mercury levels in their hair (>1ppm) had a 50% higher probability of having periodontitis than females with normal mercury levels (<1ppm). The results suggest that mercury exposure, regardless of sex, is associated with periodontitis.[21] In 1994, it was shown that the amount of tin in the ɣ1-phase is related to the emission of mercury vapor. Based on this paper, it is possible to identify the brands tested: conventional amalgams, amalgams with a reduced amount of ɣ2, and non-ɣ2-amalgams. The result is clear: non-ɣ2-amalgams emit substantially more mercury vapor than the old conventional amalgams. Using the highest emitter of the low copper amalgams as a baseline, the high copper amalgams emit 3–4 times as much mercury vapor, depending on the brand.[22]

In an investigation measuring differences in mercury vapor emissions in corroded and uncorroded samples, only one non-ɣ2-amalgam and one low copper amalgam were used. The pattern is once again confirmed, with the non-ɣ2-amalgam emitting substantially more mercury vapor than the conventional one, and corroded samples emitting more mercury vapor than those not corroded.[23] In another investigation, using the same brands of amalgam as Mahler et al.,[24] Marek studied the average values of mercury solubility in phase ɣ1 (Ag-Hg) and phase ɣ2 (Ag-Hg-Sn) with atomic absorption spectroscopy. The results showed that solubility is better in phase ɣ1 than in phase ɣ2. It was noted that the release of mercury from amalgam is smaller in phase ɣ2 than in phase ɣ1.

The release of Hg from amalgam fillings depends on the type and age of the amalgam filling.[25] Harris et al.[20] determined the migration of Hg, Ca, Zn, and Cu in teeth with amalgam fillings more than 20 years ago. They concluded that Hg (up to approximately 10 mg g(-1)) and Zn (>100 mg g(-1)) were detected in the teeth several millimeters from the location of the amalgams.

The removal of amalgam from the cavity also causes Hg release. The amount of free amalgam released from fillings depends on whether it is removed with water or through absorption. It has been reported that the amount of free mercury is greater (34.0–796μg⁄m^3) if water or suction is not used during its elimination, compared with the use of water rush (4.09-19.0 796μg⁄m^3) and the use of suction (14.0-19.0μg⁄m^3).[26]

Derand et al. reported that there is a large difference in mercury levels between polished fillings stored in a room environment and corroded fillings stored in saliva. Additionally, the simple composition frees up more mercury than do fabricated fillings.[27]

In our in vitro research, the teeth were stored in saliva, and it was found that the average values of mercury released

from teeth with class I, II, and MOD amalgam restorations were significantly different, similar to the polished and unpolished groups.

Bolsoni et al.[28] investigated the corrosion of polished and unpolished amalgam fillings over various time intervals. The corrosion products were measured with ICP-OES. They concluded that the greatest concentration of mercury occurred in the first 24 hours of the experiment, and that the corrosion of the amalgam was caused by the degradation of gamma phase 2 during amalgamation. Our research, in contrast with the findings of Bolson et al., has shown that mercury release is greater 9 months after amalgam placement; this determination of mercury release was made by ICP-OES.

Pleva et al.[29] found that the chewing surface of a 5-year-old amalgam had lost almost half of its mercury, while a 20-year-old amalgam had no mercury left on the chewing surface.

More mercury is released after chewing, and newer fillings release more mercury than older fillings.[30] The results of a study conducted by Canay et al.[31] showed that unpolished amalgam has a higher corrosion level than does polished amalgam.

Bjorkman & Lind[32] studied the influence of various factors on the evaporation of Hg from amalgam fillings. They found that rinsing the mouth with warm water for 1 minute increases the level of mercury vapor by a factor of 1.7 when the water temperature rises from 35°C to 45°C.

Loto et al.[33] reported greater release of mercury vapor in the environment of the Restorative Clinic than in other dental clinics.

The corrosion behavior and dissolution of such a structure as a set amalgam depend on the characteristics of each individual phase and on the electrochemical interaction between these phases in a special environment, such as the oral cavity during mouthguard bleaching.[34]

Fredin et al.[35] studied various aspects of mercury release from amalgam fillings under in vivo and in vitro conditions using light microscopy mercury globules. They concluded that amalgam fillings should not be considered as an appropriate filling given the long-lasting exposure to mercury vapors, which have a toxic effect on the human body.

Mercury vapors can cause various diseases in the human body. Anaerobic bacteria from periodontal disease produce H_2S and CH_3SH, which are responsible for gingivitis.[36]

According to Siblerund et al.,[37] people with amalgam fillings showed more health problems than did people without amalgam fillings. These sulfur compounds react with the mercury amalgam to produce a black pigment on the gum tissue (amalgam tattoo), consisting of HgS, which is extremely toxic and can cause oral and systemic diseases.[38]

According to Paknahad et al.,[39] amalgam fillings in patients who are exposed to Wi-Fi wave emissions release more mercury than those in patients not exposed. Leszek et al.[40] reported the deposition of mercury in various parts of the body within 29 days after the placement of amalgam restorations. They concluded that high concentrations of mercury from amalgam fillings are found in the kidneys and liver.

Conclusion

The teeth with an MOD amalgam restoration are characterized by the highest mercury levels. The more mercury is released from unpolished amalgam fillings than from polished amalgam fillings in teeth with occlusal surface cavity preparation (class I according to Black).

Acknowledgments

We thank Helen Jeays, BDSc AE, from Edanz (www.edanz.com/ac) for editing a draft of this manuscript.

Competing Interests

The authors declare that they have no competing interests.

References

1. Mutter J, Naumann J, Sadaghiani C, Walach H, Drasch G. Amalgam studies: disregarding basic principles of mercury toxicity. Int J Hyg Environ Health. 2004 Sep;207(4):391-7. doi: 10.1078/1438-4639-00305.
2. Mercury Air Quality Guidelines - Second Edition. WHO Regional Office for Europe, Copenhagen, Denmark, 2000. Available from: https://www.euro.who.int/__data/assets/pdf_file/0004/123079/AQG2ndEd_6_9Mercury.PDF
3. US Food and Drug Administration. Information for Patients About Dental Amalgam Fillings. Content current as of: 09/24/2020 Available from: https://www.fda.gov/medical-devices/dental-amalgam-fillings/information-patients-about-dental-amalgam-fillings
4. Skare I, Engqvist A. Human exposure to mercury and silver released from dental amalgam restorations. Arch Environ Health. 1994 Sep-Oct;49(5):384-94. doi: 10.1080/00039896.
5. Sweeney M, Creanor SL, Smith RA, Foye RH. The release of mercury from dental amalgam and potential neurotoxicological effects. J Dent. 2002 Jul-Aug;30(5-6):243-50. doi: 10.1016/s0300-5712(02)00040-4.
6. Berglund A. Release of mercury vapor from dental amalgam. Swed Dent J Suppl. 1992;85:1-52.
7. Bahari M, Alizadeh Oskoee P, Savadi Oskoee S, Pouralibaba F, Morsali Ahari A. Mercury release of amalgams with various silver contents after exposure to bleaching agent. J Dent Res Dent Clin Dent Prospects. 2016 Spring;10(2):118-23. doi: 10.15171/joddd.2016.019.
8. Rotstein I, Dogan H, Avron Y, Shemesh H, Steinberg D. Mercury release from dental amalgam after treatment with 10% carbamide peroxide in vitro. Oral Surg Oral Med Oral Pathol Oral Radiol Endod. 2000 Feb;89(2):216-9. doi: 10.1067/moe.2000.102160.
9. Azarsina M, Kasraei Sh, Masoum T, Khamverdi Z. Effect of surface polishing on mercury release from dental amalgam

***Corresponding author**: Prof. Violeta Vula. Department of Dental Pathology and Endodontics, Faculty of Medicine, University of Prishtina, Clinical Centre N.N. Prishtina, Kosovo. E-mail: violeta.vula@uni-pr.edu*

after treatment 16% carbamide peroxide gel. J Dent (Tehran). 2011 Winter;8(1):33-8.
10. Mutter J. Is dental amalgam safe for humans? The opinion of the scientific committee of the European Commission. J Occup Med Toxicol. 2011 Jan 13;6(1):2. doi: 10.1186/1745-6673-6-2.
11. Neghab M, Choobineh A, Hassan Zadeh J, Ghaderi E. Symptoms of intoxication in dentists associated with exposure to low levels of mercury. Ind Health. 2011;49(2):249-54. doi: 10.2486/indhealth.ms1214.
12. Leopold K, Foulkes M, Worsfold P. Methods for the determination and speciation of mercury in natural waters--a review. Anal Chim Acta. 2010 Mar 24;663(2):127-38. doi: 10.1016/j.aca.2010.01.048.
13. Brune D, Eoje DM. Man' mercury loading from a dental amalgam. Sci Total Environ. 1985; 44(1): 51-63. doi: 10.1016/0048-9697(85)90050-6
14. Toledo Bello L, Aparecida du Ana P, Santos D. Mercury Amalgam Diffusion in Human Teeth Probed Using Femtosecond LIBS. Appl Spectrosc. 2017;4:659-69. doi: 10.1177/0003702816687572
15. Toumelin-Chemla F, Lasfargues JJ. Unusual in vivo extensive corrosion of a low-silver amalgam restoration involving galvanic coupling: a case report. Quintessence Int. 2003 Apr;34(4):287-94.
16. Marek M. Dissolution of mercury from dental amalgam at different pH values. J Dent Res. 1997 Jun;76(6):1308-15. doi: 10.1177/00220345970760061101.
17. Rotstein I, Avron Y, Shemesh H, Dogan H, Mor CH, Steinberg D. Factors affecting mercury release from dental amalgam exposed to carbamide peroxide bleaching agent. Am J Dent. 2004:17(5):347-50.
18. Brownaell AM, Brent S, Brent RL, et. al. The potential adverse health effects of dental amalgams. Toxicol Rev. 2005;24:1-40. doi: 10.2165/00139709-200524010-00001.
19. UNEP 2008 annual report. Available from: https://www.unep.org/fr/node/12277
20. Harris HH, Vogt S, Eastgate H, et. al. Migration of mercury from dental amalgam through. J Synchrotron Radiat. 2008; 15(2): 123-8. doi: 10.1107/S0909049507061468.
21. Han DH, Lim SY, Sun BC, Janket SJ, Kim JB, Paik DI, Paek D, Kim HD. Mercury exposure and periodontitis among a Korean population: the Shiwha-Banwol environmental health study. J Periodontol. 2009 Dec;80(12):1928-36. doi: 10.1902/jop.2009.090293.
22. Mahler DB, Adey JD, Fleming MA. Hg emission from dental amalgam as related to the amount of Sn in the Ag-Hg (gamma 1) phase. J Dent Res. 1994 Oct;73(10):1663-8. doi: 10.1177/00220345940730101201.
23. Boyer DB. Mercury vaporization from corroded dental amalgam. Dent Mater. 1988 Apr;4(2):89-93. doi: 10.1016/s0109-5641(88)80097-6.
24. Marek M. The effect of tin on the corrosion behavior of the Ag-Hg phase of dental amalgam and dissolution of mercury. J Dent Res. 1990 Dec;69(12):1786-90. doi: 10.1177/00220345900690120101.
25. Berdouses E, Vaidyanathan TK, Dastane A, Weisel C, Houpt M, Shey Z. Mercury release from dental amalgams: an in vitro study under controlled chewing and brushing in an artificial mouth. J Dent Res. 1995 May;74(5):1185-93. doi: 10.1177/00220345950740050701.
26. Warwick R, O'Connor A, Lamey B. Mercury vapour exposure during dental student training in amalgam removal. J Occup Med Toxicol. 2013 Oct 3;8(1):27. doi: 10.1186/1745-6673-8-27.
27. Dérand T. Mercury vapor from dental amalgams, an in vitro study. Swed Dent J. 1989;13(5):169-75.
28. Bolsoni LE, Almeida RP, Viniia D, Panzeri H. [Emission microspectrometric study of the amalgam restoration-tooth interface]. Rev Odontol Univ Sao Paulo. 1990 Oct-Dec;4(4):289-92. [Article in Portuguese].
29. Pleva J. Mercury poisoning from dental amalgam. J Orthomolecular Psych. 1983;12:184-193.
30. Gay DD, Cox RD, Reinhardt JW. Chewing releases mercury from fillings. Lancet. 1979 May 5;1(8123):985-6. doi: 10.1016/s0140-6736(79)91773-2.
31. Canay S, Cehreli MC, Bilgiç S. In vitro evaluation of the effect of a current bleaching agent on the electrochemical corrosion of dental alloys. J Oral Rehabil. 2002 Oct;29(10):1014-9. doi: 10.1046/j.1365-2842.2002.00934.x.
32. Björkman L, Lind B. Factors influencing mercury evaporation rate from dental amalgam fillings. Scand J Dent Res. 1992 Dec;100(6):354-60. doi: 10.1111/j.1600-0722.1992.tb01086.x.
33. Oyapero A, Awotile A, Adenuga-Taiwo O, Enone L, Menakaya I. Managing Amalgam Phase Down: An Evaluation of Mercury Vapor Levels in a Dental Center in Lagos, Nigeria. Journal of Dental Research and Review. 2017; 4(1):4-8.
34. Marshall SJ, Marshall GW Jr. Dental amalgam: the materials. Adv Dent Res. 1992 Sep;6:94-9. doi: 10.1177/08959374920060012401.
35. Fredin B. Mercury release from dental amalgam fillings. Int J Risk Saf Med. 1994;4(3):197-208. doi: 10.3233/JRS-1994-4303.
36. Shinada K, Ueno M, Konishi C, Takehara S, Yokoyama S, Zaitsu T, Ohnuki M, Wright FA, Kawaguchi Y. Effects of a mouthwash with chlorine dioxide on oral malodor and salivary bacteria: a randomized placebo-controlled 7-day trial. Trials. 2010 Feb 12;11:14. doi: 10.1186/1745-6215-11-14.
37. Siblerud R, Mutter J. An Overview of Evidence that Mercury from Dental Fillings may be an Etiological Factor in Many Health Disorders. Journal of Biomedical Research & Environmental Sciences, Environmental contamination atmospheric chemistry. 2021;2(6): 472-85.
38. Haley BE. The relationship of the toxic effects of mercury to exacerbation of the medical condition classified as Alzheimer's disease. Med Verit. 2007;4:1510-24. doi: 10.1055/s-2007-959237.
39. Paknahad M, Mortazavi SM, Shahidi S, Mortazavi G, Haghani M. Effect of radiofrequency radiation from Wi-Fi devices on mercury release from amalgam restorations. J Environ Health Sci Eng. 2016 Jul 13;14:12. doi: 10.1186/s40201-016-0253-z.
40. Hahn LJ, Kloiber R, Vimy MJ, Takahashi Y, Lorscheider FL. Dental "silver" tooth fillings: a source of mercury exposure revealed by whole-body image scan and tissue analysis. FASEB J. 1989 Dec;3(14):2641-6. doi: 10.1096/fasebj.3.14.2636872.

International Journal of Biomedicine 12(4) (2022) 606-610
http://dx.doi.org/10.21103/Article12(4)_OA15

ORIGINAL ARTICLE

Dentistry

INTERNATIONAL JOURNAL OF BIOMEDICINE

Fracture Resistance of Cast Metal and Zirconia Posts on Endodontically Treated Teeth: An in Vitro Study

Tetore Olloni[1*], Gloria Staka[2]

[1]*Department of Prosthodontics, Faculty of Dentistry, "Hasan Prishtina" University*
[2]*Department of Prosthodontics, Faculty of Dentistry, "Hasan Prishtina" University*
Prishtina, Republic of Kosovo

Abstract

Background: Endodontically treated teeth are widely considered to be more susceptible to fracture than vital teeth and require specialized restorative treatment. The aim of this study was to estimate and compare the fracture resistance (FR) of endodontically treated teeth (ETT) restored with cast metal posts (CMP) and zirconia posts (ZP) with Universal Testing Machine (UTM).

Methods and Results: A total of 60 intact canines extracted for periodontal reasons were selected for the present study. The tooth samples were randomly divided into 2 groups based on the post type used for restoration. Group 1 tooth samples (n=30) were restored with CMP. Group 2 tooth samples (n-30) were restored with ZP. All the samples were subjected to compressive load using a UTM at a cross-head speed of 0.5 mm/min on the palatal slope at an angle of 135° to the long axis of the tooth. The maximum load necessary to fracture for each specimen was measured in Newtons (N). The results obtained showed that the difference in FR means between CMP and ZP was statistically significant (P<0.0001).

Conclusion: The FR of ZP was found to be significantly higher than those of CMP. The FR analysis with UTM is the only method that enables us to estimate the differences between the ETT restored with CMP and ZP.(**International Journal of Biomedicine. 2022;12(4):606-610.**).

Keywords: fracture resistance • endodontically treated teeth • zirconia posts • cast metal posts

For citation: Olloni T, Staka G. Fracture Resistance of Cast Metal and Zirconia Posts on Endodontically Treated Teeth: An in Vitro Study. International Journal of Biomedicine. 2022;12(4):606-610. doi:10.21103/Article12(4)_OA15.

Abbreviations

CMP, cast metal posts; **ETT**, endodontically treated teeth; **FR**, fracture resistance; **UTM**, Universal Testing Machine, **ZP**, zirconia posts.

Introduction

Endodontically treated teeth (ETT) are more susceptible to biomechanical failure than vital teeth against masticatory forces and may fracture more easily.[1] Additional factors attributed to the increased fracture risk are substantial loss of tooth structure with endodontic root access, bacteria-dentin interaction, and endodontic therapy itself.[2] In treating these teeth, posts are recommended to reinforce the teeth with extensive loss of coronal structure, which also supports the teeth under the action of occlusal forces along the roots and creates retention before placing a crown.[3,4]

In daily dental practice, adequate crown restoration is required to resume the function of the teeth, prevent the penetration of microorganisms through the end of the root canal, restore aesthetics and serve as an abutment in the fixed or removable prostheses.[5] The compatible modulus of elasticity of the post with radicular dentin has a significant role in avoiding root fracture.[6] The success of endodontic posts is based on biocompatibility, high tensile strength, good fitting accuracy, and adequate fatigue strength for favorable distribution of masticatory force.[7] Different types of posts have been proposed, from cast metal posts (CMP) to aesthetic ones.

***Corresponding author:** Tetore Olloni. Department of Prosthodontics, Faculty of Dentistry, "Hasan Prishtina" University, Prishtina, Republic of Kosovo. E-mail: tetore.olloni@gmail.com*

CMP have been accepted for their favorable physical properties, superior success rate, long-term prognosis, easy manipulation, and low cost.[8] These posts reproduce the morphology of the root canal with good accuracy.[9] However, reports of low biocompatibility, chances of corrosion, and root fracture, along with the failure to accomplish the desired aesthetics of the teeth, have prompted clinicians to look for another type of post for restoring the ETT.[10-13]

The use of dental posts with identical tooth color has directed attention toward the appearance of ETT.[14] Zirconia posts (ZP) are the foundation of many modern post concepts.[15] Zirconia, a ceramic biomaterial, is widely used because of its mechanical strength, chemical stability, esthetic outcomes, and high toughness. Apart from these favorable properties, there is a risk of root fracture due to a high modulus of elasticity.[16] The quality of cement is fundamental for post-resistance and retention on ETT, so the adhesive resin cement is indicated only when post-retention is severely impaired.[17,18] Adhesive resin cements have been preferred because they have been shown to increase the retention of the post [19] and the overall resistance against fracture of ETT.[20] Due to the low elastic modulus of the adhesive resin cement, it may act as a shock absorber, thus decreasing the risk of fracture of ETT. The types of posts have been explored by many authors. Therefore, this in vitro study aimed to estimate and compare the fracture resistance (FR) of ETT restored with CMP and ZP.

Materials and Methods

This study was conducted in the Prosthodontics Department at the University Dentistry Clinical Center of Kosovo with prior approval from the Ethical Committee (Protocol #4068/5.13.2021) of this institution. A total of 60 canines extracted for periodontal reasons, with a root length of 15-18 mm, were selected for the present study. The freshly extracted teeth were immediately placed in 5.25% NaOCl for 5 min and stored in 0.9% saline solution at room temperature (20-23° C). Teeth were used within 6 months after extraction.

The inclusion criteria were as follows: teeth with almost straight roots, completely formed apices and intact clinical crowns. The exclusion criteria were as follows: the presence of caries in the root, previous endodontic treatments, dental anomalies, and the presence of visible fracture lines in the root. Buccolingual and mesiodistal radiographs of all teeth were taken and examined to evaluate root integrity.

Any calculus or residual debris from the surface of the teeth was removed by ultrasonic scaling. Thereafter, teeth were stored in 0.9% normal saline for the rest of the study. All the tooth samples were sectioned 3mm above the cementoenamel junction. An adequate access cavity was prepared on all the teeth. The root canals were prepared and shaped up to the X3 file using a Protaper Next rotary file (ProTaper, Dentsply Maillefer, USA) and were irrigated with 2ml of 0.5% NaOCl solution between each file size. The remaining dentin layer was removed with 17% EDTA for 1 minute. The root canals were dried with absorbent paper points and obturated with ProTaper gutta-percha cones using a sealer (AH Plus, Dentsply Maillefer, USA) with cold lateral condensation. The access cavity was filled with a temporary restorative material (3M ESPE Cavit, Seefeld, Germany).

Post-space for all teeth was prepared after 7 days from obturation by the sequential use of Gates-Glidden and Pesso reamer size 1 up to size 4, keeping 4mm of gutta-percha as an apical seal. Then the finalized root canals were irrigated with 2.5% NaOCl, followed by normal saline, and dried with paper points. The tooth samples were randomly divided into 2 groups based on the post type used for restoration. A root canal impression for 2 groups was made by using a patterned resin (Duralay, Reliance Dental Manufacturing LLC, Alsip, USA).

Group1 tooth samples were restored with Co-Cr CMP (Ivoclar, Vivadent, Lichtenstein). Group 2 samples were restored with ZP using a monolithic block of Zirconium Oxide (2N99%) with CAD-CAM technology (Sirona Dental Systems, Germany). The posts were then sandblasted for 3-4 seconds with 50μm aluminum oxide powder and then cleaned with distilled water to improve the adhesion.

The post-space was thoroughly dried with absorbent paper points, and CMP and ZP were cemented with Adhesive Rezin Cement, Speed CEM Plus (Ivoclar, Vivadent, Lichtenstein). The cement was spun into the canals using a lentulo spiral (Lentulo; Dentsply Maillefer, Ballaigues, Switzerland). The posts were placed within the canal and held in position with moderate finger pressure. Excess cement was removed using a sable brush (Fig.1, Fig 2).

Fig. 1. *CMP and ZP.*

Fig. 2. *Resin cement injection.*

Final impressions were made for all the samples with polyvinylsiloxane impression material (Elite, Zhermarck). All teeth were restored with a full-coverage metal crown using type IV nickel-chromium (Wiron®99, BEGO Bremer Gold, Bremen, Germany). The crowns were cleaned with ethanol, dried, and cemented using type-1 glass-ionomer cement (GC Fuji I, GC America). The crowns were kept on the prepared samples under finger pressure for 30 sec, and excess cement was removed with a sharp instrument after 10 min.

Finally, each root was thinly covered with a silicone impression material to simulate the thickness of the periodontal ligament (Speedex, Light body, Coltène/Whaledent AG, Altstätten/ Switzerland).

Fracture resistance test

In order to receive the loads, samples were embedded parallel to their vertical axis in acrylic blocks. Loads were then applied using a UTM (H001B:1000kN, Matest, Italy) at a cross-head speed of 0.5mm/min on the palatal slope at an angle of 135° to the long axis of the tooth. The maximum

load necessary to fracture for each specimen was measured in Newtons (N) (Fig.3, Fig.4).

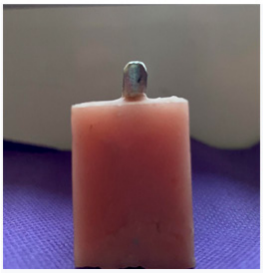

Fig. 3. *Teeth samples in acrylic block.*

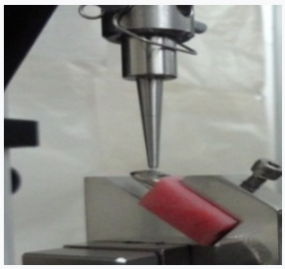

Fig. 4. *Static load application in the UTM.*

Statistical analysis was performed using statistical software package SPSS version 21.0 (SPSS Inc, Armonk, NY: IBM Corp). Data were analyzed with One-way ANOVA & Tukey's (HSD) post-hoc test. The One Sample t-Test was also applied. A probability value of $P<0.05$ was considered statistically significant.

Results

Table 1 presents descriptive statistics for CMP and ZP. In CMP and ZP, the mean FR was 141.87±13.620N and 1041.03±16.497N, respectively. A comparative analysis of the FR values between CMP and ZP groups showed that the influence of post's type on FR was significant (P=0.000) (Table 2). We have done a univariate general linear model test to which we have added Tukey's Honest Significant Difference (HSD) test to assess the significance of differences between CMP and ZP groups (Table 3). The P-value for each group comparison was less than 0.05, showing high significance (Table 3). Table 4 presents the One Sample t-Test. Thus, the difference in FR means between CMP and ZP was statistically significant (P=0.001).

Table 1.

Descriptive statistics of FR values.

Valiable	Mean	n	SD	SEM
CMP	141.87	30	13.620	2.486
ZP	1041.03	30	16.497	3.011

Table 2.

A One-Way Analysis of Variance of FR between the study groups.

	df	SS	MS	F	*P*
Between Groups	1	12127330.584	12127330.58	52997.65	0.000
Within Groups	58	13272.007	228.8277		
Total	59	12140602.59			

df- degree of freedom; SS - sum of squares; MS - mean square

Table 3.

Tukey's HSD comparison of the significance levels between the groups.

Source	Type III Sum of Squares	df	Mean Square	F	Sig.
Corrected Model	12127330.58400[a]	1	12127330.58400	5299554.774	0.000
Intercept	20989022.73067	1	20989022.73067	9172049.433	0.000
Group#	12127330.58400	1	12127330.58400	5299554.774	0.000
Error	13272.007	58	228.837		
Total	33116486.4000	60			
Corrected Total	12127463.30933	59			

a. R Squared = 1.000 (Adjusted R Squared = 1.000)

Table 4.

The One Sample t-Test.

t	df	Sig. (2-tailed)	Mean difference	95% CI for the difference	
				Lower	Upper
10.105	59	0.001	5914.5333	4743.3377	7085.7290

Discussion

The present study presented 2 posts extensively used to restore ETT and assessed their capacity to resist fracture. This study used UTM to estimate the FR of ETT restored with CMP and ZP. When analyzing the data, we focused on a significant difference between them. In this study, canines were selected as they are vulnerable to trauma because of their position.

The loading angle of 135° applied on the palatal slope was selected in order to simulate a contact angle found in Class 1 occlusion between maxillary and mandibular anterior teeth, consistent with reports of Guzy and Nikolls.[24] In our study, adhesive resin cement was used because its modulus of elasticity is comparable to dentin. A study done by Borer et al.[25] has demonstrated the successful use of adhesive resin cement, allowing for the significant chemical bonds between the dentin and the post. All samples were restored and tested with a full-coverage, cast metal crown to ensure standardization and make it more similar to the clinical situation. The crown coverage leads to an even greater distribution of masticatory forces.

In order to closely simulate the clinical situation, many studies discuss the importance of a simulated periodontal ligament.[26] Our study supports the conclusions of these studies. In our present study, each root was thinly covered with a silicone impression material to simulate the thickness of the periodontal ligament. Marchionatti et al.[27] reported that the artificial periodontal ligament had no effect on the FR of ETT when the roots were surrounded with polyvinyl siloxane. Furthermore, posts are recommended to increase the FR of ETT, and the results of our study are consistent with Kantor and

Pines,[28] and Robbins.[29] It has been reported that more rigid posts are unable to absorb stress and are, therefore, susceptible to fracture.[30,31] The present study showed a significant difference. ETT with CMP showed lower FR than ETT with ZP. The higher modulus of elasticity of CMP compared with dentin would have led to the stress concentrations and might be responsible for the fracture of ETT.[32] The result of our study contradicted the findings of Kivanç et al.,[33] in which they reported higher FR on ETT restored with CMP. Likewise, in the study by Mentik et al.,[34] the success rate of CMP was 82%. However, our results are consistent with data obtained in a study by Abduljabbar et al.,[35] which concluded that FR of ETT restored with ZP was significantly higher than ETT restored with CMP.

The observation in this study may be attributed to the fact that ZP had a higher modulus of elasticity than CMP. On the other hand, in a study by Heydecke et al.,[36] the high elastic modulus of ZP was responsible for catastrophic fractures in teeth restored with these posts. These results are supported by other studies. Rosentrit et al.[37] reported that ZP could even reinforce the tooth structure of ETT and offer better stress distribution of loads along the roots. In our present study, the ZP were custom milled, unlike in other studies, which used prefabricated ZP.[38,39] UTM is considered a valuable method to estimate the FR of ETT restored with CMP and ZP. Nevertheless, it is difficult to compare the results of this study with those of prior studies since previous studies had differences in methodology, testing procedures, and research design. The limitations of our study included the following: the static load was applied for testing samples, unlike masticatory forces. Moreover, dynamic loading, the oral environment, and temperature effects were excluded but may also be considered limitations of the study.

Finally, CMP and ZP evaluated in our study have several advantages and disadvantages. The ultimate clinical decision-making should consider the patient-related variables, such as the amount of remaining tooth structure, tooth anatomy, position, occlusion, masticatory forces, and parafunctional habits to maximize the long-term prognosis of ETT.

In conclusion, within the limitations of this study, the FR of ETT was significantly influenced by the post type. The FR of ZP was found to be significantly higher than those of CMP. The FR analysis with UTM is the only method that enables us to estimate the differences between the ETT restored with CMP and ZP. Therefore, until further studies with long-term follow-ups on CMP are available, the use of ZP with a similar elastic modulus to the dentin might provide more acceptable results in ETT.

Competing Interests

The authors declare that they have no competing interests.

References

1. Qing H, Zhu Z, Chao Y, Zhang W. In vitro evaluation of the fracture resistance of anterior endodontically treated teeth restored with glass fiber and zircon posts. J Prosthet Dent. 2007 Feb;97(2):93-8. doi: 10.1016/j.prosdent.2006.12.008.
2. Pereira JR, Neto EMR, Pamato S, Vallell AL, PaulaII VG, VidottiII HA. Fracture resistance of endodontically treated teeth restored with diferent intraradicular posts with diferent lengths. Brazilian Journal of Oral Sciences. 2013;12(1):1–4.
3. Adanir N, Belli S. Evaluation of different post lengths' effect on fracture resistance of a glass fiber post system. Eur J Dent. 2008 Jan;2(1):23-8.
4. Robbins JW, Earnest LA, Schumann SD. Fracture resistance of endodontically-treated cuspids. Am J Dent. 1993 Jun;6(3):159-61.
5. Maslamani M, Khalaf M, Mitra AK. Association of Quality of Coronal Filling with the Outcome of Endodontic Treatment: A Follow-up Study. Dent J (Basel). 2017 Jan 11;5(1):5. doi: 10.3390/dj5010005.
6. Stewardson DA, Shortall AC, Marquis PM. The effect of the elastic modulus of endodontic posts on static load failure. Int Endod J. 2011 May;44(5):458-68. doi: 10.1111/j.1365-2591.2011.01851.x.
7. Machado J, Almeida P, Fernandes S,Marques A,Vaz M. Currently used system of dental post for endodontic treatment. Procedia Structural Integrity. 2017;5: 27-33.
8. Rosenstiel SF,Land MF, Fujimoto J. Contemporary fixed prosthodontics. 4th ed. Mosby, St. Louis; 2006.
9. Akkayan B, Gülmez T. Resistance to fracture of endodontically treated teeth restored with different post systems. J Prosthet Dent. 2002 Apr;87(4):431-7. doi: 10.1067/mpr.2002.123227.
10. Glantz PO, Nilner K. The devitalized tooth as an abutment in dentitions with a reduced but healthy periodontium. Periodontol 2000. 1994 Feb;4:52-7. doi: 10.1111/j.1600-0757.1994.tb00005.x.
11. Glazer B. Restoration of endodontically treated teeth with carbon fibre posts--a prospective study. J Can Dent Assoc. 2000 Dec;66(11):613-8.
12. Luu KQ, Walker RT. Corrosion of a nonprecious metal post: a case report. Quintessence Int. 1992 Jun;23(6):389-92.
13. Meyenberg KH, Lüthy H, Schärer P. Zirconia posts: a new all-ceramic concept for nonvital abutment teeth. J Esthet Dent. 1995;7(2):73-80. doi: 10.1111/j.1708-8240.1995.tb00565.x.
14. Rosentritt M, Fürer C, Behr M, Lang R, Handel G. Comparison of in vitro fracture strength of metallic and tooth-coloured posts and cores. J Oral Rehabil. 2000 Jul;27(7):595-601. doi: 10.1046/j.1365-2842.2000.00548.x.
15. Bittner N, Hill T, Randi A. Evaluation of a one-piece milled zirconia post and core with different post-and-core systems: An in vitro study. J Prosthet Dent. 2010 Jun;103(6):369-79. doi: 10.1016/S0022-3913(10)60080-7.
16. Bateman G, Ricketts DN, Saunders WP. Fibre-based post systems: a review. Br Dent J. 2003 Jul 12;195(1):43-8; discussion 37. doi: 10.1038/sj.bdj.4810278.
17. Bonfante G, Kaizer OB, Pegoraro LF, do Valle AL. Tensile bond strength of glass fiber posts luted with different cements. Braz Oral Res. 2007 Apr-Jun;21(2):159-64. doi: 10.1590/s1806-83242007000200011.
18. Creugers NH, Käyser AF, van 't Hof MA. A meta-analysis of durability data on conventional fixed bridges. Community Dent Oral Epidemiol. 1994 Dec;22(6):448-52. doi: 10.1111/j.1600-0528.1994.tb00795.x.
19. Rosenstiel SF, Land MF, Crispin BJ. Dental luting agents: A review of the current literature. J Prosthet Dent. 1998 Sep;80(3):280-301. doi: 10.1016/s0022-3913(98)70128-3.

20. O'Keefe KL, Miller BH, Powers JM. In vitro tensile bond strength of adhesive cements to new post materials. Int J Prosthodont. 2000 Jan-Feb;13(1):47-51.
21. Mendoza DB, Eakle WS, Kahl EA, Ho R. Root reinforcement with a resin-bonded preformed post. J Prosthet Dent. 1997 Jul;78(1):10-4. doi: 10.1016/s0022-3913(97)70081-7.
22. Olcay K, Ataoglu H, Belli S. Evaluation of Related Factors in the Failure of Endodontically Treated Teeth: A Cross-sectional Study. J Endod. 2018 Jan;44(1):38-45. doi: 10.1016/j.joen.2017.08.029.
23. Saunders WP, Saunders EM. Coronal leakage as a cause of failure in root-canal therapy: a review. Endod Dent Traumatol. 1994 Jun;10(3):105-8. doi: 10.1111/j.1600-9657.1994.tb00533.x.
24. Guzy GE, Nicholls JI. In vitro comparison of intact endodontically treated teeth with and without endo-post reinforcement. J Prosthet Dent. 1979 Jul;42(1):39-44. doi: 10.1016/0022-3913(79)90328-7.
25. Borer RE, Britto LR, Haddix JE. Effect of dowel length on the retention of 2 different prefabricated posts. Quintessence Int. 2007 Mar;38(3):e164-8.
26. Kemaloglu H, Emin Kaval M, Turkun M, Micoogullari Kurt S. Effect of novel restoration techniques on the fracture resistance of teeth treated endodontically: An in vitro study. Dent Mater J. 2015;34(5):618-22. doi: 10.4012/dmj.2014-326.
27. Marchionatti AM, Wandscher VF, Broch J, Bergoli CD, Maier J, Valandro LF, Kaizer OB. Influence of periodontal ligament simulation on bond strength and fracture resistance of roots restored with fiber posts. J Appl Oral Sci. 2014 Sep-Oct;22(5):450-8. doi: 10.1590/1678-775720140067.
28. Kantor ME, Pines MS. A comparative study of restorative techniques for pulpless teeth. J Prosthet Dent. 1977 Oct;38(4):405-12. doi: 10.1016/0022-3913(77)90094-4.
29. Robbins JW. Restoration of the endodontically treated tooth. Dent Clin North Am. 2002 Apr;46(2):367-84. doi: 10.1016/s0011-8532(01)00006-4.
30. Sidoli GE, King PA, Setchell DJ. An in vitro evaluation of a carbon fiber-based post and core system. J Prosthet Dent. 1997 Jul;78(1):5-9. doi: 10.1016/s0022-3913(97)70080-5. .
31. Mannocci F, Ferrari M, Watson TF. Intermittent loading of teeth restored using quartz fiber, carbon-quartz fiber, and zirconium dioxide ceramic root canal posts. J Adhes Dent. 1999 Summer;1(2):153-8.
32. Akkayan B, Gülmez T. Resistance to fracture of endodontically treated teeth restored with different post systems. J Prosthet Dent. 2002 Apr;87(4):431-7. doi: 10.1067/mpr.2002.123227.
33. Kivanç BH, Alaçam T, Ulusoy OI, Genç O, Görgül G. Fracture resistance of thin-walled roots restored with different post systems. Int Endod J. 2009 Nov;42(11):997-1003. doi: 10.1111/j.1365-2591.2009.01609.x.
34. Mentink AG, Meeuwissen R, Käyser AF, Mulder J. Survival rate and failure characteristics of the all metal post and core restoration. J Oral Rehabil. 1993 Sep;20(5):455-61. doi: 10.1111/j.1365-2842.1993.tb01631.x.
35. Abduljabba T, Sherfudhin H, Alsaleh S, et.al. Fracture resistance of three post and core systems in endodontically treated teeth restored wit hall-ceramic crowns. King Saud University Journal of Dental Sciences. 2012;3(1):33-8.
36. Heydecke G, Butz F, Hussein A, Strub JR. Fracture strength after dynamic loading of endodontically treated teeth restored with different post-and-core systems. J Prosthet Dent. 2002 Apr;87(4):438-45. doi: 10.1067/mpr.2002.123849.
37. Rosentritt M, Fürer C, Behr M, Lang R, Handel G. Comparison of in vitro fracture strength of metallic and tooth-coloured posts and cores. J Oral Rehabil. 2000 Jul;27(7):595-601. doi: 10.1046/j.1365-2842.2000.00548.x.
38. Sorensen JA, Engelman MJ. Ferrule design and fracture resistance of endodontically treated teeth. J Prosthet Dent. 1990 May;63(5):529-36. doi: 10.1016/0022-3913(90)90070-s.
39. Butz F, Lennon AM, Heydecke G, Strub JR. Survival rate and fracture strength of endodontically treated maxillary incisors with moderate defects restored with different post-and-core systems: an in vitro study. Int J Prosthodont. 2001 Jan-Feb;14(1):58-64.

International Journal of Biomedicine 12(4) (2022) 611-616
http://dx.doi.org/10.21103/Article12(4)_OA16

ORIGINAL ARTICLE

Dentistry

INTERNATIONAL JOURNAL OF BIOMEDICINE

Serum Level of Il-2 in Patients with Type 2 Diabetes Mellitus and Periodontopathy

V. Bunjaku[1], M. Popovska[2], S. Spasovski[2], A. Spasovska-Gjorgovska[2], M. Barani[3], Sh. Mrasori[4*]

[1]UBT - Higher Education Institution, Faculty of Dentistry, Department of Oral Disease and Periodontology, Pristina, Republic Kosovo
[2]Faculty of Dentistry, University "St. Cyril and Method," Skopje, Republic of North Macedonia
[3]UBT - Higher Education Institution, Faculty of Dentistry, Department of Endodontics, Pristina, Republic Kosovo
[4]ALMA MATER EUROPEA Campus College "Rezonanca" Faculty of Dentistry, Pristina, Republic Kosovo

Abstract

The purpose of this study was to investigate the influence of low-level laser therapy (LLLT) in patients with type 2 diabetes mellitus (T2DM) and chronic periodontopathy (ChP) on serum levels of IL-2.

***Methods and Results*:** A total of 80 patients aged 35-60 years were followed; all of them had T2DM diagnosed (HbA1C≤7.5%) with ChP, where clinical attachment loss (CAL) was ≥ 4mm on at least 50% of affected teeth. All participants are divided into two groups. Group A included 40 patients who underwent conservative (non-surgical) periodontal treatment supplemented with LLLT. Group B included 40 patients who underwent only conservative therapy. Patients used oral antidiabetic medications to control glycemia: Metformin (Alkaloid, Skopje S. Macedonia) 500 mg two times a day. LLLT (Laser HF® comfort, Hager. Werken, Duisburg, Germany) was applied (660 nm, 10 mW, 8 min/day) with contact to the gingiva for five consecutive days. Serum IL-2 was determined by ELISA in 3 time intervals: at the first examination, 6 weeks, and 3 months after treatment in both groups. In Group A and Group B, at the first examination, 6 weeks after therapy, and 3 months after treatment, the serum IL-2 was 17.20±0.54 pg/ml and 17.22±0.66 pg/ml, 17.12±0.63 pg/ml and 17.17±0.63 pg/ml, and 17.03±0.64 pg/ml and 16.98±0.65 pg/ml, respectively.

In Group A, there was a significant difference between the serum IL-2 values in specified time points (first examination, 6 weeks, and 3 months after the therapy) (Friedman's ANOVA: χ^2 (n=40, df=2) = 17.22 and *P*=0.0002). In Group B, between the serum IL-2 levels, there also was a significant difference in specified time points (Friedman's ANOVA: χ^2 (n=40, df=2) = 42.33 and *P*=0.0000). The intergroup analysis, according to the temporal dynamics of the measurements, showed an evident difference between the two groups, but the serum IL-2 values in the two groups treated with and without LLLT were close, and no statistical significance was recorded between them.

Conclusion: No significant differences were recorded in the serum IL-2 levels in T2DM patients with ChP non-surgically treated with and without the application of LLLT.(**International Journal of Biomedicine. 2022;12(4):611-616.**).

Keywords: chronic periodontopathy • type 2 diabetes mellitus • IL-2 • low-level laser therapy

For citation: Bunjaku V, Popovska M, Spasovski S, Spasovska-Gjorgovska A, Barani M, Mrasori Sh. Serum Level of Il-2 in Patients with Type 2 Diabetes Mellitus and Periodontopathy. International Journal of Biomedicine. 2022;12(4):611-616. doi:10.21103/Article12(4)_OA16.

Abbreviations

ChP, chronic periodontopathy; **CAL**, clinical attachment loss; **GCF**, gingival crevicular fluid; **LLLT**, low-level laser therapy; **T2DM**, type 2 diabetes mellitus.

Introduction

Periodontal disease is a common disease in the population. It starts as gingivitis that can progress and affect the remaining structures of the periodontium, causing destructive processes, luxation, and tooth loss. The main cause of destructive inflammatory processes in the periodontium is dental plaque. The connection between plaque and the periodontium has been proven many times, and the immune response of the host has a central role.[1] However, it is considered that certain systemic diseases that have an inflammatory component can be a risk factor for periodontal disease because, through their mechanisms, they manage to change the oral microbiological environment, creating conditions for higher susceptibility to periodontopathy.[2]

During inflammation, inflammatory cytokines IL-1, IL-2, IL-8, TNF-α, and many other factors are produced, which cause an even higher inflammatory destructive reaction of the periodontium.[3]

It is considered that hyperglycemia can affect some biological pathways that stimulate the release and activation of inflammatory cytokines,[4] so poorly controlled type 2 diabetes mellitus (T2DM) negatively affects the periodontal status.[5-7] The disturbed balance between pro-inflammatory and anti-inflammatory cytokines is the cause of serious disorders in the periodontium. IL-1, IL-8, and TNF-α play a significant role in that process.[8] IL-6 can stimulate stromal cells to produce RANKL;[8,9] in contrast, IL-2 has a key role during immune homeostasis through its mediating role on T cells.[10] There is much data in the literature that confirms the connection between T2DM and periodontopathy.[11,12]

It is still a question for consideration whether diabetes affects the periodontal status or the diseased periodontium through the salivary factors and released pro-inflammatory cytokines into the gingival crevicular fluid (GCF) and worsens this systemic disease and tends toward possible complications. On the one hand, the impact of chronic periodontopathy (ChP) on the levels of glucoregulatory biomarkers in GCF[13] has been proven, and on the other hand, it is known that T2DM affects the composition of saliva and other tissue fluids that manifest in the mouth with different clinical symptomatology from the oral and periodontal aspect.[14]

In conditions of poor systemic health where T2DM and chronic periodontopathy are diagnosed, the main problem for every therapist is the choice of successful periodontal treatment. Often conventionally applied therapy is insufficient to achieve a clinical effect that would certainly regulate cytokine levels at a systemic or local level. In recent years, low-level laser therapy (LLLT) has been applied, which has been proven as an effective procedure in reducing inflammation and edema, and correcting clinical periodontal parameters.[15-17]

Histological findings of the gingival tissue treated with LLLT showed expressed healing, evident by the absence of inflammatory cells. Tissue edema could not be registered, and the number of blood vessels was reduced. Expressed collagenization and homogenization were present in the lamina propria of the gingiva.[18] Also, the correction of certain inflammatory mediators in saliva and GCF was confirmed after the application of the LLLT therapy.[19,20]

The purpose of this study was to investigate the influence of LLLT in patients with T2DM and ChP on serum levels of IL-2 as one of the inflammatory biomarkers important in the pathogenesis of periodontal disease.

Materials and Methods

We selected participants in this study by choosing suitable patients from the Department of Periodontology and Oral Diseases at the University Dental Clinical Center of Kosovo in Pristina. A total of 80 patients aged 35-60 years were followed; all of them had T2DM diagnosed (HbA1C≤7.5%) with ChP, where CAL was ≥ 4mm on at least 50% of affected teeth.

All participants are divided into two groups, A and B. Group A included 40 patients who underwent conservative (non-surgical) periodontal treatment supplemented with laser therapy. Group B included 40 patients who underwent only conservative therapy. Patients used oral antidiabetic medications to control glycemia: Metformin (Alkaloid, Skopje S. Macedonia) 500 mg two times a day. After the initial measurements and the observation of the clinical parameters, non-surgical treatment of the periodontal pockets was carried out in all study participants. Pockets were irrigated with 1% chlorhexidine gel (three times for 10 minutes). Then, LLLT was applied to the gingival part of the affected side. LLLT (Laser HF® comfort, Hager. Werken, Duisburg, Germany) was applied (660 nm, 10 mW, 8 min/day) with contact to the gingiva for five consecutive days.

To determine serum IL-2, the blood was collected after 12 hours of fasting and centrifuged for 20 minutes at 6000 rpm at 2-8°C. Serum was used for all further analyses. Serum IL-2 was determined by ELISA, based on the Biotin double antibody sandwich technology. A biotinylated detection antibody specific for Human IL-2 and Avidin-Horseradish Peroxidase (HRP) conjugate were added successively to each microplate well and incubated. The test protocol included a series of procedures that culminated in determining the optical density (OD) of each well simultaneously, using a microplate reader set at 450 nm. The OD value was proportional to the concentration of Human IL-2. Finally, a concentration of Human IL-2 in the samples was calculated by comparing the OD of the samples to the standard curve. IL-2 values in serum were determined in 3 time intervals: at the first examination, 6 weeks, and 3 months after treatment in both groups.

Statistical analysis was performed using statistical software package SPSS version 26.0 (SPSS Inc, Armonk, NY: IBM Corp). For descriptive analysis, results are presented as mean±standard deviation (SD). Student's paired t-test was applied to compare two groups for data with normal distribution. The Friedman ANOVA was used to compare three or more matched groups. A probability value of $P<0.05$ was considered statistically significant.

Ethical approval for this study was obtained from the Ethical Committee at UBT - Higher Education Institution

(Faculty of Dentistry), Pristina, Republic Kosovo. Written informed consent was obtained from all patients before inclusion in the study.

Results

Table 1 shows descriptive statistics of serum IL-2 for two study groups. In Group A and Group B, at the first examination, 6 weeks after therapy, and 3 months after treatment, the serum IL-2 was 17.20±0.54 pg/ml and 17.22±0.66 pg/ml, 17.12±0.63 pg/ml and 17.17±0.63 pg/ml, and 17.03±0.64 pg/ml and 16.98±0.65 pg/ml, respectively.

Table 1.

Serum values (pg/ml) of IL-2 in patients of two groups.

IL-2 in serum	n	Mean	Confidence -95.00%	Confidence +95.00%	Minimum	Maximum	SD
Group A							
First examination	40	17.20	17.03	17.37	16.15	18.45	0.54
6 weeks after the therapy	40	17.12	16.92	17.32	15.85	18.55	0.63
3 months after the therapy	40	17.03	16.83	17.24	15.55	18.45	0.64
Group B							
First examination	40	17.22	17.01	17.43	16.05	18.95	0.66
6 weeks after the therapy	40	17.17	16.97	17.38	16.15	18.75	0.63
3 months after the therapy	40	16.98	16.78	17.19	16.00	18.55	0.65

In Group A, there was a significant difference between the serum IL-2 values in specified time points (first examination, 6 weeks, and 3 months after the therapy) (Friedman's ANOVA: χ^2 (n=40, df=2) = 17.22 and *P*=0.0002). In Group B, between the serum IL-2 levels, there also was a significant difference in specified time points (Friedman's ANOVA: χ^2 (n=40, df=2) = 42.33 and *P*=0.0000) (Table 2).

The serum IL-2 value 6 weeks after therapy was significantly lower than at the first examination in Group A (t=2.36 and *P*=0.02), while in Group B, the difference between IL-2 levels was not significant (t=1.12 and *P*=0.27) (Table 3).

The serum IL-2 values 3 months after therapy were significantly lower than at the first examination in both groups (Group 1: t=2.50 and *P*=0.02; Group B: t=5.67 and *P*=0.00) (Table 4).

In Group A, the serum IL-2 value 3 months after therapy was slightly lower than 6 weeks after therapy (t=1.69 and *P*=0.10), while in Group B, the IL-2 level 3 months after therapy was significantly lower than 6 weeks after therapy (t=17.17 and *P*=0.000) (Table 5).

Table 2.

Differences between IL-2 values in serum in two groups at different time intervals.

IL-2 in serum	Average Rank	Sum of Ranks	Mean	SD
Group A				
First examination	2.46	98.50	17.20	0.54
6 weeks after therapy	2.00	80.00	17.12	0.63
3 months after therapy	1.54	61.50	17.03	0.64
Group B				
First examinatin	2.38	95.00	17.22	0.66
6 weeks after therapy	2.44	97.50	17.17	0.63
3 months after therapy	1.19	47.50	16.98	9.65

Table 3.

Differences in serum IL-2 values at the first examination and 6 weeks after the treatment in both groups

IL-2 in serum	Mean	SD	n	Diff.	SD Diff.	t	df	P
Group A								
First examination	17.20	0.54						
6 weeks after therapy	17.12	0.63	40	0.08	0.22	2.36	39	0.02
Group B								
First examination	17.22	0.66						
6 weeks after therapy	17.17	0.63	40	0.04	0.25	1.12	39	0.27

Table 4.

Differences in serum IL-2 values at the first examination and 3 months after the treatment in both groups

IL-2 in serum	Mean	SD	n	Diff.	SD Diff.	t	df	P
Group A								
First examination	17.20	0.54						
3 months after therapy	17.03	0.64	40	0.17	0.42	2.50	39	0.02
Group B								
First examination	17.22	0.66						
3 months after therapy	16.98	0.65	40	0.23	0.26	5.67	39	0.00

The intergroup analysis, according to the temporal dynamics of the measurements, showed an evident difference

between the two groups, but the serum IL-2 values in the two groups treated with and without LLLT were close, and no statistical significance was recorded between them.

Table 5.

Differences in serum IL-2 values 6 weeks and 3 months after the treatment in both groups

IL-2 in serum	Mean	SD	n	Diff.	SD Diff.	t	df	P
Group A								
6 weeks after therapy	17.12	0.63						
3 months after therapy	17.03	0.64	40	0.08	0.31	1.69	39	0.10
Group B								
6 weeks after therapy	17.17	0.63						
3 months after therapy	16.98	0.65	40	0.19	0.07	17.17	39	0.000

Discussion

The high-quality standard in the therapy of periodontal disease is the non-surgical treatment of the periodontium, which includes curettage of the soft wall of the periodontal pocket, removal of necrotic cementum, subgingival concretions from the root of the tooth and elimination of the complete contents (exudate, dental plaque, detritus, and microorganisms).[21] With mechanical instrumentation, there is a qualitative and quantitative change in the oral microbial flora,[22,23] which in turn results in a reduction of bacterial toxins and enzymes that change the level of local and systemic inflammatory mediators.[24] In conditions of good systemic health without comorbidities, the irritating local factors can be the cause of inflammation and destruction of the periodontium due to releasing the pro-inflammatory cytokines. Systemic diseases are an additional cause of deterioration of clinical and cytokine findings. Namely, the disturbed balance between pro- and anti-inflammatory cytokines and the immune response can be the cause of periodontal damage.[25] This study showed that serum IL-2 values in 2TDM patients treated with and without LLLT at all investigated time intervals (at 6 weeks and 3 months) after non-surgical periodontal treatment were not statistically significant. Namely, hyperglycemia, among others, affects the glycation pathway, thereby potentiating the release of inflammatory mediators at the systemic level,[26] also reflecting on the oral and periodontal tissues.

Our findings agree with the data obtained from Koçak's study.[27] But the non-surgical treatment was expected to correct the IL-2 levels, which it did after 6 weeks and 3 months in both groups. In Group A, there was a significant difference between the serum IL-2 values (first examination, 6 weeks, and 3 months after the therapy) (Friedman's ANOVA: χ^2 (n=40, df=2)=17.22 and *P*=0.0002). In Group B, between the serum IL-2 levels, there also was a significant difference in specified time points (Friedman's ANOVA: χ^2 (n=40, df=2)=42.33 and *P*=0.0000).

The authors who determined the serum biomarkers agree with these findings and confirmed that conventionally applied therapy is associated with systemic and local reduction of inflammatory markers.[28,29] In Group A, the serum IL-2 value 3 months after therapy was slightly lower than 6 weeks after therapy (t=1.69 and *P*=0.10), while in Group B, the IL-2 level 3 months after therapy was significantly lower than 6 weeks after therapy (t=17.17 and *P*=0.000).

Our results point to the fact that LLLT has no effect on the serum levels of IL-2, which has an important immune-regulatory role, promotes the growth and development of peripheral immune cells during the initiation of the (defensive) immune response, and keeps them alive as effector cells.

Researchers suggest that LLLT reduces gingival inflammation when applied as an adjunct to non-surgical treatment, calms gingival inflammation, and corrects the depth of periodontal pockets due to the anti-inflammatory, analgesic, and bio-stimulating effects.[30,31] Stadler et al.[32] registered a correction of IL-1β, IL-17, and IL-4 in GCF. The values of IL-1β and TNF-α have significantly reduced independently of blood glycemia and diabetic status in patients treated only conservatively.[33] Non-surgical periodontal treatment resulted in reduced salivary values of IL-1β and TNF-α.[34]

Based on the obtained findings and the data from several studies that showed a significant reduction of individual markers in GCF and saliva, we approach the fact that periodontal treatment effectively corrects biomarkers in local oral fluids (GCF and saliva) but not at the systemic level (serum). These changes in the oral medium are manifested through clinical improvements of the periodontium that can be partially explained by the normalization of homeostasis in tissue metabolism and inhibition of mast cell degranulation, where immune changes are in focus.

In conclusion, in our study, no significant differences were recorded in the serum IL-2 levels in T2DM patients with ChP non-surgically treated with and without the application of LLLT.

Competing Interests

The authors declare that they have no competing interests.

References

1. Graves DT, Corrêa JD, Silva TA. The Oral Microbiota Is Modified by Systemic Diseases. J Dent Res. 2019 Feb;98(2):148-156. doi: 10.1177/0022034518805739.
2. Jepsen S, Caton JG, Albandar JM, Bissada NF, Bouchard P, Cortellini P, Demirel K, de Sanctis M, Ercoli C, Fan J,

***Corresponding author**: Prof. Ass. Dr. Sh. Mrasori, PhD. ALMA MATER EUROPEA Campus College "Rezonanca "Faculty of Dentistry, Pristina, Republic Kosovo. E-mail: shefqetmrasori@gmail.com*

Geurs NC, Hughes FJ, Jin L, Kantarci A, Lalla E, Madianos PN, Matthews D, McGuire MK, Mills MP, Preshaw PM, Reynolds MA, Sculean A, Susin C, West NX, Yamazaki K. Periodontal manifestations of systemic diseases and developmental and acquired conditions: Consensus report of workgroup 3 of the 2017 World Workshop on the Classification of Periodontal and Peri-Implant Diseases and Conditions. J Clin Periodontol. 2018 Jun;45 Suppl 20:S219-S229. doi: 10.1111/jcpe.12951.

3. Das A, Sinha M, Datta S, Abas M, Chaffee S, Sen CK, Roy S. Monocyte and macrophage plasticity in tissue repair and regeneration. Am J Pathol. 2015 Oct;185(10):2596-606. doi: 10.1016/j.ajpath.2015.06.001.

4. Rabelo MS, Gomes GH, Foz AM, Stadler AF, Cutler CW, Susin C, Romito GA. Short-term effect of non-surgical periodontal treatment on local and systemic cytokine levels: Role of hyperglycemia. Cytokine. 2021 Feb;138:155360. doi: 10.1016/j.cyto.2020.155360.

5. Preshaw PM, Alba AL, Herrera D, Jepsen S, Konstantinidis A, Makrilakis K, Taylor R. Periodontitis and diabetes: a two-way relationship. Diabetologia. 2012 Jan;55(1):21-31. doi: 10.1007/s00125-011-2342-y.

6. Atieh MA, Faggion CM Jr, Seymour GJ. Cytokines in patients with type 2 diabetes and chronic periodontitis: A systematic review and meta-analysis. Diabetes Res Clin Pract. 2014 May;104(2):e38-45. doi: 10.1016/j.diabres.2014.02.002.

7. Teshome A, Yitayeh A. The effect of periodontal therapy on glycemic control and fasting plasma glucose level in type 2 diabetic patients: systematic review and meta-analysis. BMC Oral Health. 2016 Jul 30;17(1):31. doi: 10.1186/s12903-016-0249-1.

8. Sell AM, de Alencar JB, Visentainer JEL, Silva CO. Immunopathogenesis of Chronic Periodontitis. In: Periodontitis—A Useful Reference. InTech. 2017. doi: 10.5772/intechopen.69045

9. Tomás I, Arias-Bujanda N, Alonso-Sampedro M, Casares-de-Cal MA, Sánchez-Sellero C, Suárez-Quintanilla D, Balsa-Castro C. Cytokine-based Predictive Models to Estimate the Probability of Chronic Periodontitis: Development of Diagnostic Nomograms. Sci Rep. 2017 Sep 14;7(1):11580. doi: 10.1038/s41598-017-06674-2.

10. Arenas-Ramirez N, Woytschak J, Boyman O. Interleukin-2: Biology, Design and Application. Trends Immunol. 2015 Dec;36(12):763-777. doi: 10.1016/j.it.2015.10.003.

11. Taylor GW. Bidirectional interrelationships between diabetes and periodontal diseases: an epidemiologic perspective. Ann Periodontol. 2001 Dec;6(1):99-112. doi: 10.1902/annals.2001.6.1.99.

12. Lalla E, Papapanou PN. Diabetes mellitus and periodontitis: a tale of two common interrelated diseases. Nat Rev Endocrinol. 2011 Jun 28;7(12):738-48. doi: 10.1038/nrendo.2011.106.

13. Mohamed HG, Idris SB, Mustafa M, Ahmed MF, Åstrøm AN, Mustafa K, Ibrahim SO. Impact of Chronic Periodontitis on Levels of Glucoregulatory Biomarkers in Gingival Crevicular Fluid of Adults with and without Type 2 Diabetes. PLoS One. 2015 May 20;10(5):e0127660. doi: 10.1371/journal.pone.0127660.

14. Abd-Elraheem SE, El Saeed AM, Mansour HH. Salivary changes in type 2 diabetic patients. Diabetes Metab Syndr. 2017 Dec;11 Suppl 2:S637-S641. doi: 10.1016/j.dsx.2017.04.018.

15. Bunjaku V , Mrasori Sh, Grcev A, Rusevska B , Kameri A , Murtezani A , Sllamniku Z, Dragidella F. Effect of scaling, root planning and subsequent low-level laser therapy on C-reactive protein (CRP) and glycosylated haemoglobin (HbA1c) serum level in type 2 diabetes patients with chronic periodontitis. Medicus. 2017;22 (2): 147 -153.

16. Bunjaku V, Popovska M, Grcev A, Mrasori S, Kameri A, Sllamniku Z, Dragidella F. Non-surgical Periodontal Treatment and Low Level Laser Therapy (LLLT) Outcomes for Patients Suffering from Type 2 Diabetes Mellitus, Obesity and Chronic Periodontitis. Journal of International Dental and Medical Research. 2017;10(2):214-221.

17. Obradović R, Kesić L, Mihailović D, Jovanović G, Antić S, Brkić Z. Low-level lasers as an adjunct in periodontal therapy in patients with diabetes mellitus. Diabetes Technol Ther. 2012 Sep;14(9):799-803. doi: 10.1089/dia.2012.0027.

18. Obradović R, Kesić L, Mihailović D, Antić S, Jovanović G, Petrović A, Peševska S. A histological evaluation of a low-level laser therapy as an adjunct to periodontal therapy in patients with diabetes mellitus. Lasers Med Sci. 2013 Jan;28(1):19-24. doi: 10.1007/s10103-012-1058-7.

19. Mrasori S, Popovska M, Rusevska B, Shkreta M, Selani A, Bunjaku V. Effects of Low Level Laser Therapy (LLLT) on Serum Values of Interleukin 6 (IL-6) in Patients with Periodontitis and Type 2 Diabetes Mellitus (T2DM). Acta Inform Med. 2021 Mar;29(1):59-64. doi: 10.5455/aim.2021.29.59-64.

20. Bunjaku V, Popovska M, Todoroska S, Rusevska B, Cana A, Spasovski S, Spasovska-Gjorgovska A. The Role Of TNF-A in Saliva and Gingival Fluid in Patients with Chronic Periodontitis and Type 2 Diabetes Mellitus. Journal of International Dental and Medical Research 2021; 14(2): 671-679.

21. Ren C, McGrath C, Jin L, Zhang C, Yang Y. The effectiveness of low-level laser therapy as an adjunct to non-surgical periodontal treatment: a meta-analysis. J Periodontal Res. 2017 Feb;52(1):8-20. doi: 10.1111/jre.12361.

22. Diaz PI. Microbial diversity and interactions in subgingival biofilm communities. Front Oral Biol. 2012;15:17-40. doi: 10.1159/000329669.

23. Griffen AL, Beall CJ, Campbell JH, Firestone ND, Kumar PS, Yang ZK, Podar M, Leys EJ. Distinct and complex bacterial profiles in human periodontitis and health revealed by 16S pyrosequencing. ISME J. 2012 Jun;6(6):1176-85. doi: 10.1038/ismej.2011.191.

24. D'Aiuto F, Orlandi M, Gunsolley JC. Evidence that periodontal treatment improves biomarkers and CVD outcomes. J Periodontol. 2013 Apr;84(4 Suppl):S85-S105. doi: 10.1902/jop.2013.134007.

25. Garlet GP. Destructive and protective roles of cytokines in periodontitis: a re-appraisal from host defense and tissue destruction viewpoints. J Dent Res. 2010 Dec;89(12):1349-63. doi: 10.1177/0022034510376402.

26. Donath MY, Shoelson SE. Type 2 diabetes as an inflammatory disease. Nat Rev Immunol. 2011 Feb;11(2):98-107. doi: 10.1038/nri2925.

27. Koçak E, Sağlam M, Kayış SA, Dündar N, Kebapçılar L, Loos BG, Hakkı SS. Nonsurgical periodontal therapy with/without diode laser modulates metabolic control of type 2

diabetics with periodontitis: a randomized clinical trial. Lasers Med Sci. 2016 Feb;31(2):343-53. doi: 10.1007/s10103-016-1868-0.
28. Giannopoulou C, Cappuyns I, Cancela J, Cionca N, Mombelli A. Effect of photodynamic therapy, diode laser, and deep scaling on cytokine and acute-phase protein levels in gingival crevicular fluid of residual periodontal pockets. J Periodontol. 2012 Aug;83(8):1018-27. doi: 10.1902/jop.2011.110281.
29. Sanz I, Alonso B, Carasol M, Herrera D, Sanz M. Nonsurgical treatment of periodontitis. J Evid Based Dent Pract. 2012 Sep;12(3 Suppl):76-86. doi: 10.1016/S1532-3382(12)70019-2.
30. Saygun I, Karacay S, Serdar M, Ural AU, Sencimen M, Kurtis B. Effects of laser irradiation on the release of basic fibroblast growth factor (bFGF), insulin like growth factor-1 (IGF-1), and receptor of IGF-1 (IGFBP3) from gingival fibroblasts. Lasers Med Sci. 2008 Apr;23(2):211-5. doi: 10.1007/s10103-007-0477-3.
31. Qadri T, Bohdanecka P, Tunér J, Miranda L, Altamash M, Gustafsson A. The importance of coherence length in laser phototherapy of gingival inflammation: a pilot study. Lasers Med Sci. 2007 Nov;22(4):245-51. doi: 10.1007/s10103-006-0439-1.
32. Stadler AF, Angst PD, Arce RM, Gomes SC, Oppermann RV, Susin C. Gingival crevicular fluid levels of cytokines/chemokines in chronic periodontitis: a meta-analysis. J Clin Periodontol. 2016 Sep;43(9):727-45. doi: 10.1111/jcpe.12557.
33. Navarro-Sanchez AB, Faria-Almeida R, Bascones-Martinez A. Effect of non-surgical periodontal therapy on clinical and immunological response and glycaemic control in type 2 diabetic patients with moderate periodontitis. J Clin Periodontol. 2007 Oct;34(10):835-43. doi: 10.1111/j.1600-051X.2007.01127.x.
34. Kaushik R, Yeltiwar RK, Pushpanshu K. Salivary interleukin-1β levels in patients with chronic periodontitis before and after periodontal phase I therapy and healthy controls: a case-control study. J Periodontol. 2011 Sep;82(9):1353-9. doi: 10.1902/jop.2011.100472.

International Journal of Biomedicine 12(4) (2022) 617-621
http://dx.doi.org/10.21103/Article12(4)_OA17

ORIGINAL ARTICLE

Dentistry

INTERNATIONAL JOURNAL OF BIOMEDICINE

Connectivity between Frequency of Toothbrushing and Dental Caries

Valmira Maxhuni Bajgora[1], Agim Begzati[1], Lindita Maxhuni Thaçi[2*]

[1]*Department of Pediatric Dentistry, School of Dentistry, Medical Faculty, University of Prishtina, Prishtina, Kosovo*
[2]*Department of Human Ecology National Institute of Public Health, School of Medicine, Medical Faculty, University of Prishtina, Prishtina, Kosovo*

Abstract

The goal of this research was to evaluate the oral health of the children of the Roma, Ashkali, and Egyptian (RAE) community in relation to toothbrushing frequency.

***Methods and Results*:** A total of 201 children (93 boys and 108 girls) participated in this research. The decayed, missing, and filled teeth (DMFT) index of deciduous teeth and the simplified oral hygiene index (OHI-S) developed by Greene and Vermillion were evaluated in relation to toothbrushing frequency. Our research revealed an important and significant difference in toothbrushing frequency between the variables for F=3.7839 and *P*=0.0244. Children who brushed their teeth twice a day had a markedly lower DMFT index (3.15±3.29) than children who brushed their teeth less than once a day (4.86±3.81). Also, this group of children for *P*=0.02 had a markedly lower DMFT index (3.15±3.29) than children who brushed their teeth once a day (4.86±3.81). An important and significant difference was found between plaque index (PI) and toothbrushing frequency (H=7.86, *P*=0.02).

Conclusion: Difficult economic circumstances and poor oral hygiene are the main factors causing poor oral health in this group of children.(**International Journal of Biomedicine. 2022;12(4):617-621.**).

Keywords: dental caries • oral hygiene • plaque index • toothbrushing

For citation:Bajgora VM, Begzati A, Thaçi LM. Connectivity between Frequency of Toothbrushing and Dental Caries. International Journal of Biomedicine. 2022;12(4):617-621. doi:10.21103/Article12(4)_OA17

Abbreviations

DMFT, the decayed, missing, and filled teeth; **OHI-S**, the simplified oral hygiene index; **PI**, plaque index.

Introduction

Dental caries is a chronic disease and one of the most common global oral health problems. According to the World Health Organization, poor oral health may significantly affect general health and quality of life. Additionally, some oral diseases are related to chronic diseases.(1) Dental caries is the main oral health problem in most industrialized countries, affecting 60%–90% of school children and the majority of adults.(2)

Dental caries is the most widespread human disease, which not only causes disorders in dento-oral function because of its complications, but, when not treated at the right time, also seriously affects the quality of life.

Dental caries causes tooth decay as a result of bacterial activity. The color of the attacked tooth changes from yellow to black. If precautions are not taken early, inflammation occurs around the tooth leading to tooth loss or even the formation of an abscess. Dental caries is caused by specific types of bacteria that produce acids that destroy the enamel and dentin of the tooth. Different types of bacteria that normally live in the human mouth form a sticky film called dental plaque on the tooth. The plaque also contains saliva, food residues, and other natural substances. It can easily form in areas that are poorly cleaned.

The appearance of a caries lesion is determined by the coexistence of three main factors: acidogenic and acidophilic microorganisms, carbohydrates derived from the diet, and host factors.

The occurrence of dental caries is influenced by three main factors: bacterial load, susceptible tooth surface, and diet.(3) Cultural and hygiene habits are also important factors that affect the prevalence of caries.(4)

Our research focused on the Roma, Ashkali, and Egyptian (RAE) community, which has a history of being discriminated against and is one of the poorest and most disadvantaged communities in Kosovo. The RAE community has one of the poorest prospects for a better life.[5]

According to Kosovo's official statistics, there are about 8824 Roma citizens.[6] The Ashkali community is the biggest of the three communities discussed here, consisting of 15,436 citizens.[7] The Egyptian community has 11,524 members.[8] Difficult economic conditions adversely affect the health of RAE community members.[9] There is some evidence that dental caries is one of the main indicators of socioeconomic inequality.[10,11]

The goal of this research was to evaluate the oral health of the children of the RAE community in relation to toothbrushing frequency.

Materials and Methods

Ethical approval for this study was obtained from the Ethical Committee of the Medical Faculty of the University of Prishtina, Kosovo (Ref. №2602). Written informed consent was obtained from the child's parents.

A total of 201 children (93 boys and 108 girls) participated in this research. The decayed, missing, and filled teeth (DMFT) index of deciduous teeth and the simplified oral hygiene index (OHI-S) developed by Greene and Vermillion were evaluated in relation to toothbrushing frequency. Children with infectious diseases, disabled children, and uncooperative children were excluded from the study.

Clinical oral health assessment methodology

The research was conducted in primary schools, family medical centers, and other organizations where children from the RAE community were in attendance.

Dental probes, dental mirrors, and natural and artificial light sources were used for this examination. Clinical oral health status was measured using the DMFT index for deciduous teeth according to the WHO guidelines.[12]

The OHI[13] determines the presence of dental plaque on a scale of 0 to 3. Plaque is evaluated using an exploratory probe.

The index includes only six representative sites:

- the vestibular surfaces of the first maxillary molars of the right and left sides
- the vestibular surfaces of the right maxillary central incisor and the permanent left central mandibular incisor
- the lingual surfaces of the first mandibular molars

Criteria for classifying debris were as follows: 0 = no debris or stain; 1 = soft debris covering no more than one-third of the tooth surface; 2 = soft debris covering more than one-third, but no more than two-thirds, of the exposed tooth surface; and 3 = soft debris covering more than two-thirds of the exposed tooth surface.

Statistical analysis was performed using statistical software package SPSS version 21.0 (SPSS Inc, Armonk, NY: IBM Corp). For descriptive analysis, results are presented as mean (M) ± standard deviation (SD). The Kruskal-Wallis H test/one way ANOVA was used to compare three or more groups. The LSD test was used to make direct comparisons between two means from two individual groups. A probability value of $P<0.05$ was considered statistically significant.

Results

The data presented in Table 1 refer to DMFT index values in relation to toothbrushing frequency. For children who brushed their teeth only once a day, the DMFT index was 4.30±3.25. For children who brushed their teeth twice a day, this value was 3.15±3.29, whereas for children who brushed their teeth less than once a day, this value was 4.86±3.81.

Table 1.

The DMFT index and toothbrushing frequency.

Toothbrushing frequency	Mean	n	SD	Statistics (ANOVA)
Once a day	4.30	91	3.25	F=3.7839 *P*=0.0244
Less than once a day	4.86	22	3.81	
Twice a day	3.15	88	3.29	
Total	3.86	201	3.38	

Table 2 shows the differences in DMFT index values with toothbrushing frequency as an independent variable. For H=7.01 and *P*=0.03, an important and significant difference was found between the DMFT index and toothbrushing frequency. For F=3.79 and *P*=0.02, an important and significant difference between the variables was found.

Table 2.

Difference/DMFT index and toothbrushing frequency.

Toothbrushing frequency	Code	n	Rank in total
Less than once a day	1	22	2546.00
Once a day	2	91	9907.50
Twice a day	3	88	7847.50

Table 3 presents the data of Least Significant Difference (LSD) test. For *P*=0.03, children who brushed their teeth twice a day had a markedly lower DMFT index (M=3.15) than children who brushed their teeth less than once a day (M=4.86). This group of children also, for *P*=0.02, had a markedly lower DMFT index (M=3.15) than children who brushed their teeth only once a day (M=4.86). The results presented in Table 4 refer to PI values in relation to toothbrushing frequency. Children who brushed their teeth once a day had PI of 2.30±0.78. PI was 2.17±0.73 in children who brushed their teeth twice a day, and 2.57±0.51 in children who brushed their teeth less than once a day. The differences in PI values in correlation with toothbrushing frequency as an independent

variable are presented in Table 5. As for H=7.86 and *P*=0.02, an important and significant difference was found between PI and toothbrushing frequency.

Table 3.

The DMFT index and toothbrushing frequency. LSD test.

Toothbrushing frequency	{1} M=4.86	{2} M=4.30	{3} M=3.15
Once a day		0.47	0.03
Less than once a day	0.47		0.02
Twice a day	0.03	0.02	

Table 4.

Plaque index and toothbrushing frequency.

Toothbrushing frequency	Plaque index		
	Mean	n	SD
Once a day	2.30	91	0.78
Less than once a day	2.57	22	0.51
Twice a day	2.17	88	0.73
Total	2.27	201	0.74

Table 5.

Difference / plaque index and toothbrushing frequency.

Plaque index	Code	n	Rank summary
Not even once	1	22	2787.50
Once a day	2	91	9566.50
Twice a day	3	88	7947.00

Table 6.

Multiple comparisons of P-values (2-tailed) for plaque index and toothbrushing frequency.

Plaque index	Less than once R: 126.70	Once a day R: 105.13	Twice a day R: 90.31
Less than once		0.36	0.03
Once a day	0.36		0.27
Twice a day	0.03	0.27	

Multiple comparisons are presented in Table 6. Children who brushed their teeth twice a day (R: 90.31), for *P*=0.03, had a notably lower PI than children who brushed their teeth less than once a day (R: 126.70).

Discussion

Previous research established that high dental disease levels were related to differences in culture,[14] low income,[15] low education level,[16] low level of dental health knowledge,[17] inadequate oral hygiene,[18] fewer dental visits,[19] and high consumption of cariogenic food.[20]

The prevention of dental caries requires good oral hygiene, a healthy diet, limited cariogenic food, and more frequent stomatological control via regular dental visits starting at an early age. Risk factors include toothbrushing less than twice a day, frequent consumption of food rich in carbohydrates, low education level of parents, and low economic income.[21-23]

Two variables were continuously studied in relation to oral hygiene: toothbrushing frequency and the presence of dental plaque. Because dental plaque is considered to be an etiological agent of dental caries, some studies established that dental plaque control is one of the main factors in dental caries prevention, and that plaque can also be used as an indicator of oral hygiene status.

Toothbrushing with toothpaste rich in fluoride is one of the most important habits for improving oral health.

Our research revealed an important and significant difference in toothbrushing frequency between the variables for F=3.7839 and *P*=0.0244. Children who brushed their teeth twice a day had a markedly lower DMFT index (3.15±3.29) than children who brushed their teeth less than once a day (4.86±3.81). Also, this group of children for *P*=0.02 had a markedly lower DMFT index (3.15±3.29) than children who brushed their teeth once a day (4.86±3.81). Thus, our results confirm that children who brushed their teeth more frequently had lower caries prevalence.

The findings of our research showing that dental caries are related to socioeconomic conditions are consistent with several other studies conducted in other countries.[24-30] The research conducted by Leske et al.,[31] Stecksén-Blicks and Gustafsson,[32] Chesters et al.,[33] Pine et al.,[34] and Stecksén-Blicks et al.[35] were also consistent with our results. On the contrary, the research conducted by Dale,[36] Town,[37] and Etty et al.[38] showed a weak or absent relationship between toothbrushing frequency and dental caries.

An important and significant difference was also found in the OHI for H=7.86 and *P*=0.03. Children who brushed their teeth twice a day (R: 90.31), for *P*=0.03, had a markedly lower PI than children who brushed their teeth less than once a day. Our results are consistent with the results of a study conducted by Mazhari et al.[39] and Saurabh et al.[40]

In conclusion, given that the children of the RAE community live in difficult social and economic circumstances, we consider preventive programs with a special focus on children with relatively poor oral health should be implemented as a high priority.

Acknowledgments

We thank Helen Jeays, BDSc AE, from Edanz (www.edanz.com/ac) for editing a draft of this manuscript.

Competing Interests

The authors declare that they have no competing interests.

References

1. Petersen PE, Bourgeois D, Ogawa H, Estupinan-Day S, Ndiaye C. The global burden of oral diseases and risks to oral health. Bull World Health Organ. 2005 Sep;83(9):661-9.
2. Gilchrist F, Marshman Z, Deery C, Rodd HD. The impact of dental caries on children and young people: what they have to say? Int J Paediatr Dent. 2015 Sep;25(5):327-38. doi: 10.1111/ipd.12186.
3. Struzycka I. The oral microbiome in dental caries. Pol J Microbiol. 2014;63(2):127-35.
4. Petersen PE. Challenges to improvement of oral health in the 21st century--the approach of the WHO Global Oral Health Programme. Int Dent J. 2004 Dec;54(6 Suppl 1):329-43. doi: 10.1111/j.1875-595x.2004.tb00009.x.
5. Osce.Pasqyrë e komunitetit rom, ashkali dhe egjiptian të kosovës (2020; p. 4). Available online: https://www.osce.org/files/f/documents/c/c/443590_2.pdf .
6. Qendra Evropiane për Çështje të Minoriteteve në Kosovë. Community Profile: Roma Community (2020). Available online: http://www.ecmikosovo.org/uploads/Romacommunity1.pdf.
7. Qendra Evropiane për Çështje të Minoriteteve në Kosovë. Community Profile: Ashkali Community (2020). Available online: http://www.ecmikosovo.org/uploads/Ashkalicommunity1.pdf
8. Qendra Evropiane për Çështje të Minoriteteve në Kosovë. Community Profile: Egyptian Community (2020). Available online: http://www.ecmikosovo.org/uploads/Egyptiancommunity1.pdf
9. Draft Kosovo Program for Gender Equality. Available online: http://www.kryeministriks.net/repository/docs/Draft_Strategjia_per_integrimin_e_komuniteteve_2016-2020_.pdf
10. Baggio S, Abarca M, Bodenmann P, Gehri M, Madrid C. Early childhood caries in Switzerland: a marker of social inequalities. BMC Oral Health. 2015 Jul 22;15:82. doi: 10.1186/s12903-015-0066-y.
11. Zhou Y, Lin HC, Lo EC, Wong MC. Risk indicators for early childhood caries in 2-year-old children in southern China. Aust Dent J. 2011 Mar;56(1):33-9. doi: 10.1111/j.1834-7819.2010.01280.x
12. WHO: Oral Health Country, Area Profile Programme Oral Hygiene Indices. Available online: http:/www.whocollob.od.mah.se/expl/ohiintrod.html.
13. GREENE JC, VERMILLION JR. THE SIMPLIFIED ORAL HYGIENE INDEX. J Am Dent Assoc. 1964 Jan;68:7-13. doi: 10.14219/jada.archive.1964.0034.
14. Hilton IV, Stephen S, Barker JC, Weintraub JA. Cultural factors and children's oral health care: a qualitative study of carers of young children. Community Dent Oral Epidemiol. 2007 Dec;35(6):429-38. doi: 10.1111/j.1600-0528.2006.00356.x.
15. Monaghan N, Heesterman R. Dental caries, social deprivation and enhanced capitation payments for children. Br Dent J. 1999 Mar 13;186(5):238-40. doi: 10.1038/sj.bdj.4800074.
16. Kinirons M, McCabe M. Familial and maternal factors affecting the dental health and dental attendance of preschool children. Community Dent Health. 1995 Dec;12(4):226-9.
17. Szatko F, Wierzbicka M, Dybizbanska E, Struzycka I, Iwanicka-Frankowska E. Oral health of Polish three-year-olds and mothers' oral health-related knowledge. Community Dent Health. 2004 Jun;21(2):175-80.
18. Jose B, King NM. Early childhood caries lesions in preschool children in Kerala, India. Pediatr Dent. 2003 Nov-Dec;25(6):594-600.
19. Gratrix D, Taylor GO, Lennon MA. Mothers' dental attendance patterns and their children's dental attendance and dental health. Br Dent J. 1990 Jun 9;168(11):441-3. doi: 10.1038/sj.bdj.4807233.
20. Tsai AI, Chen CY, Li LA, Hsiang CL, Hsu KH. Risk indicators for early childhood caries in Taiwan. Community Dent Oral Epidemiol. 2006 Dec;34(6):437-45. doi: 10.1111/j.1600-0528.2006.00293.x.
21. Petersen PE. The World Oral Health Report 2003: continuous improvement of oral health in the 21st century--the approach of the WHO Global Oral Health Programme. Community Dent Oral Epidemiol. 2003 Dec;31 Suppl 1:3-23. doi: 10.1046/j..2003.com122.x.
22. Dusseldorp E, Kamphuis M, Schuller A. Impact of lifestyle factors on caries experience in three different age groups: 9, 15, and 21-year-olds. Community Dent Oral Epidemiol. 2015 Feb;43(1):9-16. doi: 10.1111/cdoe.12123.
23. Mejàre I, Axelsson S, Dahlén G, Espelid I, Norlund A, Tranæus S, Twetman S. Caries risk assessment. A systematic review. Acta Odontol Scand. 2014 Feb;72(2):81-91. doi: 10.3109/00016357.2013.822548.
24. Chu CH, Fung DS, Lo EC. Dental caries status of preschool children in Hong Kong. Br Dent J. 1999 Dec 11;187(11):616-20; discussion 605. doi: 10.1038/sj.bdj.4800347.
25. Davenport ES. Caries in the preschool child: aetiology. J Dent. 1990 Dec;18(6):300-3. doi: 10.1016/0300-5712(90)90127-z.
26. Blinkhorn AS. The caries experience and dietary habits of Edinburgh nursery school children. Br Dent J. 1982 Apr 6;152(7):227-30. doi: 10.1038/sj.bdj.4804790.
27. Wei SH, Holm AK, Tong LS, Yuen SW. Dental caries prevalence and related factors in 5-year-old children in Hong Kong. Pediatr Dent. 1993 Mar-Apr;15(2):116-9.
28. Holm AK, Blomquist HK, Crossner CG, Grahnén H, Samuelson G. A comparative study of oral health as related to general health, food habits and socioeconomic conditions of 4-year-old Swedish children. Community Dent Oral Epidemiol. 1975 Feb;3(1):34-9. doi: 10.1111/j.1600-0528.1975.tb00276.x.
29. Stecksen-Blicks C, Holm AK. Between-meal eating, toothbrushing frequency and dental caries in 4-year-old children in the north of Sweden. Int J Paediatr Dent. 1995 Jun;5(2):67-72. doi: 10.1111/j.1365-263x.1995.tb00167.x.
30. Holm AK. Caries in the preschool child: international trends. J Dent. 1990 Dec;18(6):291-5. doi: 10.1016/0300-5712(90)90125-x.

***Corresponding author**: Lindita Maxhuni Thaçi, Department of Human Ecology, National Institute of Public Health, School of Medicine, Medical Faculty, University of Prishtina. Prishtina, Kosovo. E- mail: lindita.maxhuni@uni-pr.edu*

31. Leske GS, Ripa LW, Barenie JT. Comparisons of caries prevalence of children with different daily toothbrushing frequencies. Community Dent Oral Epidemiol. 1976 May;4(3):102-5. doi: 10.1111/j.1600-0528.1976.tb02107.x.
32. Stecksén-Blicks C, Gustafsson L. Impact of oral hygiene and use of fluorides on caries increment in children during one year. Community Dent Oral Epidemiol. 1986 Aug;14(4):185-9. doi: 10.1111/j.1600-0528.1986.tb01530.x.
33. Chesters RK, Huntington E, Burchell CK, Stephen KW. Effect of oral care habits on caries in adolescents. Caries Res. 1992;26(4):299-304. doi: 10.1159/000261456.
34. Pine CM, McGoldrick PM, Burnside G, Curnow MM, Chesters RK, Nicholson J, Huntington E. An intervention programme to establish regular toothbrushing: understanding parents' beliefs and motivating children. Int Dent J. 2000;Suppl Creating A Successful:312-23. doi: 10.1111/j.1875-595x.2000.tb00581.x.
35. Stecksén-Blicks C, Sunnegårdh K, Borssén E. Caries experience and background factors in 4-year-old children: time trends 1967-2002. Caries Res. 2004 Mar-Apr;38(2):149-55. doi: 10.1159/000075939.
36. Dale JW. Toothbrushing frequency and its relationship to dental caries and periodontal disease. Aust Dent J. 1969 Apr;14(2):120-3. doi: 10.1111/j.1834-7819.1969.tb04290.x.
37. Town GI. The role of oral hygiene in prevention of periodontal disease and dental caries. N Z Dent J. 1979 Jan;75(339):29-33.
38. Etty EJ, Henneberke M, Gruythuysen RJ, Wöltgens JH. Influence of oral hygiene on early enamel caries. Caries Res. 1994;28(2):132-6. doi: 10.1159/000261634.
39. Mazhari F, Talebi M, Zoghi M. Prevalence of Early Childhood Caries and its Risk Factors in 6-60 months old Children in Quchan. Dental Research Journal. 2007;4(2):96~101.
40. Sharma S, Parashar P, Bansal R, Varshney AM, Shukla AK, Ahmad S, Singh D, Shukla N. Tooth brushing frequency and rinsing habits and their effects on oral hygiene index scores (OHIS) among the school children in Meerut. International Journal of Current Research. 2015;7(5):15728-15731.

International Journal of Biomedicine 12(4) (2022) 622-626
http://dx.doi.org/10.21103/Article12(4)_OA18

ORIGINAL ARTICLE

COVID-19

INTERNATIONAL JOURNAL OF BIOMEDICINE

Diffractive Phase Interferometry (DPI), CRP and COVID-19 RT-PCR Tests in COVID-19 Patients with Different Ages in AJMAN, UAE: A Comparative Study

Salah Eldin Omar Hussein*, Abd Elgadir Alamin Altoum, Ahmed L. Osman, Ayman Hussien Alfeel, Sara Ali, Marwan Ismail, Hassan M. K. I. Higazi

Department of Medical Laboratory Sciences, College of Health Sciences, Gulf Medical University, Ajman, United Arab Emirates

Abstract

***Background*:** Fast and accurate diagnosis plays an important role in controlling and further preventing COVID-19. This study was conducted in the Thumbay laboratory of Gulf Medical University (Ajman, UAE) to assess the correlations between DPI (Diffractive Phase Interferometry), COVID-19 RT-PCR, and CRP tests in COVID-19 patients of different ages and to compare the effectiveness of each parameter.

Methods and Results: A cross-sectional analytic study was conducted among 150 patients diagnosed with COVID-19 who were admitted to the Thumbay University Hospital. Their general data was collected from the LDM system, and from among the suspected patients who came to do the RT-PCR test, 230 were selected as volunteers to participate in this study, and further laboratory tests like CRP level and DPI test were done for them. The nasal swab was collected for a PCR test.

Out of 230 nasal swab samples, 150 were positive and 80 were negative for SARS-CoV-2 RNA by real-time RT-PCR assay. Among the 150 positive RT-PCR, 90 false negative DPI tests were from a sample with a high real-time RT-PCR. While 60 true positive DPI tests were positive real-time RT-PCR for swab specimens. Among the 80 negative RT-PCR, 79 were true negative and 1 was a false positive. The predictive positive value of the DPI test was 40% and the predictive negative value of the test was 98%. DPI has at least one tie between the positive actual state group and the negative actual state group. The results show weak and moderate positive correlations between CRP and the age groups.

Conclusion: The combined detection of the three indicators (RT-PCR, DPI, and CRP) are positively related to COVID-19 infection; therefore, these indicators will enable effective intervention measures to be implemented in time and the rates of severe illness and mortality to be reduced.(**International Journal of Biomedicine. 2022;12(4):622-626.**).

Keywords: Diffractive Phase Interferometry • COVID 19 • C-reactive protein • polymerase chain reaction

For citation: Hussein SEO, Altoum AEA, Osman AL, Alfeel AH, Ali S, Ismail M, Higazi HMKI. Diffractive Phase Interferometry (DPI), CRP and COVID-19 RT-PCR Tests in COVID-19 Patients with Different Ages in AJMAN, UAE: A Comparative Study. International Journal of Biomedicine. 2022;12(4):622-626. doi:10.21103/Article12(4)_OA18

Abbreviations

DPI, Diffractive Phase Interferometry; **CRP**, C-reactive protein; **RT-PCR,** reverse transcription polymerase chain reaction.

Introduction

Fast and accurate diagnosis plays an important role in controlling and further preventing COVID-19.[1] During the pandemic, scientists developed rapid tests to diagnose viral infection.[2] One of the techniques that has been implemented for the diagnosis of COVID-19 is laser-based DPI technology (Diffractive Phase Interferometry), which was developed in the UAE by QuantLase Imaging Lab to detect COVID-19 cases.[3] This is the first step in examining the suspected COVID-19 cases. DPI technique uses a laser-based technology based on optical-phase modulation, deriving a blood sample to screen the virus

within a few seconds on a large–scale population. Moreover, it is user-friendly, non-invasive, and also cost-effective.[4] This test is not used only in hospitals, but it can also be accepted in some places, in public places like cinemas, shopping malls, and travelers between different emirates of UAE. Furthermore, with a 'little hands-on training,' it can be used for testing and monitoring COVID-19 cases.[5] On the other hand, detection of SARS-CoV-2 RNA through a real-time RT-PCR assay is used to confirm the clinical diagnosis of COVID-19 by diagnostic laboratories.[6] The screening for COVID-19 is via a nasal swab; the genetic material of SARS-CoV-2 or RNA within the swab will be detected and isolated. Essentially, this technique combines reverse transcription of the RNA genetic material from the nasal swab into DNA and then amplifies these DNA targets via PCR, which helps measure the quantity of a specific virus RNA in the sample.[7]

Materials and Methods

A cross-sectional analytic study was conducted among 150 patients diagnosed with COVID-19 who were admitted to the Thumbay University Hospital. Their general data was collected from the LDM system, and from among the suspected patients who came to do the RT-PCR test, 230 were selected as volunteers to participate in this study, and further laboratory tests like CRP level and DPI test were done for them.

The nasal swab was collected for a PCR test. The patient must be seated in a comfortable position with the head tilted back slightly to make the nasal passages more accessible. A flexible plastic stick with a synthetic fiber swab is gently inserted into one of the nostrils (in some cases, samples are collected from both nostrils). The swab must go quite far back along the passage that connects the base of the nose to the back of the throat. The swab is kept in for 10-15 seconds while being rotated around to collect the sample accurately and adequately. Finally, the swab is removed slowly and gently and immediately placed in a special container to be sent for analysis in the laboratory. The whole process takes approximately 30-40 seconds.

For the CPR test, the specimen used is plasma, and the preferred collection container is an EDTA tube when the collection specimen requires 2mL of plasma. An Immunoturbidi-metric test for CRP provided by Abbott Diagnostics (Abbott Park) was evaluated. The assay is performed by testing a suspension of latex particles coated with anti-human CRP antibodies against unknown serum. The presence of a visible agglutination indicates an increase of the CRP level above the upper limit of the reference interval in the samples tested. The minimum detectable unit (analytical sensitivity) is approximately 6 mg/L (5-10 mg/L).[8]

The RT-PCR test is considered a standard for diagnosing COVID-19. The screening is conducted by assessing a nasal swab; this method is a real-time assessment to detect SARS-CoV-2 genetic material or RNA from a person's upper and lower respiratory specimens.

Laser-based DPI technology is used to examine blood samples to detect the virus. DPI technique, based on optical-phase modulation, is used to scan a blood sample for signs of surging red blood cells. DPI technology allows the health authorities to carry out large-scale screening within a few seconds to detect suspected cases of infections before they undergo a PCR swab test. All instruments should be validated by checking the precision, linearity, and accuracy according to the lab quality control protocol.

Statistical analysis was performed using statistical software package SPSS version 24.0 (SPSS Inc, Armonk, NY: IBM Corp). All values are presented (reported) as mean ± standard deviation (SD) or as number and percentage. For data with normal distribution, inter-group comparisons were performed using Student's t-test. Multiple comparisons were performed with one-way ANOVA. Correlation coefficients were calculated by linear regression analysis. A probability value of $P<0.05$ was considered statistically significant.

Written informed consent was obtained from all subjects involved in the study. Ethical approvals were obtained from the research center at College of Health Sciences, Gulf Medical University (Ajman, United Arab Emirates) before collecting data. The data was only used for study purposes without individual details identifying the patient.

Results

The study was conducted in the Thumbay laboratory of Gulf Medical University (Ajman, UAE) on 150 participants of different ages (Table 1).

Table 1.
Demographics of patients with COVID-19

Demographic parameters	Variable	Age range (years)	Patients	
			Number	%
Age group	Child group	0 – 16	4	2.7%
	Young adults	17 - 30	21	14%
	Middle-aged adults	31 - 45	89	59.3%
	Old-aged adults	Above 45	36	24%
Gender	Male	15 - 63	59	39.3%
	Female	13 - 62	91	60.7%

The results obtained showed significant differences in CRP levels in COVID-19 patients of different ages, gender, and data of PCR and DPI (Table 2).

The observed weak and moderate positive correlations between CRP and the age groups are presented in Figures 1-4.

Out of 230 nasal swab samples, 150 were positive and 80 were negative for SARS-CoV-2 RNA by real-time RT-PCR assay. Among the 150 positive RT-PCR, 90 false negative DPI tests were from a sample with a high real-time RT-PCR. While 60 true positive DPI tests were positive real-time RT-PCR for swab specimens. Among the 80 negative RT-PCR, 79 were true negative and 1 was a false positive. The predictive positive value of the DPI test was 40% and

the predictive negative value of the test was 98.8%. DPI has at least one tie between the positive actual state group and the negative actual state group. The sensitivity of the test was 98.4%, and the specificity of the test was 46.7%. The smallest cut-off value is the minimum observed test value minus 1, and the largest cut-off value is the maximum observed test value plus 1. All the other cut-off values are the averages of two consecutive ordered observed test values (Tables 3-4 and Figure 5).

Table 2.

CRP levels in COVID-19 patients of different ages, gender, and data of PCR and DPI

Parameters		CRP	P-value
Age / Years	Child	(13.1 ± 2.8)	0.0000
	Young Adults	(26.7 ± 4.3)	
	Middle-aged adults	(39.2 ± 5.9)	
	Old-aged adults	(57.4 ± 7.2)	
Gender	Male	(27.4 ± 4.1)	0.0018
	Female	(25.5 ± 3.2)	
PCR	Positive	(51.3 ± 6.3)	0.1460
	Negative	(50.1 ± 5.2)	
DPI	Swab	(33.6 ± 5.1)	0.7872
	No swab	(33.4 ± 4.9)	

Table 3.

Mathematical calculation of Sensitivity and Specificity

Sensitivity of the test:

$$\frac{True\ positive}{True\ positive\ +\ False\ negative} \times 100$$

$$\frac{60}{60+1} \times 100 = 98.4\%$$

Specificity of the test:

$$\frac{True\ negative}{True\ negative\ +\ False\ positive} \times 100$$

$$\frac{79}{79+90} \times 100 = 46.7\%$$

Predictive positive value of the test:

$$\frac{True\ positive}{True\ positive\ +\ False\ positive} \times 100$$

$$\frac{60}{60+90} \times 100 = 40\%$$

Predictive negative value of the test:

$$\frac{True\ negative}{True\ negative\ +\ False\ negative} \times 100$$

$$\frac{79}{79+1} \times 100 = 98.8\%$$

Table 4.

Sensitivity and specificity of PCR*DPI

Variable			DPI		Total
			SWAB	NO SWAB	
PCR	POSITIVE	Count	60	90	150
		% Within DPI	40%	60%	65%
	NEGATIVE	Count	1	79	80
		% Within DPI	1.25%	98.75%	35%
Total		Count	61	169	230
		% Within DPI	26.5%	73.5%	100.0%

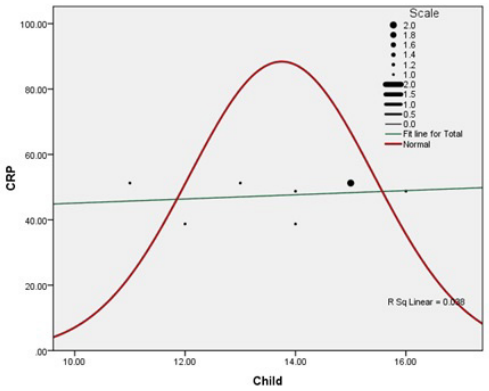

Fig. 1. *A weak positive correlation between child age group and CRP level (r=0.038, P=0.471)*

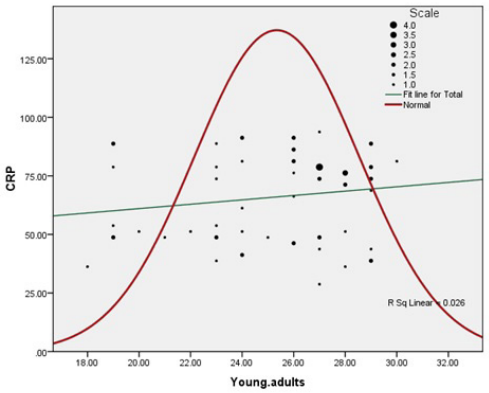

Fig. 2. *A weak positive correlation between young adult group and CRP level (r=0.026, P=0.392)*

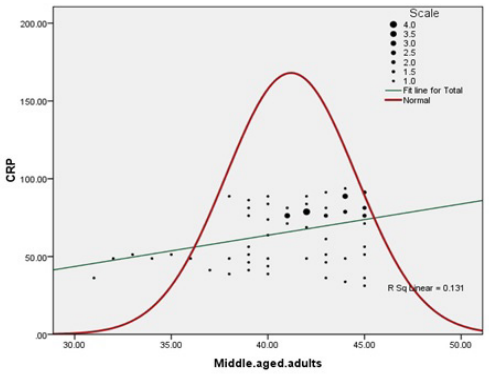

Fig. 3. *A week positive correlation between middle aged adults and CRP level (r=0.131, P=0.048)*

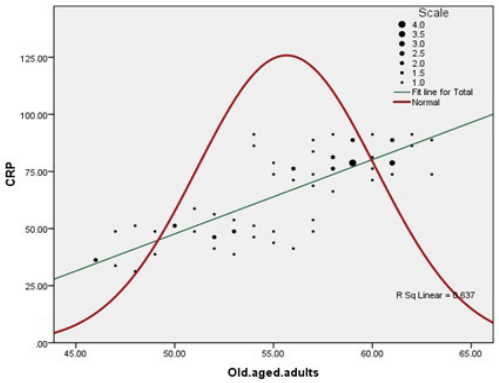

Fig. 4. *A moderate positive correlation between old-aged adults and CRP level (r=0.637, P=0.007)*

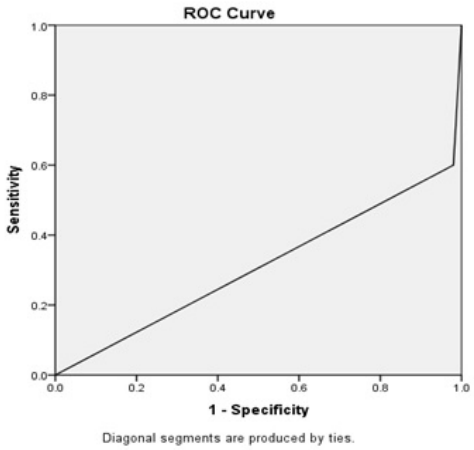

Fig. 5. *ROC curve of sensitivity and specificity.*

Discussion

The number of patients with COVID-19 is currently rapidly increasing globally, and asymptomatic patients are also the source of infection. COVID-19-related case fatality is also rapidly increasing.[8] COVID-19 is a new threat to populations, and treatment options need to be evaluated.[9] Early monitoring of key indicators was an important basis to guide treatment strategies, and early assessment of the severity of the patient's condition was of great value.[10] The new testing technology developed by QuantLase Imaging Lab helps in the early detection of COVID-19. The laser-based DPI technique is described as low-cost, user-friendly, and non-invasive, meaning mass testing can be conducted cheaply and efficiently. False positives are common in DPI, and repeat tests may be needed. A positive result means previous or other infection, though it may not be COVID-19. The principle of the laser-based DPI technique, based on optical-phase modulation, is that it can give a sign of infection within a few seconds. The procedure, known as DPI, uses lasers to identify COVIDd-19 infections within seconds. The test is done by taking a blood sample using a lancet needle, which is the same as the one used for diabetes. If it is negative, COVID-19 is ruled out. A positive DPI requires further RT-PCR, which is considered a standard for diagnosing COVID-19 in the UAE. The screening is conducted by assessing a nasal swab. This method is a real-time assessment to detect SARS-CoV-2 genetic material or RNA from a person's upper and lower respiratory specimens. CRP levels are correlated with the level of inflammation, and its concentration level is not affected by factors such as age, sex, and physical condition. This test is mandatory for patients with critical conditions who are in hospital care because the test is one of the indicators showing the body's reaction to the ongoing treatment. If the CRP, which is also recommended in the guidelines for COVID management,[11] is normal then the patient's body is reacting to the treatment positively, but if it is higher than required, checking the infection level in the body through other tests is needed.[12]

Conclusion

The proposed multiplex real-time RT-PCR methodology will enable highly sensitive detection of SARS-CoV-2 RNA. In the early stage of COVID-19, the CRP level is positively correlated with the positive PCR and could reflect disease severity, so it should be used as a key indicator for disease monitoring. CRP is a sensitive serological indicator used to evaluate the severity of COVID-19. The combined detection of the three indicators (RT-PCR, DPI, and CRP) are positively related to COVID-19 infection; therefore, these indicators will enable effective intervention measures to be implemented in time and the rates of severe illness and mortality to be reduced.

Competing Interests

The authors declare that they have no competing interests.

References

1. Taleghani N, Taghipour F. Diagnosis of COVID-19 for controlling the pandemic: A review of the state-of-the-art. Biosens Bioelectron. 2021 Feb 15; 174:112830. doi: 10.1016/j.bios.2020.112830. Epub 2020 Nov 27. PMID: 33339696; PMCID: PMC7694563
2. Al Hosany F, Ganesan S, Al Memari S, Al Mazrouei S, Ahamed F, Koshy A, Zaher W. Response to COVID-19 pandemic in the UAE: A public health perspective. J Glob Health. 2021 Mar 27; 11:03050. doi: 10.7189/jogh.11.03050. PMID: 33828834; PMCID: PMC8005306.
3. Borges LP, Martins AF, Silva BM, Dias BP, Gonçalves RL, Souza DRV, Oliveira MGB, Jesus PC, Serafini MR, Quintans JSS, Coutinho HDM, Martins N, Júnior LJQ. Rapid diagnosis of COVID-19 in the first year of the pandemic: A systematic review. Int Immunopharmacol. 2021 Dec;101(Pt

***Corresponding author:** Dr. Salah Eldin Omar Hussein. Department of Medical Laboratory Sciences, College of Health Sciences, Gulf Medical University, Ajman, United Arab Emirates. E-mail: dr.salaheldin@gmu.ac.ae*

A):108144. doi: 10.1016/j.intimp.2021.108144. Epub 2021 Sep 15. PMID: 34607235; PMCID: PMC8440261.
4. The United Arab Emirates' Government portal. Types of tests for detecting COVID-19 and testing for COVID-19. Available at: https://u.ae/en/information-and-services/justice-safety-and-the-law/handling-the-covid-19-outbreak/types-of-tests-for-detecting-covid-19-and-testing-for-covid19
5. MOHAP. COVID-19. Recent COVID-19 Information and Updates. Available at: https://mohap.gov.ae/en/covid-19
6. Ishige T, Murata S, Taniguchi T, Miyabe A, Kitamura K, Kawasaki K, Nishimura M, Igari H, Matsushita K. Highly sensitive detection of SARS-CoV-2 RNA by multiplex rRT-PCR for molecular diagnosis of COVID-19 by clinical laboratories. Clin Chim Acta. 2020 Aug;507:139-142. doi: 10.1016/j.cca.2020.04.023.
7. PureHealth. COVID-19: All You Need to Know About RT-PCR Tests and How They Can Be Conducted In The UAE Safely. Available at:https://darelhikmah.com/pcr_web/static/pure/purehealth.ae/all-you-need-to-know-about-rt-pcr-tests/index.html
8. Al Harbi M, Al Kaabi N, Al Nuaimi A, Abdalla J, Khan T, Gasmelseed H, Khan A, Hamdoun O, Weber S. Clinical and laboratory characteristics of patients hospitalised with COVID-19: clinical outcomes in Abu Dhabi, United Arab Emirates. BMC Infect Dis. 2022 Feb 8;22(1):136. doi: 10.1186/s12879-022-07059-1. PMID: 35135491; PMCID: PMC8822868
9. Ramphul K, Mejias SG. Coronavirus Disease: A Review of a New Threat to Public Health. Cureus. 2020 Mar 15;12(3):e7276. doi: 10.7759/cureus.7276. PMID: 32300496; PMCID: PMC7158591.
10. Wang L. C-reactive protein levels in the early stage of COVID-19. Med Mal Infect. 2020 Jun;50(4):332-334. doi: 10.1016/j.medmal.2020.03.007. Epub 2020 Mar 31. PMID: 32243911; PMCID: PMC7146693.
11. Ahnach M, Zbiri S, Nejjari S, Ousti F, Elkettani C. C-reactive protein as an early predictor of COVID-19 severity. J Med Biochem. 2020 Oct 2;39(4):500-507. doi: 10.5937/jomb0-27554. PMID: 33312067; PMCID: PMC7710381.
12. Nayak S, Acharjya B. VDRL test and its interpretation. Indian J Dermatol. 2012 Jan;57(1):3-8. doi: 10.4103/0019-5154.92666. PMID: 22470199; PMCID: PMC3312652.

International Journal of Biomedicine 12(4) (2022) 627-630
http://dx.doi.org/10.21103/Article12(4)_OA19

ORIGINAL ARTICLE

COVID-19

INTERNATIONAL JOURNAL OF BIOMEDICINE

Serum Procalcitonin Level and Comorbidity in Covid-19 Patients in UAE

Sara Ali*, Reem Ali, Salma Elnour, Hasan Higazi, Ahmed L. Osman, Marwan Ismail, Abdelgadir Alamin Altoum, Ayman Hussien Alfeel, Praveen Kumar Kandakurti, Salah Eldin Omar Hussein

Medical Laboratory Sciences Program, College of Health Sciences, Gulf Medical University Ajman, United Arab Emirates

Abstract

Background: Most COVID-19 patients experience a mild form of the disease, but there is a certain percentage of patients who progress to a very severe disease state that requires intensive care and invasive ventilation. In order to ensure better patient management and improved outcomes, early identification of patients who may be at a higher risk of severe infection can play an important role. The aim of this study was to assess the association between the mean procalcitonin (PCT) level and comorbidity in hospitalized patients with COVID-19.

Methods and Results: A total of 231 COVID-19-positive patients aged between 20 and 82 years (170[73.6 %] males and 61[26.4%] females) were included in this study. Serum PCT was accessed by procalcitonin assay using the Beckman Coulter UniCel DxI 800 instrument. All patients were classified into 5 groups according to age: 20-29 years - 20(8.7%), 30-39 years - 47(20.3%), 40-49 years - 72(31.2%), 50-59 years - 48(20.8%) and >60years - 44(19.0%). Eighty-seven (37.7%) patients had no chronic disease, while 144(62.3%) had comorbidities: hypertension (37[16.0%]), diabetes mellitus (44[19.0%]), a combination of diabetes mellitus with hypertension (32[13.9%]), asthma (6[2.6%]), hyperlipidemia (4[1.7%]), renal disease (1[0.4%]), and COPD (1[0.4%]). COVID-19 patients with diabetes in combination with hypertension had a statistically greater PCT level than COVID-19 patients without comorbidities (*P*=0.0273). However, there were no statistically significant differences in the mean PCT levels between other comorbidities. There were no statistically significant differences in the mean PCT level between different age categories (*P*=0.7390). The serum PCT measurement could evaluate the prognosis of the disease in some COVID-19 patients. (**International Journal of Biomedicine. 2022;12(4):627-630.**).

Keywords: procalcitonin • COVID-19 • comorbidity • diabetes mellitus • hypertension

For citation: Ali S, Ali R, Elnour S, Higazi H, Osman AL, Ismail M, Altoum AA, Alfeel AH, Kandakurti PK, Hussein SEO. Serum Procalcitonin Level and Comorbidity in Covid-19 Patients in UAE. International Journal of Biomedicine. 2022;12(4):627-630. doi:10.21103/Article12(4)_OA19

Introduction

Globally, as of 28 September 2022, there have been more than 613 million confirmed cases of COVID-19 reported to WHO.[1] Most patients experience a mild form of the disease, but there is a certain percentage of patients who progress to a very severe disease state that requires intensive care and invasive ventilation.[2,3] In order to ensure better patient management and improved outcomes, early identification of patients who may be at a higher risk of severe infection can play an important role.[4] Many studies have shown a positive correlation between increased serum procalcitonin (PCT) levels and COVID-19 severity.[5-7] Circulating PCT levels are commonly within the normal range in COVID-19 patients, as expected for a viral infection. However, increased levels have been associated with a 5-fold higher risk of evolution towards severe disease.[8] It is thought that COVID-19 progresses more quickly and severely in those with underlying medical disorders or comorbidities, frequently ending in death.[9] The aim of this study was to assess the association between the mean PCT level and comorbidity in COVID-19 hospitalized patients.

***Corresponding author:** Dr. Sara Mohammed Ali, PhD. Gulf Medical University, Ajman, United Arab Emirates. E-mail: dr.sara@gmu.ac.ae*

Materials and Methods

This is a cross-sectional study, conducted in Thumbay Hospital, Ajman, UAE, from January 2021 to October 2021. A total of 231 COVID-19-positive patients aged between 20 and 82 years (170[73.6%] males and 61[26.4%] females) were included in this study. Serum PCT was accessed by procalcitonin assay using the Beckman Coulter UniCel DxI 800 instrument. The Access PCT assay is a sequential two-step immunoenzymatic (sandwich) assay. The validation procedure was done according to CAP and CLIA for precision, accuracy, and linearity. A level of 0.5 µg/L was used as the upper limit to help determine the probability of bacterial infection, along with clinical judgement of a bacterial infection.[10]

Statistical analysis was performed using the Statistica 8.0 software package (StatSoft Inc, USA). Baseline characteristics were summarized as frequencies and percentages for categorical variables and as mean±SD for continuous variables. Inter-group comparisons were performed using Student's t-test. Multiple comparisons were performed with one-way ANOVA. Group comparisons with respect to categorical variables are performed using chi-square test. A probability value of $P<0.05$ was considered statistically significant.

The study protocol was reviewed and approved by the Ethics Committee of Gulf Medical University. All participants provided written informed consent.

Results

This study analyzed 231 SARS-CoV-2 infected patients admitted to the hospital, including 121 mild COVID-19 patients, 59 moderate COVID-19 patients, and 51 severe COVID-19 patients. All patients were classified into 5 groups according to age: 20-29 years - 20(8.7%), 30-39 years - 47(20.3%), 40-49 years - 72(31.2%), 50-59 years - 48(20.8%) and >60 years - 44(19.0%) (Table 1).

Table 1.
Age - Gender distribution.

Demographic Variable		Age range (years)	Number	%
Age group	Group 1	20 – 29	20	8.7
	Group 2	30 – 39	47	20.3
	Group 3	40 – 49	72	31.2
	Group 4	50 – 59	48	20.8
	Group 5	> 60	44	19.0
Gender	Male		170	73.6
	Female		61	26.4

Eighty-seven (37.7%) patients had no chronic disease, while 144(62.3%) had comorbidities: hypertension (37[16.0%]), diabetes mellitus (44[19.0%]), a combination of diabetes mellitus with hypertension (32[13.9%]), asthma (6[2.6%]), hyperlipidemia (4[1.7%]), renal disease (1[0.4%]), and COPD (1[0.4%]) (Table 2). The distribution of comorbidity symptoms in the different age groups is shown in Table 3.

Table 2.
Frequency of comorbidities among the COVID-19 patients.

Comorbidity	n	%
No Chronic Disease	87	37.7 %
Hypertension	37	16.0 %
Diabetes mellitus	44	19.0 %
Diabetes mellitus & Hypertension	32	13.9 %
Asthma	6	2.6 %
Hyperlipidemia	4	1.7 %
Renal disease	1	0.4 %
COPD	1	0.4 %
Multiple chronic diseases, excluding diabetes mellitus and hypertension	19	8.2 %

Table 3.
The distribution of comorbidity symptoms in the different age groups.

Symptoms		Age group / Years										*P*-value
		Group 1 (20-29)		Group 2 (30-39)		Group 3 (40-49)		Group 4 (50-59)		Group 5 (>60)		
		n	%	n	%	n	%	n	%	n	%	
Headache	Yes	12	60.0	34	72.3	47	65.3	30	62.5	27	61.4	0.7868
	No	8	40.0	13	27.7	25	34.7	18	37.5	17	38.6	
Fever	Yes	20	100	45	95.7	70	97.2	44	91.7	38	86.4	0.0995
	No	0	0	2	4.3	2	2.8	4	8.3	6	13.6	
Cough	Yes	13	65.0	29	61.7	40	55.6	26	54.2	22	50.0	0.7382
	No	7	35.0	18	38.3	32	44.4	22	45.8	22	50.0	
Fatigue	Yes	6	30.0	22	46.8	31	43.1	16	33.3	14	31.8	0.4086
	No	14	70.0	25	53.2	41	56.9	32	66.7	30	68.2	
Pneumonia	Yes	17	85.0	36	76.6	54	75.0	35	72.9	31	70.4	0.7871
	No	3	15.0	11	23.4	18	25.0	13	27.1	13	29.5	
Short of breath	Yes	14	70.0	28	59.6	50	69.4	27	56.2	24	54.5	0.3978
	No	6	30.0	19	40.4	22	30.6	21	43.8	20	45.4	
Abdominal pain	Yes	8	40.0	20	42.6	32	44.4	20	41.7	19	43.2	0.9965
	No	12	60.0	27	57.4	40	55.6	28	58.3	25	56.8	
Nausea and vomiting	Yes	10	50.0	22	46.8	42	58.3	29	60.4	22	50.0	0.6038
	No	10	50.0	25	53.2	30	42.7	19	39.6	22	50.0	

COVID-19 patients with diabetes in combination with hypertension had a statistically greater PCT level than COVID-19 patients without comorbidities (*P*=0.0273). However, there were no statistically significant differences in the mean PCT level between different age categories (*P*=0.7390) (Fig.1, Table 4)

Table 4.
PCT level among different age groups and comorbidities.

Parameters		PCT	*P-value*
Age group	Group 1	0.12±.152	0.7390
	Group 2	0.57±1.320	
	Group 3	0.51±1.838	
	Group 4	0.51±1.269	
	Group 5	0.79±2.611	
Comorbidities	Diabetes mellitus & Hypertension (n=32)	1.186 ± 3.212	0.0273*
	Diabetes mellitus (n=44)	0.654 ± 2.057	0.2262
	Hypertension (n=37)	0.292 ± 0.632	0.7948
	Multiple chronic diseases, excluding diabetes mellitus and hypertension (n=19)	0.526 ± 1.064	0.4371
No Chronic Disease (n=87)		0.336 ±0.939	

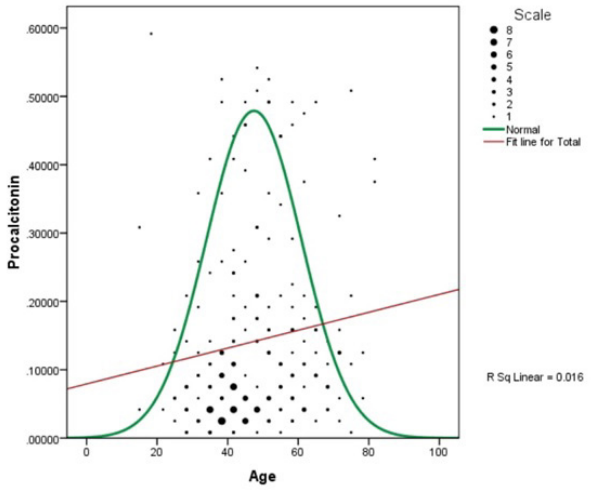

Fig. 2. *Week positive correlation between the age (year) and PCT level (µg/L) (r=0.016, P=0.107)*

Discussion

PCT is recommended as a diagnostic biomarker of infection in the febrile population and is associated with mortality.[11] In the current study, 62.3% of patients had comorbidities and 37.7% were without chronic disease. The percentage of male patients was 73.6 % and this was lower than that reported by Zhu et al.,[12] but like that reported by Yang et al.[13] (73%) and close to the data reported by Chen et al.[14] Our results showed that COVID-19 patients with diabetes in combination with hypertension had a statistically greater PCT level than COVID-19 patients without comorbidities. However, there were no statistically significant differences in the mean PCT levels between other comorbidities. No previous studies applied this comparison; we advise doing further studies to confirm these findings.

Conclusion

COVID-19 patients with diabetes in combination with hypertension have a statistically greater PCT level than COVID-19 patients without comorbidities. There are no statistically significant differences in the mean PCT level between different age categories. The serum PCT measurement could evaluate the prognosis of the disease in some COVID-19 patients.

Competing Interests

The authors declare that they have no competing interests.

References

1. WHO Coronavirus (COVID-19) Dashboard. Available at: https://covid19.who.int/
2. Mallah SI, Ghorab OK, Al-Salmi S, Abdellatif OS, Tharmaratnam T, Iskandar MA, Sefen JAN, Sidhu P, Atallah B, El-Lababidi R, Al-Qahtani M. COVID-19: breaking down a global health crisis. Ann Clin Microbiol Antimicrob. 2021 May 18;20(1):35. doi: 10.1186/s12941-021-00438-7.
3. Sanyaolu A, Okorie C, Marinkovic A, Patidar R, Younis K, Desai P, Hosein Z, Padda I, Mangat J, Altaf M. Comorbidity and its Impact on Patients with COVID-19. SN Compr Clin Med. 2020;2(8):1069-1076. doi: 10.1007/s42399-020-00363-4.
4. Langer-Gould A, Smith JB, Gonzales EG, Castillo RD, Figueroa JG, Ramanathan A, Li BH, Gould MK. Early identification of COVID-19 cytokine storm and treatment with anakinra or tocilizumab. Int J Infect Dis. 2020 Oct;99:291-297. doi: 10.1016/j.ijid.2020.07.081.
5. Lippi G, Plebani M. Procalcitonin in patients with severe coronavirus disease 2019 (COVID-19): A meta-analysis. Clin Chim Acta. 2020 Jun;505:190-191. doi: 10.1016/j.cca.2020.03.004.
6. de la Rica R, Borges M, Gonzalez-Freire M. COVID-19: In the Eye of the Cytokine Storm. Front Immunol. 2020 Sep 24;11:558898. doi: 10.3389/fimmu.2020.558898.
7. Gao Z, Xu Y, Sun C, Wang X, Guo Y, Qiu S, Ma K. A systematic review of asymptomatic infections with COVID-19. J Microbiol Immunol Infect. 2021 Feb;54(1):12-16. doi: 10.1016/j.jmii.2020.05.001.
8. Hu R, Han C, Pei S, Yin M, Chen X. Procalcitonin

levels in COVID-19 patients. Int J Antimicrob Agents. 2020 Aug;56(2):106051. doi: 10.1016/j.ijantimicag.2020.106051.
9. Sanyaolu A, Okorie C, Marinkovic A, Patidar R, Younis K, Desai P, Hosein Z, Padda I, Mangat J, Altaf M. Comorbidity and its Impact on Patients with COVID-19. SN Compr Clin Med. 2020;2(8):1069-1076. doi: 10.1007/s42399-020-00363-4.
10. Schuetz P, Beishuizen A, Broyles M, Ferrer R, Gavazzi G, Gluck EH, González Del Castillo J, Jensen JU, Kanizsai PL, Kwa ALH, Krueger S, Luyt CE, Oppert M, Plebani M, Shlyapnikov SA, Toccafondi G, Townsend J, Welte T, Saeed K. Procalcitonin (PCT)-guided antibiotic stewardship: an international experts consensus on optimized clinical use. Clin Chem Lab Med. 2019 Aug 27;57(9):1308-1318. doi: 10.1515/cclm-2018-1181.
11. Standage SW, Wong HR. Biomarkers for pediatric sepsis and septic shock. Expert Rev Anti Infect Ther. 2011 Jan;9(1):71-9. doi: 10.1586/eri.10.154.
12. Zhu J, Ji P, Pang J, Zhong Z, Li H, He C, Zhang J, Zhao C. Clinical characteristics of 3062 COVID-19 patients: A meta-analysis. J Med Virol. 2020 Oct;92(10):1902-1914. doi: 10.1002/jmv.25884.
13. Yang X, Yu Y, Xu J, Shu H, Xia J, Liu H, Wu Y, Zhang L, Yu Z, Fang M, Yu T, Wang Y, Pan S, Zou X, Yuan S, Shang Y. Clinical course and outcomes of critically ill patients with SARS-CoV-2 pneumonia in Wuhan, China: a single-centered, retrospective, observational study. Lancet Respir Med. 2020 May;8(5):475-481. doi: 10.1016/S2213-2600(20)30079-5. Epub 2020 Feb 24. Erratum in: Lancet Respir Med. 2020 Apr;8(4):e26.
14. Chen N, Zhou M, Dong X, Qu J, Gong F, Han Y, Qiu Y, Wang J, Liu Y, Wei Y, Xia J, Yu T, Zhang X, Zhang L. Epidemiological and clinical characteristics of 99 cases of 2019 novel coronavirus pneumonia in Wuhan, China: a descriptive study. Lancet. 2020 Feb 15;395(10223):507-513. doi: 10.1016/S0140-6736(20)30211-7.

International Journal of Biomedicine 12(4) (2022) 631-635
http://dx.doi.org/10.21103/Article12(4)_OA20

ORIGINAL ARTICLE

Population Health

INTERNATIONAL JOURNAL OF BIOMEDICINE

Estimating Salt Intake by Citizens of Kosovo Using 24-Hour Urine Sodium Excretion

Lindita Maxhuni-Thaçi[1], Tahire Maloku-Gjergji[1*], Burbuqe Nushi-Latifi[1], Valmira Maxhuni-Bajgora[2]

[1]Department of Human Ecology, National Institute of Public Health, School of Medicine, Medical Faculty, University of Prishtina, Prishtina, Kosovo
[2]Department of Pediatric Dentistry, School of Dentistry, Medical Faculty, University of Prishtina, Prishtina, Kosovo

Abstract

Background: The minimum physiological need for sodium is estimated to be 200-500 mg/day (about 0.5-1.25 g of salt per day) (WHO, 2012). Many studies have shown that salt consumption is the main factor in increasing blood pressure and cardiovascular disease cases.

Methods and Results: This transversal cross-sectional study was performed in Kosovo in 2019. The study included 219 people of both sexes (49.9% men and 50.2% women) aged 20–59 years. Urine was collected within 24 hours in accordance with the written instructions, and an oral explanation was provided to each research participant. Na and K in urine were analyzed using SmartLyte® autoanalyzer (Diamond Diagnostics, Holliston, Massachusetts, USA). Our results showed that the average urinary Na excretion over 24 hours in the Kosovo population was 9.52 g/24h, which corresponds to a daily salt intake of 23.8 g/24h. The average amount of urinary Na excreted in 24 hours was significantly higher in men (11.60 g/24h) than in women (7.46 g/24h) (P<0.001). Thus, the average amount of salt consumed by participants was 29.46 g/24h for men and 18.94 g/24h for women. The average urinary K excretion over 24 hours in men was 2.02 g/24h, while that in women was 1.61 g/24h (P=0.000). The Na/K ratio was significantly higher in men (6.58) than in women (5.27) (P<0.05).

Conclusion: The citizens of Kosovo consume a large amount of salt, greater than 5 g/day. In Kosovo, there has yet to be a comprehensive strategy for reducing salt consumption.(**International Journal of Biomedicine. 2022;12(4):631-635.**).

Keywords: salt • urine • sodium excretion • potassium • Kosovo

For citation: Maxhuni-Thaçi L, Maloku-Gjergji T, Nushi-Latifi B, Maxhuni-Bajgora V. Estimating Salt Intake by Citizens of Kosovo Using 24-Hour Urine Sodium Excretion International Journal of Biomedicine. 2022;12(4):631-635. doi:10.21103/Article12(4)_OA20.

Introduction

The minimum physiological need for sodium is estimated to be 200-500 mg/day (about 0.5-1.25 g of salt per day) (WHO 2012).[(1)] Many studies have shown that salt consumption is the main factor in increasing blood pressure (BP) and cardiovascular disease cases. Consuming more salt will increase the risk of heart attack, left ventricular hypertrophy, and kidney disease. Increased salt consumption and reduced liquid consumption are also associated with obesity, kidney stones, osteoporosis, and stomach cancer.[(2)]

WHO data reports show that cardiovascular diseases are the most frequently occurring diseases worldwide.[(1)] Approximately 7.1 million deaths worldwide are estimated to be caused by high BP. Additionally, one-third of disability-adjusted life years in developed countries, developing countries with high mortality rates, and developing countries with low mortality rates are attributed to high BP.[(3)]

Many studies have shown that BP can be influenced by the ratio between potassium (K) and sodium (Na). Low K levels in the blood can increase BP, while sufficient K levels obtained from fruit and vegetable consumption help

to stabilize BP.[4] Similarly, research shows the connection between salt intake and increased susceptibility to vascular diseases in patients with diabetes.[5,6]

Research shows that excessive salt intake reduces the effectiveness of hypertension drugs.[5] Because Na+ and chloride (Cl−) ions are extracellular fluid ions, the natural concentration of these two ions in food products is low. In industrially processed foods that are cooked or processed, the concentration of both ions is significantly higher than that in non-processed foods. In processed foods, Na and Cl concentrations are approximately the same or standardized, while in natural (unprocessed) foods, the concentration of Cl− ions is higher than that of Na+ ions. Foods of plant origin naturally contain more Cl− than Na+ ions, while foods of animal origin contain more Na+ than Cl− ions.[4]

In most developed countries, salt reduction can be achieved by gradually reducing the amount of salt in processed foods. Modest reductions in salt worldwide are seen as major advances in public health.[2] Guidelines for salt consumption have changed over the past decades. The Conference on Food, Nutrition and Health, organized by the US government in 1969, published the first recommendations highlighting Na's role in hypertension.[7] In 1994, the British Committee on Health and Food Policy (COMA) advised a gradual reduction in salt intake from 9 g/day to 6 g/day.[8] At the same time, the National Heart, Lung, and Blood Institute of the USA proposed a salt intake of 6 g (2440 mgNa) per day.[9] The WHO and the Food and Agriculture Organization of the United Nations, in their 2003 technical report "Diet, Nutrition and Prevention of Chronic Diseases," advise limiting salt intake to 5g/day on the basis of results from a technical report on primary prevention of essential hypertension in 1983.[10] WHO's recommendation (2012) is less than 5 grams of salt or 2 grams of sodium per person per day to prevent cardiovascular diseases.[1]

To date, no research has been conducted in this direction in Kosovo, and there is no data on salt consumption among the Kosovo population. This research highlights the amount of salt used by the citizens of Kosovo and the problems related to it. Additionally, the results of this study will inform the national strategy for reducing salt consumption.

Material and methods

Ethical approval for this study was obtained from the Ethical Committee of the Medical Faculty of the University of Prishtina, Kosovo.

Study design

This transversal cross-sectional study was performed at the country level in Kosovo in 2019. There were 219 people of both sexes (49.9% men and 50.2% women) aged 20–59 years included in the study. All participants were divided into four age groups (20–29, 30–39, 40–49, and 50–59 years). Participants' involvement in this research was voluntary. Information was distributed to each participant in written form to inform them about the purpose of the research. Each participant then provided informed consent to participate in the study.

Participants were recruited on the basis of the seven regions in Kosovo, with 31 people included from each region. The people included in the research were healthy and active, and they were randomly selected. First, in each region, the city and village were selected, then a street or a neighborhood was selected, followed by a selection of the family or adult members of that family according to the Kish method.[11]

Sample collection and analysis

Urine was collected within 24 hours in accordance with the written instructions, and an oral explanation was provided to each research participant. The first urine of the morning was discarded, and the entire amount of urine was collected for the next 24 hours using a standard bottle. The total volume of collected urine was measured.

Na and K in urine were analyzed using SmartLyte® autoanalyzer (Diamond Diagnostics, Holliston, Massachusetts, USA). The electrolyte analyzer methodology is based on measurements using ion-selective electrodes to determine the measurement values. There are six different electrodes: Na, K, chlorite, ionizing calcium, lithium, and the reference electrode. Each electrode has an ion-selective membrane that undergoes a special reaction with the corresponding ions contained in the sample being analyzed. The membrane is an ion exchanger that reacts to electrical charges by causing a potential change.

Urine Na concentrations are calculated in mmol/L and converted to grams using a conversion factor of 0.023 for Na, and 0.039 for K. Daily Na excretion was calculated by multiplying the corresponding urinary concentrations by the total urine volume. The estimated daily salt intake in grams was then calculated by multiplying the daily Na excretion by 2.54. Na/K ratio, using the 24-h urine samples, was calculated by dividing the Na concentration by the K concentration, both in mmol/L.

Statistical analysis was performed using statistical software package SPSS version 26.0 (SPSS Inc, Armonk, NY: IBM Corp).For descriptive analysis, results are presented as mean±standard deviation (SD). For data with normal distribution, inter-group comparisons were performed using Student's t-test. Multiple comparisons were performed with a one-way ANOVA. A probability value of $P<0.05$ was considered statistically significant.

Results

Out of 219 participants included in this research, the proportions of participants of each sex between age groups did not differ significantly (Table 1).

The mean 24-hour urine volume was 1.42 L in women and 1.50 L in men. The 24-hour urinary Na and K excretion was significantly higher in men than in women ($P<0.001$). The Na/K ratio was significantly higher in men (6.58) than in women (5.27) ($P<0.05$). The average amount of urinary Na excreted in 24 hours in men was 504.32 mmol/24h or 11.60 g/24h, while that in women was 324.23 mmol/24h or 7.46 g/24h. This corresponds to a daily salt intake of 29.46 g/24h for men and 18.94 g/24h for women. This difference was also significant ($P=0.000$). The average urinary K excretion over 24 hours in men was 51.68 mmol/24h or 2.02 g/24h, while

that in women was 41.40 mmol/24h or 1.61g/24h, and this difference was also significant (P=0.000) (Table 2).

Table 1.

Participant demographic data

Variable		20–29 years	30–39 years	40–49 years	50–59 years	Total
Women	n	29	26	28	27	110
	%	26.4	23.6	25.5	24.5	100.0
Men	n	27	27	29	26	109
	%	24.8	24.8	26.6	23.9	100.0
Total	n	56	53	57	53	219
	%	25.6	24.2	26	24.2	100.0

Table 2.

The 24-hour urinary Na and K excretion by sex

Parameters	Women (n=110)	Men (n=109)	P-value
Age (years)	38.44±12.32	38.98±12.01	0.741
Urine volume (L/24 h)	1.42±0.41	1.50±0.36	0.155
Na (mmol/24 h)	324.23±170.01	504.32±226.36	0.000
K (mmol/24 h)	41.40±16.33	51.68±22.35	0.000
Na (g/24 h)	7.46±3.91	11.60±5.21	0.000
K (g/24 h)	1.6±10.64	2.02±0.87	0.000
Na/K ratio	5.27±3.26	6.58±3.51	0.005
Calculated NaCl intake (g/24 h)	18.94±9.93	29.46±13.22	0.000

The average Na and K levels in 24-h urine were analyzed based on the area of residence. The results showed that the average urinary Na and K excreted over 24 hours, which was expressed in mmol/24h or g/24 h, was significantly higher in the rural population than in the urban population (P<0.001). The Na/K ratio was not significantly different between rural and urban participants. The average urinary Na excretion over 24 hours in the rural population was 454.07 mmol/24h or 10.44 g/24 h, while that in the urban population was 377.50 mmol/24h or 8.68 g/24 h. This corresponds to 26.52 g/24h of salt intake for the rural participants and 22.05 g/24 h for the urban participants (P<0.009; Table 3).

Urinary Na and K excretion over 24 hours by age group in women did not differ significantly. This also reflects the amount of salt intake. For women, the Na/K ratio showed a significant difference from that in men (P=0.011). Additionally, for men, Na and NaCl (g/24 h) values showed a significant increase with increasing age (P=0.011, Table 4).

Table 3.

The 24-hour urinary Na and K excretion by the area of residence

Parameters	Rural (n=104)	Urban (n=115)	P-value
Age (years)	39.88±11.57	37.65±12.60	0.009
Urine volume (L/24h)	1.53±0.39	1.40±0.37	0.423
Na (mmol/24 h)	454.07±216.87	377.50±215.52	0.009
K (mmol/24 h)	49.11±21.37	44.18±18.84	0.008
Na (g/24 h)	10.44±4.99	8.68±4.96	0.009
K (g/24 h)	1.92±0.83	1.72±0.73	0.010
Na/K ratio	6.11±3.20	5.74±3.64	0.071
Calculated NaCl intake (g/24 h)	26.52±12.67	22.05±12.59	0.009

Table 4.

The 24-hour urinary Na and K excretion by age group and sex

Women (years)	n	Na (mmol/24 h)	K (mmol/24 h)	Na/K ratio	Calculated NaCl intake (g/24 h)
20–29	29	284.3±101.9	37.7±14.1	4.9±2.3	16.6±5.9
30–39	26	322.3±158.3	42.5±18.9	5.5±3.8	18.8±9.2
40–49	28	302.2±134.2	46.2±14.3	4.0±1.5	17.7±7.8
50–59	27	391.8±245.2	39.3±17.4	6.8±4.3	22.9±14.3
	P	0.095	0.213	0.011	0.095
Men (years)	n	Na (mmol/24 h)	K (mmol/24 h)	Na/K ratio	Calculated NaCl intake (g/24 h)
20–29	27	402.0±201.6	42.4±18.7	6.8±4.2	23.5±11.8
30–39	27	499.9±255.9	55.0±24.7	5.9±3.2	29.2±14.9
40–49	29	511.8±184.3	52.8±20.0	6.5±3.3	29.9±10.8
50–59	26	606.8±224.9	56.7±24.1	7.1±3.3	35.4±13.1
	P	0.011	0.082	0.644	0.011

Discussion

Our study focused on assessing the daily salt intake in the Kosovo population, taking into account traditions and the culture of nutrition. To this end we measured urinary Na and K excretion over 24 hours, which was used to determine the amount of salt (e.g., NaCl) consumed by the citizens of Kosovo.

Our results showed that the average urinary Na excretion over 24 hours in the Kosovo population was high (9.52 g/day): 11.06 g/day for men and 7.46 g/day for women. When these values are converted into NaCl intake, the average amount of salt consumed by participants was 23.8 g/day: 29.46 g/day for men and 18.94 g/day for women.

In 2013, Rysha et al.[12] analyzed food consumed by children in kindergarten and children aged 1–4 years and 4–7 years in Kosovo. They showed that the Na intake values were higher than the recommended daily values for these age groups, with values ranging from 873mg for children 1–4 years old, which was 291% of the recommended daily amounts, to 1253 mg for children 4–7 years old, which was approximately 306% of the recommended daily values. Their results are consistent with those in our study.

Our findings also showed that urinary Na excretion over 24 hours among the citizens of Kosovo was higher than the results of previous research that was performed in Slovenia in 2010.[13] These results applied to both sexes. When analyzed by sex, their results showed that men excreted higher urinary Na values (220.9±86.0 mmolNa/day) than women (169.8±73.8 mmolNa/day). These results are similar to those in our study.

Our results also showed higher urinary Na excretion over 24 hours compared with a 2013 study that enrolled citizens of Novi Sad, where the average urinary Na excretion over 24 hours was 4.58 g/day.[14] This difference was evident even when their results were analyzed by sex, where the average urinary Na excretion in men was 5.58 g/day, and that of women was 3.93 g/day. These results are consistent with our results when analyzed by sex. The average urinary Na excretion over 24 hours in the population of Tromso in 2015–2016 was 3.53 g/day (4.09 g/day in men and 2.98 g/day in women)[15]. These values are lower than those of our results. However, our results were higher than those of a 2013 systematic literature review that included 51 studies from western Europe. The mean 24-hour urinary Na excretion in this review ranged from 3.28 g/day to 4.43 g/day in both sexes.[15]

Our results are also higher than those reported in a 2017 study from Turkey.[16] In this study, the average 24-hour urinary Na excretion was 252.0±92.2 mmol/day, which corresponds to a daily salt intake of 14.5±5.4 g. Published findings show that 24-hour urinary Na excretion is generally lower than the results of our research, which suggests that the citizens of Kosovo consume significantly more salt than the recommended values. This may be because the citizens of Kosovo traditionally consume a large amount of bread and pastries, meat, and meat products (e.g., sausage and dried meat), fast food, pickles, and cheese, all of which contain high amounts of salt.

The mean 24-hour urinary K excretion was lower in both sexes than the result reported for the Tromso population (3.87 g/day for men and 2.97 g/day for women). Additionally, the Na/K ratio was higher for both sexes (6.58 for men and 5.27 for women) compared with that reported for the Tromso population (1.86 for men and 1.79 for women).[15] Low K values and a high Na/K ratio contribute to an increased risk of cardiovascular disease in the population of Kosovo.

In conclusion, our results showed that the citizens of Kosovo consume a large amount of salt, greater than 5 g/day. In Kosovo, there has yet to be a comprehensive strategy for reducing salt consumption. There is an urgent to draft such a strategy as soon as possible.

Acknowledgments

We thank Jodi Smith, PhD ELS, from Edanz (www.edanz.com/ac) for editing a draft of this manuscript.

Competing Interests

The authors declare that they have no competing interests.

References

1. WHO. A/NCD/2 21 November 2012. Available from: https://apps.who.int/gb/NCDs/pdf/A_NCD_2-en.pdf
2. He FJ, MacGregor GA. A comprehensive review on salt and health and current experience of worldwide salt reduction programmes. J Hum Hypertens. 2009 Jun;23(6):363-84. doi: 10.1038/jhh.2008.144.
3. WHO Forum on Reducing Salt Intake in Populations (2006: Paris, France), World Health Organization & WHO Technical Meeting on Reducing Salt Intake in Populations (2006: Paris, France). (2007). Reducing salt intake in populations: report of a WHO forum and technical meeting, 5-7 October 2006, Paris, France. World Health Organization.
4. Morris RC Jr, Schmidlin O, Frassetto LA, Sebastian A. Relationship and interaction between sodium and potassium. J Am Coll Nutr. 2006 Jun;25(3 Suppl):262S-270S. doi: 10.1080/07315724.2006.10719576.
5. Ogihara T, Asano T, Fujita T. Contribution of salt intake to insulin resistance associated with hypertension. Life Sci. 2003 Jun 20;73(5):509-23. doi: 10.1016/s0024-3205(03)00315-1.
6. Weir MR, Fink JC. Salt intake and progression of chronic kidney disease: an overlooked modifiable exposure? A commentary. Am J Kidney Dis. 2005 Jan;45(1):176-88. doi: 10.1053/j.ajkd.2004.08.041.
7. Institute of Medicine (US) Committee on Strategies to Reduce Sodium Intake. Strategies to Reduce Sodium Intake in the United States. Henney JE, Taylor CL, Boon CS, editors. Washington (DC): National Academies Press (US); 2010.

***Corresponding author**: Tahire Maloku-Gjergji. Department of Human Ecology, National Institute of Public Health, School of Medicine, Medical Faculty, University of Prishtina. Prishtina, Kosovo. E- mail: tahire.gjergji@uni-pr.edu*

8. Department of Health. Nutritional Aspects of Cardiovascular Disease. London: HMSO,1994.
9. National High Blood Pressure Education Program Working Group report on primary prevention of hypertension. Arch Intern Med. 1993 Jan 25;153(2):186-208.
10. Diet, nutrition and the prevention of chronic diseases. World Health Organ Tech Rep Ser. 2003;916:i-viii, 1-149.
11. Kish L. A procedure for objective respondent selection within the householdıo Journal of the American Statistical Association. 1949;44:92-115.
12. Rysha A, Gjergji TM, Ploeger A. Nutritional status of preschool children attending kindergartens in Kosovo. J Health Popul Nutr. 2017 Jun 2;36(1):26. doi: 10.1186/s41043-017-0105-1.
13. Ribič CH, Zakotnik JM, Vertnik L, Vegnuti M, Cappuccio FP. Salt intake of the Slovene population assessed by 24 h urinary sodium excretion. Public Health Nutr. 2010 Nov;13(11):1803-9. doi: 10.1017/S136898001000025X.
14. Milka Popović, Unos soli u uzorku odraslog stanovnistva Novog Sada, Doktorska disertacija, Novi Sad, Godine 2013
15. Meyer HE, Johansson L, Eggen AE, Johansen H, Holvik K. Sodium and Potassium Intake Assessed by Spot and 24-h Urine in the Population-Based Tromsø Study 2015-2016. Nutrients. 2019 Jul 16;11(7):1619. doi: 10.3390/nu11071619.
16. Erdem Y, Akpolat T, Derici Ü, Şengül Ş, Ertürk Ş, Ulusoy Ş, Altun B, Arıcı M. Dietary Sources of High Sodium Intake in Turkey: SALTURK II. Nutrients. 2017 Aug 24;9(9):933. doi: 10.3390/nu9090933.

International Journal of Biomedicine 12(4) (2022) 636-639
http://dx.doi.org/10.21103/Article12(4)_OA21

ORIGINAL ARTICLE

Microbiology

INTERNATIONAL JOURNAL OF BIOMEDICINE

Detection of the bla_{VIM-2} Gene in Carbapenem-Resistant *Acinetobacter baumannii* Clinical Isolates in Sudan

Salma Mohamed[1*], Zainab Ahmed[2], Tajalseer Mubarak[2], Sara Mohamed[3], Hassan Higazi[1], Sara Ali[1]

[1]*Department of Medical Laboratory Science, Faculty of Health Sciences, Gulf Medical University, Ajman, United Arab Emirates*

[2]*Department of Microbiology, Faculty of Medical Laboratory Science, University of Science and Technology, Khartoum, Sudan*

[3]*Deparment of Internal Medicine, Faculty of Medicine, Al Neelain University, Khartoum, Sudan*

Abstract

Background: *Acinetobacter baumannii* is a *pleomorphic aerobic* Gram-negative bacillus that is notorious for having multidrug resistance traits. Carbapenem-resistant *Acinetobacter baumannii* (CRAB) is a global concern due to its ability to retain and disseminate resistance genes, which poses a threat to the spread of resistance among bacterial communities in hospital settings. The aim of our study was to evaluate the existence of the bla_{VIM-2} gene in carbapenem-resistant *Acinetobacter baumannii* clinical isolates from Sudanese hospitals.

Methods and Results: Forty clinical isolates of *Acinetobacter baumannii* were collected from June 2021 to April 2022. All isolates of *Acinetobacter baumannii* were identified via BioMérieux's Vitek-2 automated system (Marcy l'Étoile, France) and evaluated for phenotypic resistance to carbapenem, using imipenem and meropenem. The enzymatic mode of resistance was assessed by the modified Hodge test (MHT). A real-time PCR was used to detect the presence of the bla_{VIM-2} gene.

Of 40 isolates, 32(80%) were resistant to imipenem, 4(10%) were moderately resistant, and 4(10%) were susceptible to imipenem; 24(60%) were resistant to meropenem, 10(25%) were moderately resistant, and 6(15%) were susceptible to meropenem. MHT was 70% positive with imipenem use and 55% positive with meropenem use. Real-time PCR revealed that only 30% of the samples were positive for the bla_{VIM-2} gene. All bla_{VIM-2}-positive isolates were resistant to both imipenem and meropenem.

Conclusion: Resistance to carbapenem poses a serious threat, denying patients treatment options. It is essential to make continuous surveillance of these strains to prevent the development of resistant strains.(**International Journal of Biomedicine. 2022;12(4):636-639.**).

Keywords: carbapenem-resistant *Acinetobacter baumann* • bla_{VIM-2} gene • carbapenemases

For citation: Mohamed S, Ahmed Z, Mubarak T, Mohamed S, Higazi H, Ali S. Detection of the bla_{VIM-2} Gene in Carbapenem-Resistant *Acinetobacter baumannii* Clinical Isolates in Sudan. International Journal of Biomedicine. 2022;12(4):636-639. doi:10.21103/Article12(4)_OA21.

Abbreviations

CRAB, carbapenem-resistant *Acinetobacter baumannii*; **MBLs**, metallo-β-lactamases; **MHT**, modified Hodge test; **VIM**, Verona integron-borne metallo-β-lactamase.

Introduction

Acinetobacter baumannii is a pleomorphic aerobic Gram-negative bacillus that is notorious for having multidrug resistance traits. Carbapenem-resistant *Acinetobacter baumannii* (CRAB) is a global concern due to its ability to retain and disseminate resistance genes, which poses a threat to the spread of resistance among bacterial communities in hospital settings.[(1)] CRAB can render carbapenems ineffective using various enzymes known as carbapenemases.[(2)] The carbapenems are β-lactam

antimicrobial agents with an exceptionally broad spectrum of activity. The emergence of metallo-β-lactamase (MBL)-producing bacilli that are resistant to carbapenems is becoming a severe therapeutic problem.[3] Two types of MBLs, IMP and VIM, have been reported.[4] Strains producing VIM-type MBLs were originally reported in European countries.[5,6] VIM enzymes confer resistance not only to carbapenems, but to virtually all β-lactam antibiotics,[7,8] including penicillins, cephalosporins, cephamycins, and carbapenems, but not monobactams (aztreonam). Their activity is zinc dependent and is inhibited by EDTA.[6]

Currently, the VIM-type enzymes constitute the second most dominant group of ß-lactamases[9] and have been reported in different species from 23 countries worldwide.[7,10] The first metallo-β-lactamase VIM-2 in clinical isolates of *Pseudomonas aeruginosa* was collected in 1995 in Portugal.[11,12] The carbapenem-hydrolyzing β-lactamase VIM-2 shared 90% amino acid identity with VIM-1.[6] VIM-2 has been obtained from an isolate from the French Riviera region(Marseilles), 300 km from Verona, where VIM-1 had been isolated.[5] VIM-2 can be classified in the protein sequence-based subclass B1 of MBLs.[13] VIM-2 has been reported frequently from different isolates including *Acinetobacter baumannii* in Europe, United States, Latin America, and Asia.[14-16]

VIM MBLs are often encoded by mobile gene cassettes inserted into integrons,[5,6] which are sometimes located on plasmids. Most of these integrons belong to class 1, but their structures vary among isolates. The bla_{VIM-2} gene was first described in a *Pseudomonas aeruginosa*[6] isolate in France.

The aim of our study was to evaluate the existence of the bla_{VIM-2} gene in carbapenem-resistant *Acinetobacter baumannii* clinical isolates from Sudanese hospitals.

Materials and Methods

Forty clinical isolates of *Acinetobacter baumannii* were collected from June 2021 to April 2022. In this study, forty isolates of *Acinetobacter baumannii* were identified via BioMérieux's Vitek-2 automated system (Marcy l'Étoile, France) and evaluated for phenotypic resistance to carbapenem, using imipenem and meropenem. The enzymatic mode of resistance was assessed by the modified Hodge test (MHT). The primer sequence was adapted from a study by Monteiro et al.[17] (Table 1). A real-time PCR was used to detect the presence of the bla_{VIM-2} gene. The experiment was optimized and performed using a previously published protocol[18] as follows: a 25 µL reaction volume containing 5 µL of 5×FIREPol PCR Master Mix premixed (Solis BioDyne, Estonia), 1 µL optimized primers at a final concentration of 0.2 mM, 0.3 µL of the DNA template, and 18.7 µL sterile water to complete the reaction volume. The real-time PCR run was performed using the Sacycler-96 instrument (Sacacae biotechnology, Italy), which automatically calculated the derivatives of fluorescence measured at 533 nm. The real-time PCR conditions were as follows: 94°C for 10 minutes; forty cycles of 94°C for 40 seconds, 55°C for 45 seconds, 72°C for 50 seconds, and a final elongation step at 72°C for 10 minutes.

Results

Of 40 isolates, 32(80%) were resistant to imipenem, 4(10%) were moderately resistant, and 4(10%) were susceptible to imipenem; 24(60%) were resistant to meropenem, 10(25%) were moderately resistant, and 6(15%) were susceptible to meropenem (Figure 1). MHT was 70% positive with imipenem use and 55% positive with meropenem use (Figure 2). Real-time PCR revealed that only 30% of the samples were positive for the bla_{VIM-2} gene (Figure 3). All bla_{VIM-2}-positive isolates were resistant to both imipenem and meropenem.

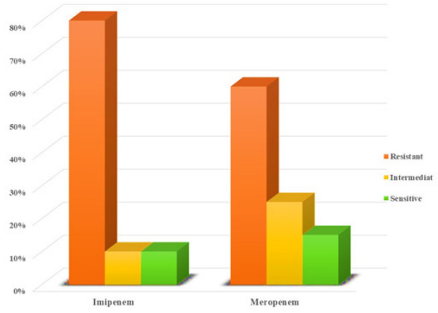

Fig. 1. *Carbapenems Susceptibility Profiles.*

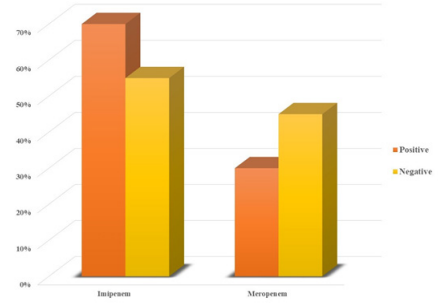

Fig. 2. *Modified Hodge test (MHT) results.*

Table 1.
Primer sequence.

	Primer	Sequence	GC%	T, C°	M.W, µg/µmol	Final Con., µM	Amp size, bp
bla_{VIM-2}	VIM-F	5'-GATGGTGTTTGGTCGCATA-3'	50.0	55.4	6024.0	0.2	382
	VIM-R	5'-CGAATGCGCAGCACCAG-3'	65.0	57.4	6160.1	0.2	

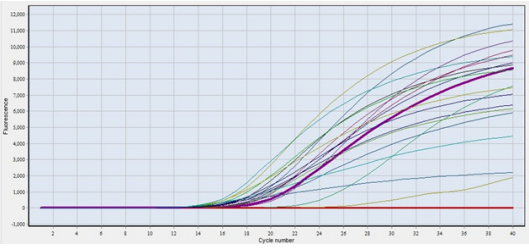

Fig. 3. *Real-time PCR detection of* bla_{VIM-2}

Discussion

Acinetobacter baumannii can cause serious, life-threatening infections, and the number of resistant strains of *Acinetobacter baumannii* isolates has increased worldwide over the last decade. WHO has declared *Acinetobacter baumannii* one of the priority pathogens.[19] All isolates in this study were resistant to one or both carbapenem antibiotics - imipenem and meropenem. In addition to structural barriers, such as cell wall permeability and lack of porins, organisms become resistant to antibiotics due to mechanical barriers, such as efflux pumps or lack or alteration of target sites, as well as by the emergence of MBL-producing bacilli.

Carbapenems are considered as last-resort antibiotics for the treatment of infections caused by multidrug-resistant, Gram-negative bacteria.[20] Susceptibility to carbapenem is typically tested using one of the antibiotics from the carbapenem family, usually imipenem or meropenem. Based on our research, we found that almost one-third of imipenem-resistant isolates were moderately resistant or sensitive to meropenem. Using only imipenem may not detect a substantial percentage of carbapenem-resistant organisms. In addition, a meropenem-sensitive isolate may carry carbapenem resistance genes that may go unnoticed, leading to further resistance spread.

Carbapenemases are groups of β-lactamases that confer resistance on carbapenem antibiotics and in some cases resistance on other classes of antibiotics, like aminoglycosides and fluoroquinolones. Enzymatic resistance is one of the most effective ways for bacteria to resist antibiotics, the evolution of enzymatic resistance is continuous with the diversity of antibiotics used for treatment.

One of the most widely used methods to detect enzyme-mediated resistance is the MHT. The principle of MHT is based on the ability of susceptible organisms to grow in the presence of an antibiotic that is enzymatically hydrolyzed by the test organism, resulting in a growth characteristic, clover-shaped zone of inhibition. In this study, MHT results also showed variation between imipenem and meropenem, with imipenem showing 70% positive MHT, suggesting that these isolates produce carbapenemase enzymes that can successfully hydrolyze imipenem antibiotics. About 45% of the isolates were MHT-positive when meropenem was used, reflecting the potency of meropenem, with a minority of isolates able to hydrolyze meropenem successfully.

Only 30% of the isolates carried the bla_{VIM-2} gene, suggesting that the bla_{VIM-2} negative isolates may have different resistance mechanisms. However, bla_{VIM-2} resides on a mobile gene cassette that is transduced by integrins with broad substrate specificity, making it a dangerous resistance element.

In conclusion, resistance to carbapenem poses a serious threat, denying patients treatment options. It is essential to make continuous surveillance of these strains to prevent the development of resistant strains.

Acknowledgments

The researchers would like to thank the National Ribat University, Al Neelain University, and the Army Hospital for making their facilities available for our practical work.

Competing Interests

The authors declare that they have no competing interests.

References

1. Lin DL, Traglia GM, Baker R, Sherratt DJ, Ramirez MS, Tolmasky ME. Functional Analysis of the *Acinetobacter baumannii* XerC and XerD Site-Specific Recombinases: Potential Role in Dissemination of Resistance Genes. Antibiotics (Basel). 2020 Jul 13;9(7):405. doi: 10.3390/antibiotics9070405.
2. Queenan AM, Bush K. Carbapenemases: the versatile beta-lactamases. Clin Microbiol Rev. 2007 Jul;20(3):440-58, table of contents. doi: 10.1128/CMR.00001-07.
3. Livermore DM, Woodford N. Carbapenemases: a problem in waiting? Curr Opin Microbiol. 2000 Oct;3(5):489-95. doi: 10.1016/s1369-5274(00)00128-4.
4. Speijer H, Savelkoul PH, Bonten MJ, Stobberingh EE, Tjhie JH. Application of different genotyping methods for Pseudomonas aeruginosa in a setting of endemicity in an intensive care unit. J Clin Microbiol. 1999 Nov;37(11):3654-61. doi: 10.1128/JCM.37.11.3654-3661.1999.
5. Lauretti L, Riccio ML, Mazzariol A, Cornaglia G, Amicosante G, Fontana R, Rossolini GM. Cloning and characterization of *bla*VIM, a new integron-borne metallo-beta-lactamase gene from a Pseudomonas aeruginosa clinical isolate. Antimicrob Agents Chemother. 1999 Jul;43(7):1584-90. doi: 10.1128/AAC.43.7.1584.
6. Poirel L, Naas T, Nicolas D, Collet L, Bellais S, Cavallo JD, Nordmann P. Characterization of VIM-2, a carbapenem-hydrolyzing metallo-beta-lactamase and its plasmid- and integron-borne gene from a Pseudomonas aeruginosa clinical isolate in France. Antimicrob Agents Chemother. 2000 Apr;44(4):891-7. doi: 10.1128/AAC.44.4.891-897.2000.
7. Sacha P, Wieczorek P, Hauschild T, Zórawski M, Olszańska D, Tryniszewska E. Metallo-beta-lactamases of Pseudomonas aeruginosa--a novel mechanism resistance to beta-lactam antibiotics. Folia Histochem Cytobiol. 2008;46(2):137-42. doi: 10.2478/v10042-008-0020-9.

***Corresponding author**: Dr. Salma Elnour Rahma Mohamed, PhD. Department of Medical Laboratory Science, Faculty of Health Sciences, Gulf Medical University, Ajman, United Arab Emirates. E-mail: dr.salmaelnour@gmu.ac.ae*

8. Bebrone C. Metallo-beta-lactamases (classification, activity, genetic organization, structure, zinc coordination) and their superfamily. Biochem Pharmacol. 2007 Dec 15;74(12):1686-701. doi: 10.1016/j.bcp.2007.05.021.
9. Santos C, Caetano T, Ferreira S, Mendo S. Tn5090-like class 1 integron carrying bla(VIM-2) in a Pseudomonas putida strain from Portugal. Clin Microbiol Infect. 2010 Oct;16(10):1558-61. doi: 10.1111/j.1469-0691.2010.03165.x.
10. Walsh TR, Toleman MA, Poirel L, Nordmann P. Metallo-beta-lactamases: the quiet before the storm? Clin Microbiol Rev. 2005 Apr;18(2):306-25. doi: 10.1128/CMR.18.2.306-325.2005.
11. Cardoso O, Leitão R, Figueiredo A, Sousa JC, Duarte A, Peixe LV. Metallo-beta-lactamase VIM-2 in clinical isolates of Pseudomonas aeruginosa from Portugal. Microb Drug Resist. 2002 Summer;8(2):93-7. doi: 10.1089/107662902760190635.
12. Cardoso O, Alves AF, Leitão R. Metallo-beta-lactamase VIM-2 in Pseudomonas aeruginosa isolates from a cystic fibrosis patient. Int J Antimicrob Agents. 2008 Apr;31(4):375-9. doi: 10.1016/j.ijantimicag.2007.12.006.
13. Bush K. Metallo-beta-lactamases: a class apart. Clin Infect Dis. 1998 Aug;27 Suppl 1:S48-53. doi: 10.1086/514922.
14. Edelstein MV, Skleenova EN, Shevchenko OV, D'souza JW, Tapalski DV, Azizov IS, Sukhorukova MV, Pavlukov RA, Kozlov RS, Toleman MA, Walsh TR. Spread of extensively resistant VIM-2-positive ST235 Pseudomonas aeruginosa in Belarus, Kazakhstan, and Russia: a longitudinal epidemiological and clinical study. Lancet Infect Dis. 2013 Oct;13(10):867-76. doi: 10.1016/S1473-3099(13)70168-3.
15. Hanson ND, Hossain A, Buck L, Moland ES, Thomson KS. First occurrence of a Pseudomonas aeruginosa isolate in the United States producing an IMP metallo-beta-lactamase, IMP-18. Antimicrob Agents Chemother. 2006 Jun;50(6):2272-3. doi: 10.1128/AAC.01440-05.
16. Dong N, Sun Q, Huang Y, Shu L, Ye L, Zhang R, Chen S. Evolution of Carbapenem-Resistant Serotype K1 Hypervirulent Klebsiella pneumoniae by Acquisition of bla_{VIM-1}-Bearing Plasmid. Antimicrob Agents Chemother. 2019 Aug 23;63(9):e01056-19. doi: 10.1128/AAC.01056-19.
17. Monteiro J, Widen RH, Pignatari AC, Kubasek C, Silbert S. Rapid detection of carbapenemase genes by multiplex real-time PCR. J Antimicrob Chemother. 2012 Apr;67(4):906-9. doi: 10.1093/jac/dkr563.
18. Mohamed SER, Alobied A, Hussien WM, Saeed MIJg. blaOXA-48 carbapenem resistant Pseudomonas aeruginosa clinical isolates in Sudan. Journal of Advances in Microbiology. 2018;10(4):1-5.
19. Mogasale VV, Saldanha P, Pai V, Rekha PD, Mogasale V. A descriptive analysis of antimicrobial resistance patterns of WHO priority pathogens isolated in children from a tertiary care hospital in India. Sci Rep. 2021 Mar 4;11(1):5116. doi: 10.1038/s41598-021-84293-8.
20. Sheu CC, Chang YT, Lin SY, Chen YH, Hsueh PR. Infections Caused by Carbapenem-Resistant *Enterobacteriaceae*: An Update on Therapeutic Options. Front Microbiol. 2019 Jan 30;10:80. doi: 10.3389/fmicb.2019.00080.

International Journal of Biomedicine 12(4) (2022) 640-643
http://dx.doi.org/10.21103/Article12(4)_OA22

ORIGINAL ARTICLE

Medicinal Plants

INTERNATIONAL JOURNAL OF BIOMEDICINE

Evaluation of Antibacterial Activity and Characterization of Phytochemical Compounds from Selected Mangrove Plants

M. Duraipandian[1*], H. Abirami[1], K. S. Musthafa[2], S. Karuthapandian[2]

[1]*PG and Research Department of Biotechnology, Vivekanandha College of Arts and Sciences for Women, Elayampalayam, Tamil Nadu, India*

[2]*Department of Biotechnology, Alagappa University, Karaikudi, Tamilnadu, India*

Abstract

The aim of this study was to investigate the antibacterial activity of n-butanol, petroleum ether, ethyl acetate, ethanol, methanol, and chloroform extracts of the sponges and leaves of different mangrove species (*Bruguiera cylindrica*, *Suaeda maritima, Ceriops decandra*, *Avicennia officinalis, Rhizophora apiculata*, *Suaeda monoica*, *Avicennia marina*, and *Rhizohora mucronata*) against *Proteus mirabilis* ATCC 7002.

Methods and Results: Agar well diffusion method was used to evaluate the antimicrobial activity of selected mangrove extracts. The active compounds from mangrove sponges and leaves with various solvents were examined under Fourier transform infrared (FTIR) spectroscopy. The ethyl acetate extracts, methanol extracts, chloroform extracts, n-butanol extracts, and petroleum ether extracts of selected mangrove leaves (*B. cylindrical*, *S. maritime*, *A. officinalis*, *S. monoica*, *A. marina*, *R. mucronata*) showed good antibacterial activity against *P. mirabilis* ATCC 7002. FTIR analysis of crude methanol extract of *S. monoica* showed the presence of amide and alkane groups in phytochemicals. For crude methanol extract of *R. mucronata*, the presence of phenol, nitro, amide, and alkane groups was revealed.

Conclusion: the results obtained revealed industrially important mangrove extracts and the functional groups of plant compounds responsible for great antibacterial activity.(**International Journal of Biomedicine. 2022;12(4):640-643.**).

Keywords: mangrove species • solvents • antibacterial activity

For citation: Duraipandian M, Abirami H, Musthafa KS, Karuthapandian S. Evaluation of Antibacterial Activity and Characterization of Phytochemical Compounds from Selected Mangrove Plants. International Journal of Biomedicine. 2022;12(4):640-643. doi:10.21103/Article12(4)_RA22

Introduction

Among billions of microorganisms, bacteria are the dominant cause of many diseases in higher eukaryotes. Bacteria are present everywhere and have various sizes and shapes. Beneficial bacteria protect the bodily functions of organisms and also have the ability to preserve the environment. But some bacteria cause deadly diseases to people. An exponential increase in bacteria that are resistant to multiple drugs against antibiotics is a critical issue.[1-3] Currently, it has been shown that bacteria are highly interactive and exhibit several social behaviors, such as swarming motility, bioluminescence, conjugal plasmid transfer, antibiotic resistance, biofilm maturation, and virulence.[4-6] The dramatically rapid and continuous emergence of antibiotic resistance in the clinical context necessitates the urgent identification of novel strategies for treating bacterial infections, including research for screening of plants for their antimicrobial activity.

Mangroves, the littoral forests of tropics and subtropics, are well known for their ecological importance. The mangrove ecosystem is characterized by highly changeable environmental conditions, such as salinity, temperature, nutrients, and tidal currents, making it one of the most productive ecosystems.[7-9] Mangroves are a rich source of several bioactive compounds (secondary metabolites) that have therapeutic significance, such as steroids, triterpenes, saponins, flavonoids, phenolic compounds, alkaloids, and tannins.[8] Recently, many studies have been directed toward investigating the biological activity of mangroves for the treatment of various diseases.[10] Due to the presence of the varied levels of bioactive compounds, research interest in mangrove plants for their therapeutic activities, including antimicrobial effects, is increasing continuously.[11-14]

***Corresponding author**: Dr. M. Duraipandian. PG and Research Department of Biotechnology, Vivekanandha College of Arts and Sciences for Women, Elayampalayam, Tamil Nadu, India E-mail: drduraipandian@vicas.org and durai2muthu@gmail.com*

The present study conducted in vitro experimental evaluation of the antibacterial activity of extracts of plant parts of *Bruguiera cylindrica* (B. *cylindrica*) [M1], *Suaeda maritima* (*S. maritima*) [M2], *Ceriops decandra* (*C. decandra*) [M3], *Avicennia officinalis* (*A. officinalis*) [M4], *Rhizophora apiculata* (*R. apiculata*) [M5], *Suaeda monoica* (*S. monoica*) [M6], *Avicennia marina* (*A. marina*) [M7], and *Rhizohora mucronata* (*R. mucronata*) [M8] in different solvent systems (methyl acetate, methanol, ethanol, n-butanol, chloroform and petroleum ether) against *Proteus mirabilis* ATCC 7002.

Proteus mirabilis (*P. mirabilis*), a kind of motile gram-negative bacteria in the Enterobacteriaceae family, is widely distributed in the environment, mainly in water, soil, and human and animal gastrointestinal tracts.[15] It is an opportunistic pathogen.[16] Among the gram-negative bacteria, *P. mirabilis* is the dominant biofilm producer in urinary tract infections, next to *E. coli*. Urease production and robust swarming motility are the 2 hallmarks of this organism. Clinically, *P. mirabilis* is most frequently a pathogen of the urinary tract, particularly in patients undergoing long-term catheterization.[17]

The aim of this study was to investigate the antibacterial activity of n-butanol, petroleum ether, ethyl acetate, ethanol, methanol, and chloroform extracts of the sponges and *leaves of different mangrove* species (M1-M8) against *P. mirabilis* ATCC 7002.

Materials and Methods

Plant collection

B. cylindrical, *S. maritime*, *C. decandra*, *A. officinalis*, *R. apiculata*, *S. monoica*, *A. marina*, *R. mucronata* were collected from the Thondi region of Rameswaram District, Tamil Nadu. The taxonomical identification of this plant was made by mangrove plants of Tamil Nadu Publication from M.S. Swaminathan Research Foundation.

Plant sample preparation and extraction methods

The fresh plant was washed under running tap water and dried in a warm place for 3 to 5 days. The samples were ground into a fine powder and the extract was prepared with different solvents, such as methanol, ethyl acetate, n-butanol, ethanol, petroleum ether, and chloroform. The extract was prepared by adding 0.5 g of sample powder in 10 ml solvents and keeping it in a shaker; then the collected solvent layer was dried in a water bath. Finally, the dried samples were kept in 2 ml Eppendorf tubes, to store for future use.

Bacterial strain

The target pathogen used in this study was *P. mirabilis* ATCC 7002, which was streaked and maintained in Luria–Bertani agar plates. For the antibacterial assay, the strain was cultivated in 2 ml of the sterile nutrient broth overnight, and 1% inoculum was subcultured for 3 hours in 2ml of sterile nutrient broth.

Antibacterial activity by the agar well diffusion method

The agar well diffusion assay was performed in nutrient agar plates. The nutrient agar medium was sterilized at 121°C for 20 minutes and poured into sterile Petri plates. The plates were allowed to solidify. Then the subcultured test pathogens were swabbed on the nutrient agar plates and kept for a few minutes for drying. Wells with 5 mm diameter were made on each plate and 100 µl of crude extract obtained from sponges and leaves of mangroves were loaded on the well. The plates were incubated for 16 hours at 30°C, and the zone of inhibition against each pathogen was measured.

FTIR analysis of crude of mangrove leaves

The active compounds from mangrove sponges and leaves with various solvents were examined under Fourier transform infrared (FTIR) spectroscopy. FTIR spectrum of crude extract mixed with potassium bromide pellet was recorded using an FTIR spectrophotometer.

Results

The shade-dried samples of sponges and leaves of mangroves were extracted with various solvents, and the weight of each crude extract was weighed in a pre-weighed Eppendorf tube.

Antibacterial activity of different extracts of mangroves against *P. mirabilis*

A total of 8 different solvent extracts of mangrove plants were tested for their antibacterial activity against *P. mirabilis.* Optimum inhibitory activity was shown by the following extracts: The crude ethyl acetate extracts of M2, M4, M6, and M8 showed inhibitory zones of 16 mm, 17 mm, 18 mm, and 17 mm, respectively (Figures 1-2, Plates 1-2).

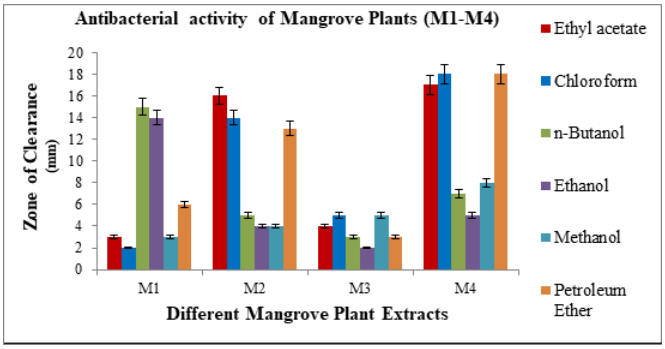

Fig. 1. *Antibacterial activity in terms of zone of inhibition of different mangrove extracts (M1 to M4) in different solvent systems*

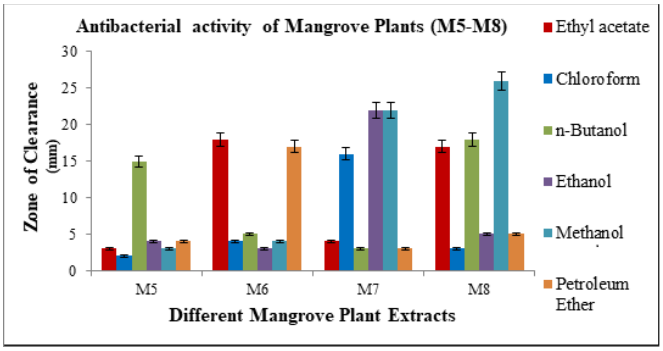

Fig. 2. *Antibacterial activity in terms of zone of inhibition of different mangrove extracts (M5 to M8) in different solvent systems*

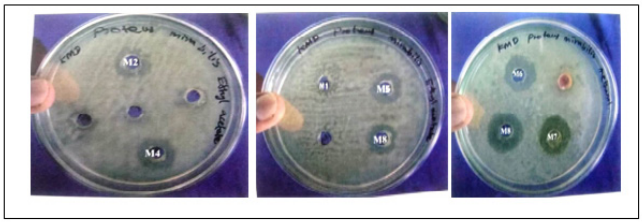

(1) (2) (3)

Plates 1-3. *The maximum antibacterial activity in terms of zone of inhibition of different mangrove extracts of M5 to M8 in ethyl acetate (2) and M6, M7 & M8 in methanol (3).*

The crude methanol extracts of M7 and M8 showed inhibitory zones of 24 mm and 26 mm, respectively (Figure 2, Plate 3) The crude n-butanol extracts of M5 and M8 showed inhibitory zones of 15 mm and 18 mm, respectively (Figure 2). The crude petroleum ether extracts of M2, M4, and M6 showed inhibitory zones of 14 mm, 18 mm, and 17 mm, respectively (Figures 1-2). Out of chloroform extracts, the crude extracts of M4 and M7 showed inhibitory zones of 18mm and 16mm, respectively (Figures 1-2). Out of ethanol extracts, the crude extracts of M1 and M7 showed inhibitory zones of 14mm and 16mm, respectively (Figures 1-2).

The FTIR spectroscopy was done to identify the functional group of the antibacterial compound present in the crude methanol extracts of M6 and M8. The FTIR peaks of methanol crude extract of M6 showed the presence of amide and alkane groups (Figure 3), whereas FTIR peaks of crude methanol extract of M8 showed the presence of phenol, amide, nitro, and alkane groups (Figure 4).

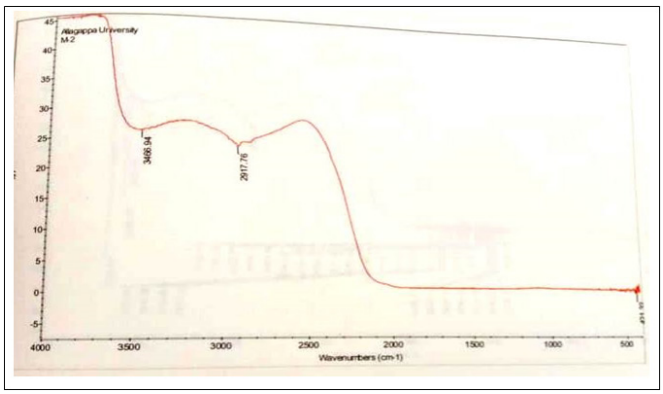

Fig. 3*. FTIR spectrum of methanol extracts of mangrove leaves of M6*

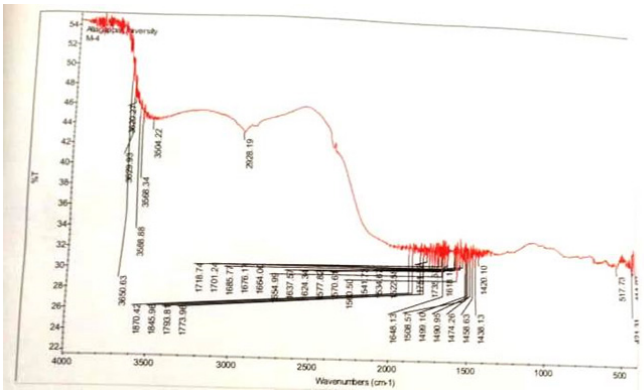

Fig. 4. *FTIR spectrum of methanol extracts of mangrove leaves of M8*

Discussion

The mangrove plants are the sources of potent drugs.[18] These drugs have many potential properties, such as antiviral, antibacterial, anthelmintic, antifungal, or antimalarial.[19-20] However, the extraction of novel natural chemical compounds from mangroves, in addition to those already known to the pharmacological compound, is still far from complete. Abeysinghe et al.[21] reported the promising antibacterial activity of *A. marina*. Moderate antibacterial activity is shown by *S. maritima* (Chenopodiaceae family) due to the presence of phenolic compounds like tannins.[22] The presence of glycosides, saponins, tannins, flavonoids, alkaloids, and terpenoids may influence the antibacterial activity of *A. officinalis*.[23] Das et al.[24] reported promising antibacterial activity due to the presence of terpenoids, phenolics, and alkaloids. Thus, pharmacological screening of natural products can be a source of innumerable therapeutic agents.[25]

In our study, different crude extracts of the selected mangrove leaves made with different solvents showed a clear zone of inhibition. The ethyl acetate extracts, methanol extracts, chloroform extracts, n-butanol extracts, and petroleum ether extracts of selected mangrove leaves (B. cylindrical, S. maritime, A. officinalis, S. monoica, A. marina, R. mucronata) showed good antibacterial activity against *P. mirabilis* ATCC 7002. FTIR analysis of crude methanol extract of *S. monoica* showed the presence of amide and alkane groups in phytochemicals. For crude methanol extract of *R. mucronata*, the presence of phenol, nitro, amide, and alkane groups was revealed.

In conclusion, the results obtained revealed industrially important mangrove extracts and the functional groups of plant compounds responsible for great antibacterial activity.

Competing Interests

The authors declare that they have no competing interests.

References

1. Walsh C. Where will new antibiotics come from? Nat Rev Microbiol. 2003 Oct;1(1):65-70. doi: 10.1038/nrmicro727.
2. Westh H, Zinn CS, Rosdahl VT. An international multicenter study of antimicrobial consumption and resistance in Staphylococcus aureus isolates from 15 hospitals in 14 countries. Microb Drug Resist. 2004 Summer;10(2):169-76. doi: 10.1089/1076629041310019.
3. Sasidharan S, Prema B, Yoga LL. Antimicrobial drug resistance of Staphylococcus aureus in dairy products. Asian Pac J Trop Biomed. 2011 Apr;1(2):130-2. doi: 10.1016/S2221-1691(11)60010-5.
4. Hentzer M, Givskov M. Pharmacological inhibition of quorum sensing for the treatment of chronic bacterial infections. J Clin Invest. 2003 Nov;112(9):1300-7. doi: 10.1172/JCI20074.
5. Rasmussen TB, Bjarnsholt T, Skindersoe ME, Hentzer M, Kristoffersen P, Köte M, et al. Screening for quorum-sensing inhibitors (QSI) by use of a novel genetic system, the

QSI selector. J Bacteriol. 2005 Mar;187(5):1799-814. doi: 10.1128/JB.187.5.1799-1814.2005.
6. Shih PC, Huang CT. Effects of quorum-sensing deficiency on Pseudomonas aeruginosa biofilm formation and antibiotic resistance. J Antimicrob Chemother. 2002 Feb;49(2):309-14. doi: 10.1093/jac/49.2.309.
7. Kathiresan K, Bingham BL. Biology of mangroves and mangrove Ecosystems. In Advances in Marine Biology. Academic Press: Cambridge, MA, USA, 2001; Volume 40, pp. 81–251.
8. Bandaranayake WM. Bioactivities, bioactive compounds and chemical constituents of mangrove plants. Wetlands Ecology and Management. 2002;10:421–52.
9. Liu L, Wang B. Protection of Halophytes and Their Uses for Cultivation of Saline-Alkali Soil in China. Biology (Basel). 2021 Apr 22;10(5):353. doi: 10.3390/biology10050353.
10. Ser HL, Tan LT, Law JW, Chan KG, Duangjai A, Saokaew S, et al. Focused Review: Cytotoxic and Antioxidant Potentials of Mangrove-Derived Streptomyces. Front Microbiol. 2017 Nov 1;8:2065. doi: 10.3389/fmicb.2017.02065.
11. Okla MK, Alamri SA, Alatar AA, Hegazy AK, Al-Ghamdi AA, Ajarem JS, et al. Antioxidant, Hypoglycemic, and Neurobehavioral Effects of a Leaf Extract of Avicennia marina on Autoimmune Diabetic Mice. Evid Based Complement Alternat Med. 2019 May 21;2019:1263260. doi: 10.1155/2019/1263260.
12. Abeysinghe PD. Antibacterial Activity of some Medicinal Mangroves against Antibiotic Resistant Pathogenic Bacteria. Indian J Pharm Sci. 2010 Mar;72(2):167-72. doi: 10.4103/0250-474X.65019.
13. Gurudeeban S, Ramanathan T, Satyavani K. Antimicrobial and radical scavenging effects of alkaloid extracts from Rhizophora zucronata. Pharm Chem J. 2013;47:50–53.
14. Mouafi FE, Abdel-Aziz SM, Bashir AA, Fyiad AA. Phytochemical analysis and antimicrobial activity of mangrove leaves (Avicenna marina and Rhizophora stylosa) against some pathogens. World Appl Sci J. 2014;29:547–554.
15. Drzewiecka D. Significance and Roles of Proteus spp. Bacteria in Natural Environments. Microb Ecol. 2016 Nov;72(4):741-758. doi: 10.1007/s00248-015-0720-6.
16. Yuan F, Huang Z, Yang T, Wang G, Li P, Yang B, Li J. Pathogenesis of Proteus mirabilis in Catheter-Associated Urinary Tract Infections. Urol Int. 2021;105(5-6):354-361. doi: 10.1159/000514097.
17. Schaffer JN, Pearson MM. Proteus mirabilis and Urinary Tract Infections. Microbiol Spectr. 2015 Oct;3(5):10.1128/microbiolspec.UTI-0017-2013. doi: 10.1128/microbiolspec.UTI-0017-2013.
18. Owhe-Ureghe UB, Ehwarieme DA, Eboh DO. Antibacterial activity of garlic and lime on isolates of extracted carious teeth. African Journal of Biotechnology. 2010;9(21):3163-3166.
19. Proksch P, Edrada RA, Ebel R. Drugs from the seas - current status and microbiological implications. Appl Microbiol Biotechnol. 2002 Jul;59(2-3):125-34. doi: 10.1007/s00253-002-1006-8.
20. Faulkner DJ. Marine pharmacology. Antonie Van Leeuwenhoek. 2000 Feb;77(2):135-45. doi: 10.1023/a:1002405815493.
21. Abeysinghe PD, Pathirana RN, Wanigatunge R. Evaluation of antibacterial activity of different mangrove plant extracts. Ruhuna Journal of Science. September 2006;1:104–112
22. Patra JK, Thatoi HN. Metabolic diversity and bioactivity screening of mangrove plants: a review. Acta Physiol Plant. 2011;33:1051–1061. doi: 10.1007/s11738-010-0667-7
23. Bhimpa V, Jaganathan P, Joel EL. Antibacterial activity and characterization of secondary metabolites isolated from mangrove plant Avicennia officinalis. Asian Pacific Journal of Tropical Medicine. 2010;3(7):412-420
24. Das SS. Qualitative determination of phytochemical constituents and antimicrobial activity of the mangrove plant Avicennia alba Blume. Int J Res Anal Rev. 2020;7(1):627-633
25. Mitra S, Naskar N, Chaudhuri P. A review on potential bioactive phytochemicals for novel therapeutic applications with special emphasis on mangrove species Phytomedicine Plus. 2021;1,100107

International Journal of Biomedicine 12(4) (2022) 644-647
http://dx.doi.org/10.21103/Article12(4)_OA23

ORIGINAL ARTICLE

Morphology

INTERNATIONAL JOURNAL OF BIOMEDICINE

Homology in Structural and Functional Organization of the Fibrous Framework of the Derma and Paraneural Connective Tissue Components

Anastasia M. Dzharu[1], Ekaterina S. Mishina[1], Mariya A. Zatolokina[1], Karina M. Borodina[1], Maksim S. Novikov[2], Ludmila M. Kachmarskaya[2]

[1]*Kursk State Medical University, Kursk, Russia*
[2]*Orel State University named after I.S. Turgenev, Orel, Russia*

Abstract

Background: The recent increase in hostilities throughout the globe is one of the main factors that damage both the skin and peripheral nerves (PN), mainly of the upper and lower extremities. The duration of treatment of the injured limb and the rate of recovery of its functions are directly related to the structural integrity of the connective tissue (CT) sheath apparatus of the PN, which further actualizes the study of its micromorphological components. The structural integrity of the peripheral nerve includes not only the preservation of its conductive component but also the membranes surrounding it, providing complete morphofunctional unity. Thus, the study of the features of their tissue organization, vascularization and innervation, with the obligatory comparison of data with homologous tissue of different topography and possible extrapolation of data, determined the purpose of this work. The aim of this study was to analyze the dynamics of changes in the fibrous components of the paraneurium and dermis in onto- and phylogenesis under the influence of various factors and to compare the data obtained for their further extrapolation.

Methods and Results: The study was conducted on mature male Wistar rats under standard vivarium conditions. The material for the study was the CT sheaths of the PN of the extremities and skin areas, 1x1 cm in size, to the depth of the subcutaneous fascia of animals. The cadaver material was taken on Days 1, 3, 7, 10, and 28 of ontogeny. The resulting biomaterial was fixed in a 10% buffered neutral formalin solution and embedded in paraffin, according to the standard method. Microtomized, the resulting histological sections were stained with hematoxylin and eosin, according to the method of Mallory and Van Gieson. A comprehensive morphological study was performed using light and electron microscopy. The study revealed the presence of two stages in the ontogeny of the CT, forming the dermis of the skin and paraneural CT structures of PN. In the first stage, structural elements are formed, considering the topography of the CT; in the second, they are differentiated, leading to a qualitative-quantitative transformation due to the appearance of a number of additional functions, an active period of body growth, and taking into account the action of various environmental factors. At earlier stages of ontogenesis, thin, flattened fibrous structures without a clear organization are observed in the field of view in the dermis of the skin. In the paraneurium, the components that form it are not sufficiently expressed. At later periods, the shape and architectonics of the fibrous component change, structurization and an increase in the thickness of the fibers occur and pronounced heterogeneity of the cellular component is observed.**(International Journal of Biomedicine. 2022;12(4):644-647.)**.

Keywords: skin dermis • connective tissue • collagen fibers • fibroblasts • regeneration • paraneural membrane

For citation: Dzharu AM, Mishina ES, Zatolokina MA, Borodina KM, Novikov MS, Kachmarskaya LM. Homology in Structural and Functional Organization of the Fibrous Framework of the Derma and Paraneural Connective Tissue Components . International Journal of Biomedicine. 2022;12(4):644-647. doi:10.21103/Article12(4)_OA23

Abbreviations

CT, connective tissue; **PN**, peripheral nerves.

Introduction

Despite significant achievements in practical neurosurgery in performing reconstructive operations on the trunks of peripheral neurons, there are still unresolved issues regarding the need to perform restorative manipulations on the connective tissue (CT) membranes surrounding the bundles of nerve fibers.[1-3] Endo-, peri-, epi- and paraneural CT sheaths of peripheral nerves (PN), having one fundamental morphological basis, perform different functions due to a

slightly different list of structural elements and topographic features.[4,5]

In domestic and foreign literature, sufficient data are presented on the structure and functions of the epi-, peri- and endoneural membranes. At the same time, data on the morphological and functional organization of the paraneural membrane are scattered and incomplete.[6,7] One of the first to study the structure of the paraneural membrane and determine its role in the peripheral nerve (sciatic nerve) was the domestic morphologist V. S. Polsky (1991). After a quarter of a century, another domestic morphologist, M. A. Zatolokina (2017), studied the paraneural apparatus of the PN of the branches of the brachial plexus in a phylogenetic aspect. In the works of foreign scientists, such as J. D. Vlok (1997), Andersen et al. (2012), O. Choquet et al. (2012), and M. Karmakar et al. (2013), data were developed that allowed the functional role of paraneural CT structures to be somewhat specified. Regarding the skin, it should be noted that external influences and any damage to internal organs (in this case, the PN of the limbs) are associated with the destruction of the constituent elements of the skin. In this regard, the study of the morphology of the constituent elements of the skin in the norm (ontogenesis) and under the influence of various factors (humid environment, physical activity) does not lose its relevance at the present time.[8-10]

The main working hypothesis of this work was that some homology is present in the structure of the fibrous base of the paraneural membrane of the peripheral nerve and the dermis of the skin. Considering the almost identical structural set of paraneurium and dermis components, the goal of this work was formulated: to analyze the dynamics of changes in the structural components of paraneurium and dermis in ontogenesis and phylogenesis under the influence of various factors and to compare the data obtained for their further extrapolation.

Materials and Methods

In vivo experiments were carried out in accordance with the legislation of the Russian Federation, in strict compliance with the European Convention for the protection of animals used for experimental and other purposes (Strasbourg, France, 1986), the provisions of Directive 2010/63/EU of the European Parliament and the Council of the European Union of 22 September 2010 on the protection of animals used for scientific purposes (Article 27), and approved by the Regional Ethics Committee of Kursk State Medical University.

The study was conducted on mature male Wistar rats under standard vivarium conditions. The material for the study was the CT sheaths of the PN of the extremities and skin areas, 1x1 cm in size, to the depth of the subcutaneous fascia of animals. The cadaver material was taken on Days 1, 3, 7, 10, and 28 of ontogeny. The resulting biomaterial was fixed in a 10% buffered neutral formalin solution and embedded in paraffin, according to the standard method. Microtomized, the resulting histological sections were stained with hematoxylin and eosin, according to the method of Mallory and Van Gieson. For scanning electron microscopy (SEM), the material, after fixation, was dehydrated in a frozen state in alcohols of increasing concentrations and mounted on a special aluminum table with conductive carbon glue, sputtered with a platinum-palladium alloy in a Quorum Q150TS sputtering unit (Germany). Next, a comprehensive morphological study was performed using light and electron microscopy (SEM - S 3400N, Hitachi, Japan). The dynamics of changes in morphometry data were assessed by such indicators as the CT density coefficient (CTDC) and the heterogeneity of the cell population. CTDC was calculated as the ratio of the area occupied by the fibers (A-f, %) to the area of interfiber gaps (A-ig, %). A-f and A-ig were determined in 30 fields of view on digitized micrographs after their geometric and optical calibration using the ImageJ 14.7a program. The heterogeneity of the cell population was assessed by karyological identification of cells visualized between the structures of the fibrous component—resident and non-resident cells were counted in 10 non-overlapping fields of view per 100 cells.

Statistical analysis was performed using using the program Statistika 10.0 (StatSoft). The mean (M) and standard error of the mean (SEM) were calculated. Differences of continuous variables were tested by the Mann-Whitney U-test. A probability value of $P \leq 0.05$ was considered statistically significant.

Results and Discussion

The main working hypothesis of this work was that homology is present in the structure of the fibrous base of the skin dermis and the paraneural apparatus of the PN. At the heart of two topographically different parts of a living organism, the skin and the paraneural membrane, is the CT, and the source of development in embryogenesis is the mesenchyme. Given this fact, it is quite logical to assume that these topographic areas are similar not only in the structure of the CT, but also in the performance of the same morphologically substantiated functions under the condition of the same external factors.

The first stage of the study, including an examination of the features of the structural organization of the fibrous component of the paraneural membrane and the dermis of the skin in laboratory animals (rats at different periods of ontogenesis), made it possible to state a similar vector direction in the dynamics of the development of the CT that forms the above indicated topographic areas.

The paraneurium of the PN of the extremities is a complex of CT, vascular, and nervous structures located between the epineurium and the fascia of the adjacent muscles and having a close morphofunctional relationship with the nerve trunk. The CT basis of the paraneurium includes its own fascial sheath and fibrillar cords extending from it, separating the fascial-cellular spaces (filled with adipose tissue) and connecting the paraneural apparatus with the fascia and interfascial spaces of the adjacent muscles. In the early stages of postnatal ontogenesis (1-3 days after birth), the fibrillar structures of the paraneurium are very poorly developed. Fascial sheath is formed by several CT fibers located relative to each other loosely and not ordered. Fibrillar strands are

not identified, fascial-cellular spaces are just beginning to form, and white adipose tissue is visualized in them with an unexpressed lobular organization.

In sections of the dermis, the fibrous component looks like thin plates with a large number of branches. The high density of the cellular component is noteworthy in comparison with the paraneural structures, where it is insignificant. The thickness of the fibrils varied from 28 to 32±0.1 nm, and the collagen fibers formed from them were 5.2±0.3 μm.

On Days 7-10 of ontogenesis, a complication of the structure of the paraneural apparatus was observed, manifested in a pronounced morphological representation of all its constituent components, as well as the structural organization of the dermis. The thickness of the fascial sheath was 2.47±0.11 μm, and that of the outgoing CT slings was 0.49±0.01 μm. The fibrous component was represented by wavy, transversely striated collagen fibers, which, when stained by the Mallory method, had a bright blue color. It should be noted that the change in the shape of collagen structures on longitudinal sections from lamellar to fibrous, on transverse sections, the shape was rounded. At the same time, the thickness of collagen fibrils was 38±1.8 nm; they were located in parallel. The cellular component was heteromorphic; several differons were identified by karyological features. The density of cells was 1.5 to 2 times higher than at the previous stage of ontogenesis.

In the late stages of ontogenesis (puberty), in the organization of both the fibrous skeleton of the dermis and the paraneurium, the rhomboid type in the arrangement of fibrous structures predominates. Thickening and spiralization of collagen fibers were observed in the dermis. On transverse sections, their shape varies from flattened to rounded. The diameter of fibrils forming collagen fibers ranged from 70 nm to 90 nm. In the structural organization of the paraneurium, a 1.7-fold thickening of its own fascial sheath and CT slings was observed. The fibers visualized in them have a spiral course, which smoothly turns into lines. Between the slings are well-defined lobules of adipose.

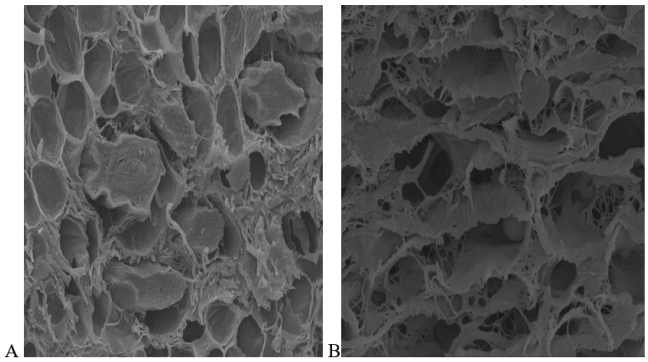

Fig. 1. *Micrograph of connective tissue (collagen fibers): A – Paraneuria; B- In the dermis of the skin. Magnification x1200. SEM.*

Thus, in the ontogeny of the CT structures of the paraneurium and the dermis of the skin, their two-stage activity was observed. In the first stage, the necessary list of structural elements was formed; in the second stage - their differentiation, which consists of a qualitative and quantitative transformation due to the appearance of several additional functions, an active period of body growth, and taking into account the action of various environmental factors.

In conclusion, the study revealed the presence of two stages in the ontogeny of the CT, forming the dermis of the skin and paraneural CT structures of PN. In the first stage, structural elements are formed, considering the topography of the CT; in the second, they are differentiated, leading to a qualitative-quantitative transformation due to the appearance of a number of additional functions, an active period of body growth, and taking into account the action of various environmental factors. At earlier stages of ontogenesis, thin, flattened fibrous structures without a clear organization are observed in the field of view in the dermis of the skin. In the paraneurium, the components that form it are not sufficiently expressed. At later periods, the shape and architectonics of the fibrous component change, structurization and an increase in the thickness of the fibers occur and pronounced heterogeneity of the cellular component is observed.

The data obtained during the work fully comply with the Lesgaft law: the form and functions are the same, which allows one to transfer the observed changes in the CT of the dermis in conditions of damage or inflammation to the paraneural CT structures. Also, it is possible to predetermine the dynamics of the course of pathological changes and disorders in the future of the functions of those structures for which the paraneurium components are fundamental (the conductive component of the PN in this case). Homologous changes in the fibrous skeleton of the dermis and paraneurium observed during ontogeny make it possible, with a certain degree of probability, to extrapolate the obtained data on changes in the dermis to the paraneural structures of the PN of the extremities.

Competing Interests

The authors declare that they have no competing interests.

References

1. Mishina ES, Zatolokina MA, Gorbunova MV, Alekseev AG, Chernomortseva ES. Comprehensive study of the structural components of the skin: from routine methods to modern microscopy methods. International Journal of Biomedicine. 2021;11(2):216-219. doi: 10.21103/Article11(2)_OA16
2. Shelupaiko VN, Borodina KM, Zatolokina MA, Zatolokina ES. [Dynamics of changes in the cellular component of the connective tissue of the paraneural structures of the sciatic nerve in the age aspect]. In the collection: "Modern problems of morphology." Proceedings of a scientific conference dedicated to the memory of Academician of the Russian Academy of Sciences, Professor Lev Lvovich Kolesnikov. 2020: 268-270. [Article in Russian].

***Corresponding author**: Prof. Mariya A. Zatolokina, PhD, ScD. Department of Histology, Embryology, and Cytology. Kursk State Medical University. Kursk, Russia. E-mail: marika1212@mail.ru*

3. Zolotenkova GV, Morozov YuE, Tkachenko SB, Pigolkin YuI. [Age-related changes in the structural and functional parameters of the skin]. Bulletin of the Baltic Federal University. I. Kant. 2014;1:132–139. [Article in Russian].
4. Mishina ES, Zatolokina MA, Ten'kov AA, Tsymbalyuk VV, Nevolko VO, Shmatko IA, Zatolokina ES. [Morphofunctional formation of the skin as an organ in the process of ontogenesis]. Bulletin of the Volgograd State Medical University. 2020;4(76):131-135. [Article in Russian].
5. Borodina KM, Zatolokina MA, Kharchenko VV, Tenkov AA, Zatolokina ES. [Features of the structural organization of the paraneural connective tissue sheath of the sciatic nerve of rats in different periods of postnatal development]. Bulletin of the Volgograd State Medical University. 2020;4(76):152-155. [Article in Russian].
6. Savenkova EN, Efimov AA, Gavrichenko EP, Kurzin LM. [The use of quantitative involutive indicators of the skin in determining the age of a person]. Bulletin of TSU. 2015; 4 (20): 824-827. [Article in Russian].
7. Fokina EN, Zagrebin VL, Fedorova OV, Tkhabit Khuda Salekh A. [Morphological aspects of skin development at different stages of prenatal ontogenesis]. Actual problems of experimental and clinical medicine. Materials of the 63rd final scientific conference of students and young scientists. 2005:124-126. [Article in Russian].
8. Fibrosis: Methods and Protocols. Edited by Laure Rittie; 2017.
9. Ghazanfari S, Khademhosseini A, Smit TH. Mechanisms of lamellar collagen formation in connective tissues. Biomaterials. 2016 Aug;97:74-84. doi: 10.1016/j.biomaterials.2016.04.028.
10. Sidgwick GP, McGeorge D, Bayat A. A comprehensive evidence-based review on the role of topicals and dressings in the management of skin scarring. Arch Dermatol Res. 2015 Aug;307(6):461-77. doi: 10.1007/s00403-015-1572-0.

International Journal of Biomedicine 12(4) (2022) 648-653
http://dx.doi.org/10.21103/Article12(4)_OA24

ORIGINAL ARTICLE

Bioethics

INTERNATIONAL JOURNAL OF BIOMEDICINE

Bioethical Knowledge and Attitudes Among Dental and Medical Students in the Medical Faculty, University of Prishtina

Fehim Haliti[1], Dion Haliti[2], Valon Hyseni[3], Valdete Haliti[4], Elena Hajdari[5], Dea Haliti[2], Naim Haliti[3*]

[1]*Department of Pediatric and Preventive Dentistry, University of Prishtina, School of Dental Medicine*
[2]*Faculty of Medicine, University of Prishtina "Hasan Prishtina"*
[3]*Department of Forensic Medicine, Faculty of Medicine, University of Prishtina, Clinical Centre N.N.*
[4]*Law Faculty, University of Prishtina*
[5]*Department of Dentistry, Faculty of Medicine, University of Prishtina "Hasan Prishtina"*
Prishtina, Kosovo

Abstract

The importance of bioethics as a formal subject has been recognized globally. The purpose of this study was to analyze undergraduate medical and dental students' knowledge, practice and attitudes regarding bioethical questions through a questionnaire. This cross-sectional study was conducted among students from the Medical Faculty who were in their first or fourth year of education. There were no differences in bioethics awareness between direction (general medicine [GM] or dentistry) or years of study among 301 GM and dental students. In this research, GM and dental students, in general, indicated a positive attitude and knowledge of bioethics.(**International Journal of Biomedicine. 2022;12(4):648-653.**).

Keywords: bioethics • dentistry • general medicine • students

For citation: Haliti F, Haliti D, Hyseni V, Haliti V, Hajdari E, Haliti D, Haliti N. Bioethical Knowledge and Attitudes Among Dental and Medical Students in the Medical Faculty, University of Prishtina. International Journal of Biomedicine. 2022;12(4):648-653. doi:10.21103/Article12(4)_OA24.

Introduction

Being a professional in our field of dentistry requires the application of bioethics. The code's introduction begins with the notion that trust is unique and vital to dentistry's role in society. More than 2,000 years ago, Hippocrates acknowledged the significance of ethics as an essential component of the medical profession — therefore, by extension, it is an also essential component of the dental profession because dentistry is central to general health.[(1)] The earliest code of bioethics was written in 1866.[(2)] The principles of ethics emphasize the dentistry profession's aspirational objectives, which are similar to those of other healthcare professions.[(3)] Bioethics is a branch of ethics associated with the systematic investigation of the aspects of human behavior in health sciences and healthcare that are based on moral principles and human values.[(4)]

Teaching professional ethics in dentistry is crucial, and appropriate goals for teaching the subject have been developed to educate student dentists on the ethical aspects of professional life and practice, enhance ethical analytical abilities among student dentists, and develop student dentists' respect and understanding for disagreement and indefiniteness. Additionally, it helps student dentists better comprehend the moral responsibility that comes with being a member of the dental profession, to encourage student dentists to continue their education in the area of professional ethics.[(5,6)]

Bioethics[(7)] should be a discipline that follows scientific progress while maintaining professional ethics and attributes. However, because of its complexity, bioethics education provides a dilemma for many teachers and scientists.

The aim of this study was to assess the knowledge and awareness of medical ethics, as well as attitudes toward the subject, among Bachelor of dentistry and general medicine

***Corresponding author**: Prof. Dr. Naim Haliti. Department of Forensic Medicine, Faculty of Medicine, University of Prishtina, Clinical Centre N.N. Prishtina, Kosovo. E-mail: naim.haliti@uni-pr.edu*

(GM) students in the first and fourth years of study in the Medical Faculty of the University of Prishtina.

Methods

We conducted a cross-sectional study among dentistry and medical undergraduate students who were attending the clinical years (first and fourth) in the Medical Faculty at the University of Prishtina between April and June 2022. A questionnaire was used to assess the extent of dental and medical students' understanding of patients' rights and dentists' legal obligations. Participants were informed about the purpose of the study and submitted written informed consent. The study was approved by the Joint Ethics Committee of the University Dentistry Clinical Center of Kosovo.

The questionnaire consisted of 34 questions divided into 6 parts. The first part comprised 5 descriptive questions about the awareness and importance of medical bioethics in GM and dental students. The second part comprised questions related to the awareness and importance of medical bioethics in GM and dental students by years of study. The third part comprised questions regarding the perspectives of GM and dental students on the main principles for a doctor's instructions. The fourth part comprised questions related to the perspectives of GM and dental students on the main principles for a doctor's instructions according to the year of studies. The fifth and sixth parts comprised questions regarding students' attitudes about dentists' duties toward patients, by direction (GM or dentistry) and year of study.

Statistical analysis was performed using statistical software package SPSS version 22.0 (SPSS Inc, Armonk, NY: IBM Corp.). Categorical variables were analyzed using the Chisquare test with the Yates' correction or, alternatively, Fisher's exact test when expected cell counts were less than 5. A probability value of $P<0.05$ was considered statistically significant.

Results and Discussion

The research included 301 students studying GM or dentistry, of whom 145(48.2%) were first-year and 156(51.8%) were fourth-year students. One hundred (33.2%) were male (Table 1).

Table 1.
General characteristics of the students involved in the research.

	General Medicine		Dentistry		Total	
	n	%	n	%	n	%
Total	170	100	131	100	301	100
Year of study						
First	82	48.2	63	48.1	145	48.2
Fourth	88	51.8	68	51.9	156	51.8
Gender						
Male	58	34.1	42	32.1	100	33.2
Female	112	65.9	89	67.9	201	66.8

Regarding the awareness of medical bioethics, and its importance, among GM and dental students, without a significant difference according to the directions (general medicine or dentistry) (P=0.73) or the year of study, 97.7% of the surveyed students believed that knowledge and implementation of bioethics are very important (Table 2). Most students reported that their medical bioethics knowledge was gained through lectures and seminars, with no significant differences based on the orientation or year of study in both directions. Knowledge of bioethics in dentistry was obtained by 81.4% of respondents in the faculty with no significant difference according to the directions or year of study, but the knowledge was reported as "sufficient" by only 50.1% of the students surveyed in the research (Tables 2 and 3).

Table 2.
Questions related to the awareness and importance of medical bioethics in GM and dental students.

Awareness and importance of medical bioethics in GM and dental students		General Medicine		Dentistry		Total		*P*-value
		n	%	n	%	n	%	
Total		170	100	131	100	301	100	
How important is bioethical knowledge and application?	It is essential to know and regularly implement it.	167	98.2	127	96.9	294	97.7	0.73
Sources of medical bioethics knowledg.	Lectures / seminars / clinical discussions	128	75.3	106	80.9	234	77.7	0.31
	Online resources (websites, online literature, etc.)	45	26.5	27	20.6	72	23.9	0.30
	Media	7	4.1	5	3.8	12	4.0	0.87
	Medical journals	10	5.9	14	10.7	24	8.0	0.19
You learned about bioethics in dental school.		133	78.2	112	85.5	245	81.4	0.15
Information about bioethics in dentistry that you received during your studies is sufficient.		96	56.5	55	42.0	151	50.2	0.02
You know the basic professional ethical principles in dentistry.		148	87.1	125	95.4	273	90.7	0.02

Table 3.
Questions related to the awareness and importance of medical bioethics in GM and dental students by year of study.

Awareness and importance of medical bioethics in GM and dental students		General Medicine					Dentistry				
		First year		Fourth year		*P*-value	First year		Fourth year		*P*-value
Total		n	%	n	%		n	%	n	%	
		82	100	88	100		63	100	68	100	
How important is bioethical knowledge and application?	It is essential to know and regularly implement it.	79	96.3	88	100	0.22	60	95.2	67	98.5	0.56
Sources of medical bioethics knowledge.	Lectures / seminars / clinical discussions	57	69.5	71	80.7	0.05	51	81.0	55	80.9	0.29
	Online resources	24	29.3	21	23.9		13	20.6	14	20.6	
	Media	2	2.4	5	5.7		1	1.6	4	5.9	
	Medical journals	1	1.2	9	10.2		3	4.8	11	16.2	
You learned about bioethics in dental school.		63	76.8	70	79.5	0.81	50	79.4	62	91.2	0.10
Information about bioethics in dentistry that you received during your studies is sufficient.		42	51.2	54	61.4	0.24	29	46.0	26	38.2	0.47
You know the basic professional ethical principles in dentistry.		69	84.1	79	89.8	0.39	57	90.5	68	100	0.03

We measured a high degree of compliance, over 90%, in questions related to the perspectives of dental students on the main principles for a doctor's instructions, with the exception of the question asking whether a dentist should avoid criticizing another dentist in the presence of patients or other health personnel, with which 87.4% of the respondents agreed, and the question of whether a dentist should report the damage caused by another dentist, with which 56.1% agreed, without significant differences (Table 4).

Relating the years of study with attitudes regarding dentists being required to report an injury caused by another dentist, agreement (Strongly agree or agree) was reported by 65.9% of first-year GM students and 43.2% of fourth-year GM students (P=0.005). First-year dental students agreed

Table 4.
Questions regarding the perspectives of GM and dental students regarding the main principles for the doctor's instructions.

Perspectives of GM and dental students on important principles for practice guidelines		General Medicine		Dentistry		Total		*P*-value
		n	%	n	%	n	%	
	Total	170	100	131	100	301	100	
The dentist should provide the greatest possible treatment for the patient's health.	Strongly Agree/ Agree	168	98.8	129	98.5	297	98.7	0.81
The dentist should practice in accordance with current medical knowledge, constantly improve skills and seek help whenever necessary.	Strongly Agree/ Agree	160	94.1	130	99.2	290	96.3	0.04
The dentist should not recommend or administer any harmful material and should provide assistance regardless of the patient's financial means, ethnic origin, or religious belief.	Strongly Agree/ Agree	165	97.1	130	99.2	295	98.0	0.36
The dentist should protect the patient's confidentiality and should not distribute the data without authorization.	Strongly Agree/ Agree	163	95.9	129	98.5	292	97.0	0.33
The dentist should not criticize another doctor in the presence of patients or other health personnel.	Strongly Agree/ Agree	145	85.3	118	90.1	263	87.4	0.29
The dentist should report any damage caused by another dentist.	Strongly Agree/ Agree	92	54.1	77	58.8	169	56.1	0.49

in 82.5% of cases, as compared with 36.8% of fourth-year students (P<0.001). In response to the statement that "The dentist should practice in accordance with current medical knowledge, constantly improve skills and seek help whenever necessary" (Strongly agree or agree), there was a significant difference only in GM students by years (P=0.02), whereas in other cases, we did not find a statistically significant difference according to the year of study (Table 5).

The following results describe students' attitudes about dentists' duties toward patients, according to the directions (general medicine or dentistry) or years of study (Tables 6 and 7). In response to "Patient care [being] your primary concern," 98.0% of students agreed (Strongly agree or agree), without significant differences between GM and dental students (P=0.93) (Table 6) and by years of study for GM (P=0.22) and dental students (P=0.95) (Table 7).

Table 5.

Questions related to the perspectives of GM and dental students regarding the main principles for the doctor's instructions according to the bioethical directions and year of study.

Perspectives of GM and dental students on important principles for practice guidelines		General Medicine					Dentistry				
		First year		Fourth year			First year		Fourth year		
		n	%	n	%	*P*-value	n	%	n	%	*P*-value
	Total	82	100	88	100		63	100	68	100	
The dentist should provide the greatest possible treatment for the patient's health.	Strongly Agree/ Agree	80	97.6	88	100	0.45	62	98.4	67	98.5	0.51
The dentist should practice in accordance with current medical knowledge, constantly improve skills and seek help whenever necessary.	Strongly Agree/ Agree	73	89.0	87	98.9	0.02	62	98.4	68	100	0.97
The dentist should not recommend or administer any harmful material and should provide assistance regardless of the patient's financial means, ethnic origin or religious belief.	Strongly Agree/ Agree	78	95.1	87	98.9	0.32	63	100	67	98.5	0.97
Dentist should protect the patient's confidentiality and should not distribute the data without authorization.	Strongly Agree/ Agree	76	92.7	87	98.9	0.10	63	100	66	97.1	0.51
The dentist should not criticize another doctor in the presence of patients or other health personnel.	Strongly Agree/ Agree	69	84.1	76	86.4	0.85	59	93.7	59	86.8	0.31
The dentist should report any damage caused by another dentist.	Strongly Agree/ Agree	54	65.9	38	43.2	0.005	52	82.5	25	36.8	<0.001

Table 6.

Questions regarding students' attitudes about dentists' duties towards patients by directions.

Students' attitudes about dentists' duties toward patients		General Medicine		Dentistry		Total		*P*-value
		n	%	n	%	n	%	
	Total	170	100	131	100	301	100	
Patient care [being] your primary concern.	Strongly Agree/ Agree	167	98.2	128	97.7	295	98.0	0.93
Treat[ing] each patient with courtesy and care.	Strongly Agree/ Agree	168	98.8	130	99.2	298	99.0	0.82
It is not important to disclose all information to the patient about their treatment.	Strongly Agree/ Agree	78	45.9	56	42.7	134	44.5	0.67
The dentist[s] must respect the dignity and privacy of the patient.	Strongly Agree/ Agree	160	94.1	126	96.2	286	95.0	0.58
Respecting the patient's requirements does not play an important role in the tasks of the dentist.	Strongly Agree/ Agree	24	14.1	20	15.3	44	14.6	0.91
The dentist cannot be responsible for the therapy prescribed for the patient.	Strongly Agree/ Agree	9	5.3	9	6.9	18	6.0	0.74
It is not necessary to involve the patient in the decision-making for the patient's treatment.	Strongly Agree/ Agree	11	6.5	18	13.7	29	9.6	0.06

Table 7.

Questions related to students' attitudes about dentists' duties towards patients by directions and year of study.

Students' attitudes about dentists' duties toward patients		General Medicine					Dentistry				
		First year		Fourth year		*P*-value	First year		Fourth year		*P*-value
		n	%	n	%		n	%	n	%	
	Total	82	100	88	100		63	100	68	100	
Patient care [being] your primary concern	Strongly Agree/ Agree	79	96.3	88	100	0.22	62	98.4	66	97.1	0.95
Treat[ing] each patient with courtesy and care	Strongly Agree/ Agree	37	45.1	41	46.6	0.97	24	38.1	32	47.1	0.39
It is not important to disclose all information to the patient about their treatment.	Strongly Agree/ Agree	75	91.5	85	96.6	0.27	63	100	63	92.6	0.08
The dentist[s] must respect the dignity and privacy of the patient	Strongly Agree/ Agree	13	15.9	11	12.5	0.68	7	11.1	13	19.1	0.30
Respecting the patient's requirements does not play an important role in the tasks of the dentist	Strongly Agree/ Agree	6	7.3	3	3.4	0.43	5	7.9	4	5.9	0.91
It is not necessary to involve the patient in the decision-making for the patient's treatment	Strongly Agree/ Agree	11	13.4	-	-	0.001	5	7.9	13	19.1	0.11

Regarding "Treat[ing] each patient with courtesy and care," agreement (Strongly agree or agree) was indicated by 99.0% of students, without significant differences between GM and dental students (*P*=0.82) (Table 6) and by years of study of GM (*P*=0.45) and dental students (*P*=0.97) (Table 7). When presented with the statement "It is not important to disclose all information to the patient about their treatment," 44.5% of the students agreed (Strongly agree or agree), without significant difference between GM and dental students (*P*=0.67) (Table 6) and by years of study among GM (*P*=0.97) and dental students (*P*=0.39) (Table 7).

The "dentist[s] must respect the dignity and privacy of the patient" statement evoked agreement by 95% of the students without significant difference between GM and dental students (*P*=0.58) (Table 6) and by years of study of GM (*P*=0.68) and dental students (*P*=0.30) (Table 7).

Agreement (Strongly agree or agree) with the statement that "Respecting the patient's requirements does not play an important role in the tasks of the dentist" was reported by 14.6% of the students without significant differences between GM and dental students (*P*=0.91) (Table 6) and by years of study of GM (*P*=0.43) and dental students (*P*=0.91) (Table 7).

Regarding the statement that "The dentist cannot be responsible for the therapy prescribed for the patient," the rate of agreement (Strongly agree or agree) was 6.0% for the students involved in this research; there were no significant differences between GM and dental students (*P*=0.74) (Table 6).

Regarding the students' attitude that patients should be involved in "decision-making for the treatment," 9.6% of the students agreed, without significant differences between GM and dental students (*P*=0.06) (Table 6) and by years of study of the dental students (*P*=0.11), whereas there was a significant difference between GM students by years of study (*P*=0.001).

The role of bioethics education in the dentistry undergraduate curriculum is essential,[8] and the value of incorporating ethics into the curriculum in Medicine has been shown previously.[9,10] Medical and dental students at the University of Prishtina study medical ethics in the first semester of the first year of study. The results of our study show that over 97% of the students surveyed believe that knowledge and implementation of bioethics are essential, with no significant differences in either direction or year, which is similar to the findings of other studies.[11] When asked about their sources of medical bioethics knowledge, it was clear that the majority of students gained it through lectures, seminars and clinical discussions, a finding that is consistent with previous studies.[12,13] Our results are comparable with those of an earlier study,[14] in which it was reported that medical students had at least a basic understanding of bioethics principles. In this study, medical and dental students showed positive attitudes regarding dentists' and doctors' duties toward patients, with no difference between the type of student or years of the study.[15]

Conclusion

By integrating bioethics into the undergraduate curriculum, future generations of dentists and doctors will be able to achieve a high level of professionalism and ethical standards.

Acknowledgment

We thank Claire Barnes, PhD, from Edanz (https://www.edanz.com/ac) for editing a draft of this manuscript.

Competing Interests

The authors declare that they have no competing interests.

References

1. Ashfaq T, Ishaq A, Shahzad F, Saleem F. Knowledge and perception about bioethics: A comparative study of private and government medical college students of Karachi Pakistan. J Family Med Prim Care. 2021 Mar;10(3):1161-1166. doi: 10.4103/jfmpc.jfmpc_103_21.
2. Code of Dental Ethics (1866). J Am Coll Dent. 2015 Fall;82(4):18-9. PMID: 27159961.
3. Berk NW. Teaching ethics in dental schools: trends, techniques, and targets. J Dent Educ. 2001 Aug;65(8):744-50.
4. Deolia SG, Prasad K, Chhabra KG, Kalyanpur R, Kalghatgi S. An Insight Into Research Ethics among Dental Professionals in A Dental Institute, India- A Pilot Study. J Clin Diagn Res. 2014 Sep;8(9):ZC11-4. doi: 10.7860/JCDR/2014/10118.4794.
5. Farooq W, Jafarey A, Arshad A. Awareness of medical ethics principles and their applications among healthcare professionals in Pakistan. Pakistan Journal of Medicine and Dentistry.2018;7:81–88.
6. J Janakiram C, Gardens SJ. Knowledge, attitudes and practices related to healthcare ethics among medical and dental postgraduate students in south India. Indian J Med Ethics. 2014 Apr 1;11(2):99-104. doi: 10.20529/IJME.2014.025.
7. Khizar B, Iqbal M. Perception of physicians and medical students on common ethical dilemmas in a Pakistani medical institute. Eubios J Asian Int Bioeth.2009;19:53–54.
8. Potter VR. Bioethics: Bridge to the future. Prentice-Hall; 1971. doi: 10.1002/sce.3730560329.
9. Prasad DK, Hegde C, Jain A, Shetty M. Philosophy and principles of ethics: Its applications in dental practice. Journal of Education and Ethics in Dentistry. 2011;1:2–6.
10. Prasad M, Manjunath C, Krishnamurthy A, et. al. Ethics in dentistry – a review. International Journal of Health Sciences and Research. 2019; 9(3):238–244.
11. Sullivan M. The new subjective medicine: taking the patient's point of view on health care and health. Soc Sci Med. 2003 Apr;56(7):1595-604. doi: 10.1016/s0277-9536(02)00159-4.
12. Ustrell-Torrent JM, Buxarrais-Estrada MR, Ustrell-TorrentRiutord-Sbert P. Ethical relationship in the dentist-patient interaction. J Clin Exp Dent. 2021 Jan 1;13(1):e61-e66.
13. Williams JR. Dental Ethics Manual (1st edition). FDI World Dental Federation; 2007. Available from: https://www.fdiworlddental.org/sites/default/files/2020-11/1-fdi_dental_ethics_manual_1st_edition_2007.pdf
14. Zhang S, Lo EC, Chu CH. Attitude and awareness of medical and dental students towards collaboration between medical and dental practice in Hong Kong. BMC Oral Health. 2015 May 2;15:53. doi: 10.1186/s12903-015-0038-2.
15. Maharani DA, Ariella S, Syafaaturrachma ID, Wardhany II, Bahar A, Zhang S, Gao SS, Chu CH, Rahardjo A. Attitude toward and awareness of medical-dental collaboration among medical and dental students in a university in Indonesia. BMC Oral Health. 2019 Jul 15;19(1):147. doi: 10.1186/s12903-019-0848-8.

International Journal of Biomedicine 12(4) (2022) 654-660
http://dx.doi.org/10.21103/Article12(4)_OA25

ORIGINAL ARTICLE

Infection Control

INTERNATIONAL JOURNAL OF BIOMEDICINE

Knowledge of Infection Control in Ultrasound Examination: A Cross-Sectional Survey Study among Sudanese Sonographic Specialists

Awadia Gareeballah*

Department of Diagnostic Radiologic Technology, College of Applied Medical Sciences, Taibah University, Al Madinah Al Munawara, Kingdom of Saudi Arabia

Abstract

Background: Ultrasonography is one of the imaging modalities associated with the risk of healthcare-associated infection. Therefore, ultrasound specialists must maintain infection control standards and adherence to ultrasound infection control guidelines.

Methods and Results: A cross-sectional survey was conducted through an online questionnaire to assess the knowledge of Sudanese sonographic specialists on infection control in ultrasonography. Participants who agreed to participate and complete the survey numbered 110. The result of the study demonstrate that the knowledge of infection control guidelines was average (26.93±3.79) among Sudanese sonographic specialists; the mean score of knowledge was 4.52±1.12 (moderate level), 12.51±1.96 (moderate level), 5.70±2.02 (low level), and 4.63±1.10 (average level) for ultrasound equipment, probe, gel bottles, and personal infection control precautions, respectively. Of the study participants, 70% knew that endovaginal and endocavitory probes were decontaminated by liquid chemical sterilant after each use, and 78.18% reported that the high-level disinfectant was used for cleaning and disinfecting equipment in contact with mucous membranes. In addition, 91.82% of participants agreed that sterile gel is highly recommended for intervention procedures, and 89.09% were aware of proper respiratory hygiene and coughing protocol. 41.82% of respondents were aware that personal protective equipment (PPE) is advised for cleaning and sanitizing ultrasonic equipment, and only 31.82% believed that non-sterile gel is insufficient if the transducer is in contact with non-intact skin.

Conclusion: The knowledge of infection control in ultrasound is average among Sudanese sonographic specialists, with a poor understanding of some ultrasound-gel infection control guidelines and safety aspects.(**International Journal of Biomedicine. 2022;12(4):654-660.**).

Keywords: infection control • sonographic specialist • transducer • gel bottle • disinfectant

For citation: Gareeballah A. Knowledge of Infection Control in Ultrasound Examination: A Cross-sectional Survey Study among Sudanese Sonographic Specialists. International Journal of Biomedicine. 2022;12(4):654-660. doi:10.21103/Article12(4)_OA25

Abbreviations

HLD, high-level disinfectant; **LLD**, low-level disinfectant**; PPE**, personal protective equipment; **TRUS**, transrectal ultrasound; **TVUS**, transvaginal ultrasound.

Introduction

Infection control and prevention are essential for patients undergoing ultrasound procedures to provide safe and outstanding quality healthcare.[1] Contaminated transducers and ultrasonic gel or coupling agents have been associated with outbreaks of infections.[2] There are several guidelines and standards for the prevention and control of ultrasound-related infections, such as the European Society of Radiology (ESR) Ultrasound Working Group, the CDC (2008), and the Australasian Society for Ultrasound in Medicine (ASUM).[3-5]

In every ultrasound examination, the general safety precautions are followed, including washing hands before and after having direct patient contact, donning PPE when necessary, maintaining clean and disinfected equipment, maintaining a clean working environment, and properly disposing of waste.[5]

***Correspondence:** Dr. Awadia Gareeballah. Department of Diagnostic Radiologic Technology, College of Applied Medical Sciences, Taibah University, Al Madinah Al Munawara, Kingdom of Saudi Arabia. E-mail: Awadhia1978@gmail.com*

The risk of infection from an ultrasonic transducer and the method of decontamination is divided into 3 main categories, according to the Spaulding Classification of the medical system risk and method of decontamination: non-critical when the device contacts intact skin, semi-critical when the device contacts a mucous membrane or non-intact skin, and critical when the medical device contacts a sterile body cavity.[6] For critical equipment decontaminated with high-level disinfectants (HLDs) or chemical sterilant, the ultrasound transducer is sensitive to heat, so the heat sterilization method is not used; a sterile transducer cover is recommended for semi-critical cleaning, followed by the HLD or chemical, and for non-critical cleaning, followed by the low-level disinfectants (LLDs).[5,6]

While the handling and administrative aspects of ultrasound coupling gels are associated with the development of nosocomial infections involving a variety of pathogenic microorganisms, there are various recommendations for reducing gel-related infections, including the policy for the use of sterile gel, non-sterile gel, and gel warmer.[7]

To the author's knowledge, there are no studies in Sudan dealing with the assessment of knowledge of infection control in ultrasound, and few studies in the literature evaluating the practice of sonographers and sonologists in ultrasound infection control; most of the surveys conducted deal with the knowledge of infection control in the radiology department in general. Therefore, this study aims to assess the awareness of infection control in ultrasound among Sudanese sonographic specialists.

Materials and Methods

A cross-sectional survey was conducted through an online questionnaire distributed among Sudanese sonographic specialists through the Google Form Platform from March to May 2022. The sampling included 110 participants who agreed to participate and completed the survey, with different ages, genders, and education levels. Ethical approval was obtained from each study participant. The study questionnaire was adapted following the guidelines and recommendations of the European Committee for Medical Ultrasound Safety, the CDC, and the ASUM.[2-4] Demographic background information, including gender, age, years of experience, and qualifications, in addition to 39 closed-ended questions dealing with knowledge of infection control in the ultrasound examination, was divided into 4 domains (cleaning and disinfecting of ultrasound equipment, transducer, ultrasound gel, and personal hygiene). The modified version of the questionnaire was validated by academic experts in ultrasound examination (consultant sonologist) with experience of more than 15 years.

The knowledge of infection control was assessed through 4 domains, including 39 close-ended questions; in each part, items/questions were classified into "Correct," which is signed by © in the tables, and "Wrong"; the possible score ranged between zero (the less pertinent to knowledge) and 39 (the most relevant to expertise). Domain 1 deals with proper cleaning and disinfecting of the equipment and was measured by 6 items/questions. Domain 2 for knowledge of the transducer cleaning and disinfecting was measured by 17 items/statements. Domain 3 assessed the ability to properly use ultrasound gel bottles, which included 10 items/reports; Domain 4 dealt with understanding personal hygiene and was measured by 6 items/questions

Statistical analysis was performed using statistical software package SPSS version 25.0 (Armonk, NY: IBM Corp.). Baseline characteristics were summarized as frequencies and percentages for categorical variables and as mean±SD for continuous variables. Mann-Whitney U test and Kruskal-Wallis test were used, respectively, to compare differences between 2 and 3 or more independent groups. Group comparisons with respect to categorical variables are performed using chi-square test. A probability value of $P<0.05$ was considered statistically significant.

Results

A total of 110 people (37 men and 73 women) participated in the study (Table 1). More than half were aged between 30 and 39 years. The majority held M.Sc. in medical diagnostic ultrasound (80.91%), followed by those with a Ph.D. in medical diagnostic ultrasound (10.0%), then a B.Sc. (7.27%), and then a diploma (1.82%). More than half (58.18%) had experience of 1-5 years, followed by those with 6-10 years (26.36%).

Table 1.
Demographic factors (N=110).

Factor	Group	N	%
Gender	Male	37	33.64
	Female	73	66.36
Age	20-29 (yrs.)	26	23.6
	30-39 (yrs.)	60	54.5
	40 (yrs.)	24	21.8
Education	Diploma	2	1.82
	B.Sc.	8	7.27
	M.Sc.	89	80.91
	Ph.D.	11	10.0
Experience	1-5 (yrs.)	64	58.18
	6-10 (yrs.)	29	26.36
	11-15 (yrs.)	10	9.09
	16-20 (yrs.)	4	3.64
	> 20 (yrs.)	3	2.73

Concerning cleaning and disinfecting the equipment, most respondents (86.40%) chose the correct answer at the start of the examination, 72.73% before and 89.09% after each patient, and 83.64% at the end of working hours; 78.18% reported that the HLD was used for cleaning and disinfecting equipment that made contact with mucous membranes. But only 41.82% knew that wearing PPE was recommended during cleaning and disinfecting the ultrasound equipment. The mean score of knowledge was 4.52±1.12 (moderate level). Thus, it can be argued that the level of knowledge of equipment among Sudanese sonographic specialists was moderate (Table 2).

Table 2.

Domain 1. The distribution of knowledge of cleaning and disinfecting of ultrasound equipment (N=110)..

Statement			N	%
The ultrasound equipment must be clean and disinfected	At the start of the examination	**Yes©**	**95**	**86.40**
		No	15	13.64
	Before each patient	**Yes©**	**80**	**72.73**
		No	30	27.27
	After each patient	**Yes©**	**98**	**89.09**
		No	12	10.91
	At the end of working hours	**Yes©**	**92**	**83.64**
		No	18	16.36
For cleaning and disinfectant of the equipment that contacts mucous membranes, which of the following is used?		**HLD©**	**86**	**78.18**
		LLD	24	21.82
Wearing PPE is recommended during cleaning and disinfecting the ultrasound equipment		**Yes©**	**46**	**41.82**
		No	30	27.27
		I don't know	34	30.91
Mean±SD (Level) = 4.52±1.12 (Moderate)				
Keys: 0-3=Low, 3.1-4.7=Moderate, 4.8-6=High; © correct answer				

Although 67.27% reported that the probe should be cleaned before examination and after each patient, only 34.55% agreed that detergent wipes before the application of disinfectants are the most effective in cleaning transducers used for non-critical ultrasound examination (intact skin) (Table 3). If the probe is used externally on unbroken skin, 85.45% reported that a cleaning step is needed, then disinfection by LLD by 74.55%, and no need to be cleaned and disinfected by 11.82%. Most specialists (83.64%) reported that using HLD is recommended when the probe is in contact with blood or body fluids. Only 46.36% said that a dedicated transducer cover was mandatory for endocavitory examinations and all interventions. About 90.91% reported that the Spaulding Classification of endovascular and endovaginal ultrasound probes is critical or semi-critical. While 70% of the participants said that the decontamination of endovaginal and endocavitory probes was done by liquid chemical sterilant after each use, only 37.27% knew that the hydrogen peroxide gas plasma is

Table 3.

Domain 2. The distribution of the knowledge concerning cleaning and disinfectant of ultrasound transducer (N=110).

Statement				N	%
The probe cleaning.	Perform after each patient			31	28.18
	Perform at the end of the day			5	4.55
	Perform before examination and after each patient©			**74**	**67.27**
Which of the following is most effective in cleaning of transducer used for non-critical ultrasound examination (intact skin)?	Soap and running water			14	12.73
	Detergent wipes before application of disinfectants©			**38**	**34.55**
	Dry paper			58	52.73
If the probe is used on intact skin, it could undergo?	A cleaning step		**Yes©**	**94**	**85.45**
			No	16	14.55
	Disinfect by low level disinfectant	**Yes©**		**82**	**74.55**
		No		28	25.45
	No clean or disinfect	Yes		13	11.82
		No©		**97**	**88.18**
How to disinfect the probe contact with blood or body fluids?	**Using high-level disinfectant©**			**92**	**83.64**
	Using low-level disinfectant			5	4.55
	Using intermediate-level disinfectant			13	11.82
Which of the following is mandatory for endocavitory probes and all interventions?	High-level disinfectant			50	45.45
	Low-level disinfectant			9	8.18
	Dedicated transducer cover©			**51**	**46.36**
It is essential to allow sufficient time for the probe to dry to attain maximum effect after disinfecting.		**Yes©**		**75**	**68.18**
		No		16	14.55
		I don't know		19	17.27
The Spaulding Classification of endovascular and endovaginal ultrasound probes.		**Critical and semi-critical©**		**100**	**90.91**
		Non-critical		10	9.09
The decontamination of endovaginal and endocavitory probes done by	heat sterilization after every use	Yes		19	17.27
		No©		**91**	**82.73**
	liquid chemical sterilant after each use	**Yes©**		**77**	70.00
		No		33	30.00
	hydrogen peroxide gas plasma after each use	**Yes©**		**41**	**37.27**
		No		69	62.73
Used of transducer cover.	Intact skin	Yes		21	19.09
		No©		**89**	**80.91**
	Skin wound and ulcer	**Yes©**		**100**	**90.91**
		No		10	9.09
	Intact infected skin	**Yes©**		**95**	**86.36**
		No		15	13.64
	TVUS and TRUS	**Yes©**		**104**	**94.55**
		No		6	5.45
	Pleural effusion and ascites drainage	**Yes©**		**75**	**68.18**
		No		35	31.82
Mean±SD (Level) = 12.51±1.96 (Moderate)					
Keys: 0-8=Low, 8.1-13.5=Moderate, 13.6-17=High; © correct answer					

used for decontamination after each use; on the other hand, 82.73% reported that heat sterilization is not used for probe decontamination. The respondents displayed good knowledge concerning the usage of transducer covers. It was found by 94.55% that transducer covers must be used in TVUS and TRUS, skin wounds and ulcers by 90.91%, intact infected skin by 86.36%, pleural effusion, and ascites drainage by 68.18%, and not used in intact skin by 80.91%. To sum up, the mean score was 12.51±1.96 (moderate level). Thus, the Sudanese sonographic specialists have good knowledge concerning the safety aspect of the probe's transducer infection control (Table 3).

Only 59.09% agreed that the larger refilled bottle carries a higher risk of contamination than the single-use one; 54.55% reported that a single-use gel bottle, once it is opened, could be discarded, and 52.73% said that if gel warmers are used, only bottles for immediate use should be warmed (Table 4).

Table 4.

Domain 3. The distribution of knowledge about avoiding contamination and correct use of ultrasound gel bottles (N=110).

Statement			N	%
The larger refilled bottle carries the risk of contamination more than the single-used one.		**Yes©**	**65**	**59.09**
		No	16	14.55
		I don't know	19	17.27
		I am not sure	10	9.09
Standard non-sterile bottles are sufficient if the transducer is in contact with non-intact skin		Yes	51	46.36
		No©	**35**	**31.82**
		I am not sure	23	20.91
		I don't know	1	0.91
Avoid contact of the gel dispensing tip with the patient or other sources of contamination.		**Yes©**	**83**	**75.45**
		No	13	11.82
		I am not sure	11	10.00
		I don't know	3	2.73
Only bottles for immediate use should be warmed if a gel warmer is used		**Yes©**	**58**	**52.73**
		No	26	23.64
		I don't know	21	19.09
		I am not sure	5	4.55
Gel bottles should be stored upside down in warmers		Yes	44	40.00
		No©	**39**	**35.45**
		I don't know	18	16.36
		I am not sure	9	8.18
For a single-use gel bottle, once it opens, it ideally should be discarded and not used for a second patient		**Yes©**	**60**	**54.55**
		No	26	23.64
		I don't know	18	16.36
		I am not sure	6	5.45
The sterile gel is highly recommended?	Non-intact skin patients	**Yes©**	**49**	**44.55**
		No	57	51.82
	Intervention procedures	**Yes©**	**101**	**91.82**
		No	7	6.36
	Endocavitory examination	**Yes©**	87	**79.09**
		No	17	15.45
	Intact skin patients	Yes	54	49.09
		No©	**50**	**45.45**
Mean±SD (Level) = 5.70±2.02 (Low)				
Keys:0-6=Low,6.1-7.9=Moderate,8-10=High; © correct answer				

However, only 35.45% disagreed that gel bottles should be stored upside down in warmers. In comparison, only 31.82% disagreed that standard non-sterile bottles are sufficient if the transducer is in contact with non-intact skin. A large percentage (75.45%) agreed with avoiding contact of the gel dispensing tip with the patient or other sources of contamination, and 91.82% agreed that sterile gel is highly recommended for intervention procedures, followed by endocavitory examination (79.09%), then non-intact skin patients by only 44.55%; however, 45.45% reported that it is not recommended for intact skin patients, for a mean score of 5.70±2.02 (low level). Thus, it can be argued that the level of knowledge of infection control when using ultrasound gel was low.

Regarding hand hygiene in ultrasound, 80% reported that it should be done before and after examination, while only 31.82% reported that the proper order of PPE is "gown–mask (respirator)–eye protection–gloves." The respiratory hygiene and cough etiquette procedure were approved as follows: 86.36% and 87.27% reported that it is important to reduce the transmission of the droplet and airborne pathogens to patients and health care, and 88.18% stated they knew that it applies to all coughing and sneezing individuals;, the total score was 4.63±1.10 (average level). Thus, it can be argued that the level of knowledge of personal hygiene was intermediate (Table 5).

Table 5.

Domain 4. The distribution of knowledge of personal hygiene among the study participants (N=110)

Statement			N	%
Hand hygiene in ultrasound should be done:	Before patient		5	4.55
	After patient		17	15.45
	Before and after examination©		**88**	**80.00**
The proper order of donning PPE is:	**gown–mask (respirator)–eye protection–gloves©**		**35**	**31.82**
	mask (respirator)–eye protection–gloves–gown		28	25.45
	gloves–eye protection–gown–mask		47	42.73
Knowledge of respiratory hygiene and cough etiquette procedure		**Yes©**	**98**	**89.09**
		No	12	10.91
Respiratory hygiene and cough etiquette procedure	Reduce the transmission of the droplet and airborne pathogens to patients	**Yes©**	**95**	**86.36**
		No	15	13.64
	Reduce the transmission of the droplet and airborne pathogens to healthcare	**Yes©**	**96**	**87.27**
		No	14	12.73
	It applies to all coughing and sneezing individual	**Yes©**	**97**	**88.18**
		No	13	11.82
Mean±SD (Level) = 4.63±1.10 (Average)				
Keys: 0-3=Low, 3.1-4.7=Average, 4.8-6=High; © correct answer				
The mean score of knowledge across all four domains was 26.93±3.79 (Average)				

The study demonstrates that there was no significant difference in the score of the knowledge of infection control in ultrasound among the study participants with respect to gender, years of experience, or education level($P>0.05$), despite the fact that the study found the score significantly differs among the different age groups, the younger age group's mean rank of knowledge score being more (64.58) than the other age groups ($P=0.001$) (Table 6).

Table 6.
Correlation between mean rank of knowledge of the study participant with demographic data.

Factor	Group	Total	
		Mean rank	χ^2 test /*P*-value
Gender	Male	47.79	χ^2 = 0.619/0.43
	Female	52.63	
Age	20-29 (yrs.)	64.58	χ^2 = 14.69/0.001
	30-39 (yrs.)	52.19	
	≥40 (yrs.)	31.71	
Education	Diploma	12.3	χ^2 = 3.91/0.27
	B.Sc.	55. 3	
	M.Sc.	51.04	
	Ph.D.	55.44	
Experience	1-5 (yrs.)	49.18	χ^2 = 0.95/0.92
	6-10 (yrs.)	51.96	
	11-15 (yrs.).	57.11	
	16-20 (yrs.)	58.62	
	>20 (yrs.)	48.17	

Discussion

It is the responsibility of every ultrasound practitioner to guarantee that cross-contamination risks have been minimized. Any equipment adopted in the environment must be safe for all patients.[2] The study found that the knowledge of infection control in ultrasound among Sudanese sonographic specialists was average. Concerning adherence to the proper method for cleaning sonographic equipment, the participants scored good knowledge; the mean score was 4.52±1.12 (moderate level). All understand that the equipment should be cleaned before and after patients, and at the end of examinations. An HLD cleans the equipment that contacts mucous or body fluids. In contrast, only 41.82% of the participants knew that wearing PPE is recommended during cleaning and disinfecting the ultrasound equipment. The participants were knowledgeable about cleaning and disinfecting ultrasound transducers. Most of them knew that when the transducer is used on intact skin, it needs a cleaning followed by an LLD; on the other hand, most of them stated that they do not require cleaning of the transducer used on intact skin, which was considered incorrect. Participants are aware that an HLD is needed when the probe comes into contact with blood or body fluids, but their knowledge was low concerning the use of a probe cover during all interventions and endocavitory examinations. In comparison to this study, Nyhsen et al.[8] assessed the practical aspect concerning the probe cleaning and decontamination in the ESR and demonstrated that a US probe cover was always used in 89% of endocavitory examinations and in 77% of the interventional procedures, which reflects more knowledge of and practice with probe cover usage than does this study.

The lens of the probe is susceptible; any abrasion or fragility of the surface of the probe reduces the performance; dry paper is one cause of abrasion in the contact surface of the probe. In this study, more than half of the participants stated that dry paper is used to clean an ultrasound probe. It is crucial to clean the transducer that is used on intact skin with a detergent wipe, followed by the LLD, which was recommended. Reprocessing of medical devices, including ultrasound transducers, is based on the Spaulding Classification system, which classifies medical devices, according to their intended use and level of disinfectant need, as critical, semi-critical, and non-critical.[1] A lack of knowledge of this classification leads to the incorrect application of appropriate methods of sterilization and disinfection, which could result in the transmission of infection from one patient to another. It was shown that 90.91% know that the Spaulding Classification of endovascular and endovaginal ultrasound probes is critical or semi-critical. These results reflect that the Sudanese sonographic specialists have adequate knowledge concerning Spaulding's classification of medical devices, thus leading to the proper use of methods of cleaning and sterilization.

Transducers used during percutaneous procedures or on non-intact skin should be protected by a single-use, sterile probe cover that matches the level of sterility utilized during the process. They should then go through LLD in between usage. If the probe cover breaks, the transducer could be tainted with blood or body fluids.[9] The respondents reflected good knowledge concerning the conditions in which the transducer covers must be used, such as TVUS and TRUS, wounds and ulcers, intact infected skin, pleural effusion, and ascites drainage.

Contaminated ultrasound gel is a source of disease transmission due to numerous processes and bacteria. According to Weist et al.,[10] improper use of the gel during routine ultrasonic scanning can lead to nosocomial skin infections caused by *Staphylococcus aureus*. According to another study, the transducer and gel's bacterial contamination rate was 42.8%.[11] Concerning infection control safety associated with gel use, the non-sterile gel should only be applied during low-risk, general inspections on healthy skin. A single-use gel bottle or sachet should be used when applying a non-sterile gel to a patient under any transmission-based precautions. A heating gel is not advised due to the possibility of bacterial contamination and growth in a warm environment. Dry heat is the ideal approach when a warm gel is required. Reusable gel bottle lids should be secured after each use, and single-use gel bottles should be discarded.[12-14] In this study, the sonographic specialists reflected poor knowledge of this safety aspect.

It is strongly recommended to use sterile gel for all semi-critical and critical US procedures, such as transducer contact with mucous membranes, contact with any body fluids (all major and minor US-guided interventional procedures), and when scanning infected or broken skin and wounds.[2] The results of this study clarified that the Sudanese sonographic specialists have good knowledge about sterile gel use, except for non-intact skin. One study done in Europe to assess the practice of infection control and decontamination of the US probe among the ESR stated that 30% of the study participants used sterile gel during endocavitory ultrasound and 77% used sterile gel during the interventional ultrasound.[8]

Hand hygiene is the easiest and most effective way to prevent infection because about 50% of health-related infections are in the hands of healthcare providers. WHO

2005 provides hand hygiene in medical care at 5 moments: before touching the patient, before cleaning or disinfecting procedures, after the risk of contact with body fluids, after touching the patient, and after touching the patient's surroundings.[15,16] Practicing respiratory hygiene and cough etiquette also reduces the risk of infection. It is important to use PPE to prevent exposure of healthcare workers and patients to infectious pathogens.[17] Most study participants were familiar with hand hygiene being performed before and after each patient and that respiratory hygiene and cough etiquette procedures apply to all coughing individuals and reduce the risk of infection to the patients and healthcare providers; unfortunately, only 31.82% knew that the right order of donning PPE is "gown–mask (respirator)–eye protection–gloves." This reflects poor knowledge concerning donning and doffing of PPE. The result of this study is consistent with Ashoor et al.,[18] who found poor knowledge among healthcare providers concerning donning of PPE; only 13.8% described the correct sequences.

No previous study concerning knowledge and awareness of infection control in ultrasound among Sudanese sonographic specialists was found. Kartaginer et al.[19] assessed the practiced infection control in ultrasound, which is hand washing, glove use, transducer cleaning, disinfection and sterilization, wearing additional protective clothing when necessary, and examination room maintenance. They found that 70% of sonographers washed their hands before examination and 83% afterward; 4% did not sheath the endocavitory probe before the procedure, and 77% wiped the transducer with a cleaning solution after patients. A survey found that some ultrasound specialists did not adhere to the most recent recommendations on how to properly disinfect transducers, wires, or ultrasound machine keyboards, and there is a lack of training from manufacturers concerning equipment cleaning and disinfecting; these discrepancies may be the cause of compliance problems and show that ultrasound practitioners need to implement a consistent approach to infection control.[20]

There were no significant differences in the degree of knowledge of infection control in ultrasound according to gender, years of experience, and education certificates among the study participants; while significant differences in knowledge scores were found among the different age groups with the younger age group having a higher score of knowledge than other age groups. This may be because the sample in this study is less than expected, despite the participants holding a Ph.D. in diagnostic ultrasound, reflecting a mean rank of the score more than a diploma, B.Sc., and M.Sc. in diagnostic ultrasound.

Conclusion

The study concluded that the knowledge of infection control among Sudanese sonographic specialists was average. In general, the Sudanese sonographic specialist has a good understanding of infection control considerations concerning the equipment and transducer cleaning and disinfecting, but poor knowledge concerning using a dedicated transducer cover during the endovaginal ultrasound. The awareness of the safety procedure of ultrasound gel is low except for avoiding contact of the gel dispensing tip with the patient or other sources of contamination and using sterile gel during the intervention and endocavitory examination. There were no appreciable differences in the level of knowledge of infection control in ultrasound among the study participants based on gender, years of experience, or educational certificates; those with a Ph.D. in diagnostic ultrasound had a higher mean rank of the score than those with a diploma, B.Sc., or M.Sc. in diagnostic ultrasound. Further training in infection control in ultrasound following the CDC and ESR recommendations is needed, mainly for infection control safety considerations of ultrasound gel and transducers.

Limitation

There is no previous study assessing the degree of knowledge of sonographic specialists concerning infection control safety during an ultrasound examination, and few studies in the literature reflect practicing infection control in ultrasound. Secondly, since this survey was online, there were some communication barriers. The number of samples in this study is lower than expected due to some network barriers in peripheral areas of Sudan. The study recommended further studies with a larger sample through an interview.

Acknowledgments

The author extends thanks to all Sudanese sonographic specialists who participate in this study, and to Professor Ahmed Abdelrahim, for his support, help, and validation of the questionnaire.

Competing Interests

The authors declare that they have no competing interests.

References

1. Moshkanbaryans L, Meyers C, Ngu A, Burdach J. The importance of infection prevention and control in medical ultrasound. Australas J Ultrasound Med. 2015 Aug;18(3):96-99. doi: 10.1002/j.2205-0140.2015.tb00207.x.
2. Nyhsen CM, Humphreys H, Koerner RJ, Grenier N, Brady A, Sidhu P, Nicolau C, Mostbeck G, D'Onofrio M, Gangi A, Claudon M. Infection prevention and control in ultrasound - best practice recommendations from the European Society of Radiology Ultrasound Working Group. Insights Imaging. 2017 Dec;8(6):523-535. doi: 10.1007/s13244-017-0580-3.
3. Rutala WA, Weber DJ; Healthcare Infection Control Practices Advisory Committee (U.S.); Centers for Disease Control and Prevention (U.S.); 2008, last update: Feburary 15, 2017. URL: https://stacks.cdc.gov/view/cdc/47378
4. Australasian Society for Ultrasound in Medicine (ASUM). Guidelines for Reprocessing Ultrasound Transducers. Australas J Ultrasound Med. 2017 Feb 23;20(1):30-40. doi: 10.1002/ajum.12042.

5. Guidelines for Infection Prevention and Control in Sonography: Reprocessing the Ultrasound Transducer. Journal of Diagnostic Medical Sonography [Internet]. 2020;36(4):381–403. URL: https://doi.org/10.1177/8756479320933256
6. WHO. Global guidelines for the prevention of surgical site infection, 2nd ed. World Health Organization; 2018.
7. Wooltorton E. Medical gels and the risk of serious infection. CMAJ. 2004 Nov 23;171(11):1348. doi: 10.1503/cmaj.1041684.
8. Nyhsen CM, Humphreys H, Nicolau C, Mostbeck G, Claudon M. Infection prevention and ultrasound probe decontamination practices in Europe: a survey of the European Society of Radiology. Insights Imaging. 2016 Dec;7(6):841-847. doi: 10.1007/s13244-016-0528-z.
9. Guideline for Ultrasound Transducer Cleaning and Disinfection. Ann Emerg Med. 2018 Oct;72(4):e45-e47. doi: 10.1016/j.annemergmed.2018.07.035.
10. Weist K, Wendt C, Petersen LR, Versmold H, Rüden H. An outbreak of pyodermas among neonates caused by ultrasound gel contaminated with methicillin-susceptible Staphylococcus aureus. Infect Control Hosp Epidemiol. 2000 Dec;21(12):761-4. doi: 10.1086/501729.
11. Kiran H., Aral M., Kıran G., Serin S., Arıkan D.C., Erkayıran U., Ekerbiçer H.C. Bacterial contamination of ultrasound probes and coupling gels in a university hospital in Turkey. Eur Res J. 2018:2149–3189. doi: 10.18621/eurj.401327.
12. Westerway SC, Basseal JM, Brockway A, Hyett JA, Carter DA. Potential Infection Control Risks Associated with Ultrasound Equipment - A Bacterial Perspective. Ultrasound Med Biol. 2017 Feb;43(2):421-426. doi: 10.1016/j.ultrasmedbio.2016.09.004.
13. GOV.UK. Guidance: Good infection prevention practice: using ultrasound gel. 2022 URL: https://www.gov.uk/government/publications/ultrasound-gel-good-infection-prevention-practice/good-infection-prevention-practice-using-ultrasound-gel.
14. Oleszkowicz SC, Chittick P, Russo V, Keller P, Sims M, Band J. Infections associated with use of ultrasound transmission gel: proposed guidelines to minimize risk. Infect Control Hosp Epidemiol. 2012 Dec;33(12):1235-7. doi: 10.1086/668430.
15. Abdella NM, Tefera MA, Eredie AE, Landers TF, Malefia YD, Alene KA. Hand hygiene compliance and associated factors among health care providers in Gondar University Hospital, Gondar, North West Ethiopia. BMC Public Health. 2014 Jan 30;14:96. doi: 10.1186/1471-2458-14-96.
16. Challenge FGPS. WHO guidelines on hand hygiene in health care: a summary. Geneva: World Health Organization. 2009;119(14):1977–2016.
17. Australian Guidelines for the Prevention and Control of Infection in Healthcare. 2010. URL: https://www.nhmrc.gov.au/about-us/publications/australian-guidelines-prevention-and-control-infection-healthcare-2010
18. Ashoor M, Alshammari S, Alzahrani F, Almulhem N, Almubarak Z, Alhayek A, Alrahim A, Alardhi A. Knowledge and practice of Protective Personal Equipment (PPE) among healthcare providers in Saudi Arabia during the early stages of COVID-19 pandemic in 2020. J Prev Med Hyg. 2022 Jan 31;62(4):E830-E840. doi: 10.15167/2421-4248/jpmh2021.62.4.2177.
19. Kartaginer R, Pupko A, Tepler C. Do Sonographers Practice Proper Infection Control Techniques? JDMS. 1997;13(6):282–7.
20. Westerway SC, Basseal JM. The ultrasound unit and infection control - Are we on the right track? Ultrasound. 2017 Feb;25(1):53-57. doi: 10.1177/1742271X16688720.

International Journal of Biomedicine 12(4) (2022) 661-666
http://dx.doi.org/10.21103/Article12(4)_OA26

ORIGINAL ARTICLE

Medical Education

INTERNATIONAL JOURNAL OF BIOMEDICINE

Assessment of Male Medical Students' Knowledge and Attitudes About Prostate Cancer and Screening at the University of Khartoum

Kamal Eldin Hussein Elhassan[1], Mohammed Eltag Mohammed[2], Nimat Hussein Elhassan[2], Abd Elgadir Alamin Altoum[3,4], Asaad MA. Babker[3,4], Ayman Hussien Alfeel[3,4], Ahmed L. Osman[3,4], Salah Eldin Omar Hussein[3,4*]

[1]*College of Medicine, Bisha University, KSA*
[2]*College of Medicine, University of Khartoum, Sudan*
[3]*College of Health Sciences, Gulf Medical University, Ajman, United Arab Emirates*
[4]*College of Medical Laboratories Science, University for Sciences and Technology, Omdurman, Sudan*

Abstract

Background: Prostate cancer (PC) is the most common cancer among men in Sudan. It was ranked fourth among all cancer treatment centers in Khartoum. This study aimed to assess knowledge and attitude toward PC among male medical students in their final and semifinal years at the University of Khartoum.

Methods and Results: A descriptive cross-sectional online survey was conducted at the University of Khartoum (Faculty of Medicine) on semifinal and final-year male medical students from March 2022 until May 2022. Data were collected from medical students, using a standardized, pretested, coded questionnaire that contained close-ended questions. The questionnaire was distributed online to the medical students using Google Forms. Knowledge levels were determined using 10 questions on risk factors, signs and symptoms, prevention, treatment, and complications of PC. A total of 131 participants received questionnaires, and the response rate was 100%. The results are presented in chronological order in the way they were analyzed, starting with sociodemographic characteristics of the participants, sources of information on PC, knowledge levels (low, medium, and high) of PC, and attitude levels (positive, negative) relating to the year of study. All medical students in the last 2 years have heard about PC, and medical students overwhelmingly (88.5%) believe that early detection of PC through screening improves survival. Almost all the respondents in our study indicated their willingness to go for PC screening (87.8%), and the rest of the respondents' attitudes about the importance of PC and treatment were positive.

Conclusion: Most students have sufficient knowledge about prostate cancer, its risk factors, complications, and treatment. Medical students are an important population in studying the determinants of screening for prostate cancer.(**International Journal of Biomedicine. 2022;12(4):661-666.**).

Keywords: prostate cancer • attitude • knowledge • medical students

For citation: Elhassan KEH, Mohammed ME, Elhassan NH, Altoum AEA, Babker AMA, Alfeel AH, Osman AL, Hussein SEO. Assessment of Male Medical Students' Knowledge and Attitudes About Prostate Cancer and Screening at the University of Khartoum. International Journal of Biomedicine. 2022;12(4):661-666. doi:10.21103/Article12(4)_OA26

Introduction

Prostate cancer (PC) is the most common cancer among men. Worldwide, an estimated 1,414,259 people were diagnosed with PC in 2020, according to cancer.net. Globally, PC is predicted to increase to approximately 1.7 million new cases and 499,000 deaths by the year 2030 because of the exponentially growing population and the large population of men who will be 65 years and older.[1] The worldwide incidence of PC differs among various geographical regions and ethnic groups.[2]

A study performed by Adeloyeon et al. on the incidence of PC in Africa showed that in 16 African countries, the PC incidence rate was 22–23.97 per 100,000 population, with a median incidence rate of 19.5 per 100,000 reported.[3] PC cancer is the most common cancer among men in Sudan. It was ranked fourth among all cancer treatment centers in Khartoum. It had the highest age-specific rate in seniors

65 and older.[4] The late presentation of cancer in Sudan, as in most developing countries, is a significant challenge to treating cancer in general, and PC in particular. Most patients present with advanced disease.

Furthermore, there is no agreement on effective strategies to reduce the risk of PC, nor on effective screening programs.[5] Screening for PC with prostate-specific antigen (PSA) testing and digital rectal examination has been extensively researched; however, with the ability of early detection in curable stages not yet established, screening is still controversial, with potentially harmful outcomes.[6] Generally, the higher the PSA level, the more likely a PC is.[7] Men at a high risk of PC are advised to begin regular PSA screening earlier, and most of those with a family history of PC are of black African/Caribbean ancestry.[7] The literature is inconsistent in PC association with PC screening knowledge, and the reasons for men refusing or attending screening are mainly unknown.[5] According to a study conducted in Sudan, the geographic distribution of cancer patients includes 19.6% of patients from Khartoum state and the same percentage from North Kordofan state, indicating that these areas have a high incidence of cancer diseases.[8]

This study aimed to assess knowledge and attitude toward PC among male medical students in their final and semifinal years at the University of Khartoum.

Materials and Methods

A descriptive cross-sectional online survey was conducted at the University of Khartoum (Faculty of Medicine) on semifinal and final-year male medical students from March 2022 until May 2022. Data were collected from medical students, using a standardized, pretested, coded questionnaire that contained close-ended questions. The questionnaire was distributed online to the medical students using Google Forms. A simple random sampling method was used to acquire the responses from the participants via the online distribution of Google Forms. The forms were sent by WhatsApp and phone number. After collecting Google Forms, we imported data into Excel to clean and prepare it for analysis. Sociodemographic characteristics were summarized in frequencies and percentages. Knowledge levels were determined using 10 questions on risk factors, signs and symptoms, prevention, treatment, and complications of PC. Each participant who could answer any of the questions from 1 to 10 was assigned a score of 1, and zero for a "no" or "don`t know" answer. The overall score was calculated for all 10 knowledge questions for each person. The maximum score was 10; any individual who had a score of 1-3 was categorized as having low knowledge, any individual who had a score of 4-7 was categorized as having medium knowledge, and any individual who had a score of 7 and above was categorized as having high knowledge. Attitudes regarding PC were assessed using 10 statements on a 3-point Likert scale: agree - 1, don`t agree - 0, and don`t know – 0. The scale was scored as agree - 1, don't know - 0 and don't agree - 0 for the positive questions, and don't agree - 1, don't know - 0 and agree - 0 for the negative statements. Out of a maximum score of 10, each participant who scored 7 and above was classified as having a positive attitude and each participant who scored 6 and below was classified as having a negative attitude. *S*tatistical analysis was performed using statistical software package SPSS version 25.0 (Armonk, NY: IBM Corp.).

Results

A total of 131 participants received questionnaires, and the response rate was 100%. The results are presented in chronological order in the way they were analyzed, starting with sociodemographic characteristics of the participants, sources of information on PC, knowledge levels (low, medium, and high) of PC, and attitude levels (positive, negative) relating to the year of study. The mean age of the participants was 23.96±0.10 years. A total of 40 participants came from a rural area, and 91 came from an urban area; most respondents (n=92) live with their families. Moreover, most of the respondents (n=93) indicated their father's education level as higher (university) and above, and their mother's education level - as higher and above indicated by 79 participants (Table 1).

Table. 1.

Demographic characteristics of respondents, the fifth- and sixth-year medical students.

Characteristics		Year of study		Total
		Fifth (batch 93)	Sixth (batch 92)	
Area	Rural	22	18	40
	Urban	49	42	91
Residency	Dormitory	13	18	31
	Other, Specify	2	2	4
	With family	54	38	92
	With relatives	2	2	4
Father's education	Elementary	1	2	3
	High school	12	13	25
	Intermediate	5	3	8
	Not educated	2	0	2
	Higher & above	51	42	93
Mother's education	Elementary	3	2	5
	High school	19	19	38
	Intermediate	2	3	5
	Not educated	4	0	4
	Higher & above	43	36	79

Observed results showed that most respondents (104/79.4%) were non-smokers. Among cigarette smokers

(n=27), about 44.4% of the respondents reported that they smoked between 5 and 10 cigarettes per day, while about 4% smoked more than 10 cigarettes per day (Figure 1).

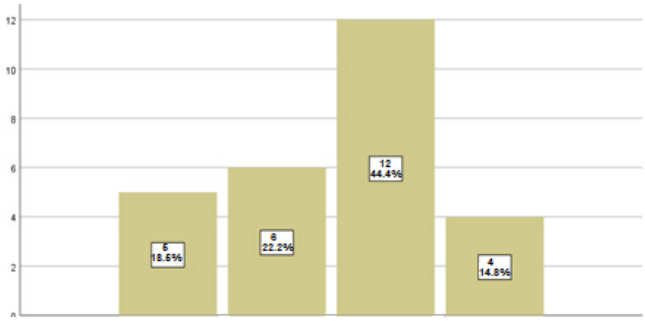

Fig. 1. *The number of cigarettes smoked per day.*

A total of 40(30.53%) respondents reported having a family history of PC. Respondents who have heard about PC indicated the following sources of information: TV (25/19.1%), social media (52/39.7%), lectures (122/93.1%), health pamphlets (32/24.4%), male dinners (10/7.6%), and others (11/8.4%) (Table 2).

Table 2.
Sources of information about PC.

Source of information	(n)	(%)
Social media	52	39.7%
Lectures	122	93.1%
Health pamphlets	32	24.4%
TV	25	19.1%
Male dinners	10	7.6%
Others	11	8.4%

Respondents who knew what PC is - 124(94.7%) (Table 3) were all able to identify the risk factors: most respondents indicated age (98.4%), family history (88.7%), and cigarette smoking (87.1%) as the most common risk factors for PC.

A total of 109(83.2%) respondents were positive that risk factors causing PC could be reduced, and 91(69.5%) could identify how the risk factors could be reduced. Most respondents (90/68.7%) identified periodic medical check-ups and better health care (90/68.7%) as the best approach to lowering PC risk. Most respondents (96/73.3%) knew the warning signs of PC, with the majority stating difficulty urinating (95/72.5%) and pain in the groin (6/4.58%) as warning signs. A total of 116(88.5%) respondents were positive that early detection could increase the chances of survival. Respondents who were positive that PC could be treated were 107(81.7%), all of whom could identify ways to treat PC (Table 3).

Almost all the respondents in our study indicated their willingness to go for PC screening (87.8%), and the rest of the respondents' attitudes about the importance of PC and treatment were positive (Table 4).

The scores were coded and summed up to provide results for participants who had positive and negative attitudes toward PC; 90(68.7%) respondents displayed a positive attitude toward PC screening (Table 5).

The associations between levels of knowledge about PC and sociodemographic factors, family history of cancer, and smoking attitude are presented as high knowledge, medium knowledge, and low knowledge. Overall, the level of knowledge of fifth-year and sixth-year students was as follows: low (0% and 1.7%, respectively), medium (28.2% and 15%, respectively), and high (71/8% and 83.3%, respectively) (Tables 6 and 7).

The levels of attitude, sociodemographic characteristics, family history of cancer, and smoking attitudes are presented as positive and negative (Table 8).

Table 3.
Distribution of respondents' responses on knowledge about PC.

Questions and Statements	Yes		No	
	(n)	(%)	(n)	(%)
Heard about PC	131	100	0	0
Could identify what PC is	124	94.7	7	5.3
Could identify risk factors	124	94.7	7	5.3
Risk factors causing PC could be reduced	109	83.2	22	16.8
Could identify how the risk factors could be reduced	91	69.5	40	30.5
Could identify early warning signs of PC	96	73.3	35	26.7
Early detection of PC could increase the chances of survival	116	88.5	15	11.5
PC could be treated	107	81.7	24	18.3
Could identify ways to treat PC	107	81.7	24	18.3
Could identify complications of PC	121	92.4	10	7.6

Table 4.
Respondents' attitudes about the importance of PC and treatment.

Statement	Agree		Don`t know		Don't agree	
	n	(%)	n	(%)	n	(%)
PC is only a problem for males of advancing age.	97	74.0	7	5.3	27	20.6
It is important to screen for PC.	117	89.3	5	3.8	9	6.9
Screening for PC can be painful.	24	18.3	38	29.0	69	52.7
Screening for PC is embarrassing.	44	33.6	13	9.9	74	56.5
Screening for PC can aggravate the disease.	10	7.6	13	9.9	108	82.4
Screening for PC will help me to be healthy.	106	80.9	12	9.2	13	9.9
Screening for PC is beneficial and will settle any ambiguities.	101	77.1	12	9.2	18	13.7
Regular examination for PC is expensive.	25	19.1	51	38.9	55	42.0
Willingness to go for PC screening.	115	87.8	3	2.3	13	9.9
I would accept any treatment if I were diagnosed with PC.	120	91.6	5	3.8	6	4.6

Table 5.
Attitude levels toward PC screening

Attitude	(n)	(%)
Positive	90	68.7
Negative	41	31.3
Total	131	100

Table 6.
Knowledge levels (low, medium, and high) of PC.

Level	(n)	(%)
High	101	77.1
Medium	29	22.1
Low	1	0.8
Total	131	100

Table 7.
Levels of knowledge about PC, sociodemographic characteristics, family history of cancer, and smoking attitude.

Characteristics		Levels of knowledge			*P*-value
		High (n)	Low (n)	Medium (n)	
Year of study	Fifth-year students	51	0	20	0.229
	Sixth-year students	50	1	9	
Area	Rural	36	0	4	0.066
	Urban	65	0	26	
Residency	With family	70	1	21	0.996
	Dormitory	25	0	6	
	With relatives	3	0	1	
	Other	3	0	1	
Father's education	Not educated	1	0	1	0.911
	Elementary	3	0	0	
	Intermediate	5	0	3	
	High school	20	0	5	
	Higher & above	72	1	20	

Table 7.

Levels of knowledge about PC, sociodemographic characteristics, family history of cancer, and smoking attitude (continued).

Characteristics		Levels of knowledge			*P*-value
		High (n)	Low (n)	Medium (n)	
Mother's education	Not educated	2	0	2	0.816
	Elementary	5	0	0	
	Intermediate	4	0	1	
	High school	31	0	7	
	Higher & above	59	1	19	
Smoking	Yes	21	1	10	0.371
	No	80	0	19	
Cancer history in family	Yes	30	0	10	0.882
	No	71	1	19	

Table 8.

Attitude statistics toward PC screening.

Characteristics		Attitude statistics				
		Neg (n)	Pos (n)	OR	95% CI	*P*-value
Year of study	Fifth-year students	22	49	0.7226	0.3445-1.5159	0.7226
	Sixth-year students	19	41			
Area	Rural	13	27	0.9231	0.4158-2.0492	0.8440
	Urban	28	63			
Smoking	Yes	7	20	0.7206	0.2778-1.8694	0.5005
	No	34	70			
Cancer history in family	Yes	11	29	0.7713	0.3396-1.7515	0.5348
	No	30	61			

Neg- Negative; Pos-Positive.

Discussion

PC is the commonest cancer in elderly males. Screening and early detection is the primary strategy to combat this disease. In much the same manner that medical educators must teach students about the nuances and uncertainties of PC screening, future physicians will eventually have to integrate this imperfect knowledge into communicating with their patients.[9] Our study was the first research among Khartoum University medical students surveyed regarding their knowledge and attitude concerning PC. Perhaps our most important finding is that all medical students in the last 2 years have heard about PC, and medical students overwhelmingly (88.5%) believe that early detection of PC through screening improves survival.

A cross-sectional study performed at the Syrian Private University between December 2020 and January 2021 was aimed to determine the knowledge level of students concerning PC. The sample included students of all years from different faculties. The data was collected by a questionnaire to measure the awareness of PC. The total number of participants was 446 from all faculties, including males and females. The percentage of students who have heard about PC was 73.1%, and those who have heard about the PSA testing was 52%. As for students of medical faculties from different years, the percentage was 62.3%, compared to non-medical faculties, where the rate was only 19.5%, indicating a low-level knowledge among non-medical students.[10]

In a study performed by Marcella et al.,[9] 1644 students were sampled at 20 medical schools using a web-based, cross-sectional survey to examine medical students' knowledge and beliefs concerning PC screening and specific determinants for their beliefs. Medical students generally were very optimistic about the benefits of screening for PC, and students' knowledge regarding PC screening shows significant improvement by class year.

Currently, results of more studies support the ability of the PSA test to detect early-stage PC,[11] but whether it should be used for screening continues to be debated,[9,12,13] as illustrated by some recommendations.[12,14]

Overall, the results of our study show that many of the respondents have a positive attitude toward PC as a disease in general, screening, as well as treatment. Almost all the respondents in our study indicated their willingness to go for PC screening (87.8%), and the rest of the respondents' attitudes about the importance of PC and treatment were positive.

In conclusion, most students have sufficient knowledge about prostate cancer, its risk factors, complications, and treatment. Medical students are an important population in studying the determinants of screening for prostate cancer.

Competing Interests

The authors declare that they have no competing interests.

References

1. Taitt HE. Global Trends and Prostate Cancer: A Review of Incidence, Detection, and Mortality as Influenced by Race, Ethnicity, and Geographic Location. Am J Mens Health. 2018 Nov;12(6):1807-1823. doi: 10.1177/1557988318798279.
2. Sekhoacha M, Riet K, Motloung P, Gumenku L, Adegoke A, Mashele S. Prostate Cancer Review: Genetics, Diagnosis, Treatment Options, and Alternative Approaches. Molecules. 2022 Sep 5;27(17):5730. doi: 10.3390/molecules27175730.
3. Adeloye D, David RA, Aderemi AV, Iseolorunkanmi A, Oyedokun A, Iweala EE, Omoregbe N, Ayo CK. An Estimate of the Incidence of Prostate Cancer in Africa: A Systematic Review and Meta-Analysis. PLoS One. 2016 Apr 13;11(4):e0153496. doi: 10.1371/journal.pone.0153496.
4. Elamin A, Ibrahim ME, Abuidris D, Mohamed KE, Mohammed SI. Part I: cancer in Sudan—burden, distribution, and trends breast, gynecological, and prostate cancers. Cancer Med. 2015 Mar;4(3):447-56. doi: 10.1002/cam4.378.
5. Saeed IE, Weng HY, Mohamed KH, Mohammed SI. Cancer incidence in Khartoum, Sudan: first results from the Cancer Registry, 2009-2010. Cancer Med. 2014 Aug;3(4):1075-84. doi: 10.1002/cam4.254.
6. Arafa MA, Rabah DM, Abdel-Gawad E, Ibrahim FK. Association of physicians' knowledge and behavior with prostate cancer counseling and screening in Saudi Arabia. Saudi Med J. 2010 Nov;31(11):1245-50.
7. Ali AA, Ibrahim FE. Incidence and geographical distribution of cancer in Radiation and Isotopes Center in Khartoum. Sudan Med Monit. 2014;9(3):109-112.
8. Arafa MA, Rabah DM, Wahdan IH. Awareness of general public towards cancer prostate and screening practice in Arabic communities: a comparative multi-center study. Asian Pac J Cancer Prev. 2012;13(9):4321-6. doi: 10.7314/apjcp.2012.13.9.4321.
9. Marcella S, Delnevo CD, Coughlin SS. A national survey of medical students' beliefs and knowledge in screening for prostate cancer. J Gen Intern Med. 2007 Jan;22(1):80-5. doi: 10.1007/s11606-006-0015-1.
10. Restum S, Alloush M, Kubtan MA. Awareness of prostate cancer: A research study on Syrian private university students, Syria. J Cancer Prev Curr Res. 2021;12(1):44-46. doi: 10.15406/jcpcr.2021.12.00452
11. Jacobsen SJ, Bergstralh EJ, Guess HA, Katusic SK, Klee GG, Oesterling JE, Lieber MM. Predictive properties of serum-prostate-specific antigen testing in a community-based setting. Arch Intern Med. 1996 Nov 25;156(21):2462-8.
12. U.S. Preventive Services Task Force. Screening for prostate cancer: recommendation and rationale. Ann Intern Med. 2002 Dec 3;137(11):915-6. doi: 10.7326/0003-4819-137-11-200212030-00013.
13. Sox HC, Mulrow C. An editorial update: should benefits of radical prostatectomy affect the decision to screen for early prostate cancer? Ann Intern Med. 2005 Aug 2;143(3):232-3. doi: 10.7326/0003-4819-143-3-200508020-00011.
14. Smith RA, Cokkinides V, von Eschenbach AC, Levin B, Cohen C, Runowicz CD, Sener S, Saslow D, Eyre HJ; American Cancer Society. American Cancer Society guidelines for the early detection of cancer. CA Cancer J Clin. 2002 Jan-Feb;52(1):8-22. doi: 10.3322/canjclin.52.1.8.

***Corresponding author**: Salah Eldin Omar Hussein. Department of Medical Laboratory Sciences, College of Health Sciences, Gulf Medical University. Ajman, United Arab Emirates. E-mail: dr.salaheldin@gmu.ac.ae*

International Journal of Biomedicine 12(4) (2022) 667-670
http://dx.doi.org/10.21103/Article12(4)_CR1

CASE REPORT

INTERNATIONAL JOURNAL OF BIOMEDICINE

Idiopathic Ventricular Tachycardia: Good Prognosis but Debilitating Symptoms

Gelu Simu, Mihai Puiu, Gabriel Cismaru*, Gabriel Gusetu, Dana Pop, Dumitru Zdrenghea, Radu Rosu

5th Department of Internal Medicine, Cardiology-Rehabilitation, "Iuliu Hatieganu" University of Medicine and Pharmacy, Cluj-Napoca, Romania

Abstract

Ventricular arrhythmias may occur in patients without anatomical heart abnormalities, a condition that is known as idiopathic ventricular arrhythmias. The most common form originates at the level of the outflow tracts. It can manifest as PVCs, non-sustained ventricular tachycardia (VT), and sustained VT. A 52-year-old female patient was admitted for 2 episodes of syncope related to a high burden of premature ventricular contractions (PVCs) and several episodes of VT with the same QRS morphology as the PVCs. A diagnosis of sustained monomorphic VT was formulated in a patient with no structural heart disease and a normal ejection fraction. Antiarrhythmic drugs such as metoprolol, propafenone, and amiodarone failed to reduce the number of PVCs, hence catheter ablation was suggested to the patient. The patient consented to the treatment, and following catheter ablation, the patient no longer experienced syncope. The 24-hour Holter ECG monitoring revealed no PVCs or VTs. PVCs and VTs from the right ventricular outflow tract (RVOT) are typically benign with a good prognosis. Catheter ablation should be employed as the definitive treatment for RVOT-VT, as our case demonstrated only partial response to antiarrhythmic drugs. (**International Journal of Biomedicine. 2022;12(4):667-670.**).

Keywords: catheter ablation • ventricular tachycardia • premature ventricular contractions • syncope • RVOT

For citation: Simu G, Puiu M, Cismaru G, Gusetu G, Pop D, Zdrenghea D, Rosu R. Idiopathic Ventricular Tachycardia: Good Prognosis but Debilitating Symptoms. International Journal of Biomedicine. 2022;12(4):667-670. doi:10.21103/Article12(4)_CR1.

Abbreviations

EAM, electroanatomical mapping; **LBBB**, left bundle branch block; **LVOT**, left ventricular outflow tract; **LVOT**, left ventricular outflow tract; **PVCs**, premature ventricular contractions; **RVOT**, right ventricular outflow tract; **RBBB**, right bundle branch block; **VT**, ventricular tachycardia.

Introduction

Ventricular tachycardia (VT) may occur in patients that have no structural impairment. Most often, in this case, the origin of tachycardia is at the outflow tract level. Arrhythmias that originate at the level of the outflow tract are represented by premature ventricular contractions (PVCs), non-sustained VT, or sustained VT. Outflow tract VTs are triggered by emotional stress, and exercise, and occur more often during the day.[1,2] ECG recognition of outflow tract VT is made by the morphology and axis in the 12 leads: broadly, RVOT-VT is suggested by an LBBB morphology with an inferior axis, while LVOT-VT is recognized by an RBBB morphology with the inferior axis.[3]

Long-term options for the treatment of outflow tract VT include antiarrhythmic drugs and catheter ablation.[3] We present the case of a young female patient with RVOT-VT and 2 syncopes with failure of antiarrhythmic drug treatment that necessitated catheter ablation for a complete cure of the arrhythmia.

***Corresponding author**: Cismaru Gabriel, MD, Ph.D. 5th Department of Internal Medicine, Cardiology-Rehabilitation, "Iuliu Hatieganu" University of Medicine and Pharmacy, Cluj-Napoca, Romania. E-mail: gabi_cismaru@yahoo.com*

Case Presentation

A 52-year-old female patient was admitted to the Department of Cardiology with palpitations and dyspnea. Palpitations were characterized by a rapid irregular rhythm, variable duration, spontaneous remission, and occurrence during both exertion and rest. In 2005, she presented with palpitations and syncope, and echocardiography revealed a normal ejection fraction and absence of valvulopathy. Due to the presence of PVCs on the ECG (Figure 1), therapy with metoprolol 50 mg per day was initiated. The patient had normal carotid arteries, a normal neurological examination, and a normal cerebral computed tomography. No other cause of syncope could be identified. After treatment with beta-blockers, symptoms persisted, so propafenone 450 mg was administered. In 2012, after seven years of treatment, the patient had a second episode of syncope. In 2005, only PVCs were discovered; all other exams were normal. Additionally, coronarography was performed, which was normal. Despite treatment with propafenone and metoprolol, the Holter ECG revealed 21,000 PVCs/24 hours (Figure 2), accompanied by episodes of nonsustained VT. Accordingly, propafenone was discontinued, and amiodarone was substituted. Under antiarrhythmic medication with amiodarone and metoprolol, she did not exhibit syncope; nonetheless, repeated Holter ECGs revealed 18,000 to 20,000 PVCs/24 hours. Catheter ablation was proposed in 2017 following an arrhythmic evaluation.

During the present hospitalization, a physical examination revealed an obese patient with a BMI of 36 kg/m^2, normal blood pressure of 110/70 mmHg and heart rate of 75 bpm, and normal lung auscultation. Her ECG showed PVCs with an LBBB morphology, inferior axis, and precordial transition in V4. Echocardiography revealed a normal left ventricular ejection fraction, normal values of left ventricular dimensions, a normal left atrium, the absence of valvulopathy, and the absence of pericardial effusion. For the quantification of PVCs, a Holter ECG revealed 18,000 PVCs with frequent episodes of nonsustained VT of 3 to 10 PVCs. After informed consent, an electrophysiological study (Figure 3) with EAM was performed. After the femoral vein was punctured, three catheters were inserted at the level of the heart: a quadripolar catheter at the level of the right ventricular apex, a decapolar catheter at the level of the coronary sinus, and a Flexibility Saint Jude catheter at the level of the RVOT. During activation mapping, the ablation catheter electrogram demonstrated a 20-ms pre-QRS local potential (Figures 4A, 4B, 5). Catheter ablation caused the elimination of PVCs and VTs, and the inability to induce VTs at the termination of the procedure (Figure 6). After the ablation, amiodarone was discontinued, and a Holter EKG 30 days after discharge revealed no PVCs; thus, metoprolol was also discontinued 24, 48, and 72-month follow-up, the patient did not take any medications, and her Holter ECG showed no PVC or syncope.

Discussion and Conclusion

VT may occur in patients with underlying heart impairment, such as ischemic heart disease,[5] dilated cardiomyopathy,[6] hypertrophic cardiomyopathy,[7] arrhythmogenic right ventricular dysplasia,[8] or in patients without structural impairment.[9] The morphology of PVCs and VTs in 12-lead derivations can provide further information on the location of the arrhythmogenic focus. Because both RVOT and LVOT are superior structures, there will be a positive QRS complex in leads D2, D3, and aVF, which corresponds to an inferior electrical axis. V1 is an anterior lead on the right side of the thorax, RVOT is also an anterior structure, and LVOT is a posterior structure relative to RVOT. When PVCs originate in the RVOT, there will be a negative QS pattern in lead V1, and when they arise in the LVOT, there will be an rS pattern in lead V1. Despite its name, RVOT is located considerably leftwards compared to LVOT. Therefore, when RVOT-VT originates from the anterior or posterior RVOT wall, the QRS complex in lead D1 will be biphasic. If the origin is towards the pulmonic valve, the QRS complex morphology in lead D1 will be QS; however, if the origin is from the right margin of RVOT, the QRS complex morphology in lead D1 will be positive. The morphology of VT in our patient was LBBB with an inferior axis. The small r wave in lead V1 and biphasic rs complex in lead D1 are consistent with the RVOT anteroseptal region origin identified by EAM. RVOT-VT is often a benign arrhythmia characterized by palpitations. However, our patient presented two syncopes due to rapid heart rates; hence, aggressive treatment with catheter ablation was recommended for a complete recovery. Viskin et al.[10] reported three patients with RVOT-VT who developed severe forms that were accompanied by syncope or cardiac arrest as a result of polymorphic VT or ventricular fibrillation. Individuals with malignant RVOT-VT had longer coupling intervals of PVCs compared to patients with benign RVOT-VT. Moreover, Shimizu et al.[11] demonstrated the electrocardiographic characteristics of malignant RVOT-VT and a correlation between a shorter coupling interval of PVCs and the risk of VT. Noda et al.[12] similarly observed shorter coupling intervals in malignant RVOT-VT types.

Chronic management of outflow tract VTs includes antiarrhythmic drugs, implantable defibrillators, or catheter ablation. Medical options include beta-blockers, verapamil, and diltiazem, which have a success rate of 20% to 50%.[13] Other antiarrhythmic medications include class IC: propafenone, flecainide, and class C: sotalol, amiodarone[14] when beta-blockers or calcium blockers are ineffective. Unfortunately, pharmacological treatment was unsuccessful in our patient, with PVC recurrence under metoprolol, propafenone, and amiodarone; therefore, catheter ablation was proposed. A history of syncope is a strong indicator that radiofrequency ablation should be considered as a therapeutic option. EAM revealed that the origin of RVOT-VT in our patient was at the anteroseptal level, with the local potential occurring 20 ms before the onset of QRS. During a 24-hour Holter ECG, radiofrequency treatments at this level rendered tachycardia uninducible and eliminated all PVCs. The patient reported neither syncope nor palpitations following catheter ablation.

Informed written consent was obtained from the patient for the publication of this case report and any accompanying medical images.

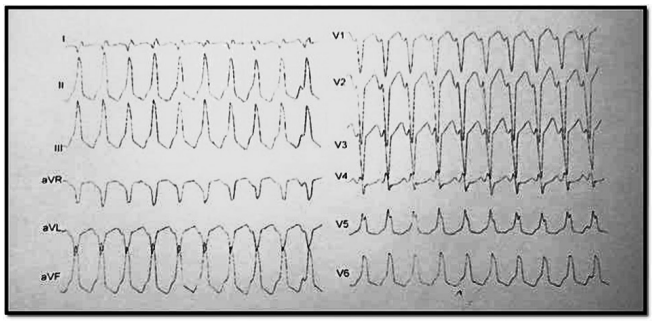

Fig. 1. *12-lead ECG during a sustained episode of ventricular tachycardia shows an LBBB morphology of the QRS with inferior axis. The biphasic pattern of QRS in lead D1 with negative QRS in leads avR and avL suggests an origin in the anterolateral RVOT.*

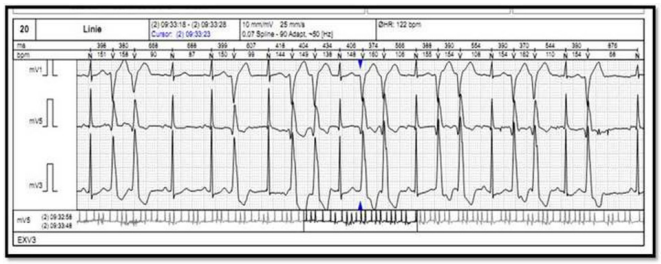

Fig. 2. *Holter ECG shows more than 21,000 PVCs/24 hours*

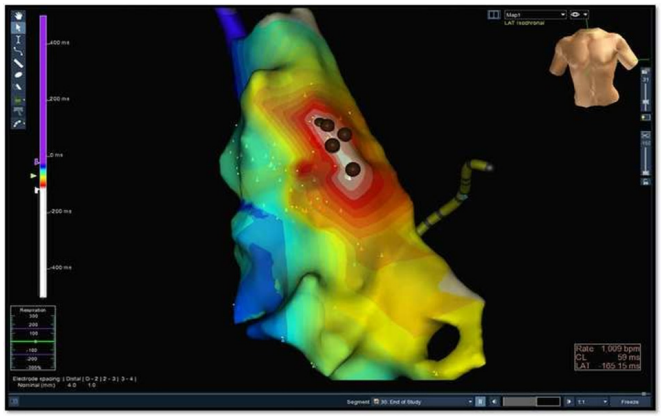

(4A)

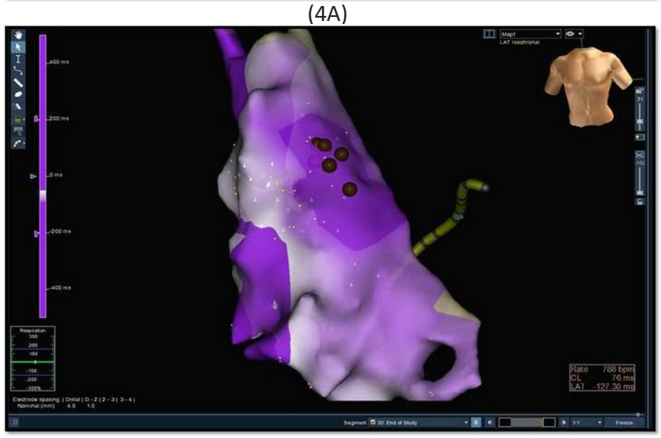

(4B)

Fig. 4. *Activation map (4A) and propagation map (4B). Both maps show the origin of PVC at the level of RVOT. Activation map shows with white color the earliest RVOT zone activated by the PVC focus. The electrical activation passes from the white zone to red→yellow→green→blue, the latest area of the RVOT being activated is the posterior RVOT. Catheter ablation (5 brown dots) at the level of the earliest electrical signal (white zone) made PVCs disappear and VT uninducible. Propagation map (4B) shows the electrical activity propagating from the anterior region of the RVOT where RF dots were placed to the latest activated zone: posterior RVOT.*

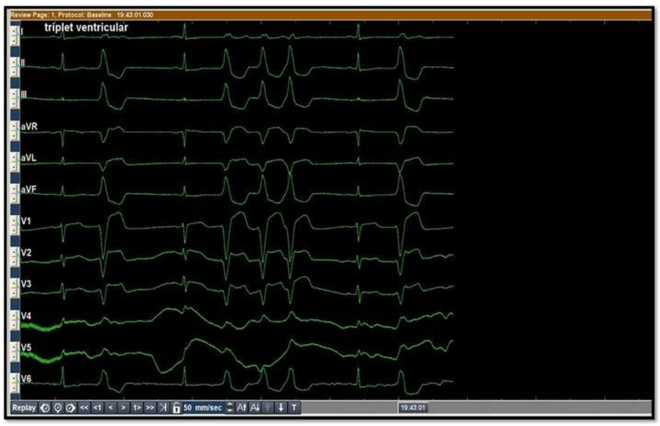

Fig. 3. *Beginning of the electrophysiological study. At the beginning of the study the patient had multiple PVCs with nonsustained episodes of VT. The morphology with LBBB pattern and inferior axis suggests origin in the RVOT.*

Fig. 5. *Local potential at the ablation target. Abl d= bipolar signal from the ablation catheter which precedes with 37 seconds the onset of QRS during PVC on 12 lead ECG. Abl uni – unipolar signal form the ablation catheter.*

Fig. 6. *12-lead ECG at the end of ablation procedure. Sinus rhythm can be seen without any PVC.*

Competing Interests

The authors declare that they have no competing interests.

References

1. Jadonath RL, Schwartzman DS, Preminger MW, Gottlieb CD, Marchlinski FE. Utility of the 12-lead electrocardiogram in localizing the origin of right ventricular outflow tract tachycardia. Am Heart J. 1995 Nov;130(5):1107-13. doi: 10.1016/0002-8703(95)90215-5.
2. Kamakura S, Shimizu W, Matsuo K, Taguchi A, Suyama K, Kurita T, Aihara N, Ohe T, Shimomura K. Localization of optimal ablation site of idiopathic ventricular tachycardia from right and left ventricular outflow tract by body surface ECG. Circulation. 1998 Oct 13;98(15):1525-33. doi: 10.1161/01.cir.98.15.1525.
3. Joshi S, Wilber DJ. Ablation of idiopathic right ventricular outflow tract tachycardia: current perspectives. J Cardiovasc Electrophysiol. 2005 Sep;16 Suppl 1:S52-8. doi: 10.1111/j.1540-8167.2005.50163.x.
4. Gard JJ, Asirvatham SJ. Outflow tract ventricular tachycardia. Tex Heart Inst J. 2012;39(4):526-8.
5. Rosu R, Cismaru G, Muresan L, Puiu M, Andronache M, Gusetu G, Pop D, Mircea PA, Zdrenghea D. Catheter ablation of ventricular tachycardia related to a septo-apical left ventricular aneurysm. Int J Clin Exp Med. 2015 Oct 15;8(10):19576-80.
6. Zeppenfeld K, Wijnmaalen AP, Ebert M, Baldinger SH, Berruezo A, Catto V, et al. Clinical Outcomes in Patients With Dilated Cardiomyopathy and Ventricular Tachycardia. J Am Coll Cardiol. 2022 Sep 13;80(11):1045-1056. doi: 10.1016/j.jacc.2022.06.035.
7. Namboodiri N, Francis J. Ventricular arrhythmias in hypertrophic cardiomyopathy--can we ever predict them? Indian Pacing Electrophysiol J. 2010 Mar 5;10(3):112-4.
8. Gabriel C, Puiu M, Rosu R, Muresan L, Rancea R, Gusetu G, Pop D, Zdrenghea D. Intracardiac ultrasound to detect aneurysm in arrhythmogenic right ventricular dysplasia/cardiomyopathy. Oxf Med Case Reports. 2018 Jan 25;2018(1):omx088. doi: 10.1093/omcr/omx088.
9. Cismaru G, Zgiia A, Istratoaie S, Puiu M, Muresan L, Cismaru A, et al. RVOT ventricular tachycardia ablation in a patient with atrial septal defect: a case report. Int J Clin Exp Med. 2020;13(10):8118-8126.
10. Viskin S, Rosso R, Rogowski O, Belhassen B. The "short-coupled" variant of right ventricular outflow ventricular tachycardia: a not-so-benign form of benign ventricular tachycardia? J Cardiovasc Electrophysiol. 2005 Aug;16(8):912-6. doi: 10.1111/j.1540-8167.2005.50040.x.
11. Knecht S, Sacher F, Wright M, Hocini M, Nogami A, Arentz T, et al. Long-term follow-up of idiopathic ventricular fibrillation ablation: a multicenter study. J Am Coll Cardiol. 2009 Aug 4;54(6):522-8. doi: 10.1016/j.jacc.2009.03.065.
12. Shimizu W. Arrhythmias originating from the right ventricular outflow tract: how to distinguish "malignant" from "benign"? Heart Rhythm. 2009 Oct;6(10):1507-11. doi: 10.1016/j.hrthm.2009.06.017.
13. Buxton AE, Waxman HL, Marchlinski FE, Simson MB, Cassidy D, Josephson ME. Right ventricular tachycardia: clinical and electrophysiologic characteristics. Circulation. 1983 Nov;68(5):917-27. doi: 10.1161/01.cir.68.5.917.
14. Mont L, Seixas T, Brugada P, Brugada J, Simonis F, Rodríguez LM, Smeets JL, Wellens HJ. Clinical and electrophysiologic characteristics of exercise-related idiopathic ventricular tachycardia. Am J Cardiol. 1991 Oct 1;68(9):897-900. doi: 10.1016/0002-9149(91)90405-a.

International Journal of Biomedicine 12(4) (2022) 671-674
http://dx.doi.org/10.21103/Article12(4)_ShC

SHORT
COMMUNICATION

INTERNATIONAL
JOURNAL
OF BIOMEDICINE

Dermatoscopic "Mimickers" of Basal Cell Carcinoma - Adnexal Skin Tumors

Reihane Bislimi Berisha[1*], Djordje Dzokic[2]

[1]*Department of Dermatology, Clinic Centre, Faculty of Medicine, University of Pristina, Prishtina, Republic of Kosovo*
[2]*Department of Plastic Surgery, Clinic Centre, Faculty of Medicine, "Ss. Cyril and Methodius" University, Skopje, Republic of North Macedonia*

Abstract

Background: Adnexal skin tumors (AST) are numerous and various, and in their appearance give dermoscopic and clinical features similar to basal cell carcinoma (BCC). Differential diagnosis is difficult, as clinical alteration seems insufficient to distinguish between BCC and many skin lesions that mimic BCC. However, the validity and usefulness of dermatoscopic criteria enable differentiation between BCC and AST. The purpose of this paper was to present the basic dermatoscopic criteria for diagnosis of BCC as well as minimally invasive methods for treatment and clinical management, with a better aesthetic outcome.

Methods and Results: This study consisted of a retrospective review of 50 skin lesions collected in our institution over a 3-year period. We analyzed the dermoscopic images of 29 skin lesions with a clinical diagnosis of BCC and 21 cases with a clinical diagnosis of AST. All lesions were assessed for the presence of various dermatoscopic criteria using a manual photo dermatoscopy system DermLite (DermLite 3, Gen). Each case was evaluated by the presence of dermatoscopic features. We compared dermatoscopic and clinical features between the BCC and AST groups.

In the AST group, there were 5(23.8%) premalignant and 16(76.2%) benign lesions. Compared to the AST group, the BCC group had a significantly higher frequency of dermatoscopic features (vascular pattern, ulceration, and additional dermatoscopic features). All lesions included in this study showed more than one of the following characteristics of BCC: arborizing vessels, short fine telangiectasia, translucency, ulceration, blue-gray globules, flecked pigmentation, and rolled borders. Cutaneous lesions with 2 or fewer dermatoscopic features of BCC were much more likely to be an adnexal tumor.

***Conclusion*:** The results of this study could be valuable for the differential diagnosis of BCC and BCC-mimicking cutaneous lesions, because dermatoscopy can be especially helpful in better describing, recognizing, and differentiating these lesions. **(International Journal of Biomedicine. 2022;12(4):671-674.)**.

Keywords: adnexal skin tumor • basal cell carcinoma • differential diagnosis

For citation: Berisha RB, Dzokic D. Dermatoscopic "Mimickers" of Basal Cell Carcinoma - Adnexal Skin Tumors. International Journal of Biomedicine. 2022;12(4):671-674. doi:10.21103/Article12(4)_ShC

Abbreviations

AST, adnexal skin tumors; **BCC**, basal cell carcinoma; **TCA**, trichloroacetic acid; **PL**, Plasma Light.

Introduction

Basal cell carcinoma (BCC) is the most common type of skin cancer and the most common neoplasm in humans.[1,2] Adnexal skin tumors (AST) are numerous and various, and in their appearance give clinical and dermatoscopic features similar to BCC, which makes differential diagnosis difficult.

Dermatoscopy is a better tool for evaluating pigmented skin lesions because it gives a magnified view of the skin layers, allowing visualization of key vascular structures that are usually not visible to the naked eye. Therefore, the dermatoscope is our third eye that connects macroscopic clinical dermatology and microscopic dermatopathology.[3] Moreover, it is essential to practice dermatoscopy at every opportunity because it provides a quick diagnosis based on specific dermatoscopic criteria.[4-8] Additionally, good knowledge of the structure and dermatoscopic criteria of BCC and their more efficient diagnosis leads to more accurate and

faster diagnoses than histopathological findings.[9-11] Most adnexal tumors are derived from hair follicles, but other ones can come from eccrine ducts or apocrine glands. AST are usually mimickers of BCC. Trichoepithelioma, pilomatricoma, epidermoid cysts, and sebaceous glands are just a few of the entities reported to dermatoscopically exhibit linear branching vessels and blue-gray globules, similar to those seen in BCC.[12-15] Arborizing telangiectasias are the typical dermoscopic feature of BCC and are common in adnexal neoplasms. Trichoepithelioma, lesions derived from the hair follicles, can be single or multiple, appearing on the face after puberty. They are filled with keratin. Indications for removal are for clinical and pathological diagnosis if there is any suspicion of malignant change.

Epidermoid sebaceous cysts are follicular nodules with a central punctum, filled with keratin, lined with stratified squamous epithelium, and of various sizes. Indications for removal are cosmetic defect and recurrent infection. Removal techniques are surgical excision with dissection, small incision (PL or 2-3 mm punch biopsy), and expression of the cyst contents and wall with pressure.

Sebaceous gland hyperplasia is a common condition of the sebaceous gland when too much oil is produced. It can be flat or slightly raised, which is not harmful. Laser surgery, fractional CO_2, excision surgery, chemical peels with TCA, retinol, and cryosurgery are treatments.[16-18] However, the value and utility of dermatoscopic data are that they enable us to distinguish between BCC and adnexal tumors. The differential diagnosis can be facilitated by the observation that the vessels of adnexal tumors are usually less focused, and pinkish-red in color. Yellow structures are very suggestive of sebaceous tumors and can help to differentiate them from other tumors that show arborizing vessels.[3]

The purpose of this paper was to present the basic dermatoscopic criteria for diagnosis of BCC as well as minimally invasive methods for treatment and clinical management, with a better aesthetic outcome.

Materials and Methods

This study consisted of a retrospective review of 50 skin lesions collected in our institution over a 3-year period. We analyzed the dermoscopic images of 29 skin lesions with a clinical diagnosis of BCC and 21 cases with a clinical diagnosis of AST. Inclusion criteria were histopathologic diagnosis of BCC and AST, the availability of clinical, dermatoscopic, and histopathology findings. The exclusion criteria were any diagnostic entity other than BCC and AST. Clinical data were obtained for each patient, including age and sex, location, and clinical appearance of the lesion. All lesions were assessed for the presence of various dermatoscopic criteria using a manual photo dermatoscopy system DermLite (DermLite 3, Gen). Each case was evaluated by the presence of dermatoscopic features. We compared dermatoscopic and clinical features between the BCC and AST groups.

In the AST group, there were 5(23.8%) premalignant and 16(76.2%) benign lesions. Compared to the AST group, the BCC group had a significantly higher frequency of dermatoscopic features (vascular pattern, ulceration, and additional dermatoscopic features). All lesions included in this study showed more than one of the following characteristics of BCC: arborizing vessels, short fine telangiectasia, translucency, ulceration, blue-gray globules, flecked pigmentation, and rolled borders. Cutaneous lesions with 2 or fewer dermatoscopic features of BCC were much more likely to be an adnexal tumor.

Ethical Approval

The study was conducted in accordance with the Declaration of Helsinki and approved by the Ethics Committee of the University Clinical Center, Pristina, Kosovo. All participants provided written informed consent.

Case Presentation 1

We present the case of a 56-year-old male patient with a round tumor behind the left ear, completely asymptomatic. This formation was round and symmetrical, 9mm in diameter, and the skin covered it except for a more pronounced vascular plexus (Figure 1a). On dermoscopic examination (DermLite Photo, 3Gen) using ultrasound gel as interface fluid, we could see branched vessels anastomoses from different calibers, located everywhere, and a red-pink lesion (Figure 1b). This is a classic clinical and dermoscopic epidermoid cyst. The yellowish-white structures would not be seen in BCC. Arborizing or "basal cell-like" vessels surrounding lesions but never reaching the center are typical for sebaceous cysts. It was decided to carry out treatment (Figure 1c) and take the biomaterial to establish the diagnosis. Through a small incision made by PL, we obtained copious whitish, pasty materials. The cyst contents and walls, as well as the clinical image after treatment, are present in Figure 1. Histopathology showed a cystic wall made up of a squamous epithelium thin cells and traces of keratin corresponding to an epidermal cyst.

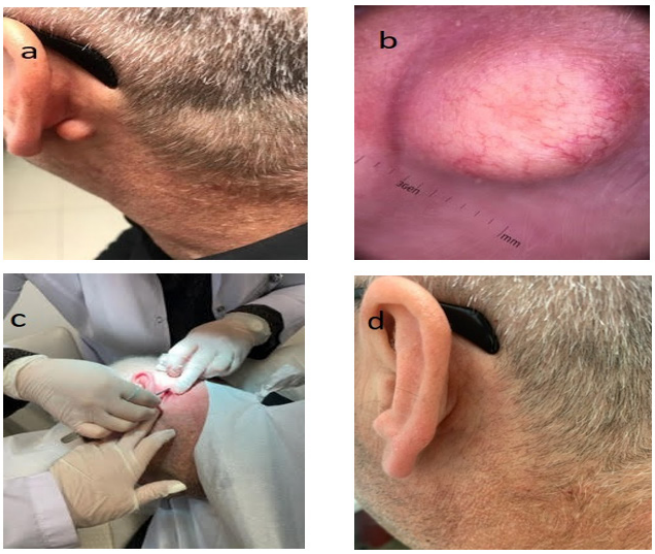

Fig. 1. *(a): Clinical image; (b): Dermoscopic image of the lesion; (c): Clinical treatment; (d): After treatment.*

Case Presentation 2

A round erythematous nodule in the *apex nasi lateral sinistra* appeared in a 25-year-old woman (Figure 2a). Dermatoscopy: a lesion with the presence of arborizing vessels, with the red-pink color of telangiectasias located on the epidermal cysts (Figure 2b). This picture can help differentiate them from the red vessels of other skin tumors, especially of BCC, and additionally show more white structureless and multiple milia-like cysts of keratin; these form the white clods. Multiple milia-like cysts are not seen in BCC and are typically clinical and dermoscopic signs of trichoepithelioma.

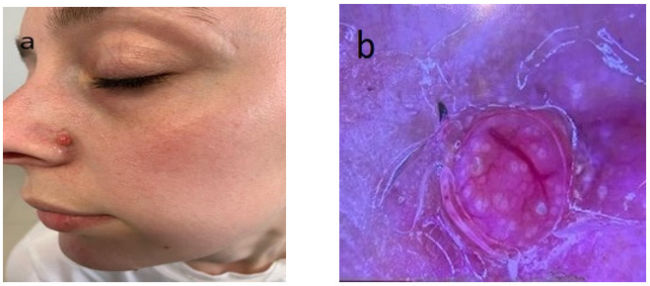

Fig. 2. *(a): Clinical image; (b): Dermoscopic image of the lesion.*

Case Presentation 3

A 73-year-old man had developed a new lesion on his forehead 9 months ago (Figure 3A). Dermoscopy of the lesion (Figure 3B) revealed the yellowish-white globules that are not seen in BCC. “Crown” or “basal cell-like” vessels seen in sebaceous gland hyperplasia surround and penetrate the lesion but never reach the center. It was decided to perform biopsy punches (3mm) to establish the diagnosis. Histopathological description of the lesion: the covering epithelium is squamous with the pigmentation of the cells of the basal layer. Signs of solar elastosis are observed in the reticular dermis. In the deeper layers, hyperplasia of the sebaceous glands is observed.

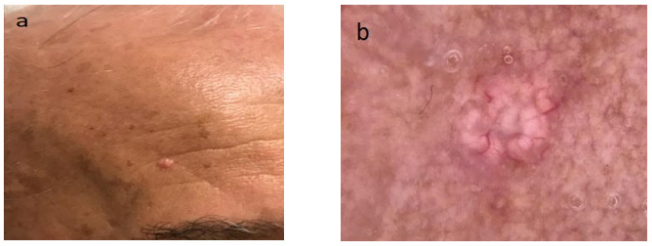

Fig. 3. *(a): Clinical image; (b): Dermoscopic image of the lesion*

Conclusion

The results of this study could be valuable for the differential diagnosis of BCC and BCC-mimicking cutaneous lesions. because dermatoscopy can be especially helpful in better describing, recognizing, and differentiating these lesions. Finally, we must be sure of the clinical diagnosis before any intervention. The dermoscopic examination is necessary for evaluating the measurement and finding of specific dermoscopic criteria, which are important to evaluate and show the value of applying dermatoscopy as a preoperative diagnostic method of treating skin lesions.

Competing Interests

The authors declare that they have no competing interests.

References

1. Del Busto-Wilhelm I, Malvehy J, Puig S. Dermoscopic criteria and basal cell carcinoma. G Ital Dermatol Venereol. 2016 Dec;151(6):642-648.
2. Álvarez-Salafranca M, Ara M, Zaballos P. Dermoscopy in Basal Cell Carcinoma: An Updated Review. Actas Dermosifiliogr (Engl Ed). 2021 Apr;112(4):330-338.. doi: 10.1016/j.ad.2020.11.011. [Article in English, Spanish]
3. Wozniak-Rito A, Zalaudek I, Rudnicka L. Dermoscopy of basal cell carcinoma. Clin Exp Dermatol. 2018 Apr;43(3):241-247. doi: 10.1111/ced.13387.
4. Enache AO, Pătrașcu V, Simionescu CE, Ciurea RN, Văduva A, Stoica LE. Dermoscopy Patterns and Histopathological Findings in Nodular Basal Cell Carcinoma-Study on 68 Cases. Curr Health Sci J. 2019 Jan-Mar;45(1):116-122. doi: 10.12865/CHSJ.45.01.16.
5. Lallas A, Apalla Z, Argenziano G, Longo C, Moscarella E, Specchio F, Raucci M, Zalaudek I. The dermatoscopic universe of basal cell carcinoma. Dermatol Pract Concept. 2014 Jul 31;4(3):11-24. doi: 10.5826/dpc.0403a02.
6. Zalaudek I, Kreusch J, Giacomel J, Ferrara G, Catricalà C, Argenziano G. How to diagnose nonpigmented skin tumors: a review of vascular structures seen with dermoscopy: part II. Nonmelanocytic skin tumors. J Am Acad Dermatol. 2010 Sep;63(3):377-86; quiz 387-8. doi: 10.1016/j.jaad.2009.11.697.
7. Kittler H, Pehamberger H, Wolff K, Binder M. Diagnostic accuracy of dermoscopy. Lancet Oncol. 2002 Mar;3(3):159-65. doi: 10.1016/s1470-2045(02)00679-4.
8. Lupu M, Caruntu C, Popa MI, Voiculescu VM, Zurac S, Boda D. Vascular patterns in basal cell carcinoma: Dermoscopic, confocal and histopathological perspectives. Oncol Lett. 2019 May;17(5):4112-4125. doi: 10.3892/ol.2019.10070.
9. Sgambato A, Zalaudek I, Ferrara G, Giorgio CM, Moscarella E, Nicolino R, Argenziano G. Adnexal tumors: clinical and dermoscopic mimickers of basal cell carcinoma. Arch Dermatol. 2008 Mar;144(3):426. doi: 10.1001/archderm.144.3.426.
10. Al Mushcab N, Husain R, Al Subaiei M, Al Qarni A, Abbas A, Al Duhileb M. Trichoblastoma mimicking basal cell carcinoma and the approach to its management: Case report.

***Corresponding author:** Reihane Bislimi Berisha. Department of Dermatology, Clinic Centre, Faculty of Medicine, University of Pristina, Prishtina, Republic of Kosovo. E-mail: reihanebislimi@hotmail.com*

Int J Surg Case Rep. 2021 Sep;86:106318. doi: 10.1016/j.ijscr.2021.106318.
11. Zaballos P, Serrano P, Flores G, Bañuls J, Thomas L, Llambrich A, Castro E, Lallas A, Argenziano G, Zalaudek I, del Pozo LJ, Landi C, Malvehy J. Dermoscopy of tumours arising in naevus sebaceous: a morphological study of 58 cases. J Eur Acad Dermatol Venereol. 2015 Nov;29(11):2231-7. doi: 10.1111/jdv.13226.
12. Zaballos P, Gómez-Martín I, Martin JM, Bañuls J. Dermoscopy of Adnexal Tumors. Dermatol Clin. 2018 Oct;36(4):397-412. doi: 10.1016/j.det.2018.05.007.
13. Lai M, Muscianese M, Piana S, Chester J, Borsari S, Paolino G, Pellacani G, Longo C, Pampena R. Dermoscopy of cutaneous adnexal tumours: a systematic review of the literature. J Eur Acad Dermatol Venereol. 2022 Sep;36(9):1524-1540. doi: 10.1111/jdv.18210.
14. Carbotti M, Coppola R, Graziano A, Verona Rinati M, Paolilli FL, Zanframundo S, Panasiti V. Dermoscopy of verrucous epidermal nevus: large brown circles as a novel feature for diagnosis. Int J Dermatol. 2016 Jun;55(6):653-6. doi: 10.1111/ijd.12948.
15. Oyasiji T, Tan W, Kane J 3rd, Skitzki J, Francescutti V, Salerno K, Khushalani NI. Malignant adnexal tumors of the skin: a single institution experience. World J Surg Oncol. 2018 May 30;16(1):99. doi: 10.1186/s12957-018-1401-y.
16. Sharma A, Paricharak DG, Nigam JS, Rewri S, Soni PB, Omhare A, Sekar P. Histopathological study of skin adnexal tumours-institutional study in South India. J Skin Cancer. 2014;2014:543756. doi: 10.1155/2014/543756.
17. Radhika K, Phaneendra BV, Rukmangadha N, Reddy MK. A study of biopsy confirmed skin adnexal tumors: experience at a tertiary care teaching hospital. Journal of Clinical and Scientific Research. 2013;2:132–138.
18. Samaila MO. Adnexal skin tumors in Zaria, Nigeria. Ann Afr Med. 2008 Mar;7(1):6-10. doi: 10.4103/1596-3519.55691.

International Journal of Biomedicine 12(4) (2022) 675-678
http://dx.doi.org/10.21103/Article12(4)_PV

POINT OF VIEW

INTERNATIONAL JOURNAL OF BIOMEDICINE

Resonant Actualization of Cultural Codes as a Determinant of Mental and Social Transformations (Part 2)

Alexander G. Kruglov*, Andrey A. Kruglov

Central Research Institute of Radiation Diagnostics
Moscow, the Russian Federation

Abstract

The cumulation of cultural codes forms and structures the integral matrix of information capacity - the cognitive thesaurus (CT) of the psyche. The dissociation of the parameters of the current balance of somatic/mental homeostasis initiates a compensatory need. The "need" extracts from the CT (actualizes) the "image" of the cultural code - a representable informational equivalent of the "need" ("dominant"). Being the content of consciousness at the time of relevance, "dominant" acquires the properties of a resonant operator, a dominant focus, forming control mental constructs. Actualization of the "dominant" initiates the activity of the "action result acceptor." For the actual dominant, the "action result acceptor" is an indicator/corrector, a frequency matching censor (resonance): perceptual dynamics of operational images of external presentation ("code key") to the parameters of the "dominant" (code). Decoding the physical parameters of the "code" provides the potential to regulate the resonant impact on the arsenal of "cultural codes" of CT through moderation of the "code key." The CT, through the "action result acceptor" (the extra-conscious regulator of the actual autonoetic forms of mental activity), programs and formats the somatic/psychic continuum of the individual. The integral matrix of the CT, having a location outside the conscious sector of the psyche, including the imperative corrector of the perceived sector of the psyche associated with the emotional register, determining/correcting the main vectors of the regulation of the life continuum, is meaningfully close to the philosophical/psychological criteria of the main cognitive regulator of the person activity, defined as the soul.(**International Journal of Biomedicine. 2022;12(4):675-678.**).

Keywords: cultural code • neuronal networks • cognitive thesaurus • spatiotemporal transformation • soul

For citation: Kruglov AG, Kruglov AA. Resonant Actualization of Cultural Codes as a Determinant of Mental and Social Transformations (Part 2). International Journal of Biomedicine. 2022;12(4):675-678. doi:10.21103/Article12(4)_PV

Abbreviations

ARA, action result acceptor; **CC**, cultural codes; **CT**, cognitive thesaurus; **GC**, generator-converter; **SPT**, spatiotemporal transformation.

Basic Part

All kinds of extra/interoceptive information in the fields of reception are converted into afferent electrical (frequency) and magnetic patterns. Afferent information undergoes spatiotemporal transformation (STT): the transformation of energy (light, sound, chemical, mechanical) of the carrier at the entrance to the system, transfer to analyzers, divergence/convergence, actualization, generation of cognitive products, displacement from consciousness, compression (reduction of redundancy while maintaining the completeness of the information).[1] The operational sequence of brain activity is as follows: the transformation of physical signals of the external environment into electromagnetic afferent flow>transformation of electromagnetic signals into mental constructs>generation of an efferent flow of control constructs of the psyche. We believe it can qualify the brain as a "generator-converter" of energy/information. The constructive result of the activity of the "generator-converter" is the nervous and cognitive constructs[2] of the psyche ("dominant") - control signals formed on the basis of redundant information and STT. In this message, "dominant" is a generalized definition of organized hierarchized constructs (packages) of cognitive information

***Corresponding author:** Alexander G. Kruglov, PhD, ScD. Central Research Institute of Radiation Diagnostics. Moscow, the Russian Federation. E-mail: krag48@mail.ru*

carriers: actual>de-actualized>repressed from conscious levels of the psyche>circulating in closed neural circuits.[3] Actualized by a compensatory need (above-threshold dissociation of the parameters of the current equilibrium of homeostasis), "dominant" becomes a resonant operator, a dominant focus, transforming into a generator of structures of mental sequences that ensure the restoration of homeostasis. In other words, "dominant" is formed and implemented as a neural association containing an encoded informational equivalent of a need with the potential to generate mental constructs upon actualization ("program" of GC).

Central generators of rhythmic activity require neither sensory inputs nor time-consistent information from outside.[4,5] The need for central generators of rhythmic activity in energy (metabolic) supply should be emphasized. The redundancy of afferent information creates the possibility of forming and structuring more than one (i.e., non-deterministic) type of behavioral activity, creating and coordinating behavioral programs implemented by neural generators. The redundancy of the information flow allows for the possibility of complication with the direct interaction of the neural generators. In other words, we believe that the brain is a "generator-converter" of energy/information of a set of neural associations that provide processes for both the "nervous" and "cognitive" sectors of the psyche aimed at ensuring the stability of somatic-psychic homeostasis. We share a common view on the storage of information in the brain in the form of frequency patterns circulating in closed neural circuits, the activity of which is reduced to a few stable states that perform the functions of information retention with error correction and reproduction of retained conditions.[3,6]

Having undergone STT and being forced out of consciousness, the "dominant" retains a stable frequency pattern of electric/magnetic parameters ("code") of the perceived and transformed image - "the informational equivalent of the object."[7] The arsenal of stored electromagnetic patterns of "dominants" (packages of information carriers) is the basic potential, the informational thesaurus of the psyche. The extraction of the "dominant" in the event of a "need" (actualization in consciousness, the acquisition of the functions of a resonant operator), along with the generation of mental constructs, initiates the mechanism of the action result acceptor (ARA). It is assumed that the ARA is implemented by a network of intercalary neurons in-ring interaction, which is a model of the future result with the expected feedback from the action results. Mismatch initiates an orienting-exploratory reaction.[8,9]

We believe that the ARA is an oscillating indicator of the coincidence/mismatch of the frequency parameters of the "code"/"code key"[10] in the "cognitive" sector of the psyche. In other words, the primary imbalance of the "current equilibrium" of somatic/mental homeostasis forms a compensatory structure: need>image (the imaginable equivalent of a "need")>motive>purposeful behavior, where the ARA is an indicator of the conformity of the matrix of "codes" (vital, social, ideal)[11] and perceptual dynamics of presented operational images, i.e., goal achievement vector.

We share the idea of human life as a spatiotemporal continuum of events, which is encoded by a continuum of neurophysiological, vegetative-emotional, and somatic-functional reactions of the whole organism.[12] The data presented earlier[13-17] allow us to determine the dynamics of the configuration and vectors of interdependent changes in the continuum of metabolism and hemodynamics, which ensure the balancing of homeostasis, both for the "norm" and the "pathology."[16] We consider the exchange continuum as a matrix of the physiological "norm," a comparison with which allows us to determine the vectors of changes in metabolism/hemodynamics in any pathology. Changes in the sets of correlation connections of the "norm" matrix are an indicator of the dynamics of vectors and the quality of metabolic connections that ensure stable hemodynamics and make up a continuum of a new (altered) level of homeostasis. For example, the transformation of signs, compositions, and vectors of metabolic regulatory relationships in hypertension reflects the mechanisms for ensuring stable hemodynamics under conditions of parametrically changed homeostasis.[13,14] That is, stable hemodynamics in hypertension is provided by a different metabolic continuum compared to the norm. Changes in metabolism/hemodynamics with "pathology" are accompanied by changes in the psyche (we do not consider the arguments of the priority of physiology/psychology). We believe that specific changes in the psyche in hypertension (and any other pathology) are an external sign of structural changes in the somatic/psychic continuum aimed at finding the boundaries of sustainable functioning. A similar mechanism forms search (adaptive, homeostatic) forms of behavior in the event of an imbalance in the sphere of social and ideal needs of the individual. The suprathreshold (boundaries of hidden frames) deviation of the socio-psychological parameters of the personality/society interrelation forms the sequence: need>goal image (a conscious need code)>motive>motivational gradient that determines the vectors and duration of goal-directed behavior structures. Achieving the goal, both tactical and at the stages of long-term attitudes, eliminates the need, and forms the parameters of temporary equilibrium in the field of ethics/aesthetics, i.e., balances the socio-psychological homeostasis. The impossibility of achieving the equilibrium parameters of homeostasis initiates orienting/search reactions, which can reach amplitudes exceeding the threshold values of both somatic and mental segments of homeostasis. The result is adaptive changes in metabolism, hemodynamics, psyche, and achievement of a range of stable functioning, equivalent to the changed parameters, defined as "pathology." Structural differences in the somatic/psychic homeostatic balance of "pathology" in comparison with "norm" (quantitative, qualitative, mental) suggest a transformation of compensatory needs and methods of their elimination. In other words, we consider "pathology" as an adaptive somatic/psychic dynamic of internal/external genesis with diverging vectors of searching for parameters of new homeostasis or development of final states.

The nosology of "pathology" determines the forms and vectors of adaptive dynamics, the structure of the transformation of compensatory needs and the arsenal of their informational equivalents ("dominants"), forming the dynamics of the somatic/psychic continuum, parametrically

different from the "norm." Considering the physical properties of the informational equivalent of the need (fixed electromagnetic and hemodynamic identification patterns), we believe that decoding the "dominant" in the period of relevance is technically possible.

The creation of a "portrait" (electromagnetic, magnetic resonance, etc.) of the decoded "dominant" (the equivalent of "need") provides the potential to regulate the resonant impact on the arsenal of "cultural codes" of CT through moderation of the "code key" to correct the equivalent of the transformed "need" in case of "pathology," which creates the possibility of a regulatory impact on the somatopsychic continuum as a whole.

We consider cultural codes (CCs) (integral images encoded in "dominant" patterns) as a fixed set of images associated with complexes of stereotypes integrated with the unconscious meaning of a thing/phenomenon in the context of culture.[3] The totality of CCs constitutes the integral matrix of the cognitive thesaurus (CT). The CT results from the cumulation of CCs formed by education, upbringing, cultural landscape, social action, and interaction.[10] The interference of the genotype and dynamics of CT determines the structure and vectors of the psychological development of the individual, the potential for creativity, and social adaptation (the structural frame of the personality).

The ARA is an indicator-corrector (frequency censor) of the limits of the admissibility of correlations: perceptual dynamics of the frequency characteristics of operational images of external presentation ("code key") to the content of the CT matrix. We believe that the integral matrix of the CT, which is outside the perceived sectors of the psyche and includes the imperative corrector/indicator (ARA) of cognitive production associated with the emotional register, determines and corrects the main vectors of the individual's life activity and is meaningfully close to the philosophical/psychological criteria of the main regulator of cognitive activity human, defined as "soul." We believe that the resonant interaction also determines the indication/correction of the frequency correspondence/inconsistency for packets of sequential perceptual information (melody, theater, taste, etc.) to the standards of CCs in the CT. Education/upbringing implants stable ethical/aesthetic standards into the psyche, which form an arsenal of cultural code elements. The increase in the number, complication, and hierarchization of CCs,[18,19] expanding the cultural potential, creates new compensatory needs, the structure of which does not always imply the possibility of their satisfaction. New needs are incentives for orienting-search behavior and an increase in the amplitude of adaptive fluctuations of the individual/society. For example, in the 18th century, the development of conceptual thinking created and scaled constructively new needs - "liberty, equality, fraternity" (with initial interference and subsequent cascading development along divergent trajectories), which became a bifurcation point that changed the social paradigm of "devotion and service" to "individualism and independence." The result was an avalanche-like growth of individual/social frustration potential and social transformations of the 18th-20th century period.[20-22]

The ARA is activated when the "dominant" is actualized, determining the behavior by the ratio of the frequency parameters of the dynamics of operational images with the "standards" (CCs) of the CT matrix arsenal. Approximation of the frequency characteristics of the images of external presentation to the boundaries of the frequency range of CCs (hidden frames) forms behavior vectors by changing the evaluative sign of indication of the ARA correspondence of the "code"/"code key," potentiated by the emotional equivalents of feedback (+, 0, -). The preconscious phase of the convergence of the frequencies of the "code"/"code key" (pre/perception) is subjectively felt as a vector emotional stress (+, 0, -) with equivalent changes in the heart rate (markers of the dynamics of the "dominant" actualization). In other words, the ARA (with an indication in the emotional register) is a vector regulator of the relation between the "dominant" (code) and the dynamics of operational images of the "code key." The ARA is an imperative corrector of cognitive activity, where the CT matrix is an arsenal of standards that determines the parameters of the ARA oscillation by the boundaries of standards (ethical, regulatory, and other codes, hidden frames). Thus, the CT matrix programs and formats the individual's life (socio/somatic/psychic) continuum, being outside the boundaries of conscious mental activity. ARA, an indicator of the CT frequency response dynamics and presented operational images, being neither energy nor a substance, determines the vectors and duration of the interaction of material information carriers ("code"/"code key"), the mechanism of interaction of which, as we believe, is an electromagnetic resonance.[10] The fundamental basis of this design is a genetic predisposition (genotype) and the integral volume of the CCs. Genetic determinism and acquired properties of the psyche (quality, volume, level of essential awareness) are a structural filter of the information received and subsequent associative structures. This filter formats the parameters of the cognitive derivative of the psyche, a symbol (image+sense), determining the semantic content of the image, vectors, and forms of purposeful behavior aimed at stabilizing socio/somatic/mental homeostasis.

Conclusion

The cumulation of CCs forms and structures the integral informative matrix of the cognitive sector of the psyche - CT. The "need," the above-threshold dissociation of the parameters of the current balance of somatic/psychic homeostasis, extracts (actualizes) the "image" of the cultural code from the CT, which is a conscious informational equivalent of the need. The actualized "code" acquires the properties of a resonant operator, a dominant focus for the time of relevance. Deciphering the physical parameters of the "code" provides the potential to regulate the resonant impact on the arsenal of "cultural codes" of CT through moderation of the "code key."

The integral informational cognitive matrix, which is outside the conscious levels of the psyche, including the ARA (the corrector of the conscious sector of the psyche) associated with the emotional register, determines the main vectors for stabilizing the socio/somatic/mental homeostasis of a person.

Through the ARA, the extra-conscious regulator of the actual (autonoetic awareness) forms of mental activity, the integral cognitive matrix programs, and formats human life as a whole, which makes it possible to consider it as a formation that is meaningfully close to the philosophical/psychological definitions of the main cognitive regulator of human life activity, formulated as the soul.

Competing Interests

The authors declare that they have no competing interests.

References

1. Shannon C. Works on information theory and Cybernetics [Raboty po teorii informatsii i kibernetike]. Trans from English. M.: Izdatel'stvo Inostrannoi Literatury.1963. [In Russian].
2. Vecker LM. Psyche and reality. Unified theory of mental processes. M.: Izdatel'stvo Smysl, 2000. [In Russian].
3. Eccles JS. An instruction-selection theory of learning in the cerebral cortex. N. Holland Biomedical Pres; 1976.
4. Sidorov AV. Central rhythm generators and functional activity neural networks of the brain. News of biomedical sciences. Minsk; 2010. [In Russian].
5. Arshavsky I, Deliagina TG, Orlovsky GN. [Central Pattern Generators: Mechanisms of the Activity and Their Role in the Control of "Automatic" Movements]. Zh Vyssh Nerv Deiat Im I P Pavlova. 2015 Mar-Apr;65(2):156-87. [Article in Russian].
6. Hopfield JJ. Neural networks and physical systems with emergent collective computational abilities. Proc Natl Acad Sci U S A. 1982 Apr;79(8):2554-8. doi: 10.1073/pnas.79.8.2554.
7. Anokhin AP. Psychic form of reflection of reality. Sofia. 1969.
8. Anokhin AP. Features of the afferent apparatus of the conditioned reflex and their significance for psychology. M. Questions of psychology.1955. [In Russian].
9. Shomes AP. Model of behavior of perception and thinking. M. Education. 2010.
10. Resonant Actualization of Cultural Codes as a Determinant of Mental and Social Transformations (Part 1). International Journal of Biomedicine. 2022;12(3):476-479. doi:10.21103/Article12(3)_PV.
11. Simonov PV. Need-information theory of emotions. M.: Voprosy Psikhologii. 1982. [In Russian].
12. Khrustalev YM. Philosophy of the psychosomatic problem. Philosophy of science and medicine. M. GEOTAR. 2009. [In Russian].
13. Kruglov AG, Gebel GY, Vasilyev AY. Impact of Intra-Extracranial Hemodynamics on Cerebral Ischemia by Arterial Hypertension (Part 1). International Journal of Biomedicine. 2012;2(2):89-95.
14. Kruglov AG, Gebel GY, Vasilyev AY. Impact of Intra-Extracranial Hemodynamics on Cerebral Ischemia by Arterial Hypertension (Part 2). International Journal of Biomedicine. 2012.2(2).96-101.
15. Kruglov AG, Utkin VN, Sherman V. Human Homeostatic Control Matrix in Norm. International Journal of Biomedicine. 2016;6(3):194-189. doi: 10.21103/Article6(3)_OA5.
16. Kruglov AG, Vasilyev AY, Sherman V. Human dynamics homeostasis control matrix in the norm with psychophisiological aspects. New York: IMRDC; 2016.
17. Kruglov AG, Utkin VN, Vasilyev AY, Kruglov AA. Spatial Synchronization of Hemodynamics and Metabolism in Norm. International Journal of Biomedicine. 2020;10(1):24-28. doi: 10.21103/Article10(1)_OA2.
18. Sumrow A. Motivation: a new look at an age-old topic. Radiol Manage. 2003 Sep-Oct;25(5):44-7.
19. Behjati M. The concept of Maslow's pyramid for cardiovascular health and its impact on "change cycle". ARYA Atheroscler. 2014 Jan;10(1):65-9.
20. Kruglov AG, Kruglov AA Adaptive Changes in the Psyche of Homo Sapiens During the Period of Singularity. (Part 1). International Journal of Biomedicine. 2020;10(2):95-100.
21. Kruglov AG, Kruglov AA. Adaptive Changes in the Psyche of Homo Sapiens during the Period of the Singularity (Part 2). International Journal of Biomedicine. 2021;11(1):68-72. doi:10.21103/Article11(1)_PV
22. Kruglov AG, Kruglov AA. Adaptive Changes in the Psyche of Homo Sapiens during the Period of the Singularity (Part 3). International Journal of Biomedicine. 2021;11(3):318-322 doi:10.21103/Article11(3)_PV.

IJBM

INTERNATIONAL JOURNAL OF BIOMEDICINE

Instructions for Authors

International Journal of Biomedicine (IJBM) publishes peer-reviewed articles on the topics of basic, applied, and translational research on biology and medicine. International Journal of Biomedicine welcomes submissions of the following types of paper: Original articles, Reviews, Perspectives, Viewpoints, and Case Reports.

All research studies involving animals must have been conducted following animal welfare guidelines such as *the National Institutes of Health (NIH) Guide for the Care and Use of Laboratory Animals*, or equivalent documents. Studies involving human subjects or tissues must adhere to the *Declaration of Helsinki and Title 45, US Code of Federal Regulations, Part 46, Protection of Human Subjects*, and must have received approval of the appropriate institutional committee charged with oversight of human studies. Informed consent must be obtained.

Pre-submissions

Authors are welcome to send an abstract or draft manuscript to obtain a view from the Editor about the suitability of their paper. Our Editors will do a quick review of your paper and advise if they believe it is appropriate for submission to our journal. It will not be a full review of your manuscript.

Manuscript Submission

Manuscript submissions should conform to the guidelines set forth in the Recommendations for the Conduct, Reporting, Editing and Publication of Scholarly Work in Medical Journals (ICMJE Recommendations), available from www.ICMJE.org.

Original works will be accepted with the understanding that they are contributed solely to the Journal, are not under review by another publication, and have not previously been published except in abstract form.

All manuscripts must be submitted through the International Journal of Biomedicine`s online submission system (www.ijbm.org/submission.php). Manuscripts must be typed, double-spaced using a 14-point font, including references, figure legends, and tables. Leave 1-inch margins on all sides. Assemble the manuscript in this order: Title Page, Abstract, Key Words, Text (Introduction, Methods, Results, and Discussion), Acknowledgments, Sources of Funding, Disclosures, References, Tables, Figures, and Figure Legends. References, figures, and tables should be cited in numerical order according to first mention in the text.

The preferred order for uploading files is as follows: Cover letter, Full Manuscript PDF (PDF containing all parts of the manuscript including references, legends, figures and tables), Manuscript Text File (MS Word), Figures (each figure and its corresponding legend should be presented together), and Tables. Files should be labeled with appropriate and descriptive file names (e.g., SmithText.doc, Fig1.eps, Table3.doc). Text, Tables, and Figures should be uploaded as separate files. (Multiple figure files can be compressed into a Zip file and uploaded in one step; the system will then unpack the files and prompt the naming of each figure. See www.WinZip.com for a free trial.)

Authors who are unable to provide an electronic version or have other circumstances that prevent online submission must contact the Editorial Office prior to submission to discuss alternate options (editor@ijbm.org).

Cover Letter

The cover letter should be saved as a separate file for upload. In it, the authors should (1) state that the manuscript, or parts of it, have not been and will not be submitted elsewhere for publication; (2) state that all authors have read and approved the manuscript; and (3) disclose any financial or other relations that could lead to a conflict of interest. If a potential conflict exists, its nature should be stated for each author. When there is a stated potential conflict of interest a footnote will be added indicating the author's equity interest in or other affiliation with the identified commercial firms.

The corresponding author should be specified in the cover letter. All editorial communications will be sent to this author. A short paragraph telling the editors why the authors think their paper merits publication priority may be included in the cover letter.

Types of articles

Original articles

Original articles present the results of original research. These manuscripts should present well-rounded studies reporting innovative advances that further knowledge about a topic of importance to the fields of biology or medicine. These can be submitted as either a full-length article (no more than 6,000 words, 4 figures, 4 tables) or a Short Communication (no more than 2,500 words, 2 figures, 2 tables). An original

article may be Randomized Control Trial, Controlled Clinical Trial, Experiment, Survey, and Case-control or Cohort study.

Case Reports

Case reports describe an unusual disease presentation, a new treatment, a new diagnostic method, or a difficult diagnosis. The author must make it clear what the case adds to the field of medicine and include an up-to-date review of all previous cases in the field. These articles should be no more than 5,000 words with no more than 6 figures and 3 tables. Case Reports should consist of the following headings: Abstract (no more than 100 words), Introduction, Case Presentation (clinical presentation, observations, test results, and accompanying figures), Discussion, and Conclusions.

Reviews

Reviews analyze the current state of understanding on a particular subject of research in biology or medicine, the limitations of current knowledge, future directions to be pursued in research, and the overall importance of the topic. Reviews could be non-systematic (narrative) or systematic. Reviews can be submitted as a Mini-Review (no more than 2,500 words, 3 figures, and 1 table) or a long review (no more than 6,000 words, 6 figures, and 3 tables). Reviews should contain four sections: Abstract, Introduction, Topics (with headings and subheadings, and Conclusions and Outlook.

Perspectives

Perspectives are brief, evidenced-based and formally structured essays covering a wide variety of timely topics of relevance to biomedicine. Perspective articles are limited to 2,500 words and usually include ≤10 references, one figure or table. Perspectives contain four sections: Abstract, Introduction, Topics (with headings and subheadings), Conclusions and Outlook.

Viewpoints

Viewpoint articles include academic papers, which address any important topic in biomedicine from a personal perspective than standard academic writing. Maximum length is 1,200 words, ≤70 references, and 1 small table or figure.

Manuscript Preparation

Title Page

The first page of the manuscript (title page) should include (1) a full title of the article, (2) a short title of less than 60 characters with spaces, (3) the authors' names, academic degrees, and affiliations, (4) the total word count of the manuscript (including Abstract, Text, References, Tables, Figure Legends), (5) the number of figures and tables, and (6) the name, email address, and complete address of corresponding author.

Disclaimers. An example of a disclaimer is an author's statement that the views expressed in the submitted article are his or her own and not an official position of the institution or funder.

Abstract

The article should include a brief abstract of no more than 200 words. Limit use of acronyms and abbreviations. Define at first use with acronym or abbreviation in parentheses. The abstract should be structured with the following headings: Background, Methods and Results, and Conclusions. The Background section should describe the rationale for the study. Methods and Results should briefly describe the methods and present the significant results. Conclusions should succinctly state the interpretation of the data. Authors should supply a list of up to four key words not appearing in the title, which will be used for indexing. The key words should be listed immediately after the Abstract. Use terms from the Medical Subject Headings (MeSH) list of Index Medicus when possible.

Main text in the IMRaD format

Introduction should describe the purpose of the study and its relation to previous work in the field; it should not include an extensive literature review.

Methods should be concise but sufficiently detailed to permit repetition by other investigators. Previously published methods and modifications should be cited by reference. A subsection on statistics should be included in the Methods section.

Results should present positive and relevant negative findings of the study, supported when necessary by reference to Tables and Figures.

Discussion should interpret the results of the study, with emphasis on their relation to the original hypotheses and to previous studies. The importance of the study and its limitations should also be discussed.

The IMRaD format does not include a separate Conclusion section. The conclusion is built into the Discussion. More information on the structure and content of these sections can be found in the Recommendations for the Conduct, Reporting, Editing and Publication of Scholarly Work in Medical Journals (ICMJE Recommendations), available from www.ICMJE.org.

Acknowledgments, Sources of Funding, and Disclosures

Acknowledgments : All contributors who do not meet the criteria for authorship should be listed in an acknowledgments section. Examples of those who might be acknowledged include a person who provided purely technical help, writing assistance, or a department chairperson who provided only general support. Authors should declare whether they had assistance with study design, data collection, data analysis, or manuscript preparation. If such assistance was available, the authors should disclose the identity of the individuals who provided this assistance and the entity that supported it in the published article.

Sources of Funding: All sources of financial support for the study should be cited on the title page, including federal or state agencies, nonprofit organizations, and pharmaceutical or other commercial sources.

Disclosure and conflicts of interest: All authors must disclose any financial or other relations that could lead to a conflict of interest. If a potential conflict exists, its nature should be stated for each author. All sources of financial support for the study should be cited, including federal or state agencies, nonprofit organizations, and pharmaceutical or other commercial sources. Please use ICMJE Form for Disclosure of Potential Conflicts of Interest (http://www.icmje.org/conflicts-of-interest/).

References

References should follow the standards summarized in the NLM's International Committee of Medical Journal Editors (ICMJE) Recommendations for the Conduct, Reporting,

Editing and Publication of Scholarly Work in Medical Journals: Sample References webpage (www.nlm.nih.gov/bsd/uniform_requirements.html) and detailed in the NLM's Citing Medicine, available from www.ncbi.nlm.nih.gov/books/NBK7256/. MEDLINE abbreviations for journal titles (www.ncbi.nlm.nih.gov/nlmcatalog/journals) should be used. The first six authors should be listed in each reference citation (if there are more than six authors, "et al" should be used following the sixth). Periods are not used in authors' initials or journal abbreviations. Examples of journal reference style:

Journal Article: Serruys PW, Ormiston J, van Geuns RJ, de Bruyne B, Dudek D, Christiansen E, et al. A Polylactide Bioresorbable Scaffold Eluting Everolimus for Treatment of Coronary Stenosis: 5-Year Follow-Up. J Am Coll Cardiol. 2016;67(7):766-76. doi: 10.1016/j.jacc.2015.11.060.

Book: Murray PR, Rosenthal KS, Kobayashi GS, Pfaller MA. Medical Microbiology. 4th ed. St. Louis: Mosby; 2002.

Chapter in Edited Book: Meltzer PS, Kallioniemi A, Trent JM. Chromosome alterations in human solid tumors. In: Vogelstein B, Kinzler KW, editors. The Genetic Basis of Human Cancer. New York: McGraw-Hill; 2002:93–113.

References should be numbered consecutively in the order in which they are first mentioned in the text. Identify references in text, tables, and legends by Arabic numerals in parentheses and listed at the end of the article in citation order.

Tables

Tables should be comprehensible without reference to the text and should not be repetitive of descriptions in the text. Every table should consist of two or more columns; tables with only one column will be treated as lists and incorporated into the text. All tables must be cited in the text and numbered in order of appearance. Tables should include a short title. Place explanatory matter in footnotes, not in the heading. Explain all nonstandard abbreviations in footnotes, and use symbols to explain information if needed. Each table submitted should be double-spaced, each on its own page. Each table should be saved as its own file as a Word Document. Explanatory matter and source notations for borrowed tables should be placed in the table footnote.

Figures and Legends

All illustrations (line drawings and photographs) are classified as figures. All figures should be cited in the text and numbered in order of appearance. Figures should be provided in .tiff, .jpeg or .eps formats. Color images must be at least 300 dpi. Gray scale images should be at least 300 dpi. Line art (black and white or color) and combinations of gray scale images and line art should be at least 1,000 dpi. The optimal size of lettering is 12 points. Symbols should be of a similar size. Figures should be sized to fit within the column (86 mm) or the full text width (180 mm). Line figures must be sharp, black and white graphs or diagrams, drawn professionally or with a computer graphics package. Legends should be supplied for each figure and should be brief and not repetitive of the text. Any source notation for borrowed figures should appear at the end of the legend. Figures should be uploaded as individual files.

Units of Measurement

Measurements of length, height, weight, and volume should be reported in metric units (meter, kilogram, or liter) or their decimal multiples. Temperatures should be in degrees Celsius. Blood pressures should be in millimeters of mercury. All measurements must be given in SI or SI-derived units. Drug concentrations may be reported in either SI or mass units, but the alternative should be provided in parentheses where appropriate.

Style and Language

The journal accepts manuscripts written in English. Spelling should be US English only. The language of the manuscript must meet the requirements of academic publishing. Reviewers may advise rejection of a manuscript compromised by grammatical errors. Non-native speakers of English may choose to use a copyediting service.

Abbreviations and Symbols

Use only standard abbreviations; use of nonstandard abbreviations can be confusing to readers. Avoid abbreviations in the title of the manuscript. The spelled-out abbreviation followed by the abbreviation in parenthesis should be used on first mention unless the abbreviation is a standard unit of measurement.

Drugs should be referred to by their generic names. If proprietary drugs have been used in the study, refer to these by their generic name, mentioning the proprietary name, and the name and location of the manufacturer, in parentheses.

Permissions

To use tables or figures borrowed from another source, permission must be obtained from the copyright holder, usually the publisher. Authors are responsible for applying for permission for both print and electronic rights for all borrowed materials and are responsible for paying any fees related to the applications of these permissions. This is necessary even if you are an author of the borrowed material. It is essential to begin the process of obtaining permission early, as a delay may require removing the copyrighted material from the article. The source of a borrowed table should be noted in a footnote and of a borrowed figure in the legend. It is essential to use the exact wording required by the copyright holder. A copy of the letter granting permission, identified by table or figure number, should be sent along with the manuscript. A permission request form is provided for the authors use in requesting permission from copyright holders.

Open Access Policy

All articles published by International Journal of Biomedicine are made freely and permanently accessible online immediately upon publication, without subscription charges or registration barriers. Articles published under an IMRDC user license are protected by copyright and may be used for non-commercial purposes. A copy of the full text of each Open Access article is archived in an online repository separate from the journal. The International Journal of Biomedicine's articles are archived in Scientific Electronic Library (Russian Science Citation Index). The authors can also self-archive the final publisher's version/PDF on personal website, departmental website, institutional repository with a link to publisher version.

Users may access, download, copy, translate, text and data mine (but may not redistribute, display or adapt) the articles for non-commercial purposes provided that users cite the article using an appropriate bibliographic citation (i.e. author(s), journal, article title, volume, issue, page numbers, DOI and the link to the definitive published PDF version on www.ijbm.org).

Article Processing Charges

When a paper is accepted for publication, the author is issued an invoice for payment of Article Processing Charge (APC). APC can be paid by the author or on their behalf, for example, by their institution or funding body.

APC helps IMRDC recover the costs of publication—including peer review management, production of the journal printed version, and online hosting and archiving, as well as inclusion in citation databases, enabling electronic citation in other journals that are available electronically. IJBM publishes all content Open Access and makes the content freely available online for researchers and readers.

IJBM charges a processing fee of $115.00 per printed black and white journal page and $230.00 per printed page of color illustrations. IJBM charges a processing fee of $94.00 per page in the case of online-only publications. For online-only publications, all illustrations submitted in color will be published in color online, at no cost to the author.

Under IJBM's existing policy, certain categories of authors are eligible for a discount. The amount of discount depends on factors such as country of origin, position of the author in the institute and quality and originality of the work. Young researchers and first time authors may also qualify for a discount. To apply for a discount, please contact our office using the 'Contact Us' page or send email to the Publisher (editor@ijbm.org) with the following information:

- Your name and institution with full address details
- Reason for applying for a waiver
- Title of your paper
- Country of residence of any co-authors.

Page Proofs

Page proofs are sent from the Publisher electronically and must be returned within 72 hours to avoid delay of publication. Generally, peer review is completed within 3-4 weeks and the editor's decision within 7-10 days of this. It is therefore very rare to have to wait more than 6 weeks for a final decision.

IMRDC Author Services

If you need help preparing a manuscript for submission, our publisher, IMRDC, offers a range of editorial services for a fee, including Advanced Editing and Translation with Editing. Please note that use of IMRDC Author Services does not guarantee acceptance of your manuscript.

It is important to note that when citing an article from IJBM, the correct citation format is **International Journal of Biomedicine.**